KIRKBRIGHT
SARGENT

Atomic Absorption
and Fluorescence Spectroscopy

535.
84
KIR

Atomic Absorption and Fluorescence Spectroscopy

G. F. Kirkbright
and M. Sargent

Academic Press
London New York San Francisco
A Subsidiary of Harcourt Brace Jovanovich, Publishers

ATOMIC ABSORPTION AND FLUORESCENCE SPECTROSCOPY

G. F. KIRKBRIGHT
Department of Analytical Chemistry,
Imperial College,
London

M. SARGENT
Thornton Research Centre,
Shell Research Limited,
Cheshire, England

1974 ACADEMIC PRESS
LONDON · NEW YORK · SAN FRANCISCO

A Subsidiary of Harcourt Brace Jovanovich, Publishers

ACADEMIC PRESS INC. (LONDON) LTD
24-28 Oval Road
London NW1 7DX

U.S. Edition published by
ACADEMIC PRESS INC.
111 Fifth Avenue,
New York, New York 10003

Copyright © 1974 by Academic Press Inc. (London) Ltd

All Rights Reserved

No part of this book may be reproduced in any form
by photostat, microfilm, or any other means, without
written permission from the publishers

Library of Congress Catalog Card Number: 74-5647

ISBN: 0-12-409750-2

PRESTON
POLYTECHNIC
59513
535.84 KIR

Printed by William Clowes & Sons Limited
London, Colchester and Beccles

Preface

The decision to prepare this volume was taken at a time (1969) when few texts devoted exclusively to analytical atomic absorption spectroscopy (AAS) had been published, and none concerned specifically with atomic fluorescence spectroscopy (AFS) was available. In the past four years several additional texts on AAS, which also contain sections on AFS, have been written. Despite the appearance of these new volumes, however, we have not been discouraged from preparation of the present volume. It was felt that there was an unfilled need for a general textbook which gave more detailed, though not indigestible, theory of both techniques, and which presented a more exhaustive consideration of instrumentation and practical techniques for the working analytical chemist as well as for the student of analytical chemistry. We recognize that it is dangerous to attempt comprehensive coverage of the theory and practice of techniques at a time when they have been developing rapidly; although it is still possible that the present volume may be rendered rapidly out of date by startling new advances in AAS and AFS, it is the opinion of the authors that while applications of the techniques continue to increase, some stabilization in the fundamentals of the instrumentation and methodology has occurred. Two exceptions which might be mentioned specifically are in the instrumentation and methodology associated with the use of non-flame cells for AAS and AFS and, the application of laser sources in AFS. Atomic fluorescence spectroscopy is considered throughout as a technique which is complementary to AAS and which holds considerable promise for many applications.

The volume deals in detail with the individual components of atomic absorption and fluorescence spectrometers (sources, atom cells, dispersive devices etc.). Sufficient fundamental theory is presented to avoid a misleading and oversimplified approach but the emphasis in the text is placed on the practice of the techniques for analysis. Although the applications literature is not exhaustive the authors feel that sufficient data is given to the reader in search of

AAS or AFS methods for a particular application; he should be able to gain an estimate of the number of alternatives possible and obtain easy access to the pertinent original publications. As mentioned at several points in the text, we consider the advent of the publication 'Annual Reports on Analytical Atomic Spectroscopy', in which comprehensive world-wide coverage of both fundamental and applications literature in both AAS and AFS is presented regularly, has rendered unnecessary any attempt at up-to-date comprehensive coverage of the applications literature in a volume of this type.

During the past decade many workers have made significant contributions to the understanding of the fundamental principles of AAS and AFS and the analytical practice of these techniques. In particular, however, we wish to pay tribute to the work of C.S.I.R.O., Australia, where analytical AAS originated in the work of Alan Walsh and his colleagues, and to Prof. C. Th. J. Alkemade, University of Utrecht, who has so often pointed the way for developments in these techniques and has made many contributions to understanding of their fundamental principles. The extensive contributions of Winefordner and co-workers at the University of Florida, which have so assisted the development of the techniques, must also be acknowledged. Perhaps to a greater extent than for many other instrumental techniques of analysis a very considerable contribution to AAS theory and practice has been made by the instrument manufacturers. In the case of several companies these contributions have been so important and sustained that the work of their employees has received international recognition.

It is a pleasure to acknowledge the encouragement given to us during preparation of this book by Professor Tom West. We wish to express our thanks to the many authors and publishers who have given permission for the reproduction of figures and other material from the original literature. We thank close colleagues for helpful discussions and acknowledge the assistance given by Mike Adams, Dai Bevan, Arthur Ward and P. J. Wilson in collection of much of the applications data given in Chapter 13. We also wish to thank Mike Adams for the preparation of the Subject Index. We are indebted to the Technical Editing staff at Thornton Research Centre, particularly Bob Taylor and Tony Shaw, for help with the preparation of manuscript and diagrams. Many secretaries have been involved with the task of preparation of draft and corrected typescripts. We particularly wish to thank Mrs. Janet Broome and Miss Maureen Coleman for their efforts in this respect. We also should thank our families for their patience and forebearance during the preparation of this book.

G. F. Kirkbright.
M. Sargent.
November, 1973.

Contents

Chapter 5 Spectral Light Sources

Chapter 6 Flames

Chapter 7 Non-flame Absorption and Fluorescence Cells

Chapter 8 Introduction of Liquid Samples into Flame Atom Cells

Chapter 9 Wavelength Selection

Chapter 10 Atomic Absorption and Fluorescence Instrumentation

Chapter 11 Practical Techniques of Atomic Absorption and Fluorescence Spectroscopy

Chapter 12 Interferences

Chapter 13 Analytical AAS and AFS Characteristics of the Elements and Applications Data

Chapter 14 Special Techniques in AAS and AFS

CHAPTER 1

Introduction

1.1 HISTORICAL ASPECTS

The techniques to be described in this book are concerned with one small region of the electromagnetic spectrum: the wavelength range extending from approximately 180 nm to 800 nm and embracing the region of visible light. Within the restrictions imposed by these somewhat arbitrary limits to "the spectrum" it may be said that the history of spectroscopy dates back over two and a half centuries to the discovery of the visible spectrum by Newton.[1] Since that time, spectroscopists at any given period have concentrated their efforts on one of two fields: analytical chemistry or the interpretation of physical and atomic properties. At the present time atomic absorption spectroscopy in particular represents a major area of interest and growth in the former field.

Following Newton's study of the spectrum of the sun was a period of almost one hundred years entirely concerned with *emission* spectroscopy. However, in 1802 Wollaston[2] reported the presence of dark bands in the continuum emission spectrum of the sun and, after a more detailed study by Fraunhofer (1814), Brewster[3] (1820) was able to ascribe them to *absorption* of radiation within the sun's atmosphere. Another forty years passed before Kirchoff and Bunsen[4,5,6] showed that one of these dark bands in the emission spectrum of the sun corresponded exactly to the yellow emission band obtained when sodium vapour is heated in a flame. Their work enabled Kirchoff to enounce the fundamental relationship between emission and absorption spectra: any species that can be excited to emit radiation at a particular wavelength will also absorb radiation at that wavelength. Thus a new technique could be added to the already well-established one of emission spectroscopy and the work of Bunsen and Kirchoff was continued and placed on a sound theoretical basis by the physicists and astronomers of the early twentieth century. Their research, which has been summarized by Mitchell and Zemansky,[7] was mainly performed with atoms at low pressures in enclosed vessels and was primarily concerned with the interpretation of atomic structure and spectra.

Although there were occasional practical applications to the study of elements present in solar and stellar atmospheres, virtually no attempt was made to apply the discoveries to practical chemical analysis; only the determination of mercury vapour in air[8] was reported as a rather exceptional example. This striking contrast with emission spectroscopy, which by the 1920s was an important analytical tool in the form of arc and spark spectrography, must be viewed in the light of two important factors. Firstly, before about 1930 the emission technique was mainly used for qualitative analysis, and there was no advantage to be gained from using absorption spectra for this purpose (in fact the reverse is true, as is witnessed by the present-day applications of the absorption technique). Secondly, even after 1930 the difficulty of making absorption measurements for quantitative analysis was considerably greater than that experienced with emission. Not only was the photographic recording of the absorption spectra more tedious, but the theory seemed to indicate that they would only prove useful for quantitative analysis if observed under very high resolution. Thus, when atomic absorption spectrometry was introduced as an analytical tool by Walsh[9,10] in 1953 and Alkemade and Milatz[11,12] in 1955, emission methods of analysis were firmly established and difficult to replace. However, these workers were able to overcome two major problems which twenty years earlier had seemed almost insuperable. The technique proposed by Walsh of measuring only the peak absorbance at the centre of the spectral line (see Section 3.5.2) removed the practical difficulty of making quantitative absorption measurements with a simple monochromating device, and the availability of photoelectric light detectors of very high sensitivity meant that it was no longer any more troublesome to record absorption rather than emission signals. By presenting this new "simple" absorption technique in combination with modern instrumentation and a high-temperature flame as the atom reservoir, Walsh in particular was able to demonstrate the advantages of atomic absorption spectrometry over emission spectrometry and flame photometry for many elements. Today a wide range of instruments is available commercially, atomic absorption is widely used in a greater range of routine determinations than the arc, spark and simple flame emission techniques, and new publications on atomic absorption spectrometry greatly outnumber those on the emission methods.

The re-emission by an atom of radiation as *fluorescence* after the absorption of light from a suitable source was first reported in 1905 when Wood[13] succeeded in exciting atomic fluorescence of the D lines of sodium vapour. He used an evacuated test tube containing sodium vapour as the atom reservoir and a gas flame containing sodium chloride as the illuminating source. The result was predicted by the classical theory of light in the same way as the resonance of standing waves observed for sound, vibrating strings, etc. Wood, therefore, termed this fluorescence "resonance radiation" and the name is still encountered today for the atomic fluorescence of resonance lines such as the D lines. Similar work was carried out with other readily volatile elements, enclosed cells again being used to contain the atomic vapour, and was mainly concerned with fundamental studies of atomic spectra. This work has been described in some detail by Mitchell and Zemansky[7] and by Pringsheim.[14]

The fluorescence of atoms in flames was first reported in 1923 by Nichols and Howes[15] for calcium, strontium, barium, lithium and sodium in a Bunsen flame. Similar observations were also reported by Badger[16] and by Mannkopff[17] for a number of other volatile elements. Further interest in the subject then appears to have lapsed until the use of atomic fluorescence spectrometry in 1956 by Boers, Alkemade and Smit[18] to study quenching processes in flames. Following this, a further report was given by Alkemade[19] in 1962 on sodium fluorescence in flames together with the suggestion that it might have analytical possibilities. This suggestion was followed up by Winefordner, Vickers and Staab[20,21] who reported the first successful analytical application of atomic fluorescence spectrometry with the determination of zinc, cadmium, and mercury. Since that time the number of publications on the technique has increased rapidly.

1.2 FUNDAMENTALS

It is worthwhile initially to outline the instrumental arrangement most commonly used for analytical absorption and fluorescence measurements, and to define some of the more widely used terms. This should avoid confusion when these terms arise in subsequent chapters.

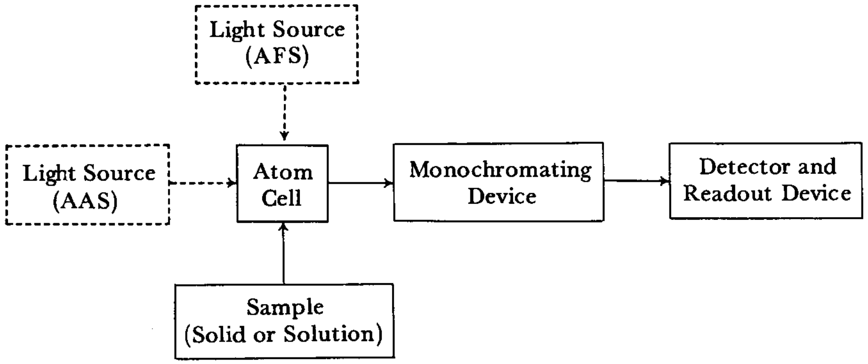

Fig. 1-1. Basic apparatus for analytical atomic spectroscopy.

The basic apparatus required is shown diagrammatically in Fig. 1-1, and a typical commercial atomic absorption spectrophotometer conforming to this arrangement is illustrated in Fig. 1-2. In order to observe atomic absorption or fluorescence signals it is necessary to have a population of free, neutral atoms of the element of interest. Thus, the most important component of the instrument is the *atom cell* or reservoir. This may take a wide variety of forms, ranging from a simple quartz cell at room temperature (for mercury) to a high-temperature flame or plasma with its ancillary equipment. If the atoms contained in this cell are to absorb radiation, and possibly to re-emit a fraction of this as fluorescence, they must be irradiated with light of the same wavelength as that of a strong absorption spectral line of the element that has been atomized. This radiation is obtained from a *light source* which may emit the spectrum of a single element, the spectra of several elements whose common analysis is frequently required or a continuum spectrum (see Section 5.1). As with the atom reservoir, the complexity of the light source and its ancillary equipment can vary considerably.

The light transmitted after the atomic absorption process has occurred, or the fluorescence emission stimulated from the atoms in the reservoir, will often be composed of radiation of both the required wavelength (i.e. the absorption line(s)) and a number of unwanted wavelengths. The latter may simply take the form of stray daylight, or may arise from other spectral lines emitted by the light source or the atom cell. It is usually necessary, therefore, to select the wavelength of the radiation from the atom cell before an attempt is made to measure the absorption or fluorescence signal. This is done with a *monochromating device*, the design of which will depend on the complexity of the instrument and the type of work to be carried out with it. For simple instruments intended only for measurements with one or two elements giving single strong spectral lines at wavelengths that can be detected a simple optical filter may suffice. On the other hand, most commercial instruments designed for maximum versatility utilize relatively complex diffraction grating monochromators (see Chapter 9).

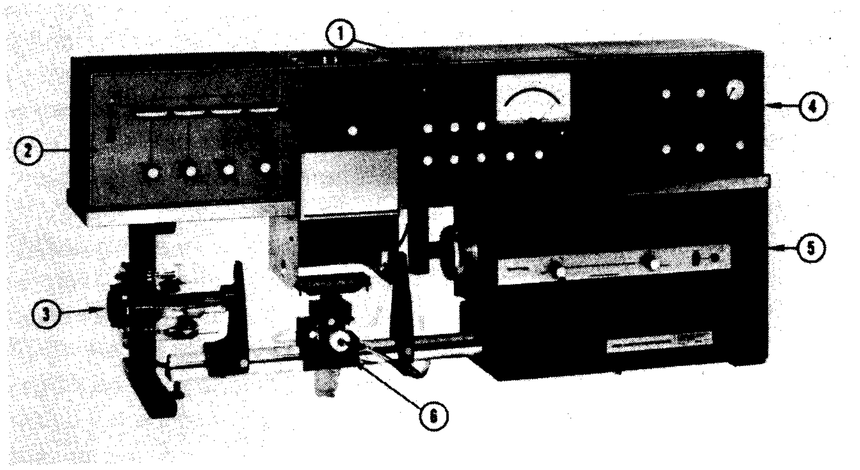

Fig. 1-2. Commercial atomic absorption spectrophotometer. 1, amplifier; 2, lamp power supply; 3, lamp turret; 4, gas control unit; 5, monochromator; 6, burner and sample nebulizer.

Whatever monochromating device is employed, it must be placed in the correct position with respect to the light source and the atom cell. In Fig. 1-1 it is shown to lie in the direct optical path from the source to the cell for absorption measurements (so that the amount of radiation absorbed is easily determined) and at 90° to this optical path for fluorescence measurements (so that fluorescence emission may be detected without interference from any radiation received direct from the light source). Although these configurations are frequently adhered to in commercial instruments for the *optical path* between light source and monochromating device, it must be remembered that the arrangement of the individual components may not be as straightforward as in Fig. 1-1; in many cases the light beam may be deflected by several mirrors or prisms so that a practically convenient instrument design is obtained. Less frequently, the optical configuration itself may vary. This is particularly true with fluorescence measurements when the relative positions of the light source and monochromating device are not of great fundamental importance provided that radiation cannot pass directly between them. Thus, if it is necessary to irradiate the atom cell with several light sources, perhaps for the simultaneous analysis of several elements, the 90° optical configuration may be changed.

Once the absorption or fluorescence signal has been obtained it must be recorded and measured. The device used to convert the radiation constituting the signal into a form that can be easily measured (and recorded if necessary) is known as the *detector*. The traditional detector is, of course, the photographic plate or film; as mentioned earlier, however, this is not very convenient for quantitative measurements and quite impracticable for absorption measurements. Hence almost all modern instruments use photoelectric devices (see Chapter 10). These convert the optical signal to an electrical signal so that a *readout device* is required in order to measure the signal. Again, this may vary considerably in complexity to range from a simple meter to measure the voltage generated by a photoelectric cell to elaborate electronic assemblies using computing techniques.

In addition to the instrumental components discussed above other more general terminology is in use the early definition of which is worthwhile. The analytical techniques utilizing the measurement of atomic absorption and fluorescence are usually referred to as respectively *atomic absorption spectrometry, spectroscopy or spectrophotometry* (*AAS*) and *atomic fluorescence spectrometry, spectroscopy or spectrophotometry* (*AFS*). The instruments used for the measurements are referred to as *spectrophotometers or spectrometers*. These different derivatives of spectr- are often used quite interchangeably in the literature but there is usually little danger of confusion arising. The observation of the presence of an element by its absorption or fluorescence spectrum is referred to as its *detection* whereas the quantitative analysis is known as its *determination*. The actual element detected or determined is frequently termed the *analyte* and it is present in the *analytical sample*, the actual composition of which may be referred to as the *sample matrix*. The word *sample* is also generally used for the solid or solution added to the atom cell, even though this may have been obtained by complicated treatment of the original analytical sample. Thus, care is sometimes necessary to avoid confusion, especially when mention is made of the *analyte concentration* in the sample. As absorption measurements in particular are made as the difference between two signals it is usually necessary to have a sample giving zero signal, that is, a *blank* which contains no analyte element. Finally, other species present in the sample or the atom cell can sometimes cause an erroneous determination of the analyte; these are known as *interferences* and are revered by analytical chemists.

The discussion of AAS and AFS necessitates frequent mention of the emission technique, and much of the nomenclature given above applies to this also. The corresponding names *atomic emission spectrometry, spectroscopy or spectrophotometry* (*AES*) are widely used; it is also common to find the technique referred to as *flame emission spectrometry, spectroscopy or spectrophotometry* (*FES*), as the flame is a widely used atom cell (in the present discussion we shall exclude traditional arc or spark emission spectrography from our definition of AES).

1.3 COMPARISON OF TECHNIQUES

It is readily recognizable from the preceding pages that essentially the same equipment and techniques may be applied to both AAS and AFS. In fact, apart from the spectral light sources, this may also apply to AES. Thus, in an analytical laboratory where inorganic trace analysis is frequently carried out by atomic spectroscopy, sufficient equipment and expertise may be available for all three techniques. It is then possible to select one of the techniques on its own merits as the most suitable for a particular determination. In view of this, it is intended to make a brief comparison of techniques by discussion of their individual advantages and disadvantages, and then to make a general comparison of all three techniques with other instrumental methods of inorganic analysis.

1.3.1 Comparison of AES, AAS and AFS

It is important first to emphasize the opinion of the authors implied above that the three techniques are complementary and no one has outstanding advantages over the other two. This is true whether comparison is based on the criterion of "limit of detection" or that of ease and convenience of analysis. First, at the time of writing there exists for each technique a group of elements for which it may provide the most sensitive method of analysis. There also remain many elements whose determination may be undertaken with equal sensitivity by two or even all three techniques. Secondly, each technique has its own instrumental and experimental advantages and disadvantages. Many are common to more than one technique, and a direct comparison may be made by detailing favourable and unfavourable points for each technique. This approach should assist when a decision is to be made concerning the technique best suited to a particular analytical service.

Advantages of AES

1. No spectral light sources are required.
2. For many elements a wide choice of sensitive analytical lines exists; many of these lines may lie in the visible region of the spectrum where intensity measurements are less complicated than in the ultraviolet region.
3. The technique can provide flexibility in dealing with a wide range of sample concentrations.
4. Qualitative as well as quantitative analysis is readily carried out.
5. Simultaneous multi-element analysis is possible.

Disadvantages of AES

1. Large changes in the intensity of the analytical signal result from small temperature changes in the atom cell.
2. Background and other line or band spectra emitted from the atom cell may cause greater interference than in the other two techniques.
3. Considerable operator skill is required routinely to obtain reliable results.
4. A high quality monochromator is essential if the technique is to be reliable and versatile.

Advantages of AAS

1. The instrumentation is simple to set up and operate because of the useful wavelength and intensity reference provided by the background light source.

2. The technique is easily automated.
3. Double-beam operation is readily arranged to provide for reduction of the effect of variation in intensity of the light source.
4. Sharp-line light sources provide better spectral selectivity than is usually obtainable with AES.
5. The analytical signal in AAS for many elements is less sensitive to temperature changes in the atom cell than it is in AES.

Disadvantages of AAS

1. A large number of relatively expensive spectral light sources are usually required. High sensitivity cannot be obtained when continuum or broad-line light sources are used with low resolution commercial instrumentation.
2. Many of the most useful absorption lines are quite far into the ultraviolet region of the spectrum where measurement is more difficult; for most elements only a few analytical lines are available.
3. When spectral interferences do occur they are less apparent than in AES and can therefore cause a more serious chance of error.
4. It is relatively difficult to obtain a long range of concentration over which linear calibration is possible.

Advantages of AFS

1. Sensitivity attainable is controlled by the intensity of the light source employed.
2. The technique is less sensitive to temperature changes in the atom cell than AES is.
3. Much of the equipment required can be less complex than that needed for AES or AAS.
4. Continuum or fairly broad-line light sources can be used with a less serious loss of sensitivity than for AAS.
5. High sensitivity is available far into the ultraviolet region of the spectrum where AES is insensitive.

Disadvantages of AFS

1. A spectral light source is required, usually one for each element, as in AAS.
2. Quenching of the fluorescence signal is greatly affected by the gas species present in the atom cell.
3. The very hot flames needed as atom cells for the determination of elements such as the refractory metals and to avoid some chemical interferences favour AES rather than AFS.

4. Scattering of light from the source may be more difficult to deal with than in AAS.
5. Although AFS usually gives a wider linear concentration range than does AAS, the extension is only on the low side of the range.
6. AFS is much less sensitive than AES for elements giving their main absorption and fluorescence lines in the visible region.

To summarize, AAS is probably the technique best suited to rapid, routine operation for analysis by relatively unskilled operators. AES is the more versatile method for use by a skilled analytical chemist in a laboratory where small numbers of non-routine determinations are required, often at short notice. AFS can provide extremely high sensitivities for certain elements less easily determined by the other two techniques, but is often said to combine some of their disadvantages.

1.3.2 Comparison with Other Instrumental Methods of Inorganic Trace Analysis

In the comparison that follows we shall be more concerned with the advantages of AAS and AFS to an analytical laboratory carrying out a reasonable volume of routine work, rather than with minor points of interest to specialized research laboratories. Perhaps the major advantage of AAS and AFS over most of the comparable techniques is their relative freedom from interferences and the need for extensive sample pretreatment. For electrochemical methods such as polarography and coulometry most types of sample require dissolution followed by a preliminary separation of the analyte to obtain sufficient selectivity. Similar disadvantages apply to molecular absorption spectrophotometry in solution, which in addition also requires the availability of many different organic reagents when a laboratory undertakes a wide range of analyses. As AAS in particular can also offer greater speed and simplicity of measurements than can these techniques, one of its early successes has been in the field of clinical and biochemical analyses where they had formerly been widely applied.

Even with instrumental techniques such as radiochemistry, automated arc spectrometry and X-ray spectrometry, AAS is able to compete in terms of lower capital cost and greater speed of analysis. This is particularly true at the present time for the former applications of these techniques where a moderate number of analyses of varying materials was required. However, the automation of AAS on a commercially viable scale has already begun and it may soon rival the large, automatic optical and X-ray spectrometers used extensively in metallurgical and other industries. Although the use of solid samples for AAS on this scale is not feasible at present it should be remembered that the direct analysis of solid samples requires the use of metallic standards to obtain freedom from matrix effects. Thus, there may be no serious disadvantage in returning to dissolution of samples with AAS determination in conjunction with standards prepared from aqueous solutions of pure reagents, particularly if the dissolution process can also be automated.

AAS and AFS exhibit some disadvantages compared to other techniques. These include the difficulty of determining major sample constituents without a large degree of dilution (with its attendant errors) and of measurement of non-metallic constituents by direct methods. At the present time a number of specific metals and sample types also present difficulties for routine analysis. Although some of the less widely applied methods, such as mass spectrometry and activation analysis, do not suffer these problems to the same extent, it should be remembered that in general they require much wider use of skilled operators. This adds greatly to the cost of the techniques. Furthermore, the current intensification of research as a result of the commercial possibilities of AES, AAS and AFS seems to be removing these problems more quickly than is the case for those inherent in other instrumental methods of inorganic analysis. Thus, it seems probable that the current rate of expansion at the expense of other techniques more traditionally used in analytical service laboratories will continue for some time.

1.4 PREVIOUS BOOKS AND REVIEWS

Until quite recently the number of textbooks on atomic absorption spectrometry was very limited. However, at the time of writing a good selection of books exclusively devoted to AAS have been published, and many review articles concerned with AAS and AFS have appeared. We shall list the books devoted entirely to atomic absorption and fluorescence with a selection of the most useful books dealing with flame photometry generally. The most useful and the most recent of the reviews and bibliographies are also indicated.

Books dealing entirely with AAS (which in some cases contain a short chapter on AFS) have been written by Elwell and Gidley,[22] Ivanov,[23] L'vov,[24] Robinson,[25] Ramirez-Munoz,[26] Slavin[27] and

Rubeska and Moldan.[28] Recently, L'vov has produced a greatly enlarged English edition[29] of his earlier monograph and this probably forms the most thorough account to-date of Russian work, with particular reference to the use of the graphite cuvette technique. Books concerned with specialized applications of AAS have also been written by Rousselet[30] (biology), Angino and Billings[31] (geology) and Christian and Feldman[32] (agriculture, biology and medicine). The most useful of the books dealing with general flame spectrometry are those by Herrmann and Alkemade,[33] Mavrodineanu and Boiteux,[34] Pungor,[35] Mavrodineanu[36] and Dean and Rains.[37] The last listed are the first two parts of a three-volume work which contain chapters by individual authors on theoretical and fundamental topics. At the time of writing no books devoted entirely to AFS have been published. The most useful and generally applicable of the many reviews concerned with AAS are those by Gilbert,[38] Walsh,[39] Mavrodineanu,[40] Slavin,[41] Kahn,[42] Koirtyohann,[43] Price,[44] West,[45] Willis[46] and Fuwa.[47] Mention must also be made of the papers presented at the Atomic Absorption Symposium held at the 1968 meeting of the ASTM. These have been published in book form,[48] as have also the plenary lectures from the 1969 AAS Symposium at Sheffield, England[49] and those of the Paris AAS Symposium in 1971.[50] More specialized reviews of AAS are also available (mainly concerned with particular applications); two recent general ones worthy of mention are by Warn[51] (comparison of AAS with other instrumental methods) and Pickett and Koirtyohann[52] (comparison of AAS with AES). The lesser current popularity of atomic fluorescence spectrometry as an analytical technique is reflected in the much smaller number of reviews published to date. Mention must be made of those by Winefordner and Mansfield,[53,54] Demers,[55] Ellis and Demers,[56] Price,[57] West,[58] Winefordner and Smith,[59] Smith[60] and Winefordner and Elser.[61] Winefordner[62] has also reviewed the relative merits of AAS and AFS.

Although bibliographies are of less immediate use than reviews, it is worth recording some of the most extensive ones. Mavrodineanu[63] has assembled 353 references on AAS with a further 87 on hollow cathode lamps, covering the period from the earliest work on the subject up to 1965. This comprehensive bibliography contains principally references on flame emission spectroscopy, many of which contain material relevant to fundamental work in AAS and AFS. It has already been extended in similar form to cover the period ending December 1968, additional earlier references also being included.[64] Of recent bibliographies, the most useful is that published annually in Perkin-Elmer's *Atomic Absorption Newsletter* by Slavin[65] and available in complete form from the manufacturer.[66] Other manufacturers have produced similar bibliographies on AAS[67,68] and AFS.[69] Another up-to-date source of references on AES, AAS and AFS is the new journal entitled *Atomic Absorption and Flame Emission Spectroscopy Abstracts.*[70] Although this was initiated only in January 1969, early volumes contain many references to publications of several previous years. Finally, the reader is directed to the biannual reviews published in *Analytical Chemistry*. Those by Margoshes and Scribner on emission spectrometry published in 1964,[71] 1966[72] and 1968[73] contain a number of references on AAS and AFS while those on flame spectrometry by Winefordner and Vickers for 1970 and 1972[74] provide the most extensive bibliographical review to date on AFS, together with an excellent section on AAS. These articles provide comprehensive notes of recent developments in the field and their high standard will no doubt be maintained in future years.

To conclude this section we include details of important works which have come to our attention since the list of books and reviews given above was compiled. *Annual Reports in Analytical Atomic Spectroscopy*, published by the Society for Analytical Chemistry, offers a comprehensive and critical annual review of the whole topic. Reynolds and Aldous[75] have written a practical guide to the experimental techniques of AAS and Price[76] has written a useful text concerned exclusively with AAS. The second volume of the work by Dean and Rains on emission and absorption spectrometry is now available[77] and deals with instrumental components and practical techniques. Parsons and McElfresh[78] have prepared an atlas of spectral lines used in flame spectroscopy.

REFERENCES

1. I. Newton, "Optics, or a Treatise of the Reflections, Refractions, Inflections and Colours of Light". 1st Ed. 1704, reissued by Dover Publications, New York, 1952.
2. W. H. Wollaston, *Phil. Trans. Roy. Soc. London,* Ser A, 1802, 92, 365.
3. D. Brewster, *Report of 2nd Meeting of British Association*, 1832, 320.
4. G. Kirchoff, *Phil. Mag.,* 1860, 20, 1.
5. G. Kirchoff and R. Bunsen, *Phil. Mag.,* 1860, 20, 89.
6. G. Kirchoff and R. Bunsen, *Phil. Mag.,* 1861, 22, 329.
7. A. C. G. Mitchell and M. W. Zemansky, "Resonance Radiation and Excited Atoms", University Press, Cambridge, 1934. (Republished 1961.)

8. T. T. Woodson, *Rev. Sci. Instr.*, 1939, **10**, 308.
9. A. Walsh, Australian Patent 23041 (1953).
10. A. Walsh, *Spectrochimica Acta*, 1955, **7**, 108.
11. C. T. J. Alkemade and J. M. W. Milatz, *Appl. Sci. Res.*, 1955, **4B**, 289.
12. C. T. J. Alkemade and J. M. W. Milatz, *J. Opt. Soc. Am.*, 1955, **45**, 583.
13. R. W. Wood, *Phil. Mag.*, 1905, **10**, 513.
14. P. Pringsheim, "Fluorescence and Phosphorescence", Interscience, New York, 1949.
15. E. L. Nichols and H. L. Howes, *Phys. Rev.*, 1923, **22**, 425 and 1924, **23**, 472.
16. R. M. Badger, *Z. Physik.*, 1929, **55**, 56.
17. R. Mannkopff, *Verhandl. d. Deutsch. Phys. Ges.*, 1933, **14**, 16.
18. A. L. Boers, C. T. J. Alkemade and J. A. Smit, *Physica*, 1956, **22**, 358.
19. C. T. J. Alkemade, *Proc Xth Colloq. Spectros. Inter., Maryland, U.S.A. 1962*, pp. 143-170. (Spartan Books, Washington, 1963.)
20. J. D. Winefordner and T. J. Vickers, *Anal. Chem.*, 1964, **36**, 161.
21. J. D. Winefordner and R. A. Staab, *Anal. Chem.*, 1964, **36**, 165.
22. W. T. Elwell and J. F. Gidley, "Atomic Absorption Spectrophotometry", 2nd ed., Pergamon Press, London, 1966.
23. N. P. Ivanov, "Atomno-absorbcionnyj Analiz", IREA, Moscow, 1966.
24. B. V. L'vov, "Atomno-absorbcionnyj Spektralnyj Analiz", Izdatelstvo "Nauka", Moscow, 1966. (Complete English translation published by U.S., A.E.C. and National Science Foundation, Report No. AEC-tr-6979, 1969.)
25. J. W. Robinson, "Atomic Absorption Spectroscopy", Dekker, New York, 1966.
26. J. Ramirez-Munoz, "Atomic Absorption Spectroscopy", Elsevier, Amsterdam, 1968.
27. W. Slavin, "Atomic Absorption Spectroscopy", Interscience, New York, 1968.
28. I. Rubeska and B. Moldan, "Atomic Absorption Spectrophotometry", Iliffe, London, 1969.
29. B. V. L'vov, "Atomic-Absorption Spectrochemical Analysis", Hilger, London, 1970.
30. F. Rousselet, "Spectrophotometry by Atomic Absorption Applied to Biology", C.D.V. and S.E.D.E.S., Paris, 1967. (In French.)
31. E. E. Angino and G. K. Billings, "Atomic Absorption Spectrophotometry in Geology", Elsevier, New York, 1968.
32. G. D. Christian and F. J. Feldman, "Atomic Absorption Spectroscopy: Applications in Agriculture, Biology and Medicine", Wiley-Interscience, New York, 1970.
33. R. Herrmann and C. T. J. Alkemade, "Flame Photometry", 2nd ed., Springer, Berlin, 1960 (in German). Translated into English as "Chemical Analysis by Flame Photometry", Interscience, New York, 1963.
34. R. Mavrodineanu and H. Boiteux, "Flame Spectroscopy", Wiley, New York, 1965.
35. E. Pungor, "Flame Photometry Theory", Van Nostrand, Princeton, 1966.
36. R. Mavrodineanu (ed.), "Analytical Flame Spectroscopy", Macmillan, London, 1970.
37. J. A. Dean and T. C. Rains (eds.), "Flame Emission and Atomic Absorption Spectrometry; Vol. 1, Theory", Dekker, New York, 1969.
38. P. T. Gilbert, *Anal. Chem.*, 1962, **34**, 210R.
39. A. Walsh, *Proc. XIIth Colloq. Spectroscop. Inter.*, Hilger and Watts, London, 1965, p. 43.
40. R. Mavrodineanu, *Encycl. Ind. Chem. Anal.*, 1966, **1**,160.

41. W. Slavin, *Appl. Spectr.*, 1966, **20**, 281.
42. H. L. Kahn in "Trace Inorganics in Water", R. A. Baker, Advances in Chemistry Series, No. 73, American Chemical Society, Washington, 1968, p. 183.
43. S. R. Koirtyohann, in "Developments in Applied Spectroscopy", ed. by W. K. Baer, A. J. Perkins and E. L. Grove, Vol. 6, Plenum Press, New York, 1968, p. 67.
44. W. J. Price, "Atomic Absorption Spectroscopy", chapter of "Spectroscopy", ed. by D. R. Browning, McGraw-Hill, New York, 1969.
45. T. S. West, *Minerals Science and Engineering*, 1969 **1**, 3 (of June issue).
46. J. B. Willis, in R. Mavrodineanu (ed.), "Analytical Flame Spectroscopy", Ch. 10, Macmillan, London, 1970.
47. K. Fuwa, in J. D. Winefordner (ed.), "Spectrochemical Methods of Analysis", Ch. 3, Wiley-Interscience, New York, 1971.
48. American Society for Testing and Materials, Atomic Absorption Spectroscopy, 443, ASTM, Philadelphia, 1969.
49. R. M. Dagnall and G. F. Kirkbright (eds.), "Atomic Absorption Spectroscopy", Butterworth, London, 1970.
50. Proc. 3rd CISAFA, Paris, Sept. 1971. Plenary lectures published in "Methodes Physiques d'Analyse", GAMS, Paris, September 1971.
51. J. R. W. Warn, *Measur. Instr. Rev.*, 1968, **15**, 505, 576, 669.
52. E. E. Pickett and S. R. Koirtyohann, *Anal. Chem.*, 1969, **41**, 28A (of issue No. 14).
53. J. D. Winefordner and J. M. Mansfield, in "Fluorescence", ed. by G. G. Guilbault, Dekker, New York, 1967.
54. J. D. Winefordner and J. M. Mansfield, *Appl. Spectros. Reviews*, 1968, **1**, 1.
55. D. R. Demers, *Appl. Spectros.*, 1968, **22**, 797.
56. D. W. Ellis and D. R. Demers, in "Trace Inorganics in Water", R. A. Baker, Advances in Chemistry Series, No. 73, Washington, 1968.
57. W. J. Price, "Atomic fluorescence spectroscopy", chapter of "Spectroscopy", ed. by D. R. Browning, McGraw-Hill, New York, 1969.
58. T. S. West, *Minerals Science and Engineering*, 1970, **2**, 31 (of January issue).
59. J. D. Winefordner and R. Smith, in R. Mavrodineanu (ed.), "Analytical Flame Spectroscopy", Ch. 11, Macmillan, London, 1970.
60. R. Smith, in J. D. Winefordner (ed.), "Spectrochemical Methods of Analysis", Ch. 4., Wiley-Interscience, New York, 1971.
61. J. D. Winefordner and R. C. Elser, *Anal. Chem.*, 1971, **43**, (4) 24A.
62. J. D. Winefordner, *Rec. Chem. Progr.*, 1968, **29**, 1.
63. R. Mavrodineanu, "Bibliography on Flame Spectroscopy Analytical Applications 1800-1966", NBS Miscellaneous Publications 281, Washington, 1967.
64. R. Mavrodineanu, in R. Mavrodineanu (ed.), "Analytical Flame Spectroscopy", Ch. 13, Macmillan, London, 1970.
65. S. Slavin, *Atomic Absorption Newsletter*, 1971, **10**, 17 (preceding parts in the issues for 1962-1970).
66. Perkin-Elmer Corporation, "Analytical Methods for Atomic Absorption", Norwalk, Connecticut (revised regularly).
67. Fisher Scientific Co. "Bibliography for Atomic Absorption Spectroscopy", Pittsburg, 1968.
68. C. A. Lermond and L. Capacho-Delgado, "Atomic Absorption Bibliography", Bausch and Lomb, Inc., Rochester, New York, 1968.
69. R. Reiss, "Atomic Fluorescence Bibliography", Aztec Instruments, Inc., South Norwalk, Conn., 1968.
70. P. R. Masek and I. Sutherland (eds.), *Atomic Absorption and Flame*

Emission Spectroscopy Abstracts, Science and Technology Agency, London. (Issued bi-monthly with annual index.)
71. B. F. Scribner and M. Margoshes, *Anal. Chem.*, 1964, 36, 329R.
72. M. Margoshes and B. F. Scribner, *Anal. Chem.*, 1966, 38, 297R.
73. M. Margoshes and B. F. Scribner, *Anal. Chem.*, 1968, 40, 223R.
74. J. D. Winefordner and T. J. Vickers, *Anal. Chem.*, 1970, 42, 206R; 1972, 44, 150R.
75. R. J. Reynolds and K. Aldous, "Atomic Absorption Spectroscopy: A Practical Guide", Griffin, London, 1970.
76. W. J. Price, "Analytical Atomic Absorption Spectrometry", Heyden and Son Ltd., London, 1972.
77. J. A. Dean and T. C. Rains (eds.), "Flame Emission and Atomic Absorption Spectrometry; Vol. 2, Components and Techniques", Dekker, New York, 1971.
78. M. L. Parsons and P. M. McElfresh, "Flame Spectroscopy: Atlas of Spectral Lines", Plenum Press, New York, 1971.

CHAPTER 2

Spectroscopic Theory

2.1 INTRODUCTION

A primary difficulty for the authors of a volume of this type is the decision whether to introduce the minimum of necessary theory, with the result that the book appears incomplete to many readers, or to give a fairly comprehensive theoretical treatment which other readers will ignore. We have attempted to compromise by dividing the theoretical part of this book into three separate sections. In this first theoretical chapter the most important points of general atomic spectroscopic theory are summarized or revised. This summary also provides an introduction to the techniques for the non-specialist reader and allows ease of reference to points of general theory in later sections. In the following two chapters more detailed quantitative discussions are presented of atomic absorption spectroscopy and atomic fluorescence spectroscopy respectively; it is hoped that this will prove sufficient for the research worker who is involved in a more fundamental approach to the techniques than are many analytical chemists. Frequent reference is made to sources of more detailed information, so that these chapters should provide a starting point for those interested in such problems as calculation of the effects of line width on absorbance, measurement of absolute concentrations of atoms, and the study of the shapes of growth curves etc.

As the notation *atomic* absorption and fluorescence spectrometry implies, we shall be mainly concerned with *atomic spectra.*[1] This type of spectrum is associated with quantized changes in atomic energy produced by variations in the orbital motions of the valence electrons. The wavelengths transporting the energy appear, in general, to be isolated; hence, the widely used term "line spectra". Although these are the most important from our point of view, it must be remembered that there are two other types of spectra that are also encountered in work concerned with AAS and AFS.

Molecular or band spectra[2] are associated with the energy changes of molecules and give rise to closely packed groups (bands) of spectral lines. They are much more complex than atomic spectra because the internal energy of a molecule comprises three independent parts—changes in vibrational and rotational energy occur in addition to electronic excitation. The main interest of these spectra in AAS and AFS lies in the interferences which they can cause in analysis; both molecular emission and absorption in the atom cell can cause inaccuracies in the measurements made at atomic lines.

The third type of spectra are *continuum spectra.** In these spectra the energy is distributed in an uninterrupted manner between all wavelengths within a given domain. A true continuum of this kind is often observed as the black-body radiation from a hot solid or liquid[3] or as the result of an atomic or molecular energy transition in which one of the energy states is unquantized.[4] Extensive, rather diffuse, band systems are also often referred to as "continua" but this should be treated as a description rather than a definition. Continua are mainly encountered in AAS and AFS as spectral light

---

* This type of spectrum is often referred to as continuous. The alternative definition of continuous spectral sources will be found in Section 5.1.1 and to avoid confusion it is better not to use continuous as an alternative to continuum.

sources which may be used over a range of wavelengths rather than only at isolated spectral lines.

2.2 ATOMIC SPECTRA AND ATOMIC ENERGY LEVELS

2.2.1 The Atom and Its Spectra

As mentioned earlier, experimental spectroscopy had achieved a considerable body of results well before the end of the last century. Thus it was recognized that the line spectra observed with spectroscopes and spectrographs were associated with atoms and that each line could be considered as "monochromatic" radiation. As light was considered to have a wave character (following the experiments of Young, Fresnel and others), each line of the spectrum was analogous to a periodic wave and its position in the spectrum could be defined in terms of its *wavelength*, λ, its *frequency*, $\nu = c/\lambda$, where c is the velocity of light, or its *wavenumber*, $\sigma = 1/\lambda$.* The velocity of light is taken as $2{\cdot}99793 \times 10^{10}$ cm/s and the frequency is measured in cycles/s, or Hertz (Hz). This gives the convenient unit of cm^{-1} for the wavenumber.† The centimetre can be used as the unit of wavelength but is inconveniently large for the *optical region* of the spectrum being discussed here. The traditional unit of wavelength is the Ångström unit ($1\ \text{Å} = 10^{-8}$ cm) but it is now being replaced by the nanometre ($1\ \text{nm} = 10^{-9}\ \text{m} = 10^{-7}$ cm; hence $1\ \text{nm} = 10\ \text{Å}$). Other units which have been fairly widely used are the micron ($1\ \mu\text{m} = 10^{-6}$ m) and the millimicron ($1\ \text{m}\mu = 1\ \text{nm} = 10^{-9}$ m). The visible region of the spectrum extends from about $\lambda = 770$ nm (red) to $\lambda = 380$ nm (violet) although optical spectra may be studied for a considerable range on either side of this. We shall be mainly concerned with the region extending from about 190 nm in the ultraviolet to 850 nm in the infrared. Finally, it should be noted that the value of c quoted above is the velocity of light in a vacuum. Thus values of λ, ν and σ evaluated with it will refer to radiation travelling through a vacuum. Since these vacuum units are the quantities related to the properties of the atom, the wavenumber (which is directly applicable to the energy levels of the atom) is usually given in tables in vacuum units. For convenience, the wavelength is normally

---

* The symbols λ, ν and σ are those most commonly used for these terms, although variations are often found in the literature.

† The reciprocal centimetre is often referred to as the Kayser, which is abbreviated to the symbol K.

quoted as its (slightly smaller*) value measured in air without correction to the vacuum wavelength.

As the number of recorded spectra increased and instruments capable of better resolution were produced, it was found that the distribution of the spectral lines of each individual element was not as random as had once been supposed. Thus it was discovered empirically that the wavelengths of the lines of the simple atomic spectra, such as those of hydrogen and the alkali metals, could be fitted to simple series formulae with great accuracy. These series were even more straightforward when the wavelengths of the lines were replaced by their vacuum wavenumbers. Furthermore, it had already been noticed that many of the lines in these simple spectra occurred in small groups named *multiplets*, such as the doublets of the alkali metals or the triplets of the alkaline earths, and in 1883 Hartley observed that there was a constant difference between the wavenumbers of the two components of some doublets (or two of the three components of some triplets). This is illustrated in Table 2-1 for some of the sodium doublets; it can be seen that the two lines of each doublet are separated by 17 cm^{-1}. Some years later, after the phenomenon of constant differences had been shown to apply to many other spectra, Ritz found that it was a direct consequence of a more general rule which he named the *combination principle*. This states that for any atom (or molecule) there is a set of *spectral terms* which are such that the vacuum wavenumber of any line of the spectrum of that species is the difference between two of the terms. It was also observed that the number of spectral terms of an atom is always much smaller than its number of spectral lines; thus the same term must appear in more than one wavenumber. This is best illustrated on a diagram, such as that in Fig. 2-1 which again uses the sodium spectrum as an example. This type of diagram is known as a *term diagram*, a *Grotrian diagram* (after its originator) or a *level diagram*. The spectral terms are represented by horizontal lines with vertical lines between them to show the spectral line corresponding to the wavenumber difference of two terms. For convenience, the term with the smallest wavenumber is taken as zero on this particular diagram. Reference to the diagram shows for example, that the term 16973 cm^{-1} appears in no less than seven line wavenumbers.

TABLE 2-1
Some sodium doublets showing constant wavenumber differences

Wavelength, nm	Wavenumber, cm^{-1}
1140·35 1138·12	8766 8783
819·48 813·33	12200 12217
616·08 615·42	16227 16244
589·59 589·00	16956 16973
568·82 568·26	17577 17594
515·36 514·91	19399 19416
498·28 497·85	20064 20081

A most important advance in the study of atomic spectra was made by Bohr shortly after the empirical discovery of the combination principle. He postulated that any atom is allowed only certain discrete and characteristic energy values, and that emission or absorption of radiation by an atom occurs when it undergoes a transition between these stationary states or *energy levels*. Furthermore, these energy levels were seen to be directly proportional to the empirical spectral terms of the atom; it had already been shown by Planck that the energy and frequency of a particular radiation are related such that

$$E = h\nu = hc\sigma \tag{2-1}$$

where E is the energy and h is a constant (6·6254 erg s) now known as *Planck's constant*. Hence the frequency of radiation corresponding to a transition of an atom between two levels (or states) of energy E_m and E_n respectively will be given by

$$\nu_{mn} = (E_m - E_n)/h$$

and the corresponding spectral terms are

$$\sigma_m = E_m/hc \quad \text{and} \quad \sigma_n = E_n/hc$$

---

* Even this value must be quoted for "standard air" since the refractive index varies slightly with location, atmospheric conditions etc.

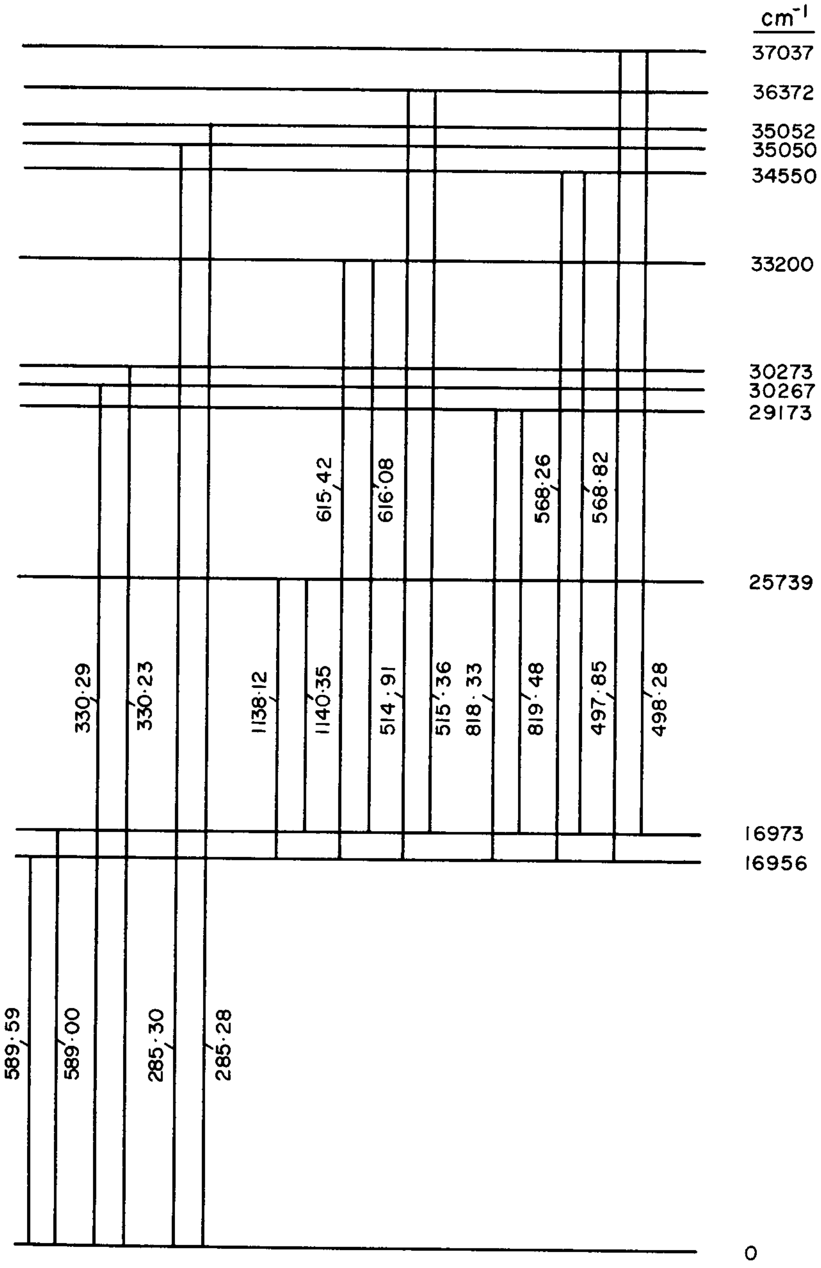

Fig. 2-1. Spectral term diagram for sodium (wavelengths of lines are given in nm).

Thus the experimental term diagrams become *energy level diagrams* of the atom simply by a change of scale.

These straightforward postulates immediately removed many of the problems existing in the interpretation of the atomic spectra that had been observed experimentally at that time. It was now obvious rather than surprising that there should be a simple relationship between the wavenumbers of many of the lines of each spectrum, and the vast number of lines in many of the spectra could be explained; even the smallest source emitting light contains a great number of atoms and these will exist in many of the different stationary states possible for that type of atom (i.e. that element). Thus, the different lines of the spectrum of that element are emitted by different atoms and not all by the same atom. This greatly simplified the task of correlating the structure of the atom and its observed spectrum.

In a similar way, the mechanism by which the different spectra could be produced was also explained by the postulates. The level of lowest energy corresponds to the spectral term with the smallest wavenumber; it is unique and is the state in which an atom will normally exist. It is referred to as the fundamental or *ground state*, whereas any level of higher energy is said to correspond to an *excited state*. A spectral line can only be emitted if the atom is in an excited state, so that energy will be released when it returns to the state of lower energy (either the ground state or an intermediate state). Thus the atom will emit radiation only after the energy required to raise it to an excited state has been provided by an external source, such as a flame, an arc, a spark, etc. On the other hand, the absorption spectrum can be obtained without such an external source as at room temperature most of the atoms are in the ground state. Hence when the atoms are irradiated with light of the correct wavelength (i.e. that corresponding to the energy difference between an excited state and the ground state) some of the energy will be absorbed to raise atoms to an excited state. This also explains the greater simplicity of an absorption spectrum compared to the corresponding emission spectrum; only a small fraction of the possible transitions for a given element will have the ground state as one of their two spectral terms.*

---

* It is, of course, possible to observe in absorption a transition which has an excited state as its lower spectral term, but only if an external source of energy is used to raise sufficient atoms to that excited state.

2.2.2 Convention and Notation

Bohr's postulates of 1913, two of which were quoted in the previous section, were based on the assumption that the energy states of an atom depended on the way in which its electrons moved about the nucleus and that this movement occurred in circular orbits; changes in angular momentum would occur in units of $h/2\pi$ when an electron moved from one orbit to another and hence the energy must also change in multiples of a fixed unit, now known as a *quantum* (or *photon*). Although this theory had proved most satisfactory in explaining the known experimental facts, the real test was whether it could be used to calculate theoretically the allowed energies of the atoms. In practice, it was found that satisfactory results were obtained only when the nucleus was accompanied by a single electron, such as with hydrogen. The revision necessary to apply the theory to all atoms and their spectra was carried out during the period 1920 to 1930. The *quantum theory* was devised to explain the structure of the atom and the way in which it gives rise to the optical spectra. At about the same time, all of the quantum theory was underpinned and explained in a logical fashion mathematically via the *quantum* or *wave mechanics*. The reader will find a useful presentation of the most important aspects of the wave mechanics in reference 1. It should be borne in mind that the quantum theory is the basis of much of the convention and notation used in any discussion of atomic spectra.

The optical spectra originate only from the positional and spin changes of electrons in the outer orbits, which with most elements are incompletely filled by electrons. These are known as the *optical electrons*. The different energy states possible for any atom are found by calculating the different orbital possibilities of its optical electrons. Each possibility corresponds to a different discrete energy of the atom as a whole and not just to energy of the electrons.* The orbits of the electrons may be readily described by a set of *quantum numbers*. These same numbers are used to calculate the number of spectral energy levels that may result from particular groups of electrons; derivations of them provide a useful notation by which the individual terms may be referenced for ease of identification. These reference numbers and symbols also indicate the order of increasing energy for groups of terms of each atom, so that the task of relating

---

* The atom will, of course, also have its translational kinetic energy but this need not be discussed in connection with the spectral energy levels on which it has no direct effect (see also Section 2.5).

experimentally measured spectral terms to their quantum number equivalents is considerably simplified.

It is usual to refer to an electron as being of a particular type depending on the orbit that it occupies. These types are indicated by the first two quantum numbers. To avoid confusion, the second quantum number is replaced by a letter* according to

$$\begin{array}{cccccc} 0 & 1 & 2 & 3 & 4 & \ldots \\ s & p & d & f & g & \ldots \end{array}$$

Thus the electrons (but more properly their orbits) are referred to as $3s$, $5d$, $2p$, etc. The combination of electrons giving rise to a particular energy of the atom is known as a *configuration*. For example, for an unexcited gallium atom it is $1s^2 2s^2 2p^6 3s^2 3p^6 3d^{10} 4s^2 4p$. The superscripts to the right of the letters indicate the number of electrons of each type. As we are only concerned with the optical electrons, this particular configuration would normally be abbreviated in spectral tables to $4p$.

The spectral term symbols are also based on the second quantum number, the same letters as above being used but in upper case; e.g. the symbol for the term corresponding to the configuration of gallium given above is P. If there is only one optical electron, as in this example, this letter must be the same as that used for the electron. When two or more optical electrons are present, their second quantum numbers are added vectorally, giving several resultant numbers. The same lettering scheme is used with these. The same type of term may thus arise from a variety of optical electron configurations and to avoid confusion the configuration should be indicated with the term, e.g. for the gallium example we should write $4p\ P$.

These terms are not directly analogous to the empirical spectral terms mentioned earlier, because the electron spin can result in each term being subdivided into further *states* (and it is these that correspond to the empirically determined spectral terms or energy levels). The individual states are indicated by a third quantum number, known as the J value, which is written as a subscript to the right of the term symbol. Thus the gallium configuration given above actually results in the states $4p\ P_{1/2}$ and $4p\ P_{3/2}$. Of these the former corresponds to the lower energy and is the ground state. The

---

* The odd choice of the first three letters is an historical result; they are related to the "sharp", "principal" and "diffuse" series of lines which may be distinguished in the sodium spectrum.

J values are useful when measurements of spectral line intensities are made, since the quantity $(2J + 1)$ is the *statistical weight*, g, of the state (see Sections 2.3 and 2.4).

The resultant electron spin of the term governs the number of possible values of J; it is used to calculate a quantity known as the *multiplicity* of the term. This usually* corresponds to the number of J values (i.e. states) for that term and is shown as a superscript to the left of the term symbol, e.g. $4p\ ^2P_{1/2}$ and $4p\ ^2P_{3/2}$ for the gallium example. In this case the term is referred to as a *doublet*; if the multiplicity were 3 it would be a *triplet*, etc. The same word *multiplet* is applied to a group of spectral lines corresponding to transitions between initial levels belonging to one term only and final levels belonging only to one other term; i.e. the upper (or lower) levels differ only in their value of J. A group of lines is designated a triplet, if the terms are triplets, but the actual number of lines will often be greater than this. For example, the calcium triplet observed between 442 and 446 nm ($4p\ ^3P$–$4d\ ^3D$) is actually composed of six lines.

2.3 THE EMISSION AND ABSORPTION OF ENERGY

2.3.1 *General*

As described in Section 2.2, for any atom there exists an extensive set of possible energy levels or states, and spectral emission or absorption results from a transition between particular pairs of these levels. The pairs between which transitions are possible are predicted by the quantum mechanics via the *selection rules*.† This results in a "picture" of the spectrum of the element with the positions of the lines indicated, but the quantum theory is also able to assist in predicting the relative *intensities* of these lines (i.e. the quantity of energy emitted or absorbed).

The intensity of a spectral line produced by a group of emitting or absorbing atoms depends on two main factors. First, given a fixed population for all energy levels (i.e. at any instant equal numbers of atoms exist in each of the possible states for a given element), the probability of any particular transition occurring will depend on the intrinsic properties of the atom as expressed by the quantum mechanics. Thus, in a group of atoms, the greater the probability of a particular transition the more intense is the corresponding spectral line. This *transition probability* is a fundamental property of the atom and is discussed below.

Secondly, the number of times a particular transition occurs will depend on the number of atoms existing at any given time with the energy of its initial level. The population of each level will depend on the properties of the group of atoms as a whole, since it must depend on the amount of energy available to the atoms. Hence, environmental factors, such as temperature and pressure, will be important and the intensity of the spectral lines will vary with the means used to obtain a population of free atoms or to excite emission lines. This effect of the distribution of atomic population is discussed in Section 2.4.

2.3.2 *The Einstein Transition Probabilities*

On the assumption that the energy levels have equal populations (or, if this is not the case, if a correction is made as described in Section 2.4) it is often possible to calculate the relative intensities of the lines of a single multiplet of a particular element by a fairly simple process using the quantum numbers of the initial and final states. The calculation is further simplified by the availability[5] of tables of the results that can be generally applied. However, the method has seen wide practical use only for certain special applications (such as the calculation of intensity ratios of hyperfine structure components; see Section 2.5.2) mainly because the results are only reliable with the lighter elements and because the restriction to a multiplet of a particular element limits the usefulness anyway.

The more common method of classifying and explaining the relative line intensities is based on Einstein's theory of radiation which defines three transition probabilities; under given conditions, the intensity of a line corresponding to a particular transition will be directly proportional to its transition probability. The transition probabilities may be calculated using quantum mechanics from first principles, in the same way that the possible states, the selection rules, etc. are derived. The calculations are complex and only possible when simplifying assumptions are made. Considerable numbers of calculated values have been published[6] but the accuracy depends on the degree of approximation and the element, and most

---

* S terms obtained from a single s-type optical electron have a multiplicity of 2 but only one J value and corresponding state, e.g. the ground state of the alkali metals. This is simply a result of the combination of numbers involved (the second J value would be $-\frac{1}{2}$ if negative quantum numbers were allowed).

† The rules are not as precise as some other parts of the quantum mechanics and certain "forbidden" lines are observed for a number of elements.

of the results have been for the lighter elements (atomic number, Z, in the range 1 to 30). In view of this many of the most useful results have been obtained experimentally from observed spectra.

Three Einstein coefficients are defined: for spontaneous emission, absorption, and stimulated emission (fluorescence) and are usually written A_{ij}, B_{ji} and B_{ij} respectively. The meaning of the subscripts should be clear from Fig. 2-2. A_{ij} is the easiest to define. It is simply the probability that an atom in state "i" will spontaneously emit a quantum ($h\nu$) and pass to the state "j". Hence A_{ij} has the unit s^{-1}. The other two coefficients are more difficult to define, as the probability of an absorption or fluorescence transition will obviously depend on the amount of incident radiation. Einstein was able to overcome this problem by defining the transition probability in these cases such that it is obtained by multiplication of the appropriate coefficient and the *radiation density* at the frequency corresponding to the particular transition (ρ_ν).* Hence $B_{ji}\rho_\nu$ and $B_{ij}\rho_\nu$ have the unit s^{-1}. Since the radiation density (ρ_ν) is energy per unit volume, it has the units erg cm^{-3} or g cm^{-1} s^{-1}. Thus B_{ji} and B_{ij} have the units cm g^{-1}. Note should be taken of this important difference between the A and B coefficients; strictly speaking only the former should be referred to as a transition probability.

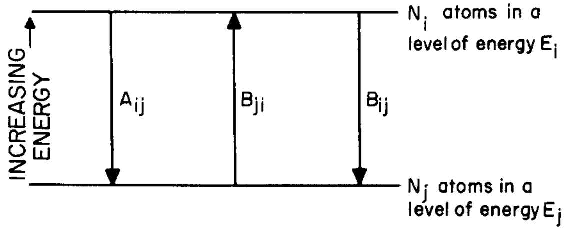

Fig. 2-2. The Einstein transition probabilities.

Einstein was able to obtain several useful relationships between the three coefficients by considering the thermodynamic equilibrium between the radiation and the atoms and comparing it with the equilibrium of a black-body radiator at the same temperature:

$$A_{ij}/B_{ij} = 8\pi h\nu^3/c^3 \qquad (2\text{-}2)$$

$$g_i B_{ij} = g_j B_{ji} \qquad (2\text{-}3)$$

where g_i and g_j are the statistical weights of the two states. These equations may also be used to relate all three transition probabilities, via A_{ij}, to the *oscillator strength* or *f-value* of the atom. This was regarded in the classical electron theory of dispersion (which preceded the quantum theory) as a measure of the degree to which the atom resembles an oscillating electron in its ability to emit and absorb a particular spectral line. The f-value is directly proportional to A_{ij}, as shown by Ladenburg's formula:

$$A_{ij} = 8\pi^2 e^2 f_{ij}/\lambda^2 mc \qquad (2\text{-}4)$$

where e and m are the electron charge and mass respectively. Substitution of the values of the constants gives

$$A_{ij} = 0{\cdot}6670 \times 10^{14} f_{ij}/\lambda^2 \qquad (2\text{-}5)$$

where A_{ij} is in s^{-1} and λ is in nm. The f-value is still widely used as it results in a convenient form for many formulae. This is particularly so since the absorption oscillator strength, f_{ji}, is related to f_{ij} by

$$g_j f_{ji} = g_i f_{ij} \qquad (2\text{-}6)$$

In view of this, tables of f-values are usually given as "gf" values which may be used for emission or absorption lines corresponding to the transition between two particular states of the atom.

2.3.3 *The Intensities of Spectral Lines*

The intensity of an emission, absorption or fluorescence line may now be expressed in terms of the number of atoms existing in its initial and/or final states. The simplest case is that for a non-self-absorbed emission line.* From the notation of Fig. 2-2, the number of transitions per second (i.e. the number of photons) corresponding to spontaneous emission will be $A_{ij} N_i$. (For convenience, N_i is usually taken as the number of atoms per unit volume, but this is not essential.) Hence, the emission intensity may be represented by

$$I_{\text{em}} = h\nu A_{ij} N_i \qquad (2\text{-}7)$$

In the case of absorption and fluorescence, the numbers of transitions are $B_{ji}\rho_\nu N_j$ and $B_{ij}\rho_\nu N_i$ respectively. The total reduction in intensity observed will depend on the difference between these two numbers.† Hence for absorption we may write

$$I_{\text{ab}} = h\nu(B_{ji}N_j - B_{ij}N_i)\rho_\nu \qquad (2\text{-}8)$$

---

* In certain cases the transition probability is defined in terms of isotropic radiation *intensity*. The coefficients are then related to the two used here by B (intensity) = $(4\pi/c)B$(density). Care should be taken not to use simultaneously equations based on different definitions of the probabilities without applying the correction factor.

* Self-absorption of spectral lines is discussed in Section 2.5.2.

† Spontaneous emission is independent of this and is not included; in practice, the two types of emission may be distinguished by suitable choice of experimental conditions (see Chapter 10).

whereas for fluorescence the intensity is simply

$$I_{fl} = h\nu B_{ij}\rho_\nu N_i \qquad (2\text{-}9)$$

As it is generally more convenient to work in terms of incident intensity rather than radiation density, we may write $I = (c/4\pi)\rho_\nu$. This assumes, however, that the incident light of intensity I is isotropic in the same way as is the spontaneously emitted light of intensity I_{em}. If, as is usually the case, the incident light is in the form of a pencil of light of solid angle Ω, the equivalent intensity will be $I_0 = (\Omega/4\pi)I$. For a beam of unit solid angle this becomes $I/4\pi$. Hence we obtain

$$I_{ab} = (h\nu/c)(B_{ji}N_j - B_{ij}N_i)I_0 \qquad (2\text{-}10)$$

$$I_{fl} = h\nu B_{ij}N_iI_0/c \qquad (2\text{-}11)$$

where B_{ji} and B_{ij} are the coefficients defined in terms of radiation density, as explained earlier.

These three expressions for I_{em}, I_{ab} and I_{fl} form the basis of most of the practical formulae used in analytical atomic spectrometry, although they are usually more useful after substitution for N_i and N_j in terms of the total number of atoms present in all states, as explained in the next section. The expressions for I_{em} and I_{fl} are more directly applicable to practical situations than that for I_{ab}; it will be seen later that other absorption expressions allowing less difficult experimental measurements are commonly used for analytical atomic absorption spectroscopy.

2.4 DISTRIBUTION OF ATOMIC POPULATION

2.4.1 General

It has already been mentioned that the relative populations of the states of the atom play a major part in determining the relative intensities of the spectral lines corresponding to the various transitions. Furthermore, these populations depend not merely on intrinsic properties of the atom, but also on the properties of the emitting or absorbing gas as a whole. If the particular type of energy in question (i.e. electronic for an atom but possibly also vibrational or rotational for a molecule) has attained equilibrium the relative populations of the quantized levels may be easily found from the Maxwell-Boltzmann Law. For some of the commonly used atom cells we may assume that thermal equilibrium does indeed exist for the atoms whose absorption or fluorescence is being measured and apply the law accordingly. In some atom cells equilibrium may exist only in certain regions or may, strictly speaking, not apply to all species present. For example, flames are widely used as atom cells and whereas the law may produce quite satisfactory results in the regions normally used for analytical measurements, this may not be the case in the primary reaction zone. Similarly, the law may give unsatisfactory results for some of the flame gas molecules in a region where it is applicable to added metal atoms.

A quite different situation exists in the case of many *electric discharges*, which are frequently used as the spectral light source for atomic absorption or fluorescence measurements and sometimes as the atom cell. Excitation in the discharge results from collisions with electrons or ions of very high energy. The Boltzmann factor $\exp -E/kT$ (see Section 2.4.2) then approaches unity and the ratio of the populations of any two levels is simply the ratio of their statistical weights, i.e.

$$N_i/N_j = g_i/g_j$$

Under these conditions the transition probability plays an even greater part than usual in determining the relative intensities of the lines, so that lines corresponding to high excitation energies may be relatively many times more intense than in, say, a flame source. As shown elsewhere, the presence of such lines in a spectral light source can have an important effect on the choice of a suitable absorption line.

2.4.2 The Maxwell-Boltzmann Law

The law states that if at an absolute temperature T there are N_i particles with energy E_i and N_j particles with energy E_j, then

$$N_i/N_j = \exp -(E_i - E_j)/kT \qquad (2\text{-}12)$$

provided that both energy states are non-degenerate. (k is the Boltzmann constant.) In fact, many of the energy states that we have regarded up to now as single levels represented by a particular value of J are actually degenerate because they further split into $(2J + 1)$ sublevels on application of a magnetic field. When there is no magnetic field (as will usually be the case in examples of interest here), each of these sublevels has the same energy. Therefore, in the notation used above, the number of particles with energy E_i is actually $(2J_i + 1)n_i$ where n_i is the population of each of the non-degenerate sublevels. Hence $N_i = g_i n_i$ and this definition of the statistical weight now becomes more logical. Since the law must be applied to non-degenerate levels of energy E_i and E_j we obtain

$$N_i/N_j = (g_i/g_j)_j(n_i/n_j) = (g_i/g_j) \exp -(E_i - E_j)/kT \qquad (2\text{-}13)$$

This general form of the law extends to any state which is non-degenerate (e.g. the ground state ${}^1S_0$ of the alkaline earths), since its statistical weight will simply be unity.

The equation obtained above is extremely useful and is widely used for calculations involving relative line intensities. However, for atomic absorption and fluorescence is often more convenient if the population of any one level (e.g. the ground state) can be expressed in terms of the total number, N, of particles present. This is easily achieved by expressing N as the sum of the populations of all levels, i.e. $N = \sum_i N_i$ (or $\sum_j N_j$, etc.). As the equation may be rewritten as

$$N_i/N_j = (g_i \exp(-E_i/kT)/(g_j \exp(-E_j/kT))$$

we have

$$N_i/N = g_i \exp(-E_i/kT)/\sum_j g_j \exp(-E_j/kT) = g_i \exp(-E_i/kT)/F(T) \qquad (2\text{-}14)$$

where $\sum_j$ is known as the *partition function,* $F(T)$, for the type of energy in question, and the difficulty of calculating it varies considerably with specific cases. With this proviso the equation applies quite generally to both atoms and molecules and to all types of energy levels.

A number of expressions for the partition function under different circumstances, and also some approximations, are available (see, for example, Ref. 2, Ch. 20-4). However, with the examples likely to be encountered in AAS and AFS it is usually more convenient with atomic spectra simply to perform the summation manually using the published g_i and E_i values for the energy levels. This is especially true when the calculation is performed for relatively low-temperature atom cells, such as flames. It should be obvious from the equation that even for temperatures as high as 3000 K, the value of N_i will be very small if E_i is more than a few electron volts, for example, if $T = 3000$ K and $E_i = 2$ eV, $\exp(-E_i/kT) = 4 \times 10^{-4}$ so that N_i is negligible compared with N. It is, therefore, rarely necessary to consider levels more than about 1 eV above ground state when the summation is carried out.

2.4.3 *Relevance of Atomic Population Distribution to AAS and AFS Measurements*

The Maxwell-Boltzmann Law only relates the population of each energy level to the total number, N, of *free neutral atoms* present. Under analytical conditions the usefulness of this information is frequently limited by inadequate knowledge of the relation between N and the actual sample concentration. The fraction of the total number of analyte atoms in the sample which N represents varies substantially depending on the analyte element, the type of sample and the nature of the absorption or fluorescence cell. The form of this relation in a given case may be of considerable interest if, for example, an absolute analysis is required. The problem is very much an experimental one, however, as the relations between the contributing factors (such as degree of ionization; volatility and stability of the compounds formed by the element; and efficiency of sample utilization) are very complex. Further discussion will be found in Section 6.5.

In spite of this difficulty, a knowledge of the *relative* distribution of sample atoms amongst the possible energy levels may still prove to be most useful. It provides a simple basis by which methods of improving sensitivity in flame absorption cells may be understood as well as assisting in the selection of the optimum absorption line for a particular element. Unfortunately, this knowledge of the relative populations of the energy levels obtained in flame atom cells has also led to a widespread misunderstanding of the comparative sensitivities of the atomic absorption and flame emission techniques. As shown in Section 2.4.2, at normal flame temperatures the atomic population of the excited state responsible for analytically useful emission of radiation is usually negligible compared to that of the ground state. This has often been quoted as proof of the belief that AAS must be considerably superior in sensitivity when compared with flame emission spectrometry (FES). That this is not the case has been clearly demonstrated by Alkemade,[7] by simple considerations from basic principles. Briefly it has been demonstrated that if experimental variables are neglected, the relative ultimate sensitivities of the two techniques depend not on the distribution of atom population caused by the flame cell, but on the effective temperature of the background light source used for AAS.

Two other fallacies that were quite common in early AAS work also resulted from an incomplete understanding of the population distribution in the atom cell, particularly of the significance of the relatively large ground-state population. In view of this, it has sometimes been stated that, if a constant free-atom population is assumed, the number of absorbing atoms will *always* be independent of temperature. In fact, this is true only for atoms such as mercury that give simple spectra in which the only low-lying level is the ground state itself. When several levels lie below *ca.* 1 eV, their relative populations will vary with temperature to produce a similar variation in the absorption at a particular line. Although the variations observed are often quite small, some combinations of statistical weights and energy levels can give rise to large changes with temperature for certain elements (e.g. tin).

Related to this problem is another which concerns the actual population of the ground state; it is often thought that at normal flame temperatures the ground state invariably has a far greater population than any other level. In fact this may not be the case for a number of elements. For example, the level of tin at 0·210 eV has a higher population than the ground state at temperatures of about 2500 K and above. For aluminium, in which the "ground state" is a doublet with a separation of 0·0139 eV, the population of the higher level is almost double that of the true ground state even below 1000 K (see also Section 11.1.1).

2.5 WIDTH OF SPECTRAL LINES

2.5.1 General

AAS used by analytical chemists at the present time is based on an experimental technique that relies for its simplicity on measuring the "peak absorbance" of a spectral line by using a spectral light source emitting a "sharp" line. The fact that even the sharpest line that can be produced has a finite width has an extremely important bearing on the application of both AAS and AFS. It introduces a number of problems in the practice of the techniques, and has resulted in considerable recent effort to produce better light sources giving greater absorption and fluorescence sensitivity. From the theoretical point of view, the fact that a spectral line may never be represented by a unique frequency (or wavelength) introduces considerable complexity into the derivation of formulae that may be used to interpret practical observations. Furthermore, this problem is recognized as one of the major difficulties encountered in any attempt to carry out absolute analyses by AAS. In view of this situation, the factors contributing to the width of a spectral line will be considered in some detail. The effects on practical AAS measurements of variations in the source (and absorption) lines will be discussed in Chapter 3.

When it is recognized that no spectral line is infinitely narrow it is no longer adequate for the purposes of AAS to represent it by the usual vertical, straight "line" of photographic spectra. A common notation for the intensity distribution of an emission line is shown in Fig. 2-3. The intensity is written as I_ν, as it is a function of the frequency ν, with a maximum value, I_0, at the central frequency of the line, ν_0. The width of the line cannot easily be quoted as the distance $\nu_1 - \nu_2$ since the position of these points is ill-defined.

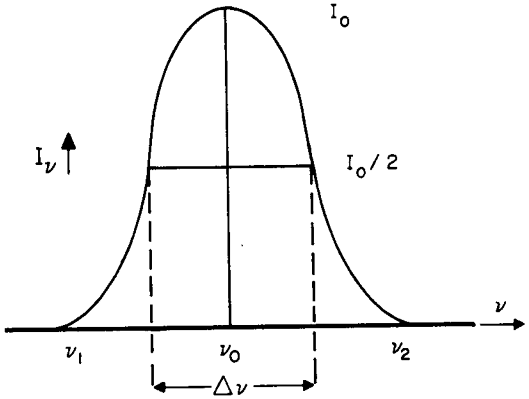

Fig. 2-3. The shape of a spectral line.

Instead, it is customary to define the breadth of any line in terms of its *half-width,* $\Delta\nu$. This is the distance between the two points on the profile where the intensity is equal to half the maximum intensity. Some authors define the half width as $\Delta\nu/2$, so that care must be taken to avoid confusion. The same nomenclature is used for absorption lines with I_ν replaced by the absorption coefficient, k_ν.

2.5.2 Line Broadening Effects

A spectral line from any source, or from any absorption or fluorescence cell, will be broadened by a number of factors. Some of these are always more important than others and the contributions of different factors will vary with the source. The most common broadening effects are listed below and an indication is given of their relative importance to AAS and AFS. It should be remembered that any numerical values quoted are merely examples and that wide variations of the different quantities may be observed in practice.

(*i*) *Natural broadening*

This is the result of the finite lifetime of any atom in any excited state. If the mean time the atom spends in a state E_i is Δt_i, then according to Heisenberg's Uncertainty Principle there will be an uncertainty ΔE_i in the value of E_i. This is defined by

$$\Delta E_i \Delta t_i = h/2\pi \tag{2-15}$$

where h is Planck's constant.

Thus, the frequency ν_0 for a transition between levels E_i and E_j given by $\nu_0 = (E_i - E_j)/h$ is no longer unique and the line has a finite width, $\Delta\nu_N$. It may be shown that

$$\Delta\nu_N = (1/\Delta t_i + 1/\Delta t_j)/2\pi \tag{2-16}$$

This equation may be simplified for a resonance line, as E_j will be the ground state with an infinitely large value of Δt_j. Furthermore, Δt_i will then be equal to the radiative lifetime* of the excited level, which for a resonance level is defined as $1/A_{ij}$. Hence

$$\Delta\nu_N = A_{ij}/2\pi \tag{2-17}$$

Thus $\Delta\nu_N$ is of the same order as A_{ij}, about $10^8\ s^{-1}$. In terms of wavelengths this would represent about 10^{-5} nm at 300 nm, which is negligible in comparison with the other factors.

(*ii*) *Doppler broadening*

This is caused by the thermal motion of the emitting or absorbing atoms. If there is a relative velocity v between the observer and an atom emitting light of frequency ν, the light received by the observer would appear to be of frequency $(\nu + d\nu)$ or $(\nu - d\nu)$, depending on the direction of motion, where $d\nu = v\,\nu/c$. As the atoms of a gas move in all directions, the observer will receive light of many slightly different frequencies. Thus the line appears broadened. The observed frequencies will have the same distribution as the velocities of the

---

* This assumes such a low pressure that the number of radiationless transitions from E_i is negligible, which may not always be true (see Sections 2.5.2 (6) and 4.5).

atoms in the gas, i.e. a Gaussian curve will represent the shape of the line.

The Doppler half-width, $\Delta\nu_D$, may be calculated from the formula

$$\Delta\nu_D = [2\sqrt{2R\ln 2}\,\nu_0\sqrt{T/M}]/c \tag{2-18}$$

where R is the gas constant, c the velocity of light and M the atomic weight of the species concerned.

After evaluation of the constants this becomes

$$\Delta\nu_D = 7{\cdot}162 \times 10^{-7}\,\nu_0\sqrt{T/M}$$

Thus the Doppler width depends on the atomic weight of the species, the temperature of the source and the wavelength of the observed line. In terms of wavelength units, it usually lies in the range 5×10^{-4} to 50×10^{-4} nm for absorption lines in the common flame cells and is somewhat smaller in the spectral light sources, which mostly operate at a rather lower temperature.

(*iii*) *Lorentz broadening*

Collision of an emitting or absorbing atom with other atoms or molecules of a foreign gas* results in a broadening, shift and asymmetry of the line profile. The resultant half-width, $\Delta\nu_L$, is known as the Lorentz, collisional or pressure-broadened width of the line. The interpretation of the collision processes in terms of the effect of the collisions on the energy levels of the atom, and hence the spectral line, is still not complete. According to the classical Lorentz theory, when an emitting or absorbing atom collides with a foreign particle there is an interruption of the vibration within the atom of an electron responsible for the spectral line. This results in a broadening of the spectral line that is directly proportional to the number of collisions per second per atom. Thus by the same reasoning that was applied to natural broadening, the value of $\Delta\nu_L$ is given by $1/\pi\tau$ (or $1/2\pi\tau$ for resonance lines) where τ is the *collisional lifetime* of the atom.† Hence, $\Delta\nu_L$ for a resonance line is given by

$$\Delta\nu_L = \sigma_L^2 N\sqrt{2\pi RT(1/M_1 + 1/M_2)}/\pi \tag{2-19}$$

where σ_L^2 is the collision cross-section for Lorentz broadening of the atom concerned (and is usually an effective value determined experimentally); N is the number of foreign species per unit volume

---

* The reason for exclusion of collisions by like atoms will be found in the next section.

† See Section 4.5.2 for the evaluation of τ.

(and is calculated from $N = 9740 \times p \times 10^{15}/T$ where p is the foreign gas pressure in torr); R is the gas constant; and M_1 and M_2 are the atomic or molecular weights of the colliding species.

The equation is useful for our purposes in that it allows a reasonable approximation to the actual value of $\Delta\nu_L$ to be calculated. However, the simple Lorentz theory is unable to deal with the accompanying shift and asymmetry of the line and even the dependence of $\Delta\nu_L$ on $T^{-1/2}$* is not in complete agreement with experimental evidence (which, however, is still of insufficient accuracy to allow complete justification of any one theory). More modern theories, which may be applied to particular regions of the line profile and particular ranges of gas pressure, have been developed to account for both the line shift and asymmetry. They have been reviewed in some detail by Breene,[8] but a useful approximation is

$$\Delta\nu_s = 0{\cdot}36\ \Delta\nu_L$$

where $\Delta\nu_s$ is the frequency shift of the line towards the red. Hence the shift of the line peak is of the same order as the collisional half-width.

The relatively high concentration of foreign molecules in flame absorption and fluorescence cells results in a value of $\Delta\nu_L$ similar to that of $\Delta\nu_D$. Hence the shift of the absorption line may be considerable and lead to a reduction in the "peak" absorbance observed at the central frequency (ν_0) of the line when a narrow, unshifted source line is used. Values of $\Delta\nu_L$ observed in low-pressure spectral sources containing only inert gas atoms are much smaller, and in devices such as hollow-cathode lamps and electrodeless discharge tubes $\Delta\nu_L$ and $\Delta\nu_s$ will usually be negligible compared with $\Delta\nu_D$. For example, the collision cross-section for broadening of the calcium 422·673 nm line by neon atoms has been found[9] to be $7{\cdot}4 \times 10^{-15}$ cm^2. If the above equation is used, and converted to wavelength units, the Lorentz half-width for a neon pressure of 10 torr is 0·00001 to 0·00003 nm depending on the temperature, whereas the Doppler half-width under the same conditions may vary from 0·002 to 0·0008 nm.

(*iv*) *Holtzmark broadening*

The term Holtzmark or resonance broadening is applied to the broadening of an excited level of an atom by interaction with atoms *of the same kind* in the ground state, provided that the two levels are linked by a strong dipole transition. Thus, the electron vibration mentioned earlier is affected not merely by the collision but by a much stronger electrostatic interaction. In fact, if the same equation is used to approximate values of the resonance half-width, $\Delta\nu_R$, (with $M_1 = M_2$ for like atoms) it is found that values of σ_R are often several hundred times greater than comparable values of σ_L. It is important to note that although Lorentz and Holtzmark broadenings result in similar intensity distributions, no line shift or asymmetry is predicated for the latter and none is observed experimentally. As with Lorentz broadening, modern theory may be used to calculate $\Delta\nu_R$ directly without recourse to experimental collision cross-sections, but variations of detail occur in the formulae depending on the theory used and the range of application.

At the level of atom concentration encountered in AAS and AFS, resonance broadening is usually of little importance despite the high values of σ_R for most elements. For example, it is uncommon to introduce into flame cells solutions exceeding a concentration of 1 M, yet even this would result[10] in resonance broadening half-widths of only ca. 10^{-5} nm. Similarly, the atom concentration within most commonly used light sources would be too low to produce significant resonance broadening. However, $\Delta\nu_R$ may not be negligible in some of the intense spectral sources used for AFS, as these are often run at high power and produce sufficient atom concentrations to give severe self-absorption even over a very small path length.

(*v*) *Stark and Zeeman broadenings*

These well-known types of spectral line broadening are usually of little importance in analytical AAS and AFS. Stark broadening results from the splitting of the electronic levels of an atom due to the presence of strong, non-uniform electric fields or large densities of moving electrons or ions. It is negligible in flames and is also considered small in hollow-cathode lamps and electrodeless discharge tubes under the conditions employed in AAS and AFS. It becomes important, however, in arcs and sparks and may be a major factor in determining their relative unsuitability for use as sharp-line sources.

Zeeman broadening is a similar splitting effect observed in the presence of a strong magnetic field. Obviously the effect will be obtained only by deliberate application of such a field, so that it is of no importance here except to mention that it might be applied to

---

* $T^{-1/2}$ at constant foreign gas pressure because of the dependence of N on T^{-1} as noted above.

produce a deliberate shift in a source or absorption line to obtain better overlap of the two.

(*vi*) *Quenching broadening*

It was mentioned earlier that radiationless transitions from the excited state of a resonance line are usually of no importance. While this may be true for a discharge within an inert gas, such as in most low-pressure spectral sources, quenching collisions can occur in flames as the result of the presence of foreign gas molecules with vibrational levels very close to the excited state of the resonance line. This may produce line broadening owing to the reduction in the lifetime of an excited atom by the same mechanism as natural broadening. The frequency distribution will have a collision rate dependence of the same type as Lorentz broadening and the half width, $\Delta\nu_Q$, for a resonance line may be determined from equation (2-19) if σ_L^2 is replaced by the quenching cross-section σ_Q^2. Values of σ_Q^2 observed experimentally are discussed in Section 4.5.4 and it will be seen that in certain flames σ_Q^2 may be sufficiently large for $\Delta\nu_Q$ to make a significant contribution to the overall broadening of many lines used in AAS and AFS.

(*vii*) *Self-absorption broadening*

This type of broadening is only of importance for lines that have their lower level at or near the ground state so that self-absorption within the source is easily induced. It is of particular relevance to analytical AAS and AFS, however, as by their very nature these techniques are mainly concerned with those spectral lines giving strong absorption. Indeed, it would appear[11,12] that self-absorption is the most serious of all the factors causing line broadening in sources used for AAS and AFS. This arises not because self-absorption itself multiplies the line width by a large factor, as it usually only increases the width by at most a factor of two or three, but because this multiplication factor is applied to the sum of all the other broadening factors. Thus self-absorption may often cause more serious line broadening of resonance lines than any other single broadening effect.

Self-absorption results in broadening of the spectral line simply because the maximum absorption occurs at the centre of the line; a greater *proportional* amount of radiation is therefore lost from the centre of an emission line than from its wings. Thus the shape of the line changes as well as its intensity, as illustrated in Fig. 2-4. The curves show the effect of increasing optical density on (a) Gaussian and (b) Lorentzian profiles for a source in which the absorbing atom concentration is uniform throughout, but the concentration of emitting atoms decreases linearly to zero between the centre and edge of the source. The effect of a given degree of self-absorption varies considerably with the model chosen for the spectral source,[13] but Fig. 2-4 is representative in that the relative increase in line width is usually somewhat greater for a collision-broadened profile than for a Doppler-broadened profile. In both cases, very high levels of self-absorption can result in self-reversal of the profile at its centre* so that a minimum is observed. Quite apart from any line width considerations, this condition can have an adverse effect on AAS and AFS sensitivities because the region of the line which is most strongly absorbed by the sample atoms is already partly lost.

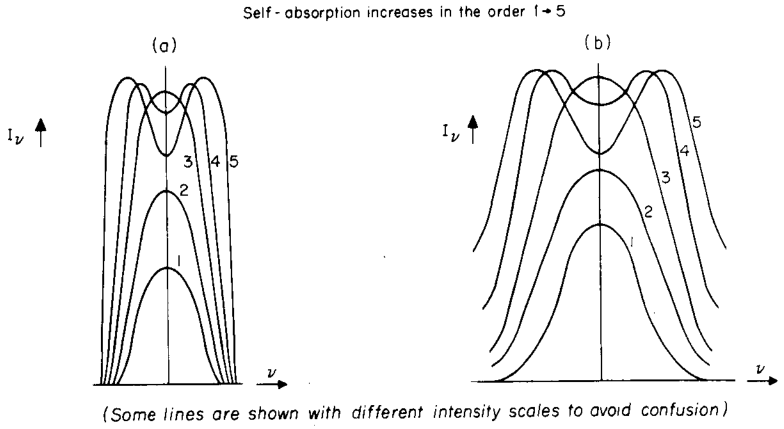

Fig. 2-4. Effect of self-absorption on line shape.[13]

As the degree of self-absorption broadening varies with the type of line broadening (of which (a) and (b) in Fig. 2-4 are only extreme cases), it is not practical to give even an approximate expression for an "absorption half-width". It is only possible to calculate a value at a particular level of absorption, and for a specific model of the atomic distribution in the source, by considering the effect of the absorption on the intensity at each point in the line profile. This must be done by representing the variation with frequency of emission intensity and absorption by complex mathematical functions

---

* Except in the special cases where the concentration of emitting atoms is uniform throughout the source or actually increases towards the edge.

of the type mentioned in Sections 2.5.3 and 3.2.1. Some typical results are plotted in Fig. 2-5, which shows the variation of the half-width ratio (self-absorbed/non-self-absorbed) with the degree of self-absorption, p. This is defined such that the doubling of p means a doubling of the self-absorption, and so on. The three cases shown are all for a uniform distribution of absorbing atoms through the source and for the following distribution of emitting atoms: (1) concentration is uniform throughout the source; (2) concentration is zero at all points except the centre of the source; (3) concentration decreases uniformly between the centre and edge of the source.

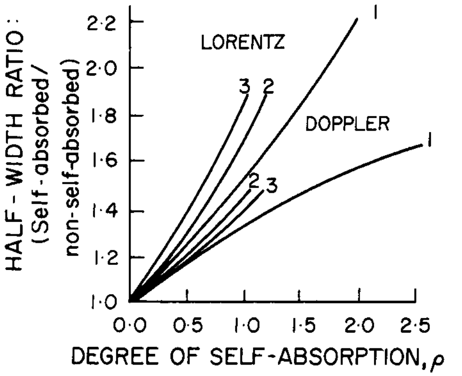

Fig. 2-5. The increase of half-width with self-absorption.[13]

(viii) Hyperfine structure effects

In the discussion so far it has been assumed that, although each separate spectral line isolated by a normal monochromator is not truly monochromatic, it can at least be represented by a single, uniform profile. In practice, when many spectral lines are examined under high resolution they are found to be made up of several closely spaced and probably partially overlapping profiles. These components, known as the hyperfine structure (hfs) of the line, are the result of small variations in the atomic energy levels due to the interaction of a nuclear spin with the spins of the electrons or to the presence of several isotopes. Thus, in many cases the "single" line will be quite complex, being made up of components due to several abundant isotopes of the element with the possibility of each of these components being further subdivided owing to the nuclear spin of the isotope. Isotopes with both atomic weight and number even (i.e. even numbers of both protons and electrons) have no nuclear spin and hence no extra subdivision of their line.

Each hfs component of a line must be considered as an individual spectral line with its own profile broadened by factors discussed above. Furthermore, the equations given in the next chapter for the calculation of absorption at a line must also be applied individually to each component. This would present no problems if the hfs components of both the emission and absorption lines were completely separated, i.e. if there was no overlap of their spectral profiles.* Unfortunately, the hfs components are very closely spaced so that the widths of the components are comparable to their separation in most common spectral sources. Unless the overlap is complete, so that the line may be regarded with fairly good accuracy as a single profile, any attempt to calculate the total line profile, after carrying out the individual line broadening calculations described above, is extremely complicated. Usually only an approximate graphical solution can be attempted.

The effect of hyperfine structure on absorption measurement is frequently neglected when, for example, line broadening estimates are made for the sharp line spectral sources used for peak absorbance measurements. This is partly because the effects on sensitivity are relatively small with most elements, and partly because the effect cannot be influenced (from the point of view of improving sensitivity) by practical measures. Thus, estimates of other broadening factors are still of some use even if the true line width due to the hfs apparently makes the Doppler, Lorentz, etc. widths appear somewhat irrelevant. However, it should be remembered that for certain aspects of absorption measurements the hfs can have important consequences and must not be overlooked (see Section 3.5.2).

2.5.3 *The Observed Line Profile and Its Measurement*

As already described, the profile of a line emitted by atoms in a spectral light source or absorbed in an absorption cell results from a combination of the factors discussed in Section 2.5.2. Unfortunately, this combination cannot be carried out by some simple addition process because the profiles are represented by complex mathematical functions. The methods used are too specialized to discuss here, but a simplified summary should prove useful in understanding

---

* In this particular context, the question of whether the spectrometer used is capable of resolving the components is irrelevant.

the effect of the different broadening factors on the complete line. The same techniques are also required in the derivation of expressions that relate the measured absorption to atomic concentration (see Section 3.2.1).

Suppose the variation in intensity with frequency for two particular types of broadening can be represented by functions of the type $I(x) = f(x)$ and $I(x) = \phi(x)$ where "x" is defined in terms of the central frequency of the profile; i.e. for any frequency ν, $x = (\nu - \nu_0)$. It may be shown that if both of these factors act at a point on the profile where $x = \nu'$, the resultant intensity at that point is given by

$$I(\nu') = \int_{-\infty}^{+\infty} f(x)\phi(\nu' - x)\,\mathrm{d}x = F(\nu') \qquad (2\text{-}20)$$

This process may be repeated for any number of broadening processes. The difficulty is that exact integration of the complex functions (i.e. mathematical expressions) represented by f, ϕ, F, etc. is impossible and approximate numerical methods must be used. These are greatly simplified if the functions can be combined in some way before attempting to carry out the integration. To do this the functions representing individual broadening factors are placed into two classes.

(*a*) *Gaussian functions* are of the form

$$f(x) = c\ \mathrm{e}^{-x^2}/\beta_2^2 \qquad (2\text{-}21)$$

where c and β_2 are constants. Doppler broadening results in a function of this type.

(*b*) *Dispersion* (*Lorentzian*) *functions* are of the form

$$f(x) = c/(1 + x^2/\beta_1^2) \qquad (2\text{-}22)$$

where c and β_1 are constants. Natural and Lorentzian broadening and the other types of broadening via collisions result in functions of this type.

If f and ϕ are both Gaussian and have the constants β_2' and β_2'', it may be shown that F is also Gaussian and has a constant given by

$$\beta_2^2 = (\beta_1')^2 + (\beta_2'')^2 \qquad (2\text{-}23)$$

Similarly, if f and ϕ are both dispersion functions, we obtain a constant for the dispersion function, F, by

$$\beta_1 = \beta_1' + \beta_1'' \qquad (2\text{-}24)$$

However, if f is Gaussian and ϕ dispersion (or vice versa), then F is known as a *Voigt function* and has both β_1 and β_2 parameters. It will obviously be a function of the form

$$F(x) = (c\ \mathrm{e}^{-x^2}/\beta_2^2)/(1 + x^2/\beta_1^2) \qquad (2\text{-}25)$$

Furthermore, if two Voigt functions are combined in the same way the result is another Voigt function whose β_1 and β_2 parameters are obtained from the two formulae given above.

Thus any symmetrical* line profile can be represented by a Voigt function. This is most important because the various half-widths are constants (for a particular profile) equivalent to the β_1 and β_2 parameters. Hence the two groups of half-widths may be added independently to give two parameters ($\Delta\nu_{\mathrm{Gauss.}}$ and $\Delta\nu_{\mathrm{Disp.}}$) which define the Voigt profile representing the actual line. Tables of the function have been calculated by evaluating the integral so that the total half-width of the Voigt profile may be obtained (see, for example, references 14 and 15).

If line widths are to be determined experimentally, it is necessary first to use a spectrometer of sufficiently high resolving power, and secondly to analyse the recorded profile by a reversal of the above procedure. This must now allow for a further line broadening factor—that due to the instrument used to observe the line, as no spectrometer can have an infinitely high resolving power. Most of the factors causing instrumental broadening may be represented by Gaussian or dispersion functions so that the *instrumental profile* will itself be a Voigt function. Although spectrometers of sufficiently high resolution are readily available,[16,17] such practical measurements are made difficult by the problems of profile analysis—since factors such as self-absorption, line asymmetry and shift and hyperfine structure add further complications. For this reason, accurate experimental values of line widths directly of interest in AAS and AFS are relatively few. It also explains why absorption techniques requiring actual measurements of absorption line profiles have seen little practical application (see Section 3.5.1). With the current interest in absolute analysis by AAS, the accurate estimation of actual line widths and the ability to record absorption line profiles remain important problems of concern to the analytical chemist.

---

* Hence the effects of collisional shift, hyperfine structure, etc. must be excluded from this treatment.

REFERENCES

1. See, for example, H. G. Kuhn, "Atomic Spectra", Longmans, Green, London, 1962.
2. See, for example, R. Mavrodineanu and H. Boiteux, "Flame Spectroscopy", Wiley, New York, 1965, Ch. 17.
3. A. G. Gaydon and H. G. Wolfhard, "Flames, Their Structure, Radiation and Temperature", 3rd ed., Chapman and Hall, London, 1970, Ch. 9.
4. A. G. Gaydon, "The Spectroscopy of Flames", Chapman and Hall, London, 1957, pp. 66-72.
5. H. E. White and A. Y. Eliason, *Phys. Rev.*, 1927, **29**, 790. (The tables are reproduced in several textbooks on atomic spectra; e.g. in ref. 1 above.)
6. W. L. Wiese, "Present status of our knowledge of atomic transition probabilities", *Proc. Xth Colloq. Spectros. Inter., Maryland, 1962*, pp. 37-56.
7. C. Th. J. Alkemade, *Applied Optics*, 1968, **7**, 1261.
8. R. G. Breene, "The Shift and Shape of Spectral Lines", Pergamon Press, Oxford, 1961.
9. N. P. Penkin and L. N. Shabanova, *Opt. Spectrosc.*, 1968, **25**, 446.
10. I. Rubeska and V. Svoboda, *Anal. Chim. Acta*, 1965, **32**, 253.
11. A. I. Bodretsova, B. V. L'vov and V. I. Mosichev, *J. Appl. Spectrosc.*, 1966, **4**, 149.
12. G. F. Kirkbright and M. Sargent, *Spectrochim. Acta*, 1970, **25B**, 577.
13. T. Tako, *J. Phys. Soc. Japan*, 1961, **16**, 2016.
14. J. T. Davies and J. M. Vaughan, *Astrophys. J.*, 1963, **137**, 1302.
15. D. G. Hummer, *Mem. Roy. Astron. Soc.*, 1965, **70**, 1.
16. S. Tolansky, "High Resolution Spectroscopy", Methuen, London, 1947.
17. P. Jacquinot, *Reports Progr. Phys.*, 1960, **23**, 268.

CHAPTER 3

Theory of Atomic Absorption Measurements

3.1 INTRODUCTION

The opportunity has been taken in several places in the preceding pages to point out the important consequences of finite spectral line-widths on the theory and practice of AAS. In order to discuss these further we find it necessary to define several parameters that may be used to represent atomic absorption and to discuss at some length the conditions under which they correspond to experimentally determined quantities. It will be seen that, in the most widely used form of AAS that has evolved, the theoretical complications, and their consequent experimental difficulties, have been reduced to the minimum for the application of atomic absorption measurements to chemical analysis. Unfortunately, restriction of the discussion to correspond to this minimum can result in considerable misunderstanding and misinterpretation of anomalies that apparently occur when the limits of the approximations are approached. Moreover, it becomes more difficult to appreciate the reasons for the choice of the absorption techniques used at present by analytical chemists and to visualize the problems involved with the development of these techniques into a sophisticated means of absolute analysis.

In view of this, we shall discuss at some length three quantities: the *absorption coefficient*; the *total absorption factor*; and the *absorbance*. The conditions under which these quantities may be used will be indicated and the boundaries of these conditions will be related to the "abnormalities" that are found in practical measurements; for example, the curvature of calibration graphs, which ideally should be straight lines. It will be seen that at the present time the widespread use of AAS is based mainly on the straightforward interpretation of *absorbance* measurements made with a sharp-line spectral source and that the other two quantities are of much less importance to the analytical chemist. Finally, the possibilities of developing AAS into an absolute analytical technique rather than into one that relies on calibration standards will be discussed.

3.2 THE ABSORPTION COEFFICIENT

3.2.1 Definition of the Absorption Coefficient, k_ν

The absorption coefficient at a discrete frequency, ν, is defined by the equation

$$I_\nu = I_\nu^0 \, \mathrm{e}^{-k_\nu L} \qquad (3\text{-}1)$$

where I_ν^0 and I_ν are the initial and final intensities of radiation of frequency ν passed through an absorption cell of length L. A plot of k_ν against frequency represents the profile of the absorption line, which is of the same form as that shown in Fig. 2-3 for an emission line. Thus, values of k_ν may only be measured directly by using a monochromating device able to resolve the profile of the absorption line; i.e. one that has a spectral bandpass considerably less than the line width.

k_ν may be expressed as a function of frequency for a general line profile by using equation (2-20). Substituting the expressions given to represent Gaussian and Lorentzian functions, and replacing the particular point ν' with a general frequency ν, we obtain

$$k_\nu = C \cdot \int_{-\infty}^{\infty} \frac{\mathrm{e}^{-x^2/\beta_2^2}}{1 + (\nu - \nu_0 - x)^2/\beta_1^2} \cdot \mathrm{d}x \qquad (3\text{-}2)$$

This may be rearranged as

$$k_\nu = C \cdot \frac{\beta_1^2}{\beta_2^2} \int_{-\infty}^{\infty} \frac{\mathrm{e}^{-(x/\beta_2)^2}}{(\beta_1/\beta_2)^2 + (\nu - \nu_0 - x)^2/\beta_2} \cdot \mathrm{d}x \qquad (3\text{-}3)$$

Equation (3-3) is considerably simplified by writing

$$y = x/\beta_2, \quad \omega = (\nu - \nu_0)/\beta_2 \quad \text{and} \quad a = \beta_1/\beta_2$$

Hence, we obtain

$$k_\nu = Ca\beta_1 \int_{-\infty}^{\infty} \frac{\mathrm{e}^{-y^2}}{a^2 + (\omega - y)^2} \cdot \mathrm{d}y \qquad (3\text{-}4)$$

Such an expression for k_ν was originally developed from the basic theories of line broadening by Voigt,[1] and a comparison with equation (3-4) allows the three constants describing the Gaussian and Lorentzian functions to be related to the half-widths of the absorption profile:

$$\beta_1 = \frac{\Delta\nu_c}{2}; \qquad \beta_2 = \frac{\Delta\nu_D}{\sqrt{2\ln 2}} \qquad (3\text{-}5)$$

and

$$C = \frac{2k_0'}{\beta_1 \pi} = \frac{2k_0'}{\pi \Delta\nu_c} \qquad (3\text{-}6)$$

where $\Delta\nu_c$ is the sum of the half-widths of the Lorentzian-type functions (i.e. $\Delta\nu_N$, $\Delta\nu_L$, $\Delta\nu_Q$ and $\Delta\nu_R$ of Section 2.5.2), $\Delta\nu_D$ is the Doppler half-width (i.e. the Gaussian function half-width) and k_0' is an ideal* quantity representing the peak absorption coefficient which would be obtained with an absorption line *broadened only by the Doppler effect.*

---

* k_0' is obviously an ideal quantity as it is impossible to obtain an absorption line without at least the Lorentzian contribution from natural broadening.

After substitution of these relations, equation (3-4) becomes

$$k_\nu = \frac{k_0' a}{\pi} \int_{-\infty}^{\infty} \frac{e^{-y^2}}{a^2 + (\omega - y)^2} \cdot dy \tag{3-7}$$

which is the form of the *Voigt expression* most widely quoted following its derivation and use by Mitchell and Zemansky.[2] Equation (3-7) relates k_ν to the number of absorbing atoms, which is included in k_0' (see Section 3.2.2), and is necessary if equation (3-1) is to be used for theoretical calculations of the variation of light absorption with concentration (*curves of growth*). For this purpose equation (3-7) must be evaluated either by using computer calculated tables of the integral,[3,4] or by replacing it with an approximate analytic expression. Several of these have been suggested, and the most recent[5,6] can give quite accurate results over a wide range of line-widths and absorption values. For example, equation (3-8)* gives k_ν/k_0' with a maximum error of only +2·5% and −5% over most conditions likely to be required.

$$\begin{aligned} k_\nu = k_0' & \left[1 - \frac{\Delta\nu_c\sqrt{\ln 2}}{\Delta}\right] \exp\left[-2{\cdot}772\left(\frac{\nu-\nu_0}{\Delta/\sqrt{\ln 2}}\right)^2\right] \\ & + \left[\frac{\Delta\nu_c\sqrt{\ln 2}}{\Delta}\right] \frac{1}{1 + 4\left(\dfrac{\nu-\nu_0}{\Delta/\sqrt{\ln 2}}\right)^2} + 0{\cdot}016\left[1 - \frac{\Delta\nu_c\sqrt{\ln 2}}{\Delta}\right] \\ & \times \left[\frac{\Delta\nu_c\sqrt{\ln 2}}{\Delta}\right] \left\{\exp\left[-0{\cdot}4\left(\frac{\nu-\nu_0}{\Delta/\sqrt{\ln 2}}\right) 2{\cdot}25\right] \right. \\ & \left. - \frac{10}{10 + \left[\dfrac{\nu-\nu_0}{\Delta/\sqrt{\ln 2}}\right]^{2{\cdot}25}}\right\} \end{aligned} \tag{3-8}$$

Δ is the observed half-width of the absorption line (resulting from all broadening effects).

3.2.2 *The Integrated Absorption Coefficient, K*

Although its dependence on frequency complicates the use of k_ν, integration of k_0 with respect to ν over the whole line results in the most useful quantity, K, which is independent of frequency. It may be shown (Mitchell and Zemansky,[2] p. 95) that K is equivalent to the quantity I_{ab}/I_0 as defined in equation (2-10). Hence we obtain

$$K = \int k_\nu \, d\nu = \frac{h\nu_0}{c}(B_{ji}N_j - B_{ij}N_i) \tag{3-9}$$

where ν_0 is the frequency at the centre of the line and the small variation of ν throughout the line has been neglected.

In many absorption cells, including flames, the value of N_i is quite small compared with that of N_j (see Section 2.4.2) so that, to a good approximation, we may simplify equation (3-9) to

$$K = \frac{h\nu_0}{c} B_{ji}N_j \tag{3-10}$$

Substitutions for B_{ji} may be made from equations (2-2) to (2-6) giving

$$K = \frac{\lambda_0^2}{8\pi}\frac{g_i}{g_j} A_{ij}N_j \tag{3-11}$$

or

$$K = \frac{\pi e^2}{mc} f_{ji}N_j \tag{3-12}$$

These equations are important as they show that K may be represented by a simple, linear relationship with N_j and that this relationship is quite independent of whatever physical processes are responsible for the formation of the absorption line. Unfortunately, it is difficult to make direct use of this fact to measure atomic populations by absorption because K can only be measured by taking the area under the actual absorption profile. It is important to remember that the value of the integrated absorption coefficient so obtained *does not* correspond to the absorption measured with a continuum source and a conventional monochromator (see Section 3.3).

Mitchell and Zemansky[2] also give an alternative integration of k_ν which shows that

$$K = \frac{2\sqrt{\ln 2}}{\sqrt{\pi}\Delta\nu_D} k_0' \tag{3-13}$$

---

* Equation (3-8) is obtained by using the notation of this book in equation (5) of reference 6.

where k'_0 is the peak absorption coefficient for a purely Doppler broadened line, as explained in Section 3.2.1. Thus, after substituting for K, we obtain

$$k'_0 = \frac{2\sqrt{\ln 2}}{\sqrt{\pi}\Delta\nu_0}\,\frac{\lambda_0^2}{8\pi}\,\frac{g_i}{g_j}\,A_{ij}N_j \qquad (3\text{-}14)$$

This equation is necessary for the calculation of curves of growth of absorption with atom concentration.

3.3 THE TOTAL ABSORPTION FACTOR, A_T

3.3.1 The Definition of A_T

In view of the difficulties already mentioned in measuring k_ν and K, it is necessary to have some other indication of how much radiation is actually absorbed during an experiment. The total absorption factor, A_T, may be calculated from a knowledge only of the amounts of light entering and leaving the absorption cell but, unlike k_ν and K, it depends on both the emission line from the source and the absorption line in the cell. Nearly all analytical AAS measurements are directly concerned with A_T as the variables normally used in AAS (percent absorption and absorbance) are both closely related to A_T.

As the total absorption factor is defined in terms of the total amount of light passing through the cell at a particular spectral line, the intensities used are integrated with respect to the complete absorption line. Hence A_T is given by

$$A_T = \frac{\text{Absorbed radiation intensity}}{\text{Incident radiation intensity}} = \frac{\Delta I}{I_0} \qquad (3\text{-}15)$$

where $\Delta I = I_0 - I$, where I is the amount of radiation leaving the cell. The *percent absorption* commonly used in AAS is defined as $[(\Delta I/I_0) \times 100]$, so that for most purposes it may be considered as an alternative notation for values of A_T.

Although A_T is easily measured experimentally, it is as difficult to relate it theoretically to the number of absorbing atoms as when k_ν is employed. In fact, it is related by expressing A_T in terms of k_ν and evaluating the integral approximately for special cases of interest in AAS. Now, by definition

$$I_0 = \int I_\nu^0 \, d\nu \quad \text{and} \quad I = \int I_\nu \, d\nu$$

so that we may rewrite equation (3-15) as

$$A_T = \frac{\int I_\nu^0 \, d\nu - \int I_\nu^0 \, e^{-k_\nu L} \, d\nu}{\int I_\nu^0 \, d\nu} \qquad (3\text{-}16)$$

by using equation (3-1). In order to proceed further it is necessary to assume that I_ν^0 will always be integrated over the same limits as k_ν is; i.e. to impose the condition that the integration will be made over the source line-width if it is narrower than the absorption line, or the absorption line-width if it is narrower than the source line. Equation (3-16) may then be rewritten as

$$A_T = \frac{\int I_\nu^0 \, d\nu \int (1 - e^{-k_\nu L}) \, d\nu}{\int I_\nu^0 \, d\nu}$$

$$= \frac{I_0 \int (1 - e^{-k_\nu L}) \, d\nu}{I_0}$$

i.e.

$$A_T = \int (1 - e^{-k_\nu L}) \, d\nu \qquad (3\text{-}17)$$

The limits of this integration are considered as a number of special cases, depending on the width of the narrower of the two lines.

3.3.2 Evaluation of A_T for a Wide Source Line

This situation applies if the background source emits a continuum or a very broad, self-absorbed line such as is obtained from an arc or flame. As the absorption line is much narrower than that from the source, we may assume that the total absorbed radiation will be given by integration of equation (3-17) across the entire absorption line, i.e. from "zero to infinity". This is quite easy for small or large values of the optical density, $k_\nu L$ (i.e. of the absorption).

(*a*) *Small $k_\nu L$*

In this case equation (3-17) may be simplified* to

$$A_T = \int_0^\infty k_\nu L \, d\nu = L \int_0^\infty k_\nu \, d\nu = LK \qquad (3\text{-}18)$$

---

* Since $(1 - e^{-x}) \rightarrow x$ as $x \rightarrow 0$.

Hence, from equation (3-12),

$$A_T = \frac{\pi e^2}{mc} f_{ji} N_j L \tag{3-19}$$

i.e. A_T will increase linearly with N_j (and therefore with the concentration of absorbing atoms*) at low optical densities.

(b) Large $k_\nu L$

When the optical density becomes sufficiently large, the central region of the line shows complete absorption. Further increases in optical density then result only in changes at the edge of the line profile, as shown in Fig. 3-1. Thus, the form of the line profile (i.e. of k_ν) is determined entirely by the edges. Under these conditions, it may be shown[2] that k_ν is adequately represented by the analytic expression

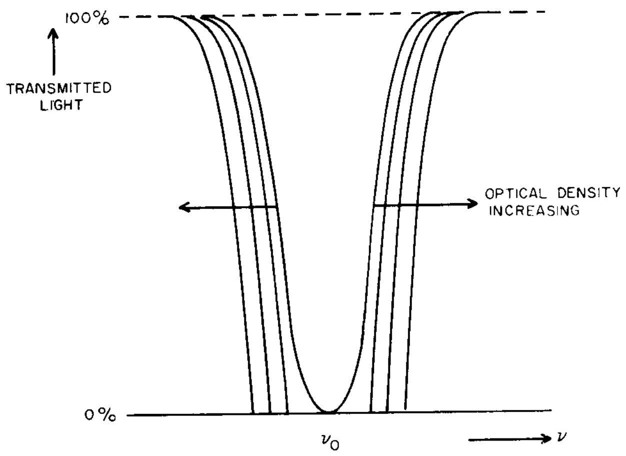

Fig. 3-1. Absorption line profile of high optical density.

$$k_\nu = \left[\frac{\Delta\nu_0 \Delta\nu_c}{4\sqrt{\pi}\sqrt{\ln 2}(\nu - \nu_0)^2}\right] k'_0 \tag{3-20}$$

Hence the complete integration of equation (3-17) is possible without undue difficulty, the resultant expression for A_T being

$$A_T = \left[\frac{k'_0 \Delta\nu_D^2 a\sqrt{\pi}L}{\ln 2}\right]^{1/2} \tag{3-21}$$

---

* But see Section 3.5.3.

After substitution for k'_0 using equation (3-13), we obtain

$$A_T = \left[\frac{2\pi e^2 \Delta\nu_D a f_{ji} N_j L}{mc\sqrt{\ln 2}}\right]^{1/2} \tag{3-22}$$

i.e. at high optical densities, A_T is proportional to the square root of the concentration of absorbing atoms.

3.3.3 Evaluation of A_T for a Sharp Line Source

This is the case when a low-current spectral lamp is used as the light source, as in most analytical AAS measurements. As the source line width, $\Delta\nu_s$, is small when compared with the width of the absorption line, we may assume that absorption will occur over the full width of the source line. Thus, the integration limits of equation (3-17) will be zero and $\Delta\nu_s$. In practice, the usual Gaussian function is converted into a triangular one and the actual integration limit is $\Delta\nu_s\sqrt{\pi}/2\sqrt{\ln 2}$.

A further consequence of using a sharp line source is that we are only concerned with the very centre of the absorption line. Thus it is valid to assume that k_ν is a constant and equal to the peak absorption coefficient of the line. This is not equal to k'_0 since the line is not purely Doppler-broadened. However, to a good approximation we may write $k_{(\nu=0)} = bk'_0$, where b is a constant of proportionality. Hence, we obtain

$$A_T = (1 - e^{bk'_0 L}) \int_0^{\frac{\Delta\nu_s\sqrt{\pi}}{2\sqrt{\ln 2}}} d\nu \tag{3-23}$$

(a) Small $k'_0 L$

Using $(1 - e^{-x}) = x$ for small values of x we obtain

$$A_T = bk'_0 L \frac{\Delta\nu_s\sqrt{\pi}}{2\sqrt{\ln 2}} \tag{3-24}$$

after performing the integration in equation (3-23). Substitution for k'_0 as before gives

$$A_T = \frac{b\Delta\nu_s}{\Delta\nu_D} \frac{\pi e^2}{mc} f_{ji} N_j L \tag{3-25}$$

i.e. A_T varies linearly with N_j.

(*b*) *Large* k'_0L

As we are now concerned only with the line centre, high optical densities will result in very strong absorption. Thus, to a good approximation, $e^{-bk'_0L} = 0$. Hence, on integration, equation (3-23) becomes

$$A_T = \frac{\Delta\nu_s\sqrt{\pi}}{2\sqrt{\ln 2}} \tag{3-26}$$

i.e. at high optical densities the absorption reaches a constant value independent of N_j.

3.4 THE ABSORBANCE, A, FOR A SHARP LINE SOURCE

An expression for the absorbance, A, may be evaluated without the need to assume limiting values of the optical density, as is required to estimate A_T. On the other hand, the derivation is only simple if a narrow source line width is assumed, i.e. if we assume that k_0 has a constant value. Thus, we restrict ourselves to the use of A with such a source; the fact that the derivation does not require an assumption based on the extreme values of $k_\nu L$ makes this expression extremely useful (see Section 3.5).

The absorbance is defined by

$$A = \log_{10}\left(\frac{I_0}{I}\right) \tag{3-27}$$

where I_0 and I are the incident and transmitted intensities at the absorption cell.

A is related to A_T by

$$A = \log_{10}\left(\frac{1}{1 - A_T}\right) \tag{3-28}$$

Thus, there is no simple relationship between the two except at low values of A_T ($< 0{\cdot}10$) when a graph of A against A_T is, to a good approximation, a straight line.

Substitution into equation (3-27) of

$$I_0 = \int_0^{\Delta\nu_s} I_\nu^0 \,.\, d\nu$$

and

$$I = \int_0^{\Delta\nu_s} I_\nu \, d\nu = \int_0^{\Delta\nu_s} I_\nu^0 \, e^{-k_\nu L} \, d\nu$$

gives

$$A = \log_{10}\left[\frac{\int_0^{\Delta\nu_s} I_\nu^0 \, d\nu}{\int_0^{\Delta\nu_s} I_\nu^0 \, e^{-k_\nu L} \, d\nu}\right] \tag{3-29}$$

If we now assume that over the limits of integration (i.e. over the narrow region at the centre of the absorption line defined by the source line-width) k_ν is a constant and equal to bk'_0 as before, we may take the exponential term outside of the integration. Hence,

$$A = \log_{10}\left[\frac{1}{e^{-bk'_0L}}\right]$$

$$= \log_{10}\,(e^{bk'_0L})$$

i.e.

$$A = 0{\cdot}434\, bk'_0L \tag{3-30}$$

Substitution for k'_0 as before gives

$$A = 0{\cdot}434\, b\, \frac{2\sqrt{\ln 2}}{\Delta\nu_D\sqrt{\pi}}\, \frac{\pi e^2}{mc} f_{ji} N_j L \tag{3-31}$$

Thus a plot of absorbance against N_j should be rectilinear over a wide concentration range (but see Section 3.5).

3.5 PRACTICAL ATOMIC ABSORPTION METHODS

3.5.1 *Historical Approach*

Atomic absorption spectroscopy has been used as a tool of fundamental research for many years, particularly in astrophysical work and for the determination of spectral constants, such as transition probabilities and oscillator strengths. Such applications require techniques that readily allow a theoretical analysis of the results, and, as mentioned several times in earlier chapters, these methods are too complex and too restricted in application to be of much use for routine chemical analysis.

From a theoretical standpoint, the most satisfactory means of applying absorption measurements is the use of equation (3-10) in conjunction with a determination of the integrated absorption coefficient, K. For this purpose the light source is a lamp whose emission intensity is of known spectral distribution, usually a continuum. The transmission of the absorption cell is then measured at a number of points on the absorption line and equation (3-1) is used to calculate k_ν at each of these frequencies. After k_ν has been plotted as a function of frequency, K corresponds to the area under the curve. Although this method has been used quite often by physicists, the experimental difficulties are great when conventional pressures and temperatures are used in the absorption cell. Under these circumstances the overall width of the absorption line will usually be only a very small fraction of a nanometre. Thus a spectrometer of extremely high resolving power is required to measure k_ν at different points on the line profile. Even when such an instrument is available (e.g., a Fabry-Perot interferometer) its use presents many practical problems. In certain cases, the problem may be considerably reduced by measuring k_ν directly with a sharp line spectral source whose emission line may be shifted slightly to allow measurements at different points on the absorption line profile. The Zeeman scanning technique, in which a strong magnetic field is applied to the spectral lamp to shift the frequency of the emission line, has been used to demonstrate this.[7] Another, perhaps more obvious solution, which has been used a number of times for theoretical studies, is to operate an absorption cell at extremely high foreign (i.e. non-absorbing) gas pressures. This produces a very wide absorption line that may be effectively resolved by a conventional spectrophotometer. Such experiments, extended to changes in temperature as well as in pressure, have proved[8] that K is quite independent of conditions in the absorption cell.

The problems of resolving the absorption line profile have also been avoided for practical applications of AAS by measuring the total absorption factor, A_T. However, as we have seen in Section 3.3, this is only simply related to concentration at very low absorption values, when it is proportional to N_j, and at very high absorption values, when it is proportional to $\sqrt{N_j}$. In the intermediate region which, in most experimental arrangements, covers a wide range of atomic populations of interest, the relationship between A_T and N_j cannot be expressed in simple analytic terms. Instead, it is necessary to compute theoretical curves of growth (of A_T against N_jL) using the Voigt expression with assumed values of the "a" parameter (see Section 3.2.2) and to compare them with experimental results.[9] Obviously, such techniques are not necessary for straightforward chemical analysis, but the lack of a constant relationship between A_T and N_j in this important region greatly reduces the usefulness of AAS with a continuum source (since it is A_T that is being measured). At very high absorption levels the $\sqrt{N_j}$ region may be passed and A_T increases more slowly than expected, eventually reaching a limiting value. This results from the fact that under these circumstances most of the effect of increasing absorption is apparent at the edges of the absorption line (as explained earlier and shown in Fig. 3-1). The narrow monochromator bandpass usually used for AAS measurements with a continuum may then mean that these changes are not detected.

Several other sophisticated techniques have also been suggested[10] in which, instead of using a continuum source to determine A_T, a line spectral source is used to measure the total absorption (the so-called "total line absorption factor A_L"). However, the applicability of these methods is again rather limited and they have not been widely used.

3.5.2 The Walsh Method of Peak Absorbance Measurements

As we have seen, most of the traditional atomic absorption methods are unsatisfactory for routine use as analytical techniques. The acceptability of AAS for such use came only after the suggestion by Walsh[11] that measurement of the absorbance, A, at the peak of the absorption line profile would give a linear relationship with concentration over a wide range of absorbance values (see equation (3-31)). In theory, such measurements should have the same freedom from the effects of changes in the absorption line profile as those of the integrated absorption coefficient, K, without the serious experimental difficulties that arise when K is measured (as it is only necessary to measure the total absorption of a sharp line spectral source).

In practice, the technique works sufficiently well with both flame and other atom cells to allow its widespread routine use. Furthermore, because measurements are made in the spectral region of strongest absorption, there is a high effective "contrast" of the absorption cell with respect to the light source. Thus, this method can also give greater sensitivity than, say, measurement of A_T with a continuum source. However, under actual experimental conditions the relationship between A and N_j is not as simple as it would appear from the discussion given above, and the range over which the absorbance varies linearly with N_j is often much smaller than might be expected. There are several possible reasons for this, not all of which will necessarily apply in every case.

1. The half-width of the emission line from the source is not always sufficiently small relative to that of the absorption line to justify the assumption that a constant value of k_ν (equal to bk'_0) may be used in the evaluation of A. This fact is not always appreciated, as it would seem that the very low pressures and the low temperatures in such sources as the hollow cathode lamp must always give a line width much narrower than that in the usual flame absorption cells. However, unless these lamps are run at low currents self-absorption of the resonance lines is easily produced for many elements and, as we have seen in Section 2.5.2(vii), this can lead to quite serious broadening of the lines. When low-temperature atom sources (such as the graphite filament) are used, the source line width may not be negligible for absorbance measurements even in the absence of self-absorption.

2. In flame absorption cells, and others with relatively high foreign gas pressures, the Lorentz shift of the absorption line peak will be considerable (see Section 2.5.2(iii)). As the source emission line is unaffected the absorbance measurement will no longer be a true peak value. This can result in a reduction of the expected absorbance by as much as 25%, depending on the absorption line profile and the extent of the shift. Willis[12] has recently attempted practical correction of absolute absorbance measurements for the effects of absorption line shift.

3. The important effects of the hyperfine structure (hfs) of many spectral lines on their effective width has already been discussed in Section 2.5.2(viii). However, our derivation of an expression for the absorbance* has assumed the existence of a single, isolated resonance line. Thus if the equation is to be rigorously applied we must use it for each individual component of the emission and absorption line rather than for the line as a whole. This always results in a lower absorbance than would be obtained with a single line, the error depending on the number of hfs components and the relative values of the component separation, the line widths and (if any) the absorption line shift. The linearity of the calibration graphs is also reduced. Both effects have been discussed in some detail by L'vov[10] who shows that the errors are minimized when the line-widths are large enough to make the hfs separation negligible. Of course, if the emission line is too wide we merely introduce a different error into the absorbance measurements. Thus, a common example will be the situation in which the absorption line is sufficiently broadened to be considered as a single component but the hfs of the emission line is important. Some values calculated for this case by L'vov are shown in Table 3-1; the further simplifying assumptions were made that the emission line consists of just two components with a pure Lorentz profile for the absorption line. It can be seen that in serious cases the absorbance may be reduced to one-third of the expected value. Practical corrections for the effect of hfs on absorbance values have recently been described by Willis.[12]

TABLE 3-1

Relative absorbance values calculated for two-component and single-component emission lines at different levels of absorption[10]

	Absorbance for a two-component emission line/Absorbance for a single-component emission line					
Ratio of hfs component separation to line-width	2:1	1:1	1:2	1:3	1:4	1:5
Absorbance for a single-component line						
0·1	0·36	0·87	1·0	1·0	1·0	1·0
0·5	0·35	0·75	0·93	0·97	0·99	1·0
1·0	0·34	0·65	0·86	0·92	0·96	0·98
1·5	0·32	0·57	0·81	0·89	0·94	0·96
2·0	0·30	0·54	0·76	0·86	0·92	0·94

4. Throughout our discussion we have related absorbance values* to the ground state population, N_j, with the implied assumption that N_j is directly proportional to the sample concentration. In practice there may be a more complex relationship owing to compound formation and dissociation in the absorption cell. This problem is particularly important with flame cells and is discussed for them in Chapter 6.

---

* And, indeed, for all of the other absorption quantities used to which this source of error also applies.

* And the other quantities.

3.5.3 *The Possibility of Absolute Analysis by Atomic Absorption Spectroscopy*

Numerous equations have been derived which, at first sight, seem to provide useful relations between atomic concentration and absorption measurements. The preceding discussion (particularly in Section 3.5.2), however, has also illustrated that in some cases the use of the equations is restricted by the extreme practical difficulties in making the required measurements, whereas in others the derivation of the expressions has involved approximations that limit their applications to certain idealized situations. It should also be mentioned that the equations include constants, such as transition probabilities, that have been determined with only poor precision for many elements and spectral lines. Finally, the expressions themselves still provide only a value of N_j in the absorption cell; in many instances relating this to the sample concentration is itself a major problem.

In view of these facts, the present situation with regard to absolute analysis may be summarized as follows. By carrying out carefully and precisely a complex set of measurements it is possible to determine with quite good accuracy the absolute concentrations of a few elements that meet fairly well the approximations required by the theoretical expressions. Furthermore, if only poor accuracy is sufficient, the measurements may be extended to a wider range of applications. Indeed, several usable techniques have been reported recently. Most interest has centred on the use of these techniques to determine the free atom fractions of various elements in the flames commonly used as absorption cells in AAS. The techniques usually involve direct application of equation (3-19) by measuring the total absorption (A_T) with a continuum source[12-15] or direct application of equation (3-31) by measuring the absorbance, A with a sharp line source.[12,15-18] It is assumed that by working at low absorption levels with carefully chosen experimental conditions, the effect of the approximations made in order to derive the theoretical relations between signal and concentration will not be significantly large in comparison with the experimental errors. However, even after allowance has been made for errors of theory and/or technique it is found that there is a consistent discrepancy between the results obtained with the two techniques. The most thorough comparison of the two techniques is that of Willis[12] who suggests that more realistic results will be obtained when a continuum source is used unless corrections are made for the effects of hyperfine structure and line shift on the peak absorbance method. He also points out the serious uncertainties that occur in many of the "*f*-values" needed in either technique.

Thus, we may conclude that the effort recently devoted to the subject has considerably clarified the nature of the problem and has indicated the most promising areas for attempts to improve the techniques. While this should make it possible to obtain reasonable results by using great care and a realistically chosen problem, it seems almost certain that these techniques will see little practical analytical application for some time to come. Compared with the simplicity, accuracy and range of application of conventional AAS using calibration by standards, they all remain impracticable for routine use.

REFERENCES

1. W. Voigt, *Münch. Ber.*, 1912, p. 603.
2. A. C. G. Mitchell and M. W. Zemansky, "Resonance Radiation and Excited Atoms", Cambridge Univ. Press, Cambridge, 1934.
3. D. W. Posener, *Australian J. Phys.*, 1959, 12, 184.
4. G. D. Finn and D. Mugglestone, *Mon. Not. R. Astr. Soc.*, 1965, 129, 221.
5. B. H. Armstrong, *J. Quant. Spec. Radiat. Transfer*, 1967, 7, 61.
6. E. E. Whiting, *J. Quant. Spec. Radiat. Transfer*, 1968, 8, 1379.
7. T. Hollander, B. J. Jansen, J. J. Plaat and C. T. J. Alkemade, *J. Quant. Spec. Radiat. Transfer*, 1970, 10, 1301.
8. J. C. Strijland and A. J. Nanassy, *Physica*, 1958, 24, 935.
9. R. B. King, B. R. Parnes, M. N. Davis and K. H. Olsen, *J. Opt. Soc. Am.*, 1955, 45, 350.
10. B. V. L'vov, "Atomic Absorption Spectrochemical Analysis", Hilger, London, 1970, Ch. 1.
11. A. Walsh, *Spectrochim. Acta*, 1955, 7, 108.
12. J. B. Willis, *Spectrochim. Acta*, 1971, 26B, 177.
13. L. De Galan and J. D. Winefordner, *J. Quant. Spec. Radiat. Transfer*, 1967, 7, 251.
14. P. J. Th. Zeegers, W. P. Townsend and J. D. Winefordner, *Spectrochim. Acta*, 1969, 24B, 243.
15. J. B. Willis, *Spectrochim. Acta*, 1970, 25B, 487.
16. S. R. Koirtyohann and E. E. Pickett, *Proc. XIIIth Colloq. Spectroscop. Intern., Ottawa, 1967*, p. 270.
17. C. S. Rann, *Spectrochim. Acta*, 1967, 23B, 827.
18. L. De Galan and G. F. Samaey, *Anal. Chimica Acta*, 1970, 50, 39.

CHAPTER 4

Theory of Atomic Fluorescence Measurements

4.1 INTRODUCTION

As absorption is the initial process that must occur before fluorescence can be observed, the expressions relating atomic fluorescence intensity to atom concentration are, naturally, similar to those already derived in Chapter 3 for atomic absorption. They are, however, more complex. This is partly due to the extra process involved; we must now account for the proportion of the absorbed energy which is re-emitted as fluorescence and allow for the possibility that the fluorescence radiation will suffer self-absorption before it can be measured. As the absolute intensity of the source radiation is of importance in AFS, any loss of this radiation due to self-absorption before it reaches the region of the cell from which fluorescence is measured will also be important. The other complicating factor is the number of different types of fluorescence that are possible. The yield of fluorescence obtained with a given absorption of radiation will vary with the type of fluorescence transition, and the effect of re-absorption of fluorescence will depend on the population of the lower level of this transition.

In view of these difficulties no attempt will be made to derive complete expressions for the fluorescence intensity in a single step. Instead, we shall first relate an ideal fluorescence intensity to the total absorption factor, A_T, derived in Chapter 3. Such a quantity has limited practical value since it is dependent on the assumptions that all absorption of the source radiation occurs within the region of the fluorescence cell actually used for measurements, and that none of the fluorescence radiation is lost by re-absorption before it can be detected. However, it will serve to illustrate the basis of more rigorous expressions without introducing many confusing correction terms. This will be followed by a discussion of the different categories of atomic fluorescence accompanied, where appropriate, by the expressions required to evaluate the fluorescence yield factor in a particular case. Finally we shall see how practical fluorescence measurements differ from the ideal case, and compare the analytical curves derived from the more rigorous expressions that may be developed with those which would be expected from the initial simple treatment.

4.2 AN IDEAL FLUORESCENCE INTENSITY

An expression for the fluorescence intensity may be obtained with little difficulty in terms of the total absorption factor, A_T, derived at some length in the previous chapter, by making the following assumptions:

1. That the particular fluorescence transition considered is excited by absorption of energy at only a single frequency.*
2. That the entire fluorescence cell is within the solid angle viewed by the detector; i.e. there will then be no region of the cell where the incident radiation is absorbed without exciting fluorescence which is measured by the detector. If this were not the case the effective incident intensity with respect to the fluorescence measurements would be less than the value where the exciting beam enters the cell (and which is used in the calculation).

---

* If more than one absorption line contributes to a particular fluorescence line, it is necessary merely to apply the equation separately to each absorption line and sum the results.

3. That no fluorescence emission is lost by reabsorption in the cell.

In this case, the integrated fluorescence intensity in a direction perpendicular to the exciting light beam is given by

$$I_F = I_0 w \frac{\Omega}{4\pi} A_T \phi \tag{4-1}$$

where I_0 is the radiant flux (expressed as energy per unit time per unit area of the fluorescence cell face on which it is incident) which excites the fluorescence under consideration; w is the width of the exciting beam of radiation; Ω is the solid angle over which the excited fluorescence is detected and measured (4π is simply the total number of radians over which fluorescence is emitted from the cell); A_T is the total absorption factor for the spectral line at which the fluorescence is excited (and therefore depends on the absorption path length through the cell as well as atom concentration); ϕ is the *fluorescence yield* (or power, or efficiency). It is the fraction of the absorbed photons which is re-emitted as fluorescence radiation.

The value of ϕ for a particular fluorescence transition will depend on the type of fluorescence (i.e. on the number of alternative paths by which the atom may return to the ground state) and on the *quenching of fluorescence* which occurs in the cell. This process is the deactivation of excited atoms by collisions with foreign atoms or molecules in the fluorescence cell, rather than as a result of a transition involving the emission of radiation. It produces an overall reduction in the fluorescence intensity measured rather than a change in the shape of calibration graphs. However, depending on the species present in the cell, quenching may result in values of ϕ far below unity, and this process is a very important factor in the selection of a suitable cell for fluorescence measurements. Quenching processes are discussed in detail in Section 4.5. The effects on ϕ of different types of fluorescence are given in the following section.

By using the equations for A_T obtained in Chapter 3, expressions for the "ideal" fluorescence intensity may be derived using equation (4-1) for the same four special cases. Thus, for a continuum source we see from equations (3-19) and (3-22) that I_F should be proportional to N_j at low optical densities and to $N_j^{1/2}$ at high optical densities. Similarly, equations (3-25) and (3-26) show that, for a sharp line source, I_F should again be proportional to N_j at low optical densities but should be independent of N_j at high concentrations. The degree of relevance of these findings to practical situations where the fluorescence intensity can no longer be considered as "ideal" will be discussed in Section 4.4.

4.3 TYPES OF ATOMIC FLUORESCENCE

The main types of atomic fluorescence process are summarized in Fig. 4-1 which shows diagrammatically the transitions involved. The energy levels are indicated by numerical subscripts used in ascending order for increasing energy. This system is used in preference to the notation of Chapter 2 to avoid confusion when the Einstein transition probabilities are applied, as in the situation discussed here the values of B_{ji} and B_{ij} applying to a particular fluorescence need not share two common energy levels. However, the distinction between B_{ji} and B_{ij} will still be clear even with this notation. Dashed lines are used on the diagrams to represent radiationless transitions

(a) Resonance fluorescence (b) Direct line fluorescence

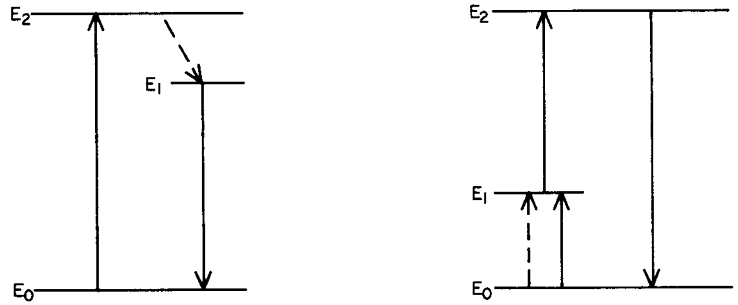

(c) Stepwise line fluorescence (d) Stepwise excited fluorescence and sensitized fluorescence

Fig. 4-1. The main types of atomic fluorescence and their electronic transitions.

(e.g. deactivation by collisions). Each of the types shown on the diagram is discussed below in more detail, although not all of them have actually been applied to analytical AFS.

4.3.1 Resonance Fluorescence

Resonance fluorescence occurs when the atom re-emits a spectral line of the same wavelength as that used for excitation. Many of the AFS measurements made by analytical chemists involve this type of fluorescence. Pure resonance fluorescence is observed only when no other types of fluorescence can occur simultaneously from the same excited state, i.e. when the selection rules allow no other transition from the excited state considered to a lower level. An example of pure resonance fluorescence without the presence of an intermediate level is shown in Fig. 4-2 for the 213·86 nm and 307·59 nm lines of zinc. Obviously, pure resonance fluorescence will not be observed unless there is a singlet ground state.

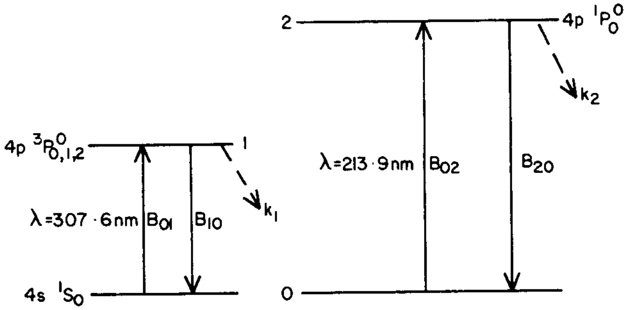

Fig. 4-2. Pure resonance fluorescence of zinc.

The yield, ϕ, of pure resonance fluorescence is easily evaluated as it is merely the ratio of the numbers of stimulated emission transitions without and with quenching of atoms in the excited state. Hence, using the Einstein transition probabilities (see Section 2.3.2) and defining as k the probability per second that an excited atom is deactivated by a quenching collision, we obtain for the zinc example shown in Fig. 4-2:

$$\phi_{307\cdot59} = \left(\frac{B_{10}}{B_{10}+k_1}\right) \quad \text{and} \quad \phi_{213\cdot86} = \left(\frac{B_{20}}{B_{20}+k_2}\right) \qquad (4\text{-}2)$$

The ease of determining ϕ when the resonance fluorescence is accompanied by fluorescence of another type may vary with the form that the latter takes. A simple example is shown for thallium in

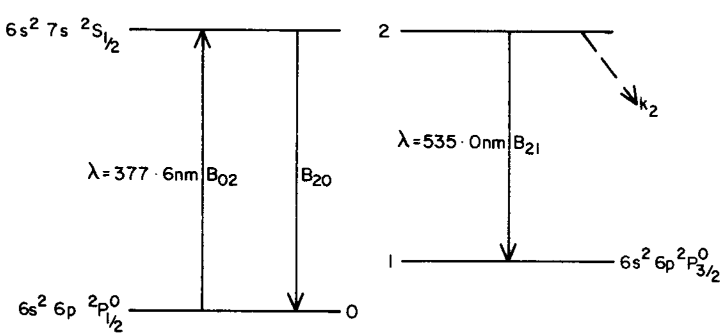

Fig. 4-3. Fluorescence from the lower thallium excited state.

Fig. 4-3. In this case excitation at the 377·6 nm resonance line produces resonance fluorescence accompanied by a further emission at 535·0 nm. In this case the yield of resonance fluorescence is given by

$$\phi_{377\cdot 6} = \frac{B_{20}}{(B_{20} + B_{21} + k_2)} \tag{4-3}$$

4.3.2 Direct Line Fluorescence

Direct line fluorescence is observed when transitions between the excited state of the resonance line and a lower intermediate level are not forbidden by the selection rules. Thus, direct line fluorescence will always occur at a longer wavelength than that of the resonance line which excites it (and which is observed simultaneously as resonance fluorescence). This situation will arise if the ground state is a multiplet, as we have already seen for thallium in Fig. 4-3. In this simple example the expression for ϕ is again easily evaluated, being*

$$\phi_{535\cdot 0} = \frac{B_{21}}{(B_{20} + B_{21} + k_2)} \tag{4-4}$$

There are other situations which can result in direct line fluorescence. For example, the ^4P excited state of the antimony resonance line lies above the ^2D state as shown in Fig. 4-4. As a result, excitation at 217·6 nm produces direct line fluorescence at 267·1 nm

---

* It should be remembered that ϕ can be defined in terms of energy rather than numbers of photons; it is then necessary to incorporate a ratio of line wavelengths whenever the absorption and fluorescence wavelengths differ as in this example (as the energies of the absorbed and emitted photons will then be different).

and 277·0 nm. Evaluation of an expression for the yield at each line is again quite straightforward. Although the direct line fluorescence is normally less intense than the resonance fluorescence at the corresponding absorption wavelength, it may well be more intense than resonance fluorescence observed at another, weaker, absorption line. Thus, in certain cases, depending on experimental conditions, the use of direct line fluorescence gives complete freedom from the effects of scattered source radiation without resulting in an unacceptable decrease in the fluorescence intensity received.

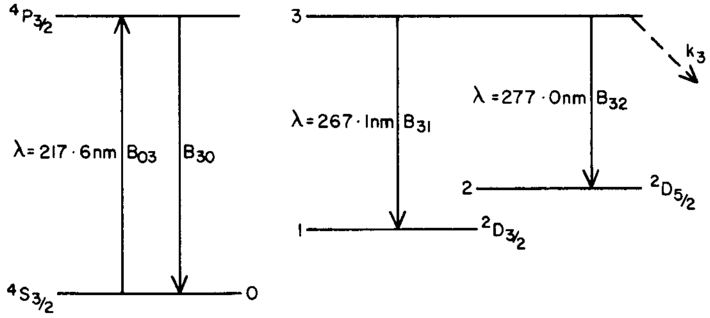

Fig. 4-4. Resonance and direct line fluorescence of antimony.

4.3.3 Stepwise Line Fluorescence

When an atom is initially excited to a higher excited state by absorption of radiation at a ground state line, it may undergo deactivation (often by a collision or other radiationless process) to a lower excited state rather than return directly to the ground state. If a transition is permitted from this level to one still lower (which will often be the ground state), stepwise line fluorescence is observed as shown in Fig. 4-1(c). For example, if sodium atoms are excited only by the 589·0 nm *D* line (this would be achieved by filtering the incident source radiation with a monochromator or a narrow-band interference filter), stepwise line fluorescence is observed at 589·6 nm provided suitable species are present to give energy transfer by collisions. This is illustrated in Fig. 4-5. The quenching rates are shown with the same notation as previously, but the vertical transitions with rates k_{12} and k_{21} represent the rates of collisional transfer of energy between the two excited states. In this particular case the splitting of the $^2P^0_0$ level is so small that k_{12} is relatively large and there is said to be good *mixing* between the $^2P^0_{1/2}$ and

$^2P^0_{3/2}$ states. When the sodium atoms are in the presence of a species which gives efficient transfer of energy by collisions, the mixing becomes fast compared to all other radiative or radiationless transitions. The populations of these two excited states are then in partial equilibrium and their ratio is practically the same as for thermal equilibrium and obeys the Boltzmann law. This allows a simple derivation of a direct expression for the ratio of fluorescence intensities concerned,[1] but its application is limited to special cases of stepwise line fluorescence such as this where the level separation is extremely small.

It will be appreciated that although the species present with the sodium atoms must give efficient collisional mixing between the excited states concerned if stepwise line fluorescence is to be observed, they should also give low quenching levels. This is essential since, with the notation of Fig. 4-5, k_{21} must at least be as large as $(k_2 + B_{20})$ for fluorescence to be observed at 589·6 nm (especially as quenching with rate k_1 will also occur at this lower excited state). As a result this particular example is not observed when an air-hydrogen flame is used as the fluorescence cell because nitrogen is an efficient quencher (see Section 4.5.3) but can be seen in an oxygen-argon-hydrogen flame because argon gives low quenching while still retaining efficient mixing capability for the two $^2P^0$ states of sodium.

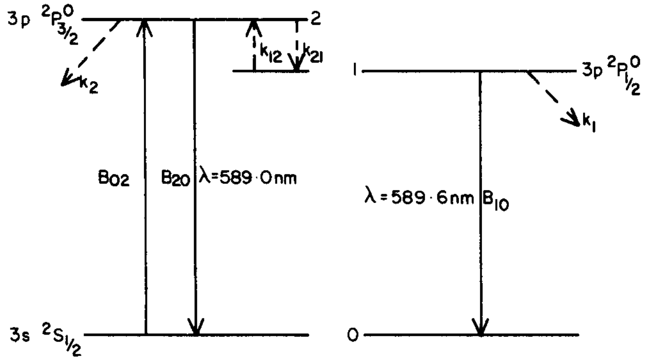

Fig. 4-5. Resonance and stepwise line fluorescence at the sodium *D* lines.

When the intermediate excited level is at much lower energy than the initial excited state it may be assumed that any mixing between the two levels is negligible; i.e. energy can be transferred to the lower level by collisional deactivation but is unlikely to return via the reverse process. However, because of the larger energy gap the deactivation may not occur in a single stage and the exact path of stepwise line fluorescence may be difficult to visualize. An example of this is shown in Fig. 4-6, again for sodium. Excitation in which only the ground state doublet at 330 nm is used produces not only resonance fluorescence at the same wavelengths but also stepwise line fluorescence at the *D* lines. It is believed that the required deactivation from the $4p\ ^2P^0$ to the $3p\ ^2P^0$ levels probably occurs via the $3d\ ^2D$ and $4s\ ^2S$ intermediate levels (not shown in the diagram) and may also give other fluorescence lines at longer wavelengths. Obviously, under these conditions, any attempt to derive an expression for the fluorescence yield at a particular wavelength will be extremely complicated. Furthermore, when the spectrum is more complicated than that of the alkali metals, there may be several alternative paths and that obtained in a particular situation may depend on the actual species responsible for the collisional deactivation.

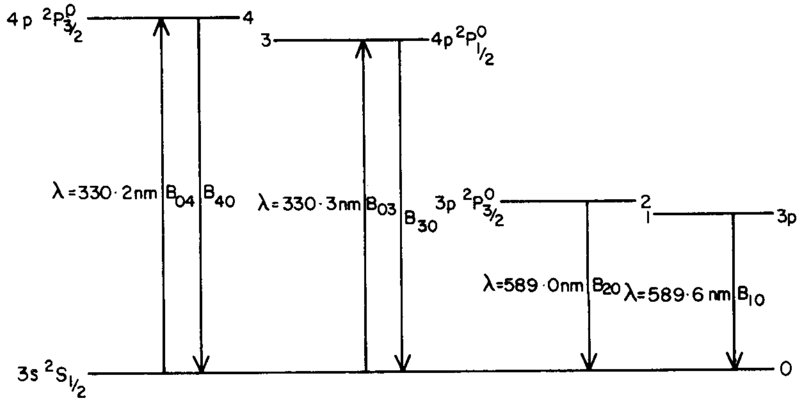

Fig. 4-6. Stepwise line fluorescence at the sodium *D* lines.

The situation can also be complicated by an energy level configuration intermediate between the types occurring in the previous two examples; i.e. where the lower excited level is neither sufficiently close to the higher one to assume an equilibrium distribution between the two nor sufficiently far below to assume that re-excitation by collision is negligible. Such an example occurs with lead, excitation at 283·3 nm to the $7s\ ^3P^0_1$ level producing stepwise line fluorescence at 368·3 nm from the $7s\ ^3P^0_0$ level. The technique needed to evaluate the rate of collisional re-excitation from $^3P_0$ to $^3P_1$ has been discussed by Jenkins[2] and is obviously complicated by the simultaneous emission of resonance and direct line fluorescence from the 7*s* $^3P_1^0$ level.

4.3.4 *Stepwise Excitation Fluorescence*

Stepwise excitation fluorescence is really the converse of stepwise line fluorescence, i.e. it occurs as the result of a stepwise absorption of energy by the atom in order to reach a particular excited state. A simple example is seen when the first level reached from the ground state is populated thermally owing to the relatively high temperature of a flame fluorescence cell. Absorption of a line involving a transition from this level can then produce excitation of fluorescence. This is seen with the thallium energy levels shown in Fig. 4-3. At sufficiently high temperatures the $6s^2\ 6p\ ^2P_{3/2}^0$ level is populated enough to give quite strong absorption at 535·0 nm so that stepwise excited fluorescence is observed at both 535·0 nm and 377·6 nm. Obviously, this type of stepwise excited fluorescence will be observed only when the lower level of the absorption line is relatively close to the ground state unless an extremely hot flame is used. In any case, the intensity is unlikely to be sufficiently intense for analytical use in most instances.

Another well-known mechanism for stepwise excited fluorescence involves the use of a very intense excitation source. An excited level reached by absorption of a ground state line may then itself act as the lower level for further absorption of another line to reach a much higher excited state. For example, absorption of the mercury 253·7 nm resonance line may be followed by absorption of the 435·8 nm line to reach the 7*s* $^3S_1$ level from which stepwise excited fluorescence is observed. Again, this is likely to be of low intensity even with an extremely bright excitation source.

Stepwise excitation fluorescence may also be observed as the exact converse of stepwise line fluorescence, i.e. absorption of the excitation radiation raises atoms to (say) the lower level of a close doublet and mixing by collisional processes involving other species present results in a population of the upper level. Thus, a fluorescence line from this level is observed, the intensity depending on the separation of the levels and the efficiency of the collisional mixing (or coupling) provided by the species concerned. A typical example will occur with the sodium levels shown in Fig. 4-5, excitation at 589·6 nm only resulting in fluorescence both at 589·6 nm (resonance) and 589·0 nm (stepwise excited) even though the latter transition involves photons of higher energy than provided

by the absorption transition. Fluorescence lines with this characteristic have recently been observed for antimony, bismuth and arsenic in flame cells and referred to as thermally assisted fluorescence[3] since the flame species involved in the mixing process have considerable thermal energy. The example of bismuth is illustrated in Fig. 4-7, excitation at 206·2 nm to the $^4P_{5/2}$ level resulting in fluorescence at 293·8 nm and 262·8 nm from the $^2P_{3/2}$ level which lies 0·12 eV higher. It can be seen that, as mentioned earlier, any attempt to write an expression for the yield of stepwise fluorescence would involve some difficulty (especially as only some of the levels are shown in most of the simplified Grotrian diagrams given here).

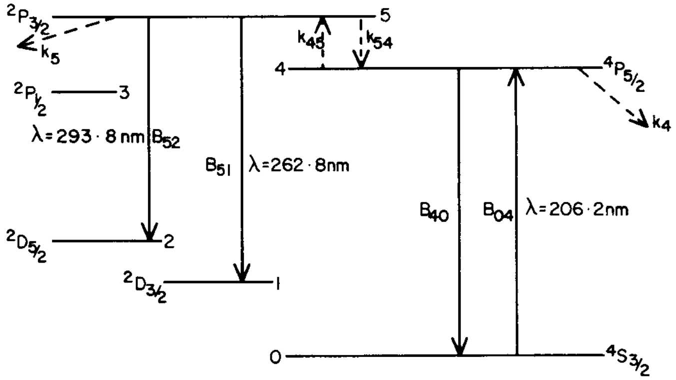

Fig. 4-7. Stepwise excited fluorescence from bismuth $^2P_{3/2}$ level.

4.3.5 *Sensitized Fluorescence*

Sensitized fluorescence* is obtained when an atom which has been excited by normal absorption of resonance radiation is able to transfer this energy to another atom during a collision, thus raising the second atom to an excited level from which a radiative transition is possible. In order to obtain sufficient collisional excitation of this kind a high concentration of the donor atoms is needed; sensitized fluorescence is thus unlikely to be observed from flame cells (especially as the energy is more likely to be lost by normal quenching collisions with the flame species). However, it has been observed in closed cells containing metal vapours at relatively high pressure. For example, if such a mixture of mercury and thallium atoms is strongly irradiated with mercury resonance radiation at 253·7 nm it is possible to observe sensitized fluorescence of thallium at the 377·6 nm and 535·0 nm lines.

---

* Sometimes referred to as photosensitized fluorescence.

4.4 CALCULATIONS OF ACTUAL FLUORESCENCE INTENSITY

It is now necessary to examine the relevance of the simple expression for fluorescence intensity derived in Section 4.2 and to discuss some recent attempts to obtain wider agreement with practical measurements. Before doing this it is useful to consider some of the assumptions made earlier in terms of the dimensions of the "standard" fluorescence cell shown in Fig. 4-8. This could be achieved in practice by making measurements with parallel light beams in order to obtain the rectangular geometry for the atom cell. As calculations usually assume conditions of uniform atomic concentration, temperature, etc. the use of a flame cell would require that the standard cell of Fig. 4-8 be situated at the centre of a flame-shielded flame (see Chapter 6). The assumption that no incident radiation is lost by absorption before it can excite useful (i.e. detected) fluorescence would be met by a cell with $\Delta L = 0$. If the condition that no fluorescence be lost by re-absorption is to apply generally, it is also necessary that $\Delta l = 0$ and l be as small as possible so that the path length over which re-absorption can occur is minimized.

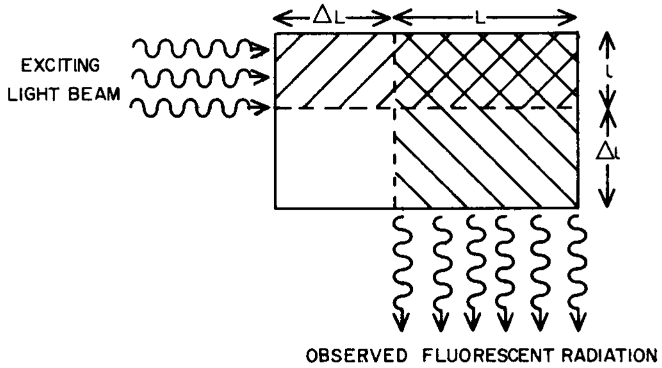

Fig. 4-8. Dimensions of a standardized fluorescence cell.

In practice it is obviously impracticable to make l sufficiently small for re-absorption to be negligible under all conditions, as the fluorescence intensity produced also depends on l (i.e. on the width of the exciting light beam). Thus equation (4-1) may be applied only when re-absorption of fluorescence is negligible; i.e. (a) at low atom concentrations, and (b) at all concentrations for direct line fluorescence (and sometimes the other types of non-resonance fluorescence) when the lower level of the fluorescence transition is far enough above the ground state for its equilibrium population to be extremely small. The analytical curves predicted by equation (4-1) will then apply and are shown in Fig. 4-9. The four asymptotes shown correspond to the four limiting cases discussed in Section 4.2; the two full curves are only obtained by numerical solution of the Voigt integral for all concentrations, as explained in Section 3.2.1. It can be seen that the limiting cases give a useful indication of the shape of the full curves. As most fluorescence measurements use resonance fluorescence, however, equation (4-1) is really only of practical interest at low concentrations. Nevertheless, AFS is a trace analysis technique and the linear dependence of fluorescence on (low) concentrations under all conditions is of considerable importance.

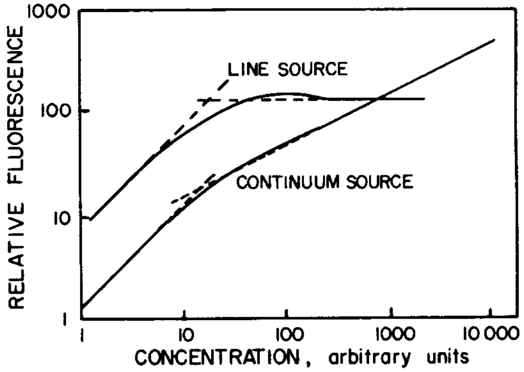

Fig. 4-9. Ideal analytical curves assuming no re-absorption of fluorescence (applicable to direct line fluorescence and certain other examples of non-resonance fluorescence).

Extension of equation (4-1) to wider concentration ranges under practically useful conditions* has been described by Hooymayers[4] for $\Delta L = 0$ and his general relation has recently been adapted to $\Delta L \neq 0$ by Zeegers and Winefordner.[5] The latter have also tested the equation experimentally and found good agreement between actual and calculated analytical curves. We shall derive the basic equation without attempting to evaluate the complex integral involving exponential terms of the absorption coefficient, k_ν.

Consider a thin layer of the standard fluorescence cell in the direction of the exciting radiation, with width dx and distance x from the edge BDF of the excitation region, as shown in Fig. 4-10.

---

* However, the derivation is carried out only for a single absorption line as with the AAS equations of Chapter 3, so that the important effect of hfs is not taken into account.

Let I_ν be the incident radiation flux of the exciting light beam expressed as energy per unit time at frequency ν per unit area and per unit frequency interval. Then from equation (3-1) the remaining radiation flux at the plane CD will be $I_\nu \exp(-k_\nu \Delta L)$. Hence, using equation (3-1) again for the region between CD and EF, the absorbed radiation at frequency ν will be proportional to $I_\nu \exp(-k_\nu \Delta L)$ $[1 - \exp(-k_\nu L)]$. If the third dimension of the cell (i.e. perpendicular to the plane of the paper in Fig. 4-10) is of length l', the integrated energy absorbed per second in the thin layer considered can be written as

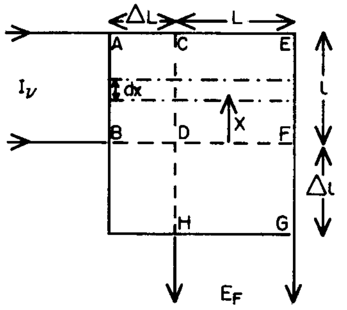

Fig. 4-10. Symbols used in the derivation of an expression for the actual fluorescence radiation E_F (see text for explanation).

$$E_A = l' \,\mathrm{d}x \int_0^\infty I_\nu \exp(-k_\nu \Delta L)\, [1\text{-}\exp(-k_\nu L)]\, \mathrm{d}\nu \qquad (4\text{-}5)$$

which we will abbreviate to

$$E_A = l' \,\mathrm{d}x\, \theta$$

Now from the definition of the fluorescence yield factor, ϕ, the fluorescence radiation emitted by the thin layer considered in a direction perpendicular to the exciting light beam and through a small solid angle Ω is simply

$$\mathrm{d}F'_{\mathrm{em}} = \frac{\Omega}{4\pi} E_A\, \phi = \frac{\Omega}{4\pi} l' \,\mathrm{d}x\, \theta\phi \qquad (4\text{-}6)$$

This will be reduced by reabsorption while travelling to the edge BDF of the excitation region to a value

$$\mathrm{d}F_{\mathrm{em}} = \frac{\Omega}{4\pi} l' \,\mathrm{d}x\, \theta\phi \exp(-k_{\nu'} x) \qquad (4\text{-}7)$$

again from equation (3-1) and where ν' is the frequency of the fluorescence line. Hence the total fluorescence radiation at frequency ν' leaving the excitation region along the line DF is obtained by integration of equation (4-7) for values of x between 0 and l, i.e.,

$$\begin{aligned} F_{\mathrm{em}} &= \int_0^l \frac{\Omega}{4\pi} l'\theta\phi \exp(-k_{\nu'} x)\, \mathrm{d}x \\ &= \frac{\Omega}{4\pi} l'\theta\phi \frac{1}{k_{\nu'}} [\exp(-k_{\nu'} x)]_0^l \qquad (4\text{-}8) \\ &= \frac{\Omega}{4\pi} l'\phi\theta \frac{1}{k_{\nu'}} [1 - \exp(-k_{\nu'} l)] \end{aligned}$$

Now by further application of equation (3-1), the radiation reaching the edge of the cell at HG after further re-absorption will be equal to $F_{\mathrm{em}} \exp(-k_{\nu'} \Delta l)$. Hence, E_F, the integrated fluorescence energy leaving the cell per second along the edge HG, is given by

$$E_F = \frac{\Omega}{4\pi} l'\theta\phi \int_0^\infty \frac{1}{k'_\nu} [1 - \exp(-k_{\nu'} l)] \cdot [\exp(-k_{\nu'} \Delta l)]\, \mathrm{d}\nu' \quad (4\text{-}9)$$

After substitution of the full expression for θ and multiplication and rearrangement* of the exponential terms within each integral, we obtain

$$\begin{aligned} E_F = \frac{\Omega}{4\pi} l'\phi \int_0^\infty I_\nu [\{1 - \exp[-k_\nu (L + \Delta L)]\} - \{1 - \exp(-k_\nu \Delta L)\}]\, \mathrm{d}\nu \\ \times \int_0^\infty \frac{1}{k_{\nu'}} \mathrm{d}_{\nu'} \times \int_0^\infty [\{1 - \exp[-k_{\nu'} (l + \Delta l)]\} - \{1 - \exp[-k_{\nu'} \Delta l]\}]\, \mathrm{d}\nu' \end{aligned} \qquad (4\text{-}10)$$

But $\int_0^\infty \frac{1}{k_{\nu'}} \mathrm{d}_{\nu'}$ may be written as $1/\int_0^\infty k_{\nu'}\, \mathrm{d}\nu$ which is simply (see Section 3.2.2) I/K where K is the integrated absorption coefficient for the fluorescence line. Hence using equation (3-11) with λ' as the wavelength of the fluorescence line, A its transition probability, g_0

---

* Using $e^a e^b = e^{a+b}$.

and g_1 the statistical weights of the lower and upper states and N_0 the population of the lower state, we obtain finally

$$E_F = \frac{\Omega}{4\pi} l'\phi \frac{8\pi}{(\lambda')^2 A N_0} \frac{g_0}{g_1}$$
$$\times \int_0^\infty I_\nu \{1 - \exp[-k_\nu (L + \Delta L)]\} - \{1 - \exp[-k_\nu \Delta L]\} \, d\nu$$
$$\times \int_0^\infty [\{1 - \exp[-k_{\nu'} (l + \Delta l)]\} - \{1 - \exp[-k_{\nu'} \Delta l]\}] \, d\nu' \tag{4-11}$$

This equation has been evaluated by Hooymayers[4] and Zeegers and Winefordner[5] for resonance fluorescence in which $\nu = \nu'$ and N_0 is equal to the ground state population of the sample element. Both found it still necessary to assume extreme cases in which the source line is either much wider than the absorption line (continuum source) or much narrower (sharp line source) in order to avoid the difficulty of defining the excitation source line profile and assigning a particular value to it for each experiment. In both reports the authors have calculated for these two special cases the full analytical curves by numerical solution of the Voigt integrals occurring in equation (4-11). They have also derived asymptotic expressions for the limiting cases of low and high concentrations using approximations for the integrals similar to those discussed in Section 3.3 for the evaluation of A_T.

Since the Voigt expressions for k_ν depend on the profile of the absorption line, as expressed* by the so-called "damping constant", a (see Section 3.2.1), the analytical curve obtained by evaluation of equation (4-11) will obviously vary with the value of a assigned to the absorption line as well as with the dimensions of the fluorescence cell. This is illustrated in Fig. 4-11 which shows curves calculated by Hooymayers[4] for different values of a with the same fluorescence cell in which $\Delta L = 0$, $L = 4l$ and $\Delta l = 3l/2$. It can be seen that the changes with different values of a are considerable. Furthermore, at high concentrations the curves differ considerably from those calculated using the "ideal" equation (see Fig. 4-9) even though part of the possible deviation from ideality has still not been included (i.e. ΔL is still zero); i.e. the continuum source curves reach a plateau instead of continuing to rise in proportion to $(N_j)^{1/2}$ whereas those for a sharp line source fall steadily instead of reaching a plateau.

Zeegers and Winefordner[5] found that for the particular example of the magnesium resonance line at 285·2 nm, their experimental conditions corresponded to an a value of 0·4. Their calculated curves for a sharp line source and an absorption line with a equal to 0·4 are shown in Fig. 4-12 for several different configurations of the fluorescence cell. It is seen that the departures from ideality increase considerably when ΔL is increased from zero. Similar effects are observed with a continuum source.

---

* From equation (3-5) it is seen that $a = \frac{\beta_1}{\beta_2} = \frac{\Delta\nu_C}{\Delta\nu_D} \cdot (\ln 2)^{1/2}$ where $\Delta\nu_C$ and $\Delta\nu_D$ are defined in Section 3.2.1.

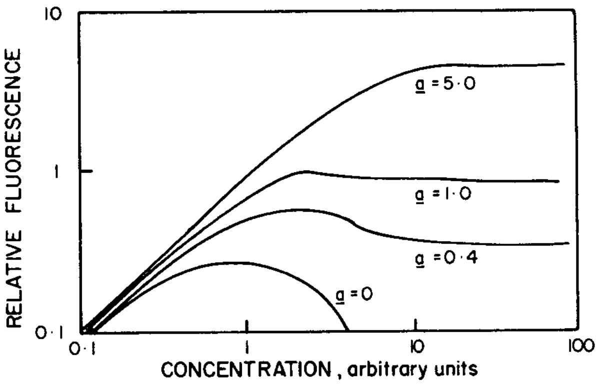

(a) Continuum source

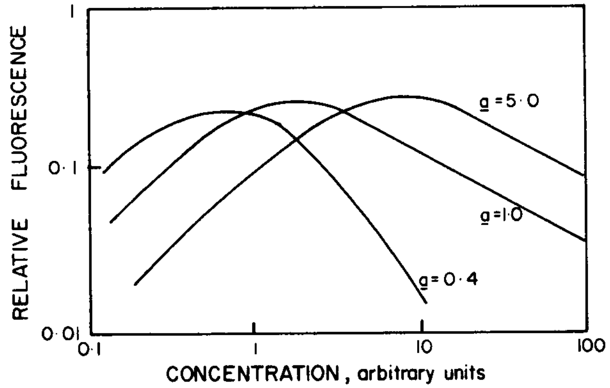

(b) Sharp line source

Fig. 4-11. Variation of calculated analytical curves with the a-parameter [ref. (4)] (single spectral line, fluorescence cell dimensions: $\Delta L = 0$, $L = 4l$, $\Delta l = 3l/2$).

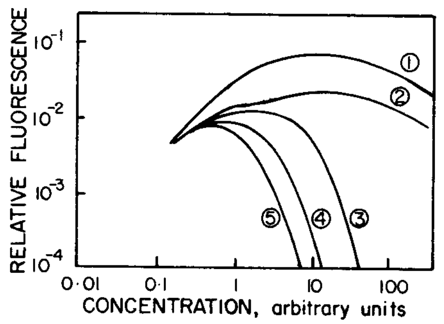

(a) $L = l = 5$ in all cases. ① $\Delta L = 0$, $\Delta l = 0$; ② $\Delta L = 0$, $\Delta l = 9{\cdot}5$; ③ $\Delta L = 1$, $\Delta l = 9{\cdot}5$; ④ $\Delta L = 3$, $\Delta l = 9{\cdot}5$; ⑤ $\Delta L = 5$, $\Delta l = 9{\cdot}5$

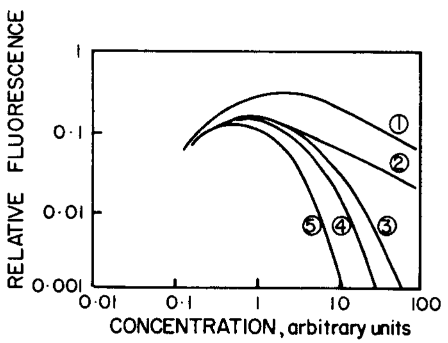

(b) $L = 10$, $l = 5$ in all cases. ① $\Delta L = 0$, $\Delta l = 0$; ② $\Delta L = 0$, $\Delta l = 9{\cdot}5$; ③ $\Delta L = 0{\cdot}5$, $\Delta l = 9{\cdot}5$; ④ $\Delta L = 1$, $\Delta l = 9{\cdot}5$; ⑤ $\Delta L = 3$, $\Delta l = 9{\cdot}5$

Fig. 4.12. Variation of calculated analytical curves with fluorescence cell dimensions for a sharp line source and a single absorption line with a-parameter equal to 0·4 [ref. (5)].

4.5 QUENCHING OF FLUORESCENCE

The quenching of fluorescence was mentioned in Section 4.2 with an indication of its important effect on the fluorescence yield observed in many practical situations. We shall now discuss in more detail the mechanism by which the process occurs and give some examples of individual quenching processes and of practical measurements which are particularly relevant to AFS. Some basic concepts necessary for a proper understanding of the principles involved will also be mentioned briefly. However, for a more thorough discussion of excitation and de-excitation processes and related topics the reader is referred to a recent, comprehensive review by Alkemade and Zeegers[6] and to the works of Laidler and Shuler,[7] Laidler,[8] and Shuler *et al.*[9] Many of the basic principles involved are discussed concisely in the textbooks of Laidler,[10] and Mavrodineanu and Boiteux.[11]

4.5.1 *Basic Concepts*

As we have seen, the fluorescence process involves the absorption of photons from a primary exciting light beam to produce an atom (or molecule) in an excited state. Up to this point in this text the main concern has been the de-excitation of this state by the re-emission of radiation (fluorescence). As there is a finite probability of such a transition occurring (the Einstein coefficient B_{ij}; see Section 2.3.2), however, there will also be a finite lifetime for the excited state before its excess energy is removed by this process. During this period it is possible for an excited species to be de-excited by other *non-radiative* processes as a result of collisional interaction with other species present in its environment. The resultant reduction in observed fluorescent power is generally referred to as *quenching* of the fluorescence. The effectiveness of quenching under particular circumstances will thus depend on the rate at which collisions occur, the type of non-radiative process involved and the efficiency of this process in removing energy from the excited species.

The fraction of absorbed photons actually re-emitted as fluorescence radiation is known as the *fluorescence yield factor,* ϕ. This is defined by the Stern-Volmer formula as

$$\phi = \frac{B_{ij}}{\text{Total probability per second of de-excitation}} \tag{4-12}$$

The total probability of de-excitation is simply the summation of B_{ij} with the *rates* of all non-radiative processes contributing to the quenching. For example, two straightforward but important examples of de-excitation processes are (a) inelastic collisions involving transfer of energy

$$A^* + B \rightleftharpoons A + B$$

and (b) reactions in which the quenching species dissociates after receiving the excess energy from the excited atom or molecule

$$A^* + CD \rightleftharpoons A + C + D$$

In these processes the superscript * is used to indicate a particle in an excited state. The symbol $\rightleftharpoons$ is used in each example as, by the

Principle of Microreversibility, the processes can proceed in either direction, that from right to left in (a) and (b) being excitation processes for A*. The *rate, r,* of each reaction is defined as the number of particles A* quenched per second per unit volume by the process. It is generally expressed in the form

$$\begin{aligned} r_1 &= k_1 [\mathrm{A}^*][\mathrm{B}] \\ r_2 &= k_2 [\mathrm{A}^*][\mathrm{CD}] \end{aligned} \tag{4-13}$$

for processes (a) and (b) respectively. k_1 and k_2 are the *rate constants* or rate coefficients for the two processes. The probabilities of a particle A* being quenched in each of these examples are thus $r_1/[\mathrm{A}^*]$ and $r_2/[\mathrm{A}^*]$ respectively. Hence, in a fluorescence experiment in which quenching occurs only by the processes (a) and (b) the yield factor is given by

$$\phi = \frac{B_{ij}}{k_1 [\mathrm{B}] + k_2 [\mathrm{CD}] + B_{ij}} \tag{4-14}$$

It can be seen from equation (4-14) that the maximum value of ϕ is unity when no quenching occurs. Note also that the effects of different quenching species are directly additive via the products of their concentrations and the rate constants. This property allows experimental measurement of the rate constants of quenching for complex situations, such as those encountered in flame cells. If only one quenching species were present its rate constant would follow directly from the measured value of ϕ, if it is assumed that its concentration and the value of B_{ij} are known. When n different quenching species act simultaneously in the flame, it is necessary to measure ϕ for each of a set of n (or more) isothermal flames having different but known compositions. All of the unknown rate constants may then be obtained from the straightforward solution of the set of simultaneous equations that results. This technique has been used to obtain the flame quenching values quoted in Section 4.5.3, although, as explained below, it is generally more useful to give the results in a form other than that of the direct rate constants.

4.5.2 Reaction Rate Theory

The fundamental relationship used in reaction rate studies is the empirical rule generally known as the *Arrhenius* law. This is usually written in the form

$$k_n = A\mathrm{e}^{-E/kT} \tag{4-15}$$

and thus relates the rate constant, k_n, of a reaction to the absolute temperature, T. A and E are constants referred to respectively as the *frequency factor* and the *activation energy* of the reaction. Since we are concerned with quenching processes that occur as the result of collisions between gaseous molecules, it is useful to interpret equation (4-15) in terms of collision theory, i.e. in terms of the number of collisions occurring between the atoms or molecules concerned. This is most simply achieved by using the *classical collision theory*, but at the expense of treating the colliding particles as hard spheres. Thus, the quantized structure of the atoms and molecules is ignored and the results calculated must be expected to differ from experimental determinations and those predicted by the *absolute reaction rate theory* which takes the internal structure into account. This more sophisticated theory is really necessary to interpret fully the quenching of excited atoms in flames, as the most important processes are known to involve conversion of the internal energy of the molecules (see Section 4.5.3). The subject is too complex to discuss here but a fairly straightforward treatment has been given by Laidler.[10] We shall, however, derive the reaction rate formulae obtained with the simple classical theory as they are still able to provide a useful format within which most measurements of quenching of atomic fluorescence are reported and interpreted.

The number of binary collisions occurring per second per unit volume in a gas mixture containing two species, A and B, considered to be hard spheres is

$$Z_{\mathrm{A,B}} = [\mathrm{A}][\mathrm{B}]\pi(r_{\mathrm{A}} + r_{\mathrm{B}})^2 \bar{v}_{\mathrm{rel}} \tag{4-16}$$

where r_{A} and r_{B} are the radii of the species A and B, and $\bar{v}_{\mathrm{rel}}$ is their average relative velocity. $Z_{\mathrm{A,B}}$ is sometimes referred to as the *collision number*, although most authors prefer to reserve this term for the number of collisions made by *one* of the species; i.e. for $Z_{\mathrm{A,B}}/[\mathrm{A}]$ or $Z_{\mathrm{A,B}}/[\mathrm{B}]$. The reciprocal of this quantity is known as the *collisional lifetime*, τ, of the particle. Thus for species A we have

$$\tau_{\mathrm{A}} = \frac{[\mathrm{A}]}{Z_{\mathrm{A,B}}} = \frac{1}{[\mathrm{B}](r_{\mathrm{A}} + r_{\mathrm{B}})^2 \bar{v}_{\mathrm{rel}}} \tag{4-17}$$

Values of τ are directly related to the spectral line widths obtained as a result of collisional or quenching broadening (see Section 2.5.2). A typical value of τ for a metal atom in a flame at 1 atm and 2500 K is about 10^{-10} second. The number of ternary collisions (i.e. between a metal atom and two flame molecules) under the same conditions is three or four orders of magnitude smaller than the number of binary collisions so that they will have a negligible effect on the value of τ.

The term $\pi(r_A + r_B)^2$ in equation (4-16) is known as the gas kinetic cross section for the process considered since it is a function of the quantity $(r_A + r_B)/2$ which, in the kinetic theory, would be the minimum distance between the two hard spheres representing A and B. In practice it is impossible to assign a definite diameter to an atom or molecule and it is customary to define a *collisional cross section* in terms of equation (4-16) *for a particular process.* Thus, the collisional cross section represents the value of $(r_A + r_B)^2$ which gives the collision frequency $(Z_{A,B})$ measured by observing the rate of the process under consideration. The collisional cross section of an atom or molecule will, therefore, vary with the process it is undergoing. It is usually written in the form $\sigma^2 = (r_A + r_B)^2$, but an alternative notation of the type, $S = \pi(r_A + r_B)^2$, is also used. As the symbol S is frequently replaced by σ, care is needed, when cross section data reported in the literature are used, to ascertain whether the values quoted include the factor π.

The collision frequency may be related to the Arrhenius equation in terms of the classical theory by writing the rate of a reaction between the particles A and B as

$$r_n = Z_{A,B}\, e^{-E/kT} = [A]\,[B]\,\pi\sigma^2 \bar{v}_{rel} e^{-E/kT} \qquad (4\text{-}18)$$

i.e. the rate is the number of particles colliding per second and having a joint energy E in excess of the mean energy. By comparison with equation (4-13), we see that the rate constant for the reaction is given by

$$k_n = \pi\sigma^2 \bar{v}_{rel} e^{-E/kT} \qquad (4\text{-}19)$$

The average relative velocity of the two particles is defined as

$$\bar{v}_{rel} = \left(\frac{8kT}{\pi\mu}\right)^{1/2} \qquad (4\text{-}20)$$

where μ is the reduced mass of the two particles; i.e.

$$\frac{1}{\mu} = \left(\frac{1}{m_A} + \frac{1}{m_B}\right)$$

Thus, we obtain finally

$$r_n = [A]\,[B]\,\sqrt{\frac{8\pi kT}{\mu}}\,\sigma^2 e^{-E/kT} \qquad (4\text{-}21)$$

and

$$k_n = \sqrt{\frac{8\pi kT}{\mu}}\,\sigma^2 e^{-E/kT} \qquad (4\text{-}22)$$

In the application of this theory to the interpretation of quenching measurements, equation (4-22) is frequently used to rewrite the Stern-Volmer formula in terms of the collisional cross section rather than the rate constant k_n (cf. equation (4-14)). Thus, measurements of ϕ for a particular atom may conveniently be tabulated as the quenching cross sections* observed with different quenching species. However, with the type of quenching measurements of interest in AFS work there is little point in considering an activation energy for the reaction and the inclusion of the exponential term in equation (4-22) is unnecessarily cumbersome. As a result of this it is convenient to define *an effective quenching cross section,* σ_Q^2 or S_Q, such that

$$k_n = \sqrt{\frac{8\pi kT}{\mu}}\,\sigma_Q^2 = \sqrt{\frac{8kT}{\pi\mu}}\,S_Q \qquad (4\text{-}23)$$

It will be noted that effective cross sections defined in this way are functions of temperature (unless the activation energy, E, is zero) and that they will automatically include any factors required to account for possible deviations of the actual value of k_n from the simple classical theory. Thus σ_Q^2 or S_Q represent a useful means of reporting experimental quenching values (see Section 4.5.3).

4.5.3 Types of Quenching Process and Experimental Results

The de-excitation processes by which quenching of excited metal atoms may occur are summarized below together with an indication of their relative importance in AFS. Experimental measurements of quenching cross sections are given where possible but relatively few data have been reported in the literature; in fact, the values given in Table 4-1 represent most of the results available at the present time.

---

* It is customary when discussing quenching processes to speak of quenching cross sections rather than collisional cross sections and this convention will generally be followed here.

TABLE 4-1
Experimentally determined quenching cross sections

	Quenching cross section,[a] σ_Q^2, Å^2									
	Quenching species									
Atom (excited level)	H_2	H_2O	O_2	N_2	CO	CO_2	Ar	Other[b]	Temperature, K	Reference
Li ($2^2P_{1/2,3/2}$)	5·2	1·9	–	6·8	12·6	9·2	≤0·3	–	1400	(*c*)
Na ($3^2P_{1/2,3/2}$)	2·9	0·5	12·3	7·0	11·9	17·0	≤0·1	–	1400	(*d*)
	2·6	0·7	10·8	6·7	13·0	15·9	–	–	2000	(*e*)
	5·1	–	–	12·9	–	–	–	3·8(HD) 3·2(D_2)	390	(*f*)
K ($4^2P_{1/2,3/2}$)	1·0	0·9	15·5	5·6	12·4	21·4	≤0·2	–	1400	(*g*)
	1·1	0·8	15·6	6·1	14·0	21·0	–	–	1900	(*h*)
K ($4^2P_{1/2}$)	–	–	–	11·2	–	–	–	–	350	(*i*)
K ($4^2P_{3/2}$)	–	–	–	12·4	–	–	–	–	350	(*i*)
K ($5^2P_{1/2,3/2}$)	19·1	4·8	–	14·3	–	–	–	–	2000	(*h*)
Rb ($5^2P_{1/2,3/2}$)	0·6	1·3	25·0	6·1	11·8	24·0	≤0·3	–	1400	(*g*)
	1·1	1·3	26·4	8·0	–	–	–	–	2000	(*j*)
Rb ($5^2P_{1/2}$)	–	–	–	11·8	–	–	–	–	300	(*k*)
Rb ($5^2P_{1/2}$)	1·9	–	–	18·5	–	–	–	1·9(HD), 1·0(D_2), < 0·3(CH_4), 0·6(CD_4), 44·3(C_2H_4), 0·6(C_2H_6)	340	(*l*)
Rb ($5^2P_{3/2}$)	–	–	–	11·5	–	–	–	–	300	(*k*)
Rb ($5^2P_{3/2}$)	1·0	–	–	13·7	–	–	–	1·6(HD), 1·6(D_2), 1·0(CH_4), 1·0(CD_4), 30·2(C_2H_4), 1·9(C_2H_6)	340	(*l*)
Cs ($6^2P_{1/2,3/2}$)	1·8	5·6	–	25·1	–	–	–	–	1400	(*g*)
Cs ($6^2P_{1/2}$)	–	–	–	24·5	–	–	–	< 0·6(CH_4)	350	(*m*)
Cs ($6^2P_{3/2}$)	–	–	–	21·9	–	–	–	–	350	(*m*)
Tl ($7^2S_{1/2}$)	0·03	1·8	13·2	6·4	13·6	32·5	⩽0·1	–	1400	(*n*)
Pb ($6p7s\ ^3P_1$)	0·4	8·0	15·0	5·7	13·0	29·0	≈ 0·0	≈ 0·0(He)	1400	(*o*)
Hg ($6\ ^3P_1$)	8·0	–	20·0	<0·3	6·5	5·0	–	–	300	(*p*)
	7·8	–	19·3	0·23	6·9	3·2	–	7·2(D_2), 0·28($^{15}N_2$), < 0·001(Xe)	296	(*q*)

---

[a] Values are effective experimental cross sections. Also the factor π is omitted even where it was included in the original source of the data (see text).

[b] The quenching species is shown in parentheses after the value of σ_Q^2.

[c] D. R. Jenkins, *Proc. Roy. Soc.*, 1968, A306, 413.

[d] Ibid., 1966, A293, 493.

[e] H. P. Hooymayers and P. L. Lijnse, *J. Quant. Spec. Radiat. Transfer*, 1969, 9, 995

[f] B. P. Kibble, G. Copley and L. Krause, *Phys. Rev.*, 1967, 159, 11.

[g] D. R. Jenkins, *Proc. Roy. Soc.*, 1968, A303, 453.

[h] H. P. Hooymayers and C. Th. J. Alkemade, *J. Quant. Spec. Radiat. Transfer*, 1966, 6, 847. Certain of the values used differ from those given in this reference having been revised subsequent to publication of the paper.

[i] D. A. McGillis and L. Krause, *Can. J. Phys.*, 1968, 46, 25.

[j] H. P. Hooymayers and P. L. Nienhuis, *J. Quant. Spec. Radiat. Transfer*, 1968, 8, 955.

[k] J. A. Bellisio, P. Davidovits and P. J. Kindlmann, *J. Chem. Phys.*, 1968, 48, 2376.

[l] E. S. Hrycyshyn and L. Krause, *Can. J. Phys.*, 1970, 48, 2761.

[m] D. A. McGillis and L. Krause, *Can. J. Phys.*, 1968, 46, 1051.

[n] D. R. Jenkins, *Proc. Roy. Soc.*, 1968, A303, 467.

[o] Ibid, 1969, A313, 551.

[p] J. P. Carrat, D. Casalta, J. L. Cojan and J. Hamel, *J. Physique*, 1966, 27, 608.

[q] J. S. Deech, J. Pitre and L. Krause, *Can. J. Phys.*, 1971, 49, 1976.

As will be seen, most of the data apply to process A(b)(ii) (see below), which is by far the most important, and are for elements giving the simplest spectra (i.e. mainly the alkali metals). Data are also included on cross sections for the mixing of excited levels (see below) as this process is closely related to quenching and the results may prove useful in certain fluorescence studies. For a more comprehensive discussion of the de-excitation processes and the literature data, the reader is referred to the review of Alkemade and Zeegers.[6]

A. Physical processes

(*a*) *Involving conversion of translational energy*, i.e. the excess electronic energy of the excited metal atom is converted into translational energy of the colliding species, no internal degrees of freedom of the latter being involved in the process.

(*i*) *Quenching by collisions with free atoms:*

$$A^* + B \rightleftharpoons A + B$$

This process is mainly of interest from the point of view of quenching by rare gas atoms. Values shown in Table 4-1 for σ_Q^2 are all less than *ca.* 0·3 Å^2 and, within the accuracy of the determinations, may be taken as almost zero. Indeed, measurements by Copley *et al.*[12] for $Na(3^2P_{1/2,3/2})$ using metal vapour in a sealed bulb at low temperature ($\leqslant$ 200°C), gave values of $<10^{-2}$ Å^2 for He, Ne, Ar, Kr and Xe. This is to be expected because transfer of kinetic energy must occur between the valence electron of the excited atom and the rare gas atom; the transfer is extremely inefficient owing to the great difference in mass of the colliding species.

(*ii*) *Quenching by collisions with free electrons:*

$$A^* + e^- \rightleftharpoons A + e^-$$

In view of the much smaller mass and higher velocity of the quenching electrons, this process should be much more efficient than (*i*) above. Direct measurements are not available but studies of the reverse excitation process[13] indicate that σ_Q^2 may be of the same order as that obtained with the major quenching process A(b)(ii) (see below). This is unlikely to be of any consequence in present applications of AFS in which flame atom cells are used, because the free electron concentration outside the primary reaction zone is relatively low in most of the flames employed. However, the process may become significant if attempts are made to use as atom cells devices such as plasmas which contain far higher electron populations.

(*iii*) *Mixing of excited states by collisions with free atoms:*

$$A^* + B \rightleftharpoons A^\dagger + B$$

This process involves the conversion, as the result of a collision, of one excited state of the atom to another (rather than to the ground state as in quenching). It has been widely observed for the doublets of the alkali metals where the energies of the two excited states are relatively close. Cross section data are shown in Table 4-2 for both processes involving collisions with other metal atoms such as

$$Na(^2P_{3/2}) + Na(^2S_{1/2}) \rightleftharpoons Na(^2P_{1/2}) + Na(^2S_{1/2})$$

and those involving collisions with rare gas atoms such as

$$Na(^2P_{3/2}) + Ar \rightleftharpoons Na(^2P_{1/2}) + Ar$$

It will be noted that the cross sections are large for Na and K, but are of the same order as quenching cross sections by process A(a)(i) for Rb and Cs where the energy difference between the doublet levels is rather larger.

(*b*) *Involving conversion of internal energy*, i.e. the excess electronic energy of the excited metal atom is converted on collision to electronic energy within another atom or molecule or to vibrational/rotational energy of the colliding molecule.

(*i*) *Quenching by collisions with other atoms:*

$$A^* + B \rightleftharpoons A + B^*$$

This can only occur with a large cross section when the two atoms have excited states of very similar energy (the slight difference during transfer being compensated for by their translational energy). It is simply the process of sensitized fluorescence described in Section 4.3.5 and, as explained there, is unlikely to be of any practical consequence in AFS work owing to the relatively low concentrations of metal atoms present in the atom cells employed.

(*ii*) *Quenching by collisions with molecules:*

$$A^* + BC \rightleftharpoons A + BC$$

As mentioned earlier, this is by far the most important process for consideration of quenching in AFS applications, and most of the data in Table 4-1 relate to it. The ability of many of the simple molecules found in flame gases to quench efficiently a wide variety

TABLE 4-2
Experimentally determined mixing cross sections

	Mixing cross sections,[a] Å^2											
	Mixing species											
Atom (excited level)	He	Ar	Na	K	H_2	N_2	HD	D_2	CH_4	Others[b]	Temperature, K	Reference
Na ($3\,^2P_{3/2} - 3\,^2P_{1/2}$)	—	—	—	—	13·4	24·2	14·0	16·6	24·5	25·8(CD_4), 30·6(C_2H_2), 30·0(C_2H_4), 30·2(C_2H_6)	390	(*c*)
Na ($3\,^2P_{3/2} - 3\,^2P_{1/2}$)	14·3	17·8	—	—	—	—	—	—	—	—	400	(*d*)
Na ($3\,^2P_{3/2} - 3\,^2P_{1/2}$)	13·1	20·6	—	—	—	—	—	—	—	—	400	(*e*)
Na ($3\,^2P_{3/2} - 3\,^2P_{1/2}$)	—	—	90	—	—	—	—	—	—	—	550	(*d*)
Na ($3\,^2P_{1/2} - 3\,^2P_{3/2}$)	—	—	—	—	25·5	45·8	26·8	31·2	47·1	48·1(CD_4), 58·0(C_2H_2), 56·6(C_2H_4), 58·0(C_2H_6)	390	(*c*)
K ($4\,^2P_{3/2} - 4\,^2P_{1/2}$)	—	—	—	—	16·9	21·0	15·6	15·9	—	—	350	(*f*)
K ($4\,^2P_{3/2} - 4\,^2P_{1/2}$)	13·0	7·0	—	79·5	—	—	—	—	—	—	360	(*g*)
Rb ($5\,^2P_{3/2} - 5\,^2P_{1/2}$)	—	—	—	—	—	2·2	—	—	—	—	300	(*h*)
Rb ($5\,^2P_{3/2} - 5\,^2P_{1/2}$)	0·032	$2{\cdot}5 \times 10^{-4}$	—	—	—	—	—	—	—	—	300	(*i*)
Rb ($5\,^2P_{3/2} - 5\,^2P_{1/2}$)	—	—	—	—	4·8	7·3	8·0	9·5	13·4	12·1(CD_4), 10·2(C_2H_4), 24·5(C_2H_6)	340	(*j*)
Rb ($5\,^2P_{1/2} - 5\,^2P_{3/2}$)	—	—	—	—	3·5	5·1	5·7	7·0	9·5	8·9(CD_4), 7·3(C_2H_4), 18·1(C_2H_6)	340	(*j*)
Cs ($6\,^2P_{3/2} - 6\,^2P_{1/2}$)	—	—	—	—	14·0	8·0	10·2	8·9	6·7	—	310	(*k*)
Cs ($6\,^2P_{3/2} - 6\,^2P_{1/2}$)	8×10^{-5}	—	—	—	—	—	—	—	—	—	300	(*i*)
Cs ($6\,^2P_{3/2} - 6\,^2P_{1/2}$)	—	$1{\cdot}6 \times 10^{-5}$	—	—	—	—	—	—	—	—	310	(*g*)

---

[a] Values are effective experimental cross sections. The factor π is omitted even where it was included in the original source of the data (see text).

[b] The quenching species is shown in parentheses after the value of the mixing cross section.

[c] M. Stupavsky and L. Krause, *Can J. Phys.*, 1968, 46, 2127.

[d] J. Pitre and L. Krause, ibid., 1967, 45, 2671.

[e] L. A. Jordan and P. A. Franken, *Phys. Rev.*, 1966, 142, 20.

[f] D. A. McGillis and L. Krause, *Can. J. Phys.*, 1968, 46, 25.

[g] L. Krause, *Appl. Optics*, 1966, 5, 1375.

[h] J. A. Bellisio, P. Davidovits and P. J. Kindlmann, *J. Chem. Phys.*, 1968, 48, 2376.

[i] A. Gallaher, *Phys. Rev.*, 1968, 172, 88.

[j] E. S. Hrycyshyn and L. Krause, *Can. J. Phys.*, 1970, 48, 2761.

[k] D. A. McGillis and L. Krause, *Can. J. Phys.*, 1968, 46, 1051.

of excited atoms is generally attributed to the ease with which the electronic energy of the atoms is converted to vibrational energy within the molecule. Although the large number of vibrational levels available in each molecule for "matching" to the atomic levels of many different metals must contribute to this effect it should be remembered that the mechanisms involved are complex; in general the proximity of a given vibrational level of a given molecule to the excited state level of the atom concerned is not necessarily a good indication of the size of the quenching cross section.

(*iii*) *Mixing of excited states by collisions with molecules:*

$$A^* + BC \rightleftharpoons A^\dagger + BC$$

Comparision of this process with A(a)(iii) is analogous to that of quenching by atoms or molecules; the existence of only a small energy difference between the mixed levels is no longer necessary for a large cross section and reference to the small number of data included in Table 4-2 will show that values of Rb and Cs are now of the same order as those for Na and K. It should be noted that, in the presence of molecules, quenching and mixing of the excited atomic states will occur simultaneously and at similar rates. This effect has not been taken into account for most of the data in Table 4-1 where results are given for overall values of σ_Q^2 for the unresolved alkali metal doublets. Although this has little practical effect on the application of the results to AFS work, it may be of considerable importance in fundamental fluorescence studies.

B. Chemical processes

Very little information is available concerning chemi-quenching, although processes of the type

$$A^* + BC \rightleftharpoons A + B + C$$

must make some contribution to the overall quenching observed for certain species present in flame gases. Zeegers[14] has estimated the quenching due to dissociation of H_2O from the rate constant of the reverse excitation process

$$H + OH + K\ (4^2S) \rightleftharpoons H_2O + K\ (5^2P)$$

and finds for an air-hydrogen flame at about 2000 K that the ratio of chemical to total quenching is *ca.* 0·1. Thus it would seem that the process is of little practical interest in analytical AFS.

REFERENCES

1. C. Th. J. Alkemade, in R. M. Dagnall and G. F. Kirkbright (eds.), "Atomic Absorption Spectroscopy", Butterworths, London, 1970, pp. 73-98.
2. D. R. Jenkins, *Proc. Roy. Soc. Lond.*, 1969, **A313**, 551.
3. R. Smith, in J. D. Winefordner (ed.), "Spectrochemical Methods of Analysis", Wiley-Interscience, New York, 1971, Ch. 4, pp. 235-282.
4. H. P. Hooymayers, *Spectrochimica Acta*, 1968, **23B**, 567.
5. P. J. Th. Zeegers and J. D. Winefordner, *Spectrochimica Acta*, 1971, **26B**, 161.
6. C. Th. J. Alkemade and P. J. Th. Zeegers, in J. D. Winefordner (ed.), "Spectrochemical Methods of Analysis", Wiley-Interscience, New York, 1971, Ch. 1, pp. 3-125.
7. K. J. Laidler and K. E. Shuler, *Chem. Rev.*, 1951, **48**, 153.
8. K. J. Laidler, "The Chemical Kinetics of Excited States", Clarendon Press, Oxford, 1955.
9. K. E. Shuler, T. Carrington and J. C. Light, *Appl. Opt.*, 1965, Suppl 2, 81.
10. K. J. Laidler, "Reaction Kinetics, Vol. 1: Homogeneous Gas Reactions", Pergamon Press, Oxford, 1963.
11. R. Mavrodineanu and H. Boiteux, "Flame Spectroscopy", Wiley, New York, 1965.
12. G. Copley, B. P. Kibble and L. Krause, *Phys. Rev.*, 1967, **163**, 34.
13. I. P. Zapesochnyi, *High Temp.*, 1967, **5**, 6.
14. P. J. Th. Zeegers, "Recombination of Radicals and Related Effects in Flames", PhD. Thesis, Utrecht, 1966.

CHAPTER 5

Spectral Light Sources

5.1 INTRODUCTION

The spectral light source forms an essential component for both atomic absorption and fluorescence spectrometry, and the optimization of its performance is of major importance if the capabilities of the two techniques are to be fully exploited. In consequence, a major part of the effort devoted to improvement of AAS and AFS instrumentation in recent years has been concerned with the light source. The results of this effort may be seen, for example, in the hollow-cathode lamps supplied as light sources with most commercial atomic absorption spectrophotometers; present-day lamps show many-fold improvements over those available for the early commercial spectrophotometers with respect to both their critical performance characteristics and their operating and storage lives. Development of light sources continues to be of major interest in this field and further improvements of the lamps described here are probable, particularly in the case of the high-intensity sources required for AFS.

5.1.1 Classification of Sources

The division of spectra into line, band and continuum types has been explained in Section 2.1. Spectral lamps used in AAS and AFS are usually referred to as line or continuum sources, the latter being applied to both true continua and those lamps emitting many closely spaced lines or bands over a wide wavelength range. The line and continuum categories may be further subdivided according to whether the lamp emits radiation *continuously* with respect to time or in short, specific bursts of energy at regular intervals, i.e. in *pulses*. Sources that are merely modulated for use with tuned detection systems (see Chapter 10) are generally classed as continuous. Thus, at the present time most sources used in AAS and AFS fall into this group. However, true pulsed operation is possible* with several types of lamps and its ability to increase the absolute intensity available from a given lamp may soon result in more widespread application of the technique.

The light sources may be further classified according to their method of construction, independently of the output characteristics. Most common in AAS and AFS are permanently† *sealed-off* lamps. These offer considerable advantages of simplicity, ease of use and good reproducibility, especially if the source requires a particularly low or high operating pressure. Many types of sealed-off lamp may be produced in a similar *demountable* form. Thus, by using, for example, removable electrodes or a tap in place of a permanent seal for the envelope, alterations may be made at any time after manufacture. This greatly facilitates investigations of the optimization of various lamp parameters or reduces the cost of providing line sources for a number of elements required only occasionally in the laboratory. Finally, several types of emission source may be classified as *consumable* as they require continuous replacement of the element of which the spectrum is required. For example, flames, arcs, plasmas and flow-through microwave discharges are described below as sources for AAS and AFS. Although such types are usually very versatile, it will be seen that they have many disadvantages which have limited their application.

Although many types of light source can be used for AAS and AFS, most are only briefly summarized here. The greater part of this chapter is devoted to a detailed description of the hollow-cathode lamp (HCL), the electrodeless-discharge lamp (EDL), the vapour-discharge lamp (VDL) and several continuum sources. These account for most of the published work in AAS and AFS and almost all analytical applications. In each case the principle and construction of the device is discussed together with its operating requirements and the characteristics of its spectral output.

5.1.2 Requirements of Light Sources Used in AAS and AFS

Some essential requirements of spectral light sources were mentioned briefly in Chapter 1 and emphasized to a certain extent in the theoretical discussion of the following chapters. We shall list the most important factors here before proceeding to a discussion and comparison of individual light sources.

For use with both AAS and AFS, it is important that the light source emit a steady uniform level of radiation to obtain an analytical signal of low noise level allowing good precision of measurement and good detection limits. In many cases it is also important that the source should show little long-term drift in emission intensity as most fluorescence spectrometers and many commercial absorption spectrometers have only single-beam operation and frequent adjustment of instrumental settings is inconvenient. In view of the need for convenience and ease of use with commercial atomic absorption spectrometers designed for large numbers of routine analyses, the spectral lamp used should also require the minimum of maintenance and adjustment to obtain optimum performance. This requirement usually necessitates the use of a permanently sealed-off source.

The characteristics of the spectra produced by sharp line sources are also important. They should be "clean", with the minimum interference to the analytical line due to the presence of spectral lines of the filler gas or impurities in the lamp. This is achieved by

---

* and sometimes essential, e.g. with many types of lasers.

† Obviously it may be possible to dismantle and re-condition some types of sealed-off lamp if suitable facilities are available.

the careful choice of the filler gas and the use of a getter in the lamp (see Section 5.2.3). The intensity of the analytical line must also be high for optimum results. In AFS it is essential that the maximum intensity is obtained, since the signal intensity (and hence the analytical signal) will be directly proportional. Even though such high intensity is not needed for AAS, a reasonably high level is required to permit low signal-noise levels and good precision to be obtained. With AAS, however, the profile of the source line is even more important than its intensity, as explained in Chapter 3. Thus, the source must be designed to avoid long path-lengths through the excited vapour; this helps to avoid self-absorption of the resonance lines which is a major source of their broadening. Similarly, the avoidance of high temperatures, pressures and current densities within the source is also an important aid to obtaining the sharpest possible source line for AAS measurements (see Section 2.5.2). With both AAS and AFS sources it is essential that the emitted resonance radiation should not pass through a cloud of cool vapour (of the analyte element) between leaving the excitation region and reaching the exit window of the lamp; this would produce self-reversal of the resonance lines, removing the central region required for both peak absorbance measurements and the efficient excitation of fluorescence.

In view of the need for sealed-off sources mentioned above and the large numbers of relatively expensive commercial lamps required in many laboratories, it is essential that such lamps should have long operating and storage lives. In many cases this has been achieved by careful attention to minor constructional details. For example, metal electrodes and silica optical windows should be fused directly to glass lamp bodies rather than attached by cemented joints. Optical windows should always be positioned so that transmission will not be reduced by formation of an opaque coating on the inner surface, particularly where volatile compounds are used or there is a possibility of the lamp being used at currents above the recommended value. Similarly, constructional materials likely to be attacked by the compound within the lamp should be avoided. For instance, the alkali metals are known to attack silica and certain types of glass. For hollow-cathode lamps of low-melting-point elements, accidental spillage from the cathode should be avoided by careful cathode construction or use of a higher melting compound or amalgam. Finally the overall construction of the lamps should be as strong as possible avoiding such obvious hazards as thin glass necks and joints.

5.2 HOLLOW-CATHODE LAMPS

5.2.1 Introduction

The hollow-cathode lamp is the most widely used of the many devices available for the production of fine line spectra and since its introduction in 1916 by Paschen[1] it has seen extensive application as a source of intense, sharp spectral lines. Several factors have been responsible for this popularity, viz: (a) lines may be produced over the whole optical region from the infrared to the vacuum ultraviolet; (b) intense spectra may be excited using only low currents; (c) extremely sharp lines are quite readily obtained; (d) the lamps and their associated power supplies are relatively simple and inexpensive to construct; (e) they give a stable, noise-free output over long periods of time. In spite of its widespread use for fifty years, the hollow-cathode lamp only became generally available commercially after the introduction of atomic absorption spectroscopy as a routine analytical method. More lamps have probably been manufactured since then than during the whole of the previous period; all commercial AAS instruments available at the present time are designed for use with these sources.

During the period from 1916 to 1955, only flow-through hollow-cathode lamps were used. This resulted from the requirement of most workers for very pure spectra which could not be obtained with sealed-off devices owing to subsequent out-gassing of the various components. There were also problems of leaking at window and electrode seals and of filler gas adsorption (see below). However, in 1955 Crosswhite, Dieke and Legagneur[2] produced a successful sealed-off iron lamp using a getter material (see below) and Walsh[3] suggested the HCL as a suitable source for AAS on the basis of the availability of a sealed device. As a result of later improvements and the less stringent requirements of spectral purity for sources used in routine AAS, most commercial lamps provided as AAS sources have been of the permanently sealed type. In view of this we shall consider the construction of these devices in detail and discuss flow-through types only briefly from the point of view of the special type of demountable HCL (see Section 5.2.6(a)).

Many different designs of HCL have been described in the literature, but the most common can generally be placed into one of two classes. The Schüler[4] lamp design uses water or liquid-air cooling of the cathode to give extremely sharp lines for fundamental applications such as ultra-high resolution studies of hyperfine structure. When line width is less critical, or for studies of high-energy lines, a hot hollow-cathode has generally proved more useful; this allows a simpler lamp design and much higher intensity. Provided that the lamp current is kept relatively low, the resonance lines are sharp enough for peak absorption measurements and all sealed-off lamps used for AAS are of this type. Thus cooled-cathode lamps will not be described here,* although they may be of some use for isotope analysis by AAS.[6,7]

5.2.2 Mechanism of the Hollow-Cathode Lamp

In general terms the hollow-cathode lamp consists of a sealed tube containing an anode, a cylindrical hollow cathode made of, or somtimes lined with, the metal whose spectrum is required, and an inert gas at a pressure of about 1 to 5 torr (depending on the gas used). When a potential of 500 to 1000 volts is applied between the electrodes a discharge of the carrier gas strikes and appears as a glowing positive column. However, at the pressure used (and for a range of 2-3 torr about it) the discharge concentrates into the hollow cathode, giving higher current densities than those normally attained in the discharge and hence intense illumination of the cathode space. The appearance of the cathode at this stage is shown in Fig. 5-1. The spectrum of the carrier gas obtained in the negative glow region shows no Stark line broadening (see Section 2.5.2) in spite of its high intensity because the potential drop between the electrodes with a steady discharge is usually only 250-300 volts. However, as the current is increased the glow occupies a larger area of the inner surface of the cathode; once the whole surface is covered a further increase in current produces an increase in the potential difference and the freedom from Stark broadening may no longer hold. With most cathode designs the current at which this occurs will usually be far in excess of other limitations to the current imposed by requirements for lamps used as AAS sources.

The low cathode-potential fall is due to the small wastage of positive ions from the hollow cathode. Thus, in conjunction with the stream of carrier gas ions directed into the cylinder by the applied field this produces a high concentration of ions within the discharge. Following acceleration by the field these ions bombard the inner surface of the cathode giving a strong sputtering action as they displace atoms from the surface. The sputtered metal atoms accumulate inside the cathode and are excited to give an emission spectrum by second-order collisions with the high concentration of excited inert gas atoms and ions. The vapour cloud of the metal atoms must be sufficiently concentrated if its spectrum is to predominate over that of the carrier gas. However, this concentration is still relatively very low so that problems of self-absorption or even resonance broadening (see Section 2.5.2) should not interfere with the excitation of an intense metal spectrum.

The sputtering mechanism of the hollow-cathode lamp explains its ability to produce intense metal spectra even when cooled to temperatures at which the vapour pressure of the metal is negligibly small. Under these conditions it is particularly important that efficient sputtering should be obtained; it may be necessary to employ argon as the inert carrier gas rather than neon or helium because it is a more effective sputtering agent owing to its greater atomic weight.* When a hot hollow cathode is used, as in AAS, the thermal vapour pressure of many metals may be considerable so that the metal pressure approaches that of the carrier gas. The metal vapour discharge may then be partly or completely self-sustaining and a very large increase in intensity of its spectrum is observed. Many of the lamps used in AAS are run close to this condition and careful adjustment of the current (i.e. vapour pressure) is important to avoid serious self-absorption and other line-broadening effects. Lamps run largely in metal vapour tend to give mostly lines of fairly low excitation energy (i.e. "arc lines") so that mainly the first spectrum is observed with few ion lines. If a "spark spectrum"

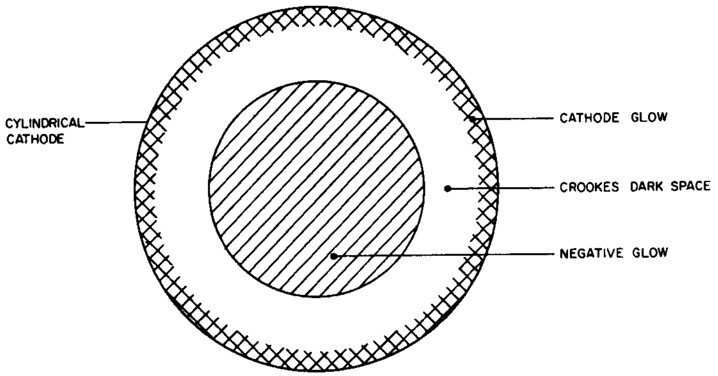

Fig. 5-1. Hollow-cathode carrier-gas discharge obtained on striking.

---

* The reader is referred to the book by Tolansky[5] for further details of this type of lamp.

* Argon 39·95, Neon 20·18, Helium 4·00.

containing many ion lines is required it is necessary to ensure excitation by collisions with an inert carrier gas having a high excitation potential, such as helium (19·7 volts).

5.2.3 *Construction of Hollow-Cathode Lamps*

It is proposed to discuss in some detail the main components of commercially available lamps rather than to describe a practical method of lamp construction. However, in a laboratory equipped with a suitable vacuum system and glass- and metal-working facilities, there should be no real difficulty in the construction of sealed lamps similar to those available from lamp manufacturers but at considerably lower cost. Practical instructions for laboratory manufacture have been published by Jones and Walsh[8] and by Bodretsova *et al.*[9] Unfortunately, details of the most recent improvements in lamp design have not always been published owing to commercial considerations. Although many useful hints can be obtained from the following pages and from the catalogues published by the larger lamp manufacturers,* it may prove necessary to carry out many measurements with each element in order to optimize parameters such as cathode dimensions and filler-gas pressure.

TABLE 5-1
Major manufacturers of hollow-cathode lamps

Atomic Spectral Lamps Pty. Ltd.,
23–31 Islington Street, Melbourne, Australia.

Cathodeon Ltd.,
Church Street, Cambridge, England.

FIVRE,
Via Panciatichi 70, Firenze-Castello, Italy.

Hitachi Ltd.,
1–4 Marunouchi, Chiyoba-Ku, Tokyo, Japan.

Dr. Kern und Sprenger GmbH.,
Post Box 751, Florenz Sartorius Strasse 5,
Gottingen, Germany.

Perkin Elmer Corp.
Instrument Division, Norwalk, Connecticut 06852, U.S.A.

Quarzlampen GmbH.,
Hanau/Main, Hoehensonnenstrasse, Germany.

Rank Precision Industries Ltd.,
98 St. Pancras Way, London, N.W.1., England.

Westinghouse Electric Corporation,
Electronic Tube Division, P.O. Box 284, Elmira,
New York 14902, U.S.A.

(*a*) *Lamp envelope and window*

The early commercial sealed hollow-cathode lamps were constructed to a design similar to that shown in Fig. 5-2 and were generally made as large as possible. The large volume was intended to increase the useful life of the lamp by minimizing the effects of leakage of air into the tube, adsorption of the filler gas onto particles sputtered from the cathode and liberation of gaseous impurities by the electrodes during use. The optical window was placed on a side arm some distance from the cathode further to reduce the possibility of deposition of sputtered metal atoms onto it (with consequent loss of transmission). The envelope was made of thin electronic grade (molybdenum) glass with thermal expansion properties similar to those of the leads to the electrodes so that a vacuum-tight seal could readily be produced.

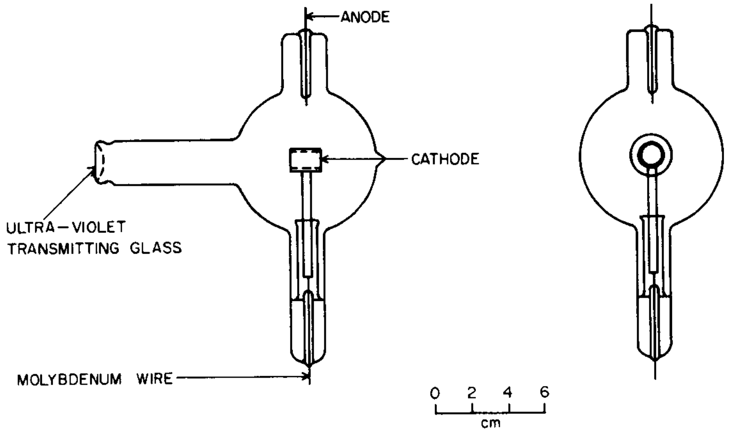

Fig. 5-2. Early design of hollow-cathode lamp for commercial atomic absorption spectrometers.

Recent improvements in lamp technology (see below) have led to the production of lamps of much smaller volume and of a more convenient design similar to that shown in Fig. 5-3. The lamp illustrated has an optical window of 25·4 mm diameter (similar to the older design), yet an overall length of only 165 mm and a maximum diameter of about 38 mm. This small size is particularly useful when several lamps are kept on "warm-up" to allow rapid interchange of elements; it also greatly reduces the storage space

---

* The major Western manufacturers of hollow-cathode lamps are listed in Table 5-1.

required for a large number of lamps. The metal-to-glass seals at the base of the lamp are protected by a plastic cover cemented to the glass, electrical connections being made via a special "lamp socket" built into this base. Use of these plastic bases, which in some designs incorporate a special fitting allowing direct attachment to the spectrometer, has greatly reduced the possibility of accidental breakage compared with the older style of lamp.

The elongated shape for the lamp body is used because it is still necessary to place the optical window a considerable distance from the cathode to avoid loss of transmission due to metal deposition.

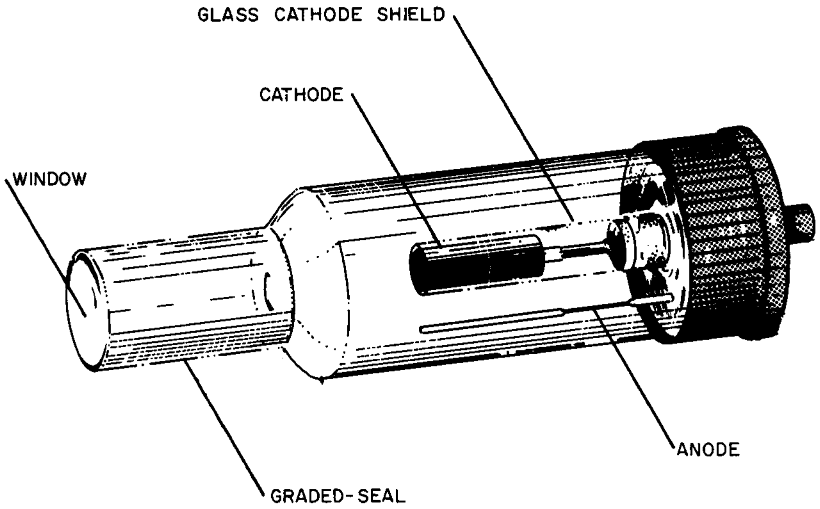

Fig. 5-3. A modern design of hollow-cathode lamp.

The narrow neck design shown in Fig. 5-3 is favoured by several manufacturers because it reduces the diameter (and hence cost) of the optical window and the graded seal which may be used with it (see below). The window material must be chosen to give adequate transmission at the wavelength of the resonance line(s) required from a particular lamp. Transmission characteristics for several window materials used in commercial lamps are shown in Fig. 5-4. Corning 7740 Pyrex glass gives good transmission above 300 nm and is used for lamps of a number of elements, including the alkali metals and many rare earth metals. It has the added advantage of being easy to seal to the electronic grade glass normally used for the lamp envelopes. However, Pyrex is unsuitable for lamps of the majority of elements, which have their best absorption lines below 300 nm and either silica or an ultraviolet transmitting glass must be used as the window material. As can be seen from Fig. 5-4, the latter is inferior to silica at all wavelengths below about 320 nm and gives very poor transmittance below 250 nm. In spite of this it has been used by several manufacturers because it can be sealed directly to the glass envelope of the lamp, whereas silica cannot (owing to the strain imposed by the large difference between the expansion coefficients of the two materials).* Early silica window lamps used a cement seal (e.g. epoxy resin) but this was rather unsatisfactory because of early leakage at the seal and also because it was not possible to obtain adequate degassing of the lamp blanks by heating them to a sufficiently high temperature. Most manufacturers now prefer to use silica windows properly sealed to the envelope via a graded seal. These are simply open-ended cylinders produced by the glass manufacturers and having silica at one end and a suitable glass at the other. The joint between the two is achieved by a special process interposing material of thermal expansion carefully graded between the two extremes. The seals are extremely reliable without being prohibitively expensive, and lamps of this type are now normally used whenever Pyrex windows are unsatisfactory.

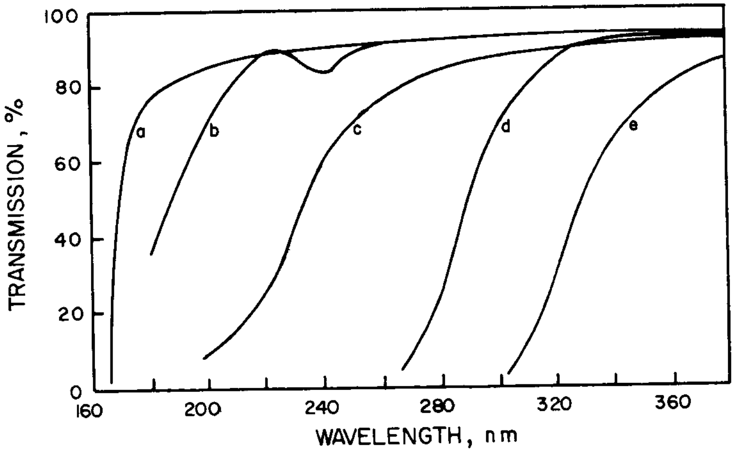

Fig. 5.4. Transmission characteristics of window materials. (a) Suprasil (optical quality silica); (b) commercial silica; (c) Corning 9741 (uv transmitting glass); (d) Corning 7740 (pyrex glass); (e) Corning 7720.

---

* Lamp envelopes of silica would be far too expensive to manufacture for normal AAS use and the silica-to-metal seal required at the electrodes also presents difficulty.

(*b*) *Electrode configuration*

Recent improvements in the design of the cathode and the other electrodes and shields associated with it have been of similar importance to those of the lamp envelope. As a result, high-quality lamps have been extended from a relatively small range of "favourable" elements to most of the elements for which AAS is a useful analytical technique. Many different cathode shapes have been suggested, some of which are shown in Fig. 5-5, but most manufacturers seem to have standardized on the narrow-bore cylindrical type (h). Those with rectangular apertures ((a), (b), (c)) give effectively a greater output of light since most spectrometers have as the dispersive element a monochromator with a rectangular entrance slit. However, there appear to be stability problems owing to concentration of the cathode glow at sharp corners. The cup-shaped designs ((c), (d)) have been quite widely used for low-melting elements as they facilitate retention of the metal within the cathode. However, most manufacturers now prefer the use of higher melting alloys or compounds in the ordinary narrow-bore cathode (h). The spherical cavity (f) is the most efficient from the electrical point of view but has not been widely used, presumably owing to difficulties of construction. Whatever the shape of the cathode, the dimensions of the hollow are quite critical if optimum performance is to be obtained (although this seems to have been overlooked in the design of some early commercial lamps). Mitchell[10] has shown that at any filler-gas pressure the ratio of resonance line intensity to unwanted ion line intensities decreases if the diameter of the bore is increased or its length decreased (see Fig. 5-6). The filler-gas pressure required also depends on the bore diameter, an approximate relationship being $d = c/p$ where p is the gas pressure (torr), d the diameter (cm) and c a constant varying between 0·5 and 10, depending on the cathode material, the type of filler gas and the operating temperature.

The cathode material also has an important effect on the operation of the lamp. Obviously it must be a reasonably good electrical conductor and in view of the fairly high operating temperature* of the types used in AAS should not melt or deform during operation. A reasonably low vapour pressure is also important to avoid rapid evaporation onto the interior surfaces of the lamp. Elements operated as liquids in the cup-type cathodes described

---

* 400-500°C may be reached near the maximum recommended operating current.

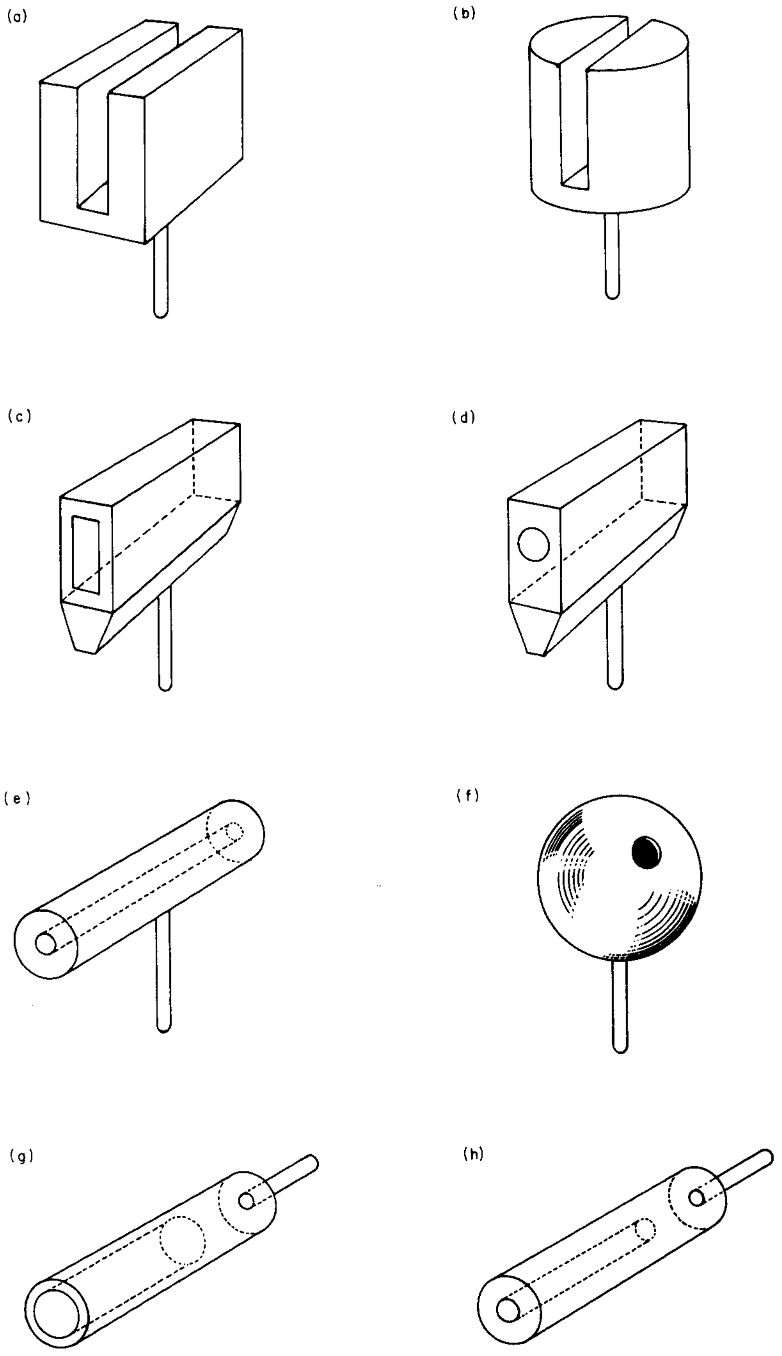

Fig. 5-5. Possible hollow-cathode shapes.

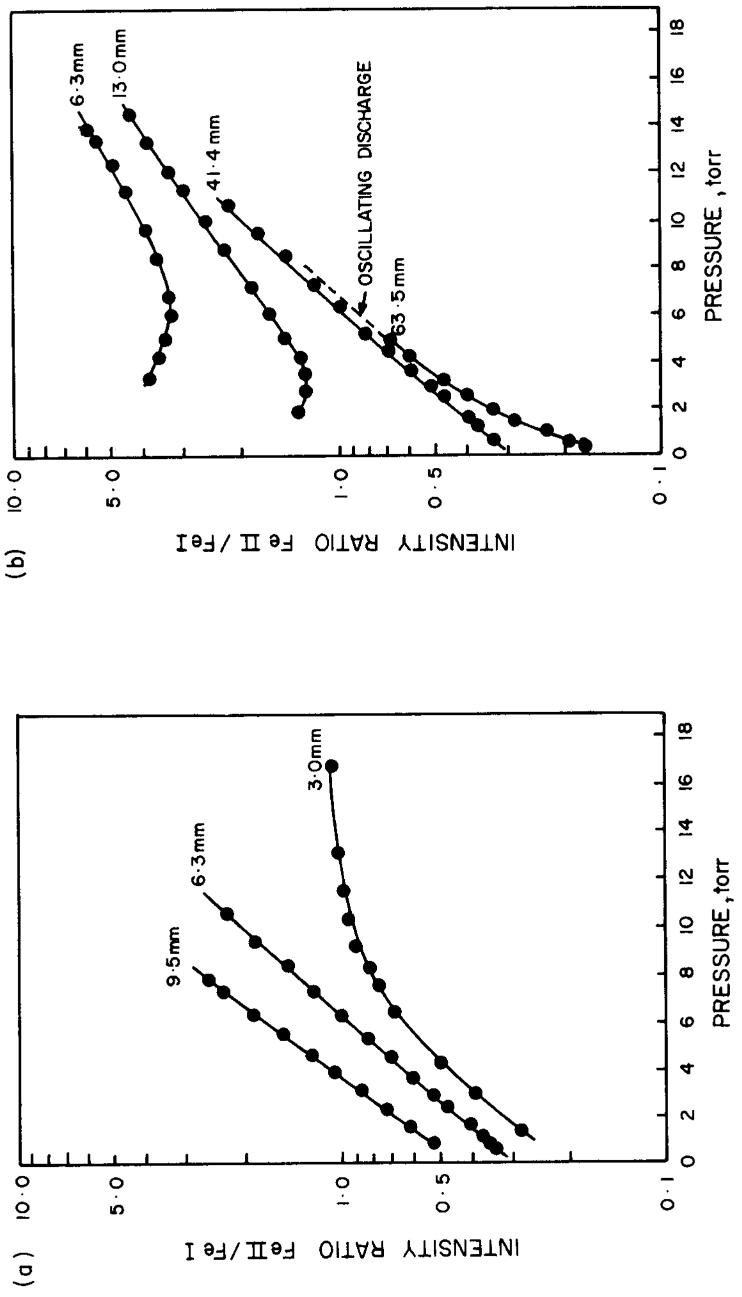

Fig. 5-6. Ratio of intensities Fe II 274·93/Fe I 273·36 at different neon pressures for a hollow-cathode at 160 mA.[10] (a) For different bore diameters, bore length 41·4 mm; (b) for different bore lengths, bore diameter 6·3 mm.

above must, of course, have relatively low vapour pressures even when molten (e.g. Ga, Pb, Sn). With many of the common metals it is possible to use the simple procedure of machining the cathode from a solid rod of the pure element. When this is not practicable owing to the cost or the physical nature of the element, a cathode shell of copper, brass, aluminium or iron may be fitted with an appropriate lining. At one time such a lining was frequently very thin and produced from foil, electrolytic plating, or deposition of a suitable salt coating. However, the sputtering process rapidly depletes such thin linings, exposing the base metal and leading to fluctuations and a gradual reduction in output intensity. Thus more satisfactory results are obtained with a fairly thick lining of a suitable alloy or salt. In fact, recent improvements to a number of "difficult" lamps have involved careful selection of the matrix used to contain the analyte element so that the rate at which it is sputtered may be closely controlled. The difficulties of producing varied matrices as alloys have been reduced considerably by using the techniques of powder metallurgy; this involves thorough mixing of the dry powders followed by sintering to produce a solid cathode lining of the correct dimensions. Strong "blocks" may be produced from even quite high melting powders by adding a lower melting bonding powder such as aluminium or copper. These techniques have also been important in the production of multi-element lamps (see Section 5.2.6(e)).

Considerable improvements have also been made to the anode design and position, although it would now seem that a quite simple arrangement works well. Some possible configurations which have been used in commercial lamps are shown in Fig. 5-7. Although types (a) and (b) were used for early commercial lamps, they are now less popular owing to the inconvenience of the side seal and connection for the anode. Types (c) and (d) are both currently available in commercial lamps, (c) having a circular anode concentric with the end of the cathode and mounted on an insulated stem. With type (d) the whole anode may be exposed in some lamps, whereas other manufacturers prefer to insulate the anode as far as the end of the cathode. These three possibilities seem to be a matter of individual preference, most manufacturers using the same design whatever the element; in practice there is probably little advantage to any one of them (except that the straight wire anode may be cheaper to produce). The selection of the anode material is also fairly straightforward, a metal such as tungsten usually being preferred. At one time titanium or zirconium was used by some manufacturers

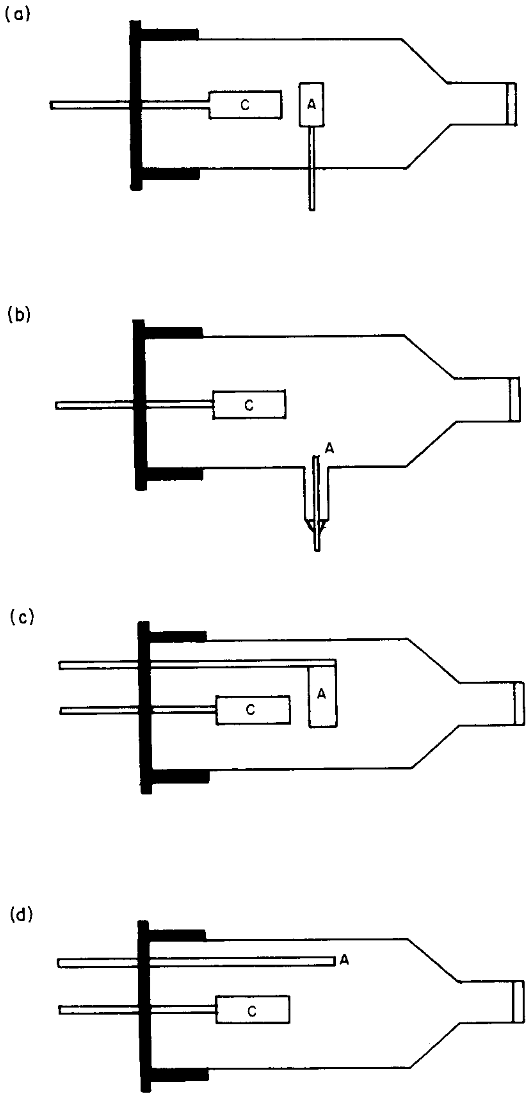

Fig. 5-7. Positions of the cathode and anode in hollow-cathode lamps.

because they actively absorb gaseous impurities in the lamp and thus act in the same way as the uranium getters incorporated in the first sealed-off lamps with much simpler lamp construction. However, it is now recognized that for the requirements of AAS light sources a getter is unnecessary if lamps are carefully constructed with adequate precautions in the selection and degassing of the materials used.

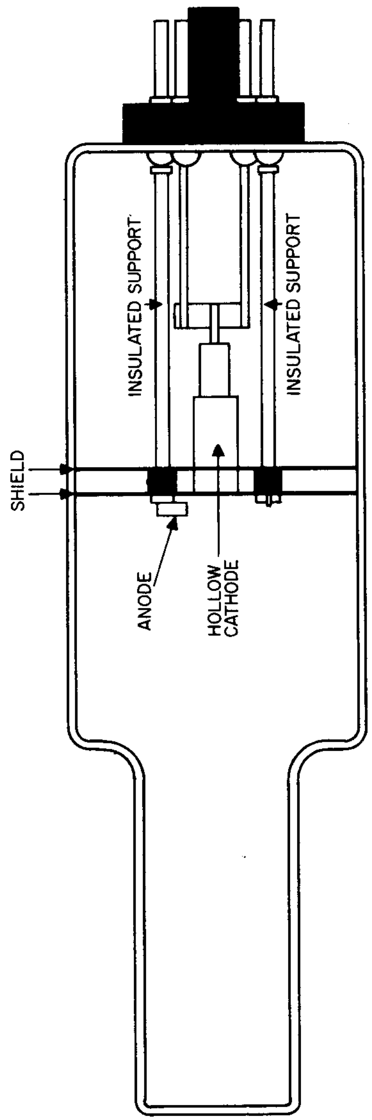

Fig. 5-8. Commercial hollow-cathode lamp with simple disc electrode shields.

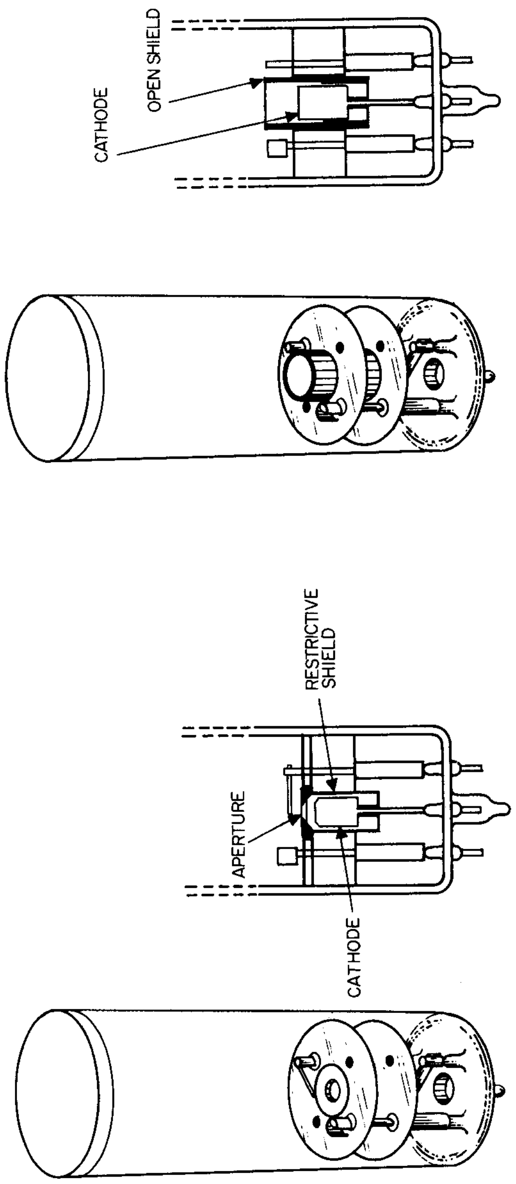

(a) (b)

Fig. 5-9. Elaborate hollow-cathode lamp shields. (a) Restrictive type; (b) open type.

Ideally, the construction of the electrodes should be such that the energy of the discharge is concentrated within the cathode, maintaining the cloud of metal vapour within a restricted area and at a uniform level of excitation. In practice this is not always possible and a cloud of weakly excited atoms may form at the mouth of the cathode or just outside it, leading to serious self-absorption of the resonance lines and a possible shortening of lamp life. To reduce this problem many commercial lamps incorporate some form of cathode shield. A simple glass shield used by Atomic Spectral Lamps Pty. Ltd. and mainly intended to prevent discharges to the outside of the cathode is shown in Fig. 5-3. A disc shield used in conjunction with a circular anode by Pye Unicam Ltd. is shown in Fig. 5-8. Ceramic shields have been used in some lamps for difficult elements. Those designed by the Perkin-Elmer Corporation are illustrated in Fig. 5-9. The restrictive type is recommended for molten or volatile metals such as lead or bismuth, whereas the open shield is used for the less volatile metals such as titanium or germanium. Manning and Vollmer[11] report that both types of shield help to restrict the metal vapour cloud to a region in front of the cathode, concentrate the discharge in the cathode cavity and reduce filler-gas cleanup.

(*c*) *Filler gas*

As mentioned earlier, the mechanism of the hollow-cathode discharge requires a low pressure of an inert gas within the lamp. The properties of the rare gases relevant to their use for this purpose are summarized in Table 5-2. The efficiency of the filler-gas ions in sputtering metal atoms from the cathode depends not only on their mass but also on their velocity. Thus, with the strength of the potential field normally present in the hollow cathode, argon is generally more effective than the heavier krypton or xenon. In view of its very low mass helium is extremely poor in its sputtering ability and is not usually used in hollow-cathode lamps of the type required for AAS. Neon, however, has a sufficiently high mass to act as an efficient sputtering agent and from a practical point of view is comparable with argon in this respect. It should also be remembered that with the uncooled lamps used in AAS, the operating temperature of the cathode may be sufficiently high to give a significant vapour pressure of a volatile element. Thus, the results obtained with a particular inert gas often vary considerably between involatile and volatile metals. Furthermore, a meaningful comparison between the different gases can only be made if the pressure is carefully optimized in each case; a change of only a few torr will often produce a very large change in the intensity of the emitted metal resonance lines.

Detailed observations of the effects of different gases and pressures have been made by Crosswhite *et al.*[2] (Fe), Mitchell[10] (Fe and U) and Bodretsova *et al.*[9] (Al, Bi, Ca, Cd, Co, Cr, Cu, Fe, Mg, Mo, Ni, Pb, Sb, Sn, Ti and Zn). Although generalized conclusions can be misleading, some comments on the results of Bodretsova *et al.* are of interest. They found that similar variations of metal line intensity with filler-gas pressure occur with He, Ne, Ar and Xe. When the gas pressure is gradually reduced with lamps of involatile metals, the resonance line intensity increases to a peak and then decreases again for most gas/metal combinations. With volatile metals the intensity generally continues to increase until the pressure is too low to maintain the discharge. In both cases the optimum pressure for neon is around 3 torr whereas that for argon is about 1 torr. The action of the other gases with different metals is less consistent, although helium generally shows similar behaviour to that of neon, and xenon to that of argon. The highest intensities were usually observed with neon and argon, although xenon gave a considerably greater intensity in a few cases (e.g. Al, Ni and Sb). Neon resulted in a considerably more intense output than that of argon for several of the involatile metals and in most other cases the two gases produced comparable metal line intensities at the optimum pressures; only in one or two examples (e.g. Ca and Pb) did argon result in a significantly higher intensity than that of neon.

TABLE 5-2
Properties of hollow-cathode filler gases

Gas	Atomic weight	Ionization potential (eV)	Excitation potential (eV)
Helium	4·00	24·580	19·818
Neon	20·18	21·559	19·619
Argon	39·95	15·755	11·548
Krypton	83·80	13·996	9·915
Zenon	131·30	12·127	8·315

In practice, only argon and neon are used as the filler gas in commercial lamps. Although neon will often produce a higher emission intensity of the metal lines, it is not an automatic choice because the spectral line emission of the inert gas itself must be considered. As explained in Section 12.3.1(c), any of these background lines lying close to a metal resonance line may lie within the spectral bandpass observed by the monochromator during an absorption measurement. As they are not absorbed by the sample atoms a loss of sensitivity and linearity of calibration graphs results. The hollow-cathode spectrum of neon is shown in Fig. 5-10 and that of argon in Fig. 5-11. The spectra consist mostly of lines of Ne(I), Ne(II), (particularly below 450 nm), Ar(I) and Ar(II) (particularly below 400 nm), although some impurity lines may be identified with both elements. When reference is made to these diagrams it should be remembered that many weaker lines of the spectra are not included. However, these will be of negligible intensity compared with those of the metal resonance lines in properly constructed lamps. In fact many of the less intense lines appearing in Figs. 5-10 and 5-11 will also be of little consequence under most circumstances. It should also be noted that in order to include these lines and retain a reasonably small diagram the higher peaks have been compressed by the recording technique while the most intense lines have been limited to an arbitrary maximum height.

When preparing a particular lamp reliable results may only be obtained if tests are carried out using both neon and argon at their optimum pressures (see above). It is then possible to examine closely the spectral region of interest, i.e. that within a few nanometres of the most sensitive resonance line, in order to decide which rare gas gives the most favourable signal-to-background ratio for the resonance line. In a few cases the choice may actually depend on the spectral bandwidth of the spectrometer in which the lamp will eventually be used. However, some general conclusions may still be drawn from Figs. 5-10 and 5-11. Argon emits rather fewer lines than neon does in the regions between 325 and 350 nm and between 580 and 700 nm, whereas neon is somewhat better between 370 and 520 nm. There is little to chose between the two in the regions below 325 nm and between 350 and 370 nm and 520 and 580 nm.

In practice, most commercial lamp manufacturers now use neon wherever possible, reserving argon for the special cases where it gives a considerably less intense background spectrum around the resonance line. The number of these special cases varies with different manufacturers and there is little doubt that personal preference still plays a part in the choice of gas. Argon was used almost exclusively in the early commercial lamps, probably because only the background spectrum was considered when the choice was made (rather

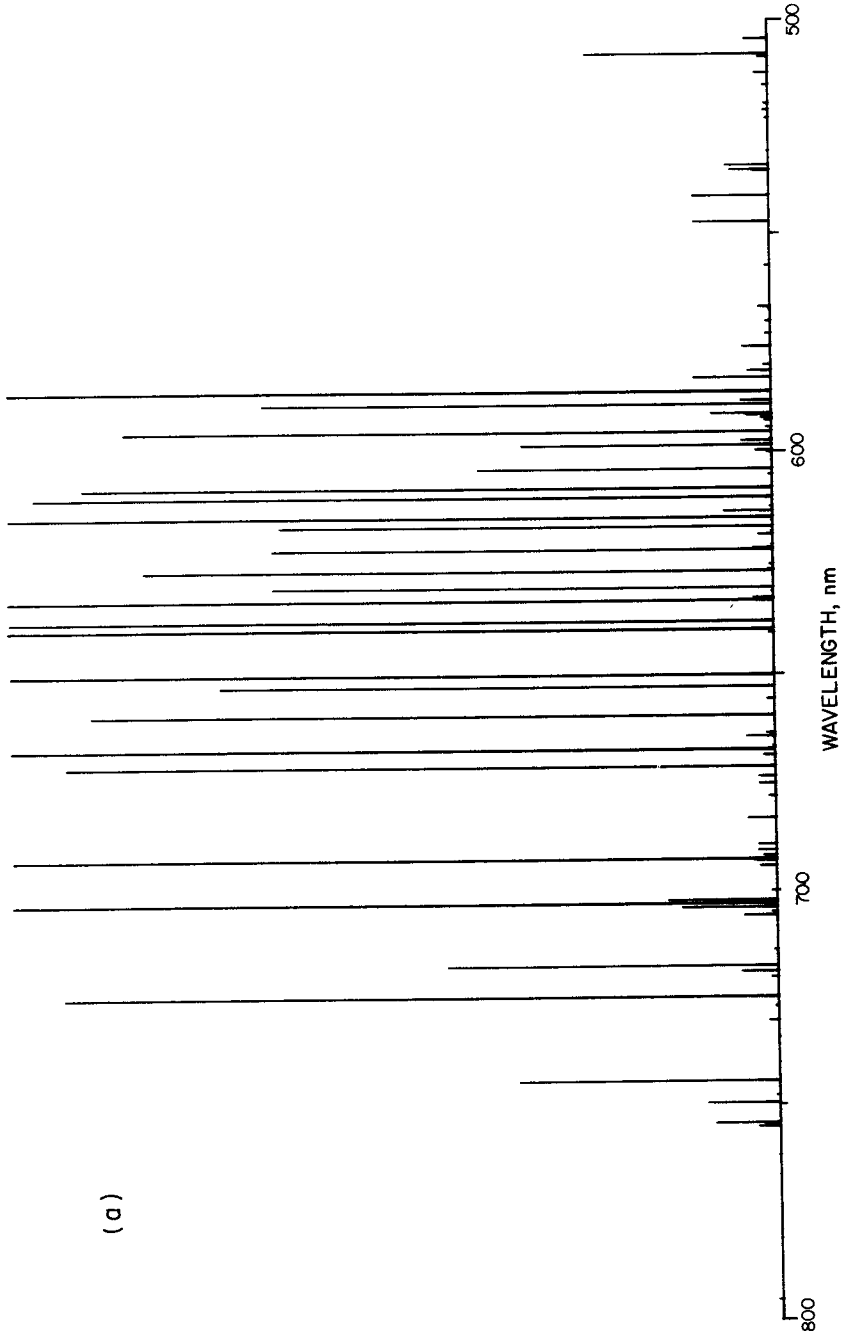

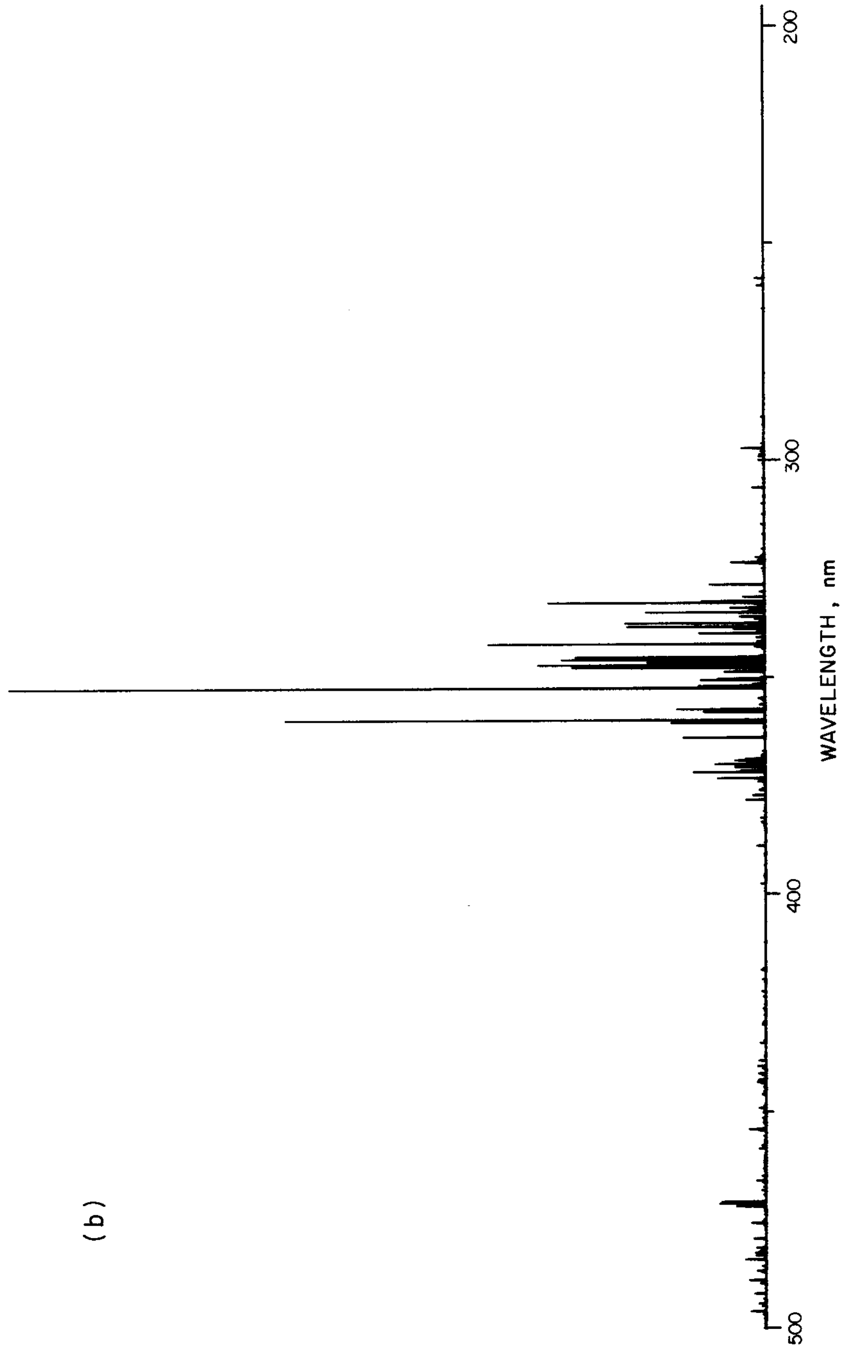

Fig. 5-10. Spectrum of neon in a hollow-cathode discharge. (a) 800-500 nm; (b) 500-200 nm. (The intensity scale from 500 to 200 nm is scale expanded 10x compared with that for 800-500 nm.)

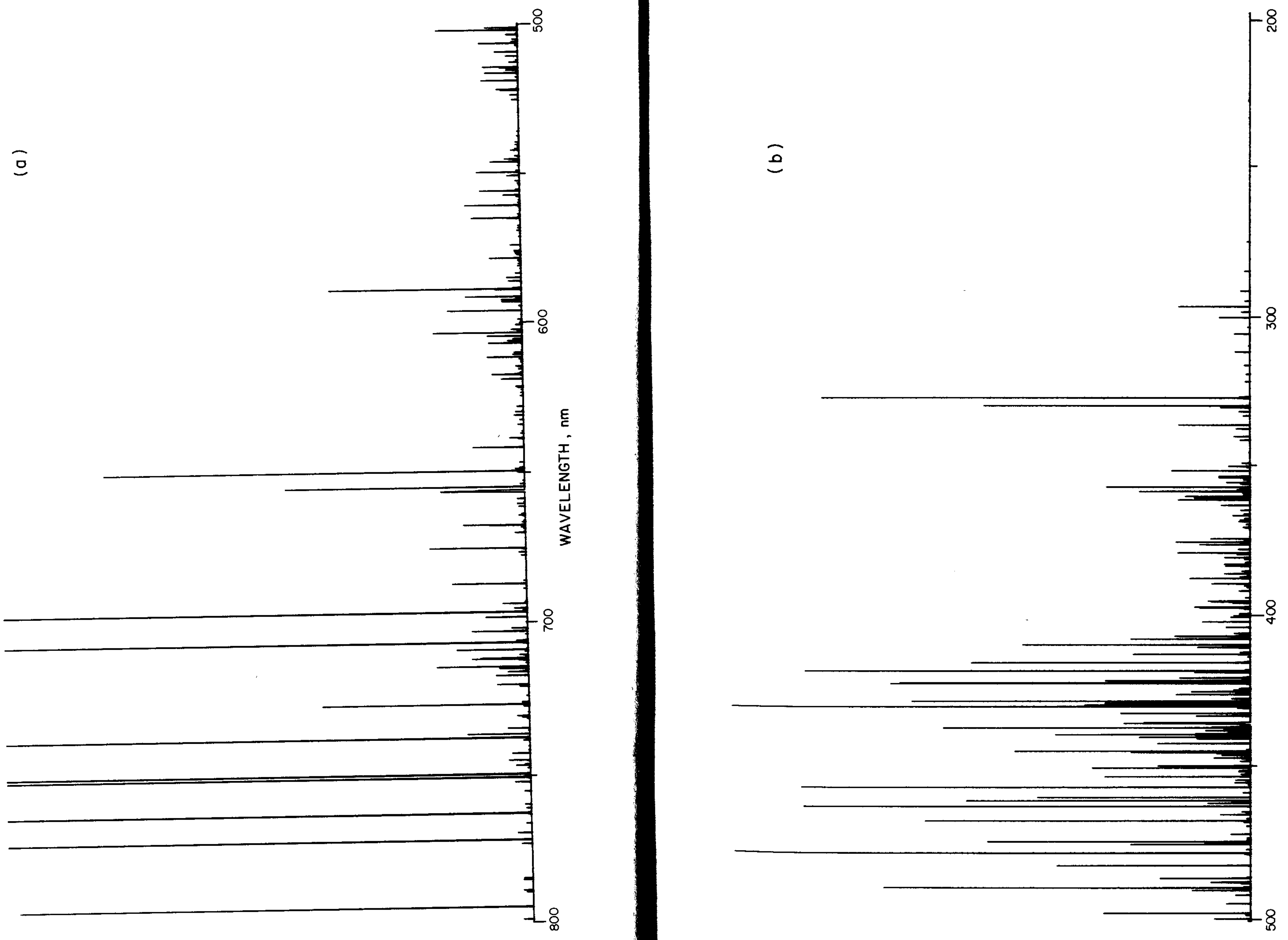

Fig. 5-11. Spectrum of argon in a hollow-cathode discharge. (a) 800-500 nm; (b) 500-200 nm.

than including also the actual intensity obtained from the metal resonance lines) and argon is seen to be as good as or even better than neon in the very important AAS ultraviolet region (i.e. below 370 nm). High-purity argon is also considerably cheaper than neon and its choice may have seemed natural at that time.

5.2.4 *Operation of Hollow-Cathode Lamps*

(*a*) *Power requirements*

A stable light source is required in both AAS and AFS to allow convenient routine operation without frequent adjustments of the spectrometer. For AAS in particular, an extremely stable source is needed to allow measurement of very small changes in its intensity at the detector (i.e. of very small absorption signals). The HCL is inherently a stable source compared with some other discharge sources owing to the design of its cathode and the fact that it operates in the glow-discharge region where the voltage across the lamp electrodes depends much more on the construction than on the lamp current. However, in most cases it is able to give sufficient stability for use in AAS only when operated from a specially designed and relatively sophisticated power supply unit. Where precise measurements are needed such a unit may be required to maintain a current stability better than 0·1% over a relatively wide range of voltage and current.

The operating voltage with most HCL designs lies in the range 150 to 300 volts and is relatively independent of the current; usually a range of less than 50 volts will cover all currents at which the lamp can be satisfactorily operated. The maximum current permissible with the conventional, sealed-off, uncooled lamps is usually about 40 or 50 mA; higher currents will overheat the cathode causing unstable operation and, in severe cases, permanent damage. In practice, most lamp manufacturers recommend a much lower maximum current to restrict the shortening of the lamp life as a result of the higher rates of metal volatilization and filler-gas "clean-up". As the starting voltage of the lamp is generally rather higher than the operating voltage, and with some designs may exceed it by as much as 150 volts, it is therefore necessary to protect the lamp* against current surges by placing a load resistor in series with it. In many cases it is convenient to place the load resistor in series with another variable resistor which may be used to adjust the operating current of the lamp, rather than to adjust it by altering the supply voltage. If the supply voltage is V_1 and the operating voltage and current selected for the lamp are V_0 and i_0 respectively, the value R_1 of the resistor required may be calculated from $R_1 = (V_1 - V_0)/i_0$. This should be clear from Fig. 5-12. For example, a 500-volt supply would be quite adequate to start and operate most commercial lamps. The load resistor required to limit to 50 mA the current of a lamp whose operating voltage is 250 volts at this current would then be 5 kΩ. Similarly, if it were necessary to operate this lamp at 10 mA (at which its operating voltage may be, say, 220 volts) a total load resistance of 28 kΩ would be needed. Thus, with a 500-volt supply a load resistance variable from about 5-50 kΩ would be sufficient for most purposes. Then even if the effective lamp resistance should drop to zero owing to a fault the maximum current through the circuit would be limited to 100 mA.

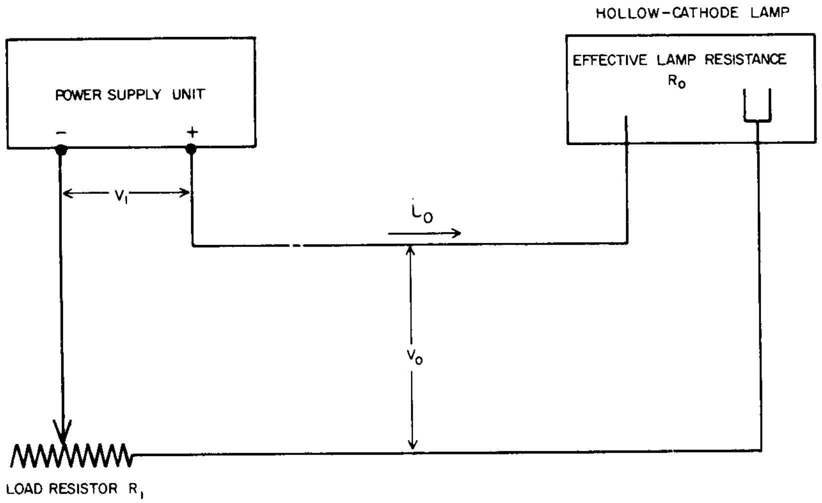

FOR LAMP : $V_0 = R_0 i_0$

FOR CIRCUIT : $V_1 = (R_0 + R_1)\,i_0$

HENCE : $V_1 = R_1 i_0 + V_0$

or $R_1 = \dfrac{V_1 - V_0}{i_0}$

Fig. 5-12. Connection of a hollow-cathode lamp to the power supply via a load resistor.

In AAS applications the lamp will be used with a power supply that minimizes the effects of voltage fluctuations in the ac mains.

---

* and the power supply unit if it is capable of supplying only small currents.

Hence the major source of instability in the lamp output will be fluctuations in its voltage/current characteristics which occur as a result of changes within the lamp itself. For example, the nature of the hollow-cathode surface and the plasma within it will be changed by the sputtering and vaporization of the metal during operation of the lamp. If a constant voltage is being applied to the electrodes the current at which the lamp is operating will change causing a fluctuation in the intensity of the light output. Thus, ideally, the lamp should be operated with a *current*-stabilized power unit which is able accurately to maintain the current supplied to the lamp at a preset value even when quite large changes occur in the voltage/current characteristics. Most of the more expensive commercial atomic absorption spectrometers now use this type of lamp supply unit.

TABLE 5-3

Effects of supply voltage on the operating stability of a hollow-cathode lamp used with a non-current-stabilized power supply unit

Supply voltage V_1	Load resistor R_1 (kΩ)	Effective lamp resistance R_0 (kΩ)	Potential drop across lamp V_0 (volts)	Lamp operating current i_0 (mA)
500	30	20	200	10
500	30	22	211·5	9·62
1000	80	20	200	10
1000	80	22	215·5	9·81
1500	130	20	200	10
1500	130	22	217·0	9·87

Where only a more simple voltage-stabilized supply is available, it is desirable to have the supply voltage (and hence the load resistor) as high as possible even though 500 volts would be adequate to run most lamps. This will then minimize the change in the current that occurs when, say, the voltage needed to sustain the discharge varies. An example to illustrate this point is given in Table 5-3. It is assumed that the load resistor (R_1) has been chosen for each of three supply voltages (V_1) to give a lamp current (i_0) of 10 mA with a discharge which "normally" has a potential drop (V_0) of 200 volts at this point. The lamp current is then calculated for each of these supply voltages and load resistors after the voltage current characteristic has changed so that the lamp would now operate at 10 mA with an applied voltage V_0 of 220 volts; i.e. the "effective resistance", R_0, of the lamp is assumed to have changed from 20 kΩ to 22 kΩ.* It can be seen that whereas a 3·8% change in the lamp operating current occurs with the 500-volt supply it is only 1·3% with the 1500-volt supply. If the lamp had been operated direct from a 200-volt supply, the current would have dropped to 200/22 = 9·1 mA, i.e. a 9% change.

It has been assumed in the preceding discussion that the hollow-cathode lamp is operating on direct current whereas, as explained elsewhere, almost all AAS and AFS spectrometers use a modulated light source with a synchronous (ac) amplifier. This is achieved in some spectrometers by placing a rotating sector (or chopper) in front of the light source. The effective intensity of the lamp will be reduced (for example, by 50% if the sector contains equal numbers of the same size open and closed segments) but this is not a serious disadvantage in AAS as the ac amplifier also gives an improvement in the stability and noise level of the signal. However, a much more convenient and effective solution to the problem is obtained by modulation of the current supplied to the lamp† and this system is used in many commercial spectrometers. Some care is then needed in the selection of the modulation frequency, waveform and peak voltage to obtain satisfactory results. The effects occurring are illustrated in Fig. 5-13. Diagram (a) shows the result of using sine-wave modulation (such as would be obtained with half-wave rectification) when the peak voltage of the supply is just high enough to start the discharge of the lamp. The lamp voltage will follow the supply voltage until the peak when the discharge initiates and the voltage of the lamp falls to a value depending on its characteristics. This value will remain fairly steady until the supply voltage has fallen again and the discharge extinguishes when the lamp voltage will again follow that of the supply until firing occurs again on the next cycle. As in dc operation the current flowing while the discharge is present will depend on the supply and lamp voltages and any impedance in series. Hence it will drop somewhat during the discharge period as the supply voltage is falling.

Referring again to diagram (a), it can be seen that under these conditions the average current supplied to the lamp is very much less than the peak current. In fact with this particular example the ratio

---

* A large change in lamp characteristics is needed to give a clear illustration; in practice, a hollow-cathode lamp in good condition would show much smaller fluctuations.

† Modulation should not be confused with pulsed operation which can be used to obtain a large increase in the output intensity of a hollow-cathode lamp. Pulsed operation is discussed in Section 5.2.4(c).

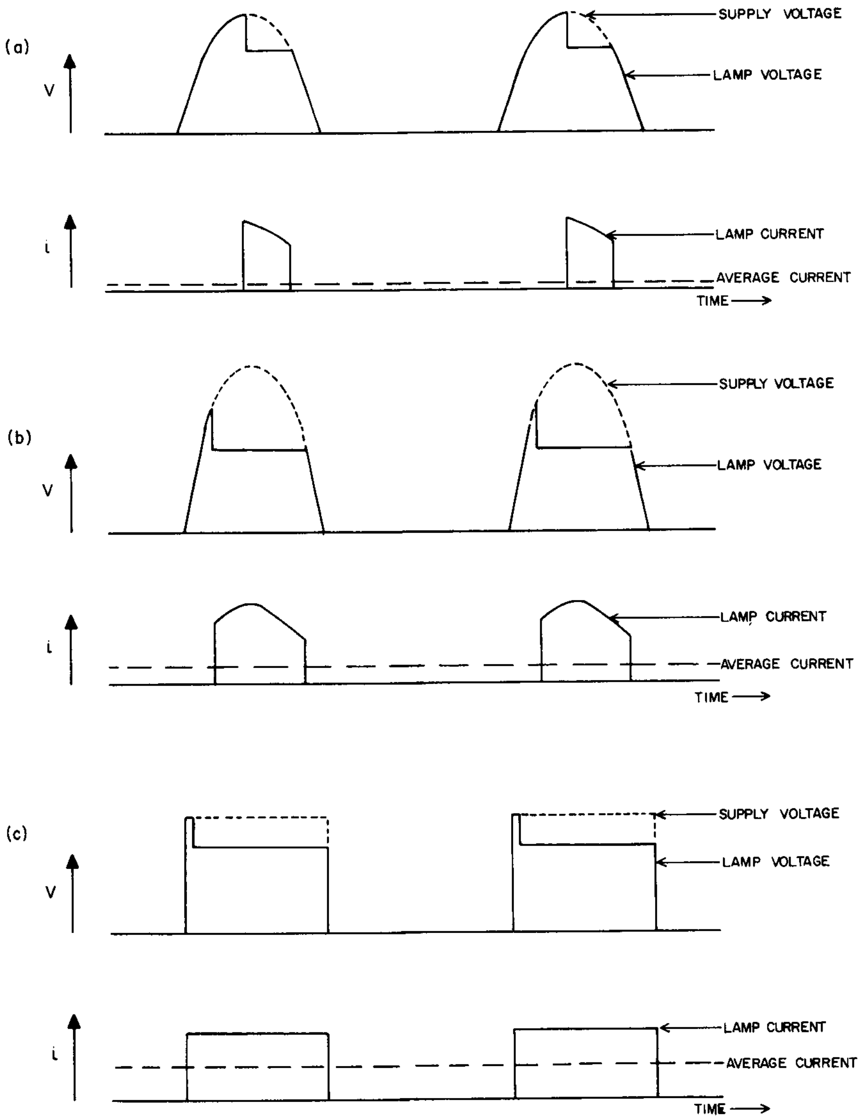

Fig. 5-13. Schematic illustration of the effects of modulation of hollow-cathode lamp power supply.

is about 10 : 1 so that if an average current of 10 mA were needed to obtain sufficient output, peak currents of around 100 mA would be necessary. Unlike dc excitation at this level, the high peak current would not lead to overheating of the cathode or serious self-absorption but it would require a higher level of ionization in the lamp and hence increase filler-gas clean-up. Thus, operation of the lamp in this way may lead to a considerable shortening of the lamp life. The peak-to-average current ratio may be reduced for a particular waveform simply by increasing the peak voltage as shown in diagram (b) of Fig. 5-13. Obviously, the discharge will now start earlier in the cycle and will be maintained for a larger and larger part of the cycle as the peak voltage is increased further. Thus, by using a sufficiently high peak voltage it would eventually be possible to maintain the discharge for almost a half-cycle, giving a ratio of just over 2 : 1. In practice, it is more satisfactory to modulate the power supply in the form of a square wave as shown in diagram (c). A peak-to-average current ratio of 2 : 1 will then always be obtained with any voltage high enough to fire the discharge (although it is advantageous to use a high supply voltage and series impedance as with dc operation).

Quite apart from the need for modulation in AAS and AFS spectrometers, the operation of the hollow-cathode lamp in this way with a current higher than the apparent average current actually improves the output intensity. This is because the relationship between intensity, I, and current, i, has been shown to be not linear but of the form $I = C\,.\,i^n$ *in the absence of self-absorption.*[2,9] C and n are constants for a particular cathode and filler gas; n usually has a value between 2 and 3 for metal lines excited by neon or argon.* The degree of self-absorption in most lamps will depend mainly on the average current so that operation of a particular lamp with a square-wave-modulated supply at an average current of 10 mA will actually give an increase in output over the same lamp operated at 10 mA dc. This should be compared with the effect of a rotating sector which must always reduce the effective intensity of the lamp. Thus, the use of this device for modulation should be avoided in a spectrometer designed for the hollow-cathode source.

(*b*) *Warm-up and lamp life*

Although most hollow-cathode lamps show a steady change in their spectral output during the useful lamp life, this is not usually of any significance during the normal periods of continuous use which in most laboratories will not exceed a few hours. However, nearly all lamps do exhibit a "warm-up" period during which the intensity

---

* A much smaller degree of enhancement would be inferred if the effect of a high peak current were calculated from plots of intensity against dc or average current supplied by manufacturers, since in many cases these are seriously distorted by self-absorption at higher currents.

drifts quite rapidly until the lamp has reached an equilibrium condition with respect to the cathode temperature and the population of analyte atoms. This effect will be observed each time the lamp is operated and may last only a few minutes or up to an hour. In view of this, many spectrometers incorporate an extra, unstabilized lamp power supply which allows one or more lamps to be run and stabilized at approximately the correct current until required for analysis of a sample. Such a device is not normally supplied with double beam spectrometers as the detection system in these compensates for any drift in intensity. This may not always be desirable, since lamps in which the metal atom population is highly temperature-dependent usually show the longest warm-up periods. These lamps may be operated under self-absorption conditions so that the actual resonance line width (and hence the peak absorption sensitivity) may change during the warm-up of the lamp; double-beam operation will not compensate for this.

The shelf-life of a lamp will depend mainly on the reliability of construction, particularly at any joints and seals; with modern techniques it may be considered as indefinite for most lamps in fairly routine use. The operating life is limited mainly by the adsorption of filler-gas onto sputtered metal atoms. The effects of loss of material from the cathode and degassing of lamp materials as they become hot during operation are generally much less important in the latest commercial lamps which are very carefully designed and constructed to minimize these factors. Although neon appears to show more rapid adsorption than the other gases this is not a critical factor in its use as a filler gas. Much more important is the choice of electrode configuration to minimize the effect of gas pressure, since this will obviously show a gradual reduction during the life of the lamp. With most elements it is then possible to obtain a useful operating life of several thousand hours at currents up to the maximum recommended by the manufacturer. It is usually possible to operate the lamp beyond this period but with reduced stability and intensity of the metal lines (although some lamps actually show an increase in output near the end of life).

(*c*) *Pulsed operation*

A major factor limiting the output intensity of the hollow-cathode sources used in AAS and AFS is, as mentioned previously, their dependence on the same discharge to atomize the sample element and to excite the atoms. Thus, any attempt to increase the level of excitation by intensifying the discharge must also produce a higher concentration of metal atoms in the cathode region with the consequent problems of self-absorption and broadening of resonance lines and shortened lamp life. One possible solution to this problem, suggested by Bodretsova *et al.*,[12] is the operation of the hollow cathode with a high-frequency power supply (e.g. 60 MHz instead of the usual dc or a few Hz ac). Although such a discharge is extremely efficient in terms of excitation it produces a lower potential drop and hence a lower energy of the ions bombarding the cathode surface than in a dc discharge. As a result, the same level of spectrum excitation may be obtained with much less sputtering of the electrode metal compared with that produced in the dc-operated lamp. Thus Bodretsova *et al.* found that, for a given degree of self-absorption and broadening of the resonance line, use of a high-frequency power supply produced a 100-fold improvement in intensity for easily sputtered metals such as magnesium and a 25-fold improvement for those metals, such as aluminium, that were difficult to sputter.

An even more impressive improvement in the intensity obtained from a standard hollow-cathode lamp was reported by Dawson and Ellis[13] using true pulsed operation of the lamp at much lower frequencies. This is a logical extension of the effect observed when the lamp power supply is modulated (see above); it simply involves increasing the pulse interval (i.e. the ratio of the period between pulses to the pulse duration) from unity to give a peak-to-average current ratio somewhat greater than the value of 2 : 1 obtained with normal square-wave modulation. It is then possible to use relatively high (peak) excitation currents while avoiding excessive thermal vaporization of the metal since the effective (average) current is only a few milliamperes. However, there is a useful limit to the value of the peak current that can be used with a particular metal (even when the effective current is kept constant by making the pulses shorter and shorter) since sputtering of the cathode material depends only on the amplitude of the pulses and eventually the stage will be reached where this process alone is able to produce a sufficiently high concentration of metal atoms for self-absorption and broadening of resonance lines to occur. Nevertheless, Dawson and Ellis[13] were able to obtain several hundred-fold improvements in observed intensity from a number of lamps without an apparent increase in self-absorption or line broadening. In fact, a later and more extensive study by Katskov *et al.*[14] has shown that the actual improvement is probably somewhat smaller than this, although still considerable.

They compared the results obtained for several lamps using normal dc operation and a power supply giving square-wave pulses at a frequency of 300 Hz with a pulse interval (see above) of 5. A Fabry-Perot interferometer was used to observe under high spectral resolution the broadening and self-absorption of the metal resonance lines. It was found that, provided the peak current of the pulses is not made too high as explained above, the "quality" of the lines is similar when the mean current of the pulsed power supply is the same as the direct current. Thus, it was possible to make a direct comparison between the intensities obtainable with the two modes of operation, as shown in Table 5-4. It can be seen that pulsed operation gives an improvement varying from about 20-fold to 130-fold depending on the metal. This variation is due to the different value of n for different metals in the equation $I = C . i^n$ (see Section 5.2.4(a)); the ratio of pulsed to dc intensity should be given simply by $(i \text{ pulsed}/i \text{ dc})^n$ and under conditions where self-absorption is insignificant it should be possible to calculate the ratio using a constant value of n for a particular lamp. This is illustrated in the last column of Table 5-4 using values of n measured by Bodretsova *et al.*[9] for conventional dc excited lamps; there is excellent agreement between the measured and calculated ratios.

TABLE 5-4
Improvements in hollow-cathode lamp intensity using a pulsed power supply[15]

Lines (nm)	i_{mean} (mA)	i_{peak} (mA)	$\left[\frac{I \text{ pulsed}}{I \text{ dc}}\right]_{\text{meas.}}$	n	$\left[\frac{I \text{ pulsed}}{I \text{ dc}}\right]_{\text{calc}}$
Ag 328·1	8	40	23	1·9	21
Al 309·3	20	100	55	2·5	56
Co 240·7	10	50	36	2·3	41
Cr 357·9	20	100	102	2·9	107
Mo 313·3	30	150	21	1·9	21
Ni 341·5	15	75	20	1·8	18
Pd 247·6	10	50	132	3·0	125
Rh 343·5	10	50	44	2·3	41
Si 251·6	30	150	26	2·0	25

More recently Mitchell and Johansson[16] have used pulsed hollow-cathode lamps as atomic fluorescence sources. As very sharp source lines are much less important than in AAS, they were able to use high peak currents without undue consideration of the relatively high atom concentrations which would consequently be sputtered. Their measurements were made with rather shorter pulses than those described above; for example, a pulse current of 190 mA corresponded to a mean current of only 8·5 mA, and they suggest that extremely high pulse currents could be obtained in this way for good fluorescence sensitivity without serious problems of overheating or self-reversal of the light source. Such short pulses also allow fluorescence measurements of very brief duration without any loss of fluorescence intensity compared with measurements made in the normal way. This technique has been used in an atomic fluorescence spectrometer for "simultaneous" multielement analysis, the different lamps being pulsed sequentially so that apparently continuous measurement of each element is obtained.

5.2.5 *Spectral Characteristics of Hollow-Cathode Lamps*

(*a*) *Line broadening and self-reversal*

The breadth and degree of self-absorption of the metal resonance lines is, as mentioned previously, one of the most important characteristics of the hollow-cathode lamp from the point of view of its use as a light source in AAS. Unfortunately, as a result of the experimental difficulties involved, relatively few measurements have been made of the line profiles that are of direct interest to AAS applications. There seems to be general agreement[9,12,17-24] that in the absence of self-absorption both metal and filler-gas lines are broadened mainly as a result of the Doppler effect. In both cases collisional (Lorentzian) broadening is the next major factor producing a line-width which generally amounts to a few percent of the Doppler width, although a similar contribution by resonance broadening has been noted[21] for some filler-gas lines and this effect may also occur with some metal lines if the atom population within the cathode increases greatly at higher operating currents. Very much larger Lorentzian line-widths have apparently been observed for certain lines of Ar(II) and Ne(II),[21,24] but these appear to result from an anomalous effect which is of no interest to AAS applications.

As the Doppler width can be readily calculated from the source temperature (see Section 2.5.2(ii)), there would seem to be little difficulty in estimating the width of a non-self-absorbed metal line simply by measuring the operating temperature of the cathode with, for example, a suitable thermocouple. However, there is considerable disagreement in the reported literature as to whether the observed Doppler temperature* is actually equal to the operating temperature

* i.e. the temperature calculated from the measured Doppler half-width using equation (2-18).

of the cathode.* This situation is complicated by the fact that measurements of the line-width are difficult and subject to considerable errors in many cases; as $\Delta\nu_D$ is proportional to $T^{1/2}$ the uncertainty in the estimated Doppler temperature may be quite large. Thermocouple measurements of the cathode wall temperature in typical modern lamps have shown a range of *ca.* 300 to 800 K at currents of about 20 to 90 mA for an iron cathode[17] and 350 to 430 K at currents of 5 to 15 mA with a calcium oxide/tungsten/titanium cathode.[23] However, the corresponding Doppler temperatures measured at the calcium 422·67 nm resonance line were reported by Yasuda[17] to be far higher (*ca.* 1300 to 2700 K for currents of 30 to 90 mA), whereas Bruce and Hannaford[23] found them virtually identical to the thermocouple values. Similarly, argon and neon lines were found by Gofmeister and Kagan[19,20] to give Doppler temperatures of 320-700 K in the current range 20-100 mA, and this is again close to the expected cathode temperature.

A much more extensive study of this problem has been made by Kreye and Roesler.[21,24] The conclusions drawn from their own line-width measurements and from their collation of ancillary data may be summarized as follows: (i) The Doppler temperature observed for the neutral filler-gas lines (i.e. ArI and NeI) is generally a good indication of the actual gas temperature. (ii) The doublet lines of ArII and NeII give similar Doppler temperatures but quartet lines show anomalously low values for reasons which are not of immediate concern. (iii) The gas temperature observed with argon is consistently about twice that observed for neon with similar lamps operated at the same discharge current. (iv) The Doppler temperature observed for a metal line is somewhat larger than that of the filler-gas lines unless there is a large interval, τ_e, between excitation and emission of the line, i.e. unless the transition probability is small. (v) It is suggested that this latter effect is due to there being insufficient time for metal atoms with high energy to come to equilibrium with the gas temperature before emission because of the relatively long interval between metal/gas atomic collisions (*ca.* 20 ns).

Some Doppler temperatures for hollow-cathode lines[21,24] are listed in Table 5-5 together with values of τ_e for the metal lines. Allowing for the general uncertainty in such measurements it can be seen that there is fair agreement between the ArI and NeI

temperatures and the thermocouple measurements reported by Yasuda[17] (argon-filled lamp) and Bruce and Hannaford[23] (neon-filled lamp). The temperatures observed for Au 479·2 and Fe 372·0 are also comparable, both of these lines having large values of τ_e, whereas those of the other metal lines with smaller values of τ_e are obviously too high to be representative of the gas temperature within the cathode. It should be noted that the value of τ_e for the calcium 422·67 nm line is about 5·4 ns.[23] Thus, if the hypothesis of Kreye and Roesler is valid, it would be expected to show a high Doppler temperature as observed by Yasuda[17] rather than a value characteristic of the cathode temperature.[23] In any event, until further data are available it would seem unwise to assume narrow Doppler line widths characteristic of the cathode temperature for many metal resonance lines, as those of interest in AAS and AFS usually exhibit large transition probabilities (i.e. small values of τ_e).

TABLE 5-5
Doppler temperature for hollow-cathode lamps[21,24]

Element[a]	Line(s)[b]	Current (mA)	Doppler temp. (K)	τ_e (ns)
Ar I	451·1 and 470·2 nm	10–25	700–1100	–
Ar I	451·1 nm	15	1200	–
Ar II	Doublets	10–25	700–1100	–
Ar II	Doublets	15	1070	–
Ar II	Quartets	10–25	400–800	–
Ar II	Quartets	15	800	–
Ne I	347·3 nm	15	640	–
Ne II	Doublets	15	590	–
Ne II	Quartets	15	350	–
Au I	312·3 nm	10–25	1500–1900	25
Au I	479·2 nm	10–25	1000–1300	70
Au I	242·8 nm	–	4700	6·5
Au I	267·6 nm	–	4700	17
Fe I	248·3 nm	–	3900	0·17
Fe I	372·0 nm	–	690	75

[a] All metal lines are for lamps with argon as filler gas.
[b] Where more than a single line is indicated temperatures have been averaged from several comparable lines.

In practice, the question of whether or not the Doppler widths of the metal resonance lines are actually characteristic of the cathode temperature is not of paramount importance in AAS applications. In either case, the possible increase in Doppler width with rising lamp temperature is insufficient for most elements to explain the serious

---

* This should not be confused with the *excitation* temperature of the spectral lines which depends on the energy provided by the excitation mechanism and in a hollow-cathode lamp is generally greatly in excess of the gas or vapour temperature.

reduction in peak absorbance values frequently observed with increasing lamp current. This is almost certainly due[9,17,18,22,23] to a rather larger increase in self-absorption broadening which occurs as a result of the higher concentration of metal atoms in the hollow-cathode bore when the operating current is increased. Both the sputtering process and thermal vaporization contribute to the enhanced production of metal atoms, their relative importance depending on the lamp design and the volatility of the analyte element. A major contribution to the improvements in modern hollow-cathode lamps has been the reduction in this effect when larger lamp currents are used to increase the intensity of the resonance line. Particularly important is the limitation of the formation of a cloud of "cool" metal atoms in front of the cathode as these will give the most serious self-absorption of the ground-state metal lines of interest in AAS and AFS. Figure 5-14 shows measurements by Bruce and Hannaford[23] of the absorbance observed through the bore and across the front of the cathode of a commercial calcium lamp. Although it was necessary to modify the cathode to allow the beam from a second source lamp to pass through, this is not expected to affect the significance of the results.

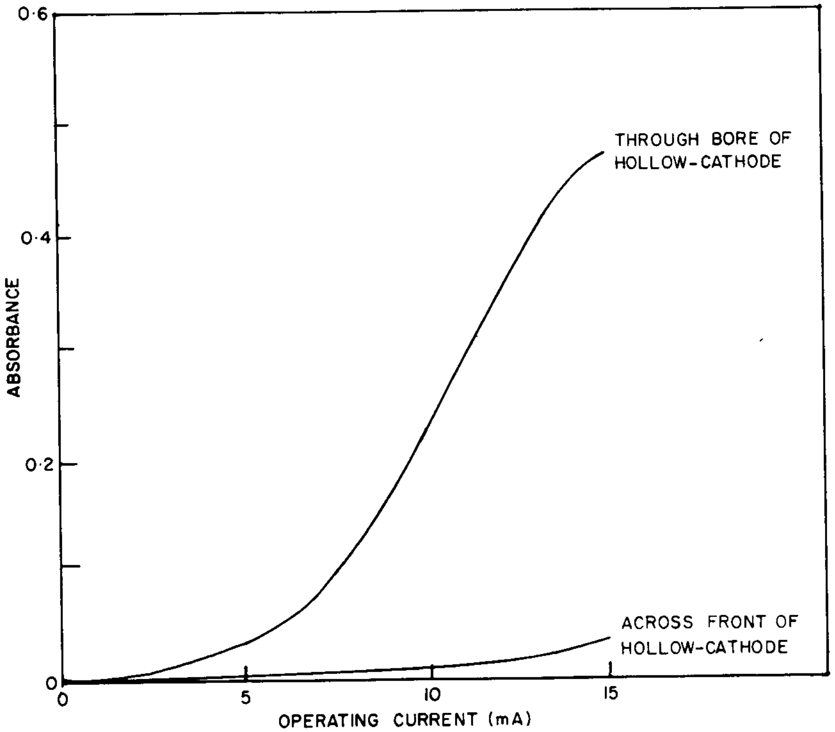

Fig. 5-14. Absorbance measured at the 422·67 nm resonance line within a calcium hollow-cathode lamp.[23]

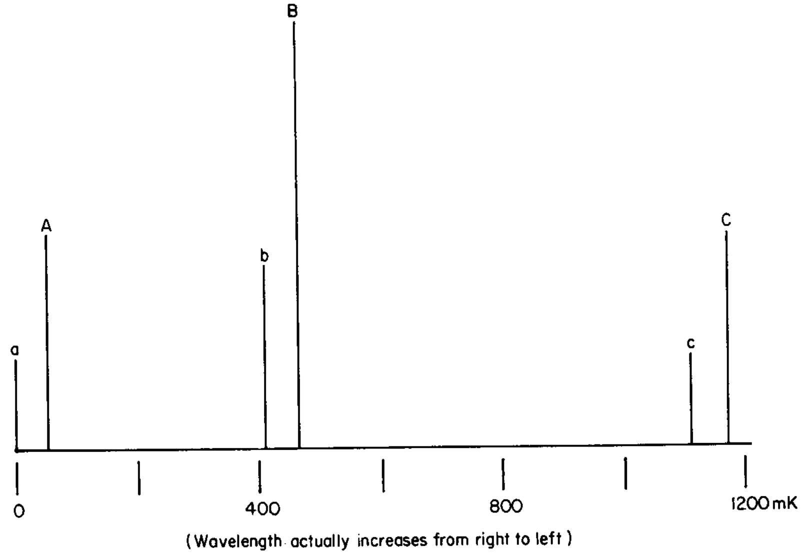

(a) Actual hyperfine structure; the heights of the lines represent the theoretical relative intensities of the components.

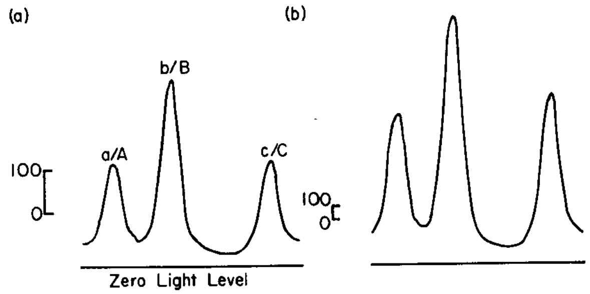

(b) Fabry-Perot spectrometer scan of the profile emitted by a hollow-cathode lamp operated at (a) 15 mA and (b) 25 mA.

Fig. 5-15. Hyperfine structure of the thallium 377·6 nm line.

The manufacturer's recommended operating current for this lamp (based on measurements of AAS sensitivity) is 4 to 5 mA, and the concentration of metal atoms within the cathode rises rapidly if this value is exceeded. The much smaller absorbance by atoms outside the cathode is an indication of efficient lamp design.

More direct evidence of the effects of self-absorption has also been obtained by actual observation of the line profiles. Analysis of the profile recorded for the calcium 422·67 nm line to deconvolute the contributions of Doppler and self-absorption broadening has confirmed[17,23] that the latter is much more important as an explanation of the increase in half-width with current, even at quite modest currents. However, as mentioned above, such measurements are difficult and involve considerable uncertainty. A much simpler qualitative assessment of the effects of self-absorption may be made by observing the relative intensities of the hyperfine components of the line[9,12,18,22] (see Section 2.5.2(vii)). Provided a high resolution spectrometer is available this technique is easily applied to most metal lines of interest* without any need to modify the source. Special cases may give additional information for particular elements, but in general the technique relies on the fact that any differences in intensity of hfs components will depend only on their relative transition probabilities (since the energy levels are very similar). Thus, if one peak is twice as intense as another the degree of

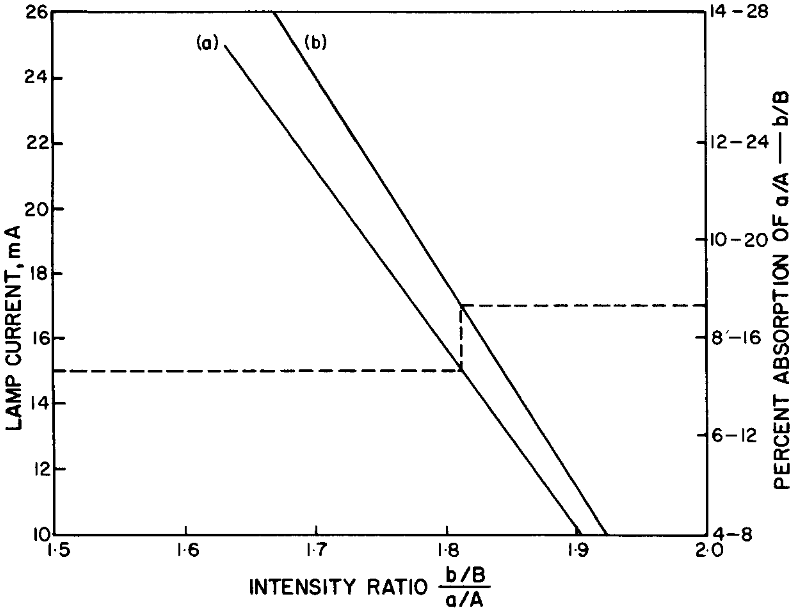

Fig. 5-16. Variation of the hfs intensity ratio of the thallium 377·6 nm line. (a) Observed experimentally for a hollow-cathode lamp at different operating currents; (b) calculated for different degrees of self absorption.

---

* Except, of course, for a few elements such as calcium which show no resolvable hfs.

absorption at these lines will be in approximately the same ratio and a rapid change in the intensity ratio occurs as self-absorption increases. The effect is clearly illustrated by the thallium 377·6 nm line,[22] the hyperfine structure of which is shown in Fig. 5-15(a). In practice, the line-width obtained from an ordinary hollow-cathode lamp results in the six components appearing as three peaks, as shown in a Fabry-Perot interferometer scan of the line (Fig. 5-15(b)). The variation with lamp current of the intensity ratio of the *a*/*A*-*b*/*B* peaks (which is theoretically 2·0 in the absence of self-absorption) is shown in Fig. 5-16. Also shown is an approximate calculated plot of the variation in the intensity ratio with different levels of self-absorption. This gives an estimate of the degree of self-absorption at a particular operating current. For example, as indicated in Fig. 5-16, the self-absorption of the *b*/*B* peak is about 17% at a current of 15 mA (the recommended lamp current is actually 20 mA).

(*b*) *Line interference*

The practical effects of non-absorbed lines appearing within the spectral bandpass of an atomic absorption spectrometer set to the wavelength of the analyte absorption line are discussed in Chapter 12; we are concerned here with the HCL characteristics producing this type of interference. It is most commonly observed when lines of the filler gas lie close to the analyte line, although the effect has also been noted for non-absorbed (i.e. non-ground-state) lines of the metal atom itself and for ionic lines of the metal. The first type is probably the easiest to avoid, or at least to reduce in severity, simply by careful choice of the gas and the lamp pressure (see Section 5.2.3(c)). Figure 5-17 shows the spectrum observed in the vicinity of the chromium 357·9 nm resonance line, (a) in an argon-filled lamp and (b) in a neon-filled lamp of modern design. The effect is such that with the argon-filled lamp the less strongly absorbed 359·4 nm chromium line actually appeared to be more sensitive. Less often it may be possible to reduce the effects of non-absorbed metal lines by a similar change in lamp construction which may enhance the resonance line intensity or reduce ionic line intensities. The latter effect is illustrated for the nickel 232·0 nm resonance line in Fig. 5-18; the drastic reduction in intensity of the nearby 231·6 nm ion line between diagrams (a) and (b) was obtained simply by reducing the pressure of the neon filler gas. It should be noted that in some cases a straightforward improvement in resonance line intensity is useful in reducing the interference as it allows a narrower spectral

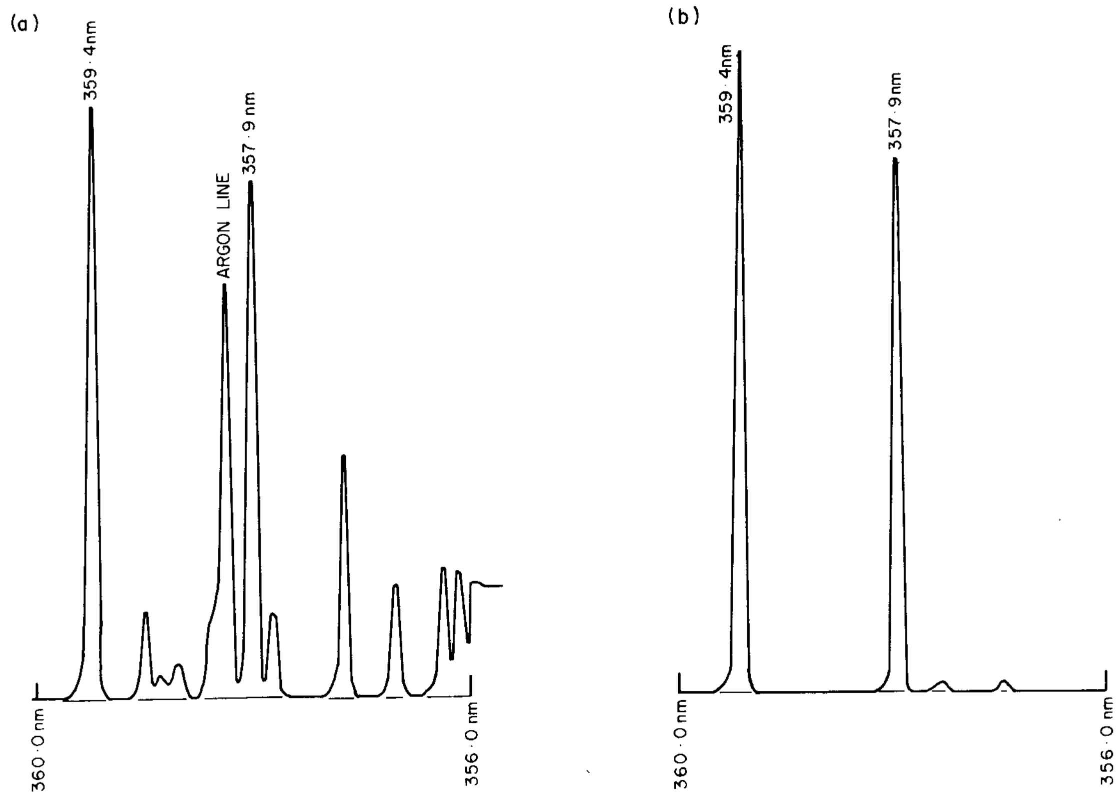

Fig. 5-17. Filler gas line interference at the chromium 357·9 nm line. (a) Spectrum from an older argon-filled lamp; (b) spectrum from a modern neon-filled lamp.[25]

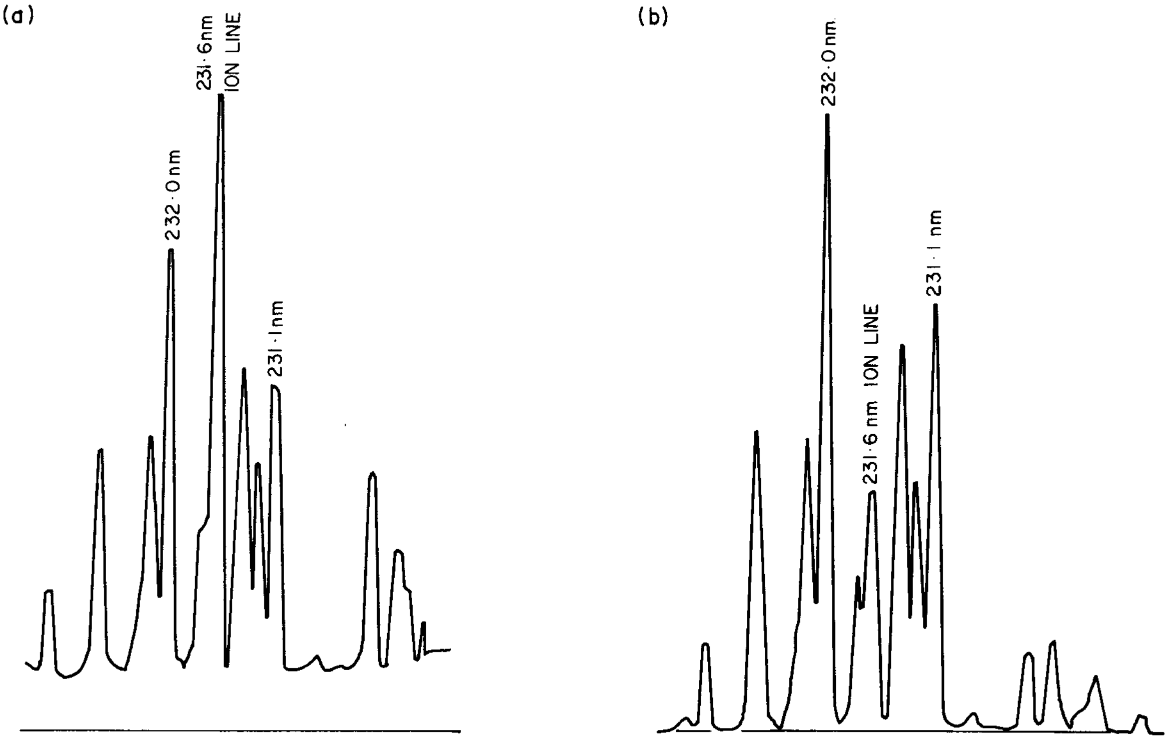

Fig. 5-18. Metal ion line interference at the nickel 232·0 nm line. (a) Spectrum from a lamp containing too high a pressure of neon; (b) spectrum from a lamp containing the correct neon pressure.[25]

bandpass to be employed while maintaining a high signal-to-noise ratio.

(*c*) *Signal-to-noise ratio*

The signal-to-noise ratio is an important factor in the selection of a source for both AAS and AFS as it limits the smallest analytical signal that can be observed and thus has a direct effect on the detection limit. A hollow-cathode lamp in good condition is inherently stable and, as discussed in Section 5.2.4(a), the effect on the output intensity of any fluctuations that may occur within the lamp can be minimized by careful construction of the power supply unit. Early studies of the application of the lamps to AAS[26,27] suggested that quite high noise levels were present and that they could not be removed or reduced by using a more stable power supply. However, it has been shown[9] that these workers almost certainly measured fluctuations not in the lamp output but in the detection circuit, probably the shot noise of the photomultiplier. This effect is illustrated in Fig. 5-19 which shows a series of signals recorded from a neon-filled iron hollow-cathode lamp operated at 50 mA (i.e. the output of the lamp is the same in each case). The

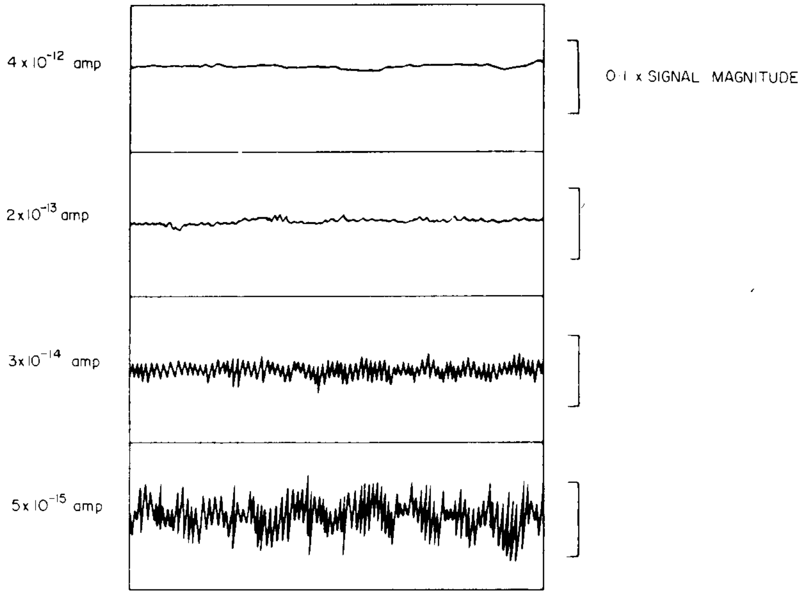

Fig. 5-19. Signal recordings of the same lamp output at different levels of incident intensity on the photomultiplier.[15]

intensity actually received at the detector was reduced in stages and it can be seen that there is an apparent increase in the "noise level of the source". As the fluctuation is about 0·1% of the signal at the highest intensity (diagram (a)), the lamp noise cannot exceed this level. Thus, a fairly high resonance line intensity is important in AAS even though the intensity has no direct effect on the sensitivity. This is particularly so for elements which have their strongest absorption lines in regions of low photomultiplier sensitivity.

5.2.6 *Special Types of Hollow-Cathode Lamp*

(*a*) *Demountable lamps*

Demountable hollow-cathode lamps are not usually supplied with commercial atomic absorption spectrometers and have seen relatively little application compared to the sealed types, although they have been described by a number of workers.[26-32] Recently, a commercial device has been introduced* which is of suitable size to replace the standard sealed-off lamps in most spectrometers without extensive modifications. The lamp (Fig. 5-20) is intended to be as versatile as possible with easily interchanged cathodes and windows and a variable anode-to-cathode distance. It is also possible to water-cool the cathode via a heat-exchanger attached to the cathode support and this, in conjunction with the continuous flow of fresh filler gas during operation, allows the use of a somewhat higher current than with a conventional lamp. As all operating parameters can also be optimized for a particular application it should be

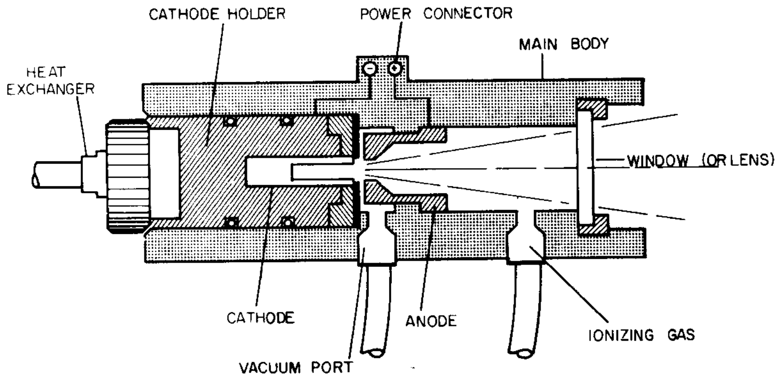

Fig. 5-20. Glomax demountable hollow-cathode lamp.

---

* Glomax Lamp, Barnes Engineering Co., Stamford, Connecticut.

possible to use this lamp as a high-intensity source for AFS as well as for specialized applications in AAS. However, for routine analyses it offers little economic advantage over conventional lamps, unless occasional determinations of many elements are likely to be required (the costs would be similar for about ten elements assuming that suitable vacuum and gas control systems are already available in the laboratory; if this were not the case the figure would exceed twenty elements).

(*b*) *High-intensity lamps*

Several lamp manufacturers refer to their standard hollow-cathode sources as "high-intensity lamps", but in the present context we are concerned with several elaborate modifications which have been suggested to allow operation of a sealed lamp at greatly increased resonance line intensity without the loss of the sharp profile. In practice, for most elements this means increasing the level of excitation without producing a higher concentration of metal atoms within the cathode; i.e. without introducing the problem of serious self-absorption.

The first and the most widely known solution to this problem was suggested by Sullivan and Walsh.[33] They used the conventional cathodic discharge to produce metal atoms at the optimum pressure but excited the cloud of atoms in front of the cathode with a second low-voltage discharge between two auxiliary electrodes. This not only gives a direct increase in the resonance line intensity prior to the onset of self-absorption but, in view of the low excitation energy available in the low-voltage auxiliary discharge, may actually enhance the resonance line intensity relative to other metal lines, filler-gas lines and ionic lines. Hence, the increased intensity of the resonance line is usually accompanied by a further improvement in the line-to-background intensity ratio. When compared with the conventional type of HCL the lamp also gives improved AAS sensitivity and calibration linearity for a number of elements. This results from the avoidance of self-absorption by a cloud of cool atoms in front of the cathode, a phenomenon often observed for the more volatile elements with early lamps of conventional design. The Sullivan and Walsh lamp, however, shows less pronounced improvement over the most modern types of conventional HCL and its use has recently been less popular. This restriction of its application has been hastened by the need to operate the lamp with a second power supply for the auxiliary discharge, especially as the small voltage drop (20-30 V) requires the use of currents up to 500 mA and hence a relatively expensive power pack.

Two attempts have been made to improve further the original Sullivan and Walsh design, one aim being to produce even sharper resonance lines for sensitive AAS measurements[34] and the other to provide an extremely intense source for atomic fluorescence.[35] Van Gelder's narrow line source[34] uses an open-ended, cylindrical hollow cathode, the discharge being struck through this cylinder between an ordinary cathode and a perforated disc anode. Metal atoms are sputtered from the inside of the hollow cathode as in a conventional lamp and the resultant resonance radiation leaves the lamp via the perforations of the anode. The discharge is constricted by a glass capillary to ensure (a) that sputtered metal atoms are restricted to an area within the cylinder where excitation can occur, and (b) that radiation is viewed only from the axis of the discharge where the excitation of sputtered atoms is most intense (i.e. where the concentration of ground-state metal atoms giving self-absorption is at its lowest).

Lowe's atomic fluorescence source[35] also uses a common anode and an open-ended cylinder for the hollow cathode. However, in this case the anode is placed behind the hollow cathode and the auxiliary (booster) cathode to one side of it so that there is no restriction of the resonance radiation leaving the lamp. A conventional, modulated discharge is struck between the anode and the hollow cathode while a high current (400 mA) dc discharge is obtained between the anode and the booster cathode. A set of restricting baffles ensures that this latter discharge can only occur through the hollow cathode (whereas in the original Sullivan and Walsh design the auxiliary discharge passes only across the front of the hollow cathode). This arrangement provides maximum excitation of metal atoms sputtered by the primary discharge, and for some elements the lamp was found to give a more than ten-fold increase in fluorescence intensity with apparently only a small increase in line-width compared with the original design.

Human and Butler[36] have described a high-intensity hollow-cathode lamp in which the auxiliary discharge is operated at microwave frequency (2450 MHz);* this has the advantage of needing only a simple wire antenna mounted within an ordinary

---

* Note that this device is quite different from both the radiofrequency HCL's described in Section 5.2.4(c) and the electrodeless microwave lamps described in Section 5.3.

hollow cathode. In use the ordinary modulated hollow-cathode discharge is used to sputter metal atoms while 10-15 watts of microwave power are applied to the antenna to boost the excitation of these atoms without increasing the normal concentration of metal atoms. It was found that at comparable absorbance sensitivities (i.e. comparable line-width/self-absorption) the auxiliary discharge was able to increase the resonance line intensity by up to 15 times.

(*c*) *Multi-element lamps*

Multi-element hollow-cathode lamps which emit resonance lines of two or more elements are useful as they can reduce the lamp cost per element and, provided suitable combinations are available, allow easier and more convenient operation in many routine analytical problems. Early multi-element lamp designs used several separate cathodes within one source,[8,37] but there were problems of alignment and of switching between the cathodes and this type has seen little application. However, several designs using a single cathode have been more successful and some of these are available commercially.

The most convenient technique with a single cathode is to construct it from a suitable alloy, but performance often deteriorates rapidly owing to preferential sputtering of one of the elements (e.g. of zinc when brass is used for a copper-zinc lamp[38]). A better approach is to press individual rings of various metals (or compounds) into a single cathode.[39,40] However, only certain combinations can be used together and the operating current must be carefully chosen to give a stable output for all elements rather than being optimized for each one. Successful multi-element lamps have been developed by the Perkin-Elmer Corporation[41-44] using sintered cathodes of mixed metal powders or intermetallic compounds. A number of lamps, containing up to seven elements, have been constructed; great care must be taken, however, in the choice of elements and materials used in a single lamp to ensure a similar useful life for each element and to avoid spectral interferences. It is also important that the group of elements should often require analysis together in a particular laboratory as these lamps often have the disadvantages of reduced intensity and limited operating conditions compared to conventional lamps. For example, the seven-element Al–Ca–Cu–Fe–Mg–Si–Zn lamp may be useful for routine blood serum analysis.

5.3. ELECTRODELESS-DISCHARGE LAMPS

5.3.1 Introduction

Although less widely used by spectroscopists than the hollow-cathode lamp, high-frequency electrodeless discharges have been recognized for many years as excellent sources of sharp-line spectra. They have several useful properties for high-resolution work and other fundamental studies, namely ease of construction, absence of electrode contamination, maintenance of the discharge at very low vapour pressures, and the need for only small amounts of the element or compound to be studied. However, their application to atomic absorption spectroscopy has been almost insignificant in comparison with the widespread use of the hollow-cathode lamp. This is undoubtedly due partly to the selection of the hollow-cathode lamp by Walsh and his co-workers (for reasons that are still largely valid) as the most suitable spectral source for their original analytical AAS work. With most elements a source line of the intensity and sharpness required for AAS is obtained with good stability and reproducibility more easily by using a hollow-cathode lamp rather than an electrodeless-discharge lamp in its present state of development. However, this is not generally the case with the type of source line required for atomic fluorescence spectroscopy, and it seems possible that the extensive development of the microwave-excited electrodeless-discharge lamp for this purpose may also lead to lamps which are useful alternatives to the HCL for routine AAS applications.

Electrodeless discharges may be excited at both *radio frequencies* (100 kHz to 100 MHz) and *microwave frequencies* (>100 MHz). The latter are a much more recent introduction as suitable power supplies have been available only during the last twenty or twenty-five years. In spite of this, most of the work by analytical chemists with these sources has used microwave excitation. This is partly due to the ready availability of suitable power supply units (originally inexpensive medical diathermy generators but more recently commercial units designed for spectroscopic applications) and partly because the properties of the microwave lamps (see below) were more appropriate for the very high output intensities required by the two groups of analytical chemists* originally concerned with the application of electrodeless-discharge lamps as spectral sources for atomic fluores-

---

* Winefordner and co-workers in the United States and West and co-workers in the United Kingdom; references to the work of both these groups will be found in the following pages.

cence spectroscopy. Radio-frequency (RF) discharges, however, have been used for fundamental fluorescence studies by many physicists because of the high stability obtainable; RF discharges may be also more suitable for obtaining resonance lines with very low self-absorption (see below).

Radio-frequency lamps have the advantage of a "skin effect" if the discharge conditions are carefully chosen. This concentrates the discharge near the tube walls so that the emitted radiation travels a negligible distance through vapour within the lamp and self-absorption and self-reversal of the resonance lines are minimized. On a more practical level, the construction of suitable RF power units is extremely well-documented and a current-stabilized supply equivalent to those used for the hollow-cathode lamp may be easily produced from widely available components (see Section 5.3.4). In contrast to this, a true "skin effect" is not normally obtained with microwave discharges and the construction of microwave generators and components involves more specialized electronic engineering. The problem of obtaining a fully stabilized unit giving stability comparable to that of hollow-cathode lamp supplies has been an important restriction on the spectroscopic application of EDL sources (see Section 5.3.5). For many applications, however, microwave excitation has two major advantages over RF excitation: both the useful operating life-time of lamps[45] and the efficiency of conversion of input power into emitted radiation[46,47] increase significantly at higher frequencies. The restricted life of RF excited lamps appears to result from absorption of the metal onto the tube walls, but even RF lamps show adequate working lives if frequencies towards the higher end of the RF range are used.[45] The rate of increase of lamp efficiency with frequency is difficult to assess, as although many different frequencies have been used for RF excitation, most work on microwave excitation has been carried out at 2450 MHz owing to the availability of commercial generators operating at this frequency. However, Jacobsen and Harrison[46] observed a sixteen-fold increase in intensity for 40 watts power when the excitation frequency was increased from 150 MHz to 3000 MHz, and Forrester *et al.*[47] reported a lamp output of 0·025 watt cm^{-2} steradian^{-1} for 95 watts input at 2450 MHz compared with 0·002 watt cm^{-2} steradian^{-1} for 1000 watts input at 70 MHz.

Although the ancillary equipment required for excitation is somewhat different for RF and microwave excitation, the basic requirements for lamp construction are rather similar. The sources are simply glass or silica envelopes containing appropriate quantities of an inert gas and the element (or one of its volatile compounds) to be excited. In view of this, constructional techniques are discussed first here, followed by separate sections dealing with the operation and characteristics of RF and microwave lamps respectively. As microwave-excited sources appear at present to be of more interest to analytical chemists these are dealt with in more detail. The reader interested in RF-excited sources as alternative absorption sources to hollow-cathode lamps or for specialized fluorescence work will, however, find adequate notes and references to serve as an introduction to the subject.

5.3.2 *Construction of Electrodeless-Discharge Lamps*

Electrodeless-discharge lamp sources suitable for both RF and microwave excitation are available commercially.* In the experience of the authors, however, manufacturers have not (at least until very recently) attempted to produce lamps to meet the specific requirements of analytical chemists, and superior sources are often produced in the laboratory, especially when very high intensity is required for sensitive atomic fluorescence measurements. As the fabrication techniques are also relatively simple, owing to the absence of electrodes, these are described below in sufficient detail for the reader wishing to undertake lamp construction in his own laboratory. This requires only simple glass-working facilities for the preparation of lamp bulbs and a small vacuum line for the filling procedure.

(*a*) *Preparation of lamp bulbs*

The most widely used materials for lamp bulbs are Pyrex glass and (for elements emitting their resonance lines below about 300 nm) transparent silica tubing. The latter is available in suitable spectroscopic grades (such as "Vitreosil" and "Suprasil") from, for example, Jencons Ltd. in the U.K., and Hanovia Lamp Division, Engelhard Industries in the U.S.A. Although both Pyrex and silica are inert to attack by RF or microwave discharges under most conditions, this is not the case with lamps of alkali and alkaline earth elements which frequently show a rapid and irreversible attack on the lamp walls.[48,49,50] The attack appears to be least serious for the heavier alkali metals (e.g. rubidium[48]) on Pyrex, but in other cases it is only

---

* For example, RF lamps have been supplied by Varian and microwave lamps by Ophthos Instrument Co., and Scintillonics-Interface Inc. in U.S.A. and EDT Supplies Ltd., EMI Electronics Ltd., Thermal Syndicate Ltd. and Southern Instruments Ltd. in U.K.

possible to use the lamps for a very short experiment. In certain cases it is possible to reduce the rate of attack by forming a protective layer of borate glass on the inside of the lamp as the metals will not react by displacement of boron owing to the much greater stability of the B—O bond compared to the Si—O bond. This may be achieved with Pyrex (borosilicate glass) by washing the inner surface of the lamp with hydrofluoric acid solution[49,50] to remove a layer of silicon and leave a borate glass surface. Alternatively, both Pyrex[48] and silica[50] may be internally glazed with a protective layer of borate glass by wetting the lamp bulbs with a saturated solution of boric acid followed by heating to a high temperature. Neither method is very effective for obtaining a long operating life, as in the former case the layer is very thin and in the latter the protective surface eventually cracks. A much more effective solution to the problem[50] involves the use of commercially available* two-ply glass having an outer layer of soda glass and an inner ply of silica-free glass intended to resist attack by sodium vapour. However, this glass is more difficult to work and seal than are conventional types and although it gives long-lived lamps with magnesium its transmission is very low at the 285 nm resonance line.

A variety of shapes have been used for the lamp bulbs but some of the more simple designs seem adequate for most purposes. Early work with RF discharges favoured cylinders one or two centimetres in diameter and perhaps 10 cm long, although bulbs with capillary sections (to produce a "thread" of discharge of great intensity) and very long cylinders (up to 2 m) were also common.[5] More recently, spherical bulbs have been popular, especially for lamps of the alkali metals,[15,48,51,52] and they allow the maximum possible output intensity while retaining the advantage of a wall discharge. Bulbs ranging in diameter from about 1 to 3 cm have been used. Frequently, cylindrical or spherical RF lamps are encased in heater units (see below) but when these are not required (i.e. for volatile elements) it is often useful to seal the lamp into a Pyrex or silica cover to protect it from draughts as the vapour pressure of a volatile metal can fluctuate significantly, even with small temperature changes.

Most work with microwave discharges has been with simple lamps made by sealing at both ends a relatively narrow, thick-walled Pyrex or fused silica tube, as shown in Fig. 5-21(a). The bulbs are usually between 3 and 10 cm long with an internal diameter of

between 5 and 15 mm. Forrester *et al.*[47] examined several more elaborate designs with additional bulbs and constrictions but found no advantages for most elements. However, they did suggest that the greatest intensity from a high-power microwave discharge could be obtained by constricting it to a diameter of about 1 mm. As even a silica capillary of this diameter would melt and seal itself under these conditions, it was necessary to use a tube of 1 mm x 4 mm cross-section. This design has not been widely used, partly because ordinary tubing is more widely available and partly because of the severe loss of line sharpness when the discharge is operated in this mode. Protective cases have not been widely used with microwave lamps as some protection from draughts is usually afforded by the cavities used for excitation (see Section 5.3.4(b)). However, the use of a vacuum jacket around the bulb has recently been found advantageous for some elements[53,54] and allows a higher and more uniform operating temperature.

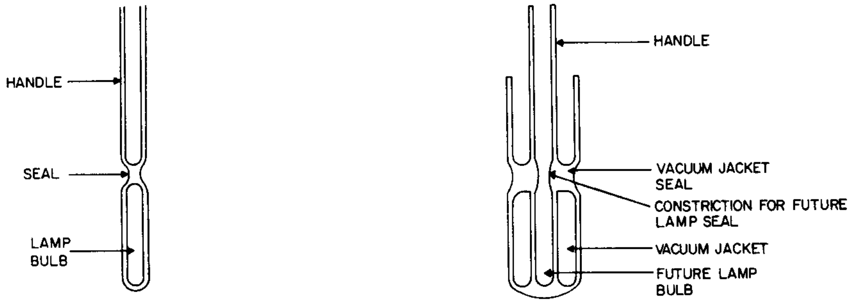

Fig. 5-21. Microwave electrodeless discharge lamps. (a) Finished lamp of simple, conventional design; (b) lamp blank with evacuated outer jacket already in place.

Some care is needed in the final preparation of lamp bulbs for both RF and microwave discharges to remove any trace contamination. Even when the spectra of such impurities are unimportant for a particular application, they may cause a significant reduction in the lamp intensity and even a serious shortening of the useful operating life. Thus it is important to clean the bulb blank thoroughly, for example by boiling it in a concentrated nitric/sulphuric acid mixture (1 : 1 v/v) and then rinsing in distilled water and drying. Subsequently, care must be taken not to touch the outside of the bulb with the hands, particularly if silica is used, as traces of oil or grease from the skin may be deposited and impair its operation. For this reason a handle permanently attached to the bulb is useful. For example, the microwave lamp shown in Fig. 5-21 simply has a short

---

* Glass Tubing and Components Ltd., Chesterfield, England; type X93.

piece of the original tubing left in place above the seal. When preparing blank bulbs, the point at which the final seal is to be made should be constricted as much as possible to minimize the heating required when the lamp is completed. This is particularly important with silica because overheating breaks down some of the silica and the oxygen produced may contaminate or even quench the discharge. In view of this, vacuum-jacketed microwave lamps should have the jacket sealed around the blank bulb[54] (as shown in Fig. 5-21(b)) rather than onto the finished lamp. The final stage of blank preparation is degassing to avoid subsequent outgassing during lamp operation. This is achieved by heating the bulb under vacuum. For obvious reasons the process must be carried out just prior to filling and is therefore discussed below in that context.

(*b*) *The vacuum line*

A simple vacuum line design is quite suitable for preparing most types of sealed-off electrodeless-discharge lamps of interest for AAS and AFS applications and the ability to achieve high vacuum conditions is not essential. It should be remembered, however, that although sealed lamps are operated at relatively high pressure (typically in the range 0·1 to 10 torr for microwave-excited lamps), a very much better vacuum is desirable to achieve effective degassing of the lamp walls. As filling of the lamps involves flushing with gas and repetitive pumping down at pressures in the region of 1 torr, a two-stage rotary pump affords a good compromise between efficient pumping in this region and a sufficiently high vacuum for degassing (typically 0·001 torr for a modern pump in good condition). Some workers have suggested[55] that a vacuum better than 10^{-6} torr is required if the lamps are to be degassed sufficiently for use as high-stability sources. It would then be necessary to use an ancillary oil or mercury diffusion pump for the degassing stage of the lamp preparation. Under these circumstances great care is needed to avoid any traces of contamination during construction and use of the vacuum line if long pump-down times are to be avoided.

A basic system suggested for preparation of sealed-off lamps is shown diagrammatically in Fig. 5-22. The cold trap, T_1, is essential, not only to avoid damage to the pump if volatile materials (e.g. iodine) are used in lamp preparation, but also to avoid contamination of the finished lamps by pump oil (the amount of oil vapour diffusing back from most commercial pumps is more than sufficient to cause detectable contamination). A simple "cold-finger" trap cooled in liquid air or nitrogen is sufficient and should be made readily demountable for cleaning if large quantities of volatile materials are used in the system. The second cold trap, T_2, is also desirable, especially if the vacuum gauges used contain mercury which would otherwise almost certainly contaminate the lamps to some extent. This trap is also a useful aid to lamp purity when ordinary commercial grade compressed gases are used for lamp preparation, as these often contain traces of oil and hydrocarbon vapours.

The filler gas is added to the system via a needle valve, NV, which should be of the precision, low-throughput type designed for vacuum use. Such a valve provides the most convenient means of adding gas to a pumped-down lamp in order to reach exactly a particular lamp pressure. It also allows an exact pressure to be set while continuous pumping proceeds; this may be useful at some stages of lamp preparation or to test particular lamp characteristics. The lamp and its connection to the vacuum line may be isolated by two valves, V_1 and V_2. These are situated to allow removal and replacement of lamps without the need to admit air to a large part of the system, as the line is intended for fairly rapid preparation of sealed lamps. However, this does mean that the lamp is not isolated from the valves by any form of trap. Thus, unless greaseless valves are available, great care must be taken during their assembly. The high-vacuum silicone greases or a more traditional type, such as Apiezon N, are suitable, but the smallest possible quantity should be used to avoid any excess entering the line; this would act as a sink for impurities and may itself act as a lamp contaminant. With Apiezon N it is useful, especially if high vacuum is to be used during degassing, to degas the grease before its application. This is easily achieved by placing some of the grease into a glass tube which is heated in hot water while

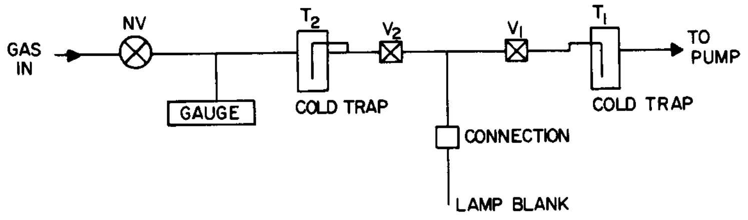

Fig. 5-22. Schematic representation of a vacuum system for the preparation of sealed electrodeless discharge lamps.

under vacuum; after cooling under vacuum the grease should be used as soon as possible.

The means of attaching the lamp blank to the vacuum system also requires some consideration. Sealing of the finished lamp is generally easier if the lamp is mounted vertically rather than horizontally. Obviously, if solid materials are to be added to a blank of the type shown in Fig. 5-21(a) it must be suspended vertically rather than mounted above the line. Attachment of the lamp blank to the line by rubber pressure tubing should be avoided as an almost inevitable source of contamination. Some workers favour direct sealing between the two, but this may present problems when only limited glass-working skill is available; furthermore, the lamp cannot be moved during the sealing process. Use of a cone- or ball-type ground joint is more convenient but still requires the sealing of part of the joint to the optical quality silica used for most lamps. Perhaps the best compromise is the use of an O-ring sealing, high-vacuum metal union. Hand-tightened components suitable for attachment to glass tubing are widely available and relatively inexpensive. They may be repeatedly resealed as no swaging of joints is necessary and the best types are quite adequate even for high vacuum (10^{-6} torr). If the O-ring is lightly greased the lamp is easily rotated to facilitate the final sealing.

The vacuum gauge indicated schematically in Fig. 5-22 may in practice take one of several forms, depending on the particular lamp preparation technique and the justifiable expense. The simplest suitable gauges are the rotatable miniature McCloud types. These have the disadvantage of precluding continuous reading of the pressure but they do give correct direct measurement with all gases and vapours and are relatively inexpensive. Mercury contamination does not occur when the gauge is isolated by a cold trap, as mentioned above. In most systems two of these gauges would be necessary, one reading *ca.* 0·001 to 1 torr and the other *ca.* 0·1 to 10 torr. Most of this range could also be covered by using the largest type of *precision* barometric gauges (not the simple types used in rough vacuum systems). These are relatively expensive and rather cumbersome, but have the advantage of continuous reading while still showing identical response to all gases and vapours. Remote reading electrical gauges are often preferred despite the need of different calibrations for each gas used in the system and the risk of serious errors when vapours are present. Care should be taken to select a commercial unit that gives adequate precision at the pressures needed for filling the lamps (for example, many Pirani gauges are unreliable above *ca.* 1 torr). A suitable electrical gauge (such as the Penning type) is generally the best choice as a monitor when high-vacuum degassing is to be used. Careful positioning of the gauge head is then required if a true indication is to be obtained of whether the lamp has reached, say, 10^{-6} torr, as errors are easily made at this degree of vacuum.

(*c*) *Materials used in lamp preparation*

Helium, neon and argon have all been used as the filler gas, although argon seems to be the most popular. It is readily available; it produces a large, stable discharge over at least* the pressure range 0·1 to 10 torr and thus allows the pressure to be optimized for the vaporization characteristics of the material used in a particular lamp. Furthermore, serious spectral interference due to its background spectrum has not been widely reported in AAS and AFS applications. As with early work on the hollow-cathode lamp (see Section 5.2.3(c)), however, direct comparisons between the three gases are rarely found in the literature. Thus, it may be worthwhile to investigate each of the gases for a particular application whenever optimum performance is essential. Ultra-high-purity (research grade) gases are unnecessary except for special applications (for example, where it is necessary to exclude the other inert gases or oxygen or nitrogen in order to obtain an extremely pure spectrum); generally "high-purity" cylinder gases are quite adequate for lamps prepared for AAS and AFS, especially if added to the lamp via a suitable trap to remove any volatile impurities.

The form in which an element is added to the lamp is of vital importance for successful lamp preparation. As there is no sputtering mechanism of the type found in the hollow cathode, the material used must produce the correct vapour pressure of the element at the operating temperature of the lamp. In many cases the range of vapour pressures for optimum performance is small and a high proportion of erratic or poor results in lamp preparation may be traced to this cause (see Section 5.3.5). Most metals will not have the correct vapour pressure at the "normal" temperature of an RF or microwave discharge and two courses of action are open: either the lamp itself may be cooled or heated, or a more suitable form of the metal may be used at the preparation stage. The former solution has

---

* Sealed microwave-excited lamps may prove difficult to initiate at pressures below about 1 torr.

been widely used for RF discharges but less so with microwave excitation (see Section 5.3.4 and 5.3.5), although the latter does offer the possibility of quite wide changes in temperature by careful choice of gas pressure, microwave cavity and operating power. Careful choice of the compound used has been widely advocated for the preparation of microwave lamps.[56-58]

It is not possible to give an exact criterion based on vapour pressure for the selection of the best compound of each metal; there is no real substitute for practical experience of preparing lamps for an actual analytical application. However, as a very general guide it can be said that materials having a vapour pressure of about 1 torr at 200-400°C will usually prove suitable. Most microwave-excited lamps described in the literature have used either the pure metal or one of its halides, or sometimes a mixture of the two. Generally the iodide is the most popular (owing to ease of handling) with the chloride as an alternative when its vapour pressure is more suitable; few lamps using the metal bromide have been reported. Although very high purity chemicals (for example, the so-called "spectroscopic grade") are unnecessary for the applications described here, it is important to avoid sealing into the lamp bulb impurities such as water or free iodine. For this reason, many workers prefer to prepare the halides when required, actually *in situ* in the lamp bulb or in an adjacent part of the vacuum line. This is particularly easy with the iodides which can often be made simply by heating a small quantity of pure iodine with a slight excess of the metal. Chlorides are best prepared by heating the metal in a stream of chlorine gas.

(*d*) *Lamp assembly*

This final stage of lamp construction involves four important steps: the cleaned and prepared lamp bulb is attached to the vacuum line and degassed; a small quantity of the metal or a suitable compound is added to the bulb; the correct pressure of filler gas is introduced; the bulb is then permanently sealed off by melting the glass or silica. Each of these steps must be carried out in the correct manner if a lamp giving optimum performance and extended operating life-time is to be obtained.

The complexity of the degassing procedure varies greatly with lamp preparation methods described by different workers. Although considerations of the operating temperature of the EDL, the required working life and spectral purity are important factors, the method of adding the metal to the lamp after degassing must be taken into account before deciding how elaborate the process should be. If the lamp is to be re-opened to the atmosphere after degassing, as recommended by West and co-workers,[58] it is obviously pointless to carry out a prolonged process at high temperatures and under high vacuum. Similarly, if degassing is to be carried out with the sample actually *in situ*, as suggested by Corliss and co-workers,[56] prolonged heating of the whole lamp is not feasible. Under these conditions it is probably adequate to flush the lamp several times with the filler gas at a pressure of a few torr while sparking the bulb with a Tesla coil. The gas discharge will then scrub water vapour and gases from the surface of the walls. After pumping the bulb down using a conventional rotary pump (i.e. to a pressure in the range 0·1 to 0·001 torr), the bulb is heated with a blow torch for a few minutes to drive off impurities situated deeper in the walls. If possible the softening point of the glass or silica should be approached. The procedure of Corliss *et al.* (where the sample is already in the lamp) is probably preferable to subsequent demounting and this process must then be carried out in two stages, heating half the tube at a time while the other half is wrapped in wet asbestos tape so that the sample remains condensed. The impurities driven from the walls* should then be flushed out with fresh filler gas.

To obtain the highest spectral purity, discharge stability and long operating life-time, a more elaborate degassing method than that described above should be used. This is also most important when EDL sources are to be operated at high temperatures to obtain discharges from relatively involatile substances such as compounds of the rare earths.[57] High-vacuum conditions (better than 10^{-6} torr) attainable with an ancillary diffusion pump are then necessary. If degassing is effected solely by heating, the lamp should be held near its softening point for 1-2 hours and it is then much more convenient to use a small demountable furnace for heating instead of a torch. Alternatively, Gleason and Pertel[55] suggest that the scrubbing process described above should be carried out with great care at 5×10^{-7} torr; they also find that excitation of a microwave discharge in a few torr of argon helps the process and gives a good indication of the extent of degassing (pure argon gives a violet plasma which becomes milky white when excessive water vapour is present on the walls of the lamp).

When extensive degassing under high vacuum is to be carried out it is also necessary to resort to a more elaborate means of introducing

* Together with oxygen formed by actual decomposition of silica at high temperatures.

the solid sample than simply placing it in a lamp bulb of the type shown in Fig. 5-21. Tomkins and Fred[57] suggested sealing the solid under vacuum into a capillary tube placed in the vacuum line. This tube may subsequently be moved into the degassed lamp and broken open by the judicious use of iron slugs and magnets. An easier solution to the problem is the use of a lamp blank with one or more side-arms, such as that shown in Fig. 5-23. This particular configuration was used by Gleason and Pertel[55] for a microwave-excited mercury lamp, but the principle is readily applied to many other applications with only minor modifications. The tube R_3 is the final lamp bulb and the sample is kept cool in R_1 while R_3 and R_2 and their connecting tube are thoroughly degassed as described above. With the unit under high vacuum, R_2 is cooled and some of the sample is driven into it by warming R_1. The absence of impurities from R_2 and R_3 is then checked, with further argon scrubbing if necessary, before adding gas at the correct pressure to the unit and sealing at the point "a". Finally, the correct amount of sample is driven into R_3 by heating R_2 before sealing the finished lamp bulb at point "b".

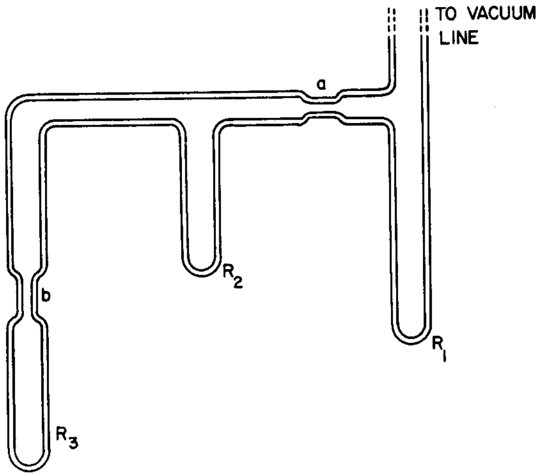

Fig. 5-23. Discharge lamp blank with side-arms for preparation of lamps with elaborate high-vacuum degassing.

Whichever method is used to introduce the sample into the lamp bulb, several general precautions should be observed. In the first place, it is not sufficient to leave a lump of solid or a few grains of powder in the bulb; the material must be heated and then recondensed on the lamp wall to degas it and drive off any water vapour which may be present. This is usually best achieved using a microburner as very little heat is required for the small amounts of solid involved. When the solid has been added directly to the final lamp bulb it is best to repeat the process several times, driving the material up and down the walls. If an iodide is prepared *in situ* it is essential to drive off any excess free iodine. Although only a few milligrammes of solid are normally added initially, even this is more than is needed (successful small microwave lamps have been prepared with as little as 0·1 microgramme of sample). Thus only a very narrow band of material needs to be left on the wall, the excess being driven out of the bulb by the heating process. There has been some discussion in the literature over the importance of the amount of material used, although until recently no attempt was made at a systematic study. For example, Worden *et al.*[59] found that curium lamps showed self-reversal when 1 mg was used but not with 100 μg; Silvester and McCarthy[60] reported that cadmium lamps gave greater intensities when containing 5 mg of solid than when 35 or 50 mg were used. On the other hand, Winefordner and co-workers[61] observed no systematic correlation between lamp performance and amounts of material in the range 0·23-10 mg.

In fact, the importance of the quantity of material depends to a large extent on the mode of lamp operation.* If the vapour pressure in an RF or microwave-excited lamp is carefully controlled by thermostating the operating temperature of the lamp with external heating (or sometimes cooling), the amount of unvaporized material left will have little effect. A number of workers appear intuitively to have obtained this condition in microwave-excited lamps where the discharge is the sole source of heat, by critical adjustment of the discharge condition, the position of the lamp in the microwave cavity, the excitation power, and the flow of cooling air. However, under these circumstances it is easier to obtain *reproducible* results if the lamp is operated so as to vaporize completely all material present in the bulb, and the amount of material added during construction then becomes of major importance. This is confirmed by a recent study reported by Cooke, Dagnall and West.[62] In order to obtain high precision and reproducibility when adding minute quantities of material to the lamps, they used the technique of preparing lamps with 5 or 10 μl aliquots of aqueous solutions. The water was

---

* This topic is discussed further in Sections 5.3.4 and 5.3.5.

removed under vacuum prior to subliming the material onto the lamp wall and then proceeding as described above. Provided suitable solutions can be prepared, this technique should prove most useful, especially when using a lamp blank with side-arm of the type discussed above. The material could be deposited on to the limb R_1 using a separate rough vacuum line before proceeding with the degassing and material transfer stages in the same way as with a more usual solid sample. The importance of adding a small, carefully controlled quantity (by whatever technique) to microwave lamps operated with complete vaporization is illustrated in Fig. 5-24. This shows the atomic fluorescence and atomic absorption signals obtained using microwave-excited zinc lamps containing small amounts of $ZnCl_2$ over a range of operating power. It can be seen that self-absorption (indicated by loss of absorption sensitivity) followed by self-reversal (indicated by loss of fluorescence sensitivity) is observed at progressively lower microwave power as the amount of material is increased.

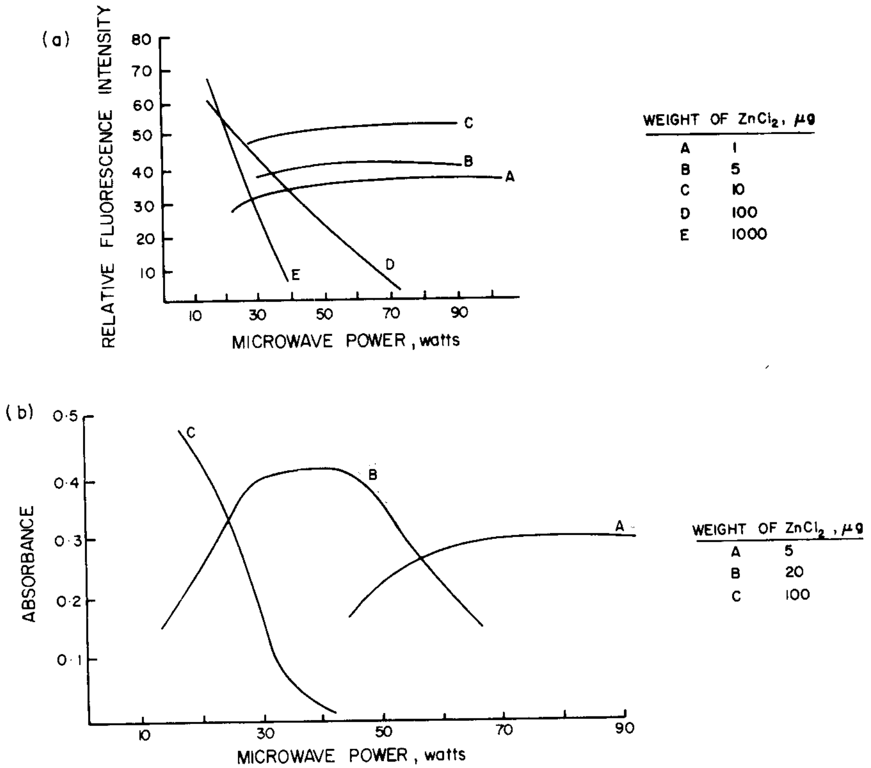

Fig. 5-24. Effect of microwave power on performance of zinc electrodeless discharge lamps containing different weights of $ZnCl_2$.[62]

Once the correct amount of sample has been placed in the degassed lamp bulb the filler gas may be added at the required pressure. Again, careful optimization for a particular application is necessary and the only general guide that can be given is that between 2 and 5 torr of argon is often a useful pressure for first consideration. If many tests are to be made to prepare a high-performance lamp it is useful to test the discharge on the vacuum line (possibly with a flow of gas at the chosen pressure), or alternatively it may be more convenient to use a demountable lamp fitted with a tap[60] for preliminary experiments. When the finished lamp is finally sealed off, care is still required to avoid unsuccessful results; it is most important to avoid excessive heating of the glass or silica. If the lamp walls have not been thoroughly degassed, sufficient impurities may be driven into the bulb to contaminate or even quench the discharge (the lamp seal is unlikely to reach such a high temperature during normal operation). An equally important effect occurs with silica lamps, irrespective of the efficiency of the degassing, and has frequently been overlooked. Owing to the high melting point of the silica, some decomposition inevitably occurs during the sealing operation and oxygen may be driven into the lamp. If a large area of silica is heated for a long period the amount of oxygen may be sufficient to quench the discharge completely, especially when unusually low filler-gas pressures are used. In fact, many "inexplicable" failures or instabilities of lamps may originate from this source.

5.3.3 Operation and Characteristics of Radio-Frequency-Excited Electrodeless-Discharge Lamps

Electrodeless-discharge lamps may be excited at radio frequencies in two modes of operation. Many spectroscopic applications have used a type of RF glow discharge for which two ring electrodes are mounted on the outside of a cylindrical lamp at a suitable distance apart.[5] It is possible to maintain these discharges over a very wide pressure range (about 10^{-3} to 10^2 torr), so that the metal vapour pressure may often be optimized without the need for an additional pressure of inert gas to support the discharge. This may be an advantage for some applications, but such sources have not been widely applied as sources for absorption or fluorescence measurements, although L'Vov[15] has used a mercury AAS source of this type operated at 145 MHz.

More recent interest for absorption and fluorescence applications has been shown in an annular type of discharge excited by positioning the lamp within the field of the coil of an RF generator. The discharge is then maintained only over a very narrow pressure range and the lamp is filled with an inert gas at the correct pressure (e.g. 1 or 2 torr of argon). Some care is needed in the choice of characteristics for the RF oscillator circuit to obtain the best results. For example, it is important to obtain a clean waveform without spurious oscillations over the whole range of currents to be used. This facilitates maintenance of a true skin discharge and also ensures that the available power is used mainly to heat the lamp envelope and to excite low energy lines (rather than unwanted non-resonance lines from higher energy levels). Similarly, although the discharge is maintained by the RF magnetic field, sufficient RF electric field must be present to initiate it. There is also a minimum frequency for any given lamp below which a discharge will not start (depending on the mean free path of an electron in the vapour for each cycle of the applied field). As the lamps have a strong negative coefficient of resistance, the oscillator should approach as closely as possible the characteristics of a constant power source; in most cases a further worthwhile improvement in lamp stability results from using a current-stabilized supply for the oscillator valves.

Lamps of this type have been described for a fairly wide range of elements, both with and without auxiliary heaters. Bell, Bloom and Lynch[48] prepared spherical lamps of 10 mm diameter for the alkali metals and operated them in the assembly shown in Fig. 5-25.* The lamp is mounted under a glass cover immediately above the exciting oscillator with a common case. Heat from the thermionic valves is thus used as an auxiliary source for the lamp and the entire package acts as an efficient heat sink to stabilize the lamp operating temperature. The temperatures shown in the diagram are the equilibrium values reached at the recommended operating current for a rubidium lamp. Although this system provides a simple, compact lamp unit, it has the disadvantage of operating properly only at the current for which the package was designed (the corresponding shell temperatures for Cs, K and Na are 40, 80 and 120°C, respectively). Thus adjustment of the lamp output by changing the excitation current is not recommended. To overcome this problem while still maintaining good temperature stability (for precise fluorescence measurements with the alkali metals), Atkinson, Chapman and Krause[49] designed a cylindrical lamp in which the base is used as a metal reservoir and is mounted in a heater block. This allows accurate independent control of the operating current and the metal vapour pressure; the discharge alone maintains the base reservoir at about 70°C and this may be gradually increased to about 200°C using the heater (which is thermostated to give stable operation). On the other hand, other workers have reported sufficient stability of spherical RF lamps for their use as sources in AAS simply by covering the bulb and coil to prevent convection currents and exclude draughts, the lamp temperature being adjusted via the excitation power. Thus L'vov and co-workers[15] have prepared convenient AAS sources for Rb, Cs, K, Na, Zn, Cd, Hg, Se and Te, while Ivanov and co-workers,[63,15] have extended the range to include As, Bi, Ca, Cu, Fe, Ga, In, Mg, Mn, Mo, P, Pb, S, Sn and Tl (owing to the low volatility of Fe, Mn, Mo and Cu it was necessary to prepare the lamps using $FeCl_2$, $MnCl_2$, MoO_3 and CuI_2). Apparently, some of these lamps are now available commercially in the USSR.[15]

The designers of the RF lamps described above have all reported that in their particular applications these sources offer a considerable improvement over more conventional alternative devices. For example, Atkinson *et al.*[49] compared their alkali metal RF lamps with commercial vapour-discharge lamps (see Section 5.4.1) as sources for sensitive atomic fluorescence measurements. From the observations at the 766·5 nm resonance line of potassium (Fig. 5-26) it is evident that the integrated intensity measured with a normal spectrometer is about twice as great for the RF lamp and shows fairly similar increases with both lamps. However, the simultaneous change in the halfwidth of the line (shown in the second diagram) is quite modest for the RF lamp, whereas there is a very sharp increase in line-width for the vapour-discharge lamp. This has a considerable effect on the observed fluorescence intensity, as illustrated in Fig. 5-27. When the potassium vapour pressure in the fluorescence cell is below 10^{-2} torr the vapour-discharge lamp produces no significant fluorescence, whereas the RF lamp is most efficient at low vapour pressures. In fact, at very low vapour pressures the absorption line is narrower than the incident exciting line from the RF lamp. Thus, as the vapour pressure in the cell is increased the broadening of the absorption line gradually matches its width to that of the exciting

---

* This design formed the basis of the Varian commercial RF lamp.

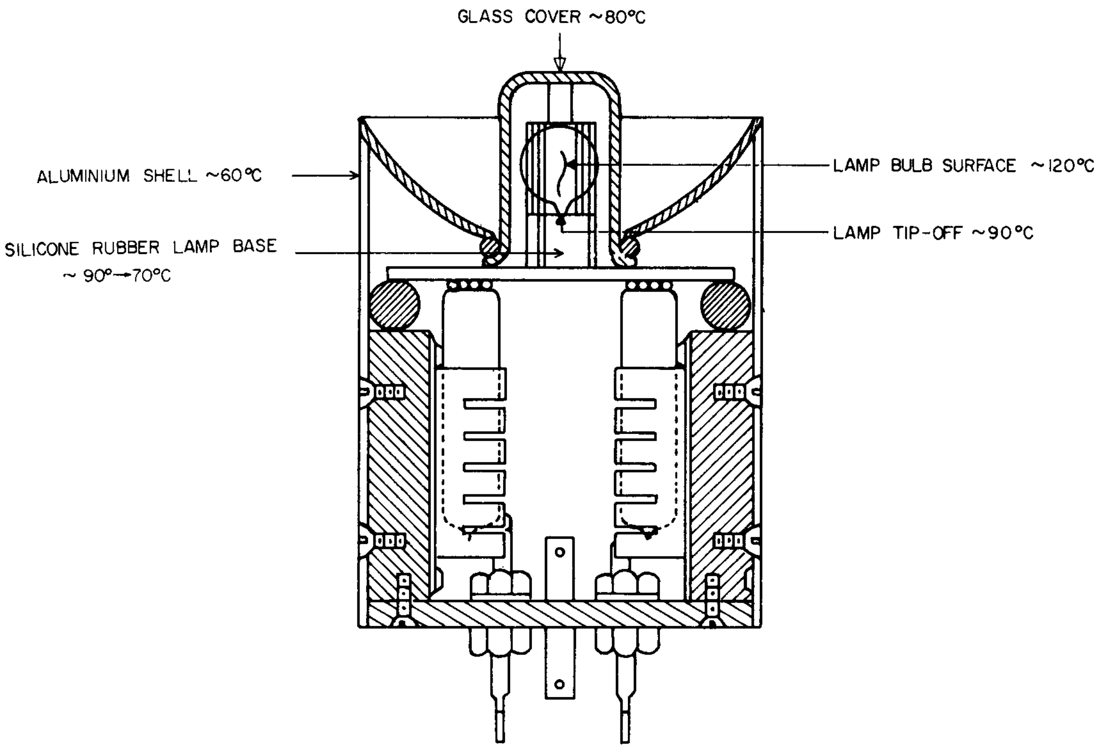

(a) Assembly used for a Rb lamp

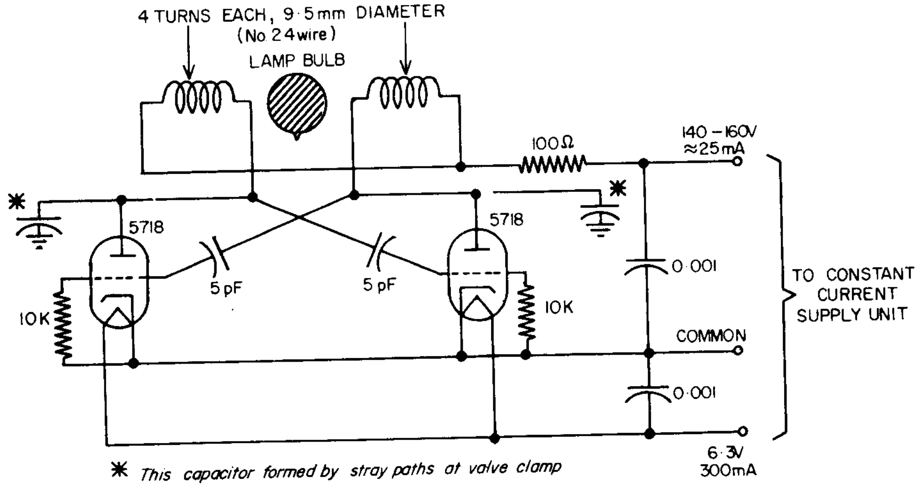

* *This capacitor formed by stray paths at valve clamp*

(b) Oscillator circuit

Fig. 5-25. Compact radio frequency exciter assembly used with alkali metal electrodeless discharge lamps.[48]

line and a small maximum in the fluorescence intensity is obtained. The second peak for the RF lamp (as well as that for the vapour-discharge lamp) results from increasing self-absorption in the fluorescence cell at higher potassium concentrations (see Section 4.4).

In a similar fashion L'Vov[15] has compared the spectral characteristics of the spherical RF lamps with those of hollow-cathode lamps from the point of view of their use as sources for AAS. He reports that, for the cadmium 228·8 nm resonance line, equal line-widths for the two sources are obtained when the intensity from the RF lamp is about 1000 times that obtained with the hollow-cathode lamp. By reducing the current to the RF lamp it was possible to improve the line sharpness considerably while maintaining a greater intensity than is available from the hollow-cathode lamp. Similarly, Ivanov *et al.*[63] reported similar AAS sensitivities for a number of metals using both hollow-cathode and spherical RF lamp sources, but the source intensity was considerably better in the latter case (e.g. a 200-300-fold improvement at the Cu 324·7 nm line). It was found that the background spectrum in these sources using xenon as filler gas was of no significance (e.g. 0·1 to 0·2% of the line intensity at the Sb 231·1 nm and Pb 283·3 nm lines). L'Vov[15] suggests that even less background emission is obtained with argon as filler gas and that lamp stability and noise are no worse than for the hollow-cathode source when the working conditions are correctly chosen.

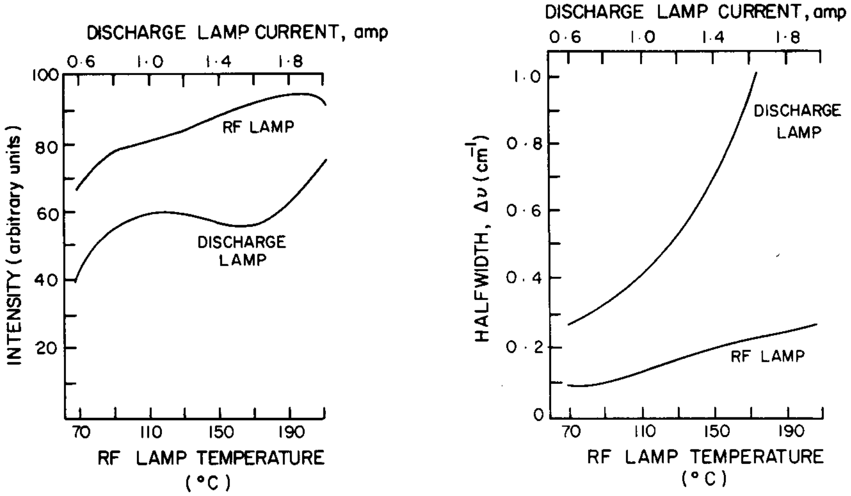

(a) Integrated relative intensities

(b) Halfwidth of the line

Fig. 5-26. The comparative effect of operating conditions on the potassium 776·5 nm resonance line for a vapour discharge lamp and a radio frequency electrodeless discharge lamp.[49]

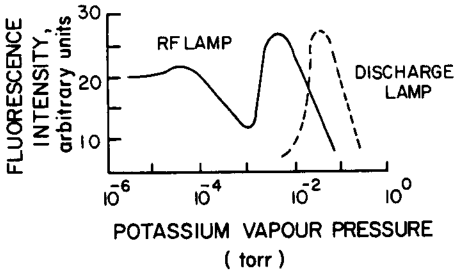

Fig. 5-27. Variation of potassium fluorescence intensity with vapour pressure, excitation at the 776·5 nm line with a radio frequency electrodeless discharge lamp or a vapour discharge lamp. (The curves are normalized to show equal peak intensities.)

5.3.4 *Operation and Characteristics of Microwave-Excited Electrodeless-Discharge Lamps*

(*a*) *Power supplies*

The construction of a microwave generator is, as mentioned above, more complex than the assembly of a dc or RF power source and requires a considerable knowledge of specialized microwave techniques. This situation has had two main consequences for the development of microwave excitation of electrodeless-discharge lamps. In the first place, although many reports are to be found in the literature describing the designs of the lamps themselves and even of suitable microwave cavities, there are very few descriptions of complete microwave generators or specialized modifications of interest to the spectroscopist. Secondly, almost all reported applications of microwave-excited lamps have used commercially available generators which are either actual medical diathermy units or "spectroscopic power supplies" produced by minor modifications to such designs. Thus, with but few exceptions, "microwave" excitation may be interpreted as excitation at the standard 2450 MHz frequency generated by the magnetron valve used in these units. However, some early generators were modified from surplus radar equipment: Jacobsen and Harrison[46] used excitation at 3000 MHz, and recently Kikuchi[64] has operated a lamp at 35 GHz (i.e.

35,000 MHz) using a klystron valve source. The following discussion deals exclusively with lamps and equipment operating at 2450 MHz.

Although medical diathermy units are readily available and relatively cheap, they may sometimes be unsuitable for use with discharge lamps intended as sources in AAS or AFS. The most serious problem is the frequent lack of any form of stabilization for the power supply to the magnetron valve; as a small percentage change in the anode voltage may alter the microwave output by 50 watts or more, such a generator can show somewhat erratic behaviour. Furthermore, the rectification of the high-voltage supply to the magnetron is sometimes rather unsatisfactory, leading to considerable mains frequency modulation of the microwave output. This may cause problems in certain spectrometers when the radiation from the lamp is chopped for use with a modulated detection system whose frequency is mains-derived. Generators sold specifically for spectroscopic use generally have a more sophisticated rectification circuit and this problem is less likely to arise. In many cases some form of stabilization for the magnetron power supply is also introduced, often by applying the voltage to the magnetron via series resistors. As explained for hollow-cathode lamp supplies (see Section 5.2.4(a)), this will minimize the change in anode current (and hence microwave power) resulting from a given fluctuation in the supply voltage. Even so it may still be advantageous to operate the generator from a voltage-stabilized power supply unit (although one with a sufficiently high power rating may not be readily available in many laboratories) and such a device should be particularly useful with generators intended for medical use.

Unfortunately, the change of magnetron power with voltage is so large that even these precautions may prove inadequate for the very stable light sources required for AAS and AFS work; a supply voltage stabilized to 0·1 per cent could still give output fluctuations of several watts for a generator with 100 to 200 watts full power rating. There also remains the effect on the anode current of changes in the load applied to the magnetron (caused by variations in discharge and lamp characteristics; see below). As the magnetron's power *vs* current characteristic is much steeper and almost a linear variation,* it would seem that more satisfactory results should be obtained by using a current-stabilized circuit for the magnetron supply. Practical considerations make the direct regulation of the magnetron current difficult, however, and until recently the authors were not aware of any commercial units or published circuits that achieve it at reasonable cost. Brandenberger[65] has pointed out a method which avoids this difficulty and has described a relatively simple modification to a commercial microwave generator. As the basic circuits of many of these units are quite similar, it should be possible to apply Brandenberger's modification without serious difficulty to currently available designs. The additional expense should be worthwhile for many applications as Brandenberger observed the output of a helium-discharge lamp operated at 50-60 watts to have a stability (long term and short term for ±5% changes in mains voltage) of about 0·1% as well as a total rms ripple of about 0·1%. It should be remembered, however, that even a current-stabilized device cannot compensate for the changes in lamp condition which are often responsible for the fluctuations in output observed with tubes containing metal vapour as well as the inert gas (see below).

As explained for the hollow-cathode source (see Section 5.2.4), when modulation of the lamp output is required use of a rotating chopper is almost always less satisfactory than direct electronic modulation of the lamp power supply. This is particularly true when electrodeless-discharge lamps are to be used as high-intensity fluorescence sources (as the chopper entails a considerable loss of the available radiation) and several commercial microwave generators are now available with facilities for modulation of the microwave output at a suitable frequency. This is achieved by modulation of the anode current of the magnetron oscillator. A relatively simple modification[66] to produce this effect involves superimposing an ac component on the dc potential of the anode using a transformer. However, this has the disadvantages[54] of working efficiently only with low-frequency sinusoidal waveforms (owing to the use of the transformer) and of frequently giving a distorted waveform on the output as a result of the relatively high dc current carried by the secondary winding of the transformer. More satisfactory results may be obtained when an adequate stabilized power supply is used for the magnetron simply by adding the desired waveform to the reference element of the circuit using a low-power signal generator. In this way it is possible to obtain reliable modulation with any waveform and at high frequencies (>100 kHz if necessary). It should be remembered, however, that with any system of modulation the electrodeless discharge lamp itself and possibly the actual emission line observed may have a considerable effect on the ease with which 100% modulation of the emitted radiation is attainable at a particular

---

* A useful rough guide for the magnetron output is that an anode current of 1 mA represents a microwave power of about 1 watt.

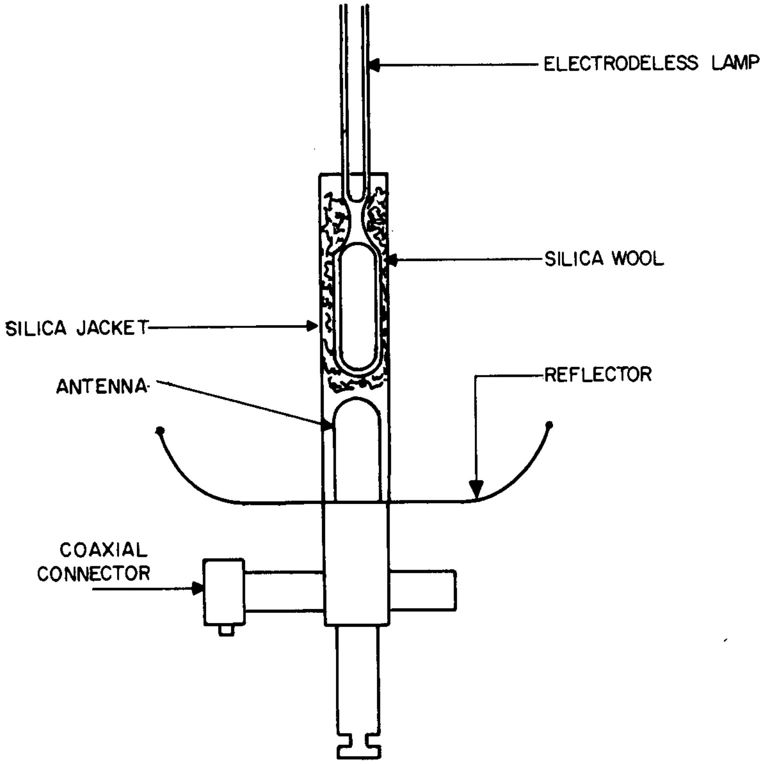

(a) Open A-type antenna with thermal insulation of the lamp body.[61]

Fig. 5-28. Operation of microwave excited electrodeless lamps with an antenna device.

frequency. For example, Phillips[67] was able to obtain 100% modulation above 150 kHz for a helium lamp, but only up to about 110 kHz for iodine-argon and mercury-helium lamps. At low frequencies (less than 100 Hz) it may be necessary to set the depth of modulation* considerably below 100% to maintain the discharge, owing to the finite lifetime of the ions in the discharge.

(*b*) *Transfer of power to the discharge*

Reliable operation of any microwave generator can only be obtained when the power is efficiently transferred to the gas in the discharge. This is achieved either by focusing the microwave radiation onto the lamp, using an antenna device with a reflector or by placing the lamp in a cavity whose resonant frequency is tuned to 2450 MHz to increase the field strength in the gas. In recent years relatively few workers have used antennae (see for example refs. 53,

---

* Modulated microwave generators usually have provision for continuous variation of the depth of modulation from 0 to 100%.

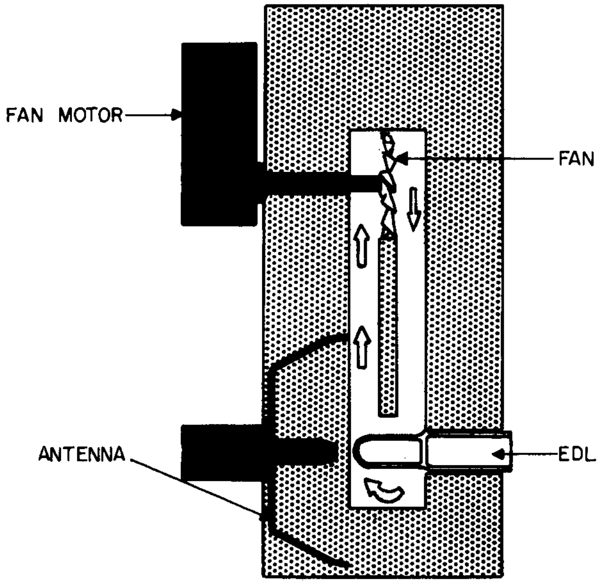

(b) A-type antenna incorporated in a temperature-stabilized lamp housing.

55, 60 and 61), an example of which is illustrated in Fig. 5-28(a). Antennae appear to be less efficient than the best of the resonant cavities and as a result of the exposed position of the lamp it is often difficult to maintain the lamp at a sufficiently high temperature to vaporize metals or their compounds (hence the insulating jacket shown in Fig. 5-28(a)). This problem appears to have been overcome in a commercial unit* which incorporates an A-type antenna in a temperature-controlled lamp housing (see Fig. 5-28(b)). It is claimed that use of a small forced air oven attached to the unit allows the lamp temperature to be maintained within ±0·1°C of a predetermined optimum value, ensuring optimum high intensities with good stability and lamp life. Furthermore, the diffuse microwave output obtained from the antenna is said to avoid the need for critical tuning and positioning of the EDL inherent in many designs of resonant cavity (see below); this simplifies operation and improves the stability of the discharge.

Most reports of microwave-excited discharge lamps concern the use of resonant cavities, usually one of a range of "standard" designs. The most popular of these are available commercially (often from

---

* Scintillonics-Interface Inc., Fort Collins, Colorado 80521, U.S.A. Based on the design of Winefordner and co-workers.

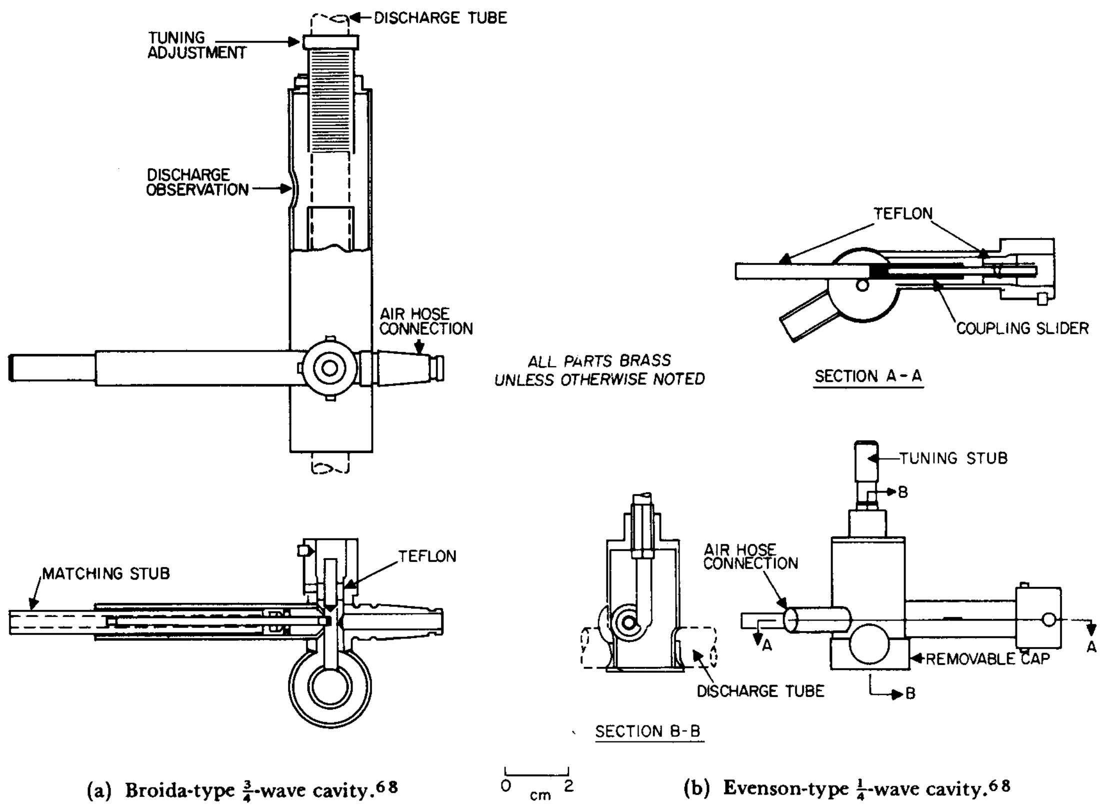

(a) Broida-type $\frac{3}{4}$-wave cavity.[68]

(b) Evenson-type $\frac{1}{4}$-wave cavity.[68]

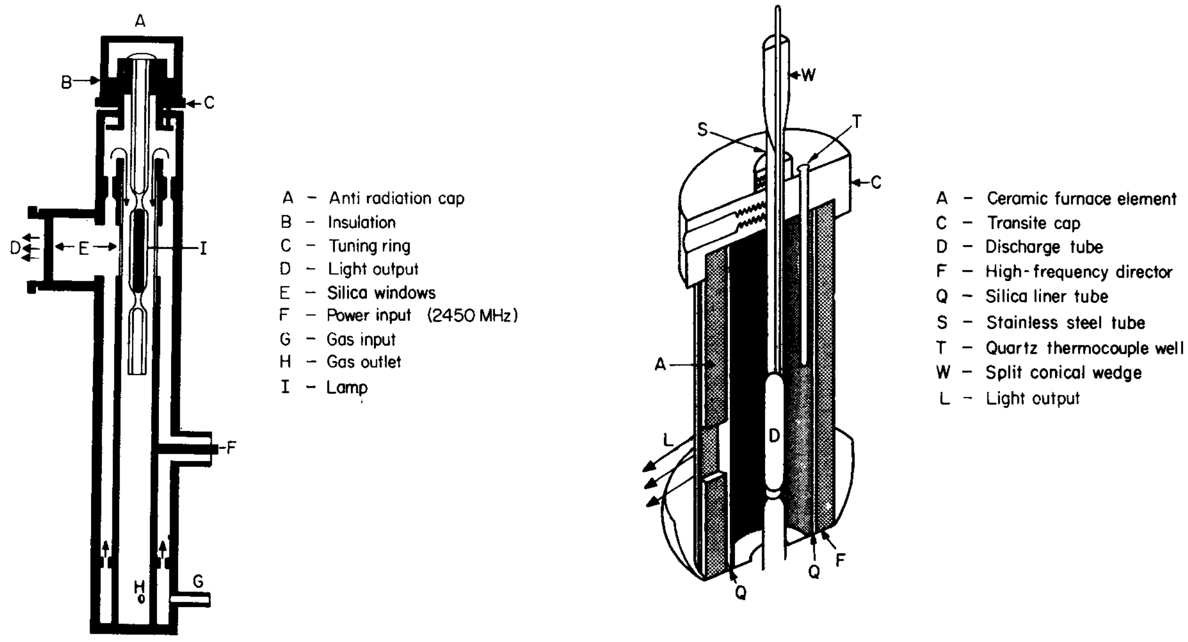

(c) Commercial $\frac{3}{4}$-wave cavity specifically designed for use with AAS and AFS sources (*EMI Electronics Ltd.*)

(d) Furnace assembly incorporating a cavity for high temperature operation of discharge lamps[57]

Fig. 5-29. Some types of cavity used in microwave excitation of electrodeless discharge lamps.

the manufacturer or distributor of a microwave generator) but they are all fairly straightforward, and construction to an existing design should present no serious difficulties. The main features of a number of the "standard" designs have been reviewed by Fehsenfeld *et al.*[68] These workers point out that the presence of a discharge within the cavity changes both the resonant frequency and the load presented by the cavity to the microwave generator. Furthermore, the properties of the discharge vary with the nature of the species present and the pressure. Hence, the most efficient designs provide both a tuning adjustment (to allow the resonant frequency of the cavity to be adjusted to the microwave frequency) and a coupling adjustment (for matching the cavity load to the generator) with sufficient degrees of variation for a wide range of discharge conditions. In some designs (including some available commercially) the coupling adjustment may give an inadequate range, or be omitted altogether. However, Schrenk *et al.*[69] have described the construction of a simple impedance-matching transformer which can be inserted between an existing cavity and input cable.

Two cavities that have been particularly widely used are illustrated in Fig. 5-29(a) and 5-29(b). They are respectively, the Broida-type $\frac{3}{4}$-wave cavity and the Evenson $\frac{1}{4}$-wave cavity. Of the two, the latter gives more efficient transfer of microwave power to the discharge over a wide range of pressures but has the disadvantage of requiring critical tuning to achieve this performance and sometimes giving arcing between the tuning stub and the coupler at this setting. McCarroll[70] has found that both these problems can be eliminated or made less serious by the addition of extension tubes $\lambda/2$ (or more) long to both sides of the cavity along the length of the discharge tube. Although both cavities have provision for forced air cooling of the lamp, the open form of the Evenson design makes it considerably more susceptible to fluctuating temperatures in the lamp than is the Broida cavity. This can prove a serious problem in obtaining good lamp stability for certain elements, since significant fluctuations in the population of metal atoms in the discharge may result. For this reason many workers have preferred to use the Broida cavity for excitation of lamps used as sources in AAS and AFS. Even so the thermal stability may be inadequate for some applications and the modified $\frac{3}{4}$-wave cavity shown in Fig. 5-29(c) should afford a further improvement. The lamp tube has a silica shield immediately adjacent to it inside the cavity, radiation leaves the cavity via a second silica window mounted on the outer wall. Thus, hot or cold air can be passed around the lamp in a carefully controlled manner using the small inlet and outlet tubes. Adjustment of the lamp power and the air flow rate (together with the actual input temperature of the air in difficult cases) allows a stable optimum temperature to be maintained for a wide range of lamps used in AAS and AFS. The cavity provides for tuning of the resonant frequency by adjustment of the coaxial gap, as in the Broida-type, but no coupling stub is fitted and in certain cases it may be advantageous to use an external matching device as mentioned above. Unlike most other designs used to date, the lamp is mounted in the cavity and held in place by a locating ring fitted to it rather than lamp and cavity being independently clamped. This should reduce the risk of relative movement between the two with the consequent possibility of significant changes occurring in the tuning of the cavity; with some critically tuned cavities vibrations in the apparatus can actually cause an unstable output via this mechanism.

As mentioned earlier, microwave-excited lamps of nonvolatile metals are usually constructed using a suitable halide to allow a sufficient atom concentration to be obtained at the "normal" operating temperature of the discharge. When this is not possible additional heating of the lamp is required. The unit shown in Fig. 5-29(d) consists of a small furnace placed on top of a microwave director and was designed by Tomkins and Fred[57] for operation of rare-earth iodide lamps at 750-800°C. The main problems with this type of high-temperature operation are those related to additional lamp outgassing and provision of sufficient cooling of insulation material at the connector between the antenna or cavity and the microwave input cable.

(*c*) *Characteristics of the discharge*

Although the main requirements* for a light source in AAS or AFS have been largely satisfied by the characteristics of microwave discharges of the permanent gases, these elements are of limited interest for analytical applications of the technique. The situation with discharges emitting the metal resonance lines is, unfortunately, somewhat less satisfactory. However, the problems mentioned here are now widely recognized and it seems likely that work currently in hand will soon result in much more reliable operation of metal

* As mentioned several times elsewhere in this book, these include easy starting with little warm-up time, high intensity (especially for AFS), narrow resonance line profiles (especially for AAS) and a stable and reproducible output.

microwave lamps. Thus, new lamps of many elements require a "running-in" period of several hours, especially those prepared using the metal and free iodine. To obtain a reproducible output on subsequent operation of the lamp, careful positioning and tuning of lamp and cavity are necessary together with a period of about 5 to 30 minutes for warm-up and stabilization during which further adjustment may be needed. Most properly constructed lamps allow initiation of the discharge (with a Tesla vacuum tester) while cold, but for a few elements it may be necessary to warm the lamp first. This may also prove helpful should a well-used lamp prove difficult to start.

Unless a lamp has deteriorated or been improperly prepared, the discharge should emit a "clean" metal spectrum. Examples of improper preparation are the presence of an iodine continuum due to a residue of free iodine in the finished lamp, and an intense mercury spectrum resulting from the use of mercury vacuum gauges without adequate trapping. Provided the correct pressure of filler gas has been used, it should be possible to obtain the metal spectrum almost completely free of background inert gas lines. In practice, the results obtained with many metals even for a well-made lamp depend very much on the way in which it is operated. The authors have found it useful to distinguish two distinct modes of operation; these also form a realistic framework into which it is possible to fit the other desirable characteristics of a lamp. In the so-called *high-intensity mode*, the inert-gas lines are usually extremely weak in comparison with those of the metal spectrum and can be completely ignored during most measurements with the metal resonance lines. This mode of operation, which is usually obtained at relatively high microwave power, also gives an extremely intense metal spectrum and with many lamps the output stability and reproducibility are limited only by those of the microwave equipment itself. Unfortunately, for very many elements the high-intensity mode of operation is also characterized by severe self-absorption broadening, or even serious self-reversal, of the metal resonance lines. Hence a lamp operated in this way may prove completely unsatisfactory as a source for AAS and, contrary to expectations from measurements of its intensity with a conventional spectrometer, give quite poor fluorescence sensitivity.

On the other hand, in the *low-intensity mode* (usually obtained at very low operating powers) there will frequently be virtually no self-absorption of metal resonance lines and the line profile is extremely sharp as the discharge conditions minimize other forms of line broadening (e.g. Doppler, pressure and Stark broadening). However, it is now found that the background inert-gas spectrum is often quite intense in comparison with the metal spectrum and may cause spectral interference with resonance lines of some elements. Furthermore, many lamps prove difficult to operate reproducibly under these conditions, frequently showing unacceptably poor stability, and the authors have found that in some cases the intensity of a metal resonance line may be no better than that obtained with similar line width and superior stability from a hollow-cathode source. The change in line-width (i.e. self absorption) when going from the low- to the high-intensity mode is illustrated in Fig. 5-30 for the thallium 377·6 nm resonance line. This diagram shows the hyperfine structure of the line, as observed with a high-resolution Fabry-Perot interferometer, under five different operating levels. As a result of the poor stability of this particular lamp in the low-intensity mode, the spectrometer was scanned rapidly while observing the spectra on an oscilloscope (each photograph shows the spectrum repeated several times; the peaks may be identified by comparison with Fig. 5-15). The very severe self-reversal with an actual decrease in the useful intensity at higher power is clearly illustrated.

The characteristics of the metal microwave-excited lamps would seem to be quite adequate for AAS and AFS sources if it were possible to operate them in the high-intensity mode at a relatively high level of excitation (i.e. input power) while maintaining minimal self-absorption of the resonance lines. At present, with the commonly used methods of preparation and operation the use of high power results in a high lamp temperature and thus in many cases a high vapour pressure of free metal atoms within the lamp. There are several ways in which it may be possible to use a high level of microwave power while maintaining a low (and, in fact, preferably the optimum) concentration of metal atoms. For example, improved methods of cooling the lamps may allow the use of high power while maintaining a lamp temperature which is sufficiently low *and* reproducible without hot or cold spots to reduce stability. On the other hand, it may prove possible to add precisely the correct amount of material to the lamp so that operation at high temperature with complete vaporization of a relatively volatile substance gives optimum performance without self-absorption. Given an even lamp temperature this would certainly give reproducible operation of the lamps. Finally, with some elements of low volatility

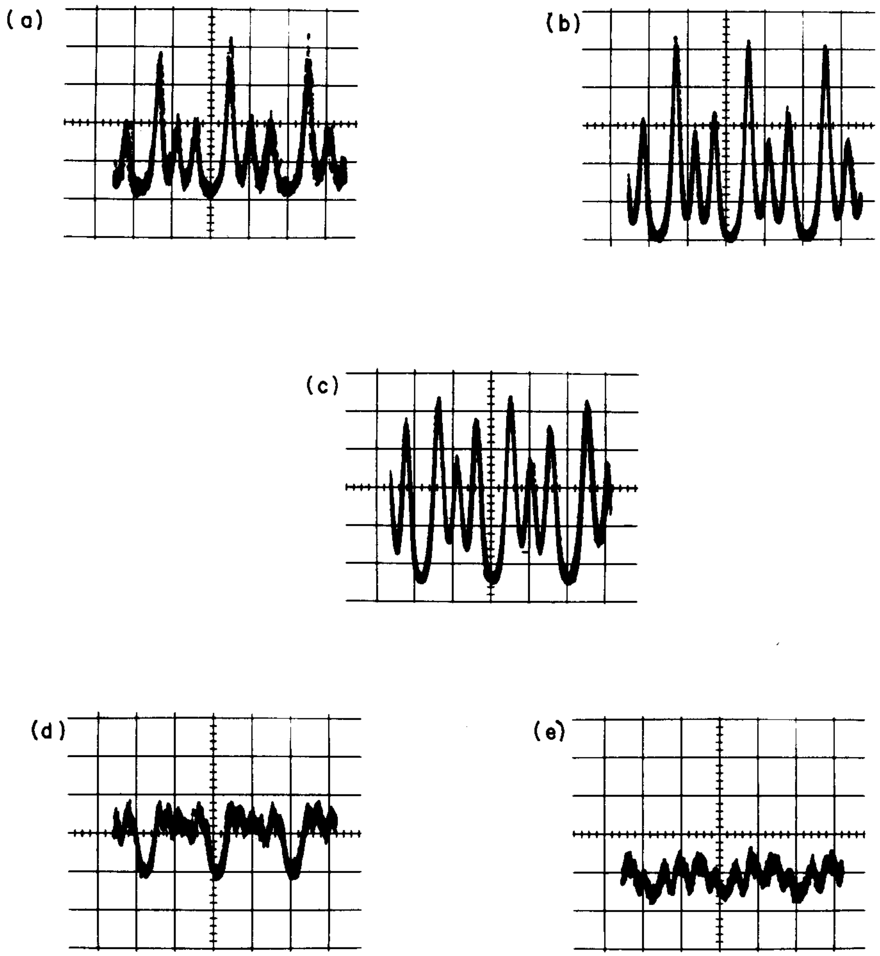

(a) Very low self-absorption (y axis 5mV/cm)
(b) Low self-absorption (y axis 20 mV/cm)
(c) Medium self-absorption (y axis 50 mV/cm)
(d) Self-reversal (y axis 50 mV/cm)
(e) Serious self-reversal (y axis 50 mV/cm)

Fig. 5-30. Fabry-Perot spectrometer scans of the thallium 377·6 line emitted by an electrodeless discharge lamp under different operating conditions[22] (cf. Fig. 5.15).

(or using their compounds of sufficiently low volatility) it may be possible to obtain good results by heating the lamp well above the temperature attained with the discharge alone. The exact vapour pressure required could then be selected and accurately maintained by control of the furnace temperature. The rather greater Doppler width of the resonance lines thus obtained would not be a serious

problem for many applications, especially with a lamp to be used as an AFS source.

5.4 OTHER LIGHT SOURCES

As mentioned at the beginning of this chapter, we shall discuss the remaining types of spectral source of interest in AAS and AFS only briefly. Some, such as the vapour-discharge lamp, were of interest in early work but are unlikely to see much further application for analytical purposes. Others, such as the laser, may well become important alternatives to the hollow-cathode lamp and electrodeless-discharge lamp as the result of future technical improvements. Several other possible sources which are unlikely ever to be of more than isolated interest for practical analytical applications will also be listed.

5.4.1 Vapour-Discharge Lamps

Vapour-discharge lamps form simple, robust sources of line spectra of the volatile elements (Cd, Cs, He, Hg, K, Na, Ne, Rb, Tl, and Zn) and for many years were the most popular commercially available* types for purposes such as spectrograph calibration. The commercial lamp shown in Fig. 5-31 is simply an inner discharge tube surrounded by an envelope to protect it from damage and draughts. The discharge tube is usually silica, but a protective layer inside a special glass is required for alkali metals to prevent attack on the surface. The envelope is usually of non-ultraviolet transmitting glass and it is then necessary to cut an opening to view the resonance lines of Zn, Cd, Hg. The discharge tube contains a small amount of the required metal, an inert gas at the correct pressure, and two tungsten electrodes for the discharge. The design shown in the diagram also incorporates starting electrodes operating via a thermistor which switches them off when the lamp reaches its normal operating temperature. These lamps may be operated with either ac or dc although Wotan lamps are intended for operation at 220-240 V ac via a choke to regulate the current passed. However, use of a stabilized power unit is almost essential for atomic fluorescence (or absorption) applications and a method of modulating the output has been described.[71]

The recommended operating current of the commercial lamps, to give stable, efficient operation is *ca.* 1·0 to 1·5 amp (depending on

* Osram G.m.b.H. ("Wotan" lamps), Munich, Germany. Phillips Gloeilampenfabriek N.V., Eindhoven, Netherlands.

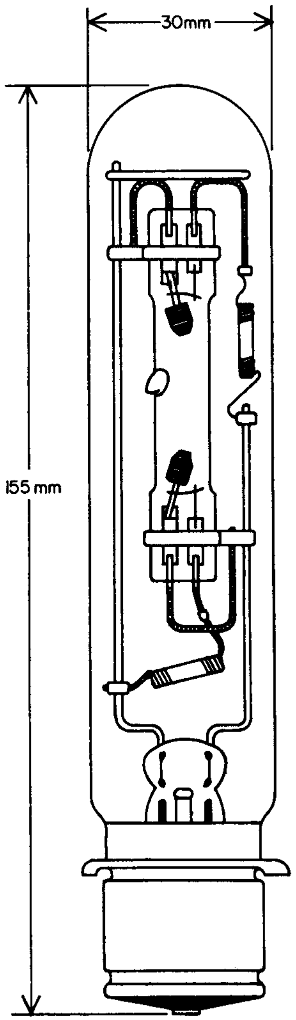

Fig. 5-31. Construction of a commercial vapour discharge lamp.

the element). However, under these conditions the resonance lines are found to be strongly self-absorbed or even self-reversed.[22,72] This is illustrated in Fig. 5-32 for the hfs components of the thallium 377·6 nm resonance line.* It can be seen that reduction of the current reduces the self-absorption and several workers have been able to use these lamps as sources for atomic fluorescence spectroscopy.[73-83]

---

* These spectra should be compared with those shown in Figs. 5-15 and 5-30 for the hollow-cathode and electrodeless-discharge lamps respectively.

The lines are still somewhat broad and the thallium lamp was found[22] to give similar line widths to those from a hollow-cathode lamp only if operated at 0·3 to 0·5 amp, when the intensity also becomes comparable. As the stability is also rather poor at these low currents (compared with the HCL source) these sources have seen little use for absorption work.[84-86]

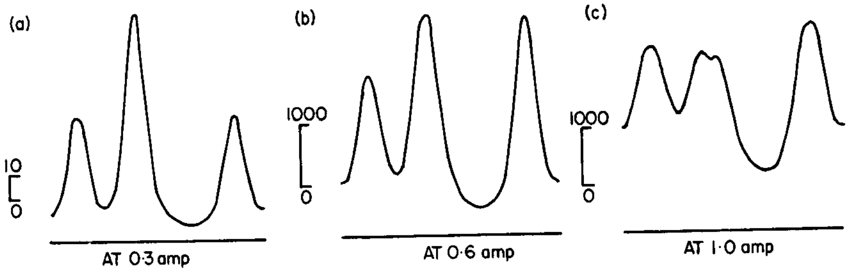

Fig. 5-32. Fabry-Perot spectrometer scans of the thallium 377·6 nm line emitted by a vapour discharge lamp at different operating currents[22] (cf. Fig. 5.15).

5.4.2 *Continuum Sources*

The continuum source is sometimes claimed to have an important advantage over all line sources for AAS and AFS work in that a single continuum lamp is sufficient for most elements. Unfortunately, as explained in earlier chapters, serious problems arise in both absorption and fluorescence applications. Thus, the sensitivity for AAS will only approach that obtained with a sharp line source if a high resolution monochromator is used, and the calibration graphs also show two distinct forms over the normal concentration range. In fluorescence work, the intensity of these sources often appears deceptively high. This is partly because the best absorption lines in some cases lie in a region of the uv where some currently available sources are well below their peak output.* Furthermore, the intensity *per unit wavelength* of most continuum sources is quite low compared with that of a line source at a strong emission line. As the bandpass of a monochromator used in AFS may easily exceed the absorption line-width by a factor of 100, conventional measurements of the source intensity with this equipment will indicate a far higher value than is actually "seen" by the absorption line of the analyte

---

* Prugger[87] has reported the variation of spectral radiance with wavelength for a number of continuum sources.

element. This effect is particularly serious when fluorescence measurements are made under conditions producing light scatter in the fluorescence cell. As scatter may be detected over the whole bandpass of the monochromator, the scatter signal will be greatly enhanced relative to the fluorescence intensity when changing from a line to a continuum source.

As a result of these problems, continuum sources have seen much less application to AAS and AFS than might otherwise be expected. Several reports have, however, appeared in the literature over the years and some of the specialized applications seem quite promising. The conventional tungsten filament lamp is really of insufficient intensity for either technique, although the more recently introduced tungsten iodide lamps with silica envelopes have been examined as absorption sources.[88] Similarly, several workers[89-91] have attempted to use the well-known hydrogen and deuterium discharge lamps as absorption sources. These are low-pressure lamps giving a far more intense continuum than does a tungsten filament between *ca.* 170 and 400 nm, with a peak output at approximately 230 nm (the deuterium is about 30% more intense than hydrogen at this wavelength). Even so their intensity is too low to allow precise atomic absorption measurements with the narrow monochromator bandpass which is frequently required.

More satisfactory results using a continuum source have been reported for the high-pressure xenon arc by a number of workers, both for AAS[92-96] and AFS.[97-104] These lamps as used in spectroscopy are usually small thick-walled silica bulbs containing two tungsten electrodes a few millimetres apart and xenon gas at a pressure of several atmospheres. Thus an extremely small bright discharge is obtained which may virtually be treated as a point source. Most of the applications mentioned above use this type of lamp with power ratings in the range 50 to 100 watts. Many other types are available for industrial purposes at power ratings of up to 20 kW, but their shape and size (and operating requirements) generally make them unsuitable for laboratory spectroscopic purposes. In any case, the power units used with such powerful lamps would generally be inadequate for the more stringent requirements of spectroscopic applications. In fact, there are many reports of work with much smaller lamps having suffered from the use of power supplies not intended for such applications. Satisfactory results in AAS or AFS can only be expected if the xenon lamp is operated with a specially designed unit giving high current stability (0·1% or better even at maximum output) and low current ripple on the dc output (this is important when synchronous detection systems are used). Operation in this way also helps to avoid sudden shifts of the arc inside the lamp, which can sometimes cause erratic changes in the lamp intensity. Suitable commercial units are available with outputs of up to 500 or 1000 watts. Some of these give only one fixed output for a lamp of a particular rating, but it is possible to obtain supplies giving a wide range of current adjustment and these are much more useful. The use of a pulsed power supply for the xenon arc has also been suggested.[105,106] As with other light sources already described, this technique allows a relatively small spectroscopic lamp to be run at currents well above its continuous rating, thus increasing the output intensity. For example, Klein[106] was able to operate a xenon lamp rated at 2·2 kW with 10 kW pulses.

5.4.3 *Lasers*

The unique properties that distinguish lasers from other optical sources may be summarized briefly as:

(i) The extremely coherent and unidirectional beam of radiation that is obtained.
(ii) The large amount of energy available over a small spectral region.
(iii) The extremely small area into which the light beam may be concentrated.

These properties offer two possibilities that are of considerable interest with respect to spectral sources for AAS and AFS. For absorption work, the coherent nature of the light beam should allow the use of much longer path lengths (either directly or by use of multiple reflection techniques through a small cell) without the usual problems of light scatter in the cell and insufficient intensity at the detector. This could result in large improvements in atomic absorption sensitivities without any other changes in current techniques. For fluorescence work, the extremely high energy that may be concentrated over the width of a resonance line and within a small area of a sample cell should produce tremendous improvements in sensitivity over anything that is possible with currently available conventional light sources.

Lasers have now been used quite widely for a number of years and their application to absorption and fluorescence studies of molecules in the gas phase has been reported in the literature. However, only very recently have any attempts been made to apply the advantages mentioned above to atomic absorption and fluorescence measurements. The explanation of this delay is quite simple. Most of the commercially produced lasers were of two types, either solid state (in which the active material is a solid such as ruby, glass, Nd-YAG, etc.) or gas (in which the active material is a permanent gas such as He/Ne, Ar, Kr, Xe, CO_2, N_2 etc.). In both cases laser action is obtained at one or perhaps several spectral lines which are characteristic of the active material. Thus, the coincidence of a laser line with a metal resonance line suitable for AAS or AFS would be quite fortuitous and rather unlikely. As a result, no attempts appear to have been made to produce a laser source for use at metal resonance lines by choosing the appropriate active material in a conventional laser. Several metal vapour lasers have been developed and the He/Cd laser is available commercially. The metal ion lines emitted by these lasers are of no direct interest in AAS or AFS and their application would still depend on the fortuitous coincidence of a laser line with a metal resonance line.

This situation has been dramatically altered by the advent of *tunable* lasers of several different types (see below).* These devices permit the laser output (in the form of a "line" whose half-width may be pre-selected and made extremely narrow if necessary) to be tuned through a given wavelength range and hence peaked at any discrete wavelength within that range. Thus, a tunable laser may be used as a sharp line source at *any* metal absorption line lying within its tuning range. Quite apart from any advantages of using a laser source as such, these devices seem to be the perfect sources for AAS and AFS; i.e. a single sharp line source which (like a continuum) can be used with many different elements and which allows the half-width of the source line to be varied over a wide range. As a result, it seems likely that once the initial drawbacks of these devices have been overcome (see below), the tunable laser will become an extremely important source in AAS and AFS. In view of this rather more space has been given to the topic than may appear warranted by the number of applications so far reported.

Perhaps the most serious deterrent to the use of a laser source for AAS and AFS at the present time is the extremely high cost of a suitable tunable laser for most elements; quite reasonably priced

---

* The term tunable as used here should not be confused with some conventional commercial lasers in which it is possible to *select* laser action at one of several spectral lines available from the active material by making an adjustment to the cavity.

commercial units are widely available but their wavelength range lies too far into the visible region for use at the absorption lines of many elements. Some of these cheaper units also give a pulsed rather than a continuous output. Their operating life may be limited if left running for an extended period. Together with the short duration of the pulses this would require some modifications to normal AAS and AFS technique.

Four distinct types of tunable laser have been reported at the time of writing, but interest in the subject is considerable and other techniques may be introduced. The four types are:

Organic dye lasers. Many commercial models are available, some being relatively simple and cheap. The principle of operation is quite straightforward and components are easily purchased for assembly of a complete system in the laboratory. Most reports of tunable laser applications actually refer to organic dye lasers. The present state of the art is summarized below.

Parametric oscillator lasers. Only one or two commercial models are available and the principle and construction is somewhat more complex than for the dye lasers. However, there is a possibility that a more versatile tunable uv output could be more readily obtained by this technique and some details are mentioned below.

Diode lasers. At present tunable diode lasers are in the development stage and give only an infra-red output. Hence they are of no further interest here.

Spin-flip Raman lasers. The comment on diode lasers also applies to these devices.

Dewey[107] has written an excellent review of all these devices with thorough coverage of the literature up to 1971, particularly for dye lasers. Part of his discussion is also relevant to AAS and AFS. Schlossberg and Kelley[108] have described in simple terms the mechanisms of the tunable lasers mentioned above and have summarized the performance achievable to the time of writing.

(*a*) *Organic dye lasers*

The development of dye lasers and early work have been reviewed by Dewey[107] and Kagan *et al.*,[109] while Bradley[110] has described some of the most recent developments and Webb[111] has discussed the mechanism of dye lasers and summarized the "state of the art".

Dye laser action is based on the optical pumping of an active material consisting of a dilute solution of an organic (dye) compound whose absorption and emission spectral bands do not overlap.

Absorption of light from the pumping source excites these molecules to excited singlet energy levels and the re-emitted fluorescence radiation produces a laser action in the cavity under suitable conditions. In practice, very fast radiationless transitions occur within the excited singlet states so that all lasing transitions occur from the bottom vibrational level of the first singlet state to the vibrational levels of the ground state, giving a broad continuous band of emission which may be between *ca.* 20 and 200 nm wide. The exact position of the band of laser radiations will depend on the structure of the dye, the concentration of the solution used, and features of the cavity (such as its path length). The wavelength ranges of some of the most important groups of laser dyes are shown in Fig. 5-33. It can be seen that the range from about 340 nm to 900 nm is fairly well covered, but the uv region of most interest in AAS and AFS is not available. Thus, the discovery of organic dyes giving laser emission further into the uv would be an important development for the direct use (see below) of tunable dye lasers for the atomic absorption and fluorescence measurements of many metals.

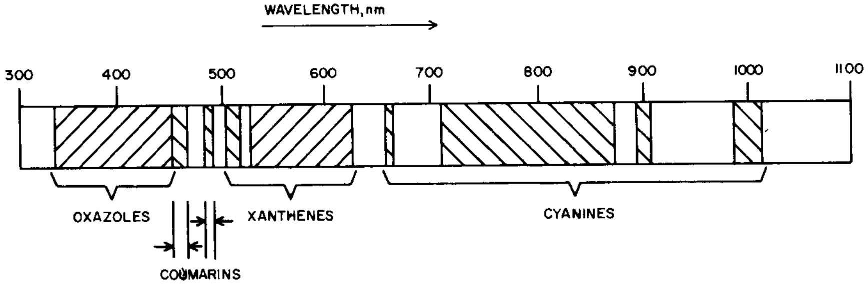

Fig. 5-33. Spectral ranges covered by the main groups of laser dyes.[110]

Early dye lasers were obtained using a pulsed conventional laser as the pumping source, the characteristics of the pumping pulse being quite critical for a successful dye laser. Subsequent investigation of the possibilities of other organic dyes and the development of special flashlamps with very short pulse rise times has allowed pumping of dye lasers without using an expensive auxiliary laser. Many relatively inexpensive commercial tunable lasers operating on this principle are now available. It should be noted that as a result of the more critical requirements for flashlamp pumped dyes some of the spectral regions shown in Fig. 5-33 may not be completely covered by this type of laser. Worden and Gough[112] have surveyed the wavelengths available from fifty-nine flashlamp pumped dyes. To avoid thermal gradients in the dye cell due to the heat transferred during pumping, it is often necessary continuously to circulate dye through the cell at a fairly high flow rate. This is particularly so with flashlamp pumping and/or when high repetition rates are required for the pulsed output, but with even a simple circulation system the thermal problem is no longer the factor limiting the maximum pulse rate and it does not prevent continuous (CW) operation of dye lasers. Until recently it was thought that CW dye lasers were not possible for a different reason. Strong intersystem crossing occurs between the energy levels of these organic molecules and leads to conversion of the excited singlet-state molecules (formed by pumping) in to excited triplet-state molecules. These have a much longer lifetime, so that an appreciable population builds up in the dye solution. As the absorption band of these molecules overlaps the singlet fluorescence band, strong absorption of the dye output can occur and eventually lead to quenching of the laser action. This also explains the need for a short pulse rise time and duration in the pumping source. However, the triplet state can easily be quenched by adding a suitable species to the dye (e.g. oxygen or cyclooctatetraene) and this technique allowed first long pulse operation of certain dyes and recently CW operation with solutions of Rhodamine 6G dye in water.[113,114] Obviously, an intense continuous source is required to pump such lasers and at present this is only possible using a very expensive argon ion laser. Thus, application to routine problems is unlikely until the overall cost can be reduced.

As mentioned earlier, the spectral width of the laser band obtained from the dye varies with different compounds but is always large compared with the width of an atomic spectral line. In some early work[109] there was a tendency to select dyes giving a fairly narrow band and to tune the laser by producing a shift in the peak of this band. This could be achieved by changing factors such as the dye concentration, the solution temperature, or the path length through the dye cell. Subsequently it was found that insertion of a spectral dispersive element into the laser cavity caused the entire output to fall into a single mode characterized by the wavelength-setting element and with a line-width equal to the spectral bandpass of the element. This is easily achieved by, for example, placing a prism between the mirrors of the cavity or by replacing one mirror with a diffraction grating. It is then possible to obtain a relatively narrow spectral line which can be tuned across the entire band over which a particular dye will lase, and it is desirable to find dyes giving as wide a band as possible. Lines narrower than 0·1 nm are produced without difficulty using a diffraction grating, but even this may be inadequate for sensitive absorption measurements. However, much sharper lines may be produced *without serious loss of laser intensity* by inserting a Fabry-Perot etalon into the cavity to reduce further the spectral bandpass. Coarse tuning is then obtained via the main grating (or, quite often, an echelle grating or another Fabry-Perot etalon of greater bandpass), while the final exact matching of the line to the desired wavelength is achieved by rotating the etalon slightly.

Spectral line-widths less than 0·001 nm can be produced in this way using just an echelle grating and one Fabry-Perot etalon.[115] By including a telescope inside the cavity to ensure that a wide, collimated beam of light is incident on each dispersive element, Hänsch[116] recently obtained a linewidth of 0·0004 nm with relative freedom from drift due to small movements of the optical components. Use of an additional Fabry-Perot interferometer external to the laser cavity further reduced the line-width to about 8×10^{-6} nm.[117] Although an extremely narrow line such as this would require considerable expertise in assembly and operation of the complete "laser unit", it can be seen that it is already possible to obtain tunable laser lines narrower than those available from most hollow-cathode lamp sources used in AAS without difficulty and using only commercially available lasers and optical components. In fact, wavelength drift of the line (from its setting on a metal resonance line) may prove more of a problem than its actual width, but even this should not be serious with the specially designed optics now available. The possibility of wavelength drift is also completely avoided in a quite different technique of locking the dye laser output to atomic resonance lines suggested by Bölger and Waysenfeld.[118] They were able to obtain "mirrors" giving high reflection coefficients only at metal resonance lines simply by generating the correct vapour pressure of an alkali metal inside a small glass cell with a wedged window. This cell could then be used as one mirror of a dye laser with an output in the correct spectral range, causing most of the laser radiation to be locked onto the frequencies of, say, the sodium or rubidium resonance lines. Thus the dye laser output is simultaneously narrowed to a line-width suitable for absorption methods and tuned to the correct wavelength without the need for any elaborate auxiliary optical components.

Although the progress in dye laser techniques described above is adequate to allow these devices to be successfully applied as light sources in both AAS and AFS (see below), one further problem remains before they can be considered as universal sources suitable for the determination of most metals. This is the availability of a completely tunable output below the present uv limit of about 360 nm and down to *ca.* 200 nm. Extension of the range of direct dye laser output below 360 nm requires the development of both suitable dyes fluorescing in this region and sufficiently intense pumping sources of even shorter wavelength. Development of pumping sources for this region should not prove difficult, as suitable flashlamps are already available for pulsed operation and many advances have recently been made in ultraviolet laser techniques[119] needed for CW pumping. Unfortunately, predictions of the likelihood of discovery of organic dyes that can be used for routine uv laser operation are not practicable at the time of writing and we can only await future developments.

However, an alternative method of obtaining a tunable uv output from a dye laser is currently receiving considerable attention and seems likely to prove most useful in the near future. This involves doubling the frequency (i.e. halving the wavelength) of laser radiation by generating second-harmonic radiation in a suitable non-linear optical material such as ADP or KDP crystals. The technique was demonstrated as long ago as 1965 and is now widely used to obtain additional spectral lines from fixed wavelength lasers, including many commercial systems. As each particular laser wavelength requires a crystal especially cut to give phase matching for normal incidence of the laser beam, application of the technique to tunable laser outputs is less satisfactory. However, it has been possible to tune dye laser outputs through relatively small uv ranges (e.g. 290 to 300 nm[120] and 280 to 290 nm[121]) using a single crystal provided the crystal is simultaneously tuned to the correct phase-matching angle for each frequency. Thus, in this way many uv metal resonance lines of interest in AAS and AFS could be covered using a single dye laser and a relatively small selection of specially cut frequency-doubling crystals. Recently Gabel and Hercher[122] reported a CW, frequency-doubled, dye laser radiation tunable from 260 to 235 nm. Unlike the previous techniques they placed the frequency doubling crystal (SHG) actually inside the dye laser cavity so that only a uv laser output was observed beyond the end mirrors. It is not clear whether the entire uv range was obtained using a single crystal or whether separate adjustment of the crystal was needed during tuning. Yet another technique currently under active investigation not only avoids any problem of resetting the device during tuning of the dye laser but also triples the fundamental frequency instead of just doubling it. This technique replaces the specially cut crystal with a relatively simple cell containing the vapour of a volatile metal (e.g. the alkali metals) and, when necessary, an inert gas to phase match the refractive indices at the input and output wavelengths.[123,124,125] Once the practical difficulties are overcome (e.g. a tendency to deposit metal films on the optical windows) it should be possible to obtain from a dye laser radiation tunable in the very important range 180 to 300 nm. Paradoxically, coverage of wavelengths *above* 300 nm may prove more difficult as this will require operation of the dye laser in the infrared region above 900 nm where currently available dyes are less satisfactory.

Some applications of dye lasers which are of direct interest to AAS and AFS have already been reported in the literature. Kuhl *et al.*[126] determined sodium vapour concentrations down to 2 ppb in an enclosed cell by absorption using a pulsed dye laser. They averaged each measurement from a number of laser shots and recorded the incident and transmitted intensity for every shot to reduce the effects of variations in the laser output. Their source line (narrowed using a Fabry-Perot interferometer) had a width of about 5×10^{-4} nm and could be set to the desired wavelength with an accuracy of about $2{\cdot}5 \times 10^{-4}$ nm. Bowman, Gibson and Sandford[127,128] have measured sodium concentrations in the upper atmosphere by using a dye laser to excite fluorescence radiation at heights as great as 100 km. Of more direct interest, Denton and Malmstadt[129] determined barium in a conventional flame cell, using a pulsed dye laser to excite fluorescence. To avoid problems of laser instability and irreproducibility it was necessary to use a relatively wide source "line" (compared with the barium absorption line in the flame) and to take data only when the laser output fell within a preselected range. It was also necessary to use an ultrasonic nebulizer producing very small droplets to avoid serious scattering problems in the flame used. A detection limit of 1 ppm Ba was obtained. Fraser and Winefordner[130,131] have carried out an extensive study of atomic fluorescence in flame cells using a pulsed dye laser pumped with a nitrogen laser as a tunable sharp line source. They measured detection limits for the elements Al, Ca, Cr, Co, Ga, In, Fe, Mn, Mo, Ni, Sr, Ti and Tl in either air-hydrogen or nitrous oxide-acetylene flames using an optical and electronic system which was rather more elaborate than that normally used for AFS work. In general terms, it was found that, with respect to detection limits and linearity of analytical curves, the system was equivalent to a conventional system using a range of sharp line sources for all elements with strong absorption lines between 360 and 650 nm, but was considerably more expensive. A major problem was the high level of scattered radiation (from the laser) received as a background to resonance fluorescence, and for a number of elements better detection limits were actually obtained by measuring at less intense non-resonance fluorescence lines. This work is treated in more detail in Chapter 14.

(*b*) *Parametric oscillator lasers*

The basic component of this type of tunable laser is a non-linear optical crystal similar to those mentioned earlier for frequency-doubling applications. Under the correct conditions the crystal is able partially to convert a high-intensity pumping source into signal and idler waves whose frequencies sum to that of the incident wave. By placing the crystal between two wavelength selective mirrors to form an optical cavity, it is possible to obtain a laser output at the signal frequency. Of particular importance is the dependence of the signal and idler frequencies on the refractive indices of the crystal. Thus, the frequency of the output may be varied by altering the temperature, rotation, or electric field of the crystal so as to vary its refractive indices, and a tunable laser is obtained. Generally a sufficient intensity is only obtained using a laser pump source, and pulsed operation is used in most cases. Continuous (CW) operation is possible, but operation is more difficult, the output is less stable, and careful design is essential.

Until recently, it was not possible to obtain a wide, continuous tuning range with one pump laser and one crystal. A commercial system,* however, is now available which provides coverage from 0·5 μm to 3·7 μm (540 to 3700 nm) using a Q-switched ND : YAG laser as pump source for a $LiNbO_3$ crystal. This range coverage is, however, only obtained by using different lines from the pump laser as the actual pump wavelength, depending on the region required. It is also necessary to use a number of different sets of special mirrors to cover the complete range quoted. Tuning is achieved by varying the temperature of the crystal using a special oven. This is claimed to give a frequency stability and resettability equal to the band-width (1 to 2·5 cm^{-1} unless an additional line-narrowing Fabry-Perot etalon is used). There appear to be no reported

---

* Chromatix, Mountain View, California, U.S.A.

applications of this type of system to AAS or AFS, partly because of the cost of these devices and partly because the available wavelengths are too long for the absorption lines of most elements. The frequencies that are available, however, would seem almost ideal for tripling to provide a tunable source in the uv region of most interest for AAS and AFS. Thus, should the metal vapour devices mentioned earlier become available for routine application, tunable parametric oscillator lasers may prove as useful as their organic dye counterparts.

5.4.4 Miscellaneous Sources

As mentioned previously, there are many types of spectral light source other than those already described here which could be applied to atomic absorption and fluorescence measurements, but very few have been considered for routine analytical work. For the sake of completeness we shall mention one or two for which AAS or AFS applications have been reported in the literature, mostly as solutions to rather non-routine problems.

Most interest has been shown in consumable sources, which are more versatile for research purposes than the other types described above. Arcs, sparks and plasmas are widely used in emission spectrography and spectrometry, but the resonance lines emitted are generally too broad for high sensitivity to be obtained in AAS and it is often difficult to obtain sufficient intensity for AFS without introducing problems of self-reversal. Since sources such as plasmas tend to be rather noisy, it is not possible to reduce these disadvantages by using high scale expansion of signals. In spite of these difficulties, Strasheim and his co-workers have made comparative tests of several of these sources, describing the use for AAS of a time-resolved spark,[132,133] and gas-stabilized dc arcs.[134,135] They reported that good precision and the ease of multi-element analysis often compensated for the much lower sensitivity (about one-third lower) compared with hollow-cathode lamp sources. A high-frequency plasma torch has also been used[136] as a source for AAS.

Flames may also be used as primary light sources for atomic absorption and fluorescence, although again sensitivity will be rather poor. It is necessary to use a hot flame at atmospheric pressure in order to obtain sufficient emission intensity from most elements, so that Doppler and Lorentz (collision) broadening will be severe. The need for quite high atom concentrations in the flame (to obtain sufficient intensity) often leads to self-absorption of resonance lines, introducing further difficulties. This is particularly true when a flame is used as the primary light source for atomic fluorescence; although the line-width is of much less importance than for absorption measurements it is necessary to obtain extremely intense emission for good AFS sensitivity. This requires a high atom concentration and results in severe self-absorption and self-reversal. Matters may be improved somewhat by using a double ("flame-shielded") flame with emitting atoms present only in the centre flame; this avoids the region of cool absorbing atoms normally present at the edge of the flame. Thus, flames offer similar advantages and disadvantages to arcs and plasmas plus the facts that their composition and operating conditions are generally uniform and well established and that no expensive power supply units are required. Flames were used as the spectral source by Alkemade and Milatz[137] for their first work on atomic absorption and since then they have been used several times for special purposes.[138-141]

REFERENCES

1. F. Paschen, *Ann. der Physik,* 1916, **50,** 901
2. H. M. Crosswhite, G. H. Dieke and C. S. Legagneur, *J. Opt. Soc. Am.,* 1955, **45,** 270.
3. A. Walsh, *Spectrochim. Acta,* 1955, **7,** 108.
4. H. Schüler, *Z. Physik,* 1926, **35** , 323.
5. S. Tolansky, "High Resolution Spectroscopy", Methuen, London, 1947; Chapter 4.
6. J. A. Goleb and Y. Yokoyama, *Anal. Chim. Acta,* 1964, **30,** 213.
7. J. A. Goleb, *Anal. Chem.,* 1963, **35,** 1978.
8. W. G. Jones and A. Walsh, *Spectrochim. Acta,* 1960, **16,** 249.
9. A. I. Bodretsova, B. V. L'Vov, E. N. Pavlovskaya and V. K. Prokof'ev, *J. Appl. Spectroscopy,* 1965, **2,** 62.
10. K. B. Mitchell, *J. Opt. Soc. Am.,* 1961, **51,** 846.
11. D. C. Manning and J. Vollmer, *Atomic Absorption Newsletter,* 1967, **6,** 38.
12. A. I. Bodretsova, B. V. L'Vov and V. I. Mosichev, *J. Appl. Spectroscopy,* 1966, **4,** 149.
13. J. B. Dawson and D. J. Ellis, *Spectrochim. Acta,* 1967, **23A,** 565.
14. D. A. Katskov, G. C. Lebedev and B. V. L'Vov, *Zh. Prikl. Spektrosk.,* 1969, **10,** 215.
15. B. V. L'Vov, "Atomic Absorption Spectrochemical Analysis", Hilger, London, 1970.
16. D. G. Mitchell and A. Johansson, *Spectrochim. Acta,* 1970, **25B,** 175.
17. K. Yasuda, *Anal. Chem.,* 1966, **38,** 592.
18. D. K. Davies, *J. Applied Phys.,* 1967, **38,** 4713.
19. V. P. Gofmeister and Yu. M. Kagan, *Opt. Spectros.,* 1968, **25,** 185.
20. *Idem,* ibid., 1969, **26,** 371.
21. W. C. Kreye and F. L. Roesler, *J. Opt. Soc. Am.,* 1970, **60,** 1100.

22. G. F. Kirkbright and M. Sargent, *Spectrochim. Acta,* 1970, **25B**, 577.
23. C. F. Bruce and P. Hannaford, ibid., 1971, **26B**, 207.
24. W. C. Kreye, *J. Opt. Soc. Am.*, 1971, **61**, 833.
25. R. J. Reynolds, *Laboratory Methods,* 1970, **81**, 197.
26. S. R. Koirtyohann and C. Feldman, *Developments in Applied Spectros.*, 1964, **3**, 180.
27. J. I. Dinnin and A. W. Helz, *Anal. Chem.*, 1967, **39**, 1489.
28. G. I. Goodfellow, *Applied Spectros.*, 1967, **21**, 39.
29. G. Rossi and N. Omenetto, *Applied Spectros.*, 1967, **21**, 329.
30. R. E. Popham and W. G. Schrenk, *Applied Spectros.*, 1968, **22**, 192.
31. G. Rossi and N. Omenetto, *Talanta,* 1969, **16**, 263.
32. G. D. Propster, paper presented at Society for Applied Spectroscopy Meeting, Chicago, May 11, 1971.
33. J. V. Sullivan and A. Walsh, *Spectrochim. Acta,* 1965, **21**, 721.
34. Z. van Gelder, *Applied Spectros.*, 1968, **22**, 581.
35. R. M. Lowe, *Spectrochim. Acta,* 1971, **26B**, 201
36. H. G. C. Human and L. R. P. Butler, *Spectrochim. Acta,* 1970, **25B**, 647.
37. A. Walsh, L.S.U. Intern. Symp. Modern Methods of Analytical Chemistry, Baton Rouge, January 1962.
38. W. T. Elwell and J. A. F. Gidley, *Anal. Chim. Acta,* 1961, **24**, 71.
39. H. Massmann, *Z. Instrumenteck.*, 1963, **71**, 225.
40. L. R. P. Butler and A. Strasheim, *Spectrochim. Acta,* 1965, **21**, 1207.
41. C. Sebens, J. Vollmer and W. Slavin, *Atomic Absorption Newsletter,* 1964, **3**, 165.
42. D. C. Manning, D. Trent and J. Vollmer, ibid., 1965, **4**, 234.
43. J. Vollmer, C. Sebens and W. Slavin, ibid., 1965, **4**, 306.
44. F. J. Fernandez, D. C. Manning and J. Vollmer, ibid., 1969, **8**, 117.
45. W. F. Meggers and F. O. Westfall, *J. Research Nat. Bur. Standards,* 1950, **44**, 447.
46. E. Jacobsen and G. R. Harrison, *J. Opt. Soc. Am.*, 1949, **39**, 1054.
47. A. T. Forrester, R. A. Gudmundsen and P. O. Johnson, ibid., 1956, **46**, 339.
48. W. E. Bell, A. L. Bloom and J. Lynch, *Rev. Sci. Instr.*, 1961, **32**, 668.
49. R. J. Atkinson, G. D. Chapman and L. Krause, *J. Opt. Soc. Am.*, 1965, **55**, 1269.
50. K. M. Aldous, R. M. Dagnall and T. S. West, *Anal. Chim. Acta,* 1969, **44**, 457.
51. R. G. Brewer, *Rev. Sci. Instr.*, 1961, **32**, 1356.
52. R. A. Franz, *Rev. Sci. Instr.*, 1963, **34**, 589.
53. K. E. Zacha, M. P. Bratzel, J. D. Winefordner and J. M. Mansfield, *Anal. Chem.*, 1968, **40**, 1733.
54. K. M. Aldous, D. Alger, R. M. Dagnall and T. S. West, *Laboratory Practice,* 1970, **19**, 587.
55. W. S. Gleason and R. Pertel, *Rev. Sci. Instr.*, 1971, **42**, 1638.
56. C. H. Corliss, W. R. Bozman and F. O. Westfall, *J. Opt. Soc. Am.*, 1953, **43**, 398.
57. F. S. Tomkins and M. Fred, *J. Opt. Soc. Am.*, 1957, **47**, 1087.
58. R. M. Dagnall and T. S. West, *Applied Optics,* 1968, **7**, 1287.
59. E. F. Worden, R. G. Gutmacher and J. G. Conway, *Applied Optics,* 1963, **2**, 707.
60. M. D. Silvester and W. J. McCarthy, *Spectrochim. Acta.* 1970, **25B**, 229.
61. J. M. Mansfield, M. P. Bratzel, H. O. Norgordon, D. N. Knapp, K. E. Zacha and J. D. Winefordner, *Spectrochim. Acta,* 1968, **23B**, 389.

62. D. O. Cooke, R. M. Dagnall and T. S. West, *Anal. Chim. Acta,* 1971, **54**, 381.
63. N. P. Ivanov, L. V. Minervina, S. V. Baranov, L. G. Pofralidi and I. I. Olikov, *J. Anal. Chem. (USSR),* 1966, **21**, 998.
64. T. T. Kikuchi, *Applied Optics,* 1972, **11**, 687.
65. J. R. Brandenberger, *Rev. Sci. Instr.*, 1971, **42**, 1535.
66. R. F. Browner, R. M. Dagnall and T. S. West, *Anal. Chim. Acta,* 1969, **45**, 163.
67. L. F. Phillips, *Rev. Sci. Instr.*, 1971, **42**, 1078.
68. F. C. Fehsenfeld, K. M. Evenson and H. P. Broida, *Rev. Sci. Instr.*, 1965, **36**, 294.
69. W. G. Schrenk, S. E. Valente and K. E. Smith, *Applied Spectros.*, 1972, **26**, 108.
70. B. McCarroll, *Rev. Sci. Instr.*, 1970, **41**, 279.
71. F. M. Hamm, T. L. Martin and P. B. Zeeman, *Anal. Chem.*, 1970, **43**, 490.
72. B. J. Russell, J. P. Shelton and A. Walsh, *Spectrochim. Acta,* 1957, **8**, 317.
73. J. D. Winefordner and R. A. Staab, *Anal. Chem.*, 1964, **36**, 165.
74. *Idem,* ibid., 1964, **36**, 1367.
75. J. M. Mansfield, J. D. Winefordner and C. Veillon, ibid., 1965, **37**, 1049.
76. G. I. Goodfellow, *Anal. Chim. Acta,* 1966, **35**, 132.
77. R. M. Dagnall, T. S. West and P. Young, *Talanta,* 1966, **13**, 803.
78. R. M. Dagnall, K. C. Thompson and T. S. West, *Anal. Chim. Acta,* 1966, **36**, 269.
79. R. S. Hobbs, G. F. Kirkbright, M. Sargent and T. S. West, *Talanta,* 1968, **15**, 997.
80. N. Omenetto and G. Rossi, *Spectrochim. Acta,* 1969, **24B**, 95.
81. T. J. Vickers and R. M. Vaught, *Anal. Chem.*, 1969, **41**, 1477.
82. P. D. Warr, *Talanta,* 1970, **17**, 543.
83. D. R. Jenkins, *Spectrochim. Acta,* 1970, **25B**, 47.
84. W. Slavin, D. J. Trent and S. Sprague, *Atomic Absorption Newsletter,* 1965, **4**, 180.
85. D. C. Manning, D. J. Trent, J. Sprague and W. Slavin, ibid., 1965, **4**, 255.
86. D. J. Trent, D. C. Manning and W. Slavin, ibid., 1965, **4**, 335.
87. H. Prugger, *Spectrochim. Acta,* 1969, **24B**, 197.
88. V. A. Fassel and V. G. Mossotti, *Anal. Chem.*, 1963, **35**, 252.
89. N. P. Ivanov and N. A. Kozyreva, *Zh. Analit. Khim.*, 1964, **19**, 1266.
90. V. L. Ginsberg and G. P. Satarina, *Zavodsk. Lab.*, 1965, **31**, 249.
91. N. P. Ivanov and N. A. Kozyreva, *Zavodsk. Lab.*, 1965, **31**, 566.
92. V. G. Mossotti and V. A. Fassel, *Spectrochim. Acta,* 1964, **20**, 1117.
93. V. A. Fassel, V. G. Mossotti, W. E. L. Grossman and R. N. Kniseley, ibid., 1966, **22**, 347.
94. M. Margoshes and M. M. Darr, *NBS Tech. Note,* 1965, **272**, 18.
95. L. de Galan, W. W. McGee and J. D. Winefordner, *Anal. Chim. Acta,* 1967, **37**, 436.
96. C. W. Frank, W. G. Schrenk and C. E. Moloan, *Anal. Chem.*, 1967, **39**, 534.
97. R. M. Dagnall, K. C. Thompson and T. S. West, *Anal. Chim. Acta,* 1966, **36**, 269.
98. D. W. Ellis and D. R. Demers, *Anal. Chem.*, 1966, **38**, 1943.
99. C. Veillon, J. M. Mansfield, M. L. Parsons and J. D. Winefordner, *Anal. Chem.*, 1966, **38**, 204.
100. D. L. Manning and P. Heneage, *Atomic Absorption Newsletter,* 1968, **7**, 80.

101. M. S. Cresser and T. S. West, *Anal. Chim. Acta,* 1970, **51**, 530.
102. *Idem, Spectrochim. Acta,* 1970, **25B**, 61.
103. D. H. Cotton and D. R. Jenkins, ibid., 1970, **25B**, 283.
104. M. P. Bratzel, R. M. Dagnall and J. D. Winefordner, *Anal. Chim. Acta,* 1970, **52**, 157.
105. A. V. Sheklein and V. A. Popov, *Zh. Nauchn. i. Prikl. Fotogr. i. Kinematogr.,* 1964, **9**, 192.
106. L. Klein, *Applied Optics,* 1968, **7**, 677.
107. C. F. Dewey, "Excitation of gases using wavelength-tunable lasers", in "Modern Optical Methods in Gas Dynamic Research", p. 221, ed. D. S. Dosanjh, Plenum Press, 1971.
108. H. R. Schlossberg and P. L. Kelley, *Physics Today,* July 1972, **25**, 36.
109. M. R. Kagan, G. I. Farmer and B. G. Huth, *Laser Focus,* September 1968, p. 26.
110. D. J. Bradley, "Recent developments in dye lasers and their applications"; paper presented at "Electro-Optics '71", Brighton, England, March 1971.
111. J. P. Webb, *Anal. Chem.,* May 1972, **44**, 30A.
112. J. T. Worden and L. Gough, *Appl. Phys. Letters,* 1971, **19**, 345.
113. D. G. Peterson, S. A. Tuccio and B. B. Snavely, *Appl. Phys. Letters,* 1970, **17**, 245.
114. A. Dienes, E. P. Ippen and C. G. Shank, *IEEE J. Quantum Electronics,* 1972, **8**, 388.
115. D. J. Bradley, A. J. F. Durrant, G. M. Gale, M. Moore and P. D. Smith, *IEEE J. Quantum Electronics,* 1968, **4**, 707.
116. T. W. Hänsch, *Applied Optics,* 1972, **11**, 895.
117. T. W. Hänsch, A. Shahin and A. L. Schawlow, *Phys. Rev. Letters,* 1971, **27**, 707.
118. B. Bölger and C. H. Weysenfeld, "Locking of organic dye laser frequency to atomic resonance lines"; paper presented at VII Inter. Quantum Electronics Conf., Montreal, May 1972.
119. W. F. Hagen, *Industrial Research,* 1972, **14**, 48.
120. B. G. Huth, G. I. Farmer, L. M. Taylor and M. R. Kagan, *Spectroscopy Letters,* 1968, **1**, 425.
121. D. J. Bradley, J. V. Nicholas and J. R. D. Shaw, *Appl. Phys. Letters,* 1971, **19**, 172.
122. C. Gabel and M. Hercher, "A continuous tunable source of coherent uv radiation"; paper presented at VII Inter. Quantum Electronics Conf., Montreal, May 1972.
123. J. F. Young, G. C. Bjorklund, A. H. Kung, R. B. Miles and S. E. Harris, *Phys. Rev. Letters,* 1971, **27**, 1551.
124. S. E. Harris and R. B. Miles, *Appl. Phys. Letters,* 1971, **19**, 385.
125. G. C. Bjorklund, D. S. Carson, S. E. Harris, A. H. Kung, R. B. Miles and J. F. Young, "Generation of ultraviolet radiation in phase-matched metal vapours"; paper presented at VII Inter. Quantum Electronics Conf., Montreal, May 1972.
126. J. Kuhl, G. Marowsley and R. Torge, *Anal. Chem.,* 1972, **44**, 375.
127. M. R. Bowman, A. J. Gibson and M. C. W. Sandford, *Nature,* 1969, **221**, 456.
128. M. C. W. Sandford and A. J. Gibson, *J. Atm. Terr. Phys.,* 1970, **32**, 1423.
129. M. B. Denton and H. V. Malmstadt, *Appl. Phys. Letters,* 1971, **18**, 485.
130. L. M. Fraser and J. D. Winefordner, *Anal. Chem.,* 1971, **43**, 1693.
131. *Idem.,* ibid., 1972, **44**, 1445.
132. A. Strasheim, *Nature,* 1964, **196**, 1194.

133. A. Strasheim and H. G. C. Human, *Spectrochim. Acta,* 1968, **23B**, 265.
134. H. G. C. Human, L. R. P. Butler and A. Strasheim, *Analyst,* 1969, **94**, 81.
135. *Idem,* paper presented at 15th Colloq. Spect. Intern, Madrid, 1969.
136. S. Greenfield, P. B. Smith, A. E. Breeze and N. M. D. Chilton, *Anal. Chim. Acta,* 1968, **41**, 385.
137. C. T. J. Alkemade and J. M. W. Milatz, *J. Opt. Soc. Amer.,* 1955, **45**, 583.
138. D. C. Manning and W. Slavin, *Atomic Absorption Newsletter,* No. 8, November 1962.
139. R. K. Skogerboe and R. A. Woodriff, *Anal. Chem.,* 1963, **35**, 1977.
140. C. S. Rann, *Spectrochim. Acta,* 1968, **23B**, 827.
141. G. F. Kirkbright and S. J. Wilson, *Analyst,* 1970, **95**, 833.

CHAPTER 6

Flames

6.1 INTRODUCTION

This chapter is concerned with the use of a flame as the atom cell in analytical atomic absorption and fluorescence spectrometers. The flame is, at present, by far the most widely used method of obtaining a population of sample (analyte) atoms in commercial atomic absorption instruments and will be discussed here in some detail. Non-flame cells, which are gradually increasing in importance, are

CHAPTER 9

Wavelength Selection

9.1 INTRODUCTION

The majority of atomic absorption or fluorescence measurements require some form of wavelength selection in the radiation that provides the signal to be processed by the spectrometer. This arises because the radiation used for the measurements is frequently accompanied by unwanted light of other wavelengths. This unwanted radiation may be simply stray daylight, a complex spectrum emitted by the light source or atom cell, or may arise from the weaker absorption lines of the analyte element which would reduce the sensitivity of AAS measurements at the main wavelength for that element (see Chapter 11). Under certain conditions, and particularly with fluorescence measurements, it is possible to use electronic methods (i.e. phase-sensitive amplifiers or solar-blind photomultipliers, as discussed in Chapter 10) to avoid detection of the unwanted light and allow useful measurements to be made without wavelength selection. Sensitive absorption measurements made in this way are, however, only possible for those elements whose atoms exhibit simple line spectra. Even in fluorescence measurements it may be difficult to obtain high signal : noise ratios for many elements by these techniques. Thus, in most reported applications of AAS and AFS, an optical monochromator device is used to preselect the radiation that is allowed to reach the photomultiplier. In commercial instrumentation the most widely used device is the traditional optical prism or grating monochromator which may be used to select any single spectral line (or, at least, a closely spaced group of lines) within a chosen wavelength range. The much simpler optical filters still commonly found in flame photometers may also sometimes be used, particularly for a number of fluorescence applications. Finally, several less widely known devices such as "resonance detectors" and "selective resonance modulation" have been applied to AAS and AFS. Each of the above techniques is described briefly in this chapter and the emphasis is placed on topics that are directly relevant to analytical spectrometry rather than on details of principle or construction. The reader is referred to specialized textbooks[1,2,3] for a more comprehensive discussion of the subject.

9.1.1 Classification of Instruments

The routine application of atomic absorption and fluorescence techniques requires only a relatively elementary knowledge of the optical instruments utilized. The particular requirements of these techniques have, however, given rise to a terminology which differs in some respects from that used in many general courses or textbooks which in other respects form an excellent introduction to the subject. Thus, it is useful to consider AAS and AFS instrumentation in perspective with respect to spectroscopic apparatus in general.

The classical method of wavelength separation involves *dispersion* of the incident radiation so that an observer may view, individually, light of any particular wavelength within the range covered by the instrument. In its simplest form such an instrument is known as a *spectroscope* and allows visual observation of the spectrum produced by the dispersing device. A permanent record may be obtained by using a *spectrograph* in which the observer's eyepiece is replaced by a camera whereby the spectrum can be photographed to produce the well-known pattern of lines on a photographic plate or film. To avoid the need to use the photographic process if just a record of light intensity at a few of these lines is required, the camera may be replaced by a *quantometer*. This replaces the photographic emulsion with a mask which allows a fine slit to be aligned with any line of the spectrum. A photocell placed behind this slit is then used to observe variations in the intensity of that line. The final development of this principle produces the *monochromator* in which a single slit and photocell is maintained in a fixed position while the spectrum is *scanned* across it by moving the dispersive element to alter the angle at which light of a particular wavelength emerges.

The spectroscope is obviously of little use for measurement of atomic absorption or fluorescence signals, while the use of a spectrograph is both inconvenient and time-consuming; it would also be somewhat impractical for routine absorption measurements which would require individual recording of line intensity with and without a sample in the atom cell. A spectrograph used with a quantometer is quite suitable for regular measurements at just one wavelength but is inconvenient if frequent wavelength changes are required. It is possible to use a quantometer with a fixed detector at each absorption line required,[4] but this becomes expensive when many wavelengths are provided and may be impractical when several closely spaced lines are to be used. Thus the monochromator is at present the most satisfactory means of obtaining a versatile, direct-reading optical system for AAS or AFS. All direct-reading photoelectric instruments (i.e. monochromator or spectrograph + quantometer) are conveniently described as *spectrometers* or *spectrophotometers*.

Each of these classical spectroscopic instruments conforms to a more or less standard arrangement of components:

(1) An entrance aperture whose image is observed separately in the spectrum for each dispersed wavelength present in the incident radiation. The most widely used aperture is a narrow rectangle, i.e. a slit. Hence the general association of a "spectrum" with the pattern of fine lines which is observed or photographed.
(2) A collimating device to produce a parallel beam of radiation from that passing through the aperture.
(3) The dispersing element which separates this radiation by giving each different wavelength a different emergent angle.
(4) A system of lenses or mirrors to focus the different wavelengths as a sharp image of the entrance aperture.

(5) A device which allows these images to be viewed, photographed or photo-electrically recorded.

The dispersing element may take a number of forms, some of which are more common than others, and the particular type used is often employed as the basis of a classification of spectroscopic instruments given above. The original dispersing element used by Newton was a transparent *prism* which, because its refractive index varies with wavelength, transmits each particular wavelength at a different angle. The prism is still employed but has to a large extent been replaced by the *diffraction grating* in which light is deflected by a pattern of fine slits at different angles according to its wavelength. This results from the wavelength-dependence of the positions and intensities of the interference patterns obtained. The interference of light may also be used in numerous other devices to obtain a dispersive element; for historical reasons these are generally referred to as *interferometers.* One or two of these devices have been applied to AAS or AFS but no further mention will be made of them here. They are best considered from our point of view merely as rather specialized types of spectrometer.

There remains a further group of wavelength separating devices which do not fall into the above classification as they do not employ a dispersive element to obtain a spectrum. Thus, we describe below several applications to AAS or AFS of devices in which the required wavelength is isolated by *absorption* of all other incident radiation before the light beam reaches the photodetector. The most widely used of these devices is the simple optical filter which depends for its action on the (molecular) absorption bands of liquid, solid or sometimes gaseous materials.* Other, more modern, instruments actually use atomic absorption by the very elements whose radiation is to be isolated as a means of detecting individual wavelengths (see Section 9.3).

9.1.2 Characteristics of Instruments

Several important characteristics are common to all classical (i.e. dispersive) spectroscopic instruments and are widely used for comparisons of performance. These refer to the *effectiveness* of the instrument for dispersing different wavelengths and to the *efficiency* with which it carries out this process, i.e. the instrument would be 100% efficient only if the intensity of each particular wavelength reaching the detector was identical to its original value as a component of the undispersed incident beam

The ability of a spectrometer to spread out different wavelengths is termed its *dispersion*. This may be measured either in terms of the *angular dispersion* of the separated beams of light as they emerge from the dispersive device or in terms of the *linear dispersion* of the separated images of the entrance aperture when they are brought to a focus at the exit aperture. Thus, if a device produces a change $\Delta\theta$ in angle for a wavelength difference $\Delta\lambda$, the angular dispersion is $\Delta\theta/\Delta\lambda$. Similarly, if two images for wavelengths separated by $\Delta\lambda$ are focused a distance Δx apart, the linear dispersion will be $\Delta x/\Delta\lambda$. A useful approximation when the changes considered are not too large is that

$$\Delta x = f\Delta\theta \qquad (9\text{-}1)$$

where f is the focal length of the optical system and is assumed to be reasonably independent of wavelength.

Equation (9-1) suggests that it should be possible to obtain separate spectral lines at the detector for any two wavelengths, no matter how small the difference between those wavelengths, simply by constructing an instrument of sufficiently large focal length. This is true, however, only if it is possible to produce an infinitely narrow entrance slit, failing which the images of the slit will become broader as the focal length is increased to obtain greater separation (of their centres). Quite apart from practical considerations such as the amount of light able to enter the instrument through an extremely narrow slit, all images are in fact diffraction patterns and have a finite minimum size which depends on the wavelength of the light as well as the construction of the instrument. Thus there is a definite limit to the ability of a particular device to separate closely spaced adjacent wavelengths; this is usually termed the *resolving power*. It is defined as $\lambda/\Delta\lambda$ where $\Delta\lambda$ is the smallest wavelength difference (at wavelength λ) which allows separation (i.e. resolution) into two distinct spectral lines.

This definition of resolving power requires qualification. Each wavelength entering the instrument is, as already explained in Chapter 2, actually a narrow region of the type shown in Fig. 2-3 in which the intensity is a maximum at the centre and gradually decreases towards zero at the edges. If the instrument was able to

---

* It is emphasized that this does not include the so-called "interference filters" (see Section 9.3.1) which are simple dispersive devices; they are, in fact, miniature interferometers.

resolve wavelength differences far smaller than the width of this region, the spectral line obtained on, say, a photographic plate would show the same distribution of intensity measured against distance along the spectrum. When this is not the case, the line obtained will have a similar appearance but the distribution will be largely a function of the instrument rather than the original wavelength distribution emitted by the source of light. This second situation will apply with the majority of light source/spectrometer combinations of interest in AAS and AFS. In any event, the variation of intensity across the width of the line means that the resolving power cannot be considered as simply a limit on one side of which two adjacent lines are completely separated while on the other side they are completely merged. Obviously it will be possible to distinguish between two adjacent peaks even when there is considerable overlap of the lines and it is necessary to decide on a practical criterion of just how close the lines can be before they can no longer be considered as resolved. Usually this is based on the fact that each observed image is actually a diffraction pattern, the "line" being the main central peak of this pattern with a succession of progressively weaker peaks on either side. The *Rayleigh criterion* states that two lines of equal intensity are just resolved if the maximum of the central peak of one line falls on the first minimum of the other. The intensity midway between the two peaks is then equal to 81% of the peak intensity. This is illustrated in Fig. 9-1. The criterion does not apply when the peaks are of unequal intensity, but it is then usual to consider the lines as resolved if at any point between the peaks the intensity falls to 81% of that of the less intense maximum.

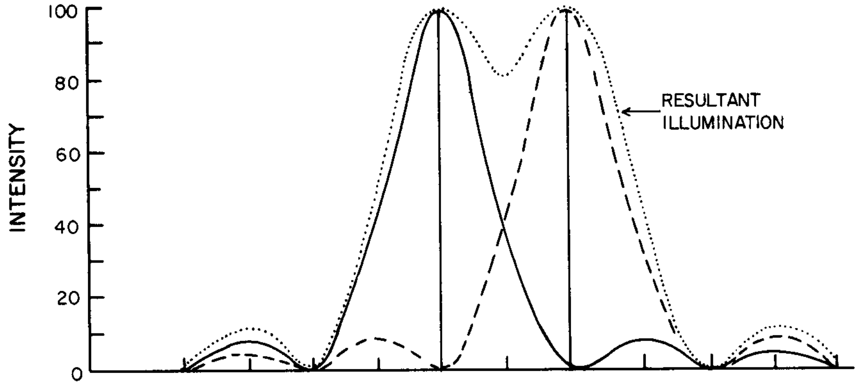

Fig. 9-1. Resultant image obtained by combination of two overlapping spectral lines in the form of diffraction patterns.

Although the resolving power bears a closer relation to practical conditions than the dispersion of an instrument, Rayleigh's criterion is really only useful when applied to very high-quality spectrometers. The actual resolution is affected by many instrumental factors such as the actual design of the instrument (assuming a given dispersion), the width of the entrance slit, the quality of the optical components, etc. Thus, in many cases the instrument may be incapable of achieving its theoretical resolving power. In both analytical atomic absorption and fluorescence spectroscopy it is much more common to refer to the capability of a monochromator in terms of its experimentally determined *bandpass.* This is simply the width of the transmitted peak as observed at the detector (i.e. on a photographic plate or on a recording obtained photoelectrically while scanning the monochromator slowly across a narrow spectral line). It is generally defined in the same way as the half-width of a spectral line (see Section 2.5), i.e. the bandpass is the width of the observed peak in wavelength units between the two points where the transmitted intensity is equal to half that at the maximum. The bandpass will obviously decrease with the width of the entrance slit, so that for monochromators it is usual to quote a value either at a given slit-width or at the smallest practicable width. The bandpass is a particularly useful concept for AAS and AFS work because not only does it give a clear picture of the capability of an instrument but it may also be applied to non-dispersive devices such as optical absorption filters.

The efficiency with which a monochromator is able to carry out the wavelength selection process is usually termed its *transmission.* This is defined as the percentage of the incident radiation that is passed by the device at the wavelength selected. As with the bandpass it is a convenient, practical term which may be applied both to dispersive and non-dispersive systems. With a monochromator transmission depends both on the design and construction of the instrument and upon the manner in which it is used. Thus, as with any optical system, the maximum radiant power that can be passed will depend on the relative values of the focal lengths and apertures of the mirrors or lenses. Similarly the amount of radiation lost during each reflection or transmission step within the device will depend on the quality of the components. Of particular importance is the width of the entrance slit; an increase not only increases the bandpass but also the transmission of the instrument. The slit and its illumination are, in fact, major factors in deciding the transmission; the relations between these factors are relatively complex. This arises because the brightness observed at the detector depends not only on the intensity of the radiation but also on the solid angle over which energy is collected. As a result, the effects of a change in the entrance slit width will depend on both the solid angle over which radiation from the light source is available and the angle over which the components of the spectrometer itself are able to collect the radiation passing through the slit. This topic is of considerable importance and is discussed further in Section 9.2.4.

9.1.3 Requirements of Instruments Used for AAS and AFS

In principle a relatively simple monochromator should suffice for most analytical atomic absorption or fluorescence measurements. In practice, however, many commercial spectrophotometers are supplied with relatively expensive, high quality grating monochromators. This is partly because such instruments are convenient to use, allow the maximum precision in measurements and enable good sensitivity to be obtained under what might otherwise be considered adverse conditions. A high-quality monochromator may also prove extremely useful if the spectrometer is to be used for flame-emission spectrometry as a means of extending the facilities available to a particular laboratory. The versatility thus obtained could account for the specifications of some instruments. Some general features are, however, desirable in any dispersive devices to be used for routine applications. These include: (1) good stability in the wavelength setting mechanism to minimize drift from the peak intensity attainable at the resonance line, (2) good stability of the slit-width setting so that changes in intensity are not caused by drift, (3) an adjustable slit width allowing the optimum value to be chosen for each application, (4) a clear and accurate wavelength calibration allowing the required resonance line to be quickly and conveniently selected, preferably with an accuracy of 0·1 nm or better, (5) a rapid wavelength changing device to facilitate changes between lines hundreds of nanometres apart, (6) entrance and exit apertures situated to allow convenient placing of auxiliary equipment. Other features that may be useful include provision of a variable speed mechanical wavelength drive to allow spectra to be scanned, an exposed slit mechanism on which an image of the light source is easily focused, and interchangeable prisms or gratings to allow optimum performance to be obtained at any wavelength.

The specific requirements for AAS and AFS differ considerably, although the same device can often be applied to both techniques with satisfactory performance. Thus, for atomic fluorescence measurements it is important that the peak transmission be relatively high to give good sensitivity. With many fluorescence cells improved sensitivity would also be obtained if light were accepted over a wide solid angle. A high transmission is frequently not necessary for atomic absorption, but sufficient light must be transmitted to obtain adequate signal : noise ratios at the photomultiplier-amplifier system. A narrow spectral bandpass is generally unnecessary for atomic fluorescence work and would frequently prove a disadvantage as (for a given size and quality of instrument) it would be obtained at the expense of high transmission. An exception may occur when fluorescence measurements are made with a continuum source. Any scattering of incident radiation that occurred would then occupy a much wider wavelength range than the fluorescence radiation. Thus, the fluorescence signal : background intensity ratio may be improved by reducing the spectral bandwidth. A narrow spectral bandpass is not essential for many atomic absorption applications but may result in improved sensitivity in certain applications. For example a reduction in bandpass can sometimes avoid detection of non-absorbing or weakly absorbing lines at wavelengths close to that of the resonance line. It may also be possible to avoid the detection of intense background radiation emitted by certain flame cells; even with modulated systems this radiation reaches the detector and can increase the noise level on the absorption signal so that precision is lost. A narrow spectral bandpass is also necessary to obtain highest sensitivity when a continuum light source is used for atomic absorption measurements.

9.2 CONVENTIONAL MONOCHROMATORS

9.2.1 General Constructional Details

A brief description of monochromator construction is given here together with details of some components. The dispersive elements (prisms and gratings) are discussed in the following sections together with some of the most commonly used optical arrangements.

Most monochromators used in atomic absorption spectrometers are of compact design and an effort is usually made to avoid optical systems requiring a case of awkward dimensions; a simple rectangular box is by far the most popular shape for integration with the remainder of the instrument. A substantial base is required to maintain accurate alignment of optical components and a well-fitting cover is needed to minimize stray light, especially if very weak fluorescence signals are to be measured. The construction of the slit mechanism is important if the full potential of the dispersive element is to be obtained, and in a monochromator this applies equally to both of the slits required. A single fixed slit width is inadequate except for very simple instruments with a limited range of application. Several manufacturers provide a choice of slit widths at low cost by the provision of a set of interchangeable plates into which stainless steel slit jaws have been fitted. A slit mechanism with movable jaws is, however, more convenient and versatile and is fitted to most instruments. The edges of the slit jaws must be straight and sharp and it is essential that they remain accurately parallel as the width is changed. In some assemblies only one jaw is moved, but symmetrical movement of both jaws is preferable as the centre of the observed line then remains in the same position. Adjustment is usually effected with a micrometer screw and this should be accurately calibrated to allow the width to be adjusted and reset to within a few μm. Complete closure of the jaws can cause damage to their edges and the mechanism should incorporate a device to prevent this. Thus an auxiliary shutter is useful to allow "zero" light levels to be registered at the detector and read-out device. In some designs the slit jaws may be partly concealed by the mechanism or by a protective cover; for many applications it is useful if an image of the light source or even of a flame absorption cell can actually be focused onto the metal plates forming the slit jaws. Ideally, the entrance and exit slit-widths should be individually optimized; monochromators used in analytical AAS and AFS, however, often have a linked mechanism so that adjustments to both are made simultaneously. In some instruments the maximum slit-width is quite small and this may prove a disadvantage for fluorescence applications where a wide spectral bandpass is quite permissible but high transmission of radiation is essential; a maximum aperture of 2-3 mm is provided with many instruments and is suitable for most applications.

Although spectrographs are available in which the dispersive element is the only optical component (principally the concave grating, which is unsuitable for scanning monochromators, see Section 9.2.3), it is generally necessary to use several lenses or

mirrors for collimating or focusing radiation within the instrument. The number of such components should be minimized because, apart from any considerations of expense, it is essential to avoid loss of radiation (by absorption, etc.), minimize stray light and maximize the contrast of the system. As a result, multi-component lenses such as those found in cameras are not used and, of course, the common coating techniques are generally impracticable if a wide wavelength range is needed. Instead of attempting to make each component perfect, it is more usual to carefully select the essential components so that their individual aberrations tend to cancel within the system.

At the present time, mirror systems are more widely used than lenses in the scanning monochromators needed for AAS and AFS. This arises because the usual disadvantage of mirrors in a spectrograph (the difficulty of providing minimum aberrations over the wide field angle needed to photograph a relatively wide region of the spectrum) no longer applies and in other respects mirrors have many advantages over lenses, particularly from the point of view of mass production at moderate cost. For example, chromatic aberrations are often a problem with lenses but cannot arise with front-surfaced mirrors. Similarly, high-quality mirror coatings are available over the whole visible and uv region, but even relatively expensive silica lenses may give considerable loss of light by absorption in wavelength regions of interest in AAS and AFS. Further losses also occur with lenses owing to surface reflections, material defects (e.g. bubbles) and other effects which are more easily avoided with mirrors. Finally, a large mirror may also be produced at substantially lower cost than an equivalent lens owing to the relative ease of mirror manufacture. The size of these components is a major factor in determining the transmission of the monochromator for a given spectral bandpass. In the past this would have been governed by the expense of the dispersive element but at the present time large replicate gratings (see Section 9.2.3) are available at quite reasonable cost. Thus the availability of large, low-cost mirrors is particularly useful for the production of large aperture* monochromators at reasonable cost. As a result it is economically feasible to use an instrument of aperture f/2 or f/3 in an atomic absorption spectrometer when f/8 or f/11 would be adequate. This not only improves the precision of measurements under adverse conditions (i.e. low-intensity light source) but also makes the spectrometer

---

* The aperture is usually expressed as an "f-number"—the ratio of focal length to effective diameter for an optical component.

much more useful for alternative application to atomic fluorescence or flame emission spectrometry.

As mentioned above, it is best to obtain a compact and convenient shape for the monochromator by the choice of a suitable optical system. This may not always be possible (particularly with prism instruments) and it may be necessary to add additional components simply to deflect the input or output beams; this is often the case where a "straight through" monochromator is required. It would also be possible to use such devices to scan the spectrum across the exit slit. In most cases, however, wavelength selection is achieved by rotation of the prism or grating. This is best carried out with a screw or gear system allowing accurate selection without backlash and reproducible operation over a long period. Wavelength calibration with dial or drum scales has been used extensively in the past; more convenient operation, however, is obtained with digital counters reading linearly in wavelength units. This is easily achieved with grating instruments (for which the dispersion does not vary greatly with wavelengths) and some prism instruments use ingenious drive mechanisms to obtain the same effect. Calibration in arbitrary units is inconvenient for routine applications where the wavelength setting is frequently changed, particularly when the calibration is not linear. Provision for fine adjustment of the wavelength setting is necessary if the instrument is to be easily set to the wavelength of a particular atomic line. Therefore, to allow rapid changes from one line to another the monochromator should be fitted with either coarse adjustment controls or a high-speed motor drive. A slow mechanical drive allowing scanning and recording of spectra is also often fitted. Several speeds are desirable to give correct matching of spectral bandpass and scan rate and the drive should be smooth to avoid vibration of the optical components.

Recently a number of modified monochromators have been reported with which it is possible to make intensity measurements at several discrete lines either while scanning rapidly or by automatic selection of lines.[5-9] These devices are useful for rapid, multi-element analysis either by AAS or AFS and may see further development. Automatic selection of lines is probably of greater interest as the rest of the spectrometer may remain unchanged (whereas rapid scanning requires that each measurement be made in an extremely small time interval). The system described by Cordos and Malmstadt[9] uses a conventional commercial monochromator and

widely available digital and logic circuit components and may be programmed to change between a large number of preset wavelengths with an accuracy of 0·02 nm. Such a device should provide worthwhile time saving in many routine applications, quite apart from its application to multi-element analysis.

9.2.2 Prism Instruments

Most early spectroscopes used a prism as the dispersive element and these devices are still used today although, as mentioned earlier, many present-day commercial monochromators used for analytical AAS or AFS employ replicate gratings. Most applications have used a prism with flat surfaces and triangular cross section and only these are mentioned here. Many other types of prism, including some with curved surfaces, have, however, also been tested for use in specialized instruments.

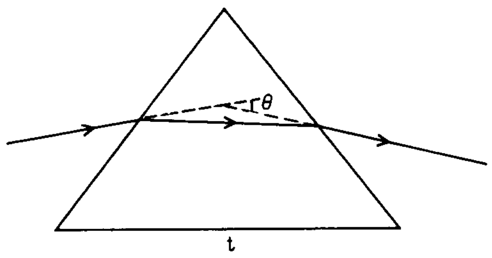

Fig. 9-2. Path of a ray through a section of a prism.

The passage of a ray of light through an isosceles prism is illustrated in Fig. 9-2. The ray is deflected as it enters and leaves the prism owing to refraction, its total deflection from the original path being known as the angle of deviation, θ. This angle assumes a minimum value when the ray passes symmetrically through the prism (i.e. enters and leaves at the same angle to the face), giving the position of minimum deviation. Under given conditions the value of θ depends on the refractive index, μ, of the prism material. Thus, as μ is a function of wavelength for a particular material, the prism acts as a dispersive element. For most spectroscopic applications, optical distortions are minimized by using the prism near to minimum deviation and also by arranging that the slit is parallel to the prism edge and using a parallel beam of light.

When a prism with a base of length t is completely illuminated by a light beam of width w it may be shown that the angular dispersion is given by

$$\frac{d\theta}{d\lambda} = \frac{t}{w}\frac{d\mu}{d\lambda} \tag{9-2}$$

and the resolving power is given by

$$\frac{\lambda}{\Delta\lambda} = t\frac{d\mu}{d\lambda} \tag{9-3}$$

where $d\mu/d\lambda$ is either found graphically or from an empirical formula such as that of Hartmann:

$$\mu = \mu_0 + C/(\lambda - \lambda_0) \tag{9-4}$$

where μ, C and λ_0 are experimentally determined constants for each material.

Hence

$$\frac{d\mu}{d\lambda} = -\frac{C}{(\lambda - \lambda_0)^2} \tag{9-5}$$

and it can be seen that both the dispersion and resolving power will decrease with increasing wavelength. It is also apparent that reducing the height of the prism (i.e. the effective value of w) will reduce the dispersion of the instrument but not its resolving power, which depends only on the length of the base. These simple rules apply only at minimum deviation and the situation is rather more complicated under other conditions. In practice it is found that the dispersion shows a rapid increase as θ is increased from its minimum value but the resolving power is reduced slightly.

Many different prism materials, including liquids, have been used successfully in the wavelength region 200 to 800 nm, but the choice for modern commercial instruments is not particularly wide. Obviously the material must have high transparency over the wavelength region of interest and this should be as wide as possible for a general purpose instrument. A high value of $d\mu/d\lambda$ is also essential to obtain good dispersion. The material should also be available in large pieces of optical quality, be easily polished, resistant to attack by air, water vapour, etc. and show a small dependence of refractive index on temperature. Optical quality glasses meet many of these requirements and are available at moderate cost in large pieces. They are widely used for instruments designed for use in the visible region and give high dispersion. Unfortunately, they are of little use for many AAS and AFS applications owing to their very low transmission in the important ultraviolet region. The useful limit lies in the range 350 to 400 nm for traditional crown-and-flint glasses and even special uv-transmitting glass cannot be used below *ca.* 300 nm. Applications in the region upwards from 200 nm generally require a quartz prism; large pieces of crystalline material are difficult to obtain, however, and may therefore be expensive. As a result, many prism instruments supplied commercially have a fused silica prism. This material gives good performance in the ultraviolet but poor dispersion in the visible region owing to a rapidly decreasing value of $d\mu/d\lambda$. Some of the more expensive prism instruments are, therefore, supplied with interchangeable glass and silica prisms. The relative dispersions of these materials in a typical commercial instrument are illustrated in Fig. 9-3.

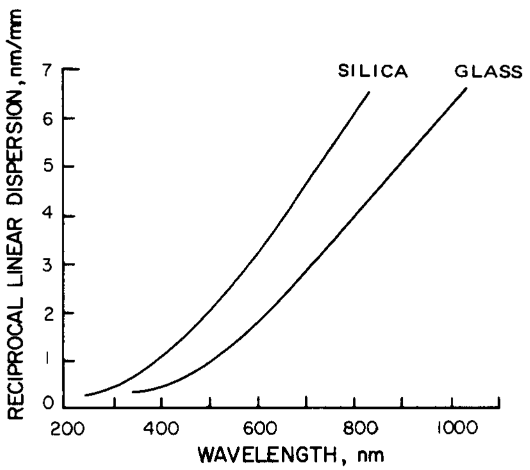

Fig. 9-3. Reciprocal linear dispersion obtained with glass and silica prisms in the same spectrometer.

Some of the classical optical arrangements used in prism instruments are illustrated in Fig. 9-4. In practice, improved performance may be obtained by elaborating on these designs. For example, use of a prism made up of several components, or instruments with two or even three separate prisms, is quite common. Those arrangements in which the entrance and exit slits appear to coincide use a tilted mirror, an off-axis mirror, or a beam deflecting device.

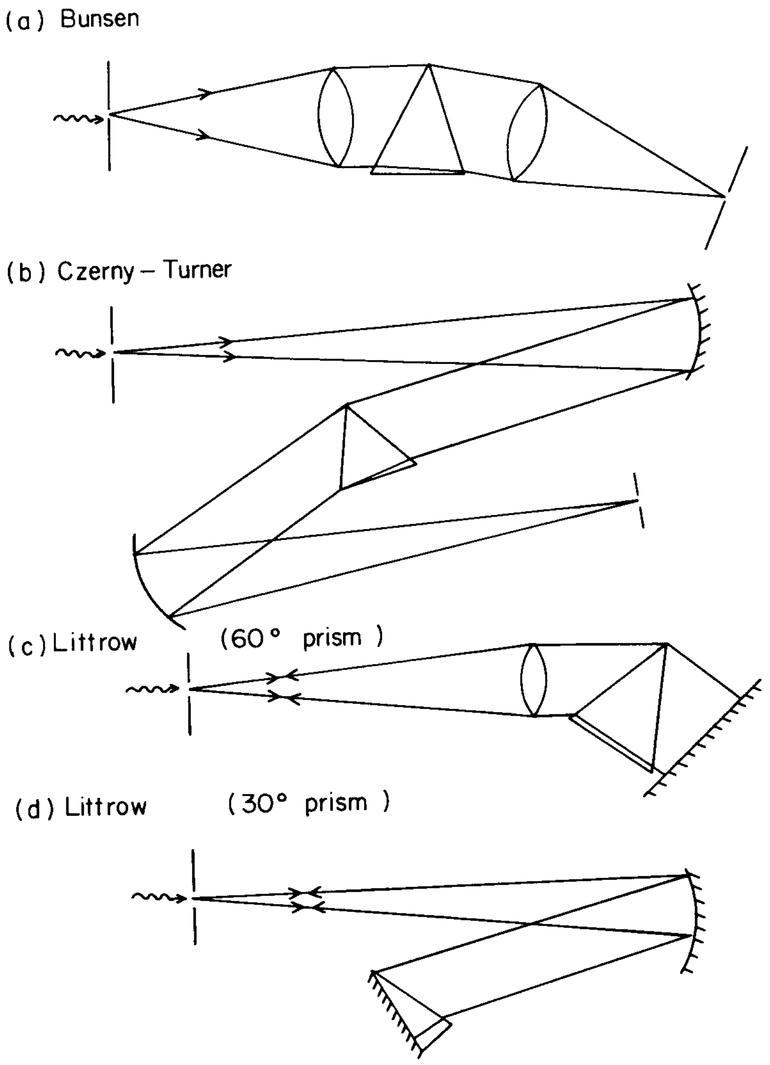

Fig. 9-4. Schematic layout of prism spectrometer systems.

9.2.3 *Grating Instruments*

As mentioned earlier, many commercial monochromators available at the present time use a diffraction grating as the dispersive element because of the availability of relatively high-quality replicate gratings at reasonable cost. (A replicate grating is simply a mass produced copy of a grating on which the spacings have been individually ruled; only the highest quality instruments are now fitted with original gratings.) Although a transmission grating would be the direct equivalent of the prism, most instruments today use front surface reflecting gratings which, like mirrors, are easily produced to cover a wide wavelength range with good performance. Concave gratings of this type ruled on concave mirrors combine the dispersive and focusing functions and thus reduce the number of components, loss of light and aberrations of the image. For this reason they are widely used for spectrographs. Plane gratings are, however, more suitable for all scanning monochromators as constant focusing conditions are maintained while the grating is rotated to scan the spectrum. Hence we shall be concerned here only with plane, reflection gratings.

A diffraction grating is simply a convenient practical method of obtaining a large number of very narrow, long apertures of the required dimensions. These apertures are of two types: those that transmit or reflect incident radiation and those that are opaque or give no reflection (depending on whether the grating is of the transmission or reflection type). When the grating is illuminated by parallel light and the transmitted or reflected radiation is brought to a focus two optical effects are obtained. The apertures produce a large number of light beams that have different path lengths but the same frequency and the same initial phase, i.e. that originate from coherent sources. Thus an interference pattern is obtained. At the same time, diffraction occurs at each of the narrow apertures (diffraction results from interference which arises from mutual interactions of different parts of the *same* wavefront so that it is observed at a single slit). As a result a combined interference and diffraction fringe pattern is seen with the characteristic intensity maxima and minima. When the grating is illuminated normally by light of wavelength λ, the principal maxima occur at angles, θ, given by the equation

$$\mu(a + b) \sin \theta = n\lambda \qquad (9\text{-}6)$$

where a and b are the widths of the two types of spaces on the grating, μ is the refractive index and n is an integer known as the order of interference.

In spectroscopic applications, the grating is illuminated by light from a slit and an image of the entrance slit is seen as a sharp line at each maximum. The spectrum may be scanned by changing the value of θ. In practice this is complicated by several factors. In the first place it can be seen from equation (9-6) that if light of wavelength

λ_1, is observed at an angle θ, this same angle will also correspond to light of a different wavelength, λ_2, in the second order, and so on. Thus, the grating will produce a series of overlapping spectra, the wavelengths observed at a given angle being such that $\lambda_1 = 2\lambda_2 = 3\lambda_3 = \ldots n\lambda_n$. Obviously the wavelength range corresponding to one order (i.e. the range without overlap) will decrease with increasing values of n. To avoid difficulty in interpretation of spectra most monochromators applied to AAS or AFS therefore use low orders, frequently the first. Even then special precautions are needed to avoid confusion from higher orders over the complete visible and uv range (see below). A second factor requiring the use of low orders is the efficiency with which dispersion is obtained; the diffraction pattern of the fringes means that approximately $1/\pi^2 n^2$ of the incident radiation goes into each order. Thus much higher transmission is obtained by using low orders, although in fact the situation can be altered by using the blazing technique (see below).

On the other hand, both the dispersion and resolving power of the grating are improved by using higher orders. The angular dispersion is given by

$$\frac{\mathrm{d}\theta}{\mathrm{d}\lambda} = \frac{n}{\mu(a+b)\cos\theta} \tag{9-7}$$

and the resolving power by

$$\frac{\lambda}{\Delta\lambda} = nN \tag{9-8}$$

where N is the total number of spaces on the grating. Thus it can be seen that if the use of high orders is impracticable it is necessary to use a grating ruled with a large number of fine spaces in order to obtain high dispersion and good resolution. Nevertheless, there is obviously a finite limit to the combination of wide wavelength range and high resolution that is possible. The popularity of grating instruments is largely due to the success with which these features have been combined at reasonable cost. Reference to equation (9-7) shows that, for a given grating and order, the dispersion is not directly dependent on wavelength. By correct design of the optical system it is possible to use the grating to give a "normal" spectrum in which the linear dispersion is constant over the whole spectral range of interest. This allows the production of monochromators having linear wavelength scales. An additional advantage is that the distance from the zero-order image to the spectral line obtained for wavelength λ is directly proportional to λ. Hence the calibration may be easily checked by noting the reading obtained at zero order (when the incident radiation is reflected or transmitted unchanged). The problem of overlap of orders has received considerable attention as even in the first order it is relatively small (e.g. the second-order image of a line 250 nm will coincide with the first-order image of one at 500 nm). A common solution is to use auxiliary filters which transmit only the (narrow) wavelength range of immediate interest. This is, however, inconvenient and reduces the efficiency of the instrument. A much more acceptable solution is to replace the simple apertures mentioned earlier by apertures formed at a controlled angle or *blaze* to the surface of the grating. This changes the diffraction properties of the grating so that for any wavelength range it is possible to direct a very high proportion of the incident radiation into a chosen order. Thus the efficiency of the grating is improved and the "ghost" spectra of other orders can be considered as of negligible intensity for many applications. The highest blaze efficiency is obtained in the first order so that this is still generally preferred, although the use of higher orders is made much more convenient than with a simple grating. Very high blaze efficiency can be obtained only over a narrow wavelength range. Thus it is usual to accept a lower peak value (perhaps 60%) in return for good efficiency over a wide wavelength range. Typically, a grating blazed at 500 nm in the first order would retain about 50% of its peak efficiency at 250 or 750 nm. As a result, some monochromators are supplied with two interchangeable gratings blazed for the uv and visible regions respectively.

Although the resolving power (and hence spectral bandpass) of a grating depends in theory only on the number and separation of the apertures, its actual performance is affected considerably by the degree of perfection achieved in the production process. Thus, loss of resolution and efficiency and increased scattered light or ghost spectral lines will be observed with poor-quality gratings. Reflection gratings require the ruling of many thousands of fine lines on to a surface that has been polished to a perfect optical finish. This is most easily achieved by coating an optically polished glass or silica plate with a layer of aluminium by vacuum-evaporation; this then allows ruling in a soft material that could not otherwise be easily optically finished. By using specially designed ruling machines and a very fine diamond point it is possible to obtain groove densities of several thousand lines per millimetre over large areas. Even with modestly

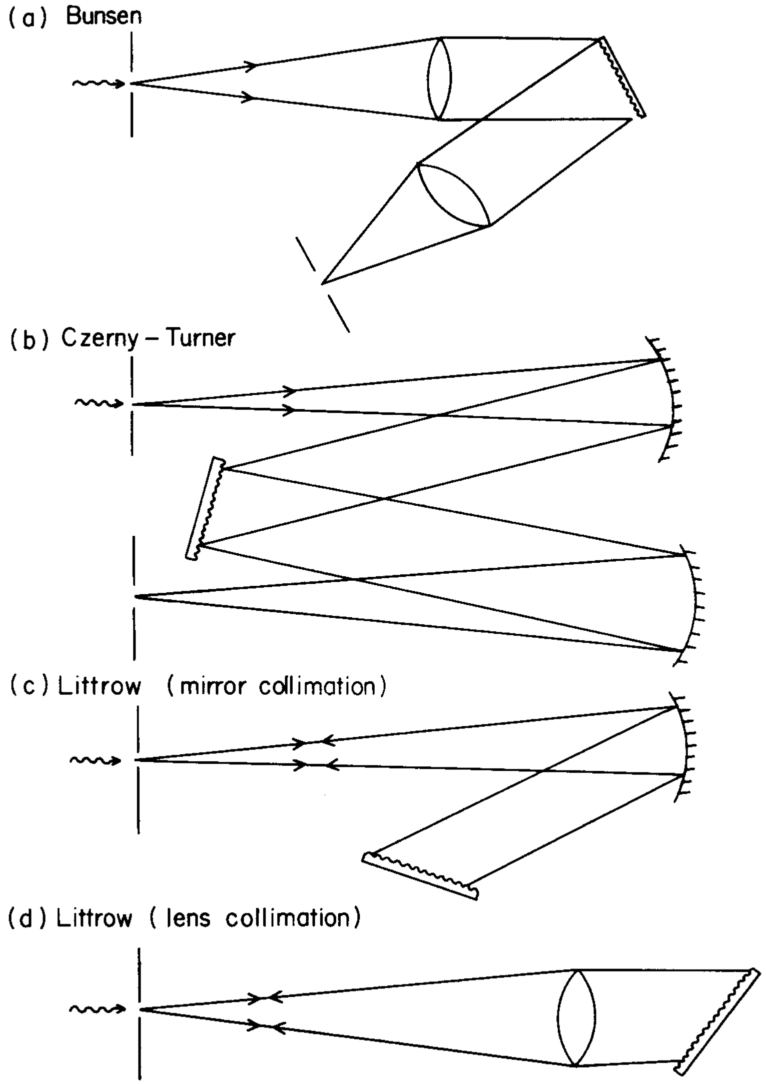

Fig. 9-5. Schematic layout of plane reflection grating spectrometric systems.

priced atomic absorption spectrometers it is possible to supply gratings of (typically) 50 x 50 mm size with more than 1000 lines/mm. Although these will be replicates, modern production techniques result in a quality almost as good as that of the original gratings.

Some of the optical arrangements that are commonly used for plane reflection gratings are illustrated in Fig. 9-5. They are

equivalent to the prism systems described in Section 9.2.2 and similar comments apply. The Czerny-Turner arrangement is particularly popular as it uses mirrors and directly provides an instrument with conveniently placed entrance and exit slits within compact dimensions.

9.2.4 Illumination of the Monochromator

Even the largest monochromators have a relatively low transmission at any given wavelength. As a result it is important to ensure that the method of illumination gives maximum utilization of the available energy, particularly for fluorescence measurements where the sensitivity may depend directly on the amount of radiation collected. To achieve this several factors must be taken into account:

(1) The intensity of the source will vary inversely with the square of its distance from the monochromator.
(2) Efficient use will only be made of the collimation system of the monochromator if it is completely illuminated, i.e. if the source subtends a solid angle at the slit that is at least as large as that subtended by the condenser.
(3) If the source has a large surface area of uniform brightness, as much as possible of that area should be included within the solid angle of radiation that reaches the collimator.
(4) If the source is of extended depth, each cross-section (taken along the optical axis) should satisfy condition (3).
(5) When the other conditions are met, use of an auxiliary condensing lens or mirror cannot further increase the brightness of the spectrum. Indeed, loss of energy will always occur at each extra optical component.

It is therefore apparent that an increase in the intensity of a spectral line cannot be obtained by using a condensing lens to focus an image of the source onto the entrance slit *unless* the source itself is too small to fill the collimator with light or the source cannot be brought sufficiently close to the slit as a result of other instrumental requirements. An exception occurs with a long source when, in general, it is possible to utilize a greater depth of source by using a lens to focus the back surface of the source on the slit. Wherever a condensing lens must be used, maximum illumination will be obtained if the lens completely fills the solid angle that can be accepted by the collimator. In some cases the aperture of silica lenses supplied with atomic absorption spectrometers is too small to meet this requirement. It is also worth remembering that with a given lens and a given (minimum) distance between the source and the slit, moving the lens closer to the slit will produce a smaller, brighter image but this does *not* increase the brightness of the observed spectral line. This arises because the energy per unit solid angle entering the monochromator is unchanged and the additional energy simply misses the collimating element and is wasted. At first sight these rules may seem somewhat complicated but it is usually possible to visualize clearly the situation with a particular monochromator simply by drawing a scale diagram of the collimator and the entrance optics, taking into account both the horizontal (across the slit) and vertical (along the length of slit) planes.

In atomic absorption applications it is nearly always necessary to use auxiliary lenses or mirrors to obtain a satisfactory optical path through the atom cell. Even though in AAS minimization of energy loss in the optical system is not as important as in AFS, careful choice of the optical system may still give improved results. For example, the entire light beam may pass through the atom cell but only part of it fall on the collimator owing to incorrect use of a lens or mirror. The absorption signal observed for a given sample added to the atom cell would then be reduced. This often occurs when an extremely small image of the background light source is focused on the slit on the assumption that full utilization of the available energy will thus be achieved. Similarly, the precision of absorption measurements may be lowered if the intensity of the source radiation reaching the detector becomes too low. This often results from incorrect use of the optical components or simply because those components are unsuitable. For example, if an atomic absorption spectrometer is designed to use a narrow parallel beam of radiation, because the absorption cell is narrow (and all of the beam must pass through the cell), this might be obtained with two small condensing lenses, one to give a parallel light beam from the source, the other to focus this beam on the monchromator slit. Loss of efficiency then occurs at two points; the first lens is too small to collect all available radiation from the lamp and the second is too small to completely fill the solid angle accepted by the collimator. This could easily be avoided, for example, by using a mirror system such as that shown in Fig. 9-6. In some cases it may, of course, be more practicable to select an optical beam that meets the requirements of the monochromator and choose the dimensions of the absorption cell accordingly.

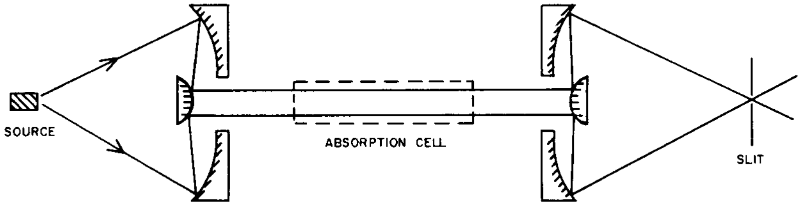

Fig. 9-6. Double inverted Cassegrain system for use with a narrow absorption cell.

9.3 OTHER MONOCHROMATING DEVICES

9.3.1 Filters

Wavelength selection by means of a small optical filter transmitting a specific resonance line is in principle an attractive alternative to the monochromator devices described in Section 9.2. This is particularly true in atomic fluorescence spectroscopy where the transmission factor attainable with a filter is often much greater than that available with a conventional monochromator. In practice, however, the number of reported applications of optical filters is relatively small. For atomic absorption spectroscopy, the relatively poor resolution of even the best filters limits their application to simple instruments suitable for the determination of a few elements which exhibit simple atomic spectra. Typical element combinations for which simple AAS instruments of this type might be designed, for example, are sodium and potassium, mercury, thallium and lead, or calcium and magnesium. In atomic fluorescence spectroscopy, filters have been used in simple spectrometers and in multi-channel instruments to provide for wavelength selection in simultaneous multi-element analysis. Possibly the relatively small interest in filters to date results from the sophisticated design of most commercial atomic absorption spectrometers; the situation may change as the use of simple instruments dedicated to specific analytical applications becomes more widespread. It is worth remembering, however, that good-quality interference filters (especially those for the uv region) are still relatively expensive and if filters are required for a number of elements this approach may prove almost as costly as the use of a simple monochromator of adequate spectral bandpass and transmission characteristics.

The traditional optical filters, used for example in molecular devices which rely on the absorption of suitable dyes added to glass, plastic, gelatine or even used alone in solution. Commercial filters of this type are available with uv transmission capability, but they are usually most suitable for application to the visible region. The dyes or pigments used in the simplest versions (such as those intended for photography) have very wide transmission bands and are rarely suitable for spectroscopic applications. More satisfactory results are obtained by using combinations of "sharp" cut-off filters which are produced by several manufacturers. These are available in two series: long wavelength (transmitting red and yellow light) and short wavelength (transmitting blue and green light). By combining a filter from the long series with one from the short series it is possible to obtain a somewhat narrower bandpass with its peak at a preselected wavelength. The bandpass is, however, still wide for many applications; even with a peak transmission of only 15-20% the half-intensity width may be of the order of 50 nm. A further disadvantage is the possibility of change of spectral characteristics owing to the large amount of energy absorbed when the filters are irradiated with unwanted wavelengths at high intensity. Therefore, these filters are unsuitable for almost all AAS applications and the majority of applications to AFS. Improved bandwidth can be obtained by combining a number of filters but the transmission is then usually too low, particularly for fluorescence measurements. A detailed tabulation of transmission and stability data for commercially available filters is included in the "Handbook of Chemistry and Physics".*

Much better results are obtained using *interference filters.* These are simple dispersive devices utilizing the interference of light for spectral isolation. Unlike the diffraction grating, different path-lengths are obtained with a semi-reflecting surface to divide the amplitude of the light beam rather than by an actual division of the wavefront. A small piece of optically flat glass or silica is coated with a semi-reflecting layer of a material that has a high reflection coefficient but gives low absorption of light. This layer is covered by a non-reflecting spacing layer and finally by a second semi-reflecting layer. The reflecting surfaces of the two outside layers are face-to-face so that multiple reflections occur between them when a beam of light is passed through the filter. As a result the emergent beam is composed of many different path-lengths and an interference fringe

---

* Published annually by the Chemical Rubber Co., Cleveland, Ohio.

pattern is observed. The positions of the transmission maxima of this pattern are found from the equation

$$2\mu d \cos\theta = n\lambda \qquad (9\text{-}9)$$

where μ is the refractive index of the spacing layer and d is its thickness. θ is the angle between the light beam and the normal to the filter surface. As the filter is usually used at 90° to the beam, equation (9-9) can be simplified to

$$2\mu d = n\lambda \qquad (9\text{-}10)$$

Thus a filter can be made with a transmission peak at any required wavelength by depositing a spacing layer with the correct value of μd. This peak will be accompanied by other transmission maxima corresponding to different orders. For example, if $\mu d = 150$ nm, the filter would transmit at 300, 600 and 900 nm. Isolation of the required peak (e.g. 600 nm) does not present problems when the maxima are so widely spaced; in some cases use of a glass base ensures transmission only at a single visible wavelength, otherwise layers of absorbing dyes may be added to the filter to "block" the unwanted peaks.

Provided the filter has been correctly manufactured and is used at 90° to the incident radiation, the bandwidth at a given spacing (i.e. value of μd) depends only on the reflection coefficient of the reflecting layers. The relationship between the two is conveniently expressed in terms of the *finesse, N,* of the filter which is the ratio of the interval between successive peaks and the bandwidth. For example, a finesse of 50 for the filter mentioned above would mean a bandwidth of 600/50 = 12 nm. If the reflection coefficient is R* the finesse is found from

$$N = \frac{\pi R^{1/2}}{1 - R} \qquad (9\text{-}11)$$

The peak transmission of the filter is also simply related to R, although the absorption coefficient, A, of the reflecting layers must also be taken into account. The fraction of incident radiation at the peak wavelength which is transmitted is given by

$$\tau_m = (1 - A - R/1 - R)^2 \qquad (9\text{-}12)$$

Some numerical values of N and τ_m for different values of R and A are given in Table 9-1.

---

* i.e. $R \times 100$ gives the percentage of light reflected by the surface.

It will be appreciated that the reflecting layers of a high-quality interference filter must show simultaneously a high value of R and a low value of A. The former is achieved relatively easily in the visible region using the traditional coating materials of silver or sometimes aluminium, but low absorption values are more difficult to obtain reproducibly even when very thin layers of metal are used. Fortunately, the situation has improved considerably in recent years as a result of the use of multiple layers of dielectric materials such as ZnS, MgF_2, Sb_2O_3 and $PbCl_2$. By correct choice of the material and the number of layers used it is possible to obtain useful filters throughout the visible and ultraviolet regions. At the present time reflecting layers combining a value of $R = 0{\cdot}98$ with $A \leqslant 0{\cdot}005$ are feasible, although such specifications are generally reserved for applications such as laser optics rather than for conventional commercial interference filters for routine use. It is also possible to reduce the bandwidth for a given peak transmission by using a wider separation (i.e. smaller wavelength interval between adjacent maxima) and relying on the blocking layers to prevent transmission at the extra harmonic peaks.

TABLE 9-1

Variation of peak transmission with reflection and absorption coefficients of reflecting materials used in interference filters

R	0·80	0·84	0·88	0·92	0·96	0·98
N	14·1	18·0	24·6	37·6	77·0	156
A	τ_m					
0·18	0·01	—	—	—	—	—
0·14	0·09	0·02	—	—	—	—
0·10	0·25	0·14	0·03	—	—	—
0·06	0·49	0·39	0·25	0·06	—	—
0·02	0·81	0·77	0·69	0·56	0·25	—
0·01	0·90	0·88	0·84	0·77	0·56	0·25
0·005	0·95	0·94	0·92	0·88	0·77	0·56
0·001	0·99	0·99	0·98	0·98	0·95	0·90

Interference filters are currently available from several manufacturers in a wide range of bandpass/transmission combinations. In the "narrow band" types of interest for AAS and AFS, typical filters for the visible region would be in the price range \$30 to \$300 with a peak transmission of about 65% for 6 to 8 nm bandpass or about 25% for 0·3 to 0·4 nm. The price will also depend on the degree of tolerance that the customer is prepared to accept in the specification of the peak transmission wavelength, as this factor is relatively difficult to control. This tolerance may be of the order of 2 nm in the cheaper filters with 6 to 8 nm bandpass, but the more expensive ultra-narrow versions can often be selected to ±0·1 nm. Although continual improvements are made in ultraviolet filters, which are now available for wavelengths down to about 200 nm, the specifications are generally somewhat poorer than in the visible region. For example, below 300 nm typical bandpass/transmission characteristics are 7-10 nm/1-5% or 23-30 nm/15-20%. As the resonance lines of many elements lie in the ultraviolet region this situation somewhat reduces the advantages of using interference filters for AAS and AFS applications.

The relatively high cost of these interference filters is also a disadvantage when wavelength selection for many elements is required. It may be possible to reduce this cost, particularly for fluorescence measurements where narrow bandpass is less important, by using a *variable interference filter.* These devices are manufactured by coating an interference filter onto a large disc (e.g. 15 cm diameter) in the form of a circular band with a continuously varying spacer thickness. The full width of the band is viewed through a slit about 1 mm wide so that as the disc is rotated a gradually changing peak wavelength is observed. Different filters are manufactured for both the visible and ultraviolet regions; a typical commercial device gives an average transmission of 40% for 20 to 25 nm bandpass, the region 450 to 700 nm being covered with a rotation of 270°.

Although interference filters have seen little use for wavelength selection in atomic absorption measurements, in atomic fluorescence spectroscopy several applications, particularly to multi-element analysis, have been reported. Mitchell and Johannson,[10] for example, utilized interference filters in a four-channel atomic fluorescence spectrometer. The filters utilized for transmission of the fluorescence radiation of each element were mounted on a rotating "filter-wheel" synchronized so that the appropriate filter passed the photomultiplier detector when the hollow-cathode lamp for that element was operated by a high-current pulse. Walsh[11] has described single and multi-channel atomic fluorescence spectrometers, the former using an interference filter and conventional monochromator, while the latter is based on a solar-blind photomultiplier (see Chapter 10).

9.3.2 Resonance Detectors

Early demonstrations[12] of the phenomenon of resonance fluorescence were made by irradiating an evacuated bulb containing a small amount of sodium metal with radiation from a sodium-discharge lamp. No radiation could be seen at 90° to the light beam until the bulb was warmed slightly to produce a low pressure of sodium vapour; under these conditions the characteristic *D*-lines are re-emitted as resonance fluorescence. In 1959, Russell and Walsh[13] suggested that this simple experiment could be used to permit the isolation of the resonance lines needed for atomic absorption measurements. All radiation from the background light source would be passed through the absorption cell and allowed to fall on a "resonance detector" containing vapour of the analyte element. A photomultiplier placed at 90° to this beam and positioned to receive fluorescence radiation generated in the detector would then respond only to changes in the analytical resonance line, just as if that line had been isolated using a conventional monochromator or filter. The advantages of this technique are immediately obvious: (1) the "bandpass" of the resonance detector is simply the width of its absorption line and under the conditions normally used the value is comparable with those obtainable only from dispersive instruments of extremely high resolution; (2) for many elements the "transmission" obtained with this narrow bandpass is much higher than could be achieved at this bandwidth by conventional techniques; and (3) unlike a conventional monochromator, it is unnecessary to select the peak wavelength manually and drift from this wavelength is impossible. In view of these advantages, considerable development of the technique has been carried out by Walsh and co-workers.[14-18] The main features are described here, although, as explained below, the advantages of application of the technique are really only realized for a few elements.

Resonance detectors are most efficient for atoms that exhibit simple spectra; a number of energy levels close to the ground state will give a complex resonance spectrum and result in poor absorption sensitivity. Thus the technique is best suited to the elements of groups I, II and III, for which the lines isolated are listed in Table 9-2. It can be seen that even in Group III several lines are detected for Al, Ga and In. The cloud of atoms in the resonance detector can be produced thermally for many metals simply by embedding a heating element in a small block of the appropriate metal (see Fig. (9-7), but in other cases it is necessary to use cathodic sputtering of

TABLE 9-2

Lines and groups of lines isolated by resonance detectors[18]

Element	Wavelength(s) of resonance radiation (nm)
Li	670·8
Na	589·0, 589·6
K	766·5, 769·9
Rb	780·0, 794·8
Cs	852·1, 894·4
Cu	324·7, 327·4
Ag	328·1, 338·3
Au	242·8, 267·6
Be	234·9
Mg	285·2
Ca	422·7
Sr	460·7
Ba	535·5
Zn	213·8
Cd	228·8
Hg	253·7
Al	308·2, 309·27, 309·28, 394·4, 396·2
Ga	287·4, 294·36, 294·42, 403·3, 417·2
In	303·9, 325·6, 325·9, 410·2, 451·1
Tl	276·8, 377·6

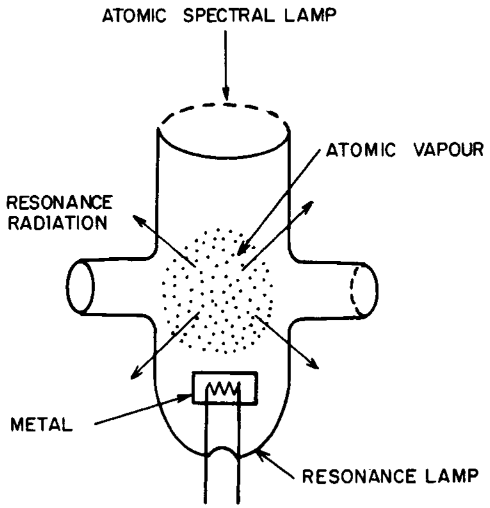

Fig. 9-7. Schematic diagram illustrating a resonance detector in which the metal atomic vapour is produced by electrical heating (from ref. 18).

the same type as in a hollow-cathode lamp (see Fig. 9-8). In practice, however, best results are obtained for most elements by using the sputtering method because the thermal types have a much longer warm-up time and require much more careful adjustment and regulation of the operating current. The current requirements of the sputtering types are similar to those of the hollow cathode lamp and the useful life is apparently as long, possibly in excess of 5000 hours.

Resonance detectors may be used for atomic absorption measurements with similar apparatus to that required when using conventional monochromators, although the best results are usually obtained with lamps having a fairly intense output. Modulation of the source is important to avoid detection of any radiation emitted spontaneously by the atoms in the resonance detector. In some respects these detectors would seem ideal for simple spectrometers, particularly of the multi-element type where several resonance detectors could view one absorption cell and automatic element selection would be easy (see Fig. 9-9). There are, however, several limitations, which will probably restrict their practical application. Perhaps the most important is the reduction in sensitivity compared with a conventional monochromator system. Optimum sensitivity will be obtained

only with the elements of group II (a single absorption line) and the absorption sensitivity decreases steadily as the number of detected lines increases. Although the "transmission factor" is good by the standards of high-resolution instruments it may be fairly low compared with the monochromators used in ordinary spectrometers. Thus resonance detectors are mostly unsuitable for fluorescence measurements. The detectors also suffer problems normally associated only with spectral sources, i.e. limited life, varying performance, a warm-up time before each operation and possible electrical instability.

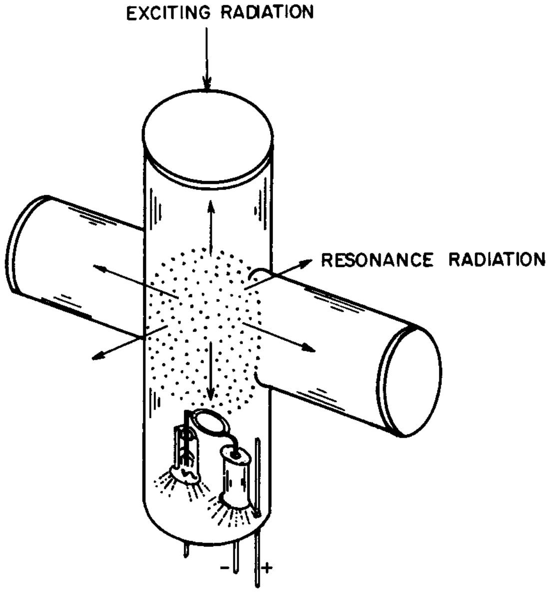

Fig. 9-8. Schematic diagram illustrating a resonance detector in which the metal atomic vapour is produced by cathodic sputtering (from ref. 18).

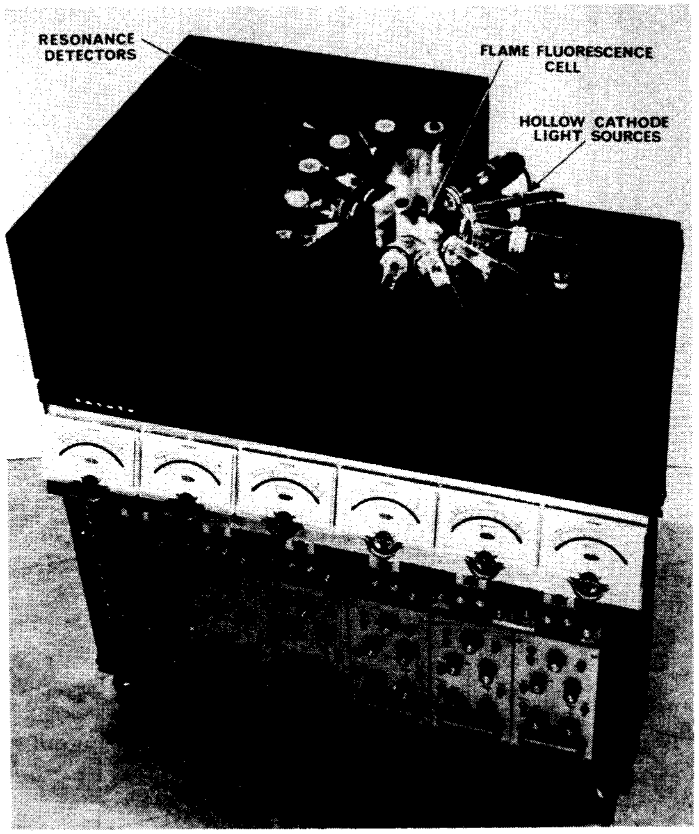

Fig. 9-9. Six-channel atomic absorption spectrophotometer incorporating resonance detectors as monochromators (from ref. 11).

9.3.3 *Selective Modulation*

Selective modulation as a means of isolating spectral lines is closely linked to the principle of the resonance detector in that the formation of an atomic vapour of the element concerned is required.

However, instead of using the resonance radiation emitted by these atoms, selective modulation requires detection of the original light beam after it has passed through the absorbing cloud. During this passage only the resonance lines of the element in the cloud will be absorbed. Hence, if the cloud of absorbing atoms can be produced periodically it is possible to modulate the radiation at the resonance lines without affecting that at any other wavelengths. A phase-sensitive detector modulated at the same frequency will, therefore, respond only to changes in intensity at the resonance lines. A demonstration of the effect of using selective modulation in this way to improve isolation of the nickel 232·0 nm resonance line is shown in Fig. 9-10. The application of this technique has been investigated by Walsh and his co-workers[18-20] and by Sebestyen.[21]

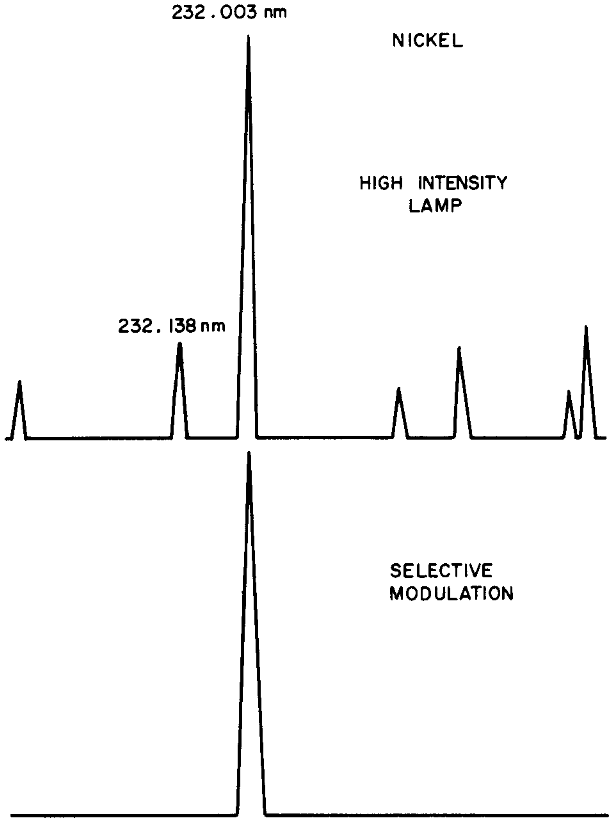

Fig. 9-10. Spectra showing isolation of the nickel resonance line at 232·003 nm by selective modulation. Lamp primary discharge: 39 mA. Lamp booster discharge: 400 mA. Modulator discharge: 20 mA.

The cloud of absorbing atoms required for selective modulation is most conveniently generated by the sputtering technique as used in hollow-cathode lamps. Modulated resonance radiation is obtained by one of three methods:

(1) Using a pulsed hollow-cathode discharge as the light source but adjusting the pulse timing and duration so that the atoms produced also act as the selective modulation medium. Figure 9-11 illustrates the manner in which a modulated signal is

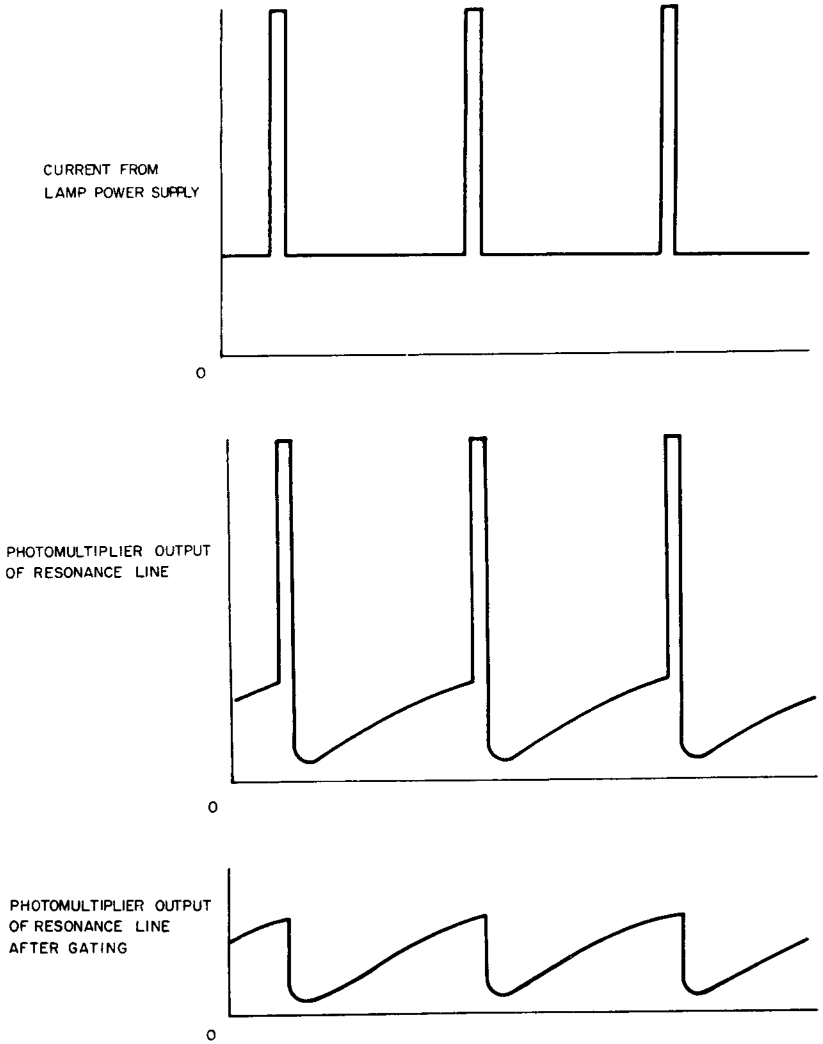

Fig. 9-11. Waveforms illustrating method of Lowe[20] for selective modulation of resonance lines by pulsed operation of a hollow-cathode lamp (from ref. 11).

obtained. The hollow cathode is operated at a steady direct current, and superimposed on this is a series of short high-current pulses. The increased sputtering due to each pulse causes a cloud of atoms of the cathode material to be formed inside and in front of the hollow cathode; by adjusting the pulse height and width it is possible to make the vapour cloud sufficiently dense to cause almost complete absorption of the resonance lines emitted by the lamp during its low dc operation. The absorption of the vapour cloud decreases between pulses and the output intensity of the resonance lines rises again to that of the dc level. The detection circuit is so arranged that there is a gating switch on the output side of the photomultiplier which is triggered by the onset of each pulse. This switch cuts out the very large increase in signal that would otherwise occur when the pulse is on. The net waveform obtained for the resonance wavelengths is thus ac in character.

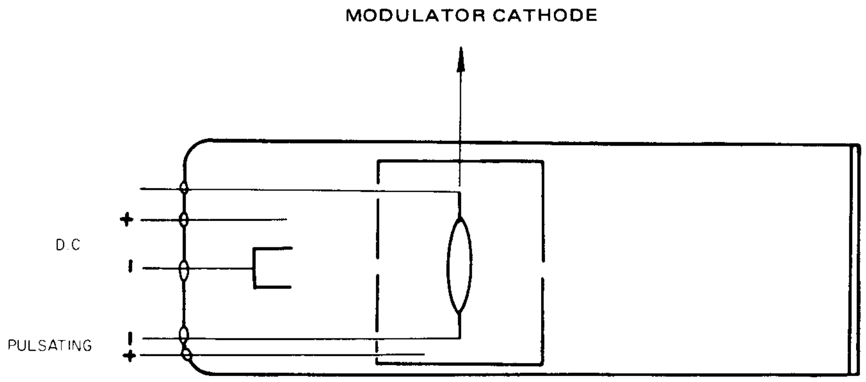

Fig. 9-12. Schematic diagram of hollow-cathode lamp incorporating internal selective modulator (from ref. 11).

(2) Using a conventional hollow-cathode discharge but with an auxiliary sputtering discharge mounted in front of the cathode to provide the cloud of cool atoms needed for selective modulation (see Fig. 9-12).

(3) Using a conventional hollow-cathode lamp with the selective modulator mounted in a separate cell in front of it (see Fig. 9-13). In almost all cases results are very poor unless a separate optical filter or a solar-blind photomultiplier is used to restrict detection of extraneous radiation and noise. The sensitivity is generally lower than with a conventional monochromator and the range and linearity of calibration are also restricted. It may be possible, however, to obtain useful absorption results for many elements by combining selective modulation with a simple (wide bandpass) conventional monochromator.

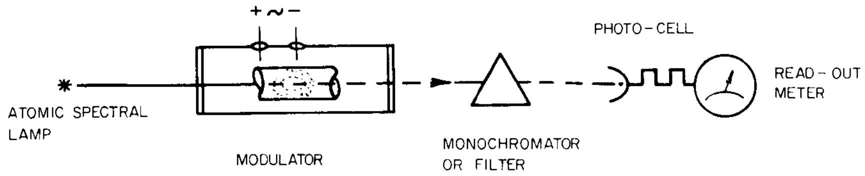

Fig. 9-13. Schematic diagram illustrating the apparatus for isolation of atomic resonance lines by selective modulation with a pulsating vapour produced by cathodic sputtering (from ref. 11).

REFERENCES

1. G. R. Harrison, R. C. Lord and J. R. Loofbourow, "Practical Spectroscopy", Prentice-Hall, Englewood Cliffs, N.J., 1948.
2. R. A. Sawyer, "Experimental Spectroscopy", Dover Publications, New York, 3rd ed., 1963.
3. R. S. Longhurst, "Geometrical and Physical Optics", Longmans, London, 2nd ed., 1967.
4. R. Mavrodineanu and R. C. Hughes, *Applied Optics,* 1968, **7,** 1281.
5. P. Buchhave and C. H. Church, ibid., 1968, 7, 2200.
6. J. B. Dawson, D. J. Ellis and R. Milner, *Spectrochim. Acta,* 1968, **23B,** 695.
7. R. Roldan, *Rev. Sci. Instrum.,* 1969, **40,** 1388.
8. R. W. Strojek, G. A. Grover and T. Kuwana, *Anal. Chem.,* 1969, **41,** 481.
9. E. Cordos and H. V. Malmstadt, ibid., 1973, **45,** 425.
10. D. G. Mitchell and A. Johannson, *Spectrochim. Acta,* 1970, **25B,** 175.
11. A. Walsh, in "Atomic Absorption Spectroscopy", eds. R. M. Dagnall and G. F. Kirkbright, Butterworths, London, 1970.
12. A. C. G. Mitchell and M. W. Zemansky, "Resonance Radiation and Excited Atoms", University Press, Cambridge, 1934.
13. B. J. Russell and A. Walsh, *Spectrochim. Acta,* 1959, **15,** 883.
14. J. V. Sullivan and A. Walsh, ibid., 1966, **22,** 1843.
15. J. A. Bowman, *Anal. Chim. Acta,* 1967, **37,** 465.
16. B. S. Rawling and J. V. Sullivan, *Trans. Inst. Min. Met.,* 1967, **76,** C238.
17. P. L. Boar and J. V. Sullivan, *Fuel,* 1967, **46,** 230.
18. J. V. Sullivan and A. Walsh, *Applied Optics,* 1968, **7,** 1271.
19. J. A. Bowman, J. V. Sullivan and A. Walsh, *Spectrochim. Acta,* 1966, **22,** 205.
20. R. M. Lowe, ibid., 1969, **24B,** 191.
21. N. A. Sebestyen, ibid., 1970, **25B,** 261.

CHAPTER 10

Atomic Absorption and Fluorescence Instrumentation

The essential components of an atomic absorption or fluorescence spectrometer and their conventional arrangement were outlined in Chapter 1. In subsequent chapters we have described in detail atom cells and methods of sample introduction, light sources and monochromating devices. One major function of every spectrometer remains to be discussed here: the detection and processing of the analytical signal. Several other topics which have not been dealt with in detail elsewhere are also included in this chapter to complete the survey of existing practical instrumentation. Our principal concern here is with techniques used at present in commercial spectrometers, although one or two other recent developments are also described. No data are included on the specifications of currently available commercial spectrometers, principally because such data rapidly become obsolescent. For information on this topic the reader is referred to the extensive advertising literature available from all manufacturers, to the annual listing in *Annual Reports on Analytical Atomic Spectroscopy** and also the advertising pages of relevant journals (particularly *Analytical Chemistry*). A comprehensive survey of atomic absorption instrumentation, which is reasonably up to date at the time of writing, has also been published.[1]

10.1 RADIATION DETECTORS

The traditional method of recording and measuring a light signal uses the photographic technique. Although this method may sometimes prove useful for special projects involving AAS or AFS it is, in general, inconvenient for measuring fluorescence signals for analytical use and would be quite impracticable for routine atomic absorption analysis. Thus, electronic devices able to convert the light signal into an electrical signal for direct reading are now generally employed. Such devices must (a) be sufficiently compact for use in the optical systems of small, modern spectrometers, (b) give sufficient sensitivity to produce stable, noise-free signals at the low levels of radiation obtainable in many fluorescence measurements or when a monochromator is used with a narrow spectral bandpass, (c) have a reasonably uniform spectral response over the wavelength range of interest and (d) be simple to use and give reliable operation over long periods. Not all of these requirements are completely met by any one detector; simplicity and low cost must often be forefeited in return for increased sensitivity in most applications of interest here.

10.1.1 Photocells

Solid state photocells are the simplest of the photoelectric radiation detectors and are widely used for light-metering applications. They rely usually on the use of photo-conductive semi-conducting materials, but in fact several types were widely used long before the introduction of semi-conducting electronic components such as the transistor. The mechanism of their photoconductivity may be understood if it is recalled that in all semi-conductors the electrons may be categorized according to the "band" of energy values in which they lie; when energy is supplied to the material by, for example, allowing light to fall upon it, some electrons in the valence band are excited into the conduction band. As the electrons lying in the conduction band are more mobile this process increases the conductivity of the material. Semi-conductors that show the photo-conductive effect include selenium, germanium, silicon, cadmium sulphide, cadmium selenide and lead sulphide. Their conductivity may be improved by introducing impurities of other elements; these can capture an electron in the conduction band and increase the time for which it remains there before returning to the valence band by recombination.

One means of utilizing the photoconductive effect to monitor light intensity is the *photovoltaic cell*. In this device a thin layer of semi-conducting material such as selenium or silicon is coated onto a metal base plate which is usually iron or aluminium (see Fig. 10-1). The semi-conductor is then overcoated with a very thin transparent layer of a precious metal such as gold, and electrodes are connected to each of the two metallic layers. A potential barrier arises at the junction between semi-conductor and metal in the absence of light and if the electrodes are connected to an external circuit no current will flow. When the junction is illuminated, however, the increase in conductivity causes the potential barrier to decrease as electrons are

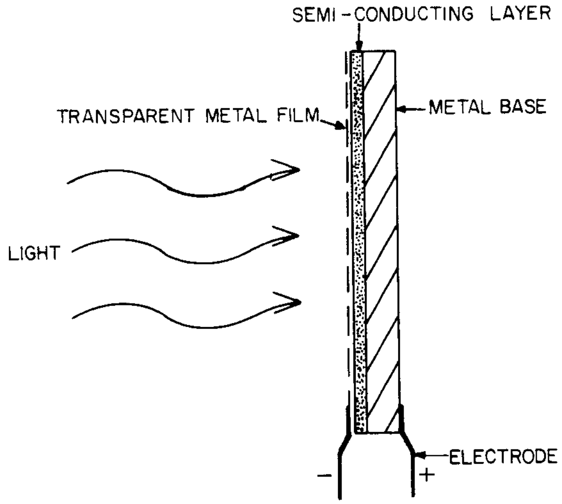

Fig. 10-1. Photovoltaic light cell.

---

* Published by Society for Analytical Chemistry, 9/10 Savile Row, London W.1.

drawn across it into the transparent metal film, which attains a negative potential compared with the metal base. This voltage depends on the type of cell and the level of illumination but is commonly of the order of a few tens of millivolts and may reach a limiting value of *ca.* 0·5 V at very high illumination. The current obtained from the cell will depend on the external resistance of the circuit, as shown in Fig. 10-2, and is usually directly proportional to the incident radiation level over only a small range unless this resistance can be maintained at a very low value. The most commonly available photocells of this type show their peak sensitivity in the visible region and usually high sensitivity can be obtained only by using a cell of large surface area (a typical cell may have a sensitivity of 0·5 mA/lumen). Thus the photovoltaic cell has seen little application to AAS or AFS in spite of its extreme simplicity and low cost.

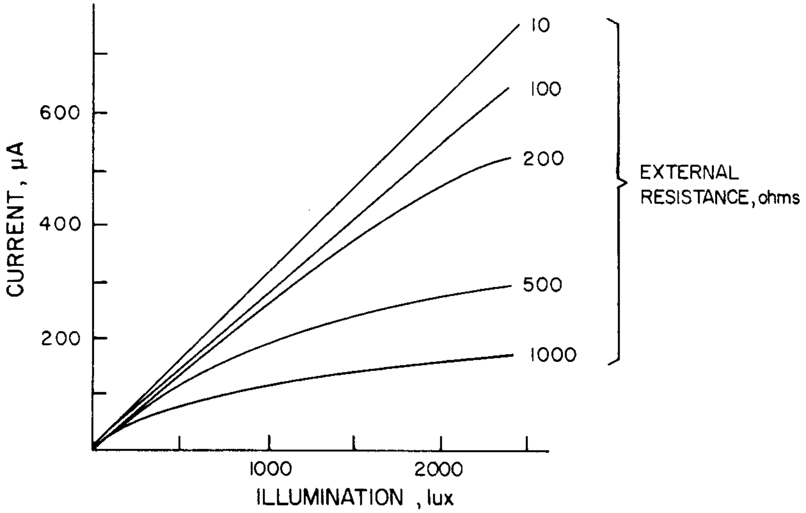

(N.B. 1 LUX IS EQUAL TO AN ILLUMINATION OF 1 LUMEN/M^2)

Fig. 10-2. Variation of current with illumination for a typical photovoltaic cell.

The photoconductive effect may also be used in *photoresistance cells*. Semi-conductors such as cadmium sulphide or lead sulphide have a very high resistance in the dark (*ca.* 1–100 MΩ). As shown in Fig. 10-3, however, this decreases rapidly on exposure to light. Thus, light intensity may be measured simply by applying a fixed potential of a few volts across the cell and noting changes in the current. High sensitivity requires a relatively large sensitive area combined with closely spaced electrodes between which the resistance may be measured. This is commonly obtained by taking a thin, flat plate of the semi-conductor and depositing onto it the electrodes in the form of a thin metal film with the configuration shown in Fig. 10-4. The spectral response curves for cadmium sulphide and lead sulphide are shown in Fig. 10-5; lead sulphide is obviously only of use for infrared measurements while even cadmium sulphide shows its peak sensitivity at rather long wavelength for most AAS and AFS applications.

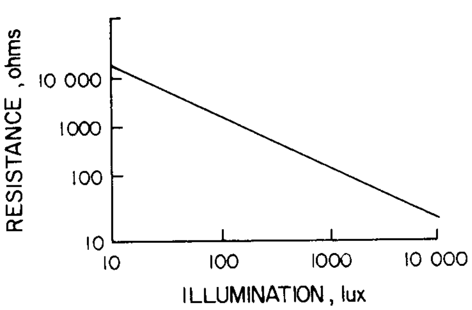

Fig. 10-3. Variation of cadmium sulphide resistance with illumination.

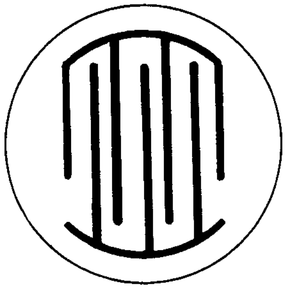

Fig. 10-4. Electrode configuration for cadmium sulphide photo-resistance cells.

Nevertheless, the sensitivity for a given size of cell is considerably better than with the photovoltaic type, a typical sensitivity being of the order of 1000 mA/lumen. Thus, cadmium sulphide cells may be of use for simple atomic absorption or fluorescence spectrometers. A possible disadvantage is the long response time of these cells which increases with decreasing illumination. Frequency response curves of a general purpose type are shown in Fig. 10-6, and it would, for example, be impossible to use a modulated system at the light levels available in usual spectrometric applications. Recent cells of this type

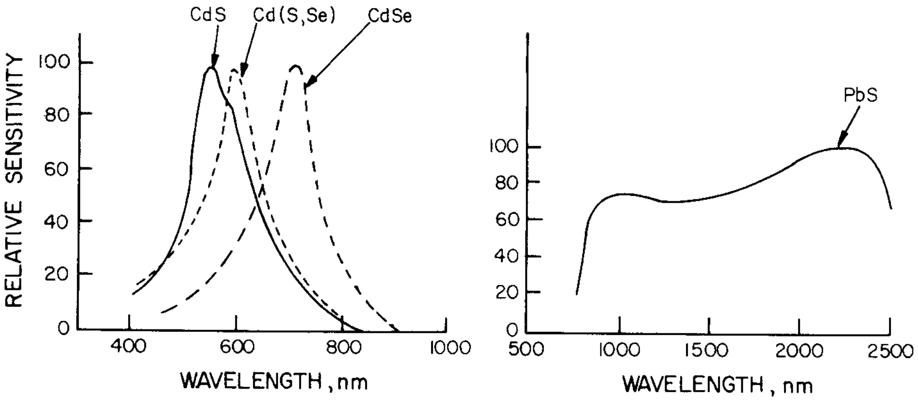

Fig. 10-5. Spectral response curves of cadmium sulphide/selenide and lead sulphide.

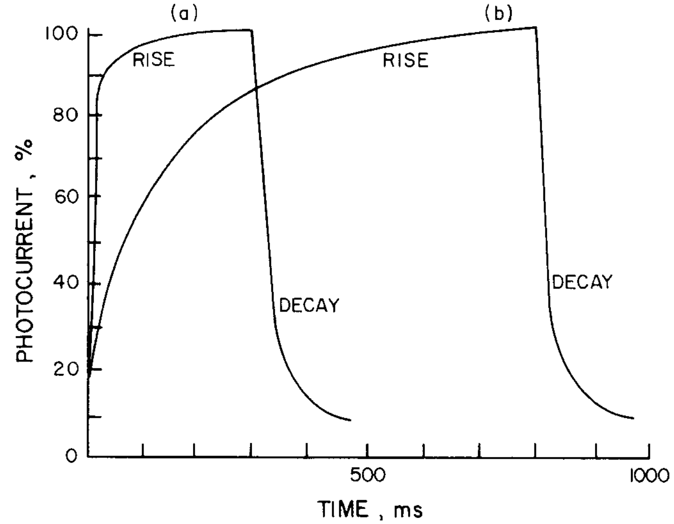

Fig. 10-6. Response time of cadmium sulphide photo-resistance cell, (a) at 1000 lux illumination, (b) at 100 lux illumination.

with low power dissipation but suitable for spectrometric applications are much better in this respect, some CdSe or Cd(S,Se) types having a response time of only a few milliseconds at 10 lux.

A modern development of the application of photoconductivity can be seen in *photo-diodes* and *photo-transistors*. In these potential barrier junctions are obtained using different types (p and n) of doped germanium or silicon crystals. A potential is applied to the cell and the current flowing depends on the level of illumination of the

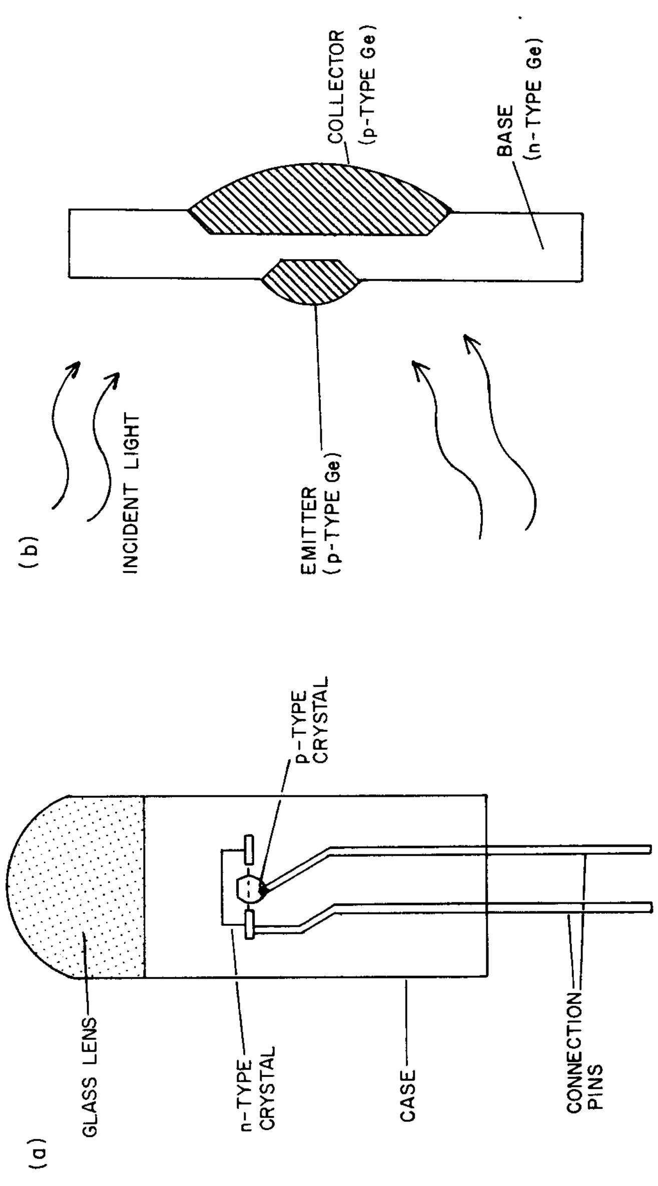

Fig. 10-7. Construction of (a) photo-diode and (b) photo-transistor.

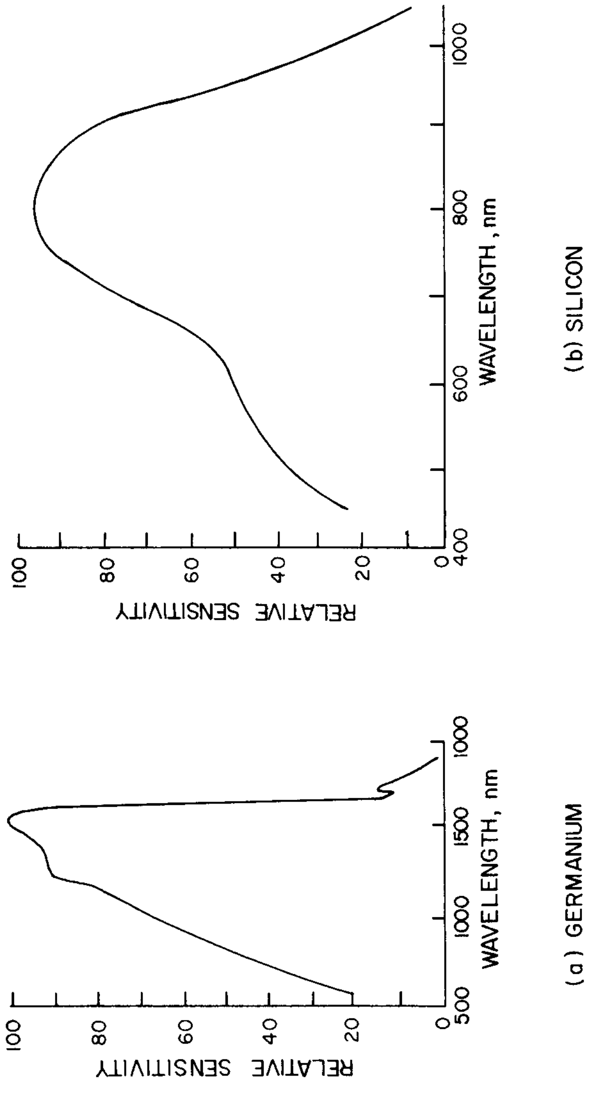

Fig. 10-8. Spectral response curves of photo-diodes and photo-transistors.

junction. Operation of the two types is similar except that the transistor incorporates an amplification factor of 400 or 500 and is therefore considerably more sensitive. Typical construction is shown in Fig. 10-7, which shows that with the transistor direct frontal illumination is not possible. The spectral response curves are shown in Fig. 10-8. It can be seen that germanium shows its peak sensitivity much further into the infrared than silicon and is thus probably less useful for application to atomic absorption or fluorescence measurements. Although the sensitivity is reasonably high (typically about 50 mA/lumen for the diode, 150 mA/lumen for the transistor) the extremely small size of these devices may limit the possibility of measurements at low light levels. Their small size may be turned to advantage in detectors used in simultaneous multi-element analysis in which a linear array of photodiodes replaces the photographic plate at the focal plane of a spectrograph. However, their frequency response is much better than that of cadmium sulphide cells (i.e. up to 50 kHz for diodes, 3 kHz for the transistors).

10.1.2 Photo-Emissive Cells

This type of detector depends upon the fact that when many metals are irradiated by photons of sufficient energy, electrons are emitted from the surface of the metal. The minimum energy required by an electron for escape is known as the work function, w, of the material, the energy of an electron emitted as the result of radiation of frequency ν being $(h\nu - w)$. Thus there is a threshold frequency, ν_0, for photoelectric emission given by $h\nu_0 = w$; radiation of lower frequency (longer wavelength) will not cause emission of electrons from that particular material. For many common metals the threshold lies well into the ultraviolet region, but for others, particularly the alkali metals, it occurs in the near ultraviolet and visible. Thus, these elements may be used to detect visible and ultraviolet radiation; it is necessary only to allow the light to fall onto a suitably shaped cathode made from an appropriate metal (or metals) and to collect the emitted electrons on an anode. Considerable effort has been applied to the development of photocathode materials and individual metals are now seldom used (except for certain specialized applications such as the detection of light in the far vacuum ultraviolet). The spectral response curves of several widely used materials are illustrated in Fig. 10-9. In many cases the short wavelength response is determined by the window material used for the photocell rather than by the cathode material itself.

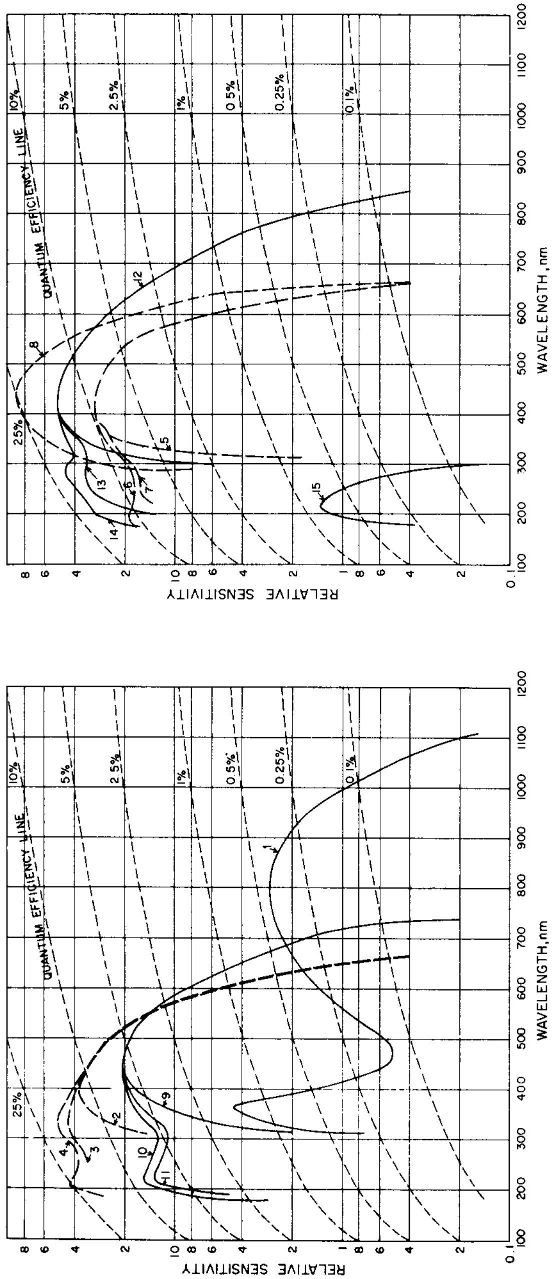

Curve	Cathode	Window*	Code
1	AgOCs	a	S1
2	SbCs	a	S4
3	SbCs	b	S5
4	SbCs	c	S19
5	SbCs Semi-	a	S11
6	SbCs transparent	c	S13
7	SbCs cathode	b	S21
8	Bialkali (KCsSb)	d	-

Curve	Cathode	Window*	Code
9	AgBiOCs	a	S10
10	AgBiOCs	c	-
11	AgBiOCs	b	-
12	Multi-alkali (NaKCsSb)	a	S20
13		b	-
14		c	-
15	CsTe	c	-

*a = borosilicate glass, b = UV transmitting glass, c = silica, d = special glass

Fig. 10-9. Spectral response curves of photocells and photomultipliers (EMI, England).

Some combinations have been assigned "S" numbers which are given in the diagram and are used by many manufacturers, but this does not apply to the more recently developed cathode materials such as CsTe or "bialkali". Not all of the combinations shown in Fig. 10-9 are available in photocells, having been developed for the photomultiplier tubes described below but they are included here for convenience.

The photoelectrons emitted by the cathode are collected on an anode while applying a sufficiently strong potential between the two electrodes. To obtain efficient collection of electrons the electrodes are placed in an envelope which is evacuated or filled with a low pressure of an inert gas. At a particular wavelength the current flowing in the external circuit is directly proportional to the intensity of illumination. The voltage applied between the anode and cathode is needed to prevent emitted electrons accumulating in a cloud, or space charge, close to the cathode and repelling electrons back to it so that no photocurrent flows. In a vacuum cell the photocurrent increases with increasing applied potential until, at the saturation voltage, all emitted electrons are collected by the anode and the current reaches a maximum value for a particular light intensity (see Fig. 10-10(a)). In gas-filled cells (usually containing less than about 1 torr of a gas such as argon) the gas atoms are ionized by collision with electrons emitted by the cathode. The original and ionization electrons are then accelerated by the applied field and undergo further collisions with other gas atoms. Thus, for each electron leaving the cathode several electrons reach the anode and an amplification effect is obtained. As the kinetic energy of the electrons depends on the potential gradient, collisions producing ionization occur more frequently as the anode voltage is increased. Hence the amplification factor increases as the anode voltage is increased and the current-voltage curve is of the form shown in Fig. 10-10(b). The applied voltage must not be allowed to reach that at which a glow discharge would initiate within the cell and the amplification factor is usually limited to a maximum of between 5 to 10 times, depending on the type of cell.

In practice, the high-vacuum type of cell is often preferred to the gas-filled type in spite of the higher photocurrent obtained from the latter. This is partly because a vacuum cell operated above its saturation voltage is very stable whereas the sensitivity of gas-filled cells is considerably affected by small changes in gas pressure or by variations in the applied voltage. Furthermore, the amplification factor may not allow measurement of weaker light signals as it is accompanied by a large increase in the *dark current*. This is the current obtained from the cell when no light is falling on the cathode and is mainly due to thermionic emission of electrons. Thus it will increase with temperature and, as it too depends on the work function of the metal, is generally larger the longer the threshold wavelength of the cathode. A typical modern vacuum-type cell would have a dark current of the order of 1 nA (although values as low as 0·005 nA are available in cells designed for operation only at low light/current levels), whereas a value of 100 nA is more usual for the gas-filled type.

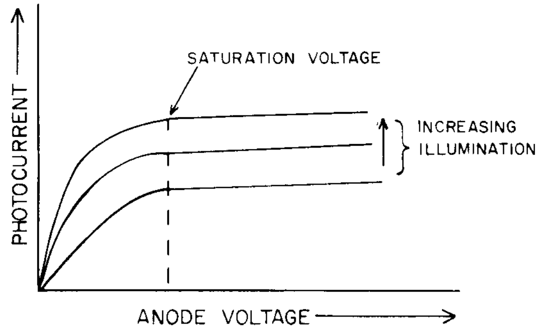

(a) HIGH-VACUUM CELL

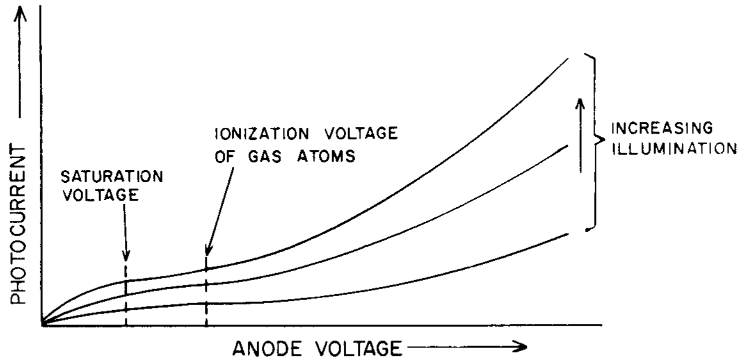

(b) GAS-FILLED CELL

Fig. 10-10. Variation of photocurrent with applied potential for photo-emissive cells.

Although both the vacuum and gas-filled types are available with a variety of spectral response and sensitivity ranges, few of these are intended for spectrometric applications. Typical sensitivities for modern commercial types are 25-50 μA/lumen for the vacuum type and 150-300 μA/lumen for the gas filled cells. These values are usually obtained with anode voltages up to 250 V for the former but below about 100 V for the latter. The high-vacuum cells have an extremely rapid response, frequencies as high as 100 MHz being usable, but the cut-off frequency is considerably lower for the gas-filled type (usually 1-10 kHz). The main disadvantage of these cells is the relative small value for the maximum cathode current which may be drawn; for some of the more sensitive types it may be as low as 1 μA. Thus if very weak light signals are to be observed the cells must be used with stable, high-gain amplifiers. The much higher currents available from photomultiplier tubes have made this combination unattractive for most applications of interest in AAS or AFS.

10.1.3 Photomultiplier Tubes

These devices represent a logical development of the photo-emissive cell. Light is detected in the same manner but, as the name implies, the cell itself incorporates an amplification system so that a much higher output current is obtained. Amplification factors in excess of 10^6 are easily achieved and extensive development has ensured very small dark currents so that extremely low light levels may be detected and measured without difficulty. As a result the photomultiplier tube is used almost exclusively for the detection of radiation in the ultraviolet and visible regions in AAS and AFS.

The amplification of the photomultiplier is obtained by using the phenomenon of secondary electron emission. The principle of this can be understood by referring to the diagrammatic representation of a photomultiplier shown in Fig. 10-11. Photoelectrons emitted by the cathode are directed not to the anode but to the first of a number of target electrodes termed dynodes. A voltage is applied between the cathode and this dynode (just as between cathode and anode in the photo-emissive cell) to ensure efficient collection of electrons at the dynode. Each of the photoelectrons striking the dynode causes several secondary electrons to be released, producing an amplification effect. These electrons are directed towards a second dynode which is again held at a more positive potential than the preceding electrode so that the process is repeated. As several dynodes are used (commercial photomultipliers are available with as many as 14 dynodes although the use of 9 or 11 is more common) the number of electrons eventually reaching the anode as a result of each electron released by the cathode is very large. The actual gain observed will depend on the number of dynodes (or "stages"), the efficiency with which the design used is able to collect all of the electrons produced, and the voltages applied between the dynodes.

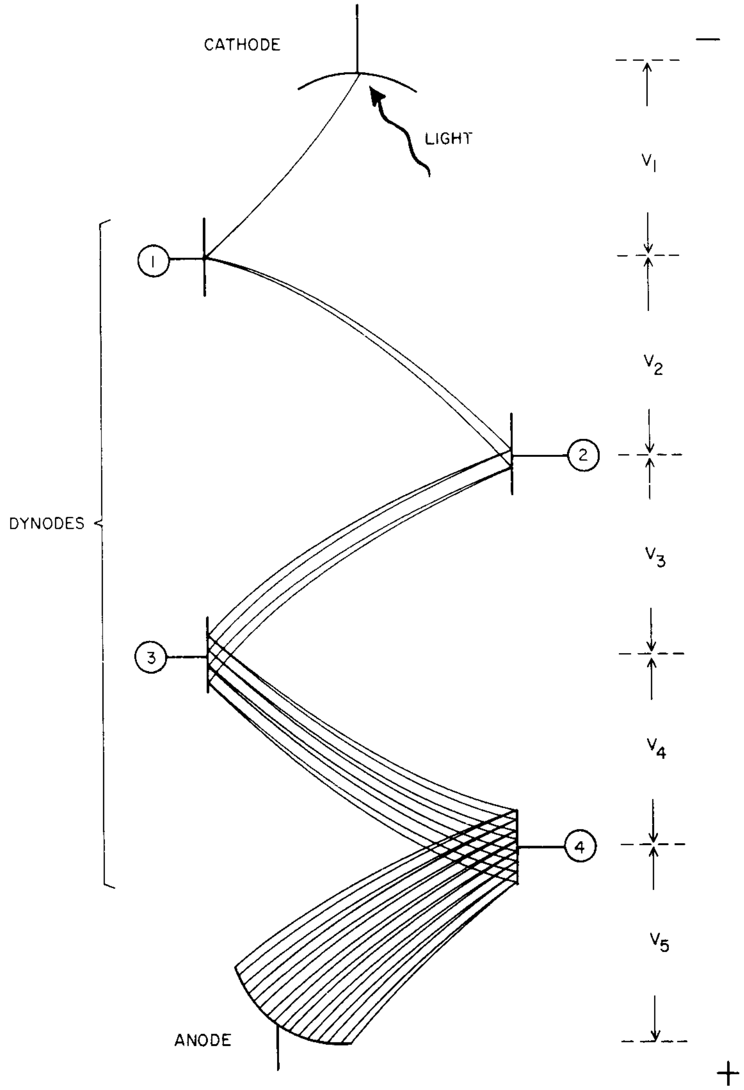

Fig. 10-11. Schematic representation of a photomultiplier tube.

The exact choice of dynode material is less critical than that of the photocathode material and SbCs is the most common, although BeCu and AgMg is also used.

The four most common designs of photomultiplier are shown in Fig. 10-12, each having certain advantages for particular applications.

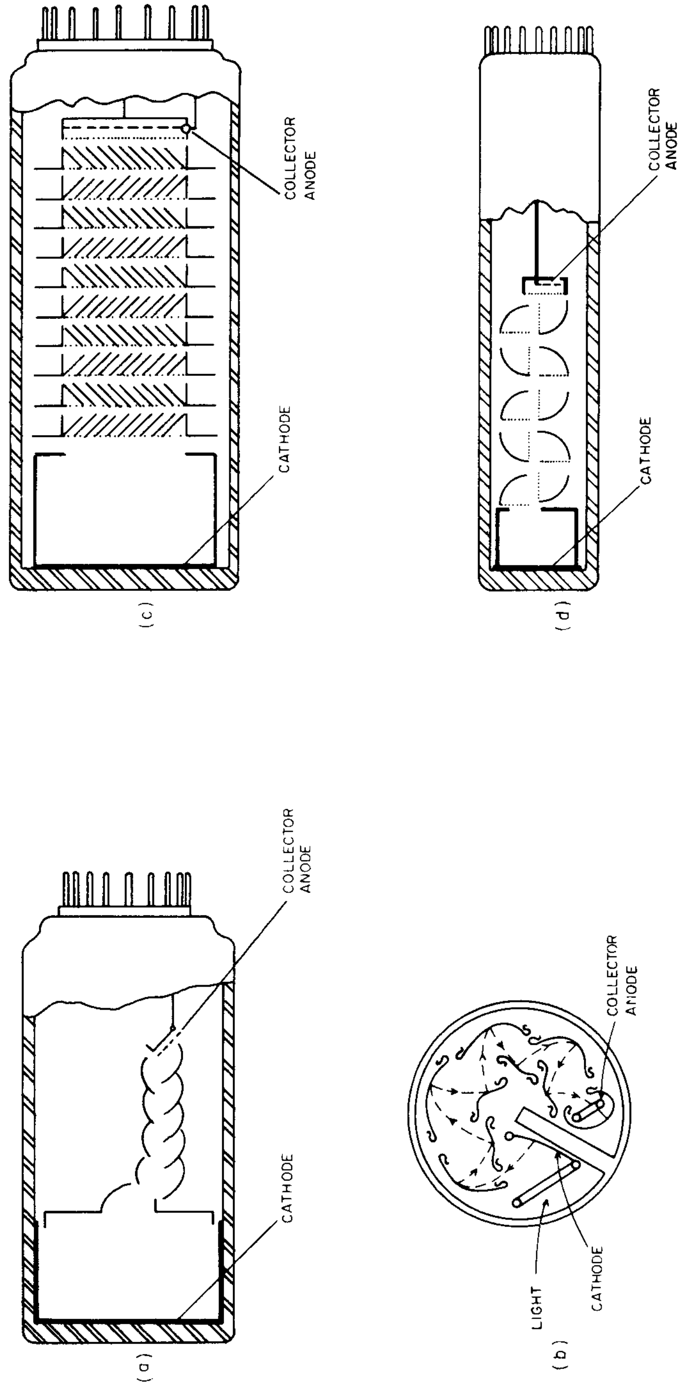

(a) LINEAR FOCUSSED (b) CIRCULAR FOCUSSED
(c) VENETIAN BLIND (d) BOX AND GRID

Fig. 10-12. Practical photomultiplier designs (EMI, England).

Thus, the venetian blind structure gives exceptionally low gain drift over long periods, the box and grid type is slightly less stable but more sensitive and more compact, the linear focused type has an extremely fast response and the circular focused type is compact and relatively inexpensive. In fact, the last-mentioned structure in side-window photomultipliers is probably the most widely used in both AAS and AFS for these reasons, even though it does not give the highest performance. The other three structures shown in Fig. 10-12 use semi-transparent cathodes, and in this case the spectral response curve of a particular cathode material may be modified (see Fig. 10-9). Not all end-window photomultipliers are necessarily of this type, however, and various modifications allowing reflecting cathodes have been used. The performance of a particular design (for a given cathode material and applied voltage) may also vary from batch to batch and between manufacturers.

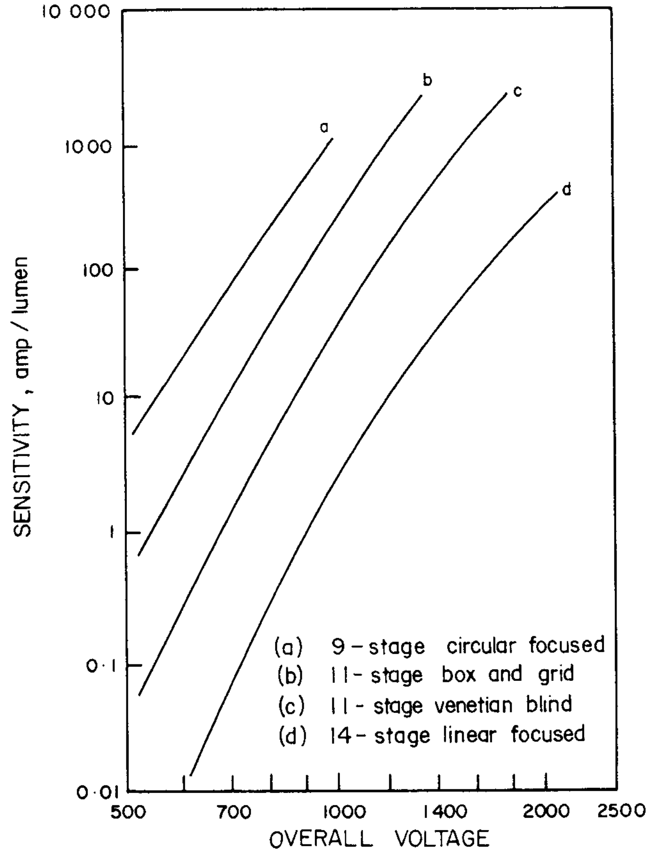

Fig. 10-13. Effect of applied voltage on photomultiplier sensitivity.

A particularly useful feature of the photomultiplier tube, apart from the large output currents at very low light levels, is the wide range over which the gain of a particular tube may be varied simply by altering the applied voltage. This effect arises because the higher the potential difference between two electrodes, the greater is the kinetic energy of the primary electron on impact and the larger the number of secondary electrons produced by each primary electron. The effect of applied voltage on sensitivity for several typical commercial photomultipliers is shown in Fig. 10-13. For most AAS and AFS applications a voltage source variable between about 500 and 1500 V is suitable, although potentials up to 2500 V may be used with some photomultipliers. In general it is best to avoid very low or very high gain values as the relative effect of the dark current may be more serious under these conditions. The highest possible gain for a particular tube (obtained with the maximum safe voltage recommended by the manufacturer) is useful in most cases only if the dark current is reduced by cooling the photomultiplier to below room temperature. As can be seen from Fig. 10-14, maximum

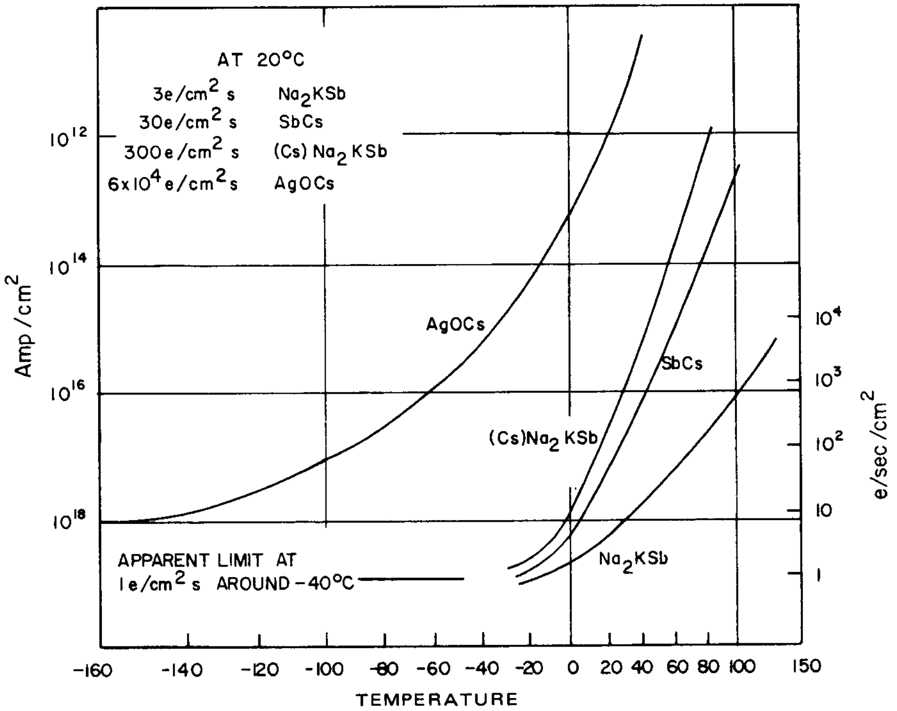

Fig. 10-14. Variation of photomultiplier cathode dark current with temperature for different cathode materials.

benefit is obtained at −40°C in most cases and at this temperature there is a very useful improvement compared with room temperature.

In view of the extremely rapid change of gain with applied voltage, it is essential to use a high-voltage power supply with high stability. As potentials up to 1500 V (at least) are desirable this unit will usually be more expensive than the photomultiplier itself and may contribute considerably to the overall cost of a spectrometer. Equally important is the method used to subdivide the applied voltage to supply the correct potentials between the dynodes and between the cathode or anode and their adjacent dynodes. In order to obtain optimum performance from the tube it should be protected from electrostatic fields by mounting it in a shield maintained at cathode potential; this requirement is obviously simplified by maintaining the cathode at earth potential and applying a high positive voltage at the anode. The output signal must then be measured via a coupling capacitor so that only pulsed or modulated light signals can be used with this system. Thus with steady light signals a high negative potential is applied to the cathode while the anode is earthed. In some spectrometers this condition is used while the tube is mounted in an earthed shield, in spite of the requirement mentioned above. In either case the applied voltage is divided using a chain of resistors (or dynode chain) as shown in Fig. 10-15. When the gain is to be varied by altering the applied voltage, it is important to maintain the cathode-to-first-dynode potential at a high value. This ensures optimum performance by using maximum gain for the first dynode, minimizes the effect of stray magnetic fields and produces the shortest response time for the tube. This is most easily achieved by replacing the first resistor with a Zener diode as shown in Fig. 10-15. Apart from this, a linear dynode chain is suitable for many applications. With pulsed operation, transient high currents may cause the build-up of an electron space charge and cause loss of linear response. This is avoided by applying a higher voltage to the last one or two dynodes. Some tubes are designed to avoid this problem at the anode and it is then necessary only to apply increased voltage at the penultimate dynode, as shown in Fig. 10-15(a).

As mentioned above, the overall sensitivity of the photomultiplier is extremely high. Maximum values of 100 to 200 A/lumen are common for the tubes used in AAS or AFS, but ratings up to 5000 A/lumen are available. It is important to remember, however, that the actual current that may be drawn from the anode is only a minute fraction of this value. An obvious limitation is the heat that can be dissipated by the components without damage. This typically limits the anode current to about 0·1 mA for compact tubes, and 0·5 or 1 mA for the larger end-window types. In practice, the maximum current that can be drawn from the anode is limited to a much smaller value by a second consideration. If the anode current approaches the value of that flowing through the dynode chain, the voltage across the last resistor in the chain (and to a lesser extent the one before it) will vary with the anode current. This effect results in

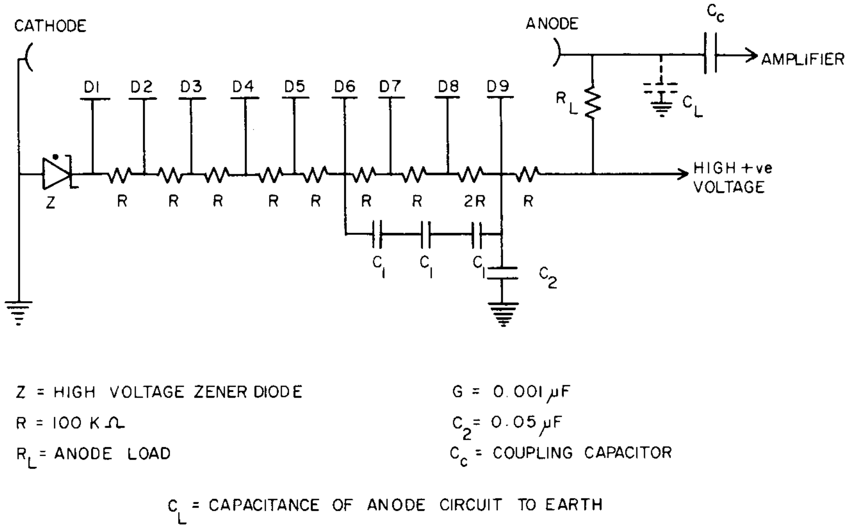

(a) For pulsed or modulated operation

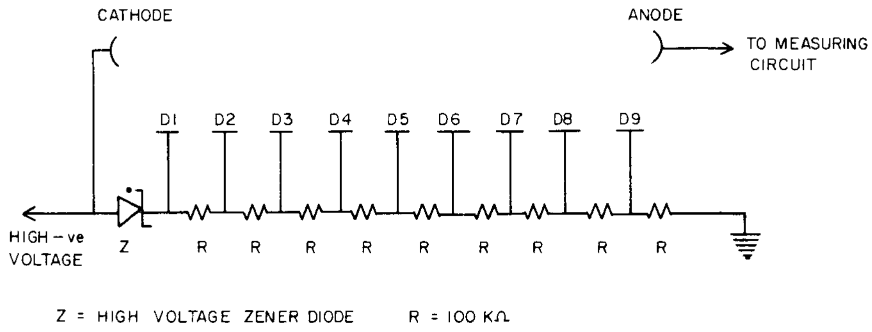

(b) For steady (d.c.) operation

Fig. 10-15. Standard dynode chains for photomultiplier operation.

an increase in overall gain with increasing anode current so that the response of the photomultiplier becomes non-linear. To reduce the problem most manufacturers recommend that the anode current be kept below about 1/10th the value of the dynode chain current or even below 1/100th if ⩾1% linearity is required. The maximum value of the dynode current is itself limited, both by heat dissipation problems (especially as the resistors are usually mounted close to the photomultiplier) and by the maximum current available from high-voltage, stable power supply units. In practice, therefore, the maximum anode current is usually in the range 1–10 μA.

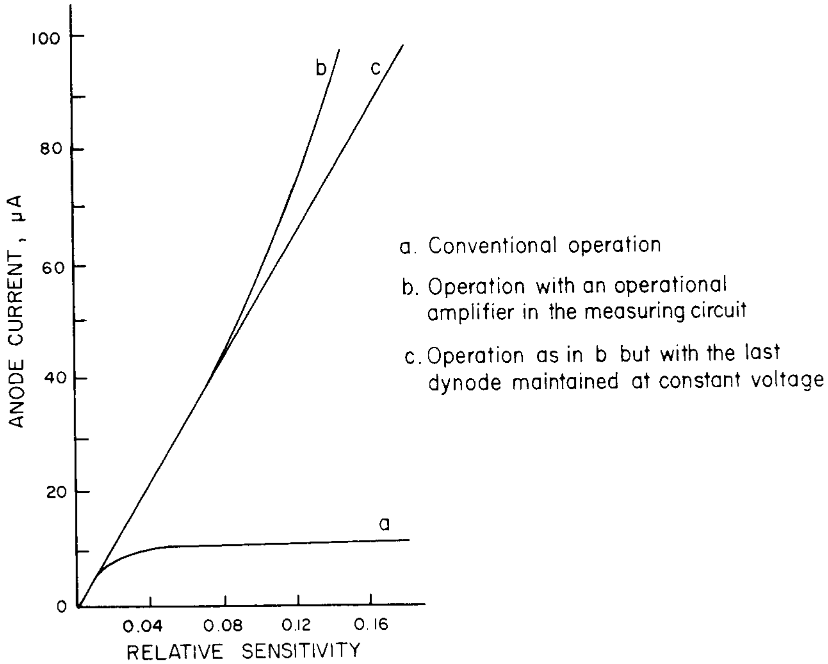

Fig. 10-16. Photomultiplier response curves at high anode currents.

These values may be increased by using higher value resistors for the last few stages of the dynode chain, the relative effect of change in anode current being reduced. Usually values of $2R$ or $3R$ are sufficient. The disadvantage of this method is that the overall voltage applied to the tube must be increased to obtain a given gain and care must be taken not to exceed the maximum rating of the tube. A more satisfactory solution is to stabilize the final dynode voltage. This is easily achieved by replacing the last resistor with a Zener diode or by using a voltage follower circuit. Use of a high anode

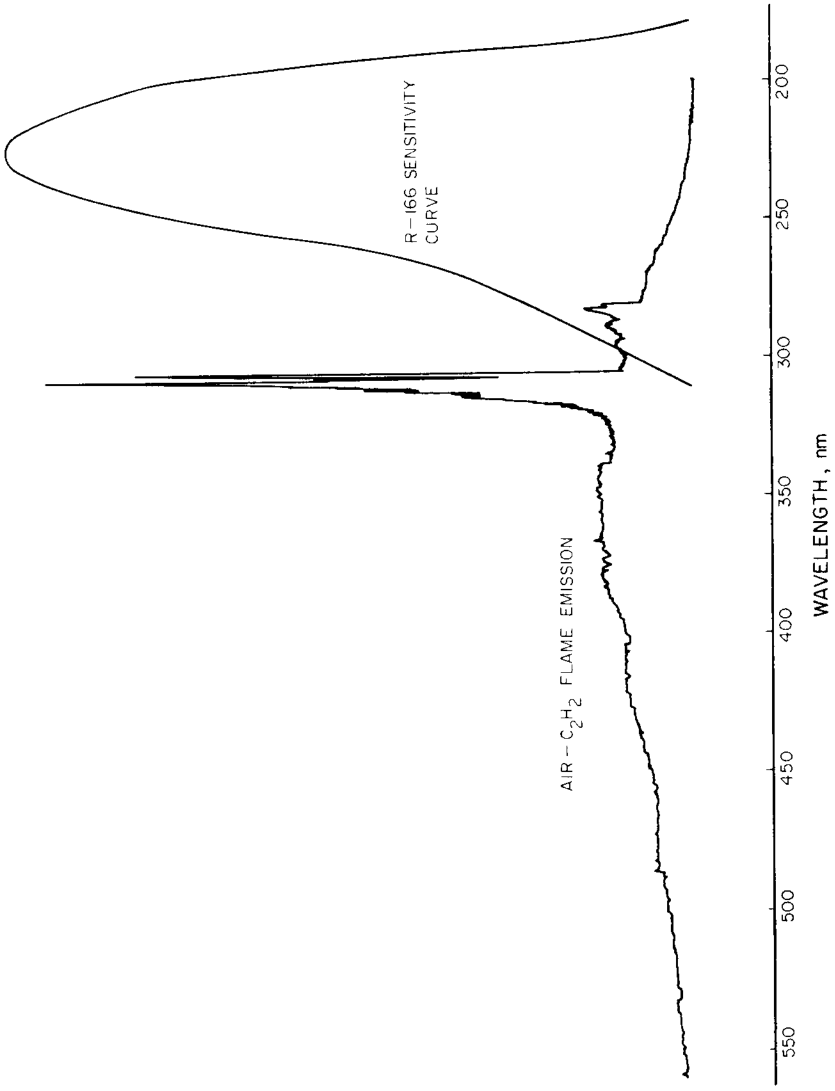

Fig. 10-17. Comparison of the background emission of an air-acetylene flame and the response of a solar-blind photomultiplier (HTV type R166).

current introduces an additional problem when the signal is measured. The voltage generated across the measuring resistor must be kept small relative to the applied voltage otherwise the effective voltage (and hence the gain) will change. Thus, if a high measuring resistor is used to allow small anode currents to be detected, the response will be non-linear as the signal increases. The problem can be avoided when operating the photomultiplier with the anode at earth potential by using an operational amplifier in the measuring circuit. This will maintain the anode at a constant "virtual earth" regardless of the photocurrent or the value of the measuring resistor. The effect of using a constant last dynode voltage together with this precaution is illustrated in Fig. 10-16.

The combination of high sensitivity and low permissible anode current obviously has the consequence that the photomultiplier must never be exposed directly to daylight when high voltage is being applied. Thus, care must be taken to avoid accidental exposure. For example if a filter is mounted directly in front of the photomultiplier housing it would be easy to remove the filter to exchange it for another without remembering to switch off the applied voltage. Although it is perfectly safe to expose a tube to daylight when the voltage is off, the most critical applications require that it be stored in the dark for several days before re-use. This arises because energy is trapped in the cathode and will, when the voltage is re-applied, appear as an excessive dark current unless time is allowed for it to dissipate. The problem of exposure to daylight is much less serious with tubes using photocathodes such as CsTe which has no response to visible light (see Fig. 10-9). These "solar-blind" photomultipliers are particularly useful for AAS or AFS applications where it is often necessary to measure only uv signals. In many circumstances (e.g. when using filters instead of a monochromator) these devices can give significantly reduced signal noise with flame atom cells. This is illustrated in Fig. 10-17, which compares the response characteristics of a solar-blind photomultiplier (HTV Type R166) with the background emission of an air-acetylene flame.

10.2 SIGNAL PROCESSING

In principle, the output current of the radiation detector could be measured directly using a micro-ammeter or recorded by applying the current across a load resistor and observing the voltage generated. In practice, however, with almost all AAS and AFS spectrometers,

some form of electronic processing of the signal is undertaken to obtain that which is finally observed by the operator. The degree of complexity involved in this operation can vary greatly, but in all cases it is intended to increase the versatility and convenience of operation of the spectrometer. We shall describe the most widely used of the available techniques, emphasizing those aspects of interest to a potential user.

10.2.1 Analogue Techniques

Until recently almost all atomic absorption and fluorescence applications involved amplification of the relatively weak signals obtained from the photocell or photomultiplier with a relatively simple analogue circuit. Apart from providing a sufficiently large current or voltage to drive a meter or chart recorder, such amplifiers facilitate operations such as backing-off unwanted signals, scale expansion of small absorption signals and, in some cases, direct conversion of logarithmic absorption signals to a linear reading. The principal requirement for such amplifiers is that they should contribute the minimum additional noise to the signal and that they should be stable; i.e. their gain should remain constant. This is usually achieved by introducing the principle of feedback so that the gain of the amplifier no longer depends on the stability of the amplifier itself (i.e. of active components such as transistors or valves) but instead on the ratio (input : output) of two passive components such as resistors (see Fig. 10-18). Even so, the signal from a photocell illuminated by a steady source of radiation will be dc and the construction of drift-free dc amplifiers is notoriously

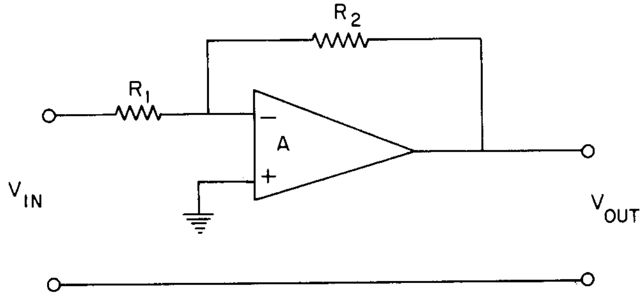

$$\text{EFFECTIVE GAIN} = \frac{V_{OUT}}{V_{IN}} = -\frac{R_2}{R_1}$$

Fig. 10-18. Feedback amplifier.

difficult. For this reason a more convenient choice is the use of a *chopper amplifier* (see Fig. 10-19). The dc input is then filtered to remove any unwanted ac components and passed through an electronic "chopper" device. This generates an ac signal (usually a square-wave form) which may be amplified using an ac amplifier tuned to the frequency of the chopper. As well as removing all dc drift components, the narrow bandwidth of such an amplifier (compared to the alternative dc amplifier) reduces the noise level of the final signal. In fact, all methods used to reduce the noise levels of measuring systems are based on narrowing the bandwidth and this important point will be considered again below. The amplified ac signal is passed through a coupling capacitor to remove any dc components and then to a second filter unit. The dc signal obtained from this may be used to drive a conventional meter or potentiometric recorder.

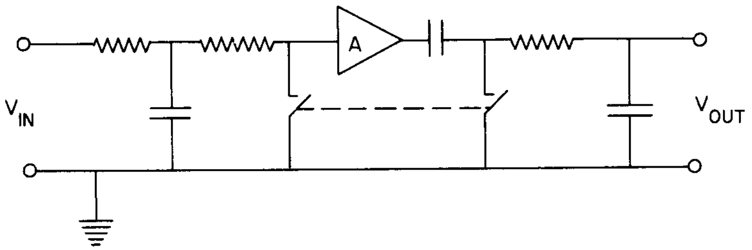

Fig. 10-19. Chopper amplifier.

In practice, simple chopper amplifiers are rarely used in absorption work and only occasionally for fluorescence measurements. This is because for optical applications considerable additional benefits may be obtained with little additional complexity by using the principle of *synchronous detection*. This is a logical extension of the chopper amplifier in which the output from the spectral light source itself is modulated so that the photodetector directly supplies an ac output. The use of modulated light sources with synchronous amplifiers is discussed further in Section 10.3.1, but briefly the technique has two main advantages for AAS and AFS. In the first place the tuned amplifier will respond only to the ac signal generated at the photodetector by the (modulated) light source so that any (dc) background emission and noise from the absorption or fluorescence cell should remain undetected. Secondly, the device used to modulate the light source can also generate a reference signal which is used to lock the amplifier exactly to the modulation frequency. It is thus possible to use an amplifier of exceptionally narrow bandwidth and to measure small signals in the presence of high noise levels.

With either type of amplifier there are several features that may be usefully incorporated into any spectrometer. For example, the gain (or perhaps attenuation) of the amplifier should be variable to allow variable scale expansion of small absorption signals. In certain cases, notably where the use of cool absorption cells results in very low signal noise levels or where very long measurement times are permissible, factors up to 100x may be usable. It is therefore useful if the controls of the instrument allow the degree of scale expansion to be easily ascertained or, at least, to be speedily reset to a predetermined value. An atomic absorption spectrometer having this facility of high, variable gain with calibrated controls is useful for measurement of small atomic fluorescence signals. In order to make full use of such facilities for either AAS or AFS the noise reduction techniques described in Section 10.3 are particularly useful. Although the more complex techniques are rarely incorporated in commercial atomic absorption spectrometers, some form of variable bandwidth is desirable for most applications. It is then possible, with a single instrument, to make full use of the high gain amplifier or to measure less demanding signals rapidly. This facility is often referred to as *signal damping*. It may involve adjustable characteristics for the ac amplifier, including incorporation of filter circuits in combination with the amplifier, but the most common approach is to pass the final dc signal through a low pass RC circuit (see Fig. 10-20) before feeding it to the meter or recorder. The time constant of the measuring device is then easily varied by changing the resistance or capacitance of the circuit. When this facility is not incorporated in the spectrometer the same effect is achieved by connecting an appropriate capacitor across the meter or recorder input terminals.

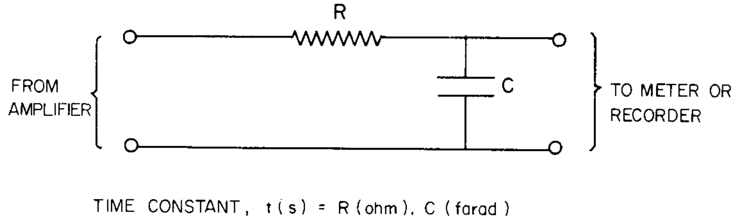

Fig. 10-20. Signal damping with a low pass RC circuit.

Despite the trend towards digital presentation of measurements (see Section 10.2.3) some commercial spectrometers with analogue circuitry still rely on the simplest read-out device, a high-quality micro-ammeter. This should have a stable movement so that the pointer will not waver unnecessarily and a large, clear scale with a mirror to facilitate accurate readings. The most useful meters of this type are calibrated with both a linear 0 to 100 scale and a logarithmic absorbance scale; unless the former is present it will be inconvenient to use the instrument for emission or fluorescence work. If the meter reads absorbance values in linear fashion across the scale it should be possible to switch out the logarithmic section of the amplifier circuit so that linear readings of emission or fluorescence signals are possible. A suitable output from the meter circuit to permit use of a potentiometric chart recorder is also useful; this output may be taken either directly as a current (to be applied to a load resistor at the recorder input) or after conversion to a convenient voltage signal (e.g. 10 mV for full-scale meter deflection). Recorder output sockets which in operation disconnect the meter are best avoided as they offer no particular advantage and sometimes prove inconvenient.

10.2.2 Photon Counting

In the preceding section we have described the standard spectrometric practice in which a photocell is used as a transducer to convert light into a steady electrical signal, be it ac or dc, which may be processed by analogue techniques. The reader will recall, however, that emission of light from any source is a series of discrete events, energy being released in small packets known as quanta or photons (see Chapter 2). The energy of the photon determines the frequency of the emitted radiation, but the intensity depends on the number of photons reaching the observer. In the traditional technique these photons are integrated into a continuous signal, but it is also possible to use the rapid response of a transducer such as the photomultiplier tube in conjunction with modern electronic instrumentation to actually count the number of photons reaching the detector. Measurement of light intensity then becomes analogous to measurement of radioactivity using, for example, a Geiger counter. An obvious advantage of such a technique for some applications is that the signal may be directly processed by digital techniques without the need for any conversion system (such as a digital voltmeter). In fact, the inherent advantages of counting techniques make "photon counting" an attractive alternative to analogue methods even for applications where the signal is not finally required in digital form. These advantages include sensitivity to low light levels, improvement of signal-to-noise ratio, better precision of measurement (in a given time interval) and the ease of integrating signals accurately over long time intervals.

taho - copper k, [illegible]

The photon counting technique was originally developed to improve measurement of low light levels[2-7] and this undoubtedly remains its most important application. Apart from the need to justify the increased cost of the instrumentation (see below) at light levels where conventional techniques give reasonable results, this situation arises because photon counting is, at present, unsuitable for measuring high light levels. The point at which it is necessary to revert to conventional current measurements is governed by the frequency response of the system. The count rate obviously increases with increasing light intensity and an error is introduced into the readings unless the system continues to resolve individual pulses as they arrive. As the emission rate of photons from the light source is random, the actual pulse rate may be greater or smaller than the average rate. Thus, the frequency response of the system must in practice be considerably faster than would be suggested by the maximum average counting rate required. In fact, it is found experimentally[7] that the photon counting system should have a frequency response at least 25 times greater than the maximum average counting rate to be measured in order to ensure less than 1% error at this rate. At present the frequency response is probably limited more by the electronic instrumentation than by the photomultiplier itself, which usually has a frequency response in the range of fifty to several hundred MHz (although it may be considerably slower for tubes with very large cathodes). With a typical tube and voltage used in AAS or AFS instrumentation a conventional current of about 0·01 μA would be equivalent to a count rate of 100 kHz and this is probably about the limit with instrumentation in present use. It may be possible, however, with more complex electronics to use a counting rate of up to 10 MHz, which with the same photomultiplier would be equivalent to a current of about 1 μA. This would then be typical of the light levels encountered in commercial atomic absorption spectrometers. Thus, at present, photon counting is of greatest interest for measurement of weak fluorescence signals, but it may soon be possible to apply its other advantages to high-precision atomic absorption measurements.

The apparatus required for a photon counting system is shown diagrammatically in Fig. 10-21. Most of the units are self-explanatory and would either be purchased individually or as a complete photon counting system. Thus, just as with the conventional use of the photomultiplier, it is useful to amplify the output before its measurement. Particular care must be taken in connecting the amplifier to the tube to avoid any loss of frequency response and it is useful if the system is able to reject any dc drift or low-frequency noise. The digital counter and printout is also self-explanatory and obviously requires a clock to control accurate counting. Similarly, a conventional chart recording is useful for applications such as scanning spectra and is easily obtained by directing the pulses to a digital-to-analogue converter. The one unit whose requirement is not obvious is the pulse-height discriminator; for low light-level measurements this is actually responsible to a considerable degree for the advantages of photon counting systems.

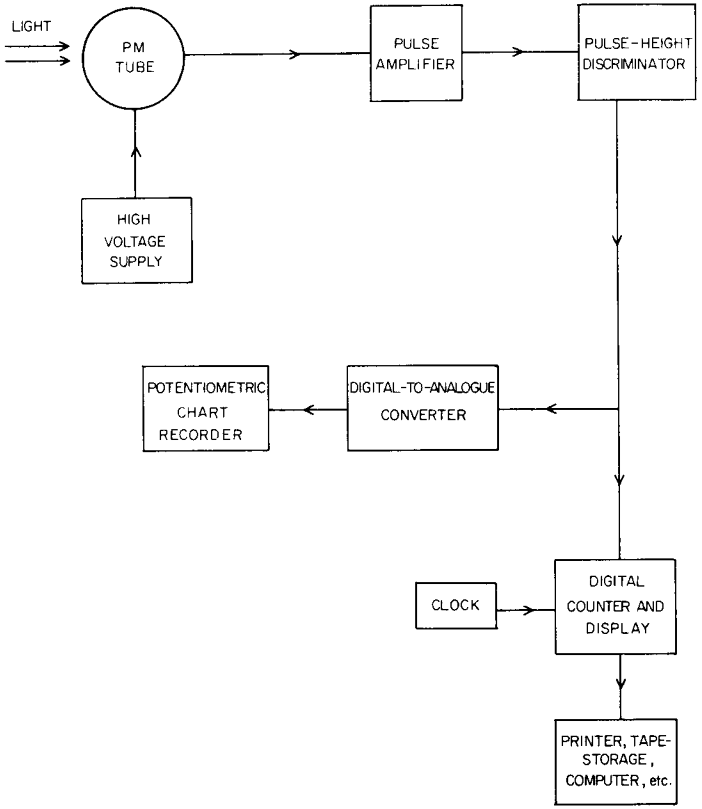

Fig. 10-21. Block diagram of a photon counting apparatus.

The pulse-height discriminator is an electronic instrument which is used to process the pulses received from the amplifier so that only those pulses lying between certain preselected values of the height (i.e. voltage) are sent to the counter and included in the measured value of the signal. Its use allows a considerable improvement in the signal-to-noise ratio obtainable from a photomultiplier tube operating at low light levels. This is possible because at these low light levels the significant noise arises not from the signal itself but from fluctuations in the photomultiplier dark current. The number of counts obtained at discrete pulse heights (i.e. within a channel set to respond only to a small voltage interval) is plotted in Fig. 10-22 against the pulse height for a typical photomultiplier tube operated with (a) a light signal applied, and (b) in the dark. It can be seen that compared with pulses arising from photons (i.e. from the signal) the background count has a disproportionately large number of very small and very large pulses. Thus, it is possible to achieve a considerable improvement in signal-to-background ratio (which is equivalent to signal-to-noise ratio for very small signals) by counting only those pulses of intermediate height. This technique supplements the use of a cooled photomultiplier, as not all dark-current pulses are

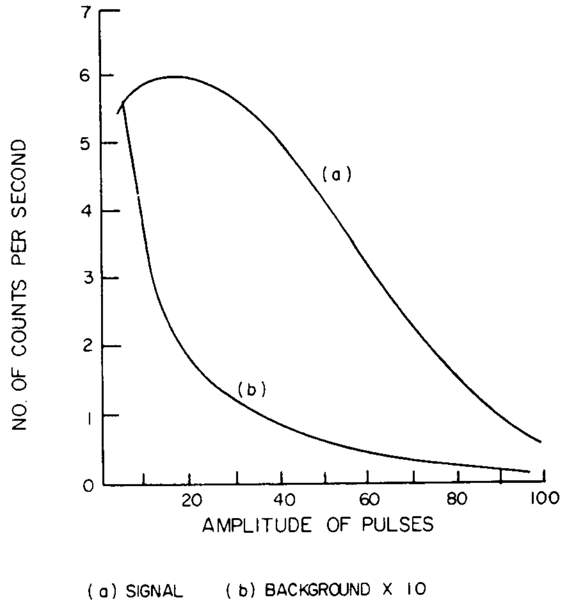

Fig. 10-22. Pulse distribution for a typical photomultiplier counting photons and background.

of thermal origin. In fact, photon counting is very efficient in this respect and when this technique is used little further improvement in signal-to-noise ratio may result when a cooled tube is employed.[8] Also, in practice, the largest reduction of background current is obtained by excluding the smallest pulses and successful results are often achieved using a discriminator in which only the smallest pulse height to be counted can be pre-selected. It should be noted that the pulse-height discriminator will also exclude some signal pulses so that the actual counting rate is reduced. The cut-off voltage of the discriminator must therefore be set in each individual case to give optimum results.

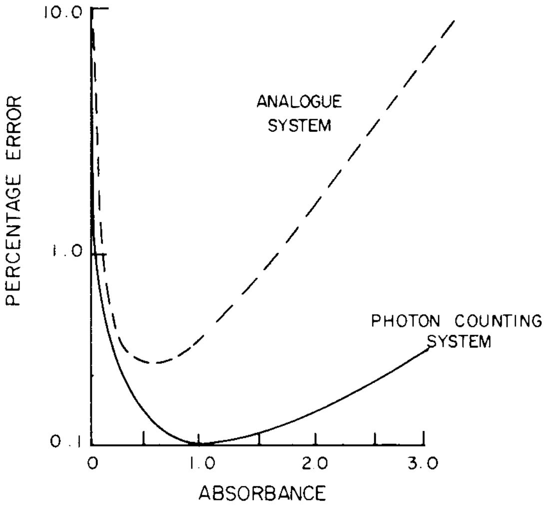

Fig. 10-23. Precision of absorbance measurements obtained by analogue and photon counting systems.[7]

Provided it could be used at convenient light levels, photon counting would also result in a considerable improvement in the precision of atomic absorption measurements. Absorption measurements are readily made by dividing the counts (for a given time) of a signal and a reference channel (subtracting any background values if necessary) the absorbance being log $(N_{\mathrm{ref}}/N_{\mathrm{signal}})$. In a routine system used for many measurements these calculations could conveniently be carried out with a small computer. As with an analogue system used for measuring absorbance values, the percentage error under given conditions will vary with the absorbance value. The overall variation is, however, much more favourable with a counting system. This is illustrated in Fig. 10-23 which shows the calculated errors for absorbance values from 0 to 3·0 units measured with an analogue system, in which it is assumed a linear scale can be read with an accuracy of 0·1%, and with a photon counting system in which a reference beam count of 2×10^6 pulses is assumed. It can be seen that not only is the error of the counting system much smaller but it has a much broader minimum. In the important range from 0·25 to 2·5 absorbance units, the analogue error varies from about 0·3 to 4·6% whereas that of the counting system is less than 0·2%. The error of the counting system is also easily made smaller still by using higher counts. The maximum number that can be made in a convenient time is limited by the frequency response of the system as in most absorption measurements there is adequate light intensity (i.e. photons/second) available. For example, if the system can handle a counting rate of 200 kHz the errors mentioned above would apply to a ten-second count. Improving the frequency response to allow a 10 MHz rate would allow a ten times greater count (of 2×10^7 pulses) in only two seconds, or a fifty times greater count over the full ten seconds. Even ten seconds is relatively rapid by the usual standards of atomic absorption measurements, so that there remains scope for still further improvement in precision.

10.2.3 Digital Readout Systems

A completely digital system for AAS or AFS would require the use of the photon counting technique described above. This technique has, in fact, seen relatively little application to AFS and, as already discussed, is at present not generally suitable for the high light levels commonly used for AAS. Nevertheless, some of the advantages of digital techniques may be obtained without resorting to photon counting, and suitable systems have already been incorporated in several commercial spectrometers. In such systems the output of the photomultiplier is measured conventionally as a continuous current but is passed into an analogue-to-digital converter to obtain a digital signal. The advantage that is taken of having the signal in digital form may then vary greatly, depending on the application and on the cost and complexity of the spectrometer.

In the simplest case, digital conversion involves no more than simply replacing the conventional panel meter used to read the absorption or fluorescence signal with a small digital voltmeter. The advantages of such a conversion for AAS or AFS are debatable. A steady voltage is more easily read from a digital display than from a meter with a scale and pointer and is clearly visible at a considerable distance from the instrument. On the other hand, users of AAS or AFS seldom need to take their readings from the far side of the laboratory and, unfortunately, are often faced with rapidly fluctuating signals which can render difficult the reading (i.e. averaging) of an ever-changing digital display. Furthermore, many operations in both AAS and AFS require "peaking" of a signal, which is undoubtedly more easily achieved with an ordinary meter. In view of these considerations, the provision of a digital readout for the spectrometer is really justified only if it forms part of a more comprehensive digital system. This system may be present both before and after the digital display itself.

There are several relatively simple operations that may usefully be performed on the analytical signal before it is displayed for the operator. For example, in atomic absorption work it is possible to convert the decrease in transmittance of the absorption cell so that it may be displayed directly as an absorbance value. Similarly, in either absorption or fluorescence work, a facility that permits the correction of non-linear calibrations to provide a direct readout of concentration is often useful. When very small absorption or fluorescence signals must be measured, significant improvements in detection limits can be obtained by integrating the signal for a fixed period rather than by using "instantaneous" readings. These and similar operations can be performed using conventional analogue techniques but the circuitry is often complex and sometimes unreliable. Thus, most of these facilities would not be incorporated in an ordinary spectrometer. Once the signal has been converted to digital form, however, a wide range of quite complex operations may be performed economically by continuing to use digital techniques. In many cases, it is possible to purchase from electronic component manufacturers complete circuit modules performing a particular function and to incorporate them into the readout circuitry of the spectrometer. Commercial atomic absorption spectrometers are now available in which these techniques allow provision of features such as switchable transmittance/absorbance readout, variable period integration of signals (e.g. from 1 to 100 seconds), or direct concentration readout at reasonable cost. The adaptability of digital circuitry may sometimes make it useful even when a conventional meter readout is desired; the signal is simply converted to digital form and the reverse operation carried out after processing to regenerate an analogue signal. In many cases, even with digital readout, a digital-to-analogue converter will be incorporated to provide an analogue output for a potentiometric recorder.

The final link in the digital system is the utilization of the processed signal. In the majority of cases this simply involves the traditional manual recording of the signal by an operator. Some commercial spectrometers are, however, already available with digital (i.e. binary coded decimal, bcd) outputs which may be connected to a printing unit of the type used in computers. Analysis results may then be directly recorded in an easily readable digital form on paper, or even be punched on to paper tape or cards for future processing by a calculating machine or computer. If a keyboard is available on the printer the operator may add appropriate notes or comments to provide a complete record of the measurements. Furthermore, if the printer incorporates a memory facility, it may be programmed for a particular routine analysis so that the desired layout, headings, sample references, etc. are obtained automatically. Thus, the spectrometer is capable of rapid production of typed sample reports.

The provision of such a system is obviously expensive; the cost of an automatic printer may easily rival that of the spectrometer itself. As a result, any operation able to justify such an outlay may well benefit from the logical extension of these facilities; i.e. processing of the spectrometer output by a computer. Provision of a small purpose-built computer is possible, but expensive. In some cases where a large time-sharing computer is available it should be possible to link the spectrometer directly, the main item of expense being development of a suitable computer programme. Provided that the work load of the spectrometer is sufficiently great, the expense of a computer system is outweighed by its potential benefits. Not only is automatic printout of results with pre-determined notes possible, but also complicated operations such as statistical analysis or storage of results for subsequent tabulation in special format. Furthermore, the computer itself is able to perform the signal processing operations mentioned above so that the spectrometer no longer requires a large part of its digital circuitry. Finally, the computer may provide a feedback to the spectrometer to allow completely automatic operation in which the computer selects samples and standards, checks unsatisfactory results, etc. Techniques described in the next section for enhancement of signal : noise ratios may also be performed or assisted by the computer. The possibilities are endless; the only limiting factors are the expense and the opportunity for breakdown of the system.

10.3 ENHANCEMENT OF SIGNAL-TO-NOISE RATIOS

It should be apparent from many of the comments made in the foregoing pages that the problem of signal noise is of major importance in both atomic absorption and atomic fluorescence spectroscopy. At the practical level it is a major factor governing the detection limit of any determination and is often an important contributor to the level of precision that may be obtained. In many cases, significant improvement in signal-to-noise ratio is attainable simply by paying scrupulous attention to optimization of instrumental parameters as described elsewhere in this book. Nevertheless, analysis of the relative factors contributing to signal noise in AAS[9] and AFS[10] shows that for certain applications it is possible to obtain further improvements even with the most carefully optimized spectrometer. In this section are described several of the techniques available. Some are either already widely used in AAS or at least easily applicable; others require complex instrumentation or knowledge of data processing techniques. In these latter cases we shall merely attempt to describe available techniques and how they may be employed.

10.3.1 Modulation of Signals

As described in Section 10.2.1, the majority of atomic absorption or fluorescence spectrometers use a synchronous or tuned amplifier in conjunction with an amplitude-modulated light source. Such a system results in improved signal-to-noise ratios for two reasons. In the first place, an ac amplification system is inherently more stable with lower noise levels. The application of source-intensity modulation, first to AAS and later to AFS, was however based on the possibility of detecting the analytical signal without interference from light emitted by the atom cell itself. In many cases this results in a much greater improvement than would be obtained simply by using ac amplification. In fact, with several elements (particularly those having their resonance lines in the visible region) atomic absorption measurements would be most inconvenient were it not for the source modulation technique. Modulation of the light-source intensity is easily achieved by placing in front of it a rotating or vibrating sector (or "chopper"). Alternatively, direct modulation may be achieved by supplying the lamp with a modulated current of the desired frequency and waveform. As explained in Chapter 5, the latter technique is preferable whenever it can be used satisfactorily with the type of lamp in question. A rotating sector may be easier to arrange and is applicable to all sources (even a second flame), but it inevitably reduces the light intensity, may restrict the usable light beam, and can sometimes prove awkward to locate within a spectrometer. It is also worth noting that use of mechanical modulation requires a completely unmodulated (i.e. dc) signal from the source itself. For example, it would not be possible to obtain successful modulation at, say, 280 Hz if the source was operated either directly from the ac mains or from a supply showing a mains ripple; the source itself would then already be completely or partially modulated at 50 or 60 Hz.

To a certain extent the advantages of a modulated light source are obtained if the signal from the detector is processed with a *tuned amplifier*, i.e. one designed to respond only to the pre-selected modulation frequency. This device is simply a combination of a narrow band electronic filter with an amplifier and appropriate feedback between the two. Its disadvantage is that in order to allow for drift of the modulation frequency a relatively wide amplifier bandwidth (>*ca.* 1 Hz) must be used. As a result the amplifier may also amplify some noise, i.e. any signal not originating directly from the modulated source. Thus, there is only limited improvement in the signal-to-noise ratio obtained, say, for atomic absorption signals in the presence of strong emission of radiation by the atom cell. The problem is avoided by using a *synchronous* or *lock-in amplifier*, which eliminates the effects of frequency drift and may therefore use a much narrower bandpass. The improvement is achieved because such devices use a *reference waveform* which is either derived from the device modulating the light source or itself controls the modulation. Thus, a feedback system within the amplifier ensures that all frequencies other than that of the reference are rejected and small variations in the absolute frequency are unimportant. When the light source is modulated electrically the same waveform generator may be used to supply both the source power supply and the amplifier. With mechanical modulation an optical link is widely used to obtain a reference waveform. This usually involves placing a miniature light bulb and photocell on opposite sides of the chopper blade. Thus, the amplitude of signal emitted by the photocell is modulated in exactly the same way as the main light beam of the spectrometer.

In practice, use of a modulation system with reference waveform allows introduction of a further stage of noise rejection. The signal and the reference not only have identical frequencies but must also be exactly in phase. Thus, by using *phase-sensitive* circuitry in the lock-in amplifier it is possible to reject any components of the final signal that are not exactly in phase with the original waveform of the modulated light source. As a result the signal-to-noise ratio is further improved. The basic layout of the phase-sensitive detector is shown in Fig. 10-24. V_s and V_r are the amplitudes of the signal and reference waveforms, respectively, after they have been processed by a tuned amplifier. V_o is the amplitude of the output and is obtained via a low-pass RC filter. The final output of the phase-sensitive amplifier is a dc signal which is often further amplified. Thus, a lock-in phase-sensitive amplifier is able to process extremely small signals in the presence of high noise levels and provide a stable, almost noise-free dc signal of useful amplitude for conventional meters or recorders.

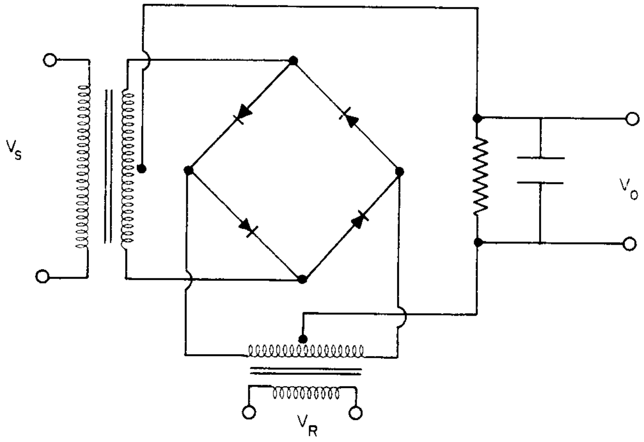

Fig. 10-24. Phase-sensitive detector using a diode detection system and a filtered output.

The modulation technique described above, in which the intensity of the spectral light source is varied, has been applied almost universally to atomic absorption and fluorescence measurements. Modulation may, however, also be achieved in other ways. Several workers[11-14] have described a *sample modulation* technique. This usually involves use of a special nebulizer assembly able to modulate the supply of sample solution to a flame. Thus, a modulated absorption or fluorescence signal is obtained with dc source radiation. The system is most advantageous in flame emission spectrometry but advantages are also claimed for application to AAS and AFS. For example an absorption signal modulated in this way is unaffected by the presence of non-absorbed source lines in the bandpass of the monochromator, as these will not be amplified by the synchronous detection system. Similarly, the background absorption of the flame will not be modulated even at the resonance wavelength of the analyte element so that measurement will be unaffected by noise or drift of the flame background. To avoid any modulation of the background it is usual to arrange that the nebulizer operates alternately with sample and blank solutions rather than with simple intermittent sample aspiration. A constant check on the zero reading is therefore also obtained. Sample modulation also has some disadvantages. For example, the modulation frequency is usually rather low owing to mechanical difficulties and the apparatus is considerably more complex than the widely used pneumatic nebulizer. It is also easier to apply the technique to total consumption nebulizer-burner units or to diffusion flames than to the premixed flames with indirect nebulizers which are of widest application for AAS or AFS. Probably the technique is of greatest use when absorption measurements must be made in regions of high background absorption (e.g. below 220 nm for the air-acetylene flame) or when a continuum source is used. In the latter case, background absorption is always a more serious problem than with sharp line sources as a result of the wider effective absorption bandpass.

It is also possible to use *wavelength modulation* in which either the wavelength of the source or of the measurement is rapidly varied. Obviously, with a sharp line source the effect is exactly the same as conventional intensity modulation and no advantage is gained. Several workers have, however, applied the technique to atomic absorption measurements with a continuum source.[15-19] An obvious advantage of such a system is that background absorption of the flame near the resonance line is automatically eliminated. The system evolved by Snelleman[15] achieved this using a small oscillating mirror within the monochromator to vary the effective wavelength setting. A disadvantage of this method is that any flame emission at the measurement wavelength is also modulated. Elser and Winefordner[16] overcame the problem by combining a similar wavelength modulation method with conventional source modulation. Their experimental system is shown diagrammatically in Fig. 10-25. They were also able to improve the signal-to-noise ratio of measurements compared with conventional modulation of a continuum source. An alternative method of wavelength modulation which also avoids modulating flame emission has been described by Svoboda.[17,18] In this case the wavelength of a continuum source is modulated with an oscillating Fabry-Perot interferometer before passing the light beam through the flame. A conventional monochromator is placed after the flame to select and isolate the wavelength of measurement in the normal way. The interferometer converts the continuum light source into a series of narrow wavelength bands (channels) each of which approximates to a sharp line spectral source. (Channel widths of a few milliangstroms are easily obtained.) The wavelengths at which these channels occur are then modulated by piezoelectrically changing the Fabry-Perot etalon plate separation. The intensity of a particular channel absorbed by the atomic species in the flame is then modulated as it passes through the wavelength of the absorption line and back (i.e. at twice the piezoelectric oscillation frequency). Even when the monochromator transmits not only the absorbed channel but nearby unabsorbed channels the atomic absorption may be detected by tuning to the appropriate frequency. Thus, the interferometer gives the continuum source the advantages of a sharp line source. Kirkbright and Troccoli[19] have employed this type of system for the direct study of atomic line profiles for calcium in different flames by absorption against the channelled spectra from the continuum (xenon) source. The experimental spectrometers used by Svoboda *et al.* and Kirkbright and Troccoli were relatively complicated and difficult to adjust. Small Fabry-Perot interferometers of high quality are now widely used in laser work, however, and these may allow easier application of the technique.

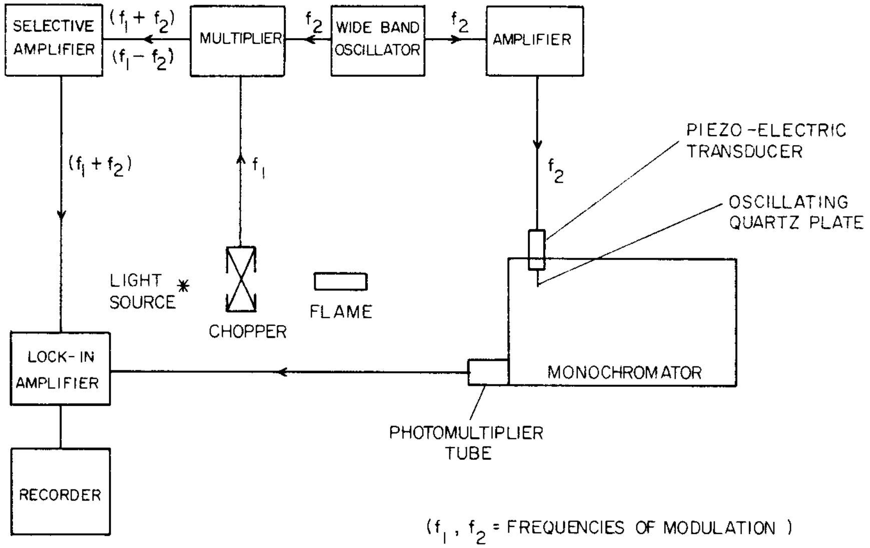

Fig. 10-25. Block diagram of experimental system for double-modulation optical scanning atomic absorption spectrometry.[10]

10.3.2 Integration and Averaging of Signals

Most atomic absorption and fluorescence spectrometers allow improved measurements of very small signals by providing a *variable damping* facility. This simply increases the response time of the system so that the effect of random signal noise on a meter or recorder is evened out and small signals may be measured more precisely. The method is cheap (it usually involves merely switching a few capacitors of different values across the output terminals) and is reasonably effective. It is, however, by no means the most efficient way of extracting signals from noise and also has some disadvantages. For example, if a sudden noise "spike" occurs with a heavily damped system there will be a considerable time lapse before the reading returns to normal. Similarly, if heavy damping is used to obtain a noise-free steady signal there will be a long waiting period after introducing a sample before the actual reading is reached. A similar delay occurs at the end of the measurement before the zero reading is regained. Some manufacturers avoid this particular problem by using "automatic damping" which is only applied when the signal has reached a steady value. This is more than a time-saving device as heavy damping often cannot be used with small samples because all of the sample would be consumed before a reading could be taken.

Integration techniques provide a more efficient alternative to heavy damping, avoid some of the disadvantages, and are still reasonably simple. If the noise is random whereas the signal is not, true integration of a combined signal and noise for a set time should reduce the noise component to zero but greatly increase the size of the signal. Even in a practical case where the noise is not completely random the signal should increase more rapidly than the noise so that the signal-to-noise ratio is increased. The simplest analogue integrator is the RC circuit of Fig. 10-20 with a very long time constant. Thus the output would be a steadily increasing voltage which is characteristic of the input voltage and the time for which the capacitor has been charging. An integrated signal is obtained simply by noting the voltage at a fixed time after starting from zero. Harrison and Berry[20] have described the application to AAS of an improved analogue integrator using an operational amplifier and incorporating an electrical relay to set the integration time. Similar devices are available commercially.

Digital integration techniques are generally more versatile and also more accurate. Provided the digital circuitry is already in use, integration is obtained merely by a suitable choice of counting times. Thus, most atomic absorption spectrometers with digital readout (or a digital accessory unit) incorporate some form of integration as standard. Usually several pre-selected integration periods in the range 1 to 100 seconds are available. As the meter will "hold" one reading until the next is available to update it, correct choice of integration period will allow easier reading of even routine measurements; continuous changing of the meter reading while the operator attempts to note an average value is then avoided. The use of digital circuitry allows several additional features to be easily incorporated. For example a zero value can be stored and automatically subtracted from all integrated readings until it is updated by the operator. Improved precision is obtained by replacing integration over one long period with an average value of the integrated values obtained over several short periods.

The technique of *signal averaging* is extremely powerful for the extraction of signals from noise and may be considered quite separately to conventional integration. It involves the sampling of a repetitive signal and storage of successive samples in a register. When each sample is taken in a completely reproducible manner the signals are cumulative whereas random noise averages to zero. In the general case the increase in signal-to-noise ratio is proportional to the square root of the number of samples. Unlike the integrator, a signal averager is able to handle a signal which is made up of many components; for example, a spectrum which is scanned repeatedly. This is achieved by using a large number of channels, each of which samples successively at a pre-determined time after the sampling procedure has been initiated (triggered). Obviously, each sampling run must start at exactly the same point on the spectrum so that a synchronizing pulse would be generated by the spectrometer. Commercial signal averagers are available but are relatively expensive when many channels are required. Their application to AAS or AFS is limited as spectral scans are not usually required. It is worth noting that if the spectrometer provides a binary (digital) output, the technique may be carried out with a small computer suitably programmed. A single channel signal averager, often called a *boxcar integrator*, is more relevant to routine absorption or fluorescence measurements, with modulated sources. It has several advantages over straightforward demodulation (with a lock-in amplifier) and measurement of the resultant "average" dc signal, either directly or after integration. Thus, instead of filtering the output of a lock-in amplifier it is possible to sample a number of output pulses and to average them. Optimum results depend on the correct selection of a number of variables in the electronic system. Nevertheless, modern circuit techniques allow incorporation of such devices into spectrometers with the minimum of external controls. For example, a system may combine sophisticated averaging and integration techniques yet present the operator with merely a digital panel meter and a switch to select intervals of 1, 10 or 100 seconds between "readings".

10.3.3 Correlation Techniques

depende de

As with integration and signal averaging, correlation analysis relies on the periodic nature of a signal compared with the random nature of noise. It is, however, even more efficient and will extract a signal that is many times smaller than its accompanying noise. The instrumentation required to achieve this is complex, although a suitably programmed small computer is again adequate; to date only one application to AAS or AFS seems to have been reported.[21] The technique involves examining the correlation (i.e. interdependence) between the signal and a delayed version of itself (auto-correlation) or between the signal and a reference (cross-correlation). For each signal, this comparison is made at a number of different time intervals. Except near zero time interval, random noise can never show any correlation, whereas any periodic signal will generate another periodic waveform. Thus, the signal is readily extracted from the noise. The advantages of correlation analysis over the techniques mentioned above, apart from this greater efficiency, include direct background correction, elimination of drift, absence of synchronizing wave (for auto-correlation) and minimization of the effects of sudden noise impulses. This last advantage may be particularly useful; it is often difficult under such conditions to read the true level of the output from, say, a lock-in amplifier, particularly when a long time-constant is used. As shown in Fig. 10-26, similar pulses have little effect on the accuracy with which a

[illegible]

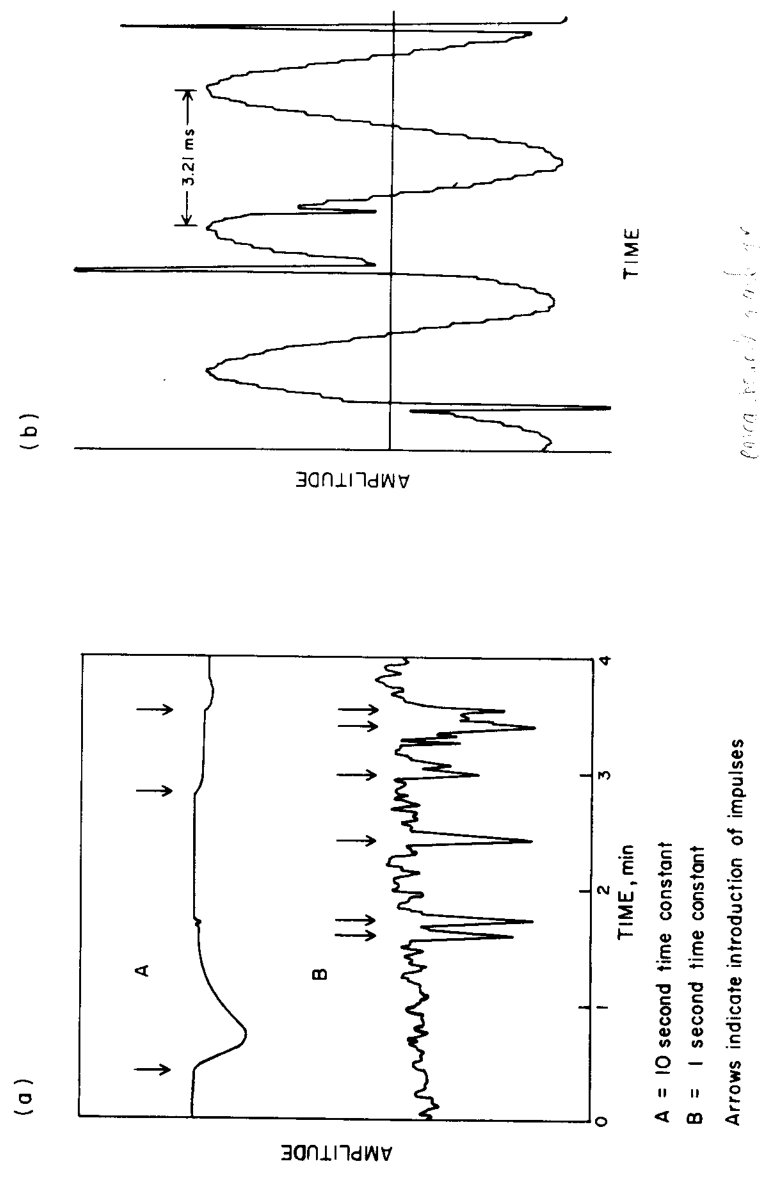

Fig. 10-26. Relative effects of impulse noise on (a) a chart recording from a lock-in amplifier and (b) a cross correlogram.[20] (In both cases the signal is the fluorescence obtained from a 100 ppm rhodium solution using a hollow-cathode lamp as source and an air-hydrogen flame.)

correlogram may be read (even if a noise peak coincided with a signal peak, the reading could merely be taken from an adjacent peak). In spite of its advantages and ease of application, the expense of the instrumentation required for correlation analysis is likely to hinder its routine application to analytical work in the near future. It is important, however, to remember the efficiency with which this and similar techniques can extract reliable data from signals that otherwise represent useless noise to the operator of a moderately priced atomic absorption spectrometer.

10.4 OPTICAL SYSTEMS

In this section we describe some of the variations that occur in the optical systems of commercial spectrometers. No attempt is made to explain fully their construction or to give comprehensive coverage, but it is hoped that the reader will obtain some guidance as to the usefulness of various features. For example, most double-beam spectrometers are claimed to have advantages over single-beam types, but at least one manufacturer lists the latter feature as an advantage over double-beam operation!

10.4.1 General Layout

Two distinct patterns are readily discernible amongst commercial atomic absorption spectrometers: the modular concept and the single-unit instrument. The former type in its classic form (see Fig. 1.2) offers maximum versatility with all optical components mounted on an accessible optical bench and ancillary units conveniently placed around them. Thus, the optical alignment is readily optimized for particular applications, components are easily changed when required and the system may often be applied in modes other than those envisaged by its designers. Such a system is ideal for research use and was quite widely available in early atomic absorption spectrometers. It is less attractive, however, in a spectrometer designed exclusively for routine analysis. The instrument requires careful alignment, components can be accidentally disturbed, lenses or mirrors may become dusty or degraded by sticky fingers, and more operator skill is required to ensure that the instrumental arrangement and operating parameters are optimized for a particular operation. Hence, routine trouble-free operation is more likely if all components are securely mounted in a single unit, optical alignment is preset by the manufacturer, and lenses, mirrors, etc., can only be disturbed by deliberate removal of a number of fixing bolts. A typical modern spectrometer based on this concept is shown in Fig. 10-27. It can be seen that even the lenses guiding the light beam through the flame have been recessed behind a metal shield to minimize the risk of soiling them. With the advent of AAS for the routine analysis of large numbers of samples this style of spectrometer has become increasingly popular and many commercial instruments now resemble the type shown in Fig. 10-27.

The trend towards a compact, easy to use spectrometer is understandable; the largest volume of sales is now for applications where this style has several advantages. The analytical chemist requiring specialized instrumentation for research purposes can probably obtain better results by purchasing individual optical, spectroscopic and electronic components from different manufacturers. The biggest problem in this respect may be the burner and nebulizer as suitable units have been developed largely for commercial atomic absorption spectrometers. Fortunately, several manufacturers supply their burners either separately or as "spares" so that no real difficulty need arise. Even the single-unit instruments show considerable variation between manufacturers as to ease of optical alignment and use, so that care is needed in the selection of a spectrometer. For example, hollow-cathode lamps usually need individual alignment owing to tolerance in manufacture. If elements are changed frequently the time required to change lamps may be an important consideration. Some instruments incorporate a movable turret or rack for several lamps, each of which may be aligned once and then moved into the correct position when required. The usefulness of this feature depends on the number of elements whose analysis is regularly required; obviously, a holder taking three lamps is inconvenient if samples are regularly analysed for elements needing six individual lamps. An alternative approach is to have a lamp-house for only a single lamp but to mount each lamp in a separate holder stored outside the spectrometer. Each lamp may then be aligned once (using adjustment screws provided on the holder) and simply be clipped into the spectrometer whenever required. This system is at its best in double-beam systems (see Section 10.4.2) where minimum warm-up of lamps is required; with single-beam spectrometers a turret holder conveniently allows lamps to be operated on "standby" and automatically switched to the main power supply when rotated into the operating position.

With either method of mounting the lamp correct alignment is

Fig. 10-27. A modern atomic absorption spectrometer constructed as a single unit.

required at some stage. The ease with which this is accomplished can vary considerably, depending on the design of the instrument. By careful positioning of the fixed optical components the manufacturer can ensure that correct alignment of the light beam with both the burner and monochromator is obtained by adjusting the lamp holder until maximum transmitted light is indicated by the readout meter. This is somewhat easier than attempting to follow the path of the light beam with pieces of white card! The adjustment of the lamp itself is probably best achieved with correctly placed screws of reasonably fine pitch but adequate length; considerable frustration results during lamp alignment with holders that are poorly designed and have inadequate provision for adjustment. Alignment is also facilitated if the optical arrangement has been carefully chosen by the manufacturer. Thus, the extent to which the path of the light beam depends on the exact position of the lamp will vary with the size and focal length of lenses and mirrors, their distance from the lamp, burner or monochromator, the size and location of beam-restricting apertures, etc.

It should not be forgotten that the flame itself is a major component of the optical system. Hence the burner should also be provided with accurate and reproducible adjustment for the vertical and lateral position of the flame. With careful design, optimization of this variable can also be made part of a simple sequence; once the light beam is correctly placed with respect to the remainder of the optical system the flame position may be set simply by adjusting the burner until maximum absorbance is observed for the element of interest. Again it is important that the available adjustment of the burner should be adequate for a wide range of conditions. This is best achieved if there is sufficient space in the burner compartment. A large burner compartment ensures ease of replacement or cleaning of the burner and allows any accessories to be fitted rapidly. Optical components, such as lenses or restricting apertures, may also then be at sufficient distance from the flame to prevent overheating and degradation.

10.4.2 Double-Beam Operation

Most early atomic absorption and fluorescence spectrometers were designed for single-beam operation, i.e. in these instruments the light passing through the absorption cell or originating from the fluorescence cell was the only radiation received at the detector. With these

systems any fluctuation in the intensity of the light source appears as an analytical signal and unless the source is very stable frequent zero checks are required. Some of the problems of drift of the light source are avoided by double-beam operation in which the detector also receives a reference light beam which has originated from the same light source but has not passed through the atom cell. Many atomic absorption spectrometers with this facility are now available commercially.

The optical arrangement of an early double-beam system is shown in Fig. 10-28. Radiation from the source is divided into two beams by a silica beam splitter at position A. The height and direction of the beams are then varied by a number of mirrors until they are merged at position B in such a way that two identical vertically adjacent beams may be passed through the monochromator. After leaving the monochromator further mirrors are used to deflect each beam to its own photomultiplier tube. The signals from these two detectors are then amplified and balanced by the readout system so that absorbance values in the sample channel are always corrected for any changes in source intensity. This system has several disadvantages; the optics are complicated, two photomultipliers (and their power supplies) are required and most important of all, there is no compensation for variations in gain of the individual photomultipliers. Much more satisfactory results are obtained with an alternative system which is now widely used. As shown in Fig. 10-29, the light beam from the light source is divided by a rotating sector, the rear surface of which is reflecting. Thus, the light is alternately passed directly into the flame or reflected backwards to a mirror which deflects the reference beam through the rear of the spectrometer. The two beams are subsequently recombined by a half-silvered mirror and pass through the monochromator to the photomultiplier as a single beam. The signal from the photomultiplier is, however, processed by an amplifier able to separate it into the reference and sample channels using the same techniques as conventional lock-in amplifiers (the two channels merely have different phase angles). Both signals could be displayed separately by the readout device but it is more common to present them simply as an absorbance signal which is automatically corrected for variations in source intensity. Several spectrometers now simultaneously present the reference beam signal on a separate meter so that it may be used as a continuous check of source intensity no matter what absorption measurements are in progress in the sample beam.

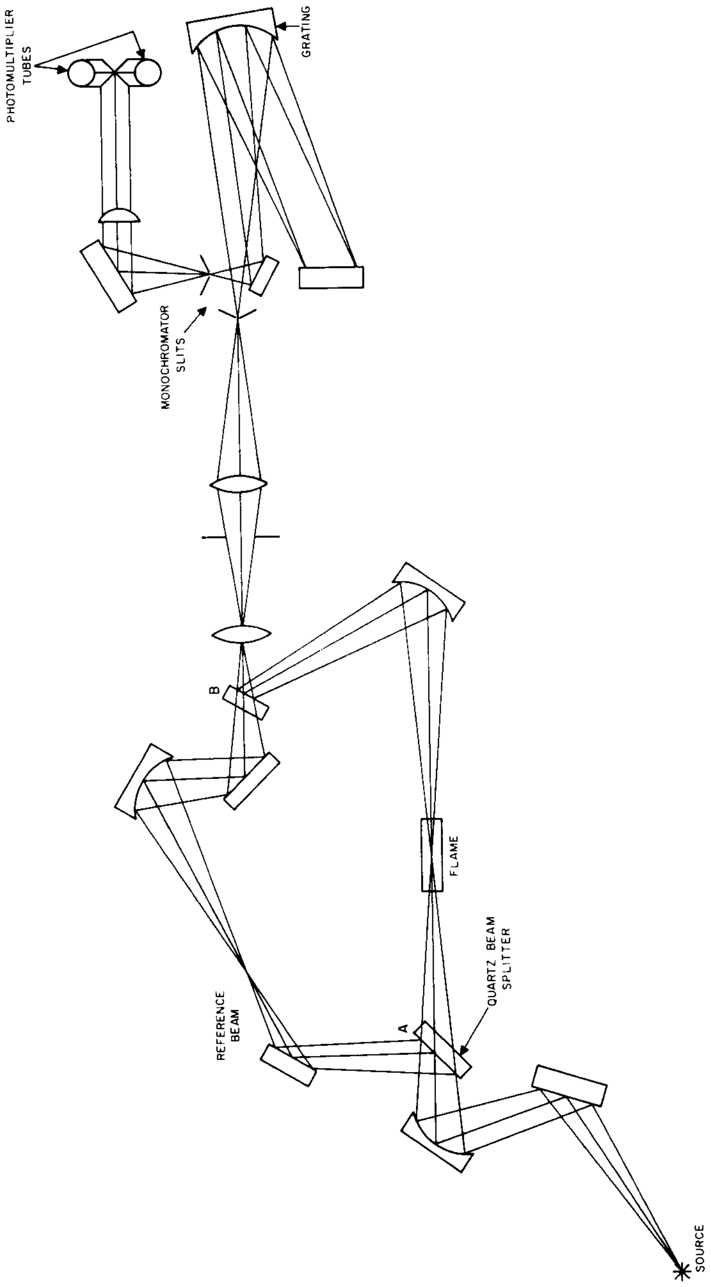

Fig. 10-28. A double-beam spectrometer using separate photomultiplier tubes for sample and reference beams.

It should be appreciated that double-beam systems only compensate for variations in source intensity; unlike solution absorption spectrophotometers the reference channel does not incorporate a "blank-cell" for correction of background absorbance. Thus, the value of double-beam operation with modern hollow-cathode lamps of high stability is sometimes questioned. On balance, there still appear to be advantages in incorporating double-beam optics in instruments designed for routine use with minimum attention. Even the best hollow-cathode lamps may show some drift of output, and all lamps require a warm-up period before a stable output is reached. Thus, with a single-beam instrument there is a tendency to run on standby as many as possible of the lamps which might be needed during the day. This may reduce their useful life; with the double-beam facility, however, the lamps need be operated only when actually in use. For almost all elements double-beam measurements may be made within a minute or two of switching on the lamp and many manufacturers provide no facilities for warm-up. Hence, no additional power supply is required and over the life of a well-used spectrometer the convenience of double-beam operation may be obtained at very little extra expense. Double-beam operation may also be particularly advantageous for atomic fluorescence measurements, which are frequently made using the more intense electrodeless discharge lamps. As discussed in Chapter 5, these sources may often be less stable than hollow-cathode lamps. It is important to remember that with both absorption and fluorescence signals the system cannot

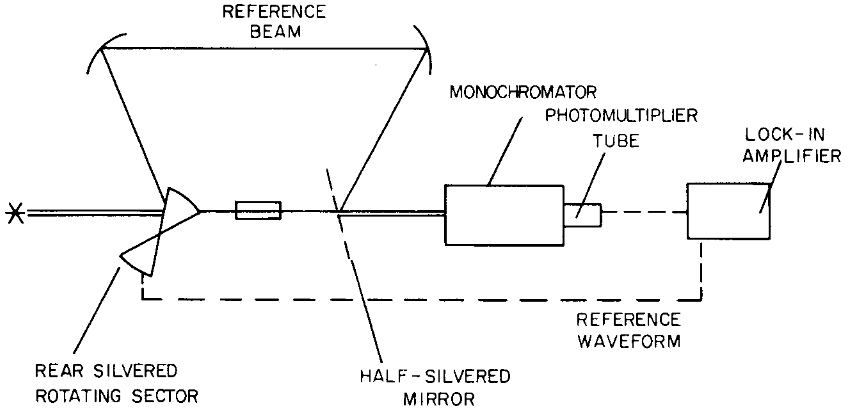

Fig. 10-29. A double-beam spectrometer using a single photomultiplier tube and electronic separation of reference and sample channels.

compensate for any variations of the source except for the total intensity of the line. For example, a sudden increase in the intensity of a lamp may be accompanied by an increase in the spectral line width. This would result in a decrease in the measured peak absorbance of a sample but there is no way in which the double-beam system described above can correct this change.

10.4.3 Background Compensation Techniques

There are two situations in which absorption by species other than the analyte atoms may prove troublesome during atomic absorption measurements and which cannot be avoided by conventional double-beam operation. As described in Chapter 6, many flames show relatively strong natural absorption of radiation in certain spectral regions, particularly at short wavelengths. Sample solutions containing high concentrations of certain anions or compounds may also absorb over relatively wide spectral bandwidths owing to either scattering of radiation or to molecular absorption. This effect is discussed further in Section 12.1.4 and 12.3.1. In either case the spurious absorption signal can prove inconvenient and may cause errors, particularly if the operator is unaware of its existence. In view of this, several attempts have been made to obtain automatic background compensation and suitable accessories are available for some commercial spectrometers. Automatic background compensation is, of course, obtained by the sample modulation techniques and some of the wavelength modulation techniques described in Section 10.3.1. These have seen little general application, however,

In one commercial system[22] the background absorbance is measured using a deuterium or hydrogen discharge lamp acting as continuum source. The lamp is placed near to the hollow-cathode lamp of a double-beam spectrometer. The optics are adjusted so that the chopper, which normally passes light from the hollow cathode alternately through the reference and flame channels, now alternately passes light from either lamp through the flame. Absorption of the broad band of continuum radiation by sample atoms is negligible but both types of radiation are absorbed equally* as the result of background effects. Thus the double-beam circuitry of the readout section automatically compensates for changes in background absorption. It should be noted that conventional double-beam operation is no longer available to compensate for variations in the hollow-cathode lamp intensity. Thus the compensation accessory is made easily demountable and is only used when necessary.

A slightly different compensation method has been described by Woodriff *et al.*[23] again using a continuum source. These workers used a polarizing beam splitter to obtain horizontal polarization of one light beam and vertical polarization of the other. The two beams may then be combined for passage through the absorption cell and monochromator but separated optically using further polarizers before being detected by a photomultiplier. This system may allow easier alignment of the two beams throughout the length of a long absorption cell such as a furnace, but probably has little advantage over the other system.

Another approach to the problem is to make background corrections using a line from the conventional hollow-cathode lamp which lies close to the resonance line but which is not absorbed by the sample atom.[24,25] As the reference line should show similar intensity variations to the resonance line, this method would have the advantages of both background correction and conventional double-beam operation. Some problems arise with this technique, however. It is often difficult to find a suitable nearby non-absorbing line and there is no guarantee that its intensity variations will always follow those of the resonance line, particularly if a line emitted by the filler gas must be used. Also, although manual corrections are readily made, a fully automatic system using this principle would require quite a complex spectrometer. In fact, it only becomes fully practicable with the type of multichannel instrument described in Section 10.4.4.

10.4.4 Multichannel Techniques

A number of attempts have been made to use either AAS or AFS for multielement analysis[26-32] and several commercial spectrometers have been designed for the rapid simultaneous determination of several elements. In most cases these instruments have seen little application to practical problems. This may be attributed to operational problems such as the size and expense of spectrometers, difficulty of maintaining the complete system in optical alignment, poor sensitivity compared with conventional single-element instruments and the effort required by an operator to manage such a system unless it is almost completely automated. There is undoubtedly a place for absorption or fluorescence spectrometers able to handle the simultaneous analysis of, say, six elements in a single

---

* As explained in Chapter 3, this is not strictly true under all conditions. Nevertheless, the system works well within the limitations imposed by other experimental factors.

sample. It seems, however, that the full benefit of such a system is only realized when it is combined with complex sample handling and data processing techniques. Thus, the complete spectrometer becomes extremely expensive and will probably only be justified when designed specifically for specialized applications. A typical example may be clinical analysis in which a single laboratory will process many samples in each of which the determination of several elements within a relatively narrow range of concentrations is required.

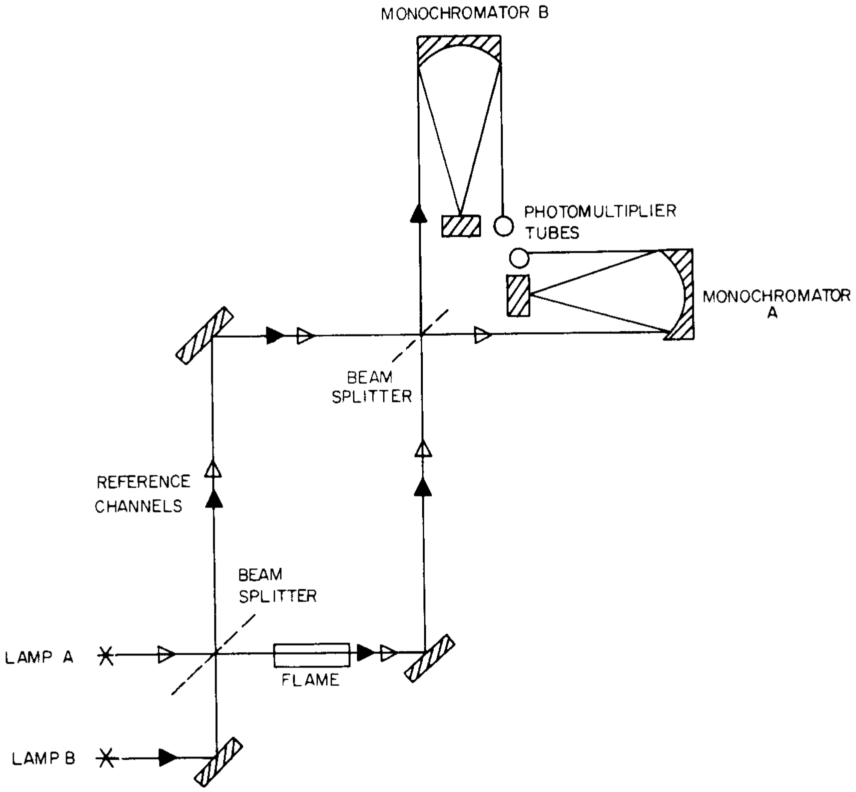

Fig. 10-30. A dual-channel, double-beam optical system.

Recently, several commercial examples have appeared of a new type of atomic absorption spectrometer which is expensive but still within the price range of a general purpose instrument. This is the double-beam, dual-channel spectrometer. As shown in Fig. 10-30 each channel has its own hollow-cathode source, monochromator and detector *and* is provided with a conventional double-beam reference channel. In some less expensive systems the second monochromator may be replaced with a tunable interference filter. Each channel also has its own readout unit so that the spectrometer may obviously be used for simultaneous two-element analysis. Of more interest for many applications, however, is the ability to program the electronics so that one channel may be used as a reference for the other. For example, if one hollow cathode is replaced by a continuum source the spectrometer provides background compensation and double-beam operation. Alternatively, both hollow cathodes may be retained but one channel set to a non-absorbed line so a different type of background correction is obtained. Similarly, one channel may be used to measure an internal standard element added to the sample and a readout obtained which is compensated for effects such as variations in nebulizer sensitivity. Such techniques also tend to minimize the effects of flame noise in certain spectral regions.

10.5 BURNER SYSTEMS

The design and construction of burners has already been described in Chapter 6 and that of nebulizers in Chapter 8; this brief section contains some comments on points of practical interest which could not be conveniently included elsewhere.

In most commercial spectrometers the position of the burner, other than fine adjustment, is selected by the designer and cannot be readily changed. A good design will ensure that the burner is easily accessible for cleaning or replacement but is well protected from draughts. At the same time protection must be provided for the operator against radiation and heat emitted by the flame and against the possibility of an explosion. The force of an explosion should be dissipated through a safety valve or bursting diaphragm to avoid any chance of disintegration of the burner or nebulizer. Probably the most useful safety feature is a removable cover across the front of the burner chamber, providing easy access when necessary while preventing accidental contact with the flame. The cover should be semi-transparent so that the operator can see the flame when adjusting gas flow or check that it is still burning. In some cases a photoelectric device is provided to switch off gases should the flame extinguish and this is particularly necessary for spectrometers designed for fully automatic operation. An extraction hood must usually be mounted over the spectrometer to remove the burnt gas. This is particularly important when using a high-temperature flame in a small laboratory or when samples are likely to produce toxic fumes. The ventilation provided is a useful safety factor against unlit gas jets. Care is needed in the choice of extractor. A low extraction rate with a large, high-temperature flame may lead to overheating of the ducting and fan. On the other hand, an excessively high extraction rate will cause draughts and may result in noisy signals.

Many atomic absorption spectrometers incorporate gas controls or offer them as an optional module but the purchaser must usually arrange suitable gas supplies. Air can be obtained from cylinders but frequent changes will be needed if, say, an air-acetylene flame is operated for long periods. It is usually more economical and more convenient to purchase a small compressor; this must be capable of supplying an adequate air flow at the relatively high pressure required by many pneumatic nebulizers while allowing sufficient margin for efficient operation of regulators. The compressor should be provided with a dust filter at its inlet and with a suitable filter to remove condensed water from the supply line. It is also advantageous to choose one of the "oil-free" types of compressor, particularly if the same regulation system is to be used with nitrous oxide. Apart from the possible use of town gas, any other gases required will be obtained from storage cylinders. Hydrogen, nitrogen, argon, etc., are stored in compressed form, propane and nitrous oxide as liquids and acetylene in special cylinders in which it is maintained as a solution in acetone. In most cases the cylinders may be used until they are empty but with acetylene a fresh cylinder should be installed when the pressure has dropped to 75-100 psi. This arises because considerable quantities of acetone distil over as the pressure falls and can significantly alter the flame characteristics. The problem can be avoided by installing a suitable filter (e.g. of activated carbon) in the acetylene line but the filter will require frequent replacement or regeneration and may prove more troublesome than simply changing the cylinder at more frequent intervals. Wherever possible all gas cylinders but particularly those containing flammable gases, should be kept in the open air. If this is impracticable, care must be taken to keep them well away from the burner and secured against accidental damage.

The storage pressure within the cylinder is relatively high, particularly with a full cylinder of compressed gas, and some form of reduction valve is required before the supply can be connected to the burner regulator unit. This is achieved almost universally with a pressure regulator which is fitted onto the outlet of the cylinder. Such regulators generally provide a variable outlet pressure together with gauges to measure both this and the cylinder pressure. Pressure control is provided by a spring-loaded diaphragm whose position is set by a regulating screw. The diaphragm maintains a constant outlet pressure (relative to the atmosphere) until the cylinder pressure falls below the value selected. In practice, the pressure drop required is often extremely large and a single diaphragm is unable to maintain a sufficiently constant pressure for spectrometric applications. For this reason it is usually desirable to use a two-stage regulator. In this a non-adjustable diaphragm reduces the cylinder pressure to a convenient pre-selected value (e.g. 100 psi) while a second adjustable diaphragm controls the final reduction to the selected operating pressure. These regulators are available in a very wide range and care must be taken to select suitable models. Points to note are: suitability for the gas (e.g. corrosion resistance); correct thread for the gas-cylinder outlet; correct inlet pressure range (the fill presure of a cylinder varies considerably depending on the gas); and correct outlet pressure range for the application (e.g. a 0-200 psi range would not be correct if 5 psi is normally required). Regulators of a similar type but with relatively low inlet pressures are available for attachment to air compressors; they are essential for satisfactory results in most applications. Regulators used with nitrous oxide are often found to "ice-up". This occurs because of the large amount of heat extracted in vaporizing the liquid gas in the cylinder and it may cause variations in output pressure.

In order to obtain optimum results in AAS or AFS a relatively complex gas-control system must be installed between the cylinder regulator and the burner. Adequate systems are provided by some manufacturers but others are less satisfactory in this respect. It may, therefore, be desirable to modify the existing system or to assemble a purpose-built unit. The following features should be incorporated.

(1) The unit should be close to the burner.
(2) Each gas should be controlled by a pressure regulator similar to that used at the cylinder. This regulator provides a final step-down in pressure to the operating value. A gauge should be available to monitor the pressure of each gas.
(3) In some cases the flow rate of the gases can be controlled adequately using a fine needle valve on the outlet of the pressure regulator. The most satisfactory results are obtained, however, by using a flow controller. Simple diaphragm units

are widely available at relatively low cost. In the present application such a controller would be supplied with gas at a constant pressure by the pressure regulator and then supply a constant flow rate of gas regardless of any fluctuations in pressure downstream (such as that due to variations in the back-pressure of the flame). A regulating screw attached to the diaphragm allows the flow rate to be varied.

(4) The flow rate of each gas must be accurately measured so that flame conditions can be set reproducibly from day to day. Most flowmeters are pressure-sensitive so that they are best installed between the pressure regulator and the needle valve or flow controller. They may then be calibrated at the operating pressure.

(5) Electrical flow transducers are available but perfectly satisfactory results are obtained using a critical orifice and manometer or a rotameter. The latter type is fitted to many commercial units. It consists of a glass or plastic tube whose bore is tapered from one end to the other. The tube is mounted vertically with the narrow end at the bottom and a small spherical or conical "float" placed inside. The float is lifted by the gas flow and the position at which it reaches a balance is characteristic of the flow rate. Different flow rates are obtained by using tubes of different bore size and/or floats of different density. The tube is either calibrated directly or else marked with an arbitrary scale and supplied with calibration graphs for different gases. It is important to bear in mind that the readings will vary with the temperature, pressure and type of gas, so that standard conditions must be used in order to obtain accurate results. The calibration will also be invalid if the rotameter is not mounted vertically. More expensive types are supplied with conical floats which spin rapidly when the rotameter is supplied with gas. Most atomic absorption spectrometers are supplied with relatively inexpensive rotameters using spherical floats, both a glass and metal ball often being placed in one rotameter to widen its useful range.

(6) The method of operating a pneumatic nebulizer is also an important consideration in designing the gas-control unit. In most cases the oxidant gas is used for nebulization. Reproducible sample addition will only be obtained if the nebulizer is operated at constant pressure. Hence, if all the oxidant is passed through the nebulizer it will not be possible to vary its flow rate. A better arrangement is to split the oxidant stream after the flow meter and to use a nebulizer that passes only a relatively small flow of gas. The rest of the oxidant may then be passed via a flow controller to the burner and its flow rate varied as required. The total flow reaching the burner will, of course, be indicated by the flow meter.

(7) The needle valves or flow controllers used to vary the gas flows should not be used to shut off the flow. Much more satisfactory operation is obtained with miniature "toggle" valves, preferably mounted on the high-pressure side of the unit. These allow the gas flows to be switched off without disturbing the flow setting and provide a simple means of rapid shut down.

(8) If the nitrous oxide-acetylene flame is used, it may be ignited and extinguished via an air-acetylene flame (see below). The control unit should therefore provide a simple means of change-over between the two oxidants. A three-way valve will suffice to change both the nebulizer and by-pass supplies, provided the same flow-control system is used for both gases. If different flow rates are required for the two gases a more complicated arrangement will be necessary. In any event, rapid change-over is necessary as an extremely sooty acetylene diffusion flame will burn while no oxidant is available.

All flames routinely used for AAS or AFS are perfectly safe provided the equipment is properly maintained and care is taken during operation, particularly when igniting or extinguishing the flame. Careful procedures are best ensured by using a standardized sequence of operations. Before attempting to light the flame the following checks should be carried out.

(1) Extractor switched on.
(2) All gas cylinders and compressor on and pressures correctly set.
(3) Nebulizer drain tube contains water (it is necessary to drain excess water from the nebulizer and at the same time provide a head of pressure to overcome the back-pressure of the flame on the burner. This is usually achieved simply by incorporating a trap with a head of several inches of water in the nebulizer drain tube).
(4) Correct flow rates preset for all gases.

When lighting the flame, the oxidant should be switched on first. As soon as the correct flow is reached the fuel gas may be switched on and the flame ignited almost immediately. To shut down, the fuel should be switched off and the oxidant left flowing for a short time to flush out any remaining fuel and to cool the burner. Owing to its somewhat higher burning velocity, most operators prefer not to use this system with the nitrous oxide-acetylene flame. Usually an air-acetylene flame is ignited as described, the fuel flow is increased to give a sooty, luminous flame, and the air is replaced by nitrous oxide. The fuel flow is then adjusted to give the required flame appearance. The reverse procedure is followed to extinguish the flame.

Fully automatic burner control units are now available which relieve the operator of the need to remember the operational sequence. A combination of electronic and servo systems is provided which switch on the gases in correct sequence, check their flows, ignite the flame and, if required, change to nitrous oxide. The flame is extinguished merely by pressing an "off" button to initiate the reverse sequence.

REFERENCES

1. C. Veillon, "Handbook of Commercial Scientific Instruments: Vol. 1, Atomic Absorption", Marcel Dekker, New York, 1972.
2. F. T. Areccki, E. Gatti and A. Sona, *Rev. Sci. Instrum.*, 1966, **37**, 942.
3. R. R. Alfano and N. Ockman, *J. Opt. Soc. Am.*, 1968, **58**, 90.
4. G. A. Morton, *Applied Optics*, 1968, **7**, 1.
5. F. Roblen, ibid., 1971, **10**, 777.
6. M. Jonas and Y. Alan, ibid., 1971, **10**, 2437.
7. H. V. Malmstadt, M. O. Franklin and G. Horlick, *Anal. Chem.*, 1972, **44**(8), 63A.
8. Y. D. Harker, J. D. Masso and D. F. Edwards, *Applied Optics*, 1969, **8**, 2563.
9. J. D. Winefordner and T. J. Vickers, *Anal. Chem.*, 1964, **36**, 1947.
10. J. D. Winefordner, M. O. Parsons, J. M. Mansfield and W. J. McCarthy, ibid., 1967, **39**, 436.
11. W. Lang, *Spectrochim. Acta*, 1967, **23A**, 471.
12. W. Trampisch and R. Herrmann, ibid., 1969, **24B**, 215.
13. K. Rüdiger, B. Gutsche, H. Kirchhof and R. Herrmann, *Analyst*, 1969, **94**, 204.
14. M. Marinkovic and T. J. Vickers, *Anal. Chem.*, 1970, **42**, 1613.
15. W. Snelleman, *Spectrochim. Acta*, 1968, **23**, 403.
16. R. C. Elser and J. D. Winefordner, *Anal. Chem.*, 1972, **44**, 698.
17. V. Svoboda, ibid., 1968, **40**, 1384.
18. G. J. Nitis, V. Svoboda and J. D. Winefordner, *Spectrochim. Acta*, 1972, **27B**, 345.
19. G. F. Kirkbright and O. E. Troccoli, *Spectrochim. Acta*, 1973, **28B**, 33.

20. W. W. Harrison and F. E. Berry, *Anal. Chim. Acta*, 1969, **47**, 415.
21. G. M. Hieftje, R. E. Bystroff and R. Lin, *Anal. Chem.*, 1973, **45**, 253.
22. H. L. Kahn, *Atomic Absorption Newsletter*, 1968, **7**, 40.
23. R. Woodriff, B. R. Culver and K. W. Olson, *Applied Spectroscopy*, 1970, **24**, 530.
24. A. C. Menzies, *Anal. Chem.*, 1960, **32**, 898.
25. J. W. Robinson, ibid., 1961, **33**, 1226.
26. L. R. P. Butler and A. Strasheim, *Spectrochim. Acta*, 1965, **21**, 1207.
27. A. Walsh, *Proc. 13th Colloq. Spec. Intern. Ottawa*, 1967, p. 257.
28. F. Brech, ibid., p. 294 and p. 1194.
29. R. Mavrodineanu and R. C. Hughes, *Applied Optics*, 1968, **7**, 1281.
30. A. Strasheim and H. G. C. Human, *Spectrochim. Acta*, 1968, **23B**, 265.
31. J. B. Dawson, D. J. Ellis and R. Milner, ibid., 1968, **23B**, 695.
32. D. G. Mitchell and A. Johansson, ibid., 1970, **25B**, 175.

CHAPTER 11

Practical Techniques of Atomic Absorption and Atomic Fluorescence Spectroscopy

In the previous chapters we have described the underlying theory of AAS and AFS and have discussed in some detail the individual components utilized in atomic absorption and fluorescence spectro-

When indirect nebulizers are employed with premixed flames the use of an adjustable nebulizer may permit greater flexibility in optimization of operating conditions. The most common of these devices provide for variation in positioning of the sample uptake capillary within the concentric nebulizing gas outlet (see Section 8.2.1). The sample uptake rate, and the yield of solution reaching the flame, may then be varied without variation in the nebulizer gas flow-rate, so that the flame volume and stability remain unchanged. It has been shown[29] that when an adjustable nebulizer of this type is used the mean drop size increases with increasing uptake rate, while the *fraction* of the sample solution reaching the burner decreases. When an adjustable nebulizer is available, therefore, the optimization of the uptake rate to produce the greatest sensitivity and precision or freedom from chemical interferences is worthwhile for a particular analytical application.

Apart from this method of variation of the nebulizer efficiency with a particular sample solution via use of an adjustable nebulizer, the efficiency of the nebulizer may usually only be further "optimized" by changing the nature of the sample solution. The addition of a water-miscible organic solvent, such as acetone or ethanol, to the aqueous sample solution usually results in some enhancement of sensitivity in AAS and AFS despite the dilution effect of the added solvent. The improvement results from increased nebulizer efficiency due to smaller mean droplet size caused by the lower surface tension of the mixed solvent and more rapid solvent evaporation from the droplets in the spray chamber (with indirect nebulizers) or in the flame (with integral nebulizer-burners). In addition, there may be less cooling of the flame by the mixed solvent compared to that which occurs with a wholly aqueous solution, although this effect will depend on whether a lean or a rich flame is employed. With mixed organic solvent/water solutions a more favourable environment may be created in the flame for the formation of atoms of the analyte or concomitant elements.[30] The organic solvent/water mixtures used in this way frequently have a higher viscosity than have aqueous solutions; this lowers the sample uptake rate of the nebulizer. However, provided the percentage of organic solvent in the solution is carefully optimized, the depression of the analytical signal which this would cause can usually be outweighed by the effect of enhanced nebulizer efficiency. In fact the lower sample uptake rate under these conditions may be an advantage when the amount of sample solution available is limited.

The use of water miscible organic solvent mixtures to enhance AAS sensitivities in premixed air-acetylene flames was investigated in an early paper by Allan.[31] Typical enhancement factors in AAS obtained for copper in organic solvent/water mixtures are shown in Table 11-1. Allan concluded that a solution containing 20% acetone + 20% isobutanol was most satisfactory, and demonstrated that the enhancements observed in this mixture were the same for magnesium, zinc, iron, manganese and copper, as would be expected if the phenomenon responsible is improved sample transport to the flame.

TABLE 11-1

Enhancement of copper absorption in a premixed air-acetylene flame by use of water-miscible solvents[a]

Solvent	Relative sensitivity
0·1 M HCl	1·0
Methanol, 40%	1·7
Ethanol, 40%	1·7
Isopropyl alcohol, 40%	1·8
Acetic acid, 10%	1·0
Dioxan, 40%	1·5
Acetone, 40%	2·0
Acetone, 80%	3·5
Acetone, 20% + isobutanol, 20%	2·35

[a] From ref. 31 (J. E. Allan, *Spectrochim. Acta*, 1961, 17, 467).

11.3 ANALYTICAL SENSITIVITY

11.3.1 Atomic Absorption Spectroscopy

The *sensitivity* attainable for the determination of an element by AAS with given instrumentation is defined as the concentration of the element (usually as ppm, μg/ml or mg/l in aqueous solution) which produces a 1% absorption signal (0·0044 absorbance) under optimum experimental conditions. This value is sometimes also referred to as the "percentual concentration limit" or "percentual sensitivity".[32,33] The sensitivity value depends primarily on the absorption path-length and the efficiency of nebulization and atomization in the absorption cell. This sensitivity value defines the slope of a linear calibration graph of absorption against concentration and hence it is frequently useful when a knowledge of the

TABLE 11-2

Sensitivity and detection limit data for different elements by AAS[a]

TABLE 11.2 (*continued*)

Element	Wavelength, nm	Flame[b]	Sensitivity, ppm/1% absorption	Detection[c] limit, ppm
Ag	328·1	A–A	0·06	0·002
Al	309·3	A–N	0·9	0·03
As	193·7	Ar–H	0·25	0·1
Au	242·8	A–A	0·2	0·02
B	249·7	A–N	40	2·5
Ba	553·6	A–N	0·3[d]	0·02
Be	234·9	A–N	0·03	0·001
Bi	223·1	A–A	0·8	0·04
Ca	422·7	A–N	0·05[d]	0·001
Cd	228·8	A–A	0·25	0·001
Ce	520·0	A–N	—	—
Co	240·7	A–A	0·15	0·01
Cr	357·9	A–A	0·1	0·003
Cs	852·1	A–A	0·3	0·05
Cu	324·7	A–A	0·1	0·002
Dy	421·2	A–N	0·8[d]	0·2
Er	400·8	A–N	0·9[d]	0·1
Eu	459·4	A–N	0·6[d]	0·04
Fe	248·3	A–A	0·1	0·01
Ga	287·4	A–N	1·2	0·1
Gd	407·8	A–N	16[d]	4
Ge	265·1	A–N	2·5	1
Hf	286·6	A–N	15	8
Hg	253·7	A–A	10	0·5
Ho	410·4	A–N	1·5[d]	0·1
In	303·9	A–A	0·9	0·05
Ir	264·0	A–N	12	2
K	766·5	A–A	0·02	0·005
La	550·1	A–N	30[d]	2
Li	670·8	A–A	0·03	0·0006
Lu	335·9	A–N	6[d]	3
Mg	285·2	A–A	0·007	0·0001
Mn	279·5	A–A	0·05	0·002
Mo	313·3	A–N	0·6	0·03
Na	589·0	A–A	0·015[d]	0·002
Nb	334·4	A–N	20[d]	1
Nd	463·4	A–N	13[d]	2
Ni	232·0	A–A	0·1	0·01
Os	290·9	A–N	1·0	0·5
Pb	283·3	A–A	0·5	0·02
Pd	247·6	A–A	0·2	0·02
Pr	495·1	A–N	22[d]	10
Pt	265·9	A–A	2·5	0·1
Rb	780·0	A–A	0·05	0·005
Re	346·0	A–N	12	1
Rh	353·5	A–A	0·5	0·03
Ru	349·9	A–A	0·5	0·3
Sb	217·6	A–A	0·6	0·1
Sc	391·2	A–N	0·65[d]	0·1
Se	196·0	Ar–H	0·25	0·1
Si	251·6	A–N	2	0·08
Sm	429·7	A–N	7[d]	2
Sn	224·6	Ar–H	0·6	0·02
Sr	460·7	A–A	0·15[d]	0·01
Ta	274·2	A–N	40	2
Tb	432·6	A–N	8[d]	3
Tc	261·6	A–A	3	—
Te	214·3	A–A	0·5	0·09
Ti	365·3	A–N	2	0·09
Tl	276·8	A–A	0·5	0·03
Tm	371·8	A–N	0·7[d]	0·2
U	358·5	A–N	50	30
V	318·4	A–N	1·5	0·06
W	400·9	A–N	20	3
Y	410·2	A–N	2[d]	0·3
Yb	398·8	A–N	0·2[d]	0·04
Zn	213·9	A–A	0·015	0·002
Zr	360·1	A–N	6	5
S	180·7	A–N	1	5[e]
P	178·3	A–N	5.4	21[f]
I	183·0	A–N	12	25[g]

[a] Perkin-Elmer, Model 403, in "Analytical Methods for Atomic Absorption Spectrophotometry", The Perkin-Elmer Corp., Norwalk, Connecticut, 1971.

[b] A–A = air-acetylene; A–N = acetylene-nitrous oxide; Ar–H = argon-hydrogen-entrained air.

[c] Defined as concentration giving deflection equal to twice the standard deviations of background (baseline) readings.

[d] In presence of excess potassium to suppress ionization.

[e] G. F. Kirkbright and P. J. Wilson, *Anal. Chem.*, 1974, in press.

[f] G. F. Kirkbright and M. Marshall, ibid., 1973, 45, 1610.

[g] G. F. Kirkbright, T. S. West and P. J. Wilson, *Atomic Absorption Newsletter*, 1972, 11, 53.

required analyte concentration range in sample and standard solutions is needed. The attainable 1% absorption sensitivity values for particular elements under optimum experimental conditions remain fairly constant between well-designed instruments of the same type. Some values obtained for different elements by AAS with a typical commercial instrument are shown in Table 11-2. For analytical work a disadvantage of using the 1% absorption sensitivity is that it yields no information concerning the attainable precision or the minimum concentration that may be determined.

Adequate analytical precision may be obtained with modern AAS instruments for many elements at solution concentrations that produce less than 1% absorption. The term *detection limit* is used to define the lowest detectable concentration of the element in the sample solution. This value is often also referred to as the "fluctuational concentration limit" or "fluctuational sensitivity".[32,33] It may be defined as that concentration of the element that produces an absorption signal equivalent to twice (or three times) the standard deviation in the noise fluctuation of the background (zero absorption) signal under the experimental conditions employed. Whether use is made of twice or three times the standard deviation in the background depends on the confidence level required (95 or 99%). Some workers also use a definition of the detection limit based on the analyte concentration required to produce an absorption signal : background noise ratio of 2; at this limit the relative standard deviation in the analysis is 50%.

The detection limit, in contrast to the 1% absorption sensitivity, thus depends on the instrumental stability and may vary considerably from instrument to instrument and from one type of sample matrix and solvent to another. The fluctuation in the signal may result from source, flame or detector noise. The contribution from fluctuation in intensity from the source depends on whether a single-beam or double-beam instrument is employed; appreciable elimination of source noise is obtained with double-beam spectrometers.[34] The source intensity arriving at the detector is subject to disturbance by the necessity to pass it through the absorption cell. When a flame cell is used the entire width of the light beam should be passed through the centre of the flame, to minimize absorption fluctuation caused by slight variations in shape of the secondary reaction zone. However, small fluctuations in flame background absorption in the interconal zone may still occur below 250 nm owing to slight changes in the fuel : oxidant ratio. In addition to this "absorption noise" from the atom cell the detector may receive appreciable emitted radiation at analyte wavelengths above *ca.* 250 nm from the flame background itself or from concomitant elements in the blank solution. As described elsewhere (Section 11.1.1) this gives rise to noise at the detector even when an a.c. source and detection system are employed. Provided that the radiation flux falling on the photomultiplier detector is sufficiently large, the detector noise may make a relatively small contribution to the overall background fluctuation level in AAS.

The detection limit defined above represents the relative value in concentration units and gives no indication of the response time of the instrument or the amount of sample solution required for a measurement. The background fluctuational level may be reduced by the use of a longer time constant (RC filtering) or by integration. As this increases the time for which the sample must be nebulized into the flame, however, no gain in absolute detection limit (weight of sample) is achieved. This absolute value depends on the relative detection limit and the minimum volume of sample required for the measurement. Typical relative detection limits obtained for different elements with a commercial double-beam AAS instrument are shown in Table 11-2.

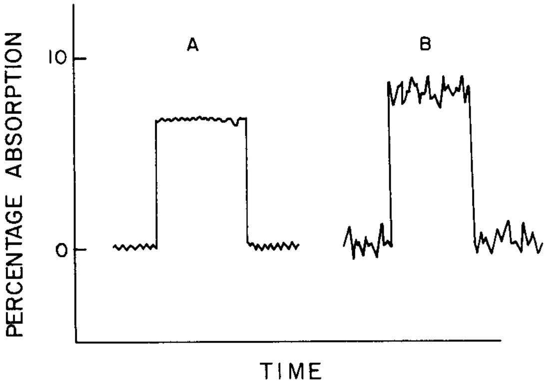

Fig. 11-5. Illustration of differing detection limits obtained for two elements A and B which exhibit similar 1% absorption sensitivities.

Two elements A and B may sometimes show similar absorption sensitivities but quite different detection limits owing to differences in the magnitude of background noise from the source, flame or detector for each element. This is illustrated in Fig. 11-5; the detection limit for element A is considerably superior to that for element B although the 1% absorption sensitivity value for element B is slightly greater than that for element A. Thus, comparisons between different elements and different instruments may sometimes be confusing and a further factor is needed to convey an estimate of the attainable precision in the absorbance range used for calibration curves (e.g. 0·1 to 0·5 absorbance).

Smith and Feldman[35] have proposed the term "*performance index*" which is defined as the aqueous concentration and relative standard deviation which yields 0·44 absorbance measured at, or normalized to, a spectral noise bandwidth of 0·25 Hz (equivalent to a 1-second time constant). In many respects this term is of more use to the analyst than the 1% absorption sensitivity or detection limit defined above. The value of 0·44 absorbance is close to that for least photometric error (0·43 absorbance) demonstrated by Ringbom,[36] while at the same time the 1% absorption sensitivity is easily obtained by dividing the concentration term in the performance index by 100 (provided that a linear relationship exists between absorbance and concentration). The detection limit may also be estimated from the relative standard deviation term in the index. Some typical values for performance index obtained with commercial instrumentation are shown in Table 11-3.[35,37]

TABLE 11-3

Values of performance index in AAS (from refs. 35 and 37)

	Performance index	
Element	% RSD	Concentration for 0·44 absorbance, ppm
Ca	0·2	6·0
Cr	0·3	5·0
Cu	0·3	2·0
Pb	0·5	10
Mg	0·44	0·8
Pt	0·30	40

11.3.2 Atomic Fluorescence Spectroscopy

The "sensitivity" of a procedure for the determination of an element by AFS is usually defined only by the relative *detection limit*, i.e. the concentration of the element in solution which produces a fluorescence signal equivalent to twice (or three times) the standard deviation in the background noise. Some workers also use a detection limit based on the concentration required to produce a signal equal to twice the maximum (peak-to-peak) noise level of the background. In AFS it is the background and noise from the atom cell and detector which principally limit the attainable detection limits. In contrast to AAS, near the detection limit in AFS the source may make a relatively minor contribution to the noise. For small signal intensities the noise level in the re-emitted fluorescence radiation (which originated from the source) is small compared to the flame flicker noise and noise at the detector due to the overall level of the flame background and shot-noise. In early fluorescence studies with intense unmodulated sources and dc amplifiers, low

TABLE 11-4

AFS detection limits for elements in flames

Element	Wavelength, nm	Flame*	Source†	Detection limit, ppm‡	Reference (see below)
Ag	328·1	Air/H_2	EDT	0·0001	*a*
Al	396·1	Argon sep. N_2O/C_2H_2	EDT	0·1	*b*
As		Ar—H_2—air	EDT	0·2	*c*
Au	267·6	Air/H_2	EDT	0·2	*a*
	242·8	O_2—H_2—Ar	H—HCl	0·005	*d*
Be	234·8	Sep. N_2O/C_2H_2	EDT	0·01	*e*
Bi	302·6	Ar—H_2—air	Iodine EDT	0·05	*f*
	306·8	N_2 sep. air/C_2H_2	EDT	0·04	*g*
Ca	422·7	Air/H_2	EDT	0·02	*a*
		H_2—air	450 W Xe	0·02	*h*
Cd	228·8	Air/H_2	EDT	0·000001	*a*
Co	240·7	Air/C_3H_8	EDT	0·005	*i*
Cr	357·9	Air/H_2	Demountable cooled HCL	1·0	*j*
Cu	324·7	Air/H_2	H—HCL	0·001	*k*
	327·4	Air/H_2	Hot HCL	0·001	*l*
Fe	248·3	Air/C_2H_2	EDT	0·009	*m*
		Ar/O_2/H_2	H—HCL	0·02	*n*
Ga	403·3 417·2	Air/H_2	H—HCl	0·5	*o*
Ge	265·1	Ar sep. N_2O/C_2H_2	EDT	0·1	*p*
Hg	253·7	O_2/H_2 org. solv	Hg pen light	0·002	*q*
In	410·5 451·1	Air/H_2	H—HCl	0·2	*o*
Mg	285·2	Air/propane	H—HCl	0·001	*r*
Mn	279·5	Air/C_2H_2	EDT	0·001	*s*
Mo	313·3	Ar. sep. N_2O/C_2H_2	EDT	0·46	*b*
Ni	232·0	Ar/O_2/H_2	H—HCl	0·003	*n*
		Air/H_2	H—HCl	0·003	*k*

TABLE 11-4 (*continued*)

Element	Wavelength, nm	Flame*	Source†	Detection limit, ppm‡	Reference (see below)
Pb	405·8	$Ar/O_2/H_2$	EDT	0·01	*t*
		Air/H_2	H—HCl	0·02	*o*
Pd	340·4	Air/H_2	H—HCL	2·0	*o*
Pt	265·9	Air/H_2	H—HCL	50	*o*
Sb	231·1	Air/C_3H_8	EDT	0·05	*u*
Se	196·0	Air/C_3H_8	EDT	0·25	*v*
Si	251·6	Ar sep. N_2O/C_2H_2	EDT	0·55	*w*
Sn	303·4	N_2 sep. $Ar/O_2/H_2$	EDT	0·1	*x*
Sr	460·7	Ar/H_2—air	EDT	0·03	*a*
Te	238·3 238·6	Air/C_3H_8	EDT	0·12	*v*
Tl	377·6	Ar/H_2—air	EDT	0·008	*a*
V	318·4	Ar sep. N_2O/C_2H_2	EDT	0·07	*b*
Zn	213·9	Air/H_2	EDT	0·00004	*a*

* Ar sep. N_2O/C_2H_2 = argon separated premixed nitrous oxide-acetylene flame; N_2 sep. air/C_2H_2 = nitrogen separated premixed air-acetylene flame.

† H—HCL = high intensity hollow-cathode lamp; EDT = electrodeless discharge tube; 450 W Xe = 450 watt xenon arc source.

‡ Detection limit usually defined as concentration resulting in S/N = 2:1.

[a] R. E. Zacha, M. P. Bratzel and J. D. Winefordner, *Anal. Chem.*, 1968, 40, 1733.

[b] R. M. Dagnall, G. F. Kirkbright, T. S. West and R. Wood, *Anal. Chem.*, 1970, 42, 1029.

[c] R. M. Dagnall, K. C. Thompson and T. S. West, *Talanta*, 1968, 15, 677.

[d] J. Matousek and V. Sychra, *Proc. Intern. Conf. AAS, Sheffield,* 1969.

[e] D. N. Hingle, G. F. Kirkbright and T. S. West, *Analyst,* 1968, 93, 522.

[f] R. M. Dagnall, K. C. Thompson and T. S. West, *Talanta,* 1967, 4, 1467.

[g] R. S. Hobbs, G. F. Kirkbright and T. S. West, *Talanta,* 1971, 18, 859.

[h] D. R. Demers and D. W. Ellis, *Anal. Chem.*, 1968, 40, 860.

[i] B. Fleet, K. V. Liberty and T. S. West, *Anal. Chim. Acta,* 1969, 45, 205.

[j] G. Rossi and N. Omenetto, *Talanta,* 1969, 16, 263.

[k] D. C. Manning and P. Heneage, *Atomic Absorption Newsletter,* 1967, 6, 124.

[l] J. I. Dinnin, *Anal. Chem.*, 1967, 39, 1491.

[m] L. Ebdon, G. F. Kirkbright and T. S. West, *Anal. Chim. Acta,* 1969, 47, 563.

[n] J. Matousek and V. Sychra, *Anal. Chem.*, 1969, 41, 518.

[o] D. C. Manning and P. Heneage, *Atomic Absorption Newsletter,* 1968, 7, 80.

[p] G. F. Kirkbright, R. M. Dagnall, T. S. West and R. Wood, *Analyst,* 1970, 95, 425.

[q] T. J. Vickers and S. P. Merrick, *Talanta,* 1968, 15, 873.

[r] T. S. West and X. K. Williams, *Anal. Chim. Acta,* 1968, 42, 29.

[s] L. Ebdon, G. F. Kirkbright and T. S. West, *Talanta,* 1970, 17, 965.

[t] R. F. Browner, R. M. Dagnall and T. S. West, *Anal. Chim. Acta,* 1970, 50, 375.

[u] R. M. Dagnall, K. C. Thompson and T. S. West, *Talanta,* 1967, 14, 1151.

[v] R. M. Dagnall, K. C. Thompson and T. S. West, *Talanta,* 1967, 14, 557.

[w] R. M. Dagnall, G. F. Kirkbright, T. S. West and R. Wood, *Anal. Chim. Acta*, 1969, 47, 407.

[x] R. F. Browner, R. M. Dagnall and T. S. West, *Anal. Chim. Acta*, 1969, 46, 207.

background hydrogen flames or inert gas separated flames were used almost exclusively to permit good detection limits to be obtained. Even with the use of a modulated source and tuned amplifier, however, the use of such low background flames results in less unwanted radiation at the detector and hence a better signal : noise ratio.

TABLE 11-5

Detection limits obtained with a six-channel atomic fluorescence spectrometer[38]

Element		Wavelength, nm	Detection limit, ppm		Linear range, ppm
Aluminium	Al	396·2	0·07	(N_2O)	0–50
Antimony	Sb	231·1	0·05		0–45
Arsenic	As	197·2	0·07	(EDL)	0–50
Barium	Ba	553·5	0·2		0–40
Cadmium	Cd	228·8	0·002		0–8
Calcium	Ca	422·7	0·0003		0–30
Chromium	Cr	357·9	0·001		0–27
Cobalt	Co	240·7	0·002		0–25
Copper	Cu	324·8	0·0006		0–9
Gold	Au	242·8	0·009		0–10
Iron	Fe	248·3	0·002		0–19
Lead	Pb	405·8	0·01	(EDL)	0–160
Magnesium	Mg	285·2	0·0001		0–8
Manganese	Mn	279·5	0·0005		0–8
Mercury	Hg	253·7	0·4	(EDL)	0–50
Molybdenum	Mo	313·3	0·06		0–30
Nickel	Ni	232·0	0·003		0–21
Silver	Ag	328·1	0·002		0–9
Strontium	Sr	460·7	0·0008		0–14
Tin	Sn	224·6	0·2		0–50
Vanadium	V	318·5	0·25	(N_2O)	0–40
Zinc	Zn	213·9	0·001		0–6

1. All data obtained in simultaneous multielement mode of operation basis with aqueous solutions using a slightly fuel-rich air-C_2H_2 flame and pulsed hollow cathode light sources unless otherwise noted. (N_2O = nitrous oxide flame; EDL = electrodeless discharge lamp.)
2. Detection limits are defined as the concentration in solution of an element which can be detected with 95% certainty. This is that quantity of the element that gives a reading equal to twice the standard deviation of a series of at least ten determinations at or near blank level.

Table 11-4 gives some AFS detection limits taken from the literature. Whilst these values all apply to flame cells, a variety of instrumentation has been used by different workers to obtain these detection limits and various authors do not necessarily present their values according to the definition of detection limits given above. Table 11-4 also gives brief details of the source and flame type used to obtain each detection limit. In addition, developments in AFS instrumentation may render these values rapidly obsolete; they are recorded here in order to demonstrate the range and flexibility of the technique. Detection limit data for AFS with non-flame cells are given in Chapter 7. Table 11-5 shows the values of detection limit obtained for various elements when a commercial six-channel atomic fluorescence spectrometer is used.[38]

11.4 INSTRUMENT OPERATION

11.4.1 Operating Procedures

General instructions for the setting up of AAS instruments, and AFS accessories that may be used with these instruments, are invariably provided by the manufacturers. These instructions include advice on the positioning of the instrument in the laboratory to avoid draughts and bright sunlight. The use of an exhaust chimney is recommended for the removal of the burnt gases which frequently contain toxic materials from the samples nebulized when flame cells are employed.

Manufacturers' recommendations concerning the details and sequence of operations to be performed in an experimental method by AAS or AFS may vary but the following outline procedure is normally performed.

(a) The source and detector power is switched on, and the source power is set to the manufacturers' recommended value (or to an experimentally predetermined optimum value). With modern hollow-cathode lamps and photomultiplier-amplifier systems very little warm-up time is required. When electrodeless discharge lamps are used as sources in AFS some additional attention to the tuning of the lamp and microwave cavity assembly to give minimum reflected power may be necessary. Moreover, the time taken to achieve intense and stable emission may vary from element to element.

(b) The source position and optical system are adjusted so that the source radiation (in AAS) or fluorescence radiation (in AFS) is incident upon the monochromator slit;* the analytical line and spectral slit-width to be employed are then selected at the monochromator.

(c) The flame is ignited and the fuel : oxidant flow rate ratio adjusted to the recommended settings. The position of the incident light beam in the flame is usually optimized by variation of the height and horizontal position of the burner relative to the light beam. Information concerning the correct procedures for igniting and extinguishing the flame is invariably provided in the instruction manual with commercial instrumentation.

(d) The burner is allowed to warm up while solvent is nebulized. During this period the burner head, burner connections and the walls of the spray chamber reach their equilibrium temperatures. This procedure is more important with indirect nebulizers than with total consumption nebulizer-burner units.

(e) The detector response is set via adjustment of the amplifier gain or photomultiplier operating voltage. In AAS the response is adjusted to obtain a reading of 100% transmission (zero absorbance) at the meter or recorder. The zero transmission (infinite absorbance) setting is checked by obstructing the light path between the source and detector with a shutter. In AFS the sensitivity is set to an established optimum setting for the sample concentration range anticipated, and any small contribution from stray or scattered light is "backed-off" electrically so that the meter or recorder reads zero deflection.

(f) Pure solvent is nebulized into the flame and the 100% and 0% transmission settings (in AAS) and zero deflection setting (in AFS) are re-checked and adjusted if necessary. The instrument may then be used for analytical absorption or fluorescence measurements.

(g) The blank, sample and standard solutions are nebulized into the flame sequentially and the absorbance or fluorescence intensity reading is noted for each. Each solution should be aspirated for sufficient time to enable the analytical signal to reach a steady value that can be measured with confidence. The time required depends on the characteristics of the nebulizer-burner assembly and on the response time setting at the detector; it would normally be *ca.* 10-20 times the effective time constant of the system (see Section 11.2.4).

(h) The nebulizer and burner assembly may be washed by aspiration of pure solvent between each sample solution measured. This is particularly important when liquid samples of high dissolved solid content are dealt with in order to minimize clogging of the burner head or nebulizer capillary. The concentration of the element determined in the sample solution is most frequently found by relating its absorbance or fluorescence intensity to the absorption or fluorescence signals produced under the same experimental conditions by solutions of known concentration. These latter values may

---

* This is readily carried out in AFS by temporarily placing a small mirror on the burner so as to deflect the source radiation through 90°.

be plotted as a "calibration graph" (or curve) of analytical signal against concentration of the element in the standard solution; the sample solution concentration is then established from this graph. Alternatively, with direct concentration read-out facilities, the meter or recorder of the detector is calibrated directly in concentration units while the solutions of known concentration are aspirated.

11.4.2 Calibration Graphs

There has been some work directed towards the possibility of absolute analysis by AAS, without the need for empirical calibration; this is discussed briefly in Sections 3.5.3 and 11.4.3. At the present time, however, absolute analysis by AAS or AFS is possible only with experimental difficulty and under very restricted analytical circumstances. In practice, when either technique is used for routine analysis, a calibration curve of the signal strength against solution concentration is employed.

As mentioned above (11.4.1) the 100% transmission in AAS, or the zero fluorescence signal in AFS, is usually set while nebulizing pure solvent or a blank solution whose composition with respect to the concomitant species matches that of the samples. If the calibration graph is known to be linear over the desired concentration range, one standard solution should ideally be sufficient to enable the calibration graph to be constructed. It is usually preferable, however, to employ several standard solutions of different concentrations in order to obtain good precision. Even when the calibration graph is known to be non-linear the use of sufficient standard solutions to construct the graph may still permit quite accurate analysis.

Under conditions for least photometric error in AAS, i.e. measurement between 0·2 and 0·7 absorbance unit, the calibration curve might typically cover a 20- to 200-fold increase in concentration above the detection limit. This often results in some inconvenience, as this range above the detection limit may correspond to the use of solutions of relatively high dissolved matrix element content which may cause nebulization or atomization difficulties. Thus, calibration curves in AAS are normally constructed for use between somewhat lower absorbance values, e.g. 0·02 to 0·5. Apart from such considerations of the photometric accuracy, the accuracy of determinations when curved calibration graphs are employed is affected by the actual shape of the curve. The rate of change of analytical signal strength with concentration governs the reliability with which the concentrations of samples producing similar absorbance values may be differentiated. The slope of the curve may vary considerably over the concentration range of interest; depending on the shape of the graph (bending away from or towards the concentration axis) the certainty with which it is possible to distinguish between samples producing high absorbances may be good or poor compared to the situation at low absorbance values. Some modern instruments used in AAS provide for correction of read-out so that absorbance values observed appear to follow a linear calibration even though the actual uncorrected calibration data are non-linear.

Frequent checks of the calibration are recommended during operation in both AAS and AFS. Standard solutions should be nebulized with each set of sample solutions to ensure that inaccurate analyses cannot result from factors such as wavelength drift, change in fuel : oxidant flow rate ratio or variable nebulizer performance.

(*a*) *AAS calibration graphs*

The dependence of the analytical absorption signal on analyte concentration has already been discussed in Section 3.3. When absorbance is measured by using a sharp-line source, i.e. in the case of the majority of practical AAS analyses, the calibration graph of absorbance against concentration should be linear over a wide range of concentration. The source line is never ideally sharp, however, and this results in a curvature of the graph towards the concentration axis; the greater the line-width the greater is the curvature and the lower the concentration at which it becomes significant. When a continuum source is employed there is no simple relationship between absorbance and concentration and the percentage absorption must be measured. As in this case the percentage absorption is directly proportional to concentration at low concentrations, and to the square root of the concentration at higher values, it is best to plot the calibration graph as log $(\Delta I/I_0)$ *vs* log (concentration); the graph has a slope of 1 at low values and of $\frac{1}{2}$ at high values. Any tendency for the slope to decrease further at very high concentrations may be reduced by increasing the bandpass of the monochromator.

The above deviations from linearity predictable from the theoretical basis of the techniques are frequently accompanied by other deviations which may be described as interference effects. As these vary with the nature of the sample rather than the instrumentation they may often prove more troublesome. These types of interference will be discussed in detail in Chapter 12, but the principal effects may be repeated in summary. When a non-absorbing spectral line is emitted by the source at a wavelength close to that of the absorption line, a reduction in sensitivity will be observed if this line is transmitted by the monochromator. The effect will progressively become more serious as the absorbance at the analytical line increases; the calibration graph bends *towards* the concentration axis. When an atom is easily ionized, the number of atoms present in the absorption cell at low sample concentrations will be seriously depleted by the formation of ions; the percentage ionization decreases with increasing concentration of atoms in the cell; the calibration graph bends *away* from the concentration axis.

(*b*) *AFS calibration graphs*

As shown in Section 4.4 the theoretical dependence of atomic fluorescence signal strength on the analyte concentration is more complex than that in AAS; fortunately the usual applications of AFS for analytical work allow a fairly simple approach from the practical viewpoint. This is based on the assumption that AFS is most frequently applicable for the measurement of low analyte concentrations in the atom cell, or that the amount of absorption occurring in the atom cell is small. The graph of concentration against fluorescence signal is then linear for both continuum and sharp-line sources. When determinations are attempted at high concentrations (the exact value depends on the element concerned) the calibration graph bends towards the concentration axis. This is partly explained by the theoretical predictions given in Section 4.4 and partly by the increasingly serious re-absorption of the resonance fluorescence signals as the atom population in the cell increases. In addition to these deviations from linearity the same type of deviation due to ionization effects will cause concavity of the calibration graphs in AFS as in AAS.

11.4.3 Other Calibration Methods

Although most routine analytical determinations by AAS and AFS are carried out with calibration graphs as described above, a number of other simple techniques are available. These methods sometimes show advantages over the conventional calibration procedure for certain analyses and the most useful ones are described below.

(*a*) *Standard additions method*

This method may be applied within the range of concentrations corresponding to linear calibration graphs. The signal is measured for the sample alone and for the sample plus aliquots of a solution of the analyte element of known concentration. The main advantage of the method in AAS and AFS is that, in effect, exact matching of the sample and "standard" solutions (sample to which known amounts of analyte element are added) is achieved automatically. This is most useful in the analysis of samples where complex matrix element effects are observed on the analytical signal. An analysis may be carried out by this method by making only two measurements, i.e. for the sample alone and for the sample plus one aliquot of standard analyte solution, but three or four measurements (sample plus one, two and three aliquots of standard analyte solution) usually result in greater accuracy. The absorbances measured for these solutions should be small in order to ensure as far as possible that the assumption of a linear relationship between absorbance and concentration is valid. The standard additions method gives incorrect results in AAS and AFS when molecular band absorption or scattering from particulate material in the flame is encountered. When this method is employed, therefore, the use of a continuum source background corrector (in AAS) or non-absorbed line (AAS or AFS) to check for this potential source of error is recommended.

(*b*) *Dilution method*

This method is an adaptation of the standard additions method that may be used in preference under certain circumstances. A measurement of the analytical signal S_1, from a volume V_1 of a solution containing a known concentration C_1 of the analyte element is made. A volume V_2 of the unknown sample, containing a concentration C_2 of analyte, is then added and a second signal, S_2, is then recorded. The unknown concentration, C_2, is then given by:

$$C_2 = C_1 \frac{S_2(V_1 + V_2)(V_2 - S_1 V_1/V_2)}{S_1}$$

Provided that sufficient accuracy is obtained with only two measurements the method is rapid and easily applied. Smaller volumes of sample solution may be used than with the addition method as it is not necessary to record a signal for the sample solution alone. Also, with concentrated sample solutions, or at least analyte solutions that produce a large analytical signal, it is not necessary to perform an additional operation to obtain sufficient dilution to reach the linear part of the calibration. This method is subject to similar errors to the standard additions method when molecular band absorption or scattered radiation is present.

(*c*) *Absolute analysis by AAS*

A technique that would allow absolute analyses by AAS would offer several advantages over the conventional methods utilizing calibration against standards. The feasibility of absolute AAS methods has been discussed by Rann,[39] de Galan[40] and de Galan and Samaey[41] and is also dealt with briefly in Section 3.5.3 of this volume. Several reports of the measurement of free atom fraction and oscillator strengths by AAS have also been made, and these measurements involve experimental difficulties similar to those of absolute analysis.[42-45] There are two principal problems associated with absolute analysis by AAS. Firstly, it is necessary that an exact theoretical expression be used to relate the experimental absorption measurements to the number of absorbing atoms. Secondly, it is necessary to calibrate experimentally the apparatus employed, both in order to evaluate all of the parameters that must be substituted into the basic equation, and to relate the number of absorbing atoms to the actual concentration of the analyte sample. Although each of these presents difficulties, the most serious from the viewpoint of the analytical chemist is the requirement of an accurate expression over a sufficiently wide range of experimental conditions, and the selection of an absorption cell in which the number of absorbing atoms can be readily related to the sample concentration. The simplest expression is that for the integrated absorption coefficient given in Section 3.2.2. As explained, however, it is difficult to use this to establish a routine analytical technique A more convenient measurement would be that of the peak absorbance obtained with the sharpest possible source line under conditions of low optical density. Even under these limited circumstances, however, the measurement cannot be applied with equal success to all elements; the absorption line used may have a hyperfine structure which is sufficiently wide or well-separated in the source and/or atom cell to cause a serious error in the measurement of the absorbance. The problem has been considered in some detail by L'Vov;[46] he suggested that measurement in a high-pressure cell might offer one solution. Under these conditions the Lorentzian broadening would result in a much wider absorption line than that obtained with other absorption cells at atmospheric pressure. The hyperfine structure would then have an insignificant effect on the absorbance measurement for a much wider range of elements and the errors due to use of a broadened source line would also be reduced.

The ease with which the number of absorbing atoms may be related to the actual sample concentration also varies with the type of absorption cell used and the analyte element. It is often possible to measure fairly accurately the proportion of the sample that actually reaches a region of the absorption cell where the analyte atoms can give rise to a signal, although the experimental technique may prove more simple for a L'Vov furnace, for example, than for a conventional premixed flame and pneumatic nebulizer. The measurement of the fraction of the sample that actually forms atoms after reaching the region in which absorption can occur, however, is more difficult. The most promising solution might be the use of an atom cell in which the free atom fraction is unity for the element concerned. With the atom cells currently available, particularly high-temperature flames, this would mean that a useful range of elements would be amenable to absolute analysis. However, after those elements have been omitted for which the lack of a suitable sharp-line source or the effect of hyperfine structure cause additional problems the range of elements becomes much smaller. Also, the combined effects of inaccuracies in the various calibrations required and deviations from the theoretical assumptions which must be made are likely to severely restrict the attainable accuracy of the results.

11.4.4 Internal Standardization in AAS

The use of an internal standard to reduce errors in flame emission spectroscopy is well established. The procedure usually adopted is to add to each of the sample and standard solutions a known amount of an internal standard element and to monitor its line emission intensity and that of the analyte element for each solution. The measurement of the two signals may be accomplished simultaneously (with a two-channel spectrometer) or sequentially (with a single-channel spectrometer). The ratio of the signal intensities is then used as a measure of the analyte concentration rather than the analyte emission intensity alone. Provided that certain criteria concerning the suitability of the element used as internal standard are fulfilled, this technique may compensate for errors otherwise incurred via changes which can occur in the rate at which sample is supplied to the flame and in flame conditions. These include change in sample viscosity and surface tension, nebulizer performance, variation of fuel : oxidant concentration ratio or change in flame geometry due to disturbance by draughts etc. It is usual in flame emission spectroscopy to select the internal standard element so that its emission wavelength, intensity and dependence of degree of atomization on flame temperature, stoicheiometry and height of observation are similar to that of the analyte element.

In AAS the use of internal standardization permits similar compensation for errors caused by variation in the nebulizer and flame characteristics. As it is preferable to measure absorption signals for both sample and internal standard simultaneously, however, a two-channel spectrometer must be employed. With this type of instrument Feldman *et al.*[47,48] have studied the use of the technique in AAS. These workers have shown that, as in flame emission work, it is necessary to use an internal standard element whose atomization process in the flame cell employed is subject to disturbances by change in nebulizer and flame characteristics in a similar manner to that of the analyte element.[49] A good example is found in the examination of the relative suitability of copper and strontium as internal standard elements in the determination of calcium by AAS. The absorbance for copper is little affected by changes in the fuel : oxidant concentration ratio supplied to the flame; the critical dependence of the absorbance for strontium on the fuel : oxidant ratio, however, is similar to that observed for the analyte element (calcium). As shown in Fig. 11-6 the analytical signal in the calcium determination may be corrected for error produced by small random changes in the fuel : oxidant ratio by using strontium as internal standard and utilizing the Ca/Sr absorbance ratio; the use of copper as internal standard results in insignificant correction. Feldman has demonstrated the advantages of the technique in practical analyses by AAS. It is claimed that approximately a two-fold improvement in precision may be obtained by using internal standardization in the determination of aluminium in cement, copper in aluminium alloy and nickel in stainless steel.[50]

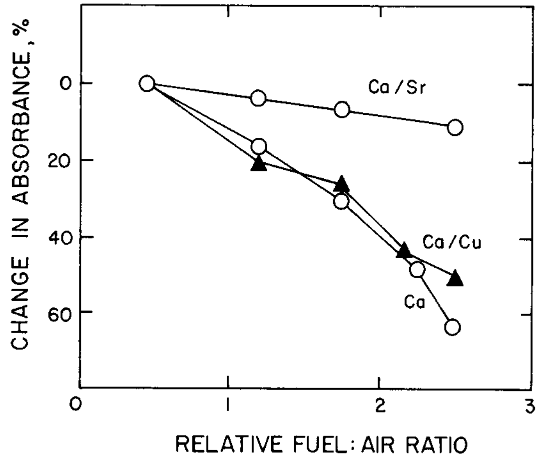

Fig. 11-6. Effect of strontium internal standard correction of effect of fuel : air rate on calcium absorbance. Use of copper internal standard does not result in appreciable correction (adapted from ref. 37).

11.4.5 Scale Expansion and Zero Suppression in AAS

For AAS work with samples that produce low absorbance readings the scale expansion technique may be employed to allow the values to be read more accurately. An auxiliary source of potential is simply used to adjust the low end of the absorbance scale (e.g. 80 to 100% on the transmission scale) to cover the full scale at the meter or recorder read-out (zero to full-scale deflection). As the scale expansion is obviously applied to both the analytical signal and the noise it is necessary to have a favourable signal : noise ratio in order to benefit fully from this technique. David[51] first modified the single-beam atomic absorption instrument of Box and Walsh in this manner to provide up to five-fold scale expansion. With double-beam instrumentation for AAS, where appreciable compensation for source noise is accomplished, larger scale expansion factors may be realized. It is frequently sufficient, when working with low absorption values and scale expansion, to plot percentage absorption (rather than absorbance) directly against concentration; only slight deviation from linearity occurs. The ability to utilize greater sample dilution if scale expansion is employed may assist in the reduction of interference effects. This effect has been demonstrated by Belcher and Brooks[52] in the determination of strontium in coal ash.

In addition to its use in recording low absorption values, the technique of scale expansion may be employed in conjunction with zero suppression in order to increase the precision obtained in the measurement of high absorption values.[53,54] The high portion of the transmission range (low absorption) is suppressed by zero adjustment and the scale is expanded so that only a small intermediate part of the percentage absorption scale is presented across the entire scale of the meter or recorder. The sample solution, and standard solutions whose percentage absorption values closely bracket that of the sample, are then nebulized into the flame.[54] In a similar manner to simple scale expansion for low absorption values, it is again usually sufficient over the small range of absorption measured to then establish the concentration of the unknown sample by plotting percentage absorption (rather than absorbance) against concentration. Results with precision as good as 0·2% have been claimed for this technique in the determination of unknown samples. Figure 11-7 shows a typical example, where the range is expanded for two solutions of similar high concentration to permit precise measurements to be made.

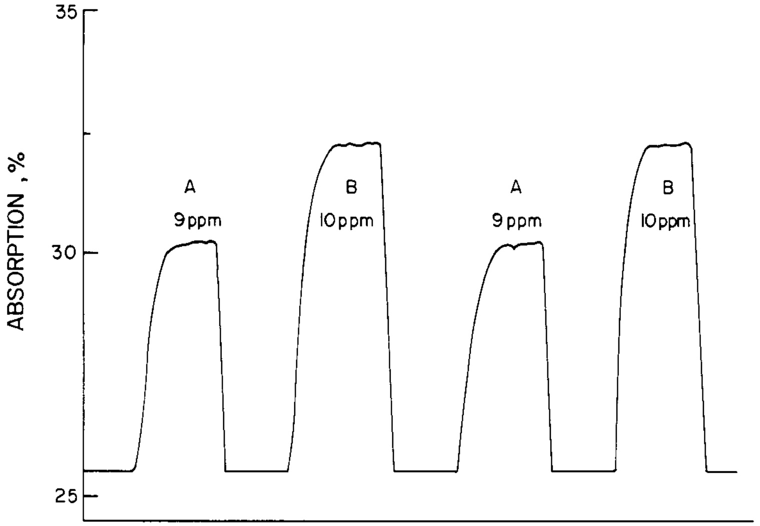

Fig. 11-7. Illustration of effect of scale expansion used with suppression of zero to permit precise determinations with solutions of similar high concentration.

11.5 PRECISION AND ACCURACY

Two types of error are recognized in any quantitative measurement. The first type is determinate or systematic error, which is attributable to a definite cause, even though the cause may not be known. Such errors are uni-directional. The magnitude may be constant from sample to sample, proportional to the size of the sample, or may vary in a complex fashion. Examples of this type of error in AAS or AFS are found in the chemical and physical interference effects on the analytical signal from concomitant elements present in samples.

The second type of error is indeterminate or *random* error brought about by the effects of uncontrolled variables. Real random errors are equally likely to cause high or low results; their existence thus causes a scatter of the results about the true value (in the absence of systematic error).

A measure of the random error is given by the *precision* of a measurement; this refers to the reproducibility obtained if the same measurement is made repeatedly. The *accuracy* of a measurement is determined by the systematic error (the deviation of the measurement from the "correct" value). Thus it is possible to carry out a precise analysis by AAS or AFS without obtaining an accurate result, but it is rare that an accurate analysis is obtained with an imprecise measurement.

11.5.1 Precision

The truly random error which is associated with a measurement is characterized by a "normal distribution" in which there is a symmetric distribution of the deviations from the true result. This situation is shown in Fig. 11.8; in the absence of systematic error the true value, A, occurs most frequently. A valid and useful estimate of the *precision* of a series of measurements is the *standard deviation*, s, of the usually small number of practical measurements (the sample),* where

$$s = \left(\frac{1}{n-1}\sum (x_i - \bar{x})^2\right)^{1/2} \qquad (11\text{-}1)$$

in which x_i is the result obtained from one measurement and $\bar{x}$ is the mean of n measurements. The summation term in this expression is inconvenient for calculating machines; if $\bar{x}$ is not known, rapid machine calculation can be achieved by using the relationship

$$\sum (x_i - \bar{x})^2 = \sum x_i^2 - \frac{1}{n}\left(\sum x_i\right)^2 \qquad (11\text{-}2)$$

If $\bar{x}$ is known a still more convenient expression for calculation is

$$\sum (x_i - \bar{x})^2 = \sum x_i^2 - n(\bar{x})^2 \qquad (11\text{-}3)$$

---

* The term *sample* refers to the small number of measurements which form part of the *population*. The term *population* refers to an infinitely large number of analytical measurements obtained from operations involving the same material. The standard deviation of a *sample*, s, is calculated using $(n - 1)$ results. The standard deviation of a population is symbolized as σ and is calculated using n results. The standard deviation of a sample is an estimate of σ.

The value of the standard deviation calculated from equation (11-3) is expressed in the same dimensions or units as the data being evaluated. It may also be expressed as the relative standard deviation, RSD, (or coefficient of variation) where

$$\mathrm{RSD} = \frac{S}{\bar{x}} \times 100 \qquad (11\text{-}4)$$

As shown in Fig. 11-8, when only random error is considered a normal distribution curve may be drawn in which the relative frequency of occurrence of a measurement, x_i, or its error, $(x_i - A)$, is plotted against multiples of the standard deviation employed. Because of the symmetrical nature of the curve there is a negative error for every positive error of the same value. The relative frequency of measurements having a small error is very great. It is found that greater than 68% of all measurements lie within the range $A \pm \sigma$, while greater than 95% and 99% of all measurements lie within the ranges $A \pm 2\sigma$ and $A \pm 3\sigma$ respectively.

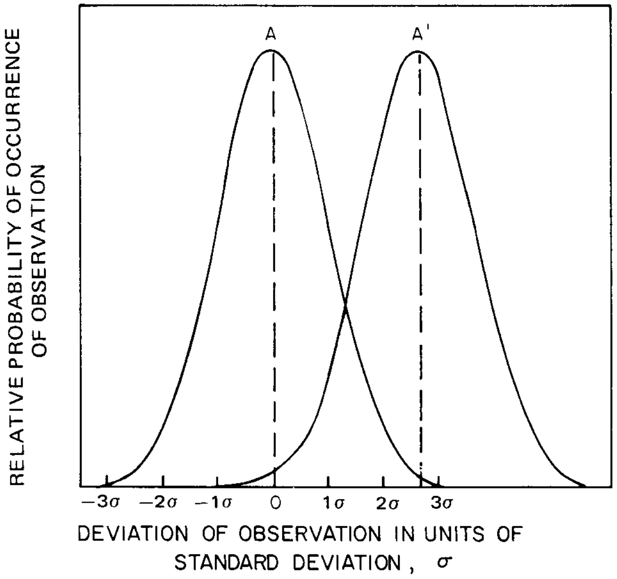

Fig. 11-8. Normal distribution curve for random error (true value A); effect of systematic error to shift curve to apparent true value A′.

In order to obtain a reliable estimate of the reproducibility of a particular determination, via calculation of the standard deviation, as many results as possible (usually more than 10) should be obtained. The overall attainable precision for a complete analytical procedure in AAS or AFS including sampling, sample pretreatment and measurement, is invariably different from that of the measurement step alone. For the purposes of the complete specification of an analytical method the overall standard deviation should be found by taking samples through the whole procedure. The standard deviation in the measurement step alone, obtained by repetitive measurements on a single prepared sample, gives an indication of the instrumental performance. An estimate of the detection limit is frequently obtained in this way, for example, by measurement of the concentration of the analyte which produces a relative standard deviation of 50%.

11.5.2 Photometric Error in Absorbance Measurement

In the technique of molecular absorption spectrophotometry in solution it is common practice to attempt to make analytical measurements between limiting absorbance values to minimize measurement error with non-linear absorbance scales. Ringbom[36] demonstrated that, when the instrumental noise in the system is constant, the variation in relative error in measurement of absorbance $\Delta A/A$ (or concentration $\Delta C/C$) with the absorbance value may be shown by differentiation of the absorbance expression to follow the curve shown in Fig. 11-9. The value of $\Delta A/A$ can thus be seen to be minimized at absorbance values between *ca.* 0·2 and 0·7 while the actual minimum on the curve occurs at about 40% transmission, i.e. $A =$ *ca.* 0·4.

In AAS, however, these limiting values for absorbance measurement are seldom adopted. High absorbance values may frequently be obtained only when the matrix element concentration in solutions of the analyte is too great to allow trouble-free routine nebulization; in addition, analytical curves in AAS are often non-linear at high absorbance values. At the low absorbance end of the scale, absorbance values considerably less than 0·2 are routinely measurable with good precision with modern instrumentation using scale expansion, signal integration or a long response time (damping). As mentioned elsewhere (Section 11.4.2), therefore, AAS calibration graphs are frequently constructed for use between *ca.* 0·02 and 0·5 absorbance unit.

With many AAS instruments the reading scale may be linear in absorbance values. In these instruments the photomultiplier output is transformed logarithmically before amplification. The photometric error then becomes more difficult to analyse because that part of the error due to the detector is proportional to the radiant power of the transmitted beam, whereas the errors in the amplification and recorder are proportional to the logarithm of the transmitted radiant power. When the linearity of the detector is good compared to that of the amplifier and recorder, the overall error will be a nearly constant fraction of an absorbance unit. The relative error is then constant across the scale and the error in determination of the analyte concentration in the sample solution decreases with increasing absorbance values (see Fig. 11-9).

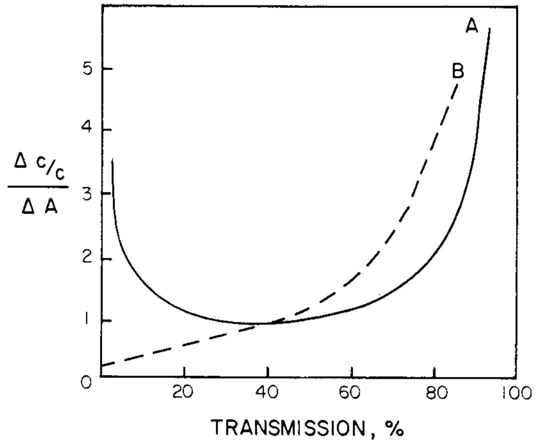

Fig. 11-9. Relative photometric error variation with percentage transmission. A, Linear transmission scale; B, linear absorbance scale.

11.5.3 Accuracy

The effect of the presence of systematic error in an analysis is to shift the most frequently observed value in the normal distribution curve (e.g. to A' in Fig. 11-8). Systematic error may be introduced at each stage of a complete analytical procedure. Loss of analyte element (or gain by contamination) may occur during sample pretreatment, or uni-directional changes in the analytical signal may be induced by the chemical or physical interference effects of concomitant materials.

Evaluation of the accuracy of an AAS or AFS procedure may be made using standard analysed samples (such as those available from the National Bureau of Standards, U.S.A., or the Bureau of Analysed Samples Ltd. in England). An alternative method is by reference of the results to those given by a well-established referee method employing a classical absolute technique or another instrumental method. The "recovery" of analyte element may also be checked by adding it in known amounts to samples and conducting the analysis in the normal fashion. In a technique for estimating inaccuracy which does not require standard additions of analyte, Youden[55] proposed the analysis of two samples of different analyte concentrations. Equal weights of each are then taken to make a third "sample" whose concentration will be the average of the two initial values. This sample is then analysed and the difference between the calculated and measured results provides an indication of the systematic error in the determinations.

11.6 PRETREATMENT OF SAMPLES

AAS and AFS are widely applicable to the analysis of many different types of solid and liquid samples where the matrix may be organic or inorganic in nature. The type of sample and the quantity available will determine the choice of the sampling procedure and the way in which the samples are prepared for analysis. Well-established sampling procedures exist for bulk samples which ensure that a homogenous sample is taken for analysis. These procedures are reviewed thoroughly in standard texts[56-58] concerned with quantitative analysis and will not be dealt with here.

In the technique of *average sampling* care must be taken that the composition of the sample is accurately representative of the average composition of the material. This type of sampling is the most common. The material to be analysed is usually a heterogeneous mineral mixture, raw material or unfinished or final product. The method of average sampling used depends on the degree of inhomogeneity and on the physical state and chemical properties of the sample. When very large amounts of material (e.g. bulk ore) are sampled, a representative raw sample is first taken. Laboratory samples may then be prepared from this by further grinding and homogenization.

In *discrete sampling* the sampling is confined to small parts of the material. For large amounts of material discrete sampling is usually easily performed. This method is used if heterogeneous parts of an otherwise homogeneous material are to be examined, e.g. oxide or sulphide inclusions in alloy castings. For such sampling from small stratified samples it may be difficult to ensure that each individual sample is representative of the material in a particular stratum.

Sampling difficulties may also be encountered when only minute amounts of solid or liquid samples of a biomedical or forensic origin are available. The usual procedure under these conditions is to obtain as many *raw* samples as possible and analyse these directly.

11.6.1 Dissolution of Samples

Once laboratory samples have been obtained care should be taken to avoid loss of the analyte element, or its gain by contamination, during any initial washing, drying or grinding of the material or on storage. The type of sample to be analysed obviously dictates the manner in which it is treated to render it suitable for analysis by AAS or AFS. The principal operation encountered for solid samples, however, is dissolution, with or without preliminary wet or dry ashing. Owing to the fact that the sample must frequently be treated with relatively large volumes of reagents during the ashing and/or dissolution procedure, care must be taken not to contaminate it with reagents containing either the analyte element or possible interfering substances. When this is known to occur, and is unavoidable, it is then essential to employ a procedure blank. If sufficient contamination occurs in this way to necessitate taking blanks through the whole procedure, the analytical precision attainable in the determination is usually substantially decreased.

Water which has been distilled in quartz apparatus or purified by ion-exchange should always be employed for dilution of sample solutions. Many acids and other reagents are available commercially in "analytical reagent" grades. It is still often advisable, however, to assume that even these reagents contain traces of the analyte element or an interferent as impurity, or that they may become contaminated from the vessels used for storage or dissolution; a procedure blank should still be undertaken. Frequently the magnitude of this blank may be decreased by pretreatment of the acids and other reagents by solvent extraction or ion-exchange procedures which remove unwanted impurities.

The material chosen for the apparatus used for the dissolution and subsequent storage of samples and standards is also frequently important, particularly in trace analysis. Adsorption of ions onto glassware from dilute standard and sample solutions is a well-known cause of inaccuracy. Dilute solutions should therefore not be stored for long periods but rather prepared fresh from more concentrated stock solutions every few days. In addition to loss of analyte by adsorption in this way, contamination of solutions can occur when previously adsorbed ions on the surface of glass containers are released on subsequent use of the vessels for sample or standard solution preparation. The apparatus itself may be attacked by the sample solutions to release contaminant species. The most common form of contamination in this way is from silicate leached from glassware. Mitchell[59] has reported the study of contamination from apparatus made from different materials. Minczewski[60] recommends the use of the following materials in order of preference: fluorinated polymers, polyethylene, quartz, platinum and glass.

The most common dissolution procedure for solid samples with an inorganic matrix is acid dissolution. The acids employed most frequently for metals, alloys and ores are HCl, H_2SO_4, HNO_3, H_3PO_4 and $HClO_4$. Phosphoric acid (H_3PO_4) is used in admixture with H_2SO_4 for some types of metallurgical sample; its possible chemical interference effect on the AAS or AFS of the analyte must be carefully checked before its use, however, particularly when large volumes are used. Hydrofluoric acid is often used in a mixture with a second acid for those samples where the formation of a stable fluoride complex assists the dissolution and aids the retention of the sample in solution.

Fusion procedures are sometimes employed for the dissolution of samples which are not readily attacked by acids. Fusion methods, however, are usually slow and it is often difficult to obtain fusion mixtures which are sufficiently free from contamination from traces of inorganic ions.

The most commonly encountered matrices that require fusion treatment for dissolution are those in which a high silicate content is expected, or for finished or part-finished refractory materials which have undergone heat treatment during processing.

11.6.2 Ashing Techniques

Both dry and wet ashing techniques are in widespread use for the destruction of organic matter in samples prior to inorganic trace analysis by AAS or other instrumental techniques. Each procedure will be briefly considered here for its suitability with different analyte elements.

(*a*) *Dry ashing*

In this technique the sample is heated in air in a suitable container at a temperature which may vary between *ca.* 400 and 800°C. The heating is usually performed by direct application of a gas flame to the base of the container. Solid samples must usually be dried in a drying oven prior to ashing and aqueous solutions are evaporated in small portions in the crucible used for the ashing procedure. When ashing of a very large amount of sample is necessary, it is advisable to weigh the sample in a weighing bottle and to ash it in portions after transference to the crucible; the weight of sample ashed is then determined by a final weighing of the bottle.

The dry ashing technique is simple, and large samples can be treated in this way. The procedure is relatively free from difficulties with contamination, although the introduction of impurities from the atmosphere must be avoided.[61] For some samples difficulty may be encountered with the retention of analyte materials by the walls of the crucible or with the subsequent dissolution of the ash (e.g., formation of acid-insoluble silicates). The most serious disadvantage of the dry ashing technique, however, occurs when the element to be determined is volatile. Thus, for example, in samples to be analysed for lead, mercury, cadmium, arsenic or selenium, dry ashing leads to partial or complete loss of the analyte element. The elements bismuth, chromium, copper, iron, nickel, vanadium and zinc may also be lost by volatilization as the metals, chlorides or organometallic compounds under certain conditions.

Some elements may be retained by the crucible employed and prove difficult to remove. Thus, Gorsuch[62] found significant retention of lead in silica crucibles above 550°C. In the presence of organic matter low recoveries of copper on dry ashing have been attributed to the retention of copper on the silica crucible employed.[50] This may be due to reduction of copper oxide and diffusion into the crucible walls of the copper metal formed. Similar difficulties have been reported for recovery of cobalt on dry ashing.[63] Thiers, Williams and Yoe,[64] however, recovered trace amounts of cobalt from blood on dry ashing for eighteen hours at 450°C. Thiers[65] recommends the following procedure for the routine analysis of biological samples with dry ashing: A liquid or solid sample in a platinum dish is heated on a hot-plate in filtered air for a period between 15 minutes and several hours, increasing the temperature gradually, until the sample has a charred appearance. The dish is then transferred to a muffle furnace and the temperature is raised from 250° to 450°C within an hour. This temperature is then maintained until the ashing is completed. If any carbon remains in the residue after prolonged ashing it may be decomposed with hot 12 M HNO_3. The ash obtained is dissolved in a small volume of hot 6 M HCl; if silica is present it should be volatilized away by evaporation with sulphuric and hydrofluoric acids.

Dry ashing is often carried out with the aid of additional oxidant. The sample may be moistened with a salt solution or a few drops of acid before combustion, or pure magnesium nitrate or acetate salt may be added as an ashing base. These procedures serve to speed the process and minimize losses by volatilization of some analyte elements, although the danger of sample contamination from trace impurities in the ashing aid used is increased. Dry combustion procedures in which an oxygen bomb[66] or oxygen flask[67] is used are frequently also employed. A particular advantage of the use of the oxygen flask technique may be the elimination of errors otherwise encountered from loss or contamination on sample transfer from the ashing vessel to the other apparatus used for storage of the sample solution. If the flask used in the technique is suitably shaped it may itself be employed as the vessel from which nebulization into the flame is effected. Belisle, Green and Winter[68] have described a flow-through oxygen flask technique which may be used with larger samples than the conventional oxygen flask method.

Gleit and co-workers[69-71] have described a low-temperature dry ashing technique which depends on radio-frequency excitation of oxygen. The active oxygen is passed over the organic material to be ashed and oxidation ensues at sample temperatures which may be maintained below 100°C. Particular advantages of this technique are the ability to retain the morphology of the sample and relative freedom from losses due to sample volatility. It is also claimed that the introduction of contamination from the container and the atmosphere are reduced. The quantitative recovery of seventeen elements after complete destruction of organic matrix material has been demonstrated using this technique. In a typical demonstration using radiotracer techniques it has been reported that selenium in alfalfa was recovered with 99% efficiency. In other work, however, incomplete recovery of the elements arsenic, selenium and mercury has been reported.[72] Two commercial assemblies utilizing this low-temperature ashing principle have been produced. This technique should find extensive application if rapid and efficient oxidation can be ensured for a wide range of matrices.

(*b*) *Wet ashing*

Organic matter may be destroyed by oxidation at lower temperatures than those used in dry ashing procedures when the technique of wet ashing is employed. The oxidizing reagents most commonly used are nitric acid, sulphuric acid and perchloric acid, either used singly or in admixture. At the lower temperatures employed the danger of loss of analyte by volatilization is decreased, although difficulty may still be encountered from loss of elements such as mercury, selenium and arsenic. The contamination risk from the presence of impurities in the digestion reagents is obviously greater than in the dry ashing procedure and the technique also requires more care in operation. From the standpoint of recovery of the analyte element, however, the wet ashing technique is usually preferable.

The most generally useful acid mixture appears to be a combination of HNO_3, H_2SO_4 and $HClO_4$; the volume ratios in which these are mixed varies according to the application and to the preference of different workers, but a mixture commonly used is $HNO_3 : H_2SO_4 : HClO_4 = 3 : 1 : 1$. While sufficient sulphuric acid is present there is little risk of explosion from the perchloric acid in this mixture and the solution may be evaporated until sulphur trioxide fumes appear. When sulphuric acid is omitted from the digestion mixture much more care must be taken to avoid explosion and the sample must not be taken to dryness; additional nitric acid is frequently added after the solution has evaporated until fumes of perchloric acid form.

Wet ashing procedures using acid mixtures containing molybdenum (VI)[73-75] or vanadium(V)[76] as a catalyst are finding increasing application. The incorporation of these catalysts is particularly useful in wet ashing where the analyte is arsenic or selenium. The procedure is rapid, only a few minutes digestion frequently being required, and appears to be very effective in minimizing loss with volatile analyte elements. Simon and co-workers[75] have investigated a variety of methods for pretreatment of urine samples before analysis and recommend this catalytic wet-digestion technique.

Johnson[77] has described the effective use of 50% H_2O_2 in conjunction with H_2SO_4 for the wet oxidation of organic matter. Other workers,[78] however, have reported loss of several elements during this procedure.

In a study of both wet and dry ashing techniques for the elements, lead, mercury, zinc, iron, strontium, chromium, antimony, molybdenum, silver, cadmium, copper, cobalt, selenium and arsenic, Gorsuch[79] found that a wet ashing procedure using HNO_3 and $HClO_4$ was generally the most satisfactory for effective recovery of these elements (except mercury).

The problems associated with destruction of organic material in samples prior to the determination of mercury have received considerable attention. Oxidation with a mixture of nitric and sulphuric acids has been employed by many workers; the temperature of the digestion mixture is maintained just below the boiling point of sulphuric acid. Wet ashing with mixtures containing perchloric acid appears to be unsuitable as loss of volatile mercury halides occurs. An oxidation procedure using 50% hydrogen peroxide has been described by Polley and Miller,[80] and other workers have employed nitric acid in the presence of potassium permanganate.[81] A variety of procedures have been described for the recovery of mercury by reduction to the element in solution using stannous chloride, hydroxylamine hydrochloride, ascorbic acid or other reductants. In some of these procedures organic matter is destroyed by prior oxidation in the same solution using strong oxidants such as potassium permanganate. The mercury may then be swept out from the solution in a current of nitrogen or argon and determined by the cold-vapour technique (see Chapter 13.4.34).

11.7 PRE-CONCENTRATION AND SEPARATION TECHNIQUES

11.7.1 Solvent Extraction

The "organic solvent effect" of increased sample transport to the flame may be usefully exploited by the solvent extraction of the analyte element into a water-immiscible solvent. This technique may also accomplish pre-concentration of the analyte element (by extraction from a large volume of aqueous solution into a small volume of organic solvent) when its concentration in the original sample solution is too low to permit its determination by AAS or AFS. The inherent spectral selectivity of AAS or AFS usually permits the use of a relatively non-selective solvent extraction system for the analyte element (in contrast to molecular absorption spectrometry in solution). However, when large amounts of matrix element or other species which give rise to chemical or physical interference are present in the aqueous sample, a degree of selectivity in the solvent extraction procedure may be useful for the elimination of these effects.

Both chelate and ion-association solvent extraction systems have been successfully employed in AAS by many workers. In most commonly employed chelate extraction procedures the pH of the aqueous sample solution is adjusted to a value suitable for formation of the complex to the extracted, and the solution is shaken with the organic solvent containing the organic chelating agent. After the phases have been allowed to separate, the organic solvent containing the chelate of the analyte element is nebulized directly into the flame for absorption or fluorescence measurements to be made.

The organic solvent chosen should not be appreciably soluble in water (to avoid problems with emulsification and slow separation) and should provide a substantial "organic solvent effect". It must also be directly combustible in the flame without the production of a smoky flame or toxic products. Aromatic solvents such as benzene or toluene generally give rise to the production of a smoky flame which may affect the analytical precision, while chlorinated solvents such as chloroform and carbon tetrachloride give rise to unpleasant and toxic combustion products. Allan[31] has reported that esters and ketones are generally satisfactory for use with the air/acetylene flame, since they produce stable flames, are completely burnt and do not contribute to the background absorption of the flame. Methyl isobutyl ketone (MIBK) has been employed extensively for solvent extraction followed by AAS (see, for example, refs. 31, 82-87) but other solvents have also commonly been employed, such as ethyl acetate,[31,83,88,89] isobutyl acetate,[90] amyl acetate,[31] propyl acetate,[31] methyl-n-amyl ketone,[91,92] methyl isopentyl ketone[93] and butanol.[90,94]

As mentioned above, unless the solvent extraction step must effect the removal of chemical or physical interferences as well as the pre-concentration of the analyte element, the most generally useful extraction methods are those that are non-selective and not critically dependent for their efficiency on the pH of the sample solution. A single set of conditions for solvent extraction (i.e. sample pH, reagent concentration) can then be applied to the pre-concentration of a range of elements. The chelating reagent that has been used most frequently in this way in AAS is ammonium pyrrolidine dithiocarbamate (APDC).[95] This reagent, which is generally used dissolved in water for direct extraction with methyl isobutyl ketone (MIBK), reacts with about 30 metal ions to form extractable metal chelates. The pH ranges over which the APDC complexes of different metal ions are formed are shown in Table 11-6. It is evident that some degree of selectivity can be introduced into solvent extraction procedures even with this "blanket" reagent by careful control of the pH of the sample solution. The APDC reagent is usually used as a 1% or 2% aqueous solution; its stability in aqueous solution depends on the pH, the rate of decomposition increasing in acid medium. It is usual to prepare the reagent solution fresh daily. Some of the typical applications of APDC extraction to AAS are given in Table 11-7.

8-Hydroxyquinoline (oxine) has also been employed for both selective and non-selective pre-concentration procedures prior to AAS determinations. The influence of pH and reagent concentration on the extraction characteristics of many metal ions is well-known from use of this reagent for gravimetry and molecular spectrophotometry in solution. In addition, the application of auxiliary masking agents, such as EDTA, cyanide or fluoride, to improve the selectivity of the extraction of particular elements has received much attention. Morrison and Freiser[96] and Stary[97] have listed conditions for the extraction of different metal ions with oxine, but the detailed extraction equilibria have not been studied for many elements. Table 11-8 shows extraction conditions for the most common elements whose pre-concentration is frequently required for AAS and which may easily be accomplished quantitatively with oxine, while Table 11-7 contains references to some published applications of oxine extraction prior to AAS determinations. 8-Hydroxyquinoline is frequently employed as a solution in chloroform for direct extraction of metal ions from aqueous solution. As chloroform may form toxic combustion products on nebulization, however, the extraction of the 8-hydroxyquinoline complexes into solvents such as ethyl acetate,[83] butanol[94] or MIBK is generally preferred.

TABLE 11-6

pH range of formation of the complexes of various metal ions with ammonium pyrrolidine dithiocarbamate[95] (APDC)

pH range	Elements forming APDC complexes
2	W
2-4	Nb, U
2-6	As, Cr, Mo, V, Te
2-8	Sn
2-9	Sb, Se
2-14	Ag, Au, Bi, Cd, Co, Cu, Fe, Hg, Ir, Mn, Ni, Os, Pb, Pd, Pt, Ru, Rh, Tl, Zn

TABLE 11-7

Some typical AAS applications employing pre-concentration or separation by solvent extraction

Organic reagent	Analyte	Solvent	Material	Reference
APDC	Cu	MIBK	Fertilizer, plants and soil	119
	Zn	MIBK	Fertilizer, plants and soil	120
	Fe, Mn, Ni	MIBK	KCl	121
	Cd, Tl, Hg	MIBK	Blood, urine	122
	Co	MIBK	Cements	123
	Co	MIBK	Plant digests	125
	Ni, Pb, Bi, Hg	MIBK	Urine	130
8-Hydroxyquinoline	Mg	MIBK	Brine, natural waters	124
	Mo	n-BuOH	Nb and Ta	94
	Cu	Ethyl acetate	Nb and Ta	88
	Mn, Co, Cu, Ni	$CHCl_3$	Brine	132
8-Hydroxyquinaldine	Mn	$CHCl_3$	Aluminous materials	133
TTA (thenoyl-trifluoroacetone)	Fe	MIBK	Urine	126
Na-DDTC (sodium diethyl dithiocarbamate)	Cd, Tl, Hg	MIBK	Blood, urine and tissue	127
	Cu	MIBK	Serum	128
Cupferron	V	MIBK	Water	131
Bathophenanthroline	Fe	MIBK	Serum	129
Diphenylthiocarbazone	Cr	MIBK	Brine	134
Toluene-3,4-dithiol	Mo	MIBK	Brine	134

Other chelating agents which may be successfully employed for pre-concentration by solvent extraction are diphenylthiocarbazone, 2-thenoyltrifluoroacetone, and cupferron (ammonium salt of *N*-nitrosophenyl hydroxylamine). Some applications of these reagents to AAS are shown in Table 11-7.

A second useful type of solvent extraction system is that based on the formation of extractable ion-association complexes between metal ions and simple inorganic ligands in aqueous solution. The ligands commonly encountered are the halides, thiocyanates and

TABLE 11-8

Practical conditions for solvent extraction of metal ions as their 8-hydroxyquinoline complexes

Metal ion	Soln. pH	Reagent conc. and solvent	Ref.
Al	4·5–11	0·1 M in $CHCl_3$	98, 99, 100
Bi	2·5–11	0·1 M in $CHCl_3$	100
Ca	>10·7	0·5 M in $CHCl_3$	100-102
	10–11	2% in MIBK	52
Cd	5·5–9·5	0·1 M in $CHCl_3$	100
		+ alcohols	103
Co(II)	4·5–10·5	0·1 M in $CHCl_3$	100
Cr(III)	6–8	Boil + excess oxine extract + $CHCl_3$	104
		0·1 M in $CHCl_3$	98
Cu	2–12	0·1% in ethyl acetate	88
Fe(III)	2–12	0·1 M in $CHCl_3$	98, 100
Hg(II)	>3	0·1 M in $CHCl_3$	100
		0·1 M in $CHCl_3$	100
Mg	10·7–13·6	0·1% in $CHCl_3$ + butylamine	105, 106 107, 108
		oxine in MIBK	
Mn(II)	6·5–10	0·1 M in $CHCl_3$	98, 100
Mo(VI)	1·0–5·5	0·01 M in $CHCl_3$	100
	4·5	1% aq. oxine, BuOH + butylamine	94
Nb(V)	6–9 (2% tartrate)	4% in $CHCl_3$	109
Ni	4–10	0·01 M in $CHCl_3$	100
	4·5–9·5	0·07 M in $CHCl_3$	98
Pb	6–10	0·1 M in $CHCl_3$	100
Pd	0–10	0·01 M in $CHCl_3$	100
Sn(IV)	2·5–5·5	0·07 M in $CHCl_3$	98
Sr	>11·5	0·5 M in $CHCl_3$	100
Th	4–10	0·1 M in $CHCl_3$	110, 100
		oxine in MIBK	110
Ti	2·5–9·0	0·1 M in $CHCl_3$	100
Tl(III)	3·5–11·5	0·01 M in $CHCl_3$	100
U(VI)	5–9	0·1 M in $CHCl_3$	111, 112, 100
		oxine in MIBK	112, 113, 114
V(V)	2–6	0·1 M in $CHCl_3$	100
		also with other solvents	66, 67 115, 116, 117
W(VI)	2·5–3·5	0·14 M in $CHCl_3$	100
Zn	4–5	0·1 M in $CHCl_3$	100
		oxine in MIBK	118
Zr(IV)	1·5–4·0	0·1 M in $CHCl_3$	100

organic phosphate esters (such as tributyl phosphate). Ion association system extraction methods usually require a strongly acidic aqueous medium for efficient extraction, and the organic solvents employed are most frequently relatively polar (esters, ketones, lower alcohols and ethers) and suitable for nebulization into flames commonly employed in AAS and AFS.

Ion association extraction procedures are generally capable of extracting higher absolute weights of metal ions in moderate volumes of solution than are organic chelate extraction procedures, and large amounts of relatively expensive reagent are not required. In addition to the use of solvent extraction for extraction of the analyte element(s) away from the bulk matrix components in the aqueous solution, therefore, with these procedures it is frequently possible to undertake the extraction of the bulk matrix element(s) to leave the analyte element in the original aqueous solution. This general approach may sometimes be chosen when pre-concentration of the analyte is unnecessary and adequate AAS or AFS sensitivity is obtained in aqueous solution. Bulk matrix element extraction may then be employed to eliminate interference by chemical or physical effects in the nebulizer or flame employed. Table 11-9 gives details of some simple ion-association procedures for different elements where the method has been shown to permit virtually quantitative extraction of the species concerned. In addition to those shown in Table 11-9, other elements may be extracted under similar conditions with varying efficiencies. Morrison and Freiser[96] have presented a more extensive compilation of data concerned with efficiency of extraction of different elements with halogen acids and other ion-association systems.

TABLE 11-9

Ion association systems for different ions shown to provide efficient extraction

Ion	Aqueous medium	Organic solvent
As(III)	11 M HCl	Benzene
Au(III)	10% HCl	Ethyl acetate
Au(III)	3 M HBr	Ethyl ether
Au(III)	7 M HI	Ethyl ether
Cd	7 M HI	Ethyl ether
	1·5 N H_2SO_4 + 1·5 M KI	Ethyl ether
Fe(III)	1 M HCl	0·1 M TOPO in cyclohexane
Fe(III)	4 M HBr	Ethyl ether
Fe(III)	6 M HCl	Ethyl ether
Fe(III)	8 M HCl	Iso-propyl ether
Ga(III)	7 M HCl	Iso-propyl ether
	3 M HCl	Tributyl phosphate
Ga(III)	7 M NH_4CNS + 0·5 M HCl	Ethyl ether
Ga(III)	5 M HBr	Ethyl ether
Ge(IV)	11 M HCl	Benzene
Hg(II)	7 M HI	Ethyl ether
In(III)	4 M HBr	Ethyl ether
In(III)	1·5 M KI + 1·5 N H_2SO_4	Ethyl ether
Mo(VI)	1 M HCl	0·1 M TOPO in cyclohexane
Mo(VI)	5 M HCl	Amyl acetate
Mo(V)	1 M NH_4CNS/0·5 M HCl	Ethyl ether
Nb(V)	11 M HCl	Di-isopropyl ketone
Nb(V)	0·6 M DBPA/1 M HNO_3	Di-n-butyl ether
Nb(V)	9 M HF + 6 M H_2SO_4	Di-isopropyl ketone
Nb(V)	10 M HF + 6 M H_2SO_4 + 2·2 M NH_4F	MIBK
Pb(II)	Excess KI/5% HCl	MIBK
Ta(V)	10 M HF + 6 M H_2SO_4 + 2·2 M NH_4F	MIBK
Sb(III)	7 M HI	Ethyl ether
Sb(V)	5 M HBr	Ethyl ether
Sb(V)	6·5-8·5 M HCl	Isopropyl ether
Sc(III)	8 M HCl	Tributyl phosphate
Sn(II)	4·6 M HF	Ethyl ether
Sn(II)	7 M HI	Ethyl ether
Sn(II)	1·5 M KI + 1·5 N H_2SO_4	Ethyl ether
Sn(IV)	3 M NH_4CNS + 0·5 M HCl	Ethyl ether
Sn(IV)	1·2-4·6 M HF	Ethyl ether
Sn(IV)	0·6 M DBPA + 1 M HNO_3	Di-n-butyl ether
Tl(I)	0·5 M HI	Ethyl ether
Tl(III)	6 M HCl	Ethyl ether
Tl(III)	$>$1 M HBr	Ethyl ether
Tl(III)	0·5 M HI	Ethyl ether
Ti(IV)	7 M HCl	0·1 M TOPO in cyclohexane
U(VI)	1 M HCl	0·1 M TOPO in cyclohexane
V(V)	pH 1·5-2·0	0·6 M TOPO in kerosene
Zn(II)	1 M NH_4CNS + 0·5 M HCl	Ethyl ether
Zr(IV)	1 M HCl	0·1 M TOPO in cyclohexane
Zr(IV)	0·06 M DBPA + 1 M HNO_3	Di-n-butyl ether

TOPO = tri-n-octylphosphine oxide; DBPA = di-n-butylphosphoric acid; MIBK = methyl iso-butyl ketone.

11.7.2 Ion Exchange

Ion-exchange procedures are applicable during pre-treatment of AAS and AFS sample solutions either to pre-concentrate the analyte element from dilute sample solutions or to remove from the sample solution other ions that may exert a chemical or physical interference effect.

The ion-exchangers most commonly employed are the high molecular-weight organic resins containing acidic or basic functional groups. Sulphonated styrene/divinylbenzene copolymer resins, such as Amberlite IR-120 and Dowex-50, are the most generally encountered types of cation exchanger. Styrene/divinylbenzene copolymers into which quaternary ammonium groups are introduced, such as Amberlite IRA-400 and Dowex-1, are commonly employed as anion exchangers. All of these resins may be employed for either batch or column techniques. The sample solution is passed onto the resin and retained in contact with it for sufficient time to ensure equilibration; non-exchanged ions may then be washed from the resin, while those ions retained must be stripped out by treatment with a suitable eluting agent which reverses the ion-exchange process.

As AAS and AFS are relatively free from interference by moderate amounts of foreign ions, it is not usually necessary for the exchanger selectively to retain only the analyte when ion-exchange techniques are used for pre-concentration of sample solutions. Retention of a group of cations or anions that includes the analyte element is usually sufficient and these ions may then be stripped from the resin with a strong acid or base. Batch operation, in which the sample solution is simply shaken with the ion-exchange resin, is frequently satisfactory for pre-concentration procedures. After filtration the analyte and other exchanged ions are stripped from the resin by treating it with the minimum necessary volume of acid or base (in order to achieve the highest possible concentration factor). In order to ensure quantitative exchange from the initial solution the pH and equilibration time used for a given resin must be carefully controlled; the same factors must also be controlled in the stripping procedure to ensure complete removal of the analyte element from the ion exchanger. In some cases the analyte ion may be difficult to remove from the resin after ion exchange. This can lead to low recoveries and contamination of subsequent samples if the same batch of ion exchanger is employed. Under these conditions it may be preferable to ash the resin to recover the analyte element.

As mentioned above, ion-exchange procedures may be employed prior to AAS or AFS determination in order to remove matrix elements from the sample solution. In this type of application relatively large amounts of ion exchanger are often required and the

TABLE 11-10

Some selected ion-exchange procedures used for the pre-concentration or separation of inorganic species prior to determination by instrumental techniques

Analyte element(s) concentrated or separated	Matrix or accompanying elements	Ion-exchange process	Reference
Si	Water	Cl-anion exch. as SiF_6^{2-}; elution with boric acid	135
Cu	Water	H-form cation exch.; elution + 5 M HCl or hot 1 M Na_2SO_3	136 137
Au, Bi, Cd	Sea water	Cl-anion exch.; elution + 0·25 M HNO_3; ash resin	138
Cs, Rb	Sea water	NH_4-form cation exchange	139
Sn	H_2O_2	H-form cation exch.; elution + 5 M HCl	140
Co	Ni	Cl-form anion exch. from HCl soln.; elute + HNO_3/HCl	141
Cu, Cd, Co, Zn and Fe	Al and Mg	Cl-form anion exch.; elution + HNO_3/HCl	142
Pt	Chlorate cell liquor	Cl-form anion exch. from HCl medium; ash resin	143
U	Uranium leach liquors	SO_4-form anion exch.	144
Rare earths	Zirconium	H-form cation exch. HF soln.; elution + 6 M HCl	145
Cu	Milk	H-form cation exch.; elution + 6% HCl	146
Cu	Mineral oils	H-form cation exch. from soln. diluted + 2-propanol; elution + 10% H_2SO_4	147
Si	Pu	Absorption of Pu on H-form cation exch. from 0·2 N HNO_3/0·05 N NH_2OH	148
Mn	U	Absorption of U on Cl-form anion exch. from 9 M HCl	149
B	Al alloys	Absorption of Al on cation exch. from pH 5 acetate soln.	150
Fluoride	Water	Acetate anion exch.; elution + 0·2 M acetic acid/0·005 M Be soln.	151

capacity of the resin to retain large amounts of the concomitant species is an important consideration. No concentration of the analyte element is obtained and, indeed, some dilution is usually inevitable as the sample solution containing the unadsorbed analyte must be completely washed from the resin.

Many descriptions of the use of ion-exchange procedures for the pre-concentration and separation of traces of inorganic ions are found in the literature. In many of these studies instrumental techniques other than AAS or AFS are used for the determination of the analyte after ion-exchange pretreatment. The practical procedures detailed may, however, be directly applicable even when the final determination is by flame spectroscopy. Table 11-10 lists some selected examples from the literature; the reader is referred to two excellent treatises devoted solely to ion exchange processes[152,153] for further detailed treatment of their analytical application.

11.7.3 Other Techniques

Precipitation techniques have found considerable application for separation and pre-concentration in trace analysis but the direct precipitation of traces of an analyte element is seldom employed (owing to the difficulty of ensuring quantitative deposition and recovery of small amounts of material). Precipitation of bulk amounts of interfering matrix elements may, however, be achieved provided that care is taken to eliminate errors due to co-precipitation of the required analyte. The phenomenon of co-precipitation may be turned to advantage for pre-concentration in trace analysis by the use of collecting or scavenging agents. In these procedures a collector precipitate is formed and co-precipitates traces of the element to be determined. This precipitate may then be filtered off and dissolved in a small volume of solution to perform the analysis. Inorganic precipitates of sparingly soluble hydroxides, sulphides or carbonates are frequently employed in this fashion. The element chosen to act as the carrier ion for precipitation should have chemical properties similar to those of the ion to be co-precipitated, and must be added to the sample solution in sufficient quantity to provide enough precipitate for filtration without special apparatus. Furthermore, it must not cause interference in the subsequent determination of the analyte by AAS or AFS. The most frequently used carrier ions are manganese, iron and aluminium, but organic precipitating agents such as 8-hydroxyquinoline and thionalide have also been employed. An advantage with the use of organic collectors, compared to inorganic reagents, is that these are usually easily purified to remove traces of inorganic ions which would otherwise cause contamination. Examples of this type of application are found in the separation and pre-concentration by Dehm *et al.*[154] of seven heavy metal impurities in inorganic salts using 8-hydroxyquinoline and thionalide with aluminium carrier, and the effective recovery of trace metals from sea water using thio-acetamide with tin and indium carriers.[155] The use of organic precipitants has been reviewed recently[156] and the application of co-precipitation techniques for analysis of sea-water has been discussed by Joyner and co-workers.[157]

Other well-established techniques for separation and pre-concentration in trace analysis include volatilization, column or paper chromatography, fire (or dry) assay (particularly for the noble elements) and electrochemical deposition. At the time of writing, however, with the possible exception of fire assay these techniques have not found extensive application prior to determinations by flame spectroscopy.

REFERENCES

1. J. E. Allan, *Spectrochim. Acta,* 1954, **10,** 800.
2. J. E. Allen, *Nature,* 1960, **187,** 1110.
3. V. G. Mossotti and V. A. Fassel, *Spectrochim. Acta,* 1964, **20,** 1117.
4. D. J. David, *Analyst,* 1961, **86,** 730.
5. J. V. Sullivan and A. Walsh, *Spectrochim. Acta,* 1965, **21,** 721.
6. J. A. Bowman, J. V. Sullivan and A. Walsh, *Spectrochim. Acta,* 1966, **22,** 205.
7. W. Slavin, "Atomic Absorption Spectroscopy", Interscience, New York, 1968, p. 120.
8. W. Slavin and D. C. Manning, *Appl. Spectrosc.,* 1965, **19,** 65.
9. L. Capacho-Delgado and D. C. Manning, *Spectrochim. Acta,* 1966, **22,** 1505.
10. H. L. Kahn and J. E. Schallis, *Atomic Absorption Newsletter,* 1968, **7,** 5.
11. T. C. Rains, in "Flame Emission and Atomic Absorption Spectrometry", eds. J. A. Dean and T. C. Rains, Marcel Dekker, New York, 1969, p. 363.
12. G. F. Kirkbright and L. Ranson, *Anal. Chem.,* 1971, **43,** 1238.
13. W. J. McCarthy, M. L. Parsons and J. D. Winefordner, *Spectrochim. Acta,* 1967, **23B,** 25.
14. R. F. Browner, R. M. Dagnall and T. S. West, *Anal. Chim. Acta,* 1970, **50,** 375.
15. R. M. Dagnall, K. C. Thompson and T. S. West, *Talanta,* 1967, **14,** 557.
16. R. S. Hobbs, G. F. Kirkbright and T. S. West, *Talanta,* 1971, **18,** 859.
17. G. Hansen, *Optik,* 1946, **1,** 227; **1,** 269.
18. P. Jacquinot, *J. Opt. Soc. Amer.,* 1954, **44,** 761; 1955, **45,** 996.
19. J. W. Perry, *J. Opt. Soc. Amer.,* 1955, **45,** 995.
20. B. J. Russell and A. Walsh, *Spectrochim. Acta,* 1959, **15,** 883.
21. J. V. Sullivan and A. Walsh, *Applied Optics,* 1968, **7,** 1271.

22. J. V. Sullivan and A. Walsh, *Spectrochim. Acta,* 1965, **21,** 721.
23. J. A. Bowman, J. V. Sullivan and A. Walsh, *Spectrochim. Acta,* 1966, **22,** 205.
24. R. M. Lowe, *Spectrochim. Acta,* 1969, **24B,** 191.
25. M. S. Cresser and T. S. West, *Spectrochim. Acta,* 1970, **25B,** 61.
26. B. V. L'Vov, "Atomic Absorption Spectroscopy", Adam Hilger, London, 1970.
27. C. Th. J. Alkemade, in "Atomic Absorption Spectroscopy", eds. R. M. Dagnall and G. F. Kirkbright, Butterworths, London, 1971.
28. M. S. Cresser, G. F. Kirkbright, M. Sargent and T. S. West, unpublished work.

28a. B. V. L'Vov, in "Atomic Absorption Spectroscopy", eds. R. M. Dagnall and G. F. Kirkbright, Butterworths, London, 1971.

29. D. A. Davies, R. Venn and J. B. Willis, *J. Sci. Ins.,* 1965, **42,** 816.
30. A. Strasheim, F. W. E. Strelow and E. Norval, *J. S. Afric. Chem. Inst.,* 1961, **20,** 25.
31. J. E. Allan, *Spectrochim. Acta,* 1961, **17,** 467.
32. J. Ramirez-Munoz, *Talanta,* 1966, **13,** 87.
33. J. Ramirez-Munoz and W. F. Ulrich, *Flame Notes, Beckman,* 1966, **1,** 33.
34. H. L. Kahn and W. Slavin, *Appl. Optics,* 1963, **2,** 931.
35. S. B. Smith Jnr. and F. J. Feldman, *8th Nat. Meeting Soc. Appl. Spectrosc.,* Anaheim, Calif. U.S.A., 1969.
36. A. Z. Ringbom, *Z. Anal. Chem.,* 1934, **115,** 332.
37. G. D. Christian and F. J. Feldman, "Atomic Absorption Spectroscopy: Applications in Agriculture, Biology and Medicine', Wiley-Interscience, New York, 1970, p. 124.
38. AFS–6 Spectrometer, Technicon Instrument Corp., Tarrytown, New York, 1971.
39. C. S. Rann, *Spectrochim. Acta,* 1968, **23B,** 827.
40. L. de Galan, *Spectrochim. Acta,* 1969, **24B,** 629.
41. L. de Galan and G. F. Samaey, *Anal. Chim. Acta,* 1970, **50,** 39.
42. B. V. L'Vov, *Spectrochim. Acta,* 1961, **17,** 761.
43. S. R. Koirtyohann and E. E. Pickett, Paper presented at XIIIth Colloq. Spectroscop. Intern., Ottawa, 1967.
44. L. de Galan and J. D. Winefordner, *J. Quant. Spec. Radiat. Transfer,* 1967, **7,** 251.
45. L. de Galan and G. F. Samaey, *Spectrochim. Acta,* 1970, **25B,** 245.
46. B. V. L'Vov, *Industrial Laboratory,* 1963, **28,** 987.
47. S. B. Smith Jnr., J. A. Blasi and F. J. Feldman, *Anal. Chem.,* 1968, **40,** 1525.
48. F. J. Feldman, J. A. Blasi and S. B. Smith Jnr., *Anal. Chem.,* 1969, **41,** 1095.
49. F. J. Feldman and S. B. Smith Jnr., *15th Spectrosc. Symp., Canada,* Toronto, 1968.
50. G. D. Christian and F. J. Feldman, "Atomic Absorption Spectroscopy: Applications in Agriculture, Biology and Medicine", Wiley-Interscience, New York, 1970, pp. 129, 192.
51. D. J. David, *Analyst,* 1961, **86,** 730.
52. C. B. Belcher and K. A. Brooks, *Anal. Chim. Acta,* 1963, **29,** 202.
53. W. Lang and R. Herrman, *Mikrochim. Acta,* 1963, 1053.
54. H. L. Kahn, *Atomic Absorption Newsletter,* 1967, **6,** 51.
55. W. J. Youden, *Ind. Eng. Chem., Anal. Ed.,* 1947, **19,** 943.
56. L. Erdey, "Gravimetric Analysis, Vol. 1", Pergamon Press, Oxford, 1963, p. 13.

57. N. H. Furman, "Scott's Standard Methods of Analysis", Van Nostrand, New York, 1939.
58. Willard and Diehl, "Advanced Quantitative Analysis", Van Nostrand, New York, 1945.
59. R. L. Mitchell, *J. Sci. Food Agric.,* 1960, **11,** 553.
60. J. Minczewski, in "Trace Characterisation", eds. W. W. Meinke and B. F. Scribner, Nat. Bureau of Standards Monograph 100, 1965.
61. N. E. Thiers, in "Trace Analysis", eds. J. H. Yoe and H. J. Koch, John Wiley, New York, 1957.
62. T. T. Gorsuch, *Analyst,* 1959, **84,** 135.
63. P. Ambler and N. Griggs, *Ind. Eng. Chem., Anal. Ed.,* 1941, **13,** 102.
64. R. E. Thiers, J. F. Williams and J. H. Yoe, *Anal. Chem.,* 1955, **27,** 1725.
65. R. E. Thiers, in "Methods of Biochemical Analysis, Vol. 5", ed. D. Glick, Interscience, New York, 1957.
66. R. A. Anduze, *Anal. Chem.,* 1957, **29,** 90.
67. W. Schöniger, *Mikrochim. Acta,* 1955, 123; 1956, 869.
68. J. Belisle, C. D. Green and L. D. Winter, *Anal. Chem.,* 1968, **40,** 1006.
69. C. E. Gleit and W. D. Holland, *Anal. Chem.,* 1962, **34,** 1454.
70. C. E. Gleit and W. D. Holland, *Anal. Chim. Acta,* 1965, **32,** 346.
71. C. E. Gleit, *Anal. Chem.,* 1965, **37,** 314.
72. C. E. Mulford, *Atomic Absorption Newsletter,* 1966, **5,** 135.
73. D. W. Bolin and O. E. Stamberg, *Ind. Eng. Chem., Anal. Ed.,* 1964, **16,** 345.
74. L. M. Cummins, T. L. Martin, G. W. Maag and D. C. Maag, *Anal. Chem.,* 1964, **36,** 382.
75. R. K. Simon, G. D. Christian and W. C. Purdy, *Amer. J. Clin. Path,* 1968, **49,** 733.
76. J. S. McNultey, *Ind. Eng. Chem., Anal. Ed.,* 1947, **19,** 809.
77. W. C. Johnson, *Analyst,* 1967, **92,** 403.
78. J. L. Down and T. T. Gorsuch, 1967, *Analyst,* 92, 398.
79. T. T. Gorsuch, *Analyst,* 1959, **84,** 135.
80. D. Polley and V. L. Miller, *Anal. Chem.,* 1955, **27,** 1162.
81. A. C. Rolfe, F. R. Russell and N. T. Wilkinson, *Analyst,* 1955, **80,** 523.
82. H. Goto, Y. Kakita and T. Furukawa, *J. Chem. Soc. Japan,* 1958, **79,** 1513.
83. J. E. Allan, *Analyst,* 1961, **86,** 530.
84. E. Berman, *Atomic Absorption Newsletter,* 1964, **3,** 111.
85. E. A. Boling, *Spectrochim. Acta,* 1966, **22,** 425.
86. D. C. Burrell, *Atomic Absorption Newsletter,* 1965, **4,** 309.
87. D. Trent and W. Slavin, *Atomic Absorption Newsletter,* 1964, **3,** 118.
88. G. F. Kirkbright, M. K. Peters and T. S. West, *Analyst,* 1966, **91,** 411.
89. R. J. Magee and A. K. Rahman, *Talanta,* 1965, **12,** 409.
90. G. F. Kirkbright, A. M. Smith and T. S. West, *Analyst,* 1967, **92,** 411.
91. J. B. Willis, *Anal. Chem..* 1962, **34,** 614.
92. L. R. P. Butler and P. M. Mathews, *Anal. Chim. Acta,* 1966, **36,** 319.
93. M. E. Morgan, *Atomic Absorption Newsletter,* 1964, **21,** 1.
94. G. F. Kirkbright, M. K. Peters and T. S. West, *Analyst,* 1966, **91,** 705.
95. H. Malissa and E. Schoffman, *Mikrochim. Acta,* 1965, 187.
96. G. H. Morrison and H. Freiser, "Solvent Extraction in Analytical Chemistry", John Wiley, New York, 1957.
97. J. Stary, "The Solvent Extraction of Metal Chelates", Pergamon Press, Oxford, 1964.
98. C. H. R. Gentry and L. G. Sherrington, *Analyst,* 1946, **71,** 432; 1950, **75,** 17.

99. J. P. Riley, *Anal. Chim. Acta*, 1958, **19**, 413.
100. J. Stary, *Anal. Chim. Acta*, 1963, **28**, 132.
101. F. Umland and K. U. Meckenstock, *Z. Anal. Chem.*, 1959, **165**, 161.
102. H. Goto and E. Sudo, *Japan Analyst* (*Bunseki Kagaku*), 1961, **10**, 171.
103. F. Umland and W. Hoffmann, *Z. Anal. Chem.*, 1954, **168**, 268.
104. A. J. Blair and D. A. Pantony, *Anal. Chim. Acta*, 1956, **14**, 545.
105. F. Umland and W. Hoffmann, *Angew. Chemie*, 1956, **68**, 704; 1957, **69**, 396.
106. F. Umland and W. Hoffmann, *Anal. Chim. Acta*, 1957, **17**, 234.
107. Y. Kekita and H. Goto, *Sci. Rep. Res. Inst., Tohoku Univ.*, 1960, **A12**, 334.
108. H. Goto and E. Sudo, *Sci. Rep. Res. Inst., Tohoku Univ.*, 1959, **A11**, 355.
109. I. P. Alimarin and I. M. Gibalo, *Vestnik Moskov. Univ., Ser. Mat., Mekh., Astr., Fiz., Khim.* 1956, **11**, No. 2, 185; 1958, **14**, No. 2, 185.
110. D. Dyrssen, *Svensk kem. Tidskr.*, 1953, **65**, 43.
111. E. P. Bullwinkel and P. Noble, *J. Amer. Chem. Soc.*, 1958, 2955.
112. D. Dyrssen and V. Dahlberg, *Acta Chem. Scand.*, 1953, **7**, 1186.
113. R. F. Clayton, W. H. Hardwick, M. Moreton-Smith and R. Todd, *Analyst*, 1958, **83**, 13.
114. W. E. Clifford, E. P. Bullwinkel, L. A. McClaine and P. Noble, *J. Am. Chem. Soc.*, 1958, **80**, 2959.
115. A. W. Ashbrook and K. Conn, *Chemist-Analyst*, 1961, **50**, 47.
116. N. Naito and K. Sugawara, *Bull. Chem. Soc., Japan*, 1957, **30**, 799.
117. E. Sudo, *J. Chem. Soc. Japan, Pure Chem. Sect.*, 1951, **72**, 817; *C.A.*, 1952, **46**, 6034.
118. Y. Kakita and H. Goto, *Sci. Rep. Res. Inst., Tohoku Univ.*, 1960, **A12**, 334.
119. J. E. Allan, *Spectrochim. Acta*, 1961, **17**, 459.
120. J. E. Allan, *Analyst*, 1961, **86**, 530.
121. S. Sprague and W. Slavin, *Atomic Absorption Newsletter*, 1964, May.
122. E. Berman, *Atomic Absorption Newsletter*, 1967, **6**, 57.
123. M. Montagut-Buscas, J. Obiols and E. Rodriguez, *Atomic Absorption Newsletter*, 1967, **6**, 61.
124. M. Suzuki, M. Yanagisawa and T. Takeuchi, *Talanta*, 1965, **12**, 989.
125. J. Stupar, *Mikrochim. Acta*, 1966, 722.
126. G. Devoto, *Russ. Med. Sarda*, 1968, **71**, 357.
127. E. Berman, *Atomic Absorption Newsletter*, 1967, **6**, 57.
128. E. Berman, *Atomic Absorption Newsletter*, 1965, **4**, 296.
129. A. Zettner, L. C. Sylvia and L. Capacho-Delgado, *Am. J. Clin. Pathol.*, 1966, **45**, 533.
130. J. B. Willis, *Anal. Chem.*, 1962, **34**, 614.
131. S. L. Sachdev, J. W. Robinson and P. W. West, *Anal. Chim. Acta*, 1967, **37**, 12.
132. R. E. Mansell and H. W. Emmel, *Atomic Absorption Newsletter*, 1965, **4**, 365.
133. R. C. Calkins, *Appl. Spect.*, 1966, **20**, 146.
134. B. Delaughter, *Atomic Absorption Newsletter*, 1965, **4**, 273.
135. R. Wickbold, *Z. Anal. Chem.*, 1959, **171**, 81.
136. B. Tuck and E. M. Osborn, *Analyst*, 1960, **85**, 105.
137. N. S. McNutt and R. H. Maier, *Anal. Chem.*, 1962, **34**, 276.
138. R. R. Brooks, *Analyst*, 1960, **85**, 745.
139. A. A. Smales and L. Salmon, *Analyst*, 1955, **80**, 37.
140. G. F. Reynolds, *Analyst*, 1957, **82**, 46.

141. A. Mizuike, Y. Iida and S. Hirano, *J. Chem. Soc. Japan, Ind. Chem. Sect.*, 1958, **61**, 1459.
142. *Idem*, ibid., 1959, **62**, 1491.
143. Y. Iida and A. Mizuike, *Japan Analyst*, 1964, **13**, 68.
144. J. N. Van Niekerk, J. F. Dewet and F. T. Wybenga, *Anal. Chem.*, 1961, **33**, 213.
145. H. J. Hettel and V. A. Fassel, *Anal. Chem.*, 1955, **27**, 1311.
146. H. A. Cranston and J. B. Thompson, *Ind. Eng. Chem., Anal. Ed.*, 1946, **18**, 323.
147. H. Buckwald and L. G. Wood, *Anal. Chem.*, 1953, **25**, 664.
148. C. E. Pietri and A. W. Wenzel, *Anal. Chem.*, 1963, **35**, 209.
149. F. Nakashima, *Anal. Chim. Acta*, 1964, **30**, 167.
150. G. F. Kirkbright, R. M. Dagnall, L. Ranson and T. S. West, unpublished work.
151. F. S. Kelso, J. M. Matthews and H. P. Kramer, *Anal Chem.*, 1964, **36**, 577.
152. O. Samuelson, "Ion Exchanges in Analytical Chemistry", John Wiley, New York, 1953.
153. J. Inczedy, "Analytical Applications of Ion Exchangers", Pergamon Press, New York, 1966.
154. R. L. Dehm, W. G. Dunn and E. R. Loder, *Anal. Chem.*, 1961, **33**, 607.
155. E. C. Mallory Jnr., in "Trace Inorganics in Water—Advances in Chemistry Series No. 73", ed. R. B. Gould, Am. Chem. Soc., Washington, D.C., 1968.
156. G. V. Miasoyedova, *Zh. Anal. Khim.*, 1966, **21**, 598.
157. T. Joyner, M. L. Healy, D. Chakravarti and T. Koyanagi, *Env. Sci. and Tech.*, 1967, **1**, 417.

lanthanum by extraction from 4-8 M HCl or HNO_3 with a 10% solution of thenoyltrifluoroacetone and nebulization of the organic phase into a nitrous oxide-acetylene flame. Grossman and Inglis[14] have described a method for the determination of Zr in hides in which the sample was dissolved in HF, ferric chloride was added to minimize interferences, and the solution was nebulized directly into a nitrous oxide-acetylene flame.

References

1. M. D. Amos and J. B. Willis, *Spectrochim. Acta,* 1966, **22,** 1325.
2. D. C. Manning, *Atomic Absorption Newsletter,* 1966, **5,** 127.
3. "Analytical Methods for Atomic Absorption Spectrophotometry", Parkin-Elmer Corp., Norwalk, Conn., U.S.A., 1971.
4. J. B. Headridge and D. P. Hubbard, *Anal. Chim. Acta,* 1967, **37,** 151.
5. W. Slavin, A. Venghiattis and D. C. Manning, *Atomic Absorption Newsletter,* 1966, **5,** 84.
6. J. I. Dinnin, *Anal. Chem.,* 1967, **39,** 1491.
7. K. E. Zacha, M. P. Bratzel, Jnr., J. D. Winefordner and J. M. Mansfield Jnr., *Anal. Chem.,* 1968, **40,** 1733.
8. J. D. Winefordner, *Anal. Chem.,* 1970, **42,** 206R.
9. V. S. Sastri, C. L. Chakrabarti and D. E. Willis, *Can. J. Chem.,* 1969, **47,** 587.
10. *Idem, Talanta,* 1969, **16,** 1093.
11. A. M. Bond, *Anal. Chem.,* 1970, **42,** 932.
12. A. M. Bond and D. R. Canterford, *Anal. Chem.,* 1971, **43,** 134.
13. R. R. Foster, *Atomic Absorption Newsletter,* 1968, **7,** 110.
14. V. B. Grossman and A. S. Inglis, *Anal. Chem.,* 1971, **43,** 1903.

CHAPTER 14

Special Techniques in AAS and AFS

14.1 INTRODUCTION

This chapter is concerned with the description of various techniques and methods in which either AAS or AFS is applied for indirect determinations or for special purposes. Thus the application of AAS for isotopic analysis and of AAS and AFS for the determination of temperatures in flame and non-flame atom cells is reviewed. The present status of the application of laser sources in AFS is also described.

14.2 APPLICATION OF INDIRECT METHODS IN ANALYSIS BY ATOMIC ABSORPTION SPECTROSCOPY*

A considerable number of elements may not be determined directly by AAS with conventional instrumentation, or may be

---

* Taken from a review by G. F. Kirkbright and H. N. Johnson, *Talanta,* **20,** 433.

determined only with low sensitivity (>5 ppm for 1% absorption) so that they are not readily determined at trace levels in solution. Thus, for example, the elements F, Cl, Br, I, S, P, C, O and N exhibit their principal resonance lines in the vacuum ultraviolet (see Table 14-1) and are not directly determinable by AAS without modified equipment (see I, S and P in Chapter 13). A second large group of elements for which direct AAS is difficult includes those elements for which, although their resonance lines lie at accessible wavelengths, it is extremely difficult to form and maintain a significant population of atoms in flame and non-flame cells. This group includes Th and Ce, for which no report of direct determination by AAS with appreciable sensitivity has been made, and in decreasing order of difficulty the elements U, B, W, Ta, La, Nb, Zr, Re, Lu, Hf Hg, Gd, Ir, Pr, Nd, Sm and Tb. In addition, the attainable sensitivity for several other elements that are frequently to be determined may be inadequate for their determination at the trace levels commonly encountered in samples to be analysed; these include As, Ge, Ti, V, Se and Te.

TABLE 14-1

Elements with principal resonance lines below 200 nm

Element	Line (nm)	Element	Line (nm)
F	95·5, 95·2	P	178·8, 178·3, 177·5
Cl	138·0, 134·7	S	182·6, 182·1, 180·7
Br	157·6, 148·9	As	197·3, 193·8, 189·0
I	183·0	Se	196·1
C	165·7, 156·1	Hg	184·9

In order to extend the range of application of AAS, and to increase the attainable sensitivity for those elements where it is inadequate for trace analysis, much attention has been devoted to the development of indirect methods of analysis for many of the elements listed above. In addition, some work has been reported for the application of indirect methods to permit the determination of organic species by AAS.

14.2.1 General Considerations

One of the principal advantages of direct methods of analysis by AAS is the high selectivity for particular elements in dilute solution. The success of indirect methods of analysis by AAS, and their applicability to practical analyses, depends on the degree to which the selectivity for the determination of the species concerned can be retained via the chemical reaction utilized before the final flame absorbance measurement. Even in those methods where some loss of selectivity is experienced owing to the nature of the initial chemical reaction employed, the ability to increase the sensitivity, or to achieve the AAS determination at all, is frequently of considerable value.

Several types of procedure may be employed in indirect determinations by AAS. In each of these the species to be determined is made to undergo a reaction with one or more other ions, and the concentration of the reaction product or of the unreacted excess of added reagent (which are directly and inversely proportional, respectively, to the concentration of the analyte species in the sample) is measured. The following specific types of procedure may be employed.

(1) Measurement of the suppression or enhancement of the atomic-absorption signal for a given element by its reaction in the flame with the species to be determined.

(2) Precipitation of the ion or compound to be determined by a second ion which is determined by AAS in the precipitate or filtrate.

(3) Formation of an ion-association or chelate complex between an organic compound or an anion to be determined and a metal or metal complex; the metal is then determined by AAS after extraction with an organic solvent.

(4) Formation of a binary or ternary heteropoly acid species between the analyte ion and other ions (one of which is usually molybdate), and determination of its concentration by AAS after separation of the complex by solvent extraction.

(5) Application of the reducing (or oxidizing) properties of the analyte species to yield an equivalent concentration of the lower (or higher) oxidation state of a metallic ion, only one oxidation state of which forms an extractable chelate complex, which may be determined by AAS.

Indirect AAS could be considered under these five headings, and this approach has been adopted elsewhere in reviews of indirect AAS methods.[1,2] However, as the analytical chemist is most frequently interested in the determination of a particular element or group of elements, indirect methods are classified here by the element determined.

14.2.2 Metals

Only rarely are the metallic elements not directly determinable by AAS; the indirect methods reported have therefore been concerned principally to provide increased sensitivity in their determination.

Aluminium

An indirect AAS method for aluminium has recently been reported.[3] The sensitivity obtained in the determination of iron by AAS is low in the fuel-rich air-acetylene flame. An enhancement of the absorbance for iron is observed in the presence of small amounts of aluminium when this fuel-rich flame is employed. The enhancement by aluminium of the absorbance produced on nebulization of a 25 ppm iron solution is linear with respect to the aluminium content of the solution in the range 0·25-1·2 ppm.

The sensitivity obtained in the determination of aluminium by this method may be varied by the nebulization of solutions containing different concentrations of iron; in this way with a 25 ppm iron solution the most sensitive working range for aluminium was found to be 0·01-0·09 ppm. Aluminium was also observed to enhance the absorbance of the elements cobalt, nickel and chromium in the flame employed. Titanium, calcium and zirconium at the same concentration levels as aluminium interfere with its determination. At concentrations equivalent to the iron concentration nickel and chromium interfere. The method is useful only for relatively pure aluminium solutions or analyses in which a separation procedure is included.

Germanium

The indirect determination of germanium by AAS, based on the formation of molybdogermanic acid (MGA) in which the molybdenum : germanium combining ratio is 12 : 1, has been described by Jakubiec and Boltz.[4] After its formation in hydrochloric acid solution at pH 1·5, the MGA complex is extracted with a mixture of 1-pentanol and diethyl ether (1 : 4 v/v). The complex is then back-extracted and decomposed by shaking the organic layer with an ammoniacal buffer at pH 9·3. The resulting molybdate may be measured by AAS at 313·2 nm in an air-acetylene flame. A sensitivity for germanium of 0·05 ppm was reported with linear calibrations up to 1·6 ppm. No interference was found for 500 ppm of Ca, Co, K, Mg, Mn, Na, Ni, Zn, acetate, chloride, perchlorate, nitrate or sulphate ions in the determination of 1·5 ppm of germanium. The maximum permissible concentrations of foreign ions for non-interference in the determination of 1·5 ppm of germanium were established as: Al, Cd, Cr(III), Cu, Mo(VI) 500 ppm; Pb 50 ppm; Fe(II), Fe(III), Ti(IV), Cr(VI), W(VI) 10 ppm; As(III), As(V), P(V) and Si interfered at any concentration.

Mercury

Mercury(II) may be converted into its anionic bromo-complex and extracted into 1,2-dichloroethane as an ion-association complex with the zinc 2,2-bipyridyl chelate cation. Yamamoto *et al.*[5] have reported the determination of the zinc content of the extract, which is equivalent to the mercury present in the sample, by AAS in an air-acetylene flame. The extraction was found to be quantitative between pH 3·5 and 5·5 and a linear calibration graph was obtained for 0·8 to 4·0 ppm of mercury in the initial aqueous phase with a sensitivity (for 1% Zn absorption) of 0·04 ppm of mercury. The following maximum permissible concentrations of foreign ions for non-interference with the determination of 2 ppm of mercury were established: Cu, 0·1 ppm; Co and I^-, 5 ppm; Cd, 15 ppm; Fe, 20 ppm; Pb, 200 ppm; Cl^-, 400 ppm.

Niobium

Kirkbright *et al.*[6] have utilized the formation of the ternary complex between niobium, phosphate and molybdate as the basis of an indirect method for the determination of niobium. The method is of the general type illustrated schematically in Fig. 14-1. As the

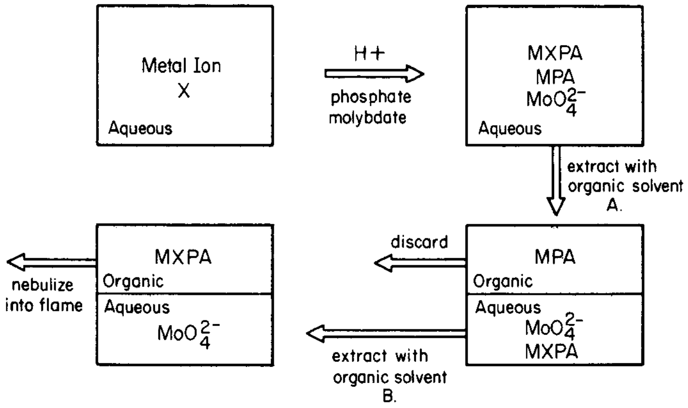

Fig. 14-1. General scheme for indirect determination of elements by AAS via formation of ternary heteropoly acids (MXPA) with phosphate and molybdate. MPA represents molybdophosphoric acid formed simultaneously with MXPA.

molybdoniobophosphoric acid (MNPA) cannot be formed in aqueous solution without the simultaneous formation of molybdophosphoric acid (MPA) a prior selective extraction of MPA is required. Both MPA and MNPA are formed in 0·5 M hydrochloric acid solution. The MPA may then be extracted with isobutyl acetate before extraction of MNPA into a single portion of n-butanol. The molybdenum associated with the niobium in the MNPA is then determined by direct AAS in the n-butanol phase which has been washed with dilute hydrochloric acid. A sensitivity of 0·015 ppm of niobium was reported, compared to a sensitivity by conventional direct AAS determination of 20 ppm for 1% absorption at the 334·4 nm line (Table 14-3); the calibration curve obtained was linear in the range 0·22-2·2 ppm of niobium. Out of twenty-seven ions studied for their interference with the determination of 1·3 ppm of niobium at the 30 to 700-fold weight ratio level, only As(V), Ge, Si, Ti, V(V) and Cr(VI) interfered. The method is sensitive because of the amplification accruing via the 11 : 1 combining ratio of molybdenum to niobium in MNPA and the "organic solvent effect" in the nebulizer of the flame spectrometer.

Thallium

Molybdophosphoric acid (MPA) has been used as a precipitant for thallium; the molybdate obtained by dissolution of the precipitate may be determined by AAS at 313·2 nm in an air-acetylene flame.[7] Thallium(I) is precipitated with MPA as $Tl_2HPMo_{12}O_{40}$ from 0·5 M perchloric acid medium. The precipitate is centrifuged, washed with perchloric acid and dissolved in 0·1 M sodium hydroxide solution. The molybdate equivalent to a definite amount of thallium is then determined. The optimum concentration range was found to be 2–20 ppm of thallium. The effect of other ions was not examined but as the method may also be used for the determination of ammonium by co-precipitation, this ion may thus interfere, as would other heavy metals which precipitate as molybdophosphates. As thallium can be determined by AAS in an air-acetylene flame with a sensitivity for 1% absorption of *ca.* 0·5 ppm at the 276·8 nm line it is doubtful whether, in view of the decreased selectivity, this method represents any advance on the direct method.

Thorium

Thorium may be determined indirectly by a method similar to that used for niobium.[8] Molybdothorophosphoric acid (MThPA) is formed in 0·15 M hydrochloric acid in the presence of excess MPA. The latter is then selectively extracted into isobutyl acetate and discarded. MThPA is extracted with n-butanol which is washed with butanol-saturated dilute hydrochloric acid. Although Kirkbright *et al.* claim to extract MThPA as such it is probable that only the MPA associated with the ternary complex was actually extracted; treatment with n-butanol has been shown to break down MThPA into thorium and MPA.[9,10] Eleven molybdenum atoms are associated with one thorium atom in the complex and the molybdenum is measured by AAS at 313·2 nm in a nitrous oxide-acetylene flame. A linear calibration curve is obtained for 1–6 ppm of thorium in the initial aqueous solution with a sensitivity of 0·063 ppm of thorium for 1% absorption. Only Zr, Fe(III), Si, As(V), Ti and Nb interfere seriously and required removal or masking.

Titanium

Titanium may be determined via its ternary heteropoly complex, molybdotitanophosphoric acid (MTPA).[11] The dissolution of the sample in hydrofluoric acid before the addition of phosphate, molybdate and acid requires the addition of aluminium to mask the excess of fluoride ion, which otherwise interferes in the determination. The excess of MPA is selectively extracted with chloroform : n-butanol (4 : 1 v/v) after formation of MTPA in 0·5 M hydrochloric acid. The MTPA is extracted with n-butanol which is then washed with butanol-saturated dilute hydrochloric acid before nebulization into a nitrous oxide-acetylene flame. Eleven molybdenum atoms are associated with two titanium atoms in the complex and the molybdenum is measured by AAS at 313·2 nm. A linear calibration curve is obtained for 0·3 to 3 ppm of titanium in the initial aqueous solution, corresponding to a sensitivity (for 1% Mo absorption) of 0·013 ppm of titanium. Interference is observed from As(V), Ge, Zr, Ta and Nb.

Ottaway *et al.*[12] have used the enhancement by titanium of the atomic absorption signal of iron in a fuel-rich air-acetylene flame to determine titanium in the range 0·01–10 ppm. The iron is nebulized as ferric sulphate in 10^{-3} M sulphuric acid. Chloride, calcium, aluminium and zirconium also give enhancements at similar concentrations. A method based on the suppression of the absorbance of strontium by titanium in the presence of oxalate ions when nebulized into a stoicheiometric air-acetylene flame has been used to determine titanium in the range 1 to 10 ppm.[13] The suppression is thought to be due to compound formation by strontium with titanium and oxalate. A solution 2×10^{-4} M in strontium and containing 100 ppm of oxalate, 10% by volume of hydrochloric acid, and the titanium, is nebulized into an air-acetylene flame. If the strontium concentration is increased higher ranges may be covered; these can, however, equally well be determined directly with a nitrous oxide-acetylene flame. A sensitivity of 0·15 ppm of titanium was recorded. Slight negative interference is experienced with EDTA, whereas Mn(II), Cu, Mg, Ca, Sn(IV) and Ni present at 200 ppm produce a small positive interference with 2 ppm of titanium. Al, Zr, H^+, Cr(III), PO_4^{3-} and F^- all interfere, and therefore the method has limited applicability but does allow determination of titanium in the presence of high hydrochloric acid concentrations. Titanium causes similar depressions in the absorbances of calcium and barium in the presence of oxalate but methods based on these effects are less sensitive.

Vanadium

Vanadium(V) has been determined indirectly by AAS via the formation of molybdovanadophosphoric acid (MVPA).[14,15] In the method of Jakubiec and Boltz[14] a mixed phosphate and molybdate reagent is added to an aliquot of the sample at pH 1·5–2·0. The excess of MPA is extracted with diethyl ether, and the MVPA complex is then extracted with an n-pentanol : diethyl ether mixture (1 : 4 v/v). The organic layer is washed with dilute hydrochloric acid, and the MVPA is decomposed by back-extraction into an ammonia-ammonium chloride buffer solution. The molybdate content of this solution, which is equivalent to the vanadium, is then determined in a reducing air-acetylene flame with a sensitivity for vanadium of 0·05 ppm for 1% absorption. The following ions caused interference in the determination of 2·17 ppm of vanadium at the concentrations indicated: Cr(III), NO_3^-, SO_4^{2-} 250 ppm, Cd, $C_2H_3O_2^-$, Cr(VI) 100 ppm; As(V), Sn(IV) 50 ppm; Ti, Si, W(VI) 10 ppm; Fe(III) 5 ppm; Fe(II) interfered at any concentration.

A method has been described which does not require back-extraction of MVPA from the organic solvent.[15] Phosphate and molybdate are added separately to the vanadium(V) solution to form MVPA in a 0·4 M nitric acid medium. An n-butanol : chloroform mixture (1 : 4 v/v) is used to extract the MPA selectively and has the advantage of forming the denser phase so that it is readily separated and discarded without the need for transfer of the sample solution. MVPA is extracted with n-butanol, which is then washed with butanol-saturated dilute acid and nebulized into a fuel-rich nitrous oxide-acetylene flame. Eleven molybdenum atoms are associated with each vanadium atom in the complex and the molybdenum is measured at 313·2 nm. A sensitivity (for 1% Mo absorption) of 0·011 ppm of vanadium was obtained with a linear calibration from 0·2 to 2·0 ppm. Interference with the determination of 0·8 ppm of vanadium was experienced from F^- (16 ppm), As(V), Sn(IV) (8 ppm); Cr(VI) (2·4 ppm); Zr (0·8 ppm); Ti and Si interfere at any concentration. A scheme has been recommended to improve the selectivity of the procedure in the presence of ions which form binary or ternary heteropolymolybdates. These ions are removed as their corresponding heteropoly acids before formation and extraction of MVPA. This is possible as vanadium exists both as V(IV) and V(V) and only V(V) apears to form the ternary heteropoly acid. Vanadium in aluminium has been determined in this manner.

14.2.3 Non-metals

Most of the published work that deals with indirect methods of analysis by AAS has been concerned with the determination of the non-metallic elements and other anionic species.

Arsenic

The reported indirect AAS methods for arsenic are all based on the formation of the binary heteropoly acid, molybdoarsenic acid (MAA). Danchik and Boltz[16] used bromine water to ensure that arsenic was present as As(V) before its reaction with molybdate at pH 1·8. The MAA was extracted with methyl isobutyl ketone (MIBK) which, after being washed with dilute hydrochloric acid, was shaken with a basic buffer solution to decompose and back-extract the MAA. The molybdenum associated with the arsenic was measured by AAS at 313·2 nm in an air-acetylene flame in the basic aqueous phase. A sensitivity of 0·07 ppm was achieved. Ramakrishna, Robinson and West[17] have described a method in which MAA formed at pH 0·9 is selectively extracted into an ethylacetate : butanol : isopentylacetate mixture (1 : 1 : 2 v/v) in the absence of MPA. A sensitivity of 0·025 ppm was reported for measurement of the associated molybdenum in a nitrous oxide-acetylene flame. The effect of 40-fold weight ratios of 40 ions was studied, none of which was found to interfere. Arsenic has been determined with a sensitivity of 1 ppm in urine.[18] In this procedure the MAA was formed at pH 1, MPA was extracted with isobutyl acetate and the pH was then increased to 2 before extraction of MAA with cyclohexane.

By judicious choice of the extraction system arsenic may be determined with high sensitivity and good selectivity via its heteropoly acid species with molybdate.

Fluorine

The presence of fluoride ion depresses the absorbance produced at 285·2 nm for magnesium in an air-coal gas flame; this effect may be utilized as the basis of an indirect AAS method.[19] The change in absorbance of the magnesium at 285·2 nm has been reported to be proportional to the fluoride concentration over the range 0·2-20 ppm of fluoride. When the concentration ratio of magnesium to fluoride in the sample solution reached 1 : 2 a constant absorbance was obtained. The method is subject to some interference, principally from phosphate and sulphate. Aluminium, oxalate and acetate also interfere at greater than 1000-fold molar ratio to fluoride.

An alternative, but less sensitive, technique based on the enhancement of zirconium absorbance by fluoride in a nitrous oxide-acetylene flame at 360·1 nm has been reported to allow the determination of fluoride in aqueous solution with a high degree of freedom from interference over the range 5-200 ppm.[19] Phosphate again interferes, but the similar enhancement observed for titanium absorption at 364·3 nm can be used for fluoride determinations in the range 40-400 ppm in the presence of phosphate.[19]

These indirect AAS methods for fluoride are considerably more rapid than the classical methods.

Chlorine

All the indirect AAS methods which have been described for the determination of chloride ion have been based on its reaction with silver nitrate. Either the excess of silver in the supernatant liquid is measured by AAS at 328 nm after removal of the silver chloride precipitate,[20-24] or the precipitate is redissolved in ammonia solution and the silver content of the ammoniacal solution is measured.[25,26,27] Chloride has been determined in serum,[20] plant liquors,[21] wine,[22] and polyvinyl chloride[23] by the first technique. A variation of this method involves the addition of a range of silver ion concentrations to aliquots of the sample containing chloride. After filtration the excess of silver in each filtrate is measured by AAS; a graph of absorbance *vs* silver concentration should then show a point of inflection at the concentration of silver equivalent to the chloride content of the original solution.

The first reported determination of chloride by AAS was based on precipitation of silver chloride, dissolution of the precipitate in ammonia solution and the determination of the silver in the resulting solution.[27] This method has been applied to the determination of chloride in titanium metal with an air-hydrogen flame[25] and to the determination of chlorine in selenium.[26]

Perchlorate

Perchlorate forms a complex with copper(I) and neocuproin (2,9-dimethyl-1,10-phenanthroline) corresponding to the composition $Cu(neocuproin)_2ClO_4$; this species is extractable into ethyl acetate. When the copper is determined by AAS at 324·7 nm the method may be applied to the determination of 12·5-125 μg of perchlorate with a sensitivity of 0·025 ppm.[28] In the determination of 3 ppm of perchlorate by this method Collinson and Boltz[28] observed interference when nitrate, ammonia, magnesium or aluminium was present at a concentration greater than 10 ppm.

Iodine

Iodine has been determined by AAS by use of a cadmium hollow-cathode lamp.[29,30] The method is based on solvent extraction into nitrobenzene of the ion-association complex formed between tris(1,10-phenanthroline)Cd(II) and iodide at pH 5; subsequent AAS determination of the cadmium content of the extract may then be made at 228·8 nm in an air-acetylene flame. The effect of a number of diverse anions upon the determination of 2×10^{-5} M iodide has been studied. Interference was experienced at concentrations greater than the molar ratios relative to cadmium indicated for the following ions: IO_4^- (0·02); ClO_3^-, ClO_4^- (0·03); NO_2^-, NO_3^- (0·1); Br^- (0·2); Cl^-, BrO_3^- (2); CN^- (10); IO_3^- (100); F^-, CO_3^{2-}, $B_4O_7^{2-}$ (1000). Christian and Feldman[31] have described the determination of iodide by utilization of its reducing action on a metal ion, coupled with extraction of the remaining oxidized form into an organic solvent and its estimation by AAS. Thus, for example, iodide reduces chromium(VI) in acid medium and the excess of chromium (VI) may be extracted from 3 M hydrochloric acid into MIBK. The absorbance of chromium(III) in the aqueous layer increases linearly and the absorbance of the unreacted chromium(VI) in the MIBK decreases linearly with increasing amounts of iodide. The reaction is slow and does not go to completion in dilute solutions. Interferences have not been studied but most reducing species, e.g. Fe^{2+}, would probably have a similar effect and thus interfere.

Selenium(IV) is reduced by iodide to elemental selenium in acid solution. When iodide is allowed to react with excess of selenium(IV) and the solution is filtered through a Millipore filter, the decrease in absorbance of the filtrate is proportional to the iodide ion concentration of the original sample solution.[31] Again, reducing species would be expected to interfere, though no results were reported for the effects of other ions.

Iodate

Iodate oxidizes iron(II) to iron(III) in acid medium; the iron(III) may be extracted into diethyl ether from 9 M hydrochloric acid solution. The absorbance of iron in the ether phase is then proportional to the iodate concentration. The solutions must be deaerated to prevent aerial oxidation. As with the reduction method for iodine, this method lacks specificity but may be useful when no other oxidizing species are present.

Nitrogen compounds

Ammonia. Bond and Willis[32] have used the enhancement of zirconium absorbance in a nitrous oxide-acetylene flame at 360·1 nm by nitrogen-containing compounds for the determination of ammonia. For ammonia, the magnitude of this enhancement was found to be proportional to the concentration of the base in the range 1×10^{-4} to 5×10^{-3} M and was used for its determination in the absence of phosphate and certain nitrogen-containing compounds. In the presence of interfering species, prior separation of the ammonia by distillation is required. The method has been applied to the determination of ammonia in biological systems.[32]

Danchik, Boltz and Hargis[7] have shown the co-precipitation of ammonium molybdophosphate with a known amount of thallium molybdophosphate and subsequent dissolution of the precipitate to provide the basis for an indirect AAS method for the determination of ammonia. The molybdate obtained by dissolution of the precipitate, which is equivalent to a known amount of thallium and ammonia, is determined at 313·2 nm in an air-acetylene flame. Molybdophosphoric acid is used as precipitant in 0·5 M perchloric acid. The method is unselective, as many heavy metals are precipitated as phosphomolybdates.

Cyanide. Cyanide may be determined via the equivalent silver associated with it in the $Ag(CN)_2^-$ complex.[33] Pieces of metallic silver are added to the solution containing the cyanide to be determined and the mixture is then shaken for one hour. The dissolved silver is determined by AAS to produce a rectilinear calibration graph for up to 3 ppm of cyanide ion. No interference is experienced from Br^-, I^-, SCN^- or SO_3^{2-} ions but $S_2O_3^{2-}$ enhances the signal. Danchik and Boltz[34] report two methods for the indirect determination of cyanide. The first is based on the formation and extraction of the dicyano-bis(1,10-phenanthroline)Fe(II) complex. The complex is extracted into chloroform, which is then evaporated, and the residue is dissolved in ethanol. The associated iron is determined by AAS in an air-acetylene flame at 248·3 nm. A sensitivity of 0·06 ppm of cyanide has been obtained by this method; the calibration graph is linear up to 5 ppm. Precipitation of silver cyanide and measurement of the excess of silver in the supernatant solution by AAS in an air-acetylene flame at 328·1 nm forms the basis of a second method. A working range of 0·3 to 2·5 ppm of cyanide has been reported with a sensitivity of 0·03 ppm.

Thiocyanate. Thiocyanate forms a dithiocyanatodipyridine copper(II) complex, $Cu_2(Py)_2(SCN)_2$, which is extractable with chloroform. The copper equivalent to the thiocyanate is determined at 324·7 nm. A sensitivity of 0·2 ppm of thiocyanate has been reported with an optimum concentration range of 7 to 18 ppm.[35] The sensitivity may be improved to 0·05 ppm by evaporating the chloroform solution almost to dryness and diluting with ethyl acetate. The optimum concentration range is then between 0·5 to 2·0 ppm.

Nitrate. A small amount of nitrate ion is extractable into MIBK when neocuproin (2,9-dimethyl-1,10-phenanthroline) is contained in the organic phase and copper(I) ions are present in the aqueous phase. The copper associated with nitrate ions in the complex, $Cu(I)(neocuproin)_2NO_3$, is measured in an air-acetylene flame at 324·7 nm.[36,37] Beer's Law is obeyed in the range 1 to 7×10^{-5} M nitrate in the aqueous phase. Nitrite and nitro-groups in organic compounds may also be determined via formation of the ion-pair with the Cu(I) neocuproin complex after their oxidation to nitrate with ceric sulphate or potassium permanganate.[38] The complex may be extracted into MIBK before measurement of the associated copper. Prior reduction of nitrite and nitro groups to amino groups by sulphamic acid permits determination of nitrate in the presence of such groups.

Phosphorus

Orthophosphate has been determined indirectly, mainly via the formation of molybdophosphoric acid (MPA) in the presence of molybdate in acid solution. The general procedure most frequently employed is illustrated in Fig. 14-2. Molybdate (ammonium or sodium salt) is added to the sample solution containing orthophosphate and the acidity is adjusted to its optimum value. The solution is mixed and allowed to stand for 5-10 minutes to ensure complete formation of MPA. The MPA is then extracted into an organic solvent which is washed either with dilute acid[39,40] to remove molybdate transferred to the organic layer, or with citrate solution to complex the excess of molybdate.[43,44] The molybdate associated with the phosphate in the complex is measured by AAS at 313·2 nm in an air-acetylene[40,46] or a nitrous oxide-acetylene flame.[17,39,47] Kumamaru *et al.*[47] employed 0·5 N hydrochloric acid to form MPA and performed the extraction with n-butyl acetate to obtain a linear, calibration graph up to 0·35 ppm of phosphorus. A general method for the determination of inorganic phosphate using 2-octanol as a solvent[44] has been applied to the determination of phosphate in fresh-water and sea-water and in blood, serum, bone, biological tissues and enzyme-containing reaction mixtures.[45] 2-Octanol was chosen as solvent after examination of n-butanol, isobutyl alcohol, 1-hexanol, 1-heptanol, 1-octanol and 2-octanol.[45] Phosphate has been determined in urine, the MPA being formed in 0·37 M hydrochloric acid and extracted into isobutyl acetate.[41] Linden *et al.*[42] have determined phosphorus in milk products and blood serum via MPA, using perchloric acid medium and MIBK as solvent, for the range 100-200 μg of phosphorus. The results obtained agreed with those established colorimetrically. Phosphate has been determined in small (0·2 ml) samples of plasma.[43] The MPA is formed at pH 1·9 in a DL-α-alanine-hydrochloric acid buffer and is extracted with MIBK. The authors claim to extract MPA with an Mo : P ratio of 15 : 1. No evidence concerning the establishment of this apparently anomalous combining ratio is given. The procedure is applicable to the determination of between 5 and 200 ppm of phosphorus.

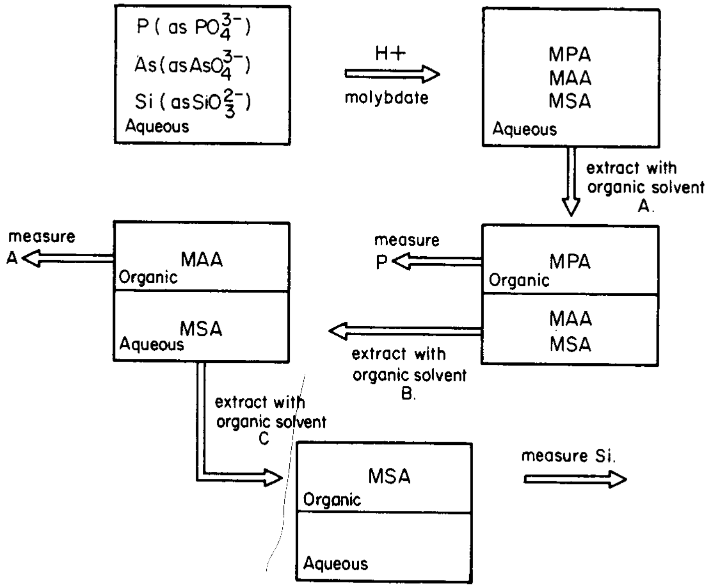

Fig. 14-2. General scheme for indirect determination of elements by AAS via formation of heteropoly acid species with molybdate.

Several schemes have been devised for the sequential determination of phosphorus, arsenic and silicon,[17] phosphorus and arsenic,[18] and phosphorus and silicon[39,40] (Fig. 14-2). All are based on the ability to extract MPA selectively. Thus MPA has been selectively extracted with isobutyl acetate after formation at pH 0·7 in nitric acid medium, to result in a final sensitivity of 0·01 ppm of phosphorus.[17] Devoto[18] used isobutyl acetate to extract MPA formed at pH 1 in an ammonium nitrate-nitric acid medium. Isobutyl acetate has also been used by Kirkbright *et al.*[39] to selectively extract MPA formed at an acidity of 0·96 M in hydrochloric acid in a single portion of solution containing phosphate and silicate, before formation of molybdosilicic acid (MSA). A sensitivity of 0·007 ppm of phosphorus and rectilinear calibration from 0·08 to 1 ppm of phosphorus were obtained by measuring the associated molybdate in the organic phase at 313·2 nm in a nitrous oxide-acetylene flame. Only W(VI) is reported to interfere out of 26 ions examined. MPA formed at pH 1·3 has also been extracted from 1·2 M hydrochloric acid medium with diethyl ether.[40] After being washed with dilute hydrochloric acid, the organic layer may be shaken with an ammoniacal buffer and the molybdate released measured in the aqueous phase by AAS in an air-acetylene flame. The optimum concentration range reported is 0·05 to 1·3 ppm of phosphorus. The use of isobutyl acetate coupled with the formation of MPA produces an extremely selective method for the determination of phosphorus by indirect AAS.

Phosphorus has been determined by several workers using the direct chemical interference of phosphate on a metal species in a flame to produce a depression of the absorption, which is a function of the phosphate concentration.[31,48,49] Orthophosphate up to $2{\cdot}5 \times 10^{-4}$ M added to 5×10^{-4} M calcium solution produces a marked depression in the absorbance obtained for calcium at 427·7 nm with a total consumption burner.[31] The limiting concentration of phosphate may be increased by increasing the calcium concentration. Singhal *et al.* have determined phosphorus in rock phosphate by depression of both calcium[49] and strontium[48] absorbance. In both cases the powdered rock phosphate is treated with a cation-exchange resin (H^+-form) before addition of calcium or strontium solution. A modification of the quinolinium molybdophosphate method has been proposed whereby total phosphorus is determined indirectly by the AAS measurement of molybdenum.[50] The familiar and well-tried gravimetric method is followed to the stage where the quinolinium molybdophosphate is formed. The precipitate is then dissolved in ammonia solution and the molybdenum determined by AAS at 313·2 nm. The method has been applied to the phosphorus analysis of Magruder collaborative fertilizer samples.[50]

Selenium

Selenium may be difficult to determine directly with high sensitivity by AAS in some flames because of strong absorption of the resonance radiation at 196 nm by the flame and optical components of the spectrometer. An indirect method has been described based on two selective reactions of selenite with 2,3-diaminonaphthalene (DAN) and palladium(II) to form the complex $Pd(DANSe)_2Cl_2$.[51] When excess of DAN is added to a solution of selenite at pH 1·5-2·5 the following reaction occurs:

(I) $C_{10}H_6(NH_2)_2 + SeO_3^{2-} + 2H_3O^+ \rightarrow C_{10}H_6N_2Se + 5H_2O$

In the presence of palladium chloride three further reactions are possible:

(II) $2\,DANSe + PdCl_2 \xrightarrow{pH \leqslant 6} Pd(DANSe)_2Cl_2$(purple)

(III) $2\,DANSe + 2PdCl_2 \xrightarrow{pH \leqslant 6} Pd_2(DANSe)_2Cl_4$(green)

(IV) $DAN + PdCl_2 \xrightarrow{pH\ 0\text{-}12}$ white polymeric complex.

Whether it is reaction II or III that occurs depends on the pH, relative concentration of reagents and also on the solvent used for the DANSe. Reaction IV always occurs and thus DANSe is removed from excess of DAN by extraction with chloroform. With chloroform as solvent the complex from reaction III is formed. The optimum calibration is from 0·05 to 1 ppm of selenium. A sensitivity of 0·017 ppm has been obtained. A study of the effect of 60-fold molar ratios of 50 ions on the determination of 0·5 ppm of selenium showed only Fe(III), Sn(IV) and Ce(IV) to interfere.

Silicon

Most indirect methods for silicon are based on the formation of molybdosilicic acid (MSA).[17,39,40,52] In one case MSA is formed at pH 1·3, extracted with a 1-pentanol : diethyl ether mixture (1 : 5 v/v) from 2M hydrochloric acid medium, and decomposed by back-extraction into a 0·1 M ammonia solution.[52] A known excess of lead(II) ion is then added to the aqueous solution to precipitate the molybdate as lead molybdate in amount equivalent to the amount of silicon present. The lead remaining in solution may be measured by AAS at 217·1 nm in an air-acetylene flame. An optimum concentration range of 0·005 to 0·07 ppm of silicon has been reported.[52] No interference was experienced from 500 ppm of Al^{3+}, NH_4^+, Fe^{3+}, Mg^{2+}, Cl^-, NO_3^-, ClO_4^- or SO_4^{2-}.

Silicon has also been determined sequentially with phosphorus[39,40] and arsenic[17] by using their respective molybdoheteropoly acids (Fig. 14-2). Kirkbright *et al.*[39] first investigated the determination of silicon by this means. They determined phosphorus as phosphate by forming MPA in 0·96 M hydrochloric acid medium and selectively extracting it into isobutyl acetate. The silicon in the same aliquot of solution is determined after the MPA extraction by adjusting the acidity of the solution of 0·15 M hydrochloric acid with 4 M ammonia solution to allow efficient formation of MSA. The MSA may then be extracted into n-butanol and the twelve molybdenum atoms associated with each silicon atom determined by AAS at 313·2 nm in a nitrous oxide-acetylene flame. A sensitivity of 0·008 ppm of silicon and an optimum concentration of 0·08 to 1 ppm of silicon are obtainable. The presence of a 100-fold weight ratio of 24 ions causes no interference in the determination of 12 μg of silicon; only arsenic(V) and germanium(IV) interfere by formation of their respective heteropoly acids. Hurford and Boltz[40] have described a similar sequential procedure in which the MSA is formed at pH 1·3 after the MPA has been extracted and is then extracted from 2 M hydrochloric acid medium with a 1-pentanol : diethyl ether mixture (1 : 5 v/v). After being washed with dilute hydrochloric acid the organic layer is shaken with basic buffer solution which extracts and decomposes the MSA. In this method the molybdenum is then measured in an air-acetylene flame. A calibration range between 0·05 and 1·1 ppm is obtained. Ramakrishna *et al.*[17] have separated MSA formed at pH 0·7 from large amounts of MPA and molybdoarsenic acid by extraction into MIBK in the presence of citrate. A sensitivity of 0·01 ppm of silicon is then obtainable, the optimum concentration range being from 0·1 to 1 ppm. Of 40 ions tested only germanium(IV) interferes with the determination of silicon.

Silicate has been determined in waste waters by atomic-absorption inhibition titration.[53] The method is based on the strong inhibition by silicate of the magnesium absorbance produced in an air-hydrogen flame. The absorbance is measured continuously while the nebulized solution is titrated; this procedure contrasts with the usual direct suppression methods when discrete sample solutions are nebulized. The sample is adjusted to pH 3-4 and passed through a cation-exchange resin (H^+-form) to remove magnesium and other interfering cations. The eluate from the column is titrated with standard magnesium solution and the titrated solution is simultaneously nebulized into an air-hydrogen flame. The end-point is detected by a sharp increase in the magnesium absorption signal at 285·2 nm. High accuracy and precision are obtained with a limit of detection of 0·1 ppm of silica. The removal of cations by ion-exchange ensures the selectivity of the method.

Sulphur

The first reported indirect AAS method for sulphur is based on the precipitation of barium sulphate on addition of excess of barium chloride to the sample solution. In this method the precipitate is dissolved in a solution of disodium EDTA and the resulting barium concentration is determined at 553·5 nm in an air-acetylene flame.[54] Lanthanum is added to prevent phosphate interference. The method has been used to estimate sulphur in urine, faeces and biological tissues after oxidation by one of several techniques.

In a procedure that avoids the necessity to dissolve the barium sulphate precipitate, a known excess of barium is added to the sample solution, and the excess is determined after the precipitation of barium sulphate.[55,56] A 0·02M hydrochloric acid medium is used to minimize loss of selectivity through co-precipitation of other ions. The error caused by the partial solubility of the precipitated barium sulphate and the incomplete reaction is overcome by calibration against standard sulphate solutions treated in a similar manner. The method has been applied to the determination of sulphate in textiles.[56] A similar method has been applied to the determination of water-soluble sulphate in acidic sulphate soils.[57] Calcium and phosphate above 30 and 10 ppm respectively interfere with the determination of 50 ppm of sulphate. A sensitivity of 1·5 ppm of sulphur has been reported for a method that involves precipitation of sulphate with barium chloride, centrifugation and measurement of the excess of barium.[58] An improvement in sensitivity is claimed to be achieved by reduction of the concentration or volume of the barium chloride solution added. The method has been applied to determination of sulphur in samples from deep mine waste water which have a high cation and sulphate concentration, and in the percolate from pyrite-bearing coalmine spoils. Good correlation has been reported between the results of the indirect AAS method and standard methods.

Sulphur in soils derived from volcanic ash is extracted with potassium dihydrogen phosphate solution; the extracted sulphur is converted into sulphate, and the organic matter is destroyed with 30% hydrogen peroxide solution and sulphate is precipitated with 15% barium chloride solution. The barium sulphate may be dissolved in a solution of EDTA (diammonium salt), and the barium measured by AAS in the presence of 1500 ppm of sodium ions to suppress barium ionization, to give a sensitivity (1% absorption) of 0·8 ppm of sulphur.[59]

Sulphur dioxide, after its preliminary conversion into sulphate with hydrogen peroxide, has been determined after precipitation and centrifugation of lead sulphate.[60] The excess of lead remaining in the supernatant liquid may be measured at 283·3 nm in an air-acetylene flame. The solution is made 25% with respect to ethanol to aid the precipitation of lead sulphate. A concentration range of 2 to 20 ppm of sulphur dioxide was recommended. Interference was experienced above the concentrations shown for the determination of 5 ppm of sulphur dioxide with the following ions Fe(III), PO_4^{3-} (0 ppm); Ba, Al (10 ppm); EDTA (20 ppm), $CH_3CO_2^-$ (250 ppm).

Sulphite or sulphur dioxide have been measured by AAS, with utilization of the high stability of the $Hg(SO_3)_2^{2-}$ complex.[61] Addition of sulphite ions to a suspension of mercury(II) oxide leads to dissolution of the oxide and formation of the soluble complex.

The amount of oxide dissolved is proportional to the increase in absorbance at 253·7 nm observed for mercury in the supernatant fluid, and is then indicative of sulphite concentration. An optimum concentration range of 12 to 84 ppm of sulphite ions (10 to 77 ppm of sulphur dioxide) with a sensitivity of 13 ppm of sulphite has been reported. The reaction is not specific and iodide, thiosulphate and thiocyanate interfere.

Sulphate has been determined by atomic-absorption inhibition titration.[62] The test solution containing 0·05-1 mg of sulphate is titrated at a constant delivery rate with standard magnesium chloride solution. The titrated solution is simultaneously nebulized into an air-hydrogen flame. The magnesium absorbance is inhibited until the concentration ratio of magnesium to sulphate approaches unity. Thereafter the graph representing increasing magnesium content becomes rectilinear and extrapolation to the base-line is used to locate the end-point. Interfering cations such as those of the alkaline earths metals are removed by passing the solution at pH 3-4 through a cation-exchanger (H^+-form). Silicate and phosphate interfere.

14.2.4 Organic Compounds

No systematic study of the determination of organic compounds by AAS appears to have been undertaken. Of the methods reported some are extremely selective and rely on the formation of a particular complex and its subsequent extraction,[63-66] while others utilize a more general reaction which can be applied for the determination of a range of compounds.[17,67]

2-Hydroxynaphthoic acid has been determined indirectly through the selective extraction of tris(1,10-phenanthroline)Ni(II)-2-hydroxynaphthoate into nitrobenzene.[66] Measurement of the nickel concentration by AAS in an air-acetylene flame as a function of the 2-hydroxynaphthoic acid concentration initially present in the aqueous phase leads to a calibration that is linear in the range from 8×10^{-5} to 4×10^{-4} M 2-hydroxynaphthoic acid. No interference is experienced from 2-naphthol.

Phthalic acid is extractable into MIBK as the ion-pair formed between bis(neocuproin) Cu(I) and the univalent anion of phthalic acid. The copper extracted is determined by AAS in an air-acetylene flame at 324·7 nm. The absorbance of the extract gives a linear relationship with the phthalic acid concentration initially present in the aqueous phase in the range 4×10^{-6} to 4×10^{-5} M.[63,64] Isophthalic and terephthalic acid do not interfere if present in amounts equimolar with the phthalic acid.

A similar method has been employed for the determination of pentachlorophenol.[65] The basis of the method is the solvent extraction into nitrobenzene of the ion-pair formed between tris(1,10-phenanthroline)Fe(III) and the pentachlorophenol anion. The iron is subsequently determined in the extract by AAS at 248·3 nm in an air-acetylene flame. A concentration range up to 3×10^{-4} M in pentachlorophenol was studied.

Vitamin B_{12} contains one atom of cobalt per molecule. On dissolution of the vitamin the cobalt may be determined by AAS at 242·5 nm. The method has formed the basis for the determination of vitamin B_{12} in pharmaceutical dosage forms.[68,69]

Christian and Feldman[31] have determined several organic compounds by a variety of methods. Glucose oxidase and ribonuclease may be determined by their depressive effect on the absorbance of calcium. The upper concentration can be increased by raising the calcium concentration. Glucose below 10^{-6} M is found to produce a marked decrease in the absorbance obtained for calcium, but above that concentration it produces an increase, up to a limiting concentration of 10^{-5} M. Glucose in the range 10^{-6} to 5×10^{-5} M was also found to give a linear enhancement in the calcium absorbance which had been depressed by the addition of a constant amount of sulphate to the solution. Ammonium pyrrolidine dithiocarbamate (APDC) has been determined by measurement of the equivalent amount of copper or cobalt with which it complexes; the complex is extracted into MIBK at pH 3. With 1 ml of 1% metal ion solution a concentration of 10^{-5} M APDC may be determined. Similarly oxine is determinable via extraction of its copper complex into MIBK or ethyl acetate from an ammonium acetate buffer at pH 6·5 and subsequent AAS measurement of the copper. With 1 ml of 10^{-4} M copper solution a concentration of 2×10^{-5} M oxine is determinable. EDTA may be determined through its action as a masking agent for the copper oxinate chelate. The decrease in absorbance of the extracted copper is proportional to the concentration of EDTA in the initial aqueous phase.

Sugar in plant materials has been determined by measurement of unreduced copper.[70] Copper is reduced in alkaline solution by the reducing sugars to form insoluble copper(I) oxide. The copper(I) oxide is centrifuged from solution and the unreduced copper(II) in solution is measured by AAS. The concentration of sugar in test solutions is determined from standard graphs prepared from known amounts of sugar.

Several organic compounds have been determined by precipitation of their silver compounds and measurement by AAS of the concentration of the excess of silver left in solution.[67] Thus iodoform, theobromine, sodium salicylate, mercaptobenzothiazole and xanthate have all been determined in this way.[67]

Non-ionic surfactants may be determined indirectly by AAS.[71,72] In one method the surfactant is precipitated as the MPA-Ba complex and the molybdenum in the supernatant liquid is assayed by AAS.[71] The molybdenum concentration is related to the quantity of surfactant by an empirical factor which must be determined for each batch and multicomponent system owing to the non-stoicheiometric nature of the precipitate. A somewhat better method, which does not require the introduction of an empirical factor, has been developed.[72] The basis is the extraction of a cobaltithiocyanate-surfactant adduct from aqueous solution into benzene, and measurement of the associated cobalt in the benzene by AAS. Pollution by non-ionic surfactants in the Atlantic has been estimated in this way with a precision better than 10%.

14.2.5 Conclusion

As shown in Table 14-2, indirect AAS methods have been reported for the determination of inorganic cations and anions in solution as well as for the organic species described above. Tables 14-3 and 14-4 illustrate that the sensitivities obtainable are usually clearly superior to those in the corresponding direct AAS determinations, where these are possible; with careful choice of experimental conditions many of the indirect methods reported exhibit sufficient selectivity for the analyte species to be applicable for practical analyses. Although several workers have described the direct determination of elements such as carbon,[73] phosphorus,[73,74] sulphur and iodine[74] in non-flame cells, and sulphur[75] and iodine[76] in the inert gas-separated nitrous oxide-acetylene flame, using the resonance lines of

TABLE 14-2

Summary of available indirect AAS methods for elements

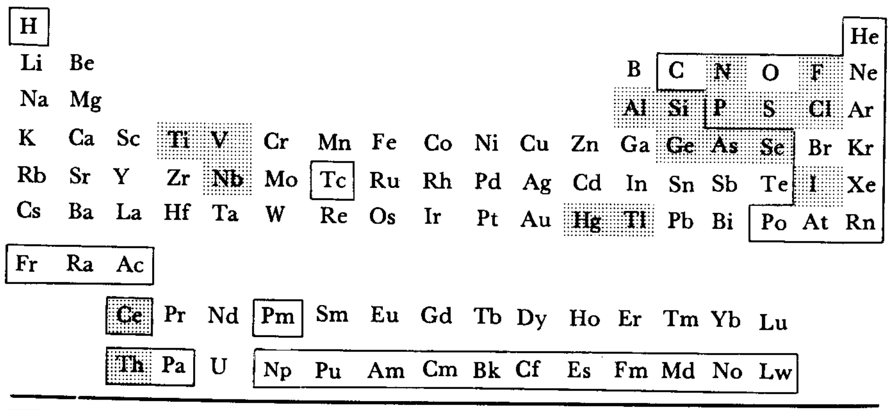

☐ Not determined by AAS with conventional equipment.

▨ Determinable by indirect AAS procedures.

TABLE 14-3

Indirect AAS methods based on formation of molybdo-heteropoly compounds

Element	Sensitivity[a] Indirect	Sensitivity[a] Direct[b]	Range, indirect, ppm	Ref.
P	0·003	250	0·04-2	44
As	0·025	0·25	0·2-2	17
Ge	0·05	2·5	0·1·6	4
Si	0·008	2·0	0·08-1·2	39
V	0·011	1·5	0·2-2	15
Nb	0·015	20	0·22-2·2	6
Th	0·063	—	1-6	8
Ti	0·013	2·0	0·3-3	11

[a] Concentration in ppm for 1% absorption

[b] From Perkin-Elmer Methods Book.

TABLE 14-4

Indirect methods based on miscellaneous procedures

Element	Sensitivity[a] Indirect	Sensitivity[a] Direct	Range, indirect, ppm	Ref.
Al		1·3	0·01-10	3
Hg	0·04	11	0·8-4	5
Tl		0·45	2-20	7
Se	0·017	2	0·05-1	51
F			0·2-20	19
Cl			0-0·4	25
ClO_4	0·025		0·5-5	28
I			0·5-5	30
CN	0·03		0·3-2·5	34
SCN	0·2		7-18	35

[a] Concentration in ppm to give 1% absorption.

these elements in the vacuum ultraviolet, these procedures require modified or specialized instrumentation and have not yet found widespread application.

14.3 ISOTOPE ANALYSIS BY ATOMIC ABSORPTION SPECTROSCOPY

Atomic absorption spectrometry may be utilized to advantage in the study of the isotopic composition of various elements. In order to view the isotopic splitting and hyperfine structure components of atomic lines by emission spectroscopy instrumentation of high resolving power is required and the broadening processes occurring in the source must be minimized. While for many elements the latter requirement also holds for AAS measurements, by this technique isotopic composition may be studied with apparatus of modest resolving power similar to that employed in many commercially available atomic absorption spectrophotometers.

The general approach involves the use of a light source emitting radiation of a single isotope of the element studied and measurement of the absorption of this radiation at one of the ground state lines of this isotope by an atomic vapour of the sample isotope mixture produced in a flame or non-flame cell. Alternatively the sample isotope mixture itself may be used in a light source such as a sputtering cell or high-frequency electrodeless discharge lamp. The absorption of the radiation emitted by one of the isotopes in the sample is then observed for the atomic vapour produced from a single isotope of the element (usually in a non-flame absorption cell).

Whichever method is employed the wavelength separation between the lines for the two or more isotopes of the element studied must be sufficient to preclude significant "spectral overlap" of the emission and absorption profiles. In order to achieve this it may be necessary to operate the radiation source and absorber cell at low pressure, temperature and optical thickness to achieve narrow line profiles. L'Vov[77] has concluded that isotopic analysis is only possible for twelve elements; this was deduced from a consideration of the isotope shift of the resonance lines of various elements and an estimate of the degree of overlap between the isotope components assuming minimal Doppler broadening in a hollow-cathode source cooled with liquid nitrogen. The elements for which isotopic analysis is possible under these conditions are Ar, B, He, Hg, Li, Ne, Os, Pb, Pt, Re, Tl and U. While some of these elements (e.g. the rare gases,

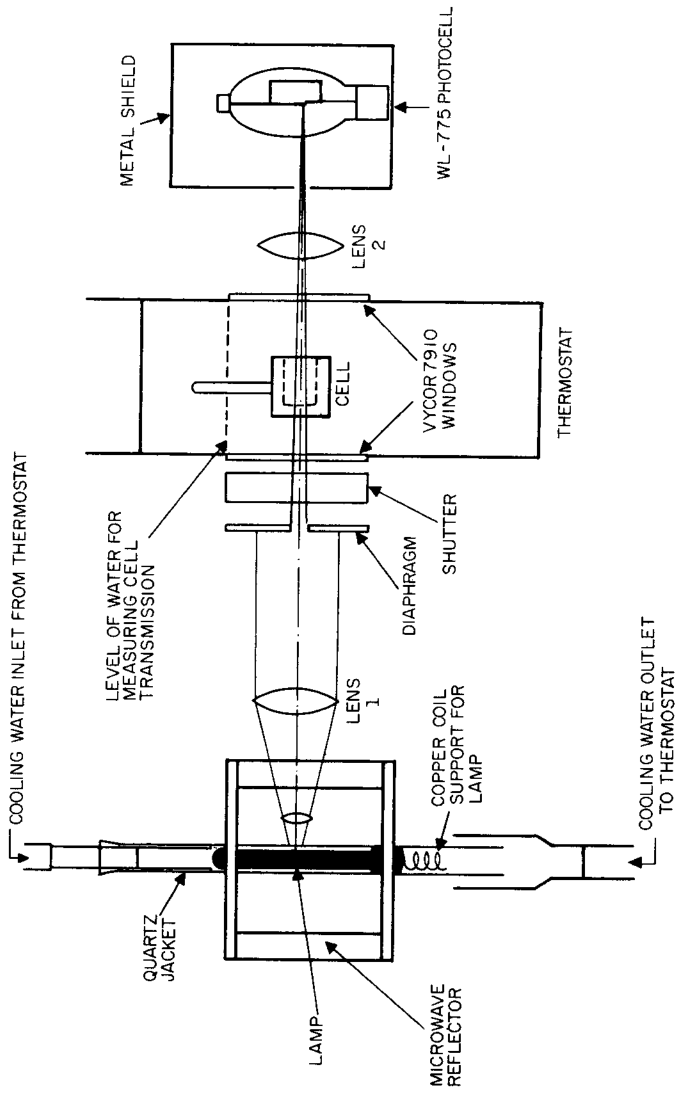

Fig. 14-3. Optical system for mercury isotope AAS used by Osborn and Gunning.[78]

Hg and Li) are either already monatomic gases or easily converted into atomic vapour in low temperature emission or absorption cells for isotopic measurements, others (e.g. B, Os, Pt) are less readily atomized and few observations of their isotopic composition have been made by AAS. The following section reviews briefly the application of AAS to the study of isotopic composition of the more easily atomized elements.

Mercury

AAS was applied to the determination of the Hg^{202} isotope in mercury by Osborn and Gunning.[78] As shown in Fig. 14-3 these workers employed as the light source a water-cooled microwave-excited electrodeless-discharge lamp containing the Hg^{202} isotope. Radiation at the Hg 253·7 nm line was passed through the vapour of the mercury sample contained in a silica cell maintained at a constant temperature which could be varied between 12 and 40°C. Under these conditions there was little overlap between the Hg^{202} emission line and the absorption lines of the other mercury isotopes; the results obtained for Hg samples containing widely differing concentrations of the Hg^{202} isotope were in good agreement with those obtained by mass spectrometry.

Lead

Kirchof[79] has described a method for the determination of the stable isotopes of lead by using the absorption of the hyperfine components of the Pb 283·3 and 405·8 nm resonance lines. Samples and standards containing known isotopic mixtures were incorporated into hollow cathodes used as primary radiation sources. The Pb^{208} (or Pb^{206}) content in the sample could be determined by measuring the absorbance of this radiation by lead vapour known to contain only Pb^{208} (or Pb^{206}). The absorbing vapour was produced by cathodic sputtering in a second hollow-cathode discharge. Figure 14-4 shows the absorption calibration curves obtained for Pb^{208}; the Pb 283·3 nm resonance line from the source hollow-cathode containing a Pb^{206}/Pb^{208} mixture is here absorbed by atomic vapour of the Pb^{208} isotope in the absorption cell. The absorption sensitivity is seen to be proportional to the concentration of the Pb^{208} isotope and to the operating current in the absorption cell. The examination by this technique of various geological samples containing varying Pb^{208} and Pb^{206} concentrations gave results which were in good agreement with those obtained by mass spectrometry.

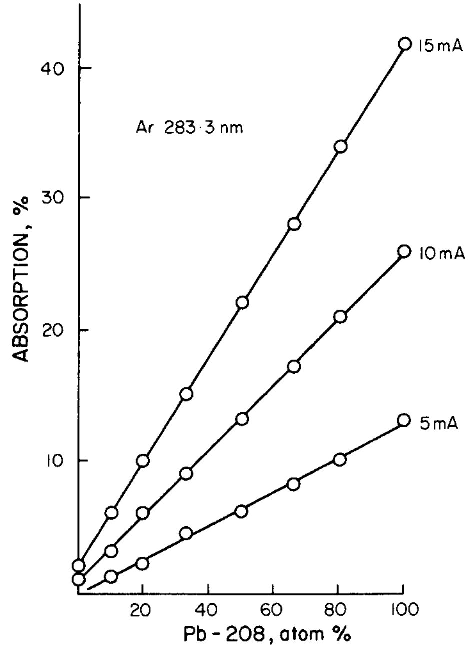

Fig. 14-4. Variations of absorption with Pb^{208} content of the Pb 283·3 nm resonance line from a Pb^{206}/Pb^{208} hollow-cathode source by Pb^{208} in a hollow-cathode absorption cell. Current values are those for the absorption cell. Argon carrier gas pressure 1·5 torr.

Brimhall[80] has demonstrated that it is possible to utilize a conventional long path air-acetylene flame for examination of the isotopic composition of lead sample solutions using a commercially available flame spectrophotometer and three different hollow-cathode lamps each enriched with a particular isotope. Three aqueous standard solutions, each likewise enriched in one of the three lead isotopes and containing a total of 10 ppm Pb were also employed. Figure 14-5 shows the instrument response obtained for each standard solution using each of the three sources. The absorption signal is dependent on the isotopic composition of the solution examined although overlapping absorption occurs. From the absorption signals measured using each of the three sources, it is possible to calculate the isotopic concentrations in a sample solution by solving a set of three simple simultaneous equations.

Lithium

The lithium 670·8 nm line is a doublet ($^2P_{3/2} \rightarrow {}^2S_{1/2}$, $^2P_{1/2} \rightarrow {}^2S_{1/2}$) in which the two components have a separation of approximately 350 mK (0·015 nm). The isotope shift between Li^6 and Li^7 is

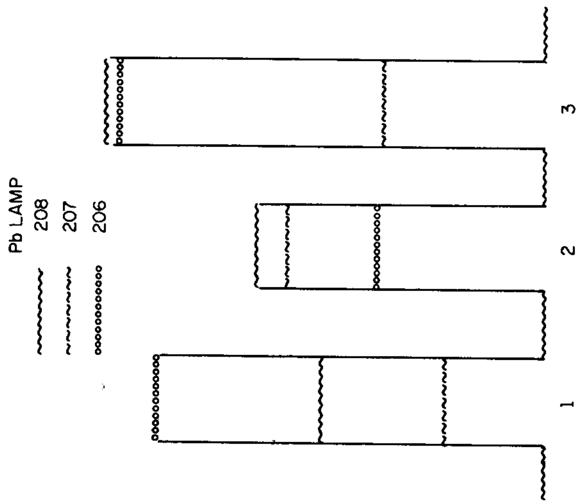

Standard	Concentration of isotope, ppm		
	Pb^{206}	Pb^{207}	Pb^{208}
1.	9·74	0·069	0·192
2.	0·216	9·240	0·548
3.	0·012	0·041	9·947

Fig. 14-5. Absorption response obtained for standard solutions 1, 2 and 3 for hollow-cathode lamps enriched in Pb^{206}, Pb^{207} and Pb^{208} respectively.

also near to this value; one of the Li^6 hyperfine components is therefore almost exactly coincident with one of the Li^7 lines (see Fig. 14-6). Even with a sharp line source of a single lithium isotope and a narrow absorption line profile in a suitable absorbing cell, spectral overlap interference results in the absorption of Li^6 radiation by Li^7 and vice versa. In early work Zaidel and Korennoi[81] described a method for lithium isotope analysis in which the radiation from Li^6 or Li^7 enriched hollow-cathode lamp sources absorbed by the lithium sample nebulized into an air-acetylene flame was measured. The difficulty of the overlap of the Li^6 and Li^7 lines was overcome by making simultaneous measurement of the total lithium content of the flame by flame emission spectroscopy; the isotope composition of samples was determined using standards of known composition to prepare calibration graphs on which Li^6 or Li^7 absorbance was plotted versus the relative concentration of Li^6 (i.e. $[Li^6]/[Li^6]+[Li^7]$).

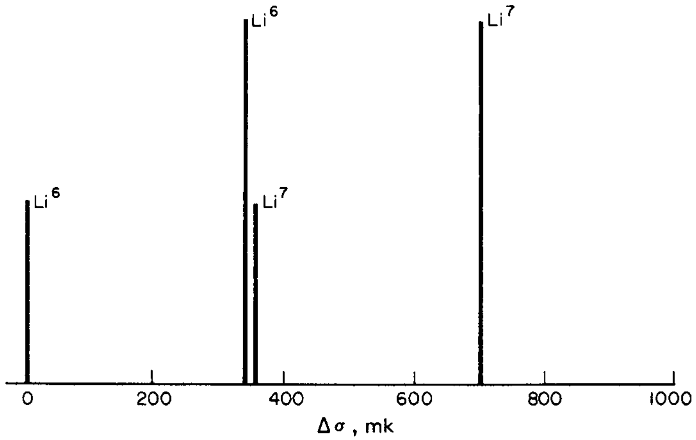

Fig. 14-6. Fine structure of the lithium 670·8 nm doublet.

In another study of lithium isotope composition Zaidel and Korennoi[82] utilized the technique of "isotope filtration". In this method the lithium sample was introduced into the flame and the total line emission at 670·8 nm from both isotopes was passed through Li^7 vapour contained in a heated tube. The Li^7 vapour absorbs the radiation emitted by the Li^7 isotope in the flame and also part of that from the Li^6 isotope owing to the absorption overlap. The Li^6 isotope is then determined from a calibration graph of the intensity of the transmitted (Li^6) radiation versus Li^6

concentration; linear calibration graphs were obtained over the range 2 to 91% Li^{6}.

Manning and Slavin[83] have described the determination of Li^{6} and Li^{7} by AAS using an air-acetylene flame as the absorption cell and an oxy-hydrogen source flame into which Li^{6} and Li^{7} isotopes were introduced separately and alternately. These workers observed that small variations in the total lithium content of sample solutions did not significantly affect the accuracy of the determination. Manning and Slavin have also reported work in which excess Li^{7} isotope was added to the sampling flame to absorb the strong Li^{6} component (at the weaker overlapping Li^{7} absorption line) from the Li^{6} emission in the source flame. The measured and known absorption by the excess Li^{7} was subtracted from the absorption produced by the sample containing excess Li^{7}; the net absorbance with a Li^{6} source flame after the subtraction is attributable to Li^{6} in the sample. Between 0·0001 and 0·1% Li^{6} may be determined in this way.

Goleb and Yokoyama[84] have determined the natural abundance ratio Li^{7}/Li^{6} by AAS using Li^{6} and Li^{7} in separate water-cooled hollow cathodes as the light sources, and a Schüler-Gollnow water-cooled hollow-cathode sputtering chamber to atomize samples. Li^{6} and Li^{7} absorption readings were obtained by passing radiation from each source independently through the sputtering chamber containing vapour of either samples or standards. The analytical calibration graph was established by plotting the ratio of the absorbances for Li^{6} and Li^{7} against Li^{6} concentration; over the narrow range of concentrations studied (2·5 to 10% Li^{6}) a straight line calibration graph was obtained. The result obtained for the Li^{7}/Li^{6} natural abundance ratio (12·1 ± 3·3%) compared favourably with the mass spectrometric value of 12·3.

Uranium

The determination of U^{238} and U^{235} isotopes by AAS has been described by Goleb.[85,86] In an early paper the U 591·54 and 502·74 nm lines, for which the isotope shifts are 0·007 nm and 0·01 nm respectively, were employed. With these large isotope shifts no absorption overlap problems were encountered when using a water-cooled, single-isotope, hollow-cathode lamp as light source and a water-cooled, open-ended cylindrical hollow-cathode sputtering cell for samples. Table 14-5 shows the absorption results for standards at the 591·54 and 502·74 nm lines. It was suggested that samples could be examined directly as solids inserted into the absorption tube. In the report of a later, more detailed study Goleb[86] described a similar procedure using Schüler-Gollnow water-cooled hollow-cathode lamp light sources for each isotope and a water-cooled hollow-cathode absorption cell. An isotope filtration method was finally adopted,

TABLE 14-5

Incident uranium light absorbed by a uranium hollow-cathode discharge tube used as an absorption source[a]

Composition of uranium		Incident light absorbed, %	Uranium line, nm
Emission tube	Absorption tube		
99·3% U^{238} 0·7% U^{235}	99·3% U^{238} 0·7% U^{235}	60	591·540
7·0% U^{238} 93·0% U^{235}	99·3% U^{238} 0·7% U^{235}	5	591·540
99·3% U^{238} 0·7% U^{235}	99·3% U^{238} 0·7% U^{235}	42	502·738
7·0% U^{238} 93·0% U^{235}	99·3% U^{238} 0·7% U^{235}	3	502·738

[a] From ref. 85.

TABLE 14-6

Comparison of atomic absorption and mass spectrographic results for uranium isotope analysis[a]

(Samples sputtered in emission tube)

	Uranium-238 (at-%)			
Sample no.	Atomic absorption	Mass. spectr.	Dev. (at-%)	Rel. dev. (%)
1. 50 (mg) Metal	78·8	79·7	0·90	1·1
2. 50 (mg) Metal	60·3	59·9	0·40	0·7
3. 50 (mg) Metal	51·5	50·4	1·10	2·2
4. 50 (mg) Metal	40·6	39·5	1·10	2·8
5. 50 (mg) Metal	19·6	19·1	0·50	2·6
6. 50 (mg) Metal	5·60	5·59	0·01	0·2
7. 50 (mg) U$_3$O$_8$	49·8	50·4	0·60	1·2
8. 36 (mg) U$_3$O$_8$ (92 at-% U-236)	2·41	2·38	0·03	1·3
9. 1 (mg) Uranyl nitrate (98 at-% U-234)	0·58	0·60	0·02	3·3

[a] From ref. 86.

however, in which radiation emitted from samples and standards in the hollow-cathode discharge was absorbed selectively by the pure uranium isotope contained in the absorption cell. The percentage transmission was then related to the isotope concentration of the sample placed in the source tube. The calibration graph obtained using this method for the determination of U^{238} shows that good correlation between the experimental data and the theoretical relationship was observed; results for the analysis of samples containing between 0·58 and 78·8% of U^{238} agreed well with mass spectrometric values. Table 14-6 shows a comparison of AAS and mass spectrometric results. An advantage of the isotope filtration technique is that samples can be used in the emission tube in metallic, oxide or compound form.

Boron

Goleb[86] has described an attempt to determine the boron natural abundance ratio, B^{11}/B^{10}, by AAS using similar instrumentation and procedures to those employed for his work with the uranium isotopes. With single isotope sources no difference in absorption at the B 249·6 and 249·7 nm lines was observed when different isotopes were used in the absorption discharge cell. Goleb attributed this to the fact that the half-widths of the lines were greater than the isotopic displacements. L'Vov has commented that the comparatively high temperature of the hollow cathodes and the use of xenon as filler gas may be responsible for the negative results obtained. Because of the high current density and the poor thermal conductivity of boron the gas temperature within the hollow cathodes could be 400-500°C, and the line broadening by xenon would be large compared with that obtained if neon had been employed; both factors would result in overlapping absorption owing to increases in the half-widths of the isotopic components relative to the isotopic displacement.

Helium

L'Vov and Mosichev[87] examined the isotopic composition of mixtures of He^3 and He^4 using a gas discharge absorption cell providing sufficient excitation to obtain an atomic population in the ^3S level. The absorption at 1083·0 nm due to the transition $2^3S - 2^3P_{0,1,2}$ may then be observed using a He^3 or He^4 high-frequency gas discharge lamp as light source. This technique is necessary to avoid the use of the resonance lines of helium which lie in the vacuum ultraviolet. The isotope shift of each of the three lines of the multiplet is 1180 mK and is similar to the separation of the lines of the multiplet (1070 mK); therefore some overlap of the isotope components occurs. Self-absorption of the emission line from the source was found to lead to deviation from linearity in the calibration graph for He^4 but this did not prevent successful analysis under carefully controlled experimental conditions.

14.4 LASER-EXCITED ATOMIC FLUORESCENCE SPECTROSCOPY

The source power delivered to the atom cell in AFS is relatively low when vapour-discharge lamps, hollow-cathode lamps, electrodeless-discharge tubes or continuum sources are employed. As the magnitude of the fluorescence signal is proportional to the source power transferred to the sample atoms in the flame or non-flame cell employed, any method whereby source power delivery may be increased would have a beneficial effect on sensitivity in AFS. As pointed out by Fraser and Winefordner,[88] the use of a stable, repetitively pulsed source of excitation with a small duty cycle, i.e. small ratio of on-to-off time, might permit an increase in the fluorescence signal-to-noise ratio owing primarily to decreased noise; during the short on-time the signal may be of the same magnitude as the average signal obtained using a continuously operated source, whereas the noise would be small because of the small number of random photo-detector pulses from dark current, flame background emission, etc.[89] Thus the high peak power output from a repetitively pulsed, tunable laser should provide for high power delivery to an analytical atom cell and permit the attainment of high detection sensitivity. This type of system should in most respects be the ideal source for analytical AFS; the general characteristics of the most suitable lasers available at present have been discussed in Section 5.4.3.

Denton and Malmstadt[90] have described the use of a ruby laser-pumped tunable organic dye laser for excitation of atomic fluorescence of barium in a flame. The experimental arrangement employed is shown in Fig. 14-7. The ruby laser was fitted with a cryptocyanine saturable Q-switch cell; second harmonic generation was achieved in a 10 mm KDP crystal. A 5×10^{-4} M solution of 2′,7′-dichlorofluorescein at pH 11 was used in the 10 mm dye laser cell. Beam splitter and photodiode assemblies were employed to monitor the output power of both the ruby and dye laser. A spectrograph was employed to assist in setting up the system. The ruby rod was allowed to equilibrate thermally for one minute between each firing. The problem of scatter of the intense source radiation by water droplets or salt particles in the flame was overcome by use of an ultrasonic nebulizer-burner system which produced a very fine mist to ensure complete desolvation and conversion of the sample into atomic vapour. A linear atomic fluorescence calibration graph was constructed in the concentration range 1 to 10 ppm of barium at the Ba 553·5 nm resonance line.

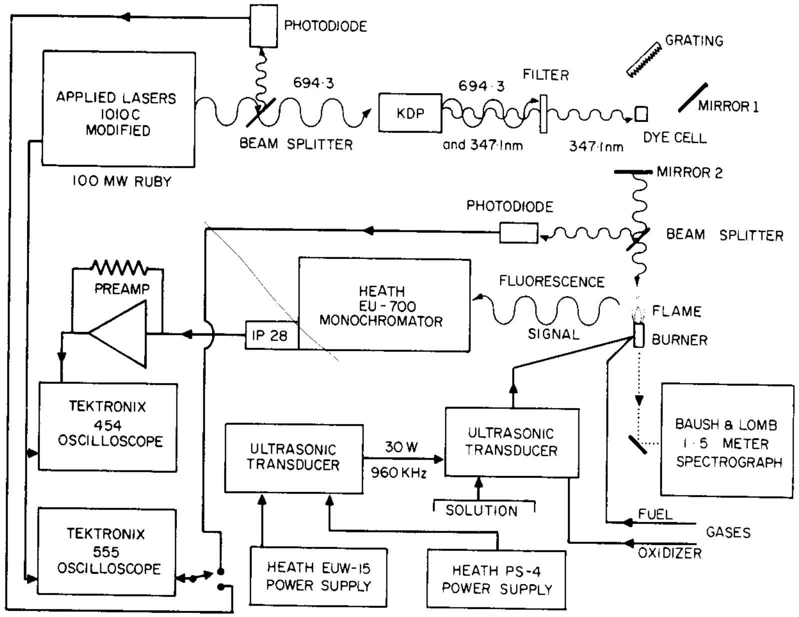

Fig. 14-7. Diagram of experimental arrangement for laser excited AFS used by Denton and Malmstadt.[90]

Fraser and Winefordner[88,91] have reported the use of a faster repetition rate pulsed system utilizing a nitrogen laser-pumped tunable dye laser for excitation of atomic fluorescence from a wide range of elements in air-hydrogen, air-acetylene and nitrous oxide-acetylene flames. A block diagram of the experimental system used is shown in Fig. 14-8. The peak power output of the dye laser over a spectral band-width of 0·1–1 nm is *ca.* 10 kW, the average power output of the dye laser is *ca.* 0·001 W, the pulse half-width is 2–8 ns, and the repetition rate is 1–30 Hz depending on the dye used. Ten dyestuffs were used, each covering a spectral range of about 30 nm in order to provide a system tunable over the range 360 to 650nm. Figure 14-9 shows the output radiant flux and wavelength range covered by each of the ten laser dyes used. As the output of the tunable dye laser can be varied over a range of 10-30 nm, depending on the dye, it is possible to wavelength scan the output of the dye laser. This provides a convenient means of correcting for any background scatter signals and obtaining spectral information by the use of a fast response photomultiplier tube and a boxcar integrator capable of aperture gate widths of the order of 10 ns. Figure 14-10 demonstrates the wavelength scanning facility and shows the spectral distribution (obtained by varying the dye laser wavelength) over a wavelength range of *ca.* 1 nm centred on 422·7 nm and the relative signal magnitude (mV or V) obtained by deliberate scattering of the incident radiation or nebulizing water and Ca solution into an air-hydrogen flame. With this laser technique, therefore, atomic fluorescence is effectively excited with a wide line source with a power output of 10 kW, i.e. during the laser "on-time" fluorescence is excited with a source having an effective black body temperature of 75,000 K at 400 nm and during the "off-time" no signal or noise

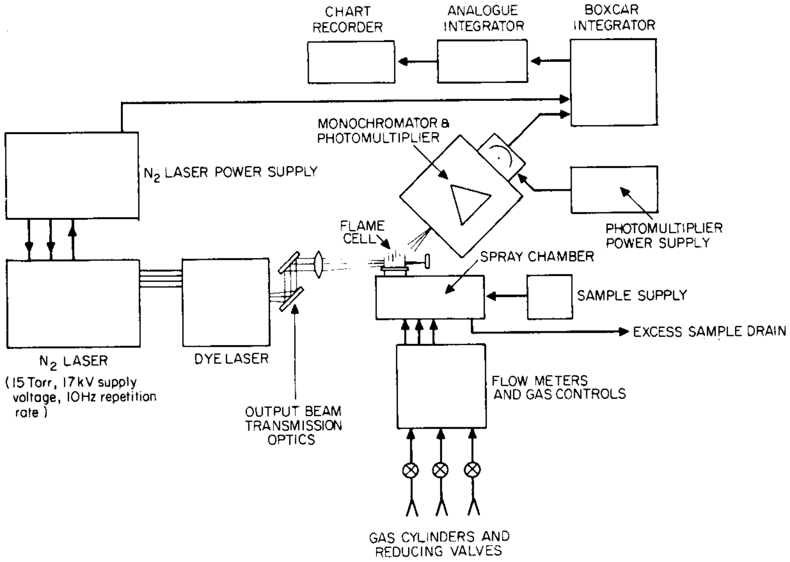

Fig. 14-8. Block diagram of experimental system used for laser-excited flame AFS by Fraser and Winefordner.[91]

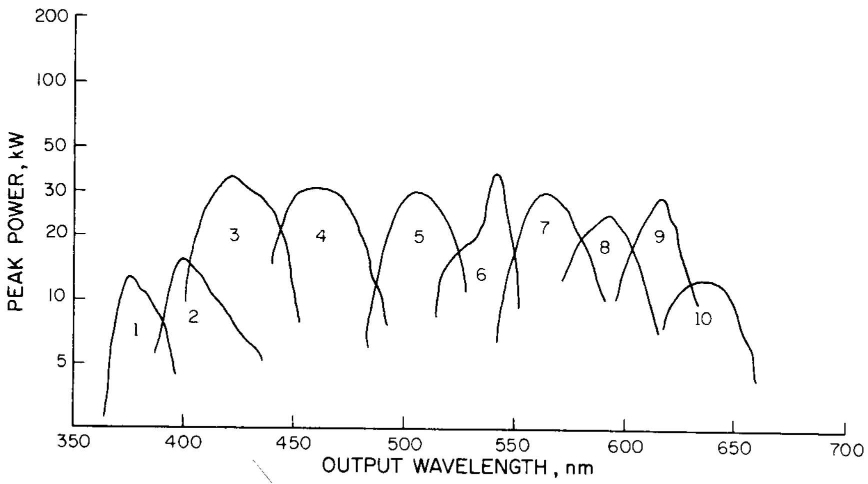

Fig. 14-9. Output radiant flux and wavelength range of laser dyes used by Fraser and Winefordner.[91]

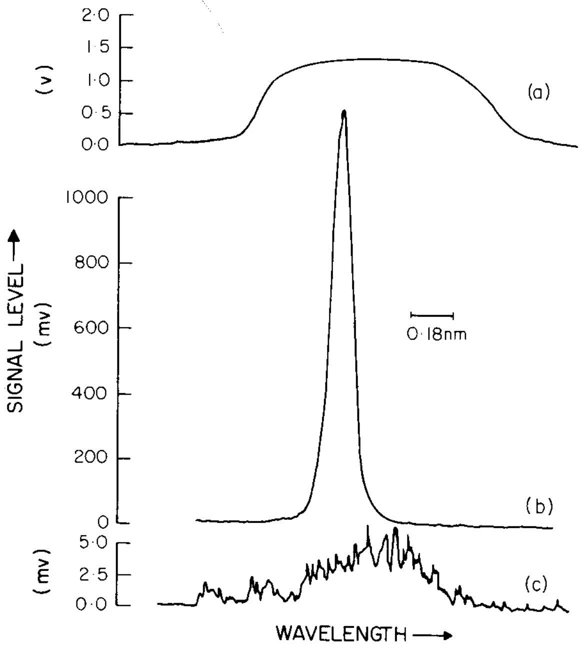

Fig. 14-10. (a) Spectrometer slit function obtained by wave-length scanning the dye laser radiation scattered from a Teflon sheet used in place of the flames (monochromator wavelength set at 422·7 nm). (b) Spectral distribution of fluorescence radiation of Ca (1000 μg/ml) obtained by varying the dye laser wavelength over about 1 nm surrounding 422·7 nm (monochromator wavelength set at 422·7 nm). Solution aspiration rate is 4 ml/min. (c) Spectral distribution of scattered radiation by the flame gases obtained by varying the dye laser wavelength over about 1 nm surrounding 422·7 nm (monochromator wavelength set at 422·7 nm).

is being measured. With a duty cycle of *ca.* 10^{-7}, i.e. with the laser "on" for only 1 part in 10^7 parts, random noise effects from flame flicker, electronic measurement noise and fluctuations in sample introduction are negligible at most concentrations. Fraser and Winefordner have pointed out that the resonance fluorescence signal: noise ratio at high concentrations is dependent on shot noise in the signal owing to the randomness in the emission of photons, pulse-to-pulse amplitude variations in the dye laser output and also scatter noise. At low concentrations, i.e. near the limit of detection, the resonance fluorescence signal:noise ratio is primarily dependent on scatter noise from particles and optical inhomogeneities in the flame gases.

Linear analytical fluorescence calibration graphs were constructed by Fraser and Winefordner for fluorescence of Al, Ca, Co, Cr, Ga, In, Fe, Mn, Mo, Ni, Sr, Ti and Tl over three or four orders of magnitude concentration range. Resonance and non-resonance fluorescence effects were utilized. The corresponding detection limits obtained in this work are shown in Table 14-7. The values of the detection limits obtained for Al, Ga, In and Ti are equal to, or better than, any reported values by any other flame spectroscopic method, and the values for Cr, Mn, Ni, Mo and Tl are within a factor of 10 of those obtained by any other flame method; of the remaining values only those for Ca, Co, Sr and Fe are not within a factor of ten of other flame spectroscopic methods. Although it might be expected from the use of a "wide-line" source (0·1–1·0 nm) for excitation of fluorescence, for the elements investigated no appreciable spectral interference resulting from simultaneous excitation of atomic fluorescence from other elements was observed in this work. The limits of detection obtained may be substantially improved by reducing the laser beam scatter noise to the extent where the principal noise limitation arises from photon noise due to the atomizer background and from detector noise. A limitation of the present dye laser excitation system is the lower useful wavelength limit of 360 nm which precludes the possibility of excitation of intense fluorescence for many elements.

With the laser excitation system two-photon excitation fluorescence was observed for Cd and Zn.[91] In this process two photons are absorbed simultaneously of combined energy equal to the difference in energy between the two energy levels involved in the absorption process. Thus the two-photon excitation fluorescence of Cd involves excitation of analyte atoms with intense radiation at 457·6 nm (or of

TABLE 14-7

Limits of detection by laser excited atomic fluorescence[91]

Element	Type of fluorescence[a]	Type of flame Ox(1/min)/F(1/min)[b]	Mono-chromator slit, μm	Dye type[c]	Analytical line, nm[d]	Energy levels, cm^{-1}[e]	gf Value[f]	Limit of detection, ppm[g]	Upper limit, ppm[h]
Al	RF	$N_2O(14·5)/C_2H_2(6·5)$	150	17/66B	394·4	0-25348	0·15	1×10^{-1}	2×10^{2}
	E-RF	$N_2O(14·5)/C_2H_2(6·5)$	150	17/66B	396·1	112-25348	0·31	3×10^{-2}	1×10^{2}
	N-DLF	$N_2O(14·5)/C_2H_2(6·5)$	150	17/66B	394·4/396·1	0-25348/112-25348	0·15/0·31	5×10^{-3}	2×10^{2}
Ca	RF	$Air(7·5)/H_2(15·2)$	250	17/52	422·7	0-23652	0·28	5×10^{-3}	5×10^{1}
Cr	RF	$Air(7·5)/H_2(11·8)$	150	17/66D	357·8	0-27935	1·60	2×10^{-2}	2×10^{1}
	RF	$Air(7·5)/H_2(11·8)$	150	17/66D	359·3	0-27820	1·40	2×10^{-2}	2×10^{1}
Co	E-RF	$N_2O(12·0)/C_2H_2(6·4)$	100	17/66D	357·5	816-28777	0·22	5×10^{1}	ND[i]
	AS-DLF	$N_2O(12·0)/C_2H_2(6·4)$	100	17/66D	347·4/357·5	0-28777/816-28777	0·64/0·22	2×10^{-1}	2×10^{2}
Ga	RF	$Air(7·5)/H_2(20·0)$	150	17/66B	403·2	0-24788	0·24	1×10^{-1}	5×10^{2}
	N-DLF	$Air(7·5)/H_2(20·0)$	150	17/66B	403·2/417·2	0-24788/826-24788	0·24/0·53	2×10^{-2}	2×10^{1}
In	RF	$Air(7·5)/H_2(18·3)$	250	17/66B	410·4	0-24373	0·47	1×10^{-2}	5×10^{1}
	N-DLF	$Air(7·5)/H_2(18·3)$	250	17/66B	410·5/451·1	0-24373/2213-24373	0·47/0·66	2×10^{-3}	5×10^{1}
Fe	RF	$Air(7·5)/H_2(11·8)$	250	17/66D	372·0	0-26875	0·52	3×10^{-1}	2×10^{3}
Mn	RF	$Air(7·5)/H_2(20·0)$	150	17/66B	403·0	0-24802	0·33	1×10^{-2}	2×10^{1}
Mo	RF	$N_2O(12·0)/C_2H_2(6·4)$	100	17/66D	379·8	0-26321	1·30	1×10^{1}	1×10^{2}
	RF	$N_2O(12·0)/C_2H_2(6·4)$	100	17/66D	390·3	0-25614	0·47	3×10^{-1}	1×10^{2}
Ni	E-RF	$Air(14·3)/C_2H_2(2·6)$	200	17/66D	361·0	880-28569	0·15	2×10^{0}	5×10^{2}
	E-AS-DLF	$Air(14·3)/C_2H_2(2·6)$	200	17/66D	361·0/352·4	880-28569/205-28569	0·15/0·85	5×10^{-2}	2×10^{2}
Sr	RF	$Air(7·5)/H_2(15·2)$	150	17/53	460·7	0-21698	0·27	1×10^{-2}	2×10^{1}
Ti	E-RF	$N_2O(14·5)/C_2H_2(6·5)$	150	17/66B	399·8	387-25388	1·50	1×10^{-1}	2×10^{2}
Tl	RF	$Air(14·3)/C_2H_2(2·3)$	200	17/66D	377·6	0-26478	0·22	1×10^{0}	5×10^{1}
	N-DLF	$Air(14·3)/C_2H_2(2·3)$	200	17/66D	377·6/535·0	0-26478/7793-26478	0·22/0·92	2×10^{-2}	1×10^{2}

[a] RF = resonance fluorescence involving ground state. E-RF = thermally assisted resonance fluorescence involving excited lower state. N-DLF = Stokes direct line fluorescence involving ground lower state in absorption process. AS-DLF = anti-Stokes direct line fluorescence involving ground lower state in fluorescence process. E-AS-DLF = excited anti-Stokes direct line fluorescence involving excited lower states for both absorption and fluorescence processes.

[b] Ox(1/min)/F(1/min) = oxidant (flow rate)/fuel (flow rate).

[c] Dye types as designated by manufacturer of dye laser (AVCO Everett Research Laboratories).

[d] If only one line is listed, the absorption and fluorescence lines are identical.

[e] Taken from C. H. Corliss and W. R. Bozman, "Experimental Transition Probabilities for Spectral Lines of Seventy Elements", NBS Monograph 53, U.S. Government Printing Office, Washington, D.C., 1962 (and from W. F. Meggers, C. H. Corliss and B. F. Scribner, "Tables of Spectral-Line Intensities", NBS Monograph 32, Part I, U.S. Government Printing Office, Washington, D.C., 1961).

[f] Taken from C. H. Corliss and W. R. Bozman (see footnote e).

[g] Concentration resulting in a signal-to-rms noise of 2.

[h] Highest concentration of analyte resulting in a signal deviating from linearity by no more than 5%.

[i] Not determined.

two different lines of comparable total energy) and observation of the cadmium resonance line at 228·8 nm.

The nitrogen pumped dye laser system has also been used by Winefordner and co-workers in a study of the laser excited atomic fluorescence determination of the rare-earth elements in a premixed nitrous oxide-acetylene flame.[92] Both resonance and non-resonance fluorescence was studied; the appreciable ionization of many of the rare-earth elements in the nitrous oxide-acetylene was also found to

TABLE 14-8

Detection limits obtained for the rare-earth elements by laser-excited atomic and ionic fluorescence spectrometry (from ref. 92)

Element	Wavelength, nm[a]	Detection limit, ppm	
		AFS[b,c]	IFS[c]
Ce	569·92	n.d.	
	394·21 (371·64)		0·5
Dy	418·68 (418·68)	0·6	
	353·60 (364·54)		0·3
Er	400·80 (400·80)	0·5	
	337·27 (369·26)		2·5
Eu	462·72 (459·40)	0·02	
	393·05 (420·50)		0·2
Gd	368·41 (368·41)	5	
	336·22 (376·84)		0·8
Ho	410·38 (405·39)	0·15	
	——— ———		n.d.
Lu	513·51 (465·80)	3	
	——— ———		n.d.
Nd	489·69 (463·42)	2	
	424·74 (430·36)		40
Pr	495·14 (495·14)	10	
	430·58 (427·23)		1
Sm	429·67 (375·64)	0·6	
	373·91 (366·14)		0·15
Tb	433·84 (432·65)	1·5	
	350·92 (370·28)		0·5
Tm	409·42 (371·79)	0·1	
	379·58 (376·13)		5
Yb	346·44 (398·80)	0·01	
	328·94 (369·42)		0·03

[a] Laser excitation wavelength given in parentheses.

[b] 1000 ppm of potassium as KCl added to suppress ionization.

[c] n.d. = not detectable at 500 ppm.

permit observation of resonance and non-resonance fluorescence for the ionic species. The detection limits obtained on nebulization of aqueous solutions of the rare-earths are shown in Table 14-8. These values, except for erbium, are within a factor of three of the best values reported by AAS. The authors point out, however, that because in the majority of cases non-resonance fluorescence was utilized, AFS should be superior to AAS for the practical determination of rare-earth mixtures, i.e. when spectral interferences may possibly be encountered. The laser-excited AFS detection limits reported to date are inferior to those attainable by flame emission spectroscopy for six elements (Dy, Er, Eu, Ho, Nd and Pr) and are similar to the FES values for the other elements. As few spectral interferences occur in the determination of the rare-earths by flame emission spectroscopy in high-temperature flames (owing to the simplicity of the emission spectra obtained[93,94,95]) at the time of writing FES is probably preferable to AAS or AFS for the determination of these elements.

14.4.1 Saturation Effects with Laser Excitation

In flame AAS and AFS with continuum sources and with dilute atomic vapours the integral of the atomic absorption coefficient, A_T, is generally dependent only on the wavelength and the optical density of the absorber (equation 3-17). This is strictly correct, however, only in the limit of zero incident light flux, i.e. when the incident radiation does not cause significant population of the excited state relative to the ground state. This is a good approximation only for low incident light fluxes available from conventional sources such as hollow-cathode or electrodeless-discharge lamps. When the source flux is very high, however, as in laser excitation, this expression does not provide an accurate description of the attenuation of the light beam. Under these conditions *the absorption coefficient becomes also a function of the incident radiant flux density* (non-linear absorption).[96-103] The intense radiation may then induce in the sample a state of near-saturation of the energy levels in which the excited state population becomes substantially equal to that of the ground state. Winefordner and co-workers,[102,103] and Piepmeier[104,105] have described the theoretical and practical consequences of the occurrence of saturation in AFS for a broad-band laser excitation source and a monochromatic laser excitation source respectively. With a high incident radiation flux, where the integrated absorption coefficient becomes a function of the source irradiance, a more correct expression for the integrated absorption coefficient at low concentrations is given by[97,102]

$$A_T = \int (1 - \exp(-k_\nu \,.\, E^s_\nu \,.\, l)\, \mathrm{d}\nu = c_1 N_T \left[\frac{(E^s_{\nu mn})\ \text{saturation}}{E^s_{\nu mn} + (E^s_{\nu mn})\ \text{saturation}} \right] \tag{14-1}$$

where $(E^s_{\nu mn})$ saturation is the source spectral irradiance at ν_{mn}, the frequency of the transition, for which the steady state integrated absorption coefficient is reduced by a factor of two over the low light flux absorption coefficient,[97] $E^s_{\nu mn}$ is the spectral irradiance of the excitation source, N_T is the total number of atoms per unit volume of flame gases, and c_1 is a factor including fundamental constants and atomic parameters.

If $E^s_{\nu mn} \ll (E^s_{\nu mn})_{\text{saturation}}$ the equations given in Chapter 4 relating fluorescence signal strength to source irradiance apply. However, when the available source irradiance $E^s_{\nu mn}$ is much greater than that required for saturation, $(E^s_{\nu mn})_{\text{saturation}}$, the expression for the fluorescence flux, F_{nm}, is given for a broad-band laser source by

$$F_{nm} = A_{mn} \,.\, N^* = c_2\, Y_{mn} N_T \left[\frac{(E^s_{\nu mn})\ \text{saturation}}{h\nu_{mn}} \right] \tag{14-2}$$

Which is independent of $E^s_{\nu mn}$, the source irradiance. A_{mn} is the Einstein spontaneous transition probability, N^* is the number of atoms per unit volume in the excited state (in excess of the thermal population of the level), Y_{mn} is the quantum yield of the fluorescence process and c_2 is a proportionality constant.

Thus above a certain value of the source irradiance there is a *non-linear* dependence between the fluorescence flux and the spectral irradiance of the source; the condition is approached in which the fluorescence flux becomes independent of the source spectral irradiance. Effectively the vapour becomes transparent to a further increase in $E^s_{\nu mn}$. There is still a linear dependence for a dilute vapour, however, on the concentration of absorbing atoms. This effect of working close to saturation conditions, and the observation by Piepmeier[104,105] and Winefordner *et al.*[102-103] that under these conditions the fluorescence flux is influenced very little by collisional quenching, have several consequences of great importance from an analytical point of view. These are:

(1) The fluorescence signal is not greatly influenced by the source stability. The saturation effect above a certain value of $E^s_{\nu mn}$

ensures that any pulse-to-pulse variation in the source irradiance does not affect the stability of the fluorescence signal.

(2) The linearity of the fluorescence working curve is extended to higher concentrations. At saturation the medium becomes transparent at ν_{mn} because the excited and ground state populations are similar and further absorption in the irradiated volume cannot occur. If the irradiance of the source is such that the atomic system can be kept at saturation for any value of N, the fluorescence flux will be linearly related to N, and the calibration curves will have a slope of unity even at high optical densities. If the medium is transparent self-absorption cannot take place, also the source irradiance is no longer a function of the length along the absorption path, L (see Chapter 4 and Fig. 4-10). Obviously this consideration of transparency under saturation conditions applies only for the irradiated volume; the factors of self-absorption and self-reversal must still be considered for the post-filter effect produced in any unilluminated volume between the fluorescing volume and the detector. Winefordner *et al.*[106] have demonstrated this effect of increased linear range by varying the spectral irradiance of the laser source with neutral density filters and/or by defocusing the laser spot on the flame. Figure 14-11 shows the resonance fluorescence growth curves for indium and strontium obtained at high and low spectral irradiance obtained by defocusing the source.

(3) The proportional dependence of fluorescence signal on the quantum efficiency which is observed at low irradiance is removed under saturation conditions. Thus, provided that the atomization efficiency does not change, the magnitude of the saturated fluorescence signal would not be expected to be greater in the oxygen-argon-hydrogen flame than in a hydrocarbon flame containing nitrogen in spite of the large difference in quantum yield for these flames. Thus the nitrous oxide-acetylene flame is just as effective as other flames from this viewpoint and can be used for AFS to maximize atomization efficiency and minimize chemical interferences without the penalty of lower quantum yield experienced under low irradiance conditions.

Piepmeier[104] has pointed out that the use of high source irradiance with a laser may result in deterioration in detection limits owing to the fact that scattered light is proportional to the source irradiance. The greater possibilities for employment of non-resonance transitions when a laser source is used for excitation, however, should minimize this possible disadvantage. In addition it is possible to improve the fluorescence-to-scattering intensity ratio by enlarging the laser beam in the flame.[102] It is, however, necessary to reach a compromise between scattering and signal stability. As there is a

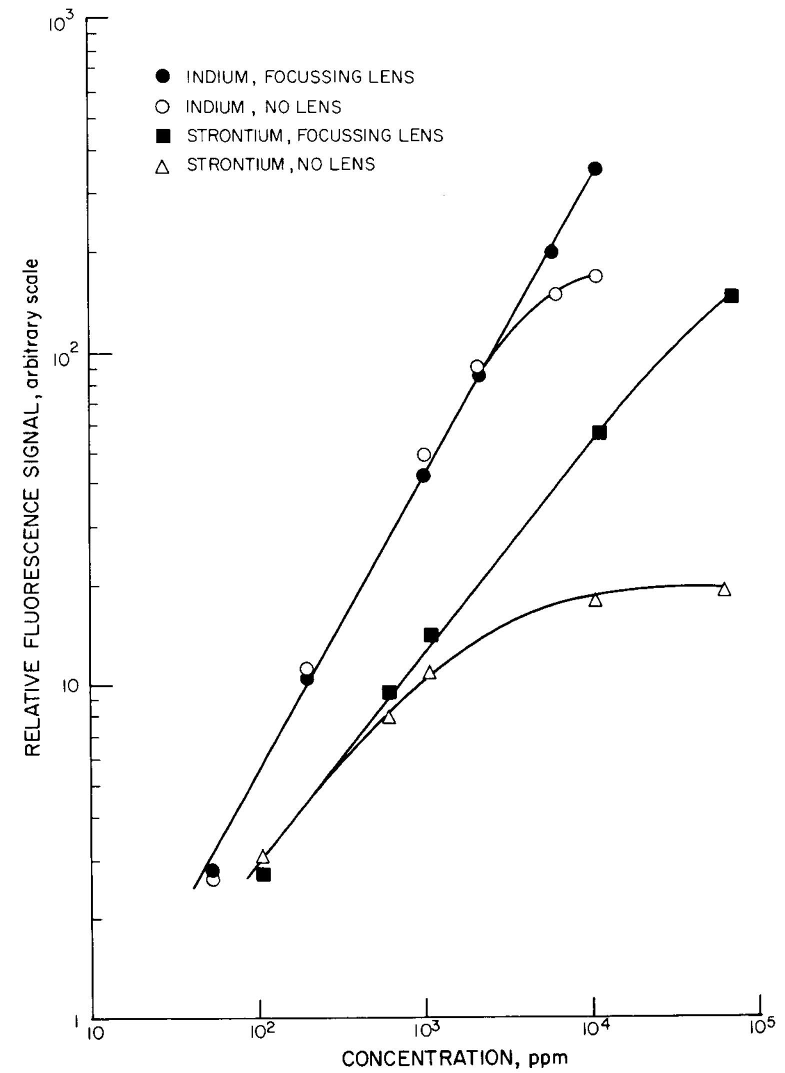

Fig. 14-11. Resonance fluorescence calibration curves for indium and strontium. The fluorescence signals for the different curves are not reported on the same scale.

limiting value of the fluorescence radiance, even if the source irradiance is increased indefinitely, it is apparent that it is the signal : noise ratio rather than the signal itself which should be maximized.

Current developments in AFS using laser excitation lend credence to earlier claims that this type of source is probably ideal in many respects; the fundamental advantages of using high source irradiance described above should certainly lead to the more widespread adoption of these sources for practical AFS measurements.

14.5 MEASUREMENT OF FLAME TEMPERATURES BY AAS AND AFS

In the study of atomization processes and interference phenomena encountered in analytical atomic spectroscopy it is often necessary to have a knowledge of the temperature within the flame or non-flame atom cell employed. It is frequently not satisfactory to assume the temperature in the atom cell under investigation from literature values for similar cells. In flames, for example, the measured temperature will depend on the values of the gas flow-rate and the design of burner head used and considerable misinterpretation may occur if literature values for a particular flame temperature are used to treat experimental data obtained with different apparatus. Except for some thermocouple methods of measurement, which may often be unsatisfactory owing to the influence of the sensing element on the atom cell environment and measured temperature, the two most widely used spectroscopic techniques of temperature measurement are the line reversal and two-line emission procedures. Both of these methods require special apparatus and are frequently time-consuming.[107,108,109] Additionally both methods require that atomic emission can be stimulated from a species (often Na in the line-reversal technique and Fe for two-line emission) added to the atom cell. Although little work has been reported to date concerned with the temperature of atomic vapours produced in non-flame cells, this latter requirement of these methods renders them of little value for these purposes. There exists, therefore, a need for simple spectroscopic techniques of temperature measurement which are applicable to flame and non-flame atom cells and which require mainly absorption and fluorescence instrumentation similar to that used by many workers undertaking studies of atomization processes and interference effects. Two such techniques have been reported; these depend on the measurement of relative absorption and fluorescence respectively at two atomic lines of the analyte element introduced into the atom cell.

14.5.1 Two-line Atomic Absorption Method

Browner and Winefordner[110] have described a straightforward atomic absorption technique for temperature measurement using a simple uncalibrated continuum light source (quartz iodine lamp). The method is applicable directly, with no modification required, to any atomic absorption spectrometer possessing a monochromator that will allow the use of a spectral band-pass of *ca.* 0·04 nm.

The two-line absorption method depends on the measurement of the absorption at each of two lines for an element introduced into the sample flame. One of these lines originates from the ground state and the other is chosen to originate from a thermally populated level less than 1 eV above the ground state. The ratio of these absorption signals may then be applied to calculate the effective electronic excitation temperature of the atoms within the flame. At low optical density the relative absorption, α, of the radiation from a continuum light source by atoms in the light path is given by

$$\alpha = \frac{\phi_A}{\phi_0} = \frac{\pi e^2 l \lambda_0^2 n f}{m s c^2} \qquad (14\text{-}3)$$

where e and m are the electronic charge and mass, c is the velocity of light, l is the absorption path length, λ_0 is the peak absorption wavelength, n is the concentration of atoms at the lower energy level involved in the transition, f is the absorption oscillator strength, ϕ_0 is the radiant flux of the continuum source transmitted with only a blank introduced into the flame, ϕ_A is the radiant flux from the source absorbed by the analyte atoms in the flame, and s is the spectral band-width of the monochromator. Equation (14-3) only holds provided that s is greater than, or equal to, $4\Delta\lambda_a$, where $\Delta\lambda_a$ is the total half-width of the absorption line.

At high optical densities, equation (14-3) becomes

$$\alpha = \frac{1}{s}\left[\frac{2\pi e^2 l \lambda_0^2 n f a \, \Delta\lambda_D}{m c^2 (\ln 2)^{1/2}}\right]^{1/2} \qquad (14\text{-}4)$$

where $\Delta\lambda_D$ is the Doppler half-width of the line, and a is the damping constant (see Chapter 3.2). By substitution for *a* and neglecting the natural line width, equation (14-4) becomes

$$\alpha = \frac{1}{s}\left[\frac{2\pi e^2 l\lambda_0^2 nf\Delta\lambda_L}{mc^2}\right]^{1/2} \tag{14-5}$$

where $\Delta\lambda_L$ is the Lorentz (collisional) half-width.

Equations (14-4) and (14-5) are not valid at very high optical densities (α greater than *ca.* 0·3) because at these values parts of the absorption line wings may extend beyond the spectral band-width of the monochromator.

When thermal equilibrium exists in the atomic vapour the relative populations n_0 and n_1 of two electronic levels 0 and 1 are given by

$$\frac{n_1}{n_0} = \frac{g_1}{g_0}\exp\left[\frac{E_0 - E_1}{kT}\right] \tag{14-6}$$

where E_0 and E_1 are the energy levels of states 0 and 1 and g_0 and g_1 their statistical weights, k is the Boltzmann constant and T is the absolute temperature. Atoms with degenerate ground states have one or more electronic levels close to the ground state. For a particular atom with a degenerate ground state it is possible to relate accurately the relative absorption at the resonance line and at a non-ground-state line to the relative populations of these levels by combining equations (14-4) and (14-6). At low optical densities the temperature is then given by

$$T = \frac{E_1 - E_0}{k\ln\left[\left(\frac{g_1 f_1}{g_0 f_0}\right)\left(\frac{\lambda_1}{\lambda_0}\right)^2\left(\frac{\alpha_0}{\alpha_1}\right)\right]} \tag{14-7}$$

and at high optical densities by

$$T = \frac{E_1 - E_0}{k\ln\left[\left(\frac{g_1 f_1}{g_0 f_0}\right)\left(\frac{\lambda_1}{\lambda_0}\right)^2\left(\frac{\alpha_0}{\alpha_1}\right)^2\left(\frac{\Delta\lambda_{L_1}}{\Delta\lambda_{L_0}}\right)\right]} \tag{14-8}$$

where α_0 and α_1 refer to the relative absorption signals at the lines of wavelengths λ_0 and λ_1, whose lower states have energies E_0 and E_1 and whose collisional half-widths are $\Delta\lambda_{L_0}$ and $\Delta\lambda_{L_1}$. To achieve optimum signal levels for the measurement, the energy separation of states 0 and 1 should not be too great (less than 1 eV for temperatures less than 4000 K) and the absorption oscillator strengths must be comparable. Only relative values of the f values are required in order to obtain an absolute electronic excitation temperature at low optical densities. If the low optical density region is used, however, this limits both α_0 and α_1 to *ca.* $< 0{\cdot}03$; at these low values of α unacceptable errors in the temperature measurement may result. If the high optical density region is used it is apparently necessary to know the ratio of the collisional half-widths. Browner and Winefordner[110] were able to show from curve of growth measurements with In in a number of flames of different temperatures and composition that the ratio of the collisional half-widths, $\Delta\lambda_{L_1}/\Delta\lambda_{L_0}$, given by the intersection point of the low and high optical density asymptotes for each curve, was identical with α_1/α_0 within the limits of experimental accuracy. Thus

TABLE 14-9

Experimental values of Lorentz half-width ratios from growth curves for indium (from ref. 110)

Flame	Temperature, K	$\Delta\lambda_{L_{451\cdot1}}/\Delta\lambda_{L_{410\cdot2}}$ (= α'_1/α'_0)[a]	α_1/α_0 Low O.D.[a]	α_1/α_0 High O.D.[a]
$Ar/O_2/H_2$	2098 (R)[b]	0·56	0·56	0·58
	2250 (R)	0·69	0·71	0·66
Air/C_2H_2	2430 (R)	0·76	0·78	0·73
	2470 (R)	0·78	0·77	0·74
N_2O/C_2H_2	2995 (Fe)[c]	0·90	0·85	0·91

[a] Values of $\Delta\lambda_{L_{451\cdot1}}/\Delta\lambda_{L_{410\cdot2}}$ from the growth curves and of α_1/α_0 measured at low optical densities (O.D.) have an error of approximately 10%. The error in the ratio of α_1/α_0 at high optical densities (O.D.) is about 1%.

[b] R = reversal temperature.

[c] Fe = iron two-line temperature.

$$\frac{\Delta\lambda_{L_1}}{\Delta\lambda_{L_0}} = \frac{\alpha'_1}{\alpha'_0} = \frac{\alpha_1}{\alpha_0} \tag{14-9}$$

where the values of α' refer to the intersection points of the high- and low-density asymptotes. The experimental data obtained in different flames to show that α'_1/α'_0 is equal to α_1/α_0 for indium are shown in Table 14-9. On substitution for $\Delta\lambda_{L_1}/\Delta\lambda_{L_0}$, equation (14-6) for high optical densities becomes identical to equation (14-5) for low optical densities. This equation may then be used up to α values of *ca.* 0·3 without the need to evaluate $\Delta\lambda_{L_1}/\Delta\lambda_{L_0}$. In order to obtain high sensitivity $dT/d(\alpha_0/\alpha_1)$ should be small and thus widely different α values should be measured. This leads to poor precision in the ratio α_0/α_1, however, and to obtain good precision the approximate range $1{\cdot}1 \gtrsim \alpha_0/\alpha_1, \gtrsim 5$ was recommended. When the two-line absorption method is applied with Ga, In and Tl this results in restriction of the working ranges of temperature to Ga, 650-2200 K; In, 1200-3500 K and Tl, 3650-7750 K. Table 14-10 lists some temperatures obtained by Browner and Winefordner for different flames using the two-line absorption method and values obtained by the same workers for the same flames using other spectroscopic methods. Systematic and random errors of about 1% were claimed for the technique.

TABLE 14-10

Temperature of flames measured by two-line atomic absorption method (from ref. 110)

Flame	Gas flow rates ($1\ \mathrm{min}^{-1}$)		Temperature (K)	
	Fuel	Oxidant	Absorption method	Other methods[a]
$Ar/O_2/H_2$	6·2	O_2-2·1[b] Ar-13·2	2078	2098 (R)
	6·2	O_2-2·6[b] Ar-13·2	2260	2250 (R)
Air/C_2H_2	1·3	9·5[b]	2452	2430 (R)
	1·3	9·5[c]	2473	2470 (R)
N_2O/C_2H_2	4·5	8·2[d]	2961	2995 (Fe)

[a] R = reversal temperature, Fe = iron two-line temperature.

[b] Flame shielded Meker burner. Same gas flows through outer and inner flames.

[c] 50-mm slot burner.

[d] 10-mm diameter capillary burner.

The two-line absorption technique should prove to be of great value in the measurement of electronic excitation temperatures in non-emissive atom cells such as graphite rod and tube devices.

14.5.2 *The Two-line Atomic Fluorescence Method*

Omenetto, Benetti and Rossi[111] have described four possible methods whereby flame electronic excitation temperature measurements may be made by atomic fluorescence spectroscopy. These methods may be related to the processes shown schematically in Fig. 14-12 for thallium. When the flame is irradiated by a continuum source (compact arc or broad line vapour-discharge lamp) from which suitable excitation wavelengths are selected with filters, the following possibilities present themselves:

(a) It may be shown[112] that the ratio of the anti-Stokes fluorescence (F_{20}) to direct line fluorescence (F_{21}) at low atomic concentrations (no self-absorption) is given by

$$\frac{F_{20}}{F_{21}} = \frac{E(\lambda_{12})f_{12}}{E(\lambda_{02})f_{02}} \cdot \left(\frac{\lambda_{12}}{\lambda_{02}}\right)^3 \cdot \frac{n_1}{n_0} \cdot \frac{\phi_{20}}{\phi_{21}} \qquad (14\text{-}10)$$

where the $E(\lambda)$ values represent the spectral irradiance of the excitation source at the wavelengths concerned, the f values are the corresponding oscillator strengths of the lines, λ_{12} and λ_{02} are the central wavelengths of the observed transitions, n_1 and n_0 are the atomic concentrations in the corresponding states and ϕ_{20} and ϕ_{21} are the quantum efficiencies of the fluorescence processes considered. Alkemade[112] has also demonstrated that $\phi_{20}/\phi_{21} = A_{20}/A_{21}$ where A_{20} and A_{21} are the Einstein transition probabilities. Furthermore, for thermal equilibrium conditions n_1 and n_0 are related via the Boltzmann distribution. Thus equation (14-10) becomes

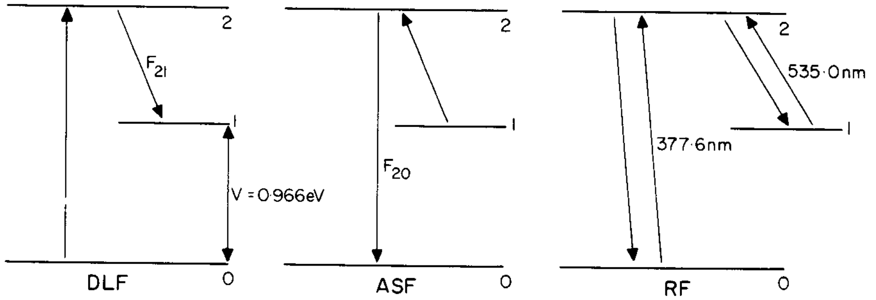

Fig. 14-12. Schematic diagram of the fluorescence process for thallium in flames. DLF = direct-line fluorescence; ASF = anti-Stokes fluorescence; RF = resonance fluorescence.

$$\frac{F_{20}}{F_{21}} = \frac{E(\lambda_{12})}{E(\lambda_{02})} \cdot \left[\frac{\lambda_{12}}{\lambda_{02}}\right]^5 . 10 \exp\left[\frac{-5040 V_1}{T_f}\right] \qquad (14\text{-}11)$$

where V_1 is the excitation energy of level 1 above the ground state. Hence, solving for T_f the flame temperature,

$$T_f = \frac{5040 V_1}{\left[\ln \dfrac{E(\lambda_{12})}{E(\lambda_{02})} + 5 \ln \dfrac{\lambda_{12}}{\lambda_{02}} - \ln \dfrac{F_{20}}{F_{21}}\right]} \qquad (14\text{-}12)$$

The experimental data required to calculate the flame temperature are the spectral irradiances of the source at the excitation wavelengths and the intensities of the anti-Stokes and direct-line fluorescence signals.

(b) The thermodynamic radiation law implies that the ratio $E(\lambda_{12})\backslash E(\lambda_{02})$ corresponds to the temperature T of a black body. A temperature T_c, often called the colour temperature, can therefore be formally assigned to the continuum source. Using Wien's law it can be written

$$\frac{E(\lambda_{12})}{E(\lambda_{02})} = \frac{\lambda_{12}^{-5} \exp\left(\dfrac{-h\nu_{12}}{kT_c}\right)}{\lambda_{02}^{-5} \exp\left(\dfrac{-h\nu_{02}}{kT_c}\right)}$$

$$= \lambda_{12}^{-5}\,\lambda_{02}^{5} \exp\left(\frac{V_1}{kT_c}\right) \tag{14-13}$$

where ν_{12} and ν_{02} are the central frequencies of the transitions and k is the Boltzmann constant. By substitution into equation (14-11),

$$\frac{F_{20}}{F_{21}} = 10 \exp\left[5040 V_1 \left(\frac{1}{T_c} - \frac{1}{T_f}\right)\right] \tag{14-14}$$

Thus when the intensity of the anti-Stokes fluorescence equals that of the direct-line fluorescence the colour temperature of the source will be equal to the flame temperature. If the colour temperature of the source could be varied continuously a value of unity for F_{20}/F_{21} could be achieved. In practice several values of F_{20}/F_{21} can be obtained by changing the filter transmission characteristics and these values may be used to construct a graph of F_{20}/F_{21} against $1/T$; the straight line obtained may then be extrapolated to $\ln(F_{20}/F_{21}) = 0$.

(c) If the temperature of one flame is known by independent measurement, the measurement of the ratio F_{20}/F_{21} provides a means of calculating the temperature of several other flames. If equation (14-11) is written for two temperatures T_{f_1} (known) and T_{f_2} (unknown), we may simplify to

$$\log\left(\frac{F_{20}}{F_{21}}\right)_{T_{f_1}} \Big\backslash \log\left(\frac{F_{20}}{F_{21}}\right)_{T_{f_2}} = \frac{5040 V_1}{T_{f_2}} - \frac{5040 V_1}{T_{f_1}} \tag{14-15}$$

The use of this relationship then permits the calculation of T_{f_2}.

Methods of flame temperature measurement based on (a) and (b) require the accurate calibration of the relative efficiency of the monochromator and detector system at the wavelengths λ_{12} and λ_{02}, and the ratio of the spectral irradiances of the source must be measured experimentally. It should be pointed out, however, that a knowledge of the transition probabilities for the lines used is not required; this represents an advantage over many other methods. Omenetto and co-workers[111] described a fourth method of flame temperature measurement by AFS based on determination of the ratio F_{21}^{*}/F_{21}, where F_{21}^{*} is the number of $2 \rightarrow 1$ transition/s due to excitation involving thermal assistance between levels 0 and 1, and F_{21} is the number of direct $2 \rightarrow 1$ fluorescence transition/s due to excitation via $0 \rightarrow 2$. This results in an equation similar to that used in method (a) but requiring a knowledge of the *gf* values of the transitions studied. Method (c) does not require the separate calibration of the monochromator and detector assembly or the measurement of the source irradiance.

TABLE 14-11

Values for electronic excitation temperatures of various premixed flames obtained by two-line atomic fluorescence methods (from ref. 111)

		Flame temperatures (K)			
		Fluorescence (thallium)			
Gas mixture	Method	(a)	(d)	Reversal (thallium)	Two-line (iron)[a]
Air Hydrogen	9·8 1/min 11·6 1/min	2070	2085	2090	2160
Air Acetylene (nitrogen-separated)	9·8 1/min 1·5 1/min	2435	(2440)[b]	2440	ND[c]
Air Acetylene	9·8 1/min 1·5 1/min	2540	2530	2540	2480
Nitrous oxide Acetylene (nitrogen-separated)	7·2 1/min 4·7 1/min	2860[d]	2870[d]	2850	2820
Nitrous oxide Acetylene	7·2 1/min 4·7 1/min	3085[d]	3090[d]	3070	3000

[a] Iron line pairs used: 3733·32/3734·87; 3820·43/3895·66 (air-hydrogen). 3722·56/3734·87 (air-acetylene). 3722·56/3749·49 (nitrous oxide-acetylene) after Kirkbright *et al.* (ref. 109).

[b] Temperature obtained by the "line reversal" method and used for the calculation of the other flame temperatures.

[c] ND = not determined. Consistent data could not be obtained.

[d] Philips metal vapour discharge lamp used as excitation source.

Omenetto and co-workers used concentrations of between 50 and 200 ppm of thallium for temperature measurements and did not find significant dependence of the measured temperatures on thallium concentration. Table 14-11 shows values of the thallium electronic excitation temperature obtained in various flames by the AFS methods (a) and (c) described above. Good agreement was obtained between these values and those from the line-reversal method with thallium and the two-line emission method with iron. The temperature values in Table 14-11 obtained by method (c) were calculated taking the line-reversal temperature of the nitrogen-separated air-acetylene flame as the known temperature. From the coefficient of variation of fluorescence measurements for air-acetylene and air-hydrogen flames (1·6 and 3% for F_{21} and 3% and 2·2% for F_{20} respectively) and the estimated precision in the instrumental calibration (*ca.* 5%) a possible overall precision of about 1-2% was claimed by the authors. The AFS methods probably require greater care in the instrument calibration and fluorescence measurements using the continuum source than does the AAS method described in Section 14.5.1.

REFERENCES

1. D. F. Boltz, in E. L. Grove and A. J. Perkins, "Developments in Applied Spectroscopy", Vol. 7A, p. 222, Plenum Press, New York, 1969.
2. M. Pinta, *Méthodes Phys. Anal.*, 1970, **6**, 268.
3. J. M. Ottaway, D. T. Coker and B. Singleton, *Talanta*, 1972, **19**, 787.
4. R. J. Jakubiec and D. F. Boltz, *Anal. Chem.*, 1969, **41**, 78.
5. Y. Yamamoto, T. Kumamaru, Y. Hayashi and Y. Otani, *Anal. Letters*, 1968, **1**, 955.
6. G. F. Kirkbright, A. M. Smith and T. S. West, *Analyst*, 1968, **93**, 292.
7. R. S. Danchik, D. F. Boltz and L. G. Hargis, *Anal. Letters*, 1968, **1**, 891.
8. G. F. Kirkbright, A. P. Rao and T. S. West, *Spec. Letters*, 1969, **2**, 69.
9. V. F. Barkovskii and T. V. Velikanova, *Russ. J. Inorg. Chem.* (English Transl.), 1970, **15**, 829.
10. *Idem*, ibid., 1966, **11**, 1230.
11. G. F. Kirkbright, A. M. Smith, T. S. West and R. Wood, *Analyst*, 1969, **94**, 754.
12. J. M. Ottaway, D. T. Coker and J. A. Davies, *Anal. Letters*, 1970, **3**, 385.
13. C. L. Chakrabarti and M. Katyal, *Anal. Chem.*, 1971, **43**, 1302.
14. R. J. Jakubiec and D. F. Boltz, *Anal. Letters*, 1968, **1**, 347.
15. H. N. Johnson, G. F. Kirkbright and T. S. West, *Analyst*, 1972, **97**, 696.
16. R. S. Danchik and D. F. Boltz, *Anal. Letters*, 1968, **1**, 901.
17. T. V. Ramakrishna, J. W. Robinson and P. W. West, *Anal. Chim. Acta*, 1969, **45**, 43.
18. G. Devoto, *Boll. Soc. Ital. Biol. Sper.*, 1968, **44**, 425.
19. A. M. Bond and T. A. O'Donnell, *Anal. Chem.*, 1968, **40**, 560.
20. H. Bartels, *At. Absorption Newsletter*, 1967, **6**, 132.
21. J. B. Ezell, Jr., *ibid.*, 1967, **6**, 84.
22. M. D. Garrido, C. Llagund and J. Carrindo, *Am. J. Enol. Viticult.*, 1971, **22**, 44.

23. E. D. Truscott, *Anal. Chem.*, 1970, **42**, 1657.
24. Y. Tofuku and S. Hirano, *Bunseki Kagaku*, 1971, **20**, 142.
25. H. Fujinuma, K. Kasama, K. Takeuchi and S. Hirano, ibid., 1970, **19**, 1487.
26. W. Reichel and L. Acs, *Anal. Chem.*, 1969, **41**, 1886.
27. U. Westerlund-Helmerson, *At. Absorption Newsletter*, 1966, **5**, 97.
28. W. J. Collinson and D. F. Boltz, *Anal. Chem.*, 1968, **40**, 1896.
29. Y. Yamamoto, T. Kumamaru, Y. Hayashi and Y. Otani, *Bunseki Kagaku*, 1968, **17**, 92.
30. T. Kumamaru, *Bull. Chem. Soc. Japan*, 1969, **42**, 956.
31. G. D. Christian and F. J. Feldman, *Anal. Chim. Acta*, 1968, **40**, 173.
32. A. M. Bond and J. B. Willis, *Anal. Chem.*, 1968, **40**, 2087.
33. E. Jungreis, *Israel J. Chem.*, 1969, **7**, 583.
34. R. S. Danchik and D. F. Boltz, *Anal. Chim. Acta*, 1970, **49**, 567.
35. *Idem*, *Anal. Chem.*, 1968, **40**, 2215.
36. T. Kumamaru, E. Tao, N. Okamoto and Y. Yamamoto, *Bull. Chem. Soc. Japan*, 1965, **38**, 2204.
37. Y. Yamamoto, T. Kumamaru, Y. Hayashi and Y. Otani, *Bunseki Kagaku*, 1969, **18**, 359.
38. M. E. Houser and M. I. Fauth, *Microchem. J.*, 1970, **15**, 399.
39. G. F. Kirkbright, A. M. Smith and T. S. West, *Analyst*, 1967, **92**, 411.
40. T. R. Hurford and D. F. Boltz, *Anal. Chem.*, 1968, **40**, 379.
41. G. Devoto, *Boll. Soc. Ital. Biol. Sper.*, 1968, **44**, 424.
42. G. Linden, S. Turk and B. Tarodo de la Fuente, *Chem. Anal.*, 1971, **53**, 244.
43. J. A. Parsons, B. Dawson, E. Callahan and J. T. Potts, Jr., *Biochem. J.*, 1970, **119**, 791.
44. W. S. Zaugg and R. J. Knox, *Anal. Chem.*, 1966, **38**, 1759.
45. *Idem*, *Anal. Biochem.*, 1967, **20**, 282.
46. W. S. Zaugg, *At. Absorption Newsletter*, 1967, **6**, 63.
47. T. Kumamaru, Y. Otani and Y. Yamamoto, *Bull. Chem. Soc. Japan*, 1967, **40**, 429.
48. K. C. Singhal, A. C. Banerji and B. K. Banerjee, *Technology* (*Sindri*), 1968, **5**, 117.
49. K. C. Singhal and B. K. Banerjee, *Technology* (*Sindri*), 1968, **5**, 239.
50. J. R. Melton, W. L. Hoover, P. A. Howard and V. S. Green, *J. Assoc. Offic. Anal. Chemists*, 1971, **54**, 373.
51. H. K. Y. Lau and P. F. Lott, *Talanta*, 1971, **18**, 303.
52. L. A. Trudell and D. F. Boltz, *Mikrochim. Acta*, 1970, 1220.
53. R. W. Looyenga and C. O. Huber, *Anal. Chem.*, 1971, **43**, 498.
54. D. A. Roe, D. S. Miller and L. Lutwak, *Anal. Biochem.*, 1966, **15**, 313.
55. B. Magyar and F. Santos, *Helv. Chim. Acta*, 1969, **52**, 820.
56. R. Dunk, R. A. Mostyn and H. C. Hoare, *At. Absorption Newsletter*, 1969, **8**, 79.
57. J. A. Varley and P. Y. Chin, *Analyst*, 1970, **95**, 592.
58. F. Y. Borden and L. H. McCormic, *Soil. Soc. Am. Proc.*, 1970, **34**, 705.
59. G. G. Galindo, H. Applet and E. B. Schalscha, ibid., 1969, **33**, 974.
60. S. A. Rose and D. F. Boltz, *Anal. Chim. Acta*, 1969, **44**, 239.
61. E. Jungreis and Z. Anavi, ibid., 1969, **45**, 190.
62. R. W. Looyenga and C. O. Huber, ibid., 1971, **55**, 179.
63. T. Kumamaru, Y. Hayashi, N. Okamoto, E. Tao and Y. Yamamoto, ibid., 1966, **35**, 524.
64. T. Kumamaru, ibid., 1968, **43**, 19.

65. Y. Yamamoto, T. Kumamaru and Y. Hayashi, *Talanta*, 1967, **14**, 611.
66. Y. Yamamoto, T. Kumamaru, Y. Hayashi and Y. Otani, *Bull. Chem. Soc. Japan*, 1969, **42**, 1774.
67. H. K. L. Gupta and D. F. Boltz, *Microchem. J.*, 1971, **16**, 571.
68. D. G. Berge, R. T. Pflaum, D. A. Lehman, and C. W. Franck, *Anal. Letters*, 1968, **1**, 613.
69. F. J. Diaz, *Anal. Chim. Acta*, 1972, **58**, 455.
70. A. L. Potter, E. D. Ducay and R. M. Macready, *J. Assoc. Offic. Anal. Chemists*, 1968, **51**, 748.
71. J. C. Sheridan, E. P. K. Lau and B. Z. Senkowski, *Anal. Chem.*, 1969, **41**, 247.
72. J. Courtot-Coupez and A. Le Bihan, *Anal. Letters*, 1969, **2**, 567.
73. A. Walsh, *Proc. Xth Colloq. Spectrosc. Internationale*, p. 127, Hilger, 1962.
74. B. V. L'Vov and A. D. Khartsyzov, *Zh. Prikl. Spektr.*, 1969, **11**, 413.
75. G. F. Kirkbright and M. Marshall, *Anal. Chem.*, 1972, **44**, 1228.
76. G. F. Kirkbright, T. S. West and P. J. Wilson, *At. Absorption Newsletter*, 1972, **11**, 53.
77. B. V. L'Vov, "Atomic Absorption Spectrochemical Analysis", Hilger, London, 1970, p. 260.
78. K. R. Osborn and H. E. Gunning, *J. Opt. Soc. Am.*, 1955, **45**, 552.
79. H. Kirchof, *Spectrochim. Acta*, 1969, **24B**, 235.
80. W. H. Brimhall, *Anal. Chem.*, 1969, **41**, 1349.
81. A. N. Zaidel and E. P. Korennoi, *Opt. i. Spektrosk.*, 1961, **10**, 570.
82. A. N. Zaidel and E. P. Korennoi, *Zav. Lab.*, 1963, **29**, 1449.
83. D. C. Manning and W. Slavin, *At. Absorption Newsletter*, 1962, **1**, 39.
84. J. A. Goleb and Y. Yokoyama, *Anal. Chim. Acta*, 1964, **30**, 213.
85. J. A. Goleb, *Anal. Chem.*, 1963, **35**, 1978.
86. J. A. Goleb, *Anal. Chim. Acta*, 1966, **34**, 135.
87. B. V. L'Vov and V. I. Mosichev, *Zh. Prikl. Spektrosk.*, 1966, **4**, 491.
88. L. M. Fraser and J. D. Winefordner, *Anal. Chem.*, 1971, **43**, 1693.
89. J. D. Winefordner, *Accounts Chem. Res.*, 1969, **2**, 361.
90. M. B. Denton and H. V. Malmstadt, *Appl. Phys. Letters*, 1971, **18**, 485.
91. L. M. Fraser and J. D. Winefordner, *Anal. Chem.*, 1972, **44**, 1444.
92. N. Omenetto, N. N. Hatch, L. M. Fraser and J. D. Winefordner, *Anal. Chem.*, 1973, **45**, 195.
93. A. P. D'Silva, R. N. Kniseley, V. A. Fassel, R. H. Curry and R. B. Myers, *Anal. Chem.*, 1964, **36**, 532.
94. D. N. Hingle, G. F. Kirkbright and T. S. West, *Analyst*, 1969, **94**, 864.
95. R. N. Kniseley, C. C. Butler and V. A. Fassel, *Anal Chem.*, 1969, **41**, 1494.
96. T. J. McDrath, in "Modern Optical Methods in Gas Dynamic Research", ed. D. S. Dosanjh, Plenum Press, New York, 1971.
97. M. Hercher, *Appl. Optics*, 1967, **6**, 947.
98. M. Hercher, W. Chu and D. L. Stockman, *I.E.E.E. J. Quantum Elect.*, 1968, **QE4**, 954.
99. L. Huff and L. G. DeShafer, *J.O.S.A.*, 1970, **60**, 157.
100. F. Gires, *I.E.E.E. J. Quantum Elect.*, 1966, **QE2**, 624.
101. C. R. Guiliano and L. D. Hess, *I.E.E.E. J. Quantum Elect.*, 1967, **QE3**, 358.
102. N. Omenetto, P. Benetti, L. P. Hart, J. D. Winefordner and C. Th. J. Alkemade, *Spectrochim. Acta*, 1973, **28B**, 289.
103. J. D. Winefordner, *Proc. 4th International Conf. on Atomic Spectroscopy*, Toronto, 1973.

104. E. H. Piepmeier, *Spectrochim. Acta*, 1972, **27B**, 431.
105. E. H. Piepmeier, *Spectrochim. Acta*, 1972, **27B**, 445.
106. N. Omenetto, L. P. Hart, P. Benetti and J. D. Winefordner, *Spectrochim. Acta*, 1973, **28B**, 301.
107. A. G. Gaydon and H. G. Wolfhard, "Flames, Their Structure, Radiation and Temperature", Chapman and Hall, London, 3rd ed., 1970.
108. R. H. Tourin, "Spectroscopic Gas Temperature Measurements", Elsevier, Amsterdam, 1966.
109. G. F. Kirkbright, M. Sargent and S. Vetter, *Spectrochim. Acta*, 1970, **25B**, 465.
110. R. F. Browner and J. D. Winefordner, *Anal. Chem.*, 1972, **44**, 247.
111. N. Omenetto, P. Benetti and G. Rossi, *Spectrochim. Acta*, 1972, **27B**, 453.
112. C. T. J. Alkemade, *Pure Appl. Chem.*, 1970, **23**, 73.

Subject Index